UNIVERSIDAD DE GRANADA
Departamento de Química Orgánica

Diseño, síntesis y evaluación de estructuras bidimensionales orgánicas como nuevos dispositivos en Electrónica Molecular

MEMORIA DE TESIS DOCTORAL

presentada por

ANA MARTÍN LASANTA

para optar al título de

DOCTOR EN QUÍMICA

Con mención DOCTOR INTERNACIONAL

Granada, Septiembre de 2013

El doctorando ANA MARTÍN LASANTA y los directores de la tesis JUAN MANUEL CUERVA CARVAJAL, LUIS ALVAREZ DE CIENFUEGOS RODRÍGUEZ y DELIA MIGUEL ALVAREZ, garantizamos, al firmar esta tesis doctoral, que el trabajo ha sido realizado por el doctorando bajo la dirección de los directores de la tesis y hasta donde nuestro conocimiento alcanza, en la realización del trabajo, se han respetado los derechos de otros autores a ser citados, cuando se han utilizado sus resultados o publicaciones.

Granada, Septiembre 2012

Director/es de la Tesis   Doctorando

Fdo.: Juan Manuel Cuerva Carvajal   Fdo.: Ana Martín Lasanta

Fdo.: Luis Álvarez de Cienfuegos Rodríguez

Fdo.: Delia Miguel Álvarez

Los doctores JUAN MANUEL CUERVA CARVAJAL, LUIS ALVAREZ DE CIENFUEGOS RODRÍGUEZ y DELIA MIGUEL ALVAREZ,

CERTIFICAN:

Que la presente memoria titulada *"Diseño, síntesis y evaluación de estructuras bidimensionales orgánicas como nuevos dispositivos en Electrónica Molecular"* ha sido realizada en el Departamento de Química Orgánica de la Universidad de Granada, bajo su dirección, por la licenciada ANA MARTIN LASANTA y autorizan su presentación para que sea calificada como Tesis Doctoral con mención de Doctor Internacional.

Granada, Septiembre 2013.

Fdo.: Dr. Juan Manuel Cuerva Carvajal

Fdo.: Dr. Luis Álvarez de Cienfuegos Rodríguez

Fdo.: Dr. Delia Miguel Álvarez

ORGANIZACIÓN DE LA MEMORIA

El trabajo realizado durante la presente Tesis Doctoral se ha organizado en dos bloques que corresponden a dos líneas de investigación diferentes que se desarrollan en el grupo. El primero está dedicado al diseño, síntesis y caracterización de moléculas orgánicas como nuevos dispositivos en electrónica molecular y recoge los capítulos 1 y 2. El segundo bloque (capítulo 3) incluye el trabajo realizado en el campo de la química de radicales mediada por complejos de Ti(III) en la que el grupo tiene una dilatada experiencia. Al comienzo de cada capítulo se incluye una introducción y el objetivo de cada proyecto. El desarrollo de cada uno de los objetivos comprende los antecedentes y la discusión de los resultados así como las conclusiones, perspectivas y la parte experimental.

En el capítulo 1 denominado *"Towards the synthesis of carbon networks based on graphyne substructures"* se presenta una introducción que pretende mostrar el creciente interés de la comunidad científica en el desarrollo de alótropos bidimensionales del carbono y algunas de las metodologías que se han llevado a cabo para sintetizar fragmentos de grafeno y estructuras relacionadas como el grafino. A continuación, se exponen los resultados obtenidos en la síntesis de subestructuras anisotrópicas del grafino con malla de tetrabenzociclina que podrían actuar como cables moleculares desconectados electrónicamente aunque unidos covalentemente (objetivo 1). En este primer capítulo también se incluyen los primeros esfuerzos dedicados a la síntesis de estructuras 2D-conductoras mediante una aproximación supramolecular (objetivo 2).

Como los dehidrobenzoanulenos, los oligómeros lineales tipo fenilacetileno son subestructuras del grafino. La libertad conformacional de estos oligómeros nos ha permitido desarrollar subestructuras del grafino no planas. En el capítulo 2, titulado *"Synthesis and characterization of graphyne-based helical scaffolds"* se incluyen los resultados obtenidos en el desarrollo de hélices con estructura de *o-phenylene-ethynylene* (*o*PE) siguiendo dos estrategias diferentes: la restricción conformacional mediante la formación de enlaces covalentes (objetivo 1) y la inducción de la estructura helicoidal mediante la formación de complejos Ag(I)- alquino (objetivo 2). Dichos estudios han generado resultados muy esperanzadores dirigidos al desarrollo de complejos organometálicos quirales con ligandos helicoidales con potenciales propiedades como catalizadores como se recoge en el apartado de conclusiones y trabajo futuro.

En el tercer capítulo titulado *"Ti/Pd-mediated Michael-type conjugated additions", t*ras una introducción que pretende proporcionar una visión general de los fundamentos, reactividad y aplicaciones a la síntesis de la química del cloruro de bis(ciclopentadienil)titanio(III), se presentan los resultados obtenidos en el desarrollo de nuevas metodologías de síntesis para la formación de carbo- y heterociclos de cinco y seis miembros mediante reacciones de adición tipo Michael. El uso combinado de los metales de transición Ti/Pd ha permitido la formación de nuevos enlaces C-C a partir de pronucleófilos alílicos estables como son los carbonatos y carboxilatos.

Por último, de manera resumida y en forma de anexos, se han incluido otros resultados obtenidos durante el desarrollo de esta Tesis Doctoral.

RESUMEN

Capítulo 1: HACIA LA SÍNTESIS DE REDES BIDIMENSIONALES CONDUCTORAS DE CARBONO

El carbono atómico es una especie de vida corta que se estabiliza en varias estructuras multiatómicas con distintas configuraciones moleculares llamadas *alótropos*. Muchos autores consideran el descubrimiento de los fullerenos y los nanotubos, el evento desencadenante de la "fiebre del carbono" auspiciada poco después por el aislamiento del grafeno. Aunque a lo largo de estos años, los intereses y esfuerzos dedicados al estudio y la fabricación de los compuestos de carbono se han diversificado en innumerables campos de investigación, los polímeros de carbono bidimensionales han sido unos de los grandes protagonistas como consecuencia de las nuevas y fascinantes propiedades geométricas, ópticas y electrónicas predichas y medidas para el grafeno.

Aunque las síntesis en superficie de grafenos (redes de átomos con hibridación sp^2) están proporcionando resultados muy prometedores, la fabricación de mallas que incluyan combinaciones de átomos de carbono con distinta hibridación sigue estando limitada a la síntesis orgánica "clásica". De entre la infinidad de los alótropos de carbono 2D con mallas mixtas ($sp+sp^2$) imaginables, el grafino y el grafidiino son los más populares debido a las predicciones teóricas publicadas sobre sus propiedades electrónicas, especialmente como conductores moleculares con potenciales aplicaciones en Electrónica Molecular.

La Electrónica Molecular es una rama de la nanotecnología que se centra en el estudio y empleo de moléculas para fabricar dispositivos electrónicos. El transporte electrónico es por tanto un tema central en el que los denominados cables moleculares son los protagonistas. Un problema práctico de la Electrónica Molecular es conseguir que los sistemas tengan estabilidad mecánica y por consiguiente electrónica. La detección de un efecto estocástico de "encendido-apagado" (*blinking*) de los dispositivos electrónicos unimoleculares construidos en microscopios de efecto túnel (STM) desató un gran debate sobre cómo mejorar la estabilizad de estos dispositivos. En este contexto, nuestro grupo de investigación ha demostrado de forma teórica que moléculas con más de un contacto presentan mayor estabilidad mecánica y propiedades conductoras. Animados por estos resultados nos propusimos sintetizar una estructura 2D conductora con malla de tetrabenzociclina que permitiera aumentar el número de contactos con una superficie metálica así como comportarse como un conjunto de cables moleculares.

La estrategia sintética para construir una red de este tipo se ha basado en dos reacciones: la reacción de acoplamiento de Sonogashira para crecer el esqueleto molecular y la reacción de metátesis de alquinos para cerrar la malla. La síntesis de la subunidad estructural más pequeña de esta red se ha llevado a cabo con éxito tras varias optimizaciones estructurales y de condiciones de reacción para la etapa de cierre del anillo. Desafortunadamente los múltiples intentos de extender la estructura han resultado infructuosos. Sin embargo, la caracterización espectroscópica de los productos finales e intermedios de las moléculas sintetizadas apoyan la hipótesis de partida de que los cables moleculares unidos covalentemente en posición *meta* están débilmente conectados electrónicamente. Un problema inherente al modelo de red diseñado es que no permite solventar la gran limitación de la solubilidad concomitante a la "planarización" de la estructura molecular, ni aliviar la tensión de anillo de las estructuras "poli-fusionadas". Por eso, como trabajo futuro, proponemos un nuevo diseño de malla que tiene en cuenta ambos factores.

Dentro del proyecto dirigido a construir redes moleculares bidimensionales conductoras, también se han realizado los primeros esfuerzos dedicados a la síntesis de estructuras 2D-conductoras mediante una aproximación supramolecular. Esta segunda aproximación se basa en la capacidad de autoensamblaje de las bases nitrogenadas adenina y timina. Los resultados obtenidos, aunque muy preliminares, sugieren que para sintetizar estructuras extensas, hay que mejorar la solubilidad de los productos de partida o emplear técnicas de síntesis en fase sólida. Además, para reforzar el proceso de autoensamblaje, se proponen otros pares de moléculas capaces de formar tres enlaces de hidrógeno para los cuáles las constantes de asociación descritas son varios órdenes de magnitud mayores.

Capítulo 2: SÍNTESIS Y CARACTERIZACIÓN DE ESTRUCTURAS HELICOIDALES π-CONJUGADAS

Las funciones de las macromoléculas biológicas como son las proteínas y el ADN dependen de su estructura tridimensional que está definida de forma general por interacciones no covalentes como son el enlace de hidrógeno, el π-stacking, las interacciones electrostáticas y las interacciones solvofóbicas. Combinando las guías de la naturaleza con las herramientas desarrolladas por la química orgánica sintética y la química supramolecular, se pueden encontrar en bibliografía una gran variedad de polímeros con estructura tridimensional definida. Aunque son muchas las posibilidades, las hélices son probablemente el motivo estructural 3D más frecuente y estudiado.

En el campo de la química, se denomina *foldámeros* a los oligómeros moleculares capaces de adoptar estructuras ordenadas en disolución mediante interacciones no covalentes entre sus monómeros. Como las benzociclinas, los oligómeros de fenilacetileno son moléculas que constituyen en el esqueleto del grafino. En concreto, los polímeros de *meta*- (*m*PE) y *orto*-fenilacetileno (*o*PE) permiten generar estructuras tridimensionales de grafino gracias a la libertad conformacional de su esqueleto. En este segundo capítulo, hemos desarrollado dos proyectos centrados en el estudio y caracterización de subestructuras del grafino basadas en oligómeros de *orto*-fenilacetileno que adoptan una estructura tridimensional de hélice.

Nuestro primer objetivo ha perseguido cerrar la estructura mínima (1 *loop*) de hélices con esqueleto de cable molecular, restringiendo la libertad conformacional de los oligómeros mediante la formación de enlaces covalentes entre los dos anillos apilados. Utilizando tetrámeros de *o*PE funcionalizados con distintas cadenas laterales, hicimos un sondeo de reacciones de macrociclación. Afortunadamente, la reacción de doble esterificación de los tetrámeros funcionalizados con grupos hidroximetil dio lugar a los macrociclos deseados. Un estudio teórico (cálculos DFT) sobre la termodinámica del proceso ha revelado que gran parte del éxito de esta ciclación reside en la existencia de un enlace de hidrógeno intramolecular que preorganiza la estructura favoreciendo la formación del monociclo frente a otras especies poliméricas. Posteriormente, también hemos cerrado la estructura helicoidal utilizando la reacción de metátesis de alquenos catalizada por el catalizador de Grubbs de primera generación.

Además del grupo funcional conector, la localización del mismo, el número de puntos de unión y la longitud-naturaleza de la "grapa" son factores que determinan el éxito de la macrociclación así como las propiedades estructurales de los productos (flexibilidad del esqueleto y tamaño de la cavidad). Para el análisis de las propiedades de las hélices sintetizadas se han llevado a cabo varios estudios. Las propiedades geométricas se estudiaron en estado sólido (cristalización y resolución de las estructuras de rayos X). De los espectros de absorción y fluorescencia se pudo comprobar el mantenimiento de la flexibilidad y delocalización electrónica (aromaticidad) del esqueleto de *o*PE tras la ciclación. Un estudio teórico (DFT) realizado sobre un compuesto modelo ha revelado el comportamiento pseudoelástico para estas hélices bajo estrés mecánico.

Para fijar la estructura de la hélice en un sentido (quiralidad en eje; notación M, P), se ha utilizado un ácido-*L*-tartárico en el que los grupos hidroxilo están protegidos con grupos pivaloilo. Para tres sustratos di-funcionalizados y uno tetrafuncionalizado con cuatro grupos hidroximetil, se obtuvieron mezclas diastereoenriquecidas cuya composición se determinó mediante experimentos de dicroísmo circular (CD) y HPLC quiral. La determinación de la configuración M, P de las mezclas de diastereisómeros, se hizo en base a la simulación de los resultados experimentales mediante cálculos de TD-DFT. El aislamiento de una única hélice de quiralidad M, se consiguió cerrando un esqueleto de *o*PE, primero con una "grapa" quiral que definió un eje preferente y, después, haciendo más rígida la estructura con una segunda "grapa" formada mediante la reacción de metátesis de alquenos.

A la luz de los resultados anteriores, proponemos que estos macrociclos de esqueleto conjugado cuya estructura helicoidal es permanente, podrían emular las propiedades de un soleniode molecular si se utilizaran para construir un dispositivo electrónico unimolecular. Por otro lado, también podrían comportarse como muelles moleculares sometidos a compresión-tracción mecánica ya que su estructura helicoidal es flexible y capaz de recuperar la conformación inicial cuando se deja de aplicar la fuerza.

La extensión de esta metodología de cierre covalente a otras geometrías se consiguió con éxito para las hélices con estructura romboidal quiral con la "grapa" de *L*-tartrato. Otros esqueletos de polifenilcarbazol se cerraron utilizando como reacción de cierre la metátesis de alquenos. Sin embargo la extensión de esta metodología a estructuras de *o*PE con varias vueltas resultó muy complicada debido a la limitada solubilidad de los productos polihidroxilados de partida.

Esta estrategia de cierre covalente, nos proporcionó una nueva colección de nuevos macrociclos de tamaño definido que podrían actuar como ligandos. La integración de metales en la cavidad de un "poro molecular" es uno de los métodos habituales para obtener complejos organometálicos y, en última instancia, catalizadores. Por eso, comenzamos a explorar la capacidad de quelación de estos macrociclos con una colección de metales. De entre los distintos metales probados, los metales carbófilos Ag(I) y Au(I) dieron lugar al movimiento de las señales de los hidrógenos aromáticos que se atribuyó a la formación de un complejo de coordinación. Más interesante fue descubrir que la Ag(I) podían inducir el plegamiento helicoidal de los oligómeros de *o*PE abiertos.

Los resultados de RMN de protón y carbono de los ligandos libres y los complejos generados, proporcionaron información muy útil sobre el modo de coordinación preferente de la Ag(I). En consonancia con los precedentes descritos en bibliografía para el enlace Ag(I)-alquino, confirmamos que los tetrámeros de *o*PE con tres enlaces triples actúan como ligandos π-donores. La obtención de un cristal nos ha permitido confirmar que, en estado sólido, el ión Ag(I) se encuentra coordinado dentro de la cavidad del macrocilo mediante tres enlaces η-2 a los tres alquinos (coordinación trigonal plana ligeramente distorsionada). La geometría óptima generada mediante cálculos de DFT reproduce con éxito la estructura cristalina obtenida aunque predice distancias ligeramente mayores para los enlaces Ag(I)-alquino.

Con el fin de estudiar la fortaleza de la interacción Ag(I)-alquino, hemos realizado valoraciones utilizando ^{1}H-RMN, espectroscopia de *UV-vis* y CD. Los resultados de las valoraciones sugieren que la capacidad de coordinación de estos macrociclos es discreta en términos de energía libre y depende en gran parte del tamaño de la cavidad que generan, de la flexibilidad del esqueleto cíclico y de la geometría de coordinación preferente de la Ag(I).

Como se ha mencionado, durante los estudios de quelación de las hélices con el ión Ag(I), observamos que este metal parecía inducir el plegamiento helicoidal de los oligómeros abiertos de *o*PE. Un estudio sistemático realizado en seis nuevos ligandos con libertad conformacional (abiertos) y no sustituidos con cadenas laterales (sólo anillos de benceno y alquinos) confirmó la capacidad de la Ag(I) para generar la estructura tridimensional en hélice siempre y cuando los tres alquinos estén localizados en *orto*. Además, un crecimiento exponencial del valor de la constante de unión/plegamiento puso de manifiesto efectos cooperativos para los ligandos con más de tres alquinos (sitios de unión). Las geometrías optimizadas (DFT) de los complejos catiónicos (es decir, sin tener en cuenta el contraión BF_4^-), sugieren que el ión Ag(I) puede coordinarse de distantas formas a tres o cuatro grupos alquino, i.e. coordinación tetrahédrica o trigonal plana. Curiosamente, algunas de las geometrías calculadas sugieren la formación de contactos Ag-Ag para los ligandos con 6 alquinos o más.

Dado el éxito de la aproximación supramolecular a la síntesis de estructuras helicoidales mediante coordinación con sales de Ag(I) y la magnitud de las constantes de asociación medidas, por último, hemos realizado un estudio sobre la cinética de plegamiento y el efecto de la coordinación, en una familia de hélices con características espectroscópicas peculiares. Para ello, hemos utilizado como "sonda fluorescente" grupos pireno. El pireno es una molécula fluorescente que se utiliza habitualmente como sensor porque forma excímeros. Se denominan excímeros a los dímeros de vida corta que se forman en estado excitado entre dos moléculas iguales y que presentan propiedades espectroscópicas únicas.

En el último estudio de este capítulo, hemos sintetizado cuatro nuevas hélices que comprenden un grupo pirenil en al menos uno de los extremos. Mediante RMN de protón hemos corroborado que esta nueva familia de hélices mantiene las genuinas características de coordinación (i.e. plegamiento) con la Ag(I) observadas en los *o*PE estudiados con anterioridad. Además, hemos realizado un estudio de fluorescencia en tiempo resuelto que proporciona información cuantitativa sobre la cinética de

plegamiento de estos *o*PE en disolución y que demuestra inequívocamente que la presencia de Ag(I) estabiliza la conformación helicoidal. Además, durante estos estudios observamos que los ligandos que tienen grupos metoxilo en su estructura se coordinan a la plata con constantes de asociación mucho mayores y manteniendo la disposición helicoidal. Este descubrimiento afortunado abre la posibilidad de desarrollar una nueva familia de *helicatos* ditópicos más estables, chirales y capaces de coordinarse otros metales. Como trabajo futuro, pretendemos desarrollar una nueva familia de ligandos cambiando el grupo metoxilo por otras cadenas laterales quirales y el átomo de oxígeno por otros heteroátomos.

<u>Capítulo 3: ADICIONES CONJUGADAS TIPO MICHAEL MEDIADAS POR EL SISTEMA MULTIMETÁLICO Pd/Ti.</u>

La química de radicales libres es una de las herramientas más útiles en Química Orgánica para la formación de enlaces C-C. El cloruro de bis(ciclopentadienil)titanio(III) ha demostrado ser un reactivo excelente en el campo de la química de radicales libres. La especie activa de Ti(III) (i.e. [Cp$_2$TiCl]) se genera fácilmente por agitación *in situ* de un complejo comercial de titanio(IV), Cp$_2$TiCl$_2$, con un metal reductor. Además este reactivo de transferencia monoelectrónica es un ácido de Lewis suave, altamente oxofílico. Tal combinación de propiedades lo convierten en un reactivo de síntesis muy útil como demuestra su variada reactividad hacia epóxidos, haluros alílicos y propargílicos y aldehídos α,β-insaturados. Además, el cloruro de bis(ciclopentadienil)titanio(III) combinado con reactivos que actúan como fuente de átomo de hidrógeno ha dado lugar al desarrollo de nuevas metodologías de reducción de radicales carbonados. Sorprendentemente, el agua ha resultado ser un excelente reactivo fuente de átomo de hidrógeno en combinación con el cloruro de bis(ciclopentadienil)titanio(III).

Otra de las sinergías más éxitosas del titanoceno, se ha traducido en el desarrollo de metodologías que combinan las ventajas de la química de radicales libres y la de los metales de transición, a las que nuestro grupo ha contribuido significativamente. En este contexto, hemos desarrollado un método eficiente para la alilación intramolecular tipo Michael de grupos carbonilo α,β-insaturados, a partir de carbonatos y carboxilatos alílicos (pronucleófilos). El uso combinado en cantidades catalíticas de complejos de Ti/Pd ha permitido la síntesis de carbo- y heterociclos de cinco y seis miembros con rendimientos moderados y generalmente buenas diastereoselecciones. Además, hemos realizado varias pruebas mecanísticas que confirman que esta reacción transcurre mediante una vía radicalaria.

CHAPER I. Towards the synthesis of 2D conducting carbon networks.

1.1. Introduction

1.1.1. Carbon and its flat allotropes

Atomic carbon is a very short-lived species stabilized in various multi-atomic structures with different molecular configurations called *allotropes*.[1] The three traditional carbon allotropes are amorphous carbon (Figure 1g), graphite (Figure 1b) and diamond (Figure 1a). But in the last decades, several other exotic allotropes have been discovered, such as fullerenes (Figure 1d-f),[2] carbon nanotubes (Figure 1h),[3] graphene (Figure 1b, one carbon sheet),[4] lonsdaleite (Figure 1c),[5] glassy carbon,[6] carbon nanofoam,[7] chaoite (carbyne)[8] and so on (Figure 1, right). Carbon ability to form virtually an infinite number of compounds is largely due to the varied types of bonds it can form and the number of different elements it can join in bonding. In order to deal with the apparently inflationary number of discovered and hypothetical carbon allotropes, Koga *et al.* proposed a classification scheme for all-carbon materials according to the type of hybridization of the valence orbitals (Figure 1, left) and a related tentative ternary carbon allotropy diagram (Figure 2).[9]

[1] "Allotrope", IUPAC Gold Book Electronic version, http://goldbook.iupac.org/A00243.html.

[2] The solid-state manifestation of fullerenes is called fullerite. H.W. Kroto, J.R. Heath, S.C. O'Brien, R.F. Curl, R.E. Smaliey, *Nature* **1985**, *318*, 162–163.

[3] (a) S. Iijima, *Nature* **1991**, *354*, 56-58; (b) S. Iijima, T. Ichihashi, *Nature* **1993**, *363*, 603-605.

[4] K. S. Novoselov, A. K. Geim, S. V. Morozov, D. Jiang, Y. Zhang, S. V. Dubonos, I. V. Grigorieva, A. A. Firsov, *Science* **2004**, *306*, 666-669.

[5] Lonsdaleite or hexagonal diamond is an allotrope of carbon with a hexagonal lattice. In nature, it forms when meteorites containing graphite strike the Earth. It was first identified in 1967 from the Canyon Diablo meteorite. C. Frondel, U. B. Marvin, *Nature* **1967**, *214*, 587–589.

[6] Glassy carbon or vitreous carbon is a non-graphitizing carbon which combines glassy and ceramic properties with those of graphite. (a) R. E. Franklin, *Proc. Roy. Soc., A* **1951**, *209*, 196-218; (b) J. C. Lewis, B. Redfern, F. C. Cowlard, *Solid-State Electronics* **1963**, *6*, 251–254; (c) P. J. F. Harris, *Philosophical Magazine* **2004**, *84 (29)*, 3159–3167.

[7] Carbon nanofoam is a low-density cluster-assembly of carbon atoms strung together in a loose three-dimensional network. Each cluster is about 6 nanometers wide and consists of about 4000 carbon atoms linked in graphite-like sheets that are given negative curvature. A. V. Rode, S. T. Hyde, E. G. Gamaly, R. G. Elliman, D. R. McKenzie, S. Bulcock, *Appl. Phys. A* **1999**, *69 (7)*, S755–S758.

[8] The "missing link" in the story of carbon allotropy was a one-dimensional (chain-like) polymer coined as carbyne. (a) V. I. Kasatochkin, A. M. Sladkov, N. M. Popov, Y. P. Kudryavtsev, V. V. Korshak, *Dokl. Akad. Nauk, USSR* **1967**, *177*, 358. Chaoite or white carbon is a mineral discovered in shock-fused graphite gneiss from the Ries crater in Bavaria. From its electron diffraction pattern, the mineral has been considered to have a carbyne structure. (b) A. El Goresy, G. Donnay, *Science* **1968**, *161*, 363–364. Some references concerning the polemic about the existence of carbyne and its related mineral chaoite. (c) A. G. Whittaker, P. L. Kintner, *Science* **1969**, *165*, 589-591; (d) A. G. Whittaker, G. M. Wolten, *Science* **1972**, *178*, 54-56; (e) P. P. K. Smith, P. R. Buseck, *Science* **1982**, *216*, 984-986. The first synthesis of a long-chain acetylenic bond species: (f) R. Eastmond, T. R. Johnson, D. R. M. Walton, *Tetrahedron* **1972**, *28*, 4601-4616; (g) R. J. Lagow *et al. Science* **1995**, *267*, 362-367.

[9] R. B. Heimann, S. E. Evsyukov, Y. Koga, *J. Chem. Phys.* **1997**, *35*, 1654-1658.
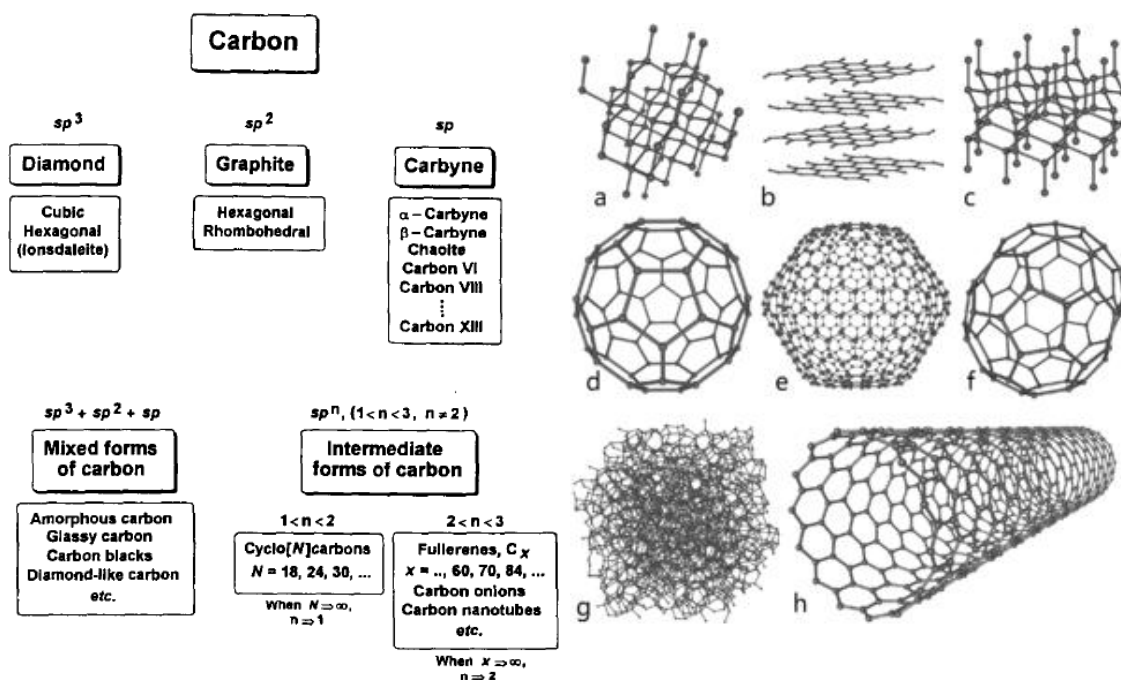
Figure 1. *Classification scheme for all-carbon materials according to the type of hybridization (left).*
[From ref. 9] Some carbon allotropes: a) diamond, b) graphite, c) lonsdaleite, d) C_{60}, e) C_{540}, f) C_{70},
g) amorphous carbon and h) single-walled carbon nanotube (right). [From "allotropes of carbon" in
Wikipedia]

In such schemes, each unique valence state (sp^3-, sp^2-, and sp-hybridization) belongs to a distinct archetypical allotropic form that is characterized by its polymeric connectivity.[10] Hence, the sp^3-type of hybridization corresponds to a spatial (3D) polymer of carbon represented by diamond. The sp^2-type of hybridization corresponds to a planar (2D) polymer represented by graphite. Finally, the sp-type of hybridization corresponds to a linear (1D) chain-like polymer of carbon represented by carbyne.[11] All other forms of carbon are considered transitional carbon forms and have been divided into two groups: mixed forms of carbon and intermediate carbon forms.[12]

---

[10] According to this classification, fullerenes and their derivatives have to be considered zero-dimensional since their closed-cage molecules do not lend themselves to polymeric structures connected by directional bonds but only to van der Waals-type interactions. See e.g.: P.D.W. Boyd, C.A. Reed *Acc. Chem. Res*. **2005**, *38*, 235-242.

[11] To obtain an overview about the molecular polyynes isolated and characterized to date see: (a) S. Szafert, J. A. Gladysz, *Chem. Rev.* **2003**, *103*, 4175–4205; (b) S. Szafert, J. A. Gladysz, *Chem. Rev.* **2006**, *106*, PR1–PR33; (c) W. A. Chalifoux, R. R. Tywinski, *Nat. Chem.* **2010**, *2*, 967-971.

[12] The fractional degree of hybridization found in intermediate carbon forms is due to the curvature of their frameworks causing the carbon skeleton to be strained. For instance, the degree of hybridization of carbon atoms in C60 the most in-depth studied member of the fullerene family, was reported to be 2.28. See: R. C. Haddon, *Phil. Trans. Roy. Soc. London, Ser. A.-Phys. Sci. Eng.* **1993**, *343*, 53-62.
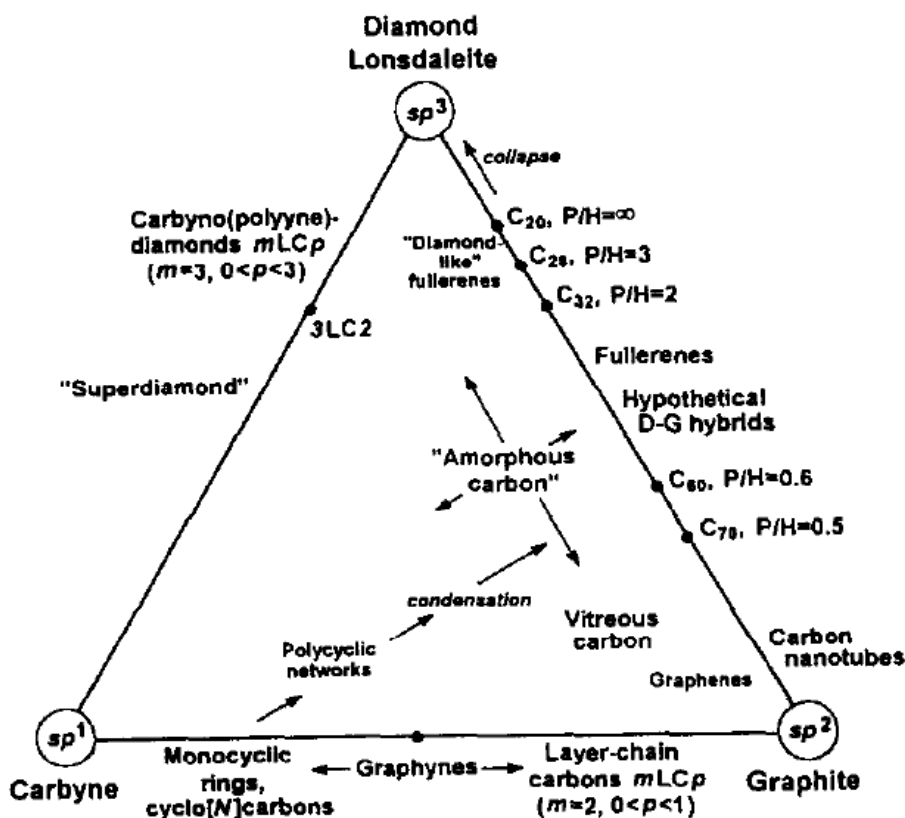
13

Figure 2. *Ternary "phase" diagram of carbon allotropes. [From ref. 9]*

The demonstration that fullerenes are stable carbon molecules because of their high kinetic stabilization has fuelled world-wide efforts to prepare new molecular and polymeric carbon allotropes[13] of fundamental interest in nanosciences and technology.[14] On the other hand, since successful preparation of graphene by mechanical cleavage from graphite in 2004,[4] the paradigm of 2D nanomaterial has rapidly risen to be one of the hottest stars in materials science, chemistry and physics due to its many exciting and unusual electronic, optic and geometric characteristics.[15]

1.1.2. Synthesis of graphene fragments

---

[13] F. Diederich, *Nature* **1994**, *369*, 199-207.

[14] T. N. Hoheisel, S. Schrettl, R. Szilluweit, H. Frauenrath, *Angew. Chem. Int. Ed.* **2010**, *49*, 6496-6515.

[15] To read more about graphene, see e.g.: (a) C. N. R. Rao, A. K. Sood, K. S. Subrahmanyam, A. Govindaraj, *Angew. Chem. Int. Ed.* **2009**, *48*, 7752-7777; (b) M. J. Allen, V. C. Tung, R. B. Kaner, *Chem. Rev.* **2010**, *110,* 132–145; (c) D. R. Dreyer, R. S. Ruoff, C. W. Bielawski, *Angew. Chem. Int. Ed.* **2010**, *49*, 9336-9344. About other graphene-like materials: M. Xu, T.Liang, M. Shi, H. Chen, *Chem. Rev.* **2013**, *113*, 3766–3798.
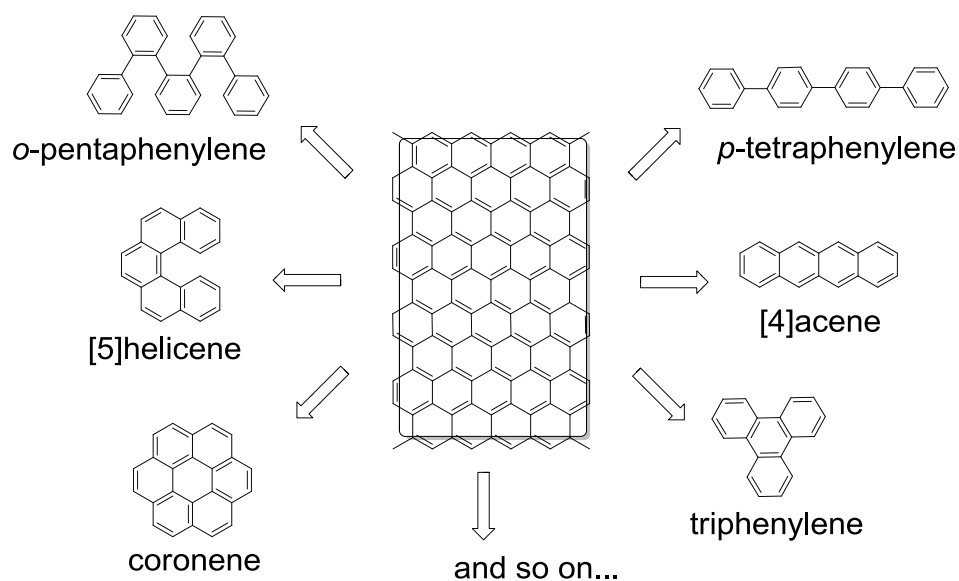
Figure 3. *Some polycyclic aromatic hydrocarbons (PAHs) and polyaromatic molecules that can be considered graphene fragments.*

When chemists, who tend to think of compounds and covalent bonds, look at the structure of a carbon allotrope they instantaneously dissect the molecular structure into repeating units and speculate about routes to synthesize these fascinating materials (Figure 3).[16] In the field of "graphene total synthesis", Müllen *et al.* have made an impressive work.[17] This group has developed a highly productive stepwise strategy based on repetitive Diels-Alder addition of acetylenes to tetraphenylcyclopentadienone derivatives and subsequent planarization by a cascade of intramolecular oxidative cyclodehydrogenations (Scholl reaction).[18] Following such synthetic path, huge oligophenylene dendrimers have been transformed into nanographenes and graphene nanoribbonds (GNRs) with different sizes, geometries and peripheral topologies.[19] As a representative example, a well-defined nanographene sheet with 222 carbon atoms was generated in this way (Scheme 1).[20]

[16] J. Sakamoto, J. van Heijst, O. Lukin, A. D. Schlüter, *Angew. Chem. Int. Ed.* **2009**, *48*, 1030-1069.

[17] To read about other chemical methods for the production of GNRs, see e.g.: J. Deng, B. Wang, Y. Shi, Q. Song, A. Wang, L. Hao, B. Luo, X. Li, Z. Wang, F. Wang, L. J. Zhi, *Macromol. Chem. Phys.* **2012**, *213*, 1033-1050.

[18] (a) F. Morgenroth, E. Reuther, K. Müllen, *Angew. Chem. Int. Ed.* **1997**, *36*, 631-634; (b) V. S. Iyer, M. Wehmeier, J. D. Brand, M. A. Keegstra, K. Müllen, *Angew. Chem. Int. Ed.* **1997**, *36*, 1604-1607.

[19] (a) J. Wu, W. Pisula, K. Müllen, *Chem. Rev.* **2007**, *107*, 718-747; (b) X. Feng, W. Pisula, K. Müllen, *Pure Appl. Chem.* **2009**, *81* (12), 2203-2224.

[20] C. D. Simpson, J. D. Brand, A. J. Berresheim, L. Przybilla, H. J. Rader, K. Müllen, *Chem. Eur. J.* **2002**, *8*, 1424-1429.
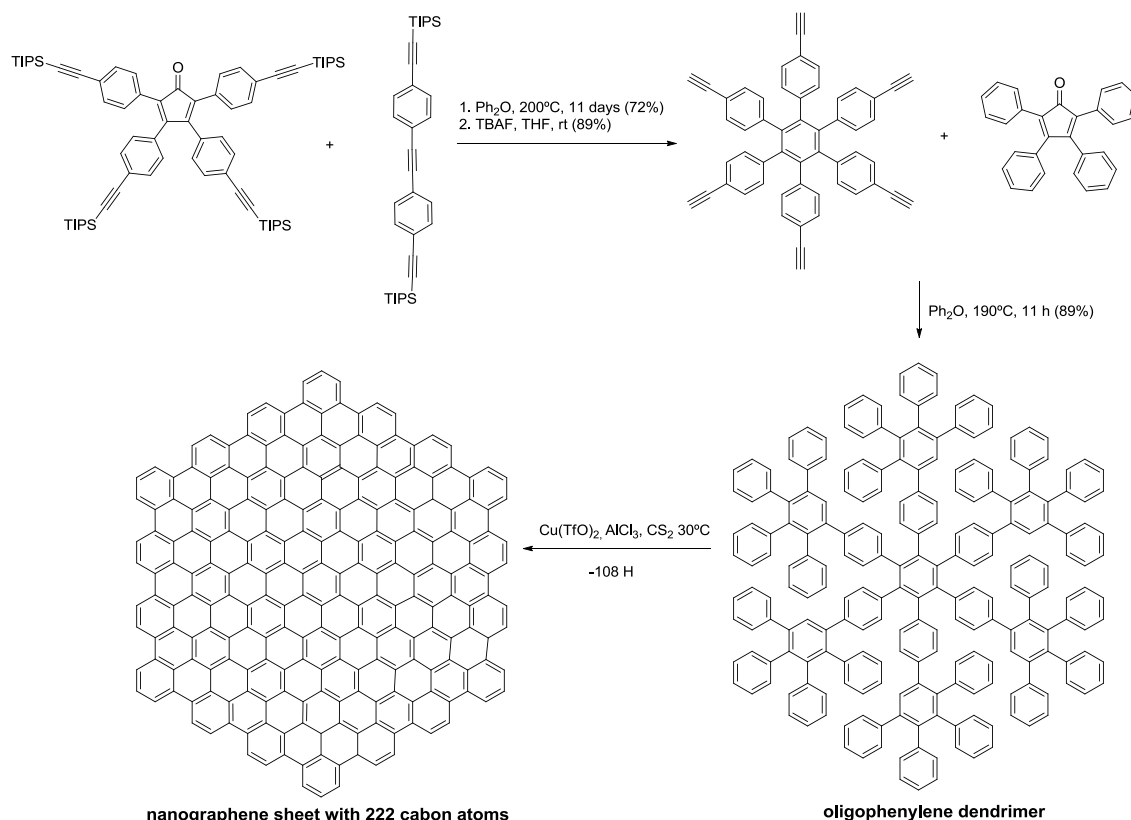
Scheme 1. *Synthetic pathway developed by Müllen et al. involving repetitive Diels–Alder aditions for the preparation of graphene fragments. [From ref. 21]*

Although the oligophenylene dendrimers are monodisperse, shape-persistent, carbon-rich molecular nanostructures,[21] their conversion into the corresponding flat polycyclic aromatic hydrocarbons (PAHs) renders to intractable and insoluble material assigned as the desired products based on mass spectrometric evidences and AFM or STM characterizations.[22] Together with the use of STM and AFM for analytical purposes, the employment of these tools to create covalent bonds between molecules adsorbed on appropriate solid substrates has raised their interest in the last few years.

Following the seminal work of Hla *et al.* in which iodobenzenes were coupled to biphenyls on a Cu(111) surface (Ullman coupling) using a homebuilt UHV-STM,[23] several C-C bond forming reactions have been successfully performed on reactive solid substrates. For example, 6,11-dibromo-1,2,3,4-tetraphenyltriphenylene monomer has been transformed into chevron-type GNRs on a Au(111) surface in a two thermal activation step process: biradical formation and C-C coupling first, then cyclodehydrohalogenation (Figure 4).[24]

[21] H. Zhang, P. C. M. Grim, P. Foubert, T. Vosch, P. Vanoppen, U. M. Wiesler, A. J. Berresheim, K. Müllen, F. C. De Schryver, *Langmuir* **2000**, *16*, 9009-9014.

[22] (a) F. Jaeckel, M. D. Watson, K. Müllen, J. P. Rabe, *Phys. Rev. Lett.* **2004**, *92*, 188303; (b) H. J. Rader, A. Rouhanipour, A. M. Talarico, V. Palermo, P. Samor, K. Müllen, *Nat. Mater.* **2006**, *5*, 276-279; (c) T. Boehme, C. D. Simpson, K. Müllen, J. P. Rabe, *Chem. Eur. J.* **2007**, *13*, 7349-7357.

[23] (a) S.W. Hla, L. Bartels, G. Meyer, K.-H. Rieder, *Phys. Rev. Lett.* **2000**, *85*, 2777-2780; (b) S.W. Hla, G. Meyer, K.-H. Rieder, *Chem. Phys. Lett.* **2003**, *370*, 431-436.

[24] J. Cai, P. Ruffieux, R. Jaafar, M. Bieri, T. Braun, S. Blankenburg, M. Muoth, A. P. Seitsonen, M. Saleh, X. Feng, K.Müllen and R. Fasel, *Nature*, **2010**, *466*, 470–473.
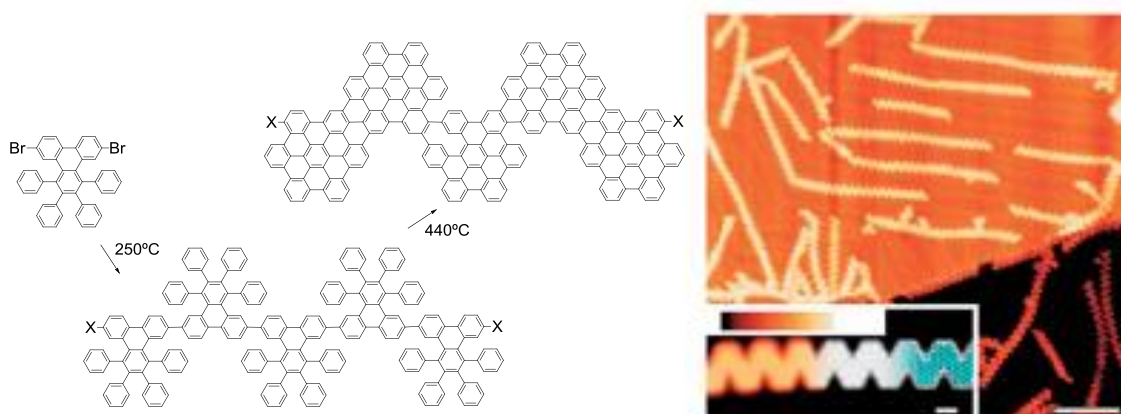
Figure 4. Reaction scheme from 6,11-dibromo-1,2,3,4-tetraphenyltriphenylene monomer to chevron-type GNRs (left). STM image of chevron-type GNRs fabricated on a Au(111) surface. [From ref. 25]

Four years ago, Bieri *et al.*[25] fabricated the first example of one-atom-thick porous graphene (a 2D polyphenylene superhoneycomb framework with an uniform pore spacing of 7.4 Å) on a Ag(111) surface by homolytically cleavage of carbon–halogen bonds (Figure 5, left). Following the same methodology, Gottfried *et al.*[26] have recently reported a new hexagonal porous graphene cutout (called hyperbenzene) consisting of 18 phenylene units and characterized by a large diameter of 21.3 Å (Figure 5, right).
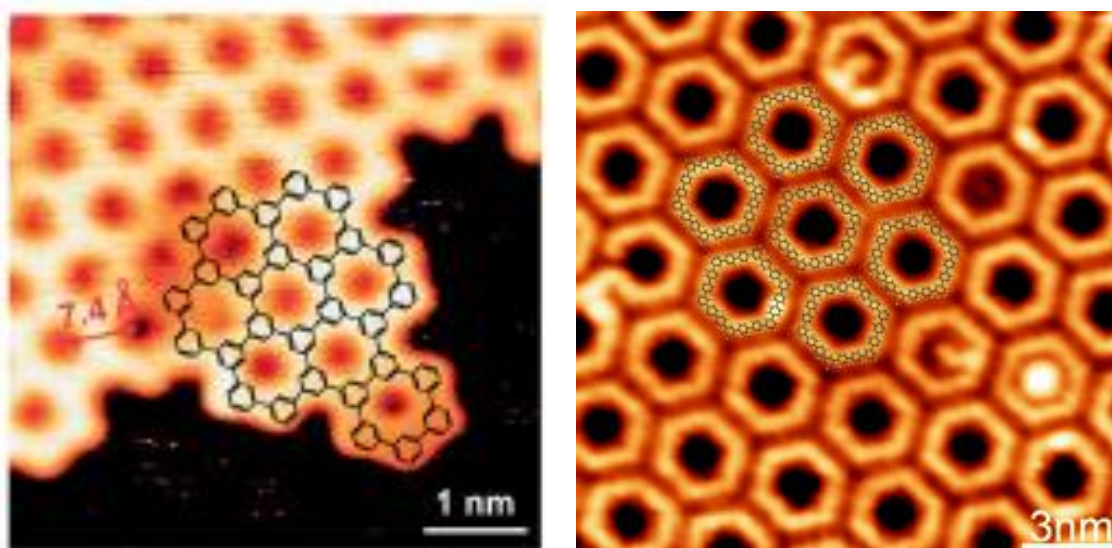

Figure 5. High-resolution STM image of an edge of the one-atom-thick porous graphene (left). [From ref. 26] High-resolution STM image of the porous graphene cutout hyperbenzene. (right). [From ref. 27]

1.1.3. Other 2D all-carbon allotropes[27]

Before the isolation of graphene, indeed more that 50 years ago, the interest of scientists in 2D all-carbon polymers was already a intense research field due to the wide range of planar allotropes with different meshes that can be envisioned combining sp and sp^2 carbon atoms.[28] Although these networks

[25] M. Bieri, M. Treier, J. Cai, K. Aït-Mansour, P. Ruffieux, O. Gröning, P. Gröning, M. Kastler, R. Rieger, X. Feng, K. Müllen, R. Fasel, *Chem. Commun.* **2009**, 6919-6921.

[26] Q. Fan, J. Zhu, J. Kuttner, G. Hilt, J. M. Gottfried *Angew. Chem.* **2013**, *125,* 4766-4770*.*

[27] Q. Tang, Z. Zhou, Z Chen, *Nanoscale,* **2013**,*5*, 4541-4583.

[28] (a) A.T. Balaban, C. C. Rentia, E. Ciupitu, *Rev. Roum. Chim.* **1968**, *13*, 231-247; (b) R. Hoffmann, T. Hughbanks, M. Kertsz, P. H. Bird, *J. Am. Chem. Soc.* **1983**, *105*, 4831-4832; (c) R. H. Baughman, H. Eckhardt, M. Kertsz, *J. Chem. Phys.* **1987**, *87*, 6687-6699; (d) K. M. Merz, Jr. R. Hoffmann, A.T. Balaban *J.*

were never actually realized, drawings of them have been published repeateadly.[29] From the infinite variety of 2D conjugated backbones that can be envisioned, graphyne and graphdiyne are probably the most popular (Figure 6).[30,31]
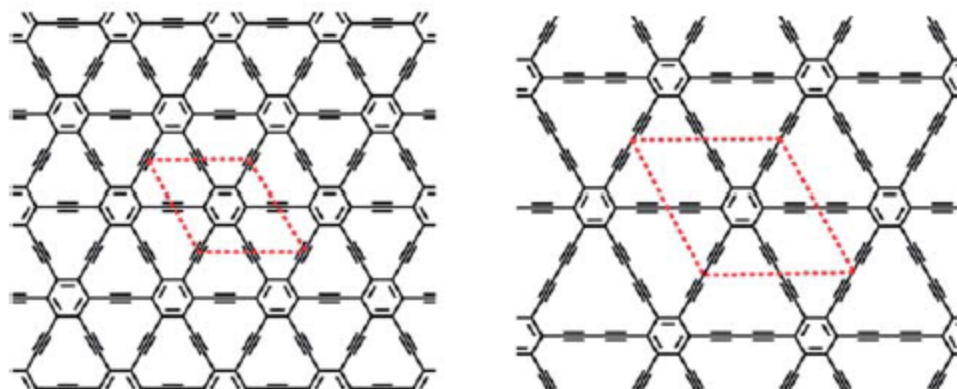

Figure 6. *Structure of 2D graphyne (left) and graphdiyne (right). The red parallelogram drawn represents a unit cell. [From ref. 28]*

Graphyne was firstly predicted in 1987 by Baughman *et al.*[32] Ideal graphyne is an infinite one-atom-thick planar sheet in which triple bonds connect benzene rings comprising weakly antiaromatic 12-membered rings (Figure 6 left).[33] Structurally, graphyne layers have the same hexagonal symmetry (*p6m*) as graphene, and the energy-minimized graphyne structure has an optimized crystal parameter of a = b = 6.86 Å, c = 6.72 Å, γ = 120º, and an interlayer distance of 3.3 Å.[34] Graphdiyne, proposed by Haley *et al.* in 1997,[35] can be considered a graphyne in which an extra alkyne unit increases the pore size of the network to approximately 2.5 Å (Figure 6 right).

Due to the structural resemblance, both infinite structures exhibit similar properties such as extreme hardness, high thermal resistance, and conductivity or superconductivity. The binding energies of graphyne (7.95 eV per atom) and graphdiyne (7.78 eV per atom) are comparable to those of graphite (8.66 eV per atom) or fullerene C60 (8.22 eV per atom) in the LDA level, indicating the structural stability of both carbon materials.[36] The presence of triple bonds in graphyne or graphdiyne makes the π-electron more localized, leading to a non-zero gap.[37] Both 2D graphyne and graphdiyne sheet are direct bandgap semiconductors with band gaps of 0.52–0.53 eV at the local spin density approximation (LSDA) level, while more accurate hybrid exchange–correlation functional obtains a larger gap of 0.96 eV for graphyne and 1.22 eV for graphdiyne.[38] Interestingly, a recent theoretical work has shown that some graphyne substructures with rectangular symmetry (e.g. the so-called 6,6,12-graphyne) are in some

Am. Chem. Soc. **1987**, *109*, 6742-6748; (e) R. L. Johnston, R. Hoffmann, *J. Am. Chem. Soc.* **1989**, *111*, 810-819

[29] J. Sakamoto, J. van Heijst, O. Lukin, A. D. Schlüter, *Angew. Chem. Int. Ed.* **2009**, *48*, 1030-1069.

[30] M. M. Haley, *Pure Appl. Chem.* **2008**, *80* (3), 519-532.

[31] Related planar networks constructed via Stone-Wales transformation known as haeckelites and pentaheptites and several single-atom-thick periodic carbon lattices of mixed sp^2+sp hybridations have been thouroughtly theoretically studied and some of their molecular analogs synthesized. See e.g.: Bruno Masenelli, Patrice Mélinon, *From Small Fullerenes to Superlattices: Science and Applications,* Pan Standford Publishing Pte. Ltd: **2013**.

[32] R. H. Baughman, H. Eckhardt and M. Kertesz, *J. Chem. Phys.* **1987**, *87*, 6687–6699.

[33] (a) K. Tahara, T. Yoshimura, M. Sonoda, Y. Tobe, R. V. Williams, *J. Org. Chem.* **2007**, *72*, 1437-1442; (b) J. Juselius;D. Sundholm, *Phys. Chem. Chem. Phys.* **2001**, *3*, 2433-2437.

[34] (a) J. Kang, J. Li, F. Wu, S.-S. Li, J.-B. Xia, *J. Phys. Chem. C*, **2011**, *115*, 20466–20470; (b) S. W. Cranford, M. J. Buehler, *Carbon*, **2011**, *49*, 4111–4121; (c) Q. Peng, W. Ji, S. De, *Phys. Chem. Chem. Phys.* **2012**, *14*, 13385–13391.

[35] M. M. Haley, S. C. Brand, J. J. Pak, *Angew. Chem.Int. Ed.* **1997**, *36*, 836–838.

[36] N. Narita, S. Nagai, S. Suzuki, K. Nakao, *Phys. Rev. B: Condens. Matter*, **1998**, *58*, 11009–11014.

[37] M. Kondo, D. Nozaki, M. Tachibana, T. Yumura, K. Yoshizawa, *Chem. Phys.* **2005**, *312*, 289–297.

[38] Y. Jiao, A. J. Du, M. Hankel, Z. H. Zhu, V. Rudolph, S. C. Smith, *Chem. Commun.* **2011**, *47*, 11843–11845.

aspects more versatile than graphene due to its directional anisotropy and its nonequivalent Dirac points (Figure 7).[39]
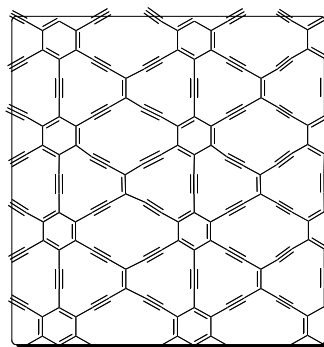

Figure 7. Structure of the 6,6,12-graphyne.

Concerning the synthesis of this type of carbon allotropes, Li *et al.* tried to grow graphdiyne on a Cu(111) surface via a cross-coupling reaction using hexa-ethynylbenzene as the monomer in the presence of pyridine at 60ºC for 72h.[40] Although promising in a first glance, the graphdiyne-type 2D-polymer obtained was a multilayers solid with a thickness of about 1 mm. The fact that multilayers of graphdyine were obtained instead of a one-atom-thick 2D structure can be related with the ability of alkynes to give other topochemical reactions forming enynes[41] and Bergman-type reaction products[42] as have been reported in other studies.

The results obtained in the innovative work reported by Li are a good example of the compromises that have to be made in the synthesis of one-atom-thin networks regarding lateral extension and detailed proof of structure on the molecular level. For example, irregularly cross-linked (anisotropic) films could never be obtained when mechanisms of bond formation require complicated transient relative orientations or the strictly distinction between growth-directions.[43] Attempts to construct new carbon phases with high level of structure perfection and in higher amounts are largely determined by organic synthesis.[44] Moreover, a lot of knowledge about the potential properties of the larger flat entities can be extracted from their smaller cut-outs.

1.1.4. The Organic Chemistry Approach to graphyne: Small Fragments by Covalent Synthesis

Dehydrobenzo[12]annulene ([12]DBA) **1** is considered the smallest unit of graphyne (Figure 8). In addition to being a graphyne mimic, [12]DBAs have garnered some interest in recent years as ligands for organometallic chemistry,[45] as hosts for binding guest molecules, as probes for investigating weak induced ring currents,[46] as precursors to other carbon-rich materials[47] and due to their self-assembly capability to form well-defined nanometer-scale structures.[48]

[39] D. Malko, C. Neiss, F. Vines, A. Gorling, *Phys. Rev. Let.*, **2012**, *108*, 086804.

[40] (a) G. Li, Y. Li, H. Liu, Y. Guo, Y. Li, D. Zhu, *Chem. Commun.* **2010**, *46*, 3256–3258; (b) H. Liu, J. Xu, Y. Li, Y. Li, *Acc. Chem. Res.* **2010**, *43*, 1496–1508.

[41] (a) T. Takami, H. Ozaki, M. Kasuga, T. Tsuchiya, A. Ogawa, Y. Mazaki, D. Fukushi, M. Uda, M. Aono, *Angew. Chem. Int. Ed.* **1997**, *36*, 2755-2757; (b) A. Miura, S. De Feyter, M. M. S. Abdel-Mottaleb, A. Gesquiere, P. C. M. Grim, G. Moessner, M. Sieffert, M. Klapper, K.Müllen, F. C. De Schryver, *Langmuir* **2003**, *19*, 6474-6482.

[42] D. G. de Oteyza, P. Gorman, Y.-C. Chen, S. Wickenburg, A. Riss, D. J. Mowbray, G. Etkin, Z. Pedramrazi, H.-Z. Tsai, A. Rubio, M. F. Crommie, F. R. Fischer, *Science* **2013**, *340*,1434-1437.

[43] An interesting the synthesis of a quasi-2D-polymer based on the antracene photodimerization of a rigid cyclic compound has been developed by Schülter et al. following the Staudinger's polymerization concept. P. Kissel, R. Erni, W. B. Schweizer, M. D. Rossell, B. T. King, T. Bauer, S. Götzinger, A. D. Schlüter, J. Sakamoto, *Nat. Chem.* **2012**, *4*, 287.

[44] F. Diederich, M. Kivala, *Adv. Mater.* **2010**, *22*, 803–812.

[45] W. J. Youngs, C. A. Tessier, J. D. Bradshaw, *Chem. Rev.* **1999**, *99*, 3153-3180.

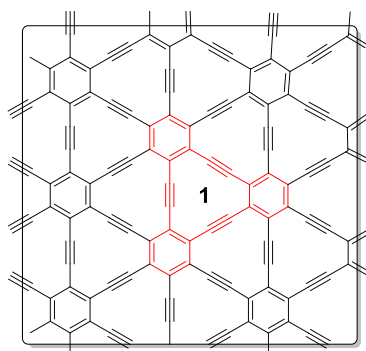[46] N. Z. Huang, F. Sondheimer, *Acc. Chem. Res.* **1982**, *15*, 96.

Figure 8. *Dehydrobenzo[12]annulene ([12]DBA)* **1** *(red) as the smallest unit of graphyne.*

Since its initial preparation in 1966 in the laboratories of Eglinton[49] and Staab[50] via cyclooligomerization of the copper salt of *o*-iodo-phenylacetylene, several approaches to the synthesis of [12]DBA and related fused macrocycles marked a renaissance in annulene synthesis that continues to this day.[51] Most of the reactions used are transition-metal-mediated coupling reactions mediated by Pd(0) (Sonosgashira coupling)[52] or Cu(I) (Stephens-Castro coupling and their modifications)[53] but other synthesis via pinacol coupling[54] and alkyne metathesis[55] have also been utilized. An even more exotic strategy to afford [12]DBA was the thermolysis of benzo[1,2-c:3,4-c':5,6-c''] tricinnoline through a one-meter silica tube at 780°C/0.005 Torr which gave the unsubstitued [12]DBA in a poor 8% yield.[56]

Regardless of the reaction employed, three different approaches render the general retrosynthetic plan to obtain **1** and related poly-fused compounds: the intermolecular cyclotrimerization, the intramolecular cyclization and the intermolecular cyclization. Despite cyclotrimerization seems the most direct route to synthesize **1**, very low yields (ca. 30%)[57] attributed to the insolubility of [12]DBA and the simultaneous formation of other oligomers such as the tetrabenzocycline (TBC) **2** represent two major drawbacks (Scheme 2).[58]

[47] E. L. Spitler, C. A. Johnson II, M. M. Haley. *Chem. Rev.* **2006***, 106*, 5344-5386.

[48] (a) K. Tahara, S. Furukawa, H. Uji-i, T. Uchino, T. Ichikawa, J.Zhang, W. Mamdouh, M. Sonoda, F. C. De Schryver, S.De Feyter, Y. Tobe, *J. Am. Chem. Soc.* **2006**, *128*, 16613;(b) S. Lei, K. Tahara, X. Feng, S. Furukawa, F. C. De Schryver, K. Müllen, Y. Tobe, S. De Feyter, *J. Am. Chem. Soc.* **2008**, *130*, 7119; (c) K. Tahara, S. Lei, J. Adisoejoso, S. De Feyter, Y. Tobe, *Chem. Commun.* **2010**, *46*, 8507; (d) K. Tahara, S. Okuhata,J. Adisoejoso,S. Lei, t. Fujita, S. De Feyter, Y. Tobe *J. Am. Chem. Soc.* **2009**, *131*, 17583-17590.

[49] I. D. Campbell, G. Eglinton, W. Henderson, R. A. Raphael. *J. Chem. Soc., Chem. Commun* **1966***,* 87.

[50] H. A. Staab, F. Graf. *Tetrahedron Lett.* **1966***,*751.

[51] For excelent reviews: (a) E. L. Spitler, C. A. JohnsonII, M. M Haley*, Chem. Rev.* **2006**, *106*, 5344. (b) M. Iyoda, J. Yamakawa, M. J. Rahman *Angew. Chem. Int. Ed.* **2011**, *50*, 10522-10553.

[52] R. Chinchilla, C. Najera, *Chem. Soc. Rev.* **2011**, *40*, 5084–5121; (b) R. Chinchilla, C. Najera, *Chem. Rev.* **2007**, *107*, 874–922.

[53] D. C. Owsley, C. E. Castro.*Organic Syntheses*, **1988**, *6*, 916.

[54] T. Yoshimura, A.Inaba, M. Sonoda, K. Tahara, Y. Tobe, R. V. Williams, *Org. Lett.* **2006**, *8* (14), 2933-2936.

[55] O. S. Miljanic, K. P. C. Vollhardt, G. D. Whitener, *SynLett,* **2003**, 29-34.

[56] J.W. Barton, M.K. Shepherd, *Tetrahedron Lett.* **1984**, *25*, 4967.

[57] Higher and lower yields can be found in literature depending on the reaction used and the specific substitution pattern on the [12]DBA core.

[58] Owing to their similarity in composition, structure, and solubility, it is often difficult (or impossible) to isolate the desired macrocycle from the crude mixture. See for example: D. Zhang, C. A. Tessier, W. Youngs, J. *Chem. Mater.* **1999**, *11*, 3050-3057.
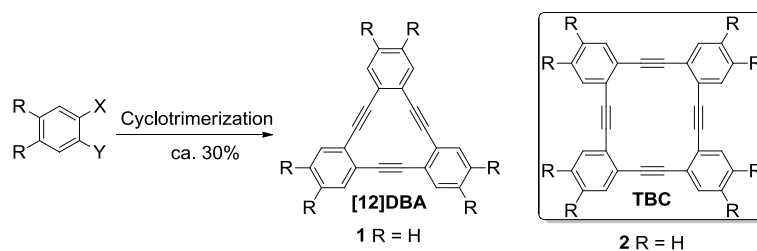
Scheme 2. *Intermolecular cyclotrimerization strategy to obtain **1**. Structure of the TBC **2** (inset).*

Probably, the more representative example of how to settle such shortcomings is represented by the "precipitation-driven alkyne metathesis" strategy developed in Moore´s laboratory which afforded only the alkoxy [12]DBA **1b** in 86% yield (Scheme 3).[59] The increased efficiency of such cyclotrimerization is not only due to the improvement of the macrocycle solubility with long alkyl side chains[60] but also to the precipitation of the diarylacetylene **3** which serves as the driving force to shift the equilibrium to the kinetically and thermodynamically favoured product.[61] Despite being a clearly smart solution, the usefulness of such methodology to construct wider systems is not so evident.
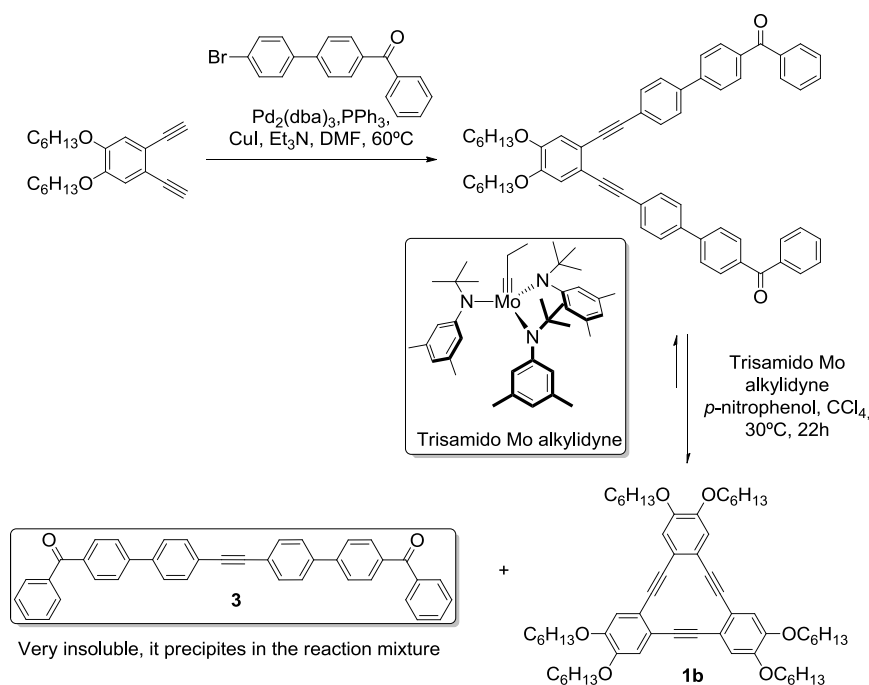
Scheme 3. *High-throughput alkyne metathesis to obtain **1b** due to the concomitant precipitation of **3**.*

To minimize the formation of side products, [12]DBA **1** has also been assembled via a sequential approach (Scheme 4). After cross-coupling reactions and manipulation of functional groups to obtain the precursor **4**, intramolecular cyclization under high dilution conditions furnished **1** as the sole product in 69% yield[62] while the intramolecular cyclization reported by Iyoda *et al.*[63] led to **1** in 51% yield.

---

[59] W.; Brombosz, S. M.; Mendoza, J. L.; Moore, J. S. *J. Org. Chem.* **2005**, *70*, 10198-10201.

[60] When R≠H, yields typically increase to ca. 40-50%.

[61] Zhang, W.; Moore, J. S. *J. Am. Chem. Soc.* **2005**, *127*, 11863- 11870.

[62] J. M. Kehoe, J. H. Kiley, J. J. English, C. A. Johnson, R. C. Petersen, M. M. Haley*, Org. Lett.,* **2000**, *2*(7), 969–972.

[63] M. Iyoda, S. Sirinintasak, Y. Nishiyama, A. Vorasingha, F. Sultana, K. Nakao, Y. Kuwatani, H. Matsuyama, M. Yoshida, Y. Miyake *Synthesis* **2004**, *9*, 1527-1531.
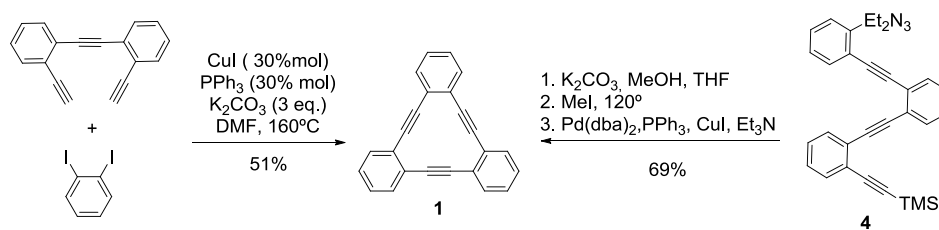
Scheme 4. *Sequential approach to 1.*

A recent work from Milch *et al.* makes a comparative analysis in which the three possible retroanalysis (cyclotrimerization, inter- and intramolecular cyclizations) are explored in terms of isolated yields to afford a methoxocarbonyl substitued [12]DBA using the same reaction (the insertion of acetylene gas via Sonogashira coupling).[64]
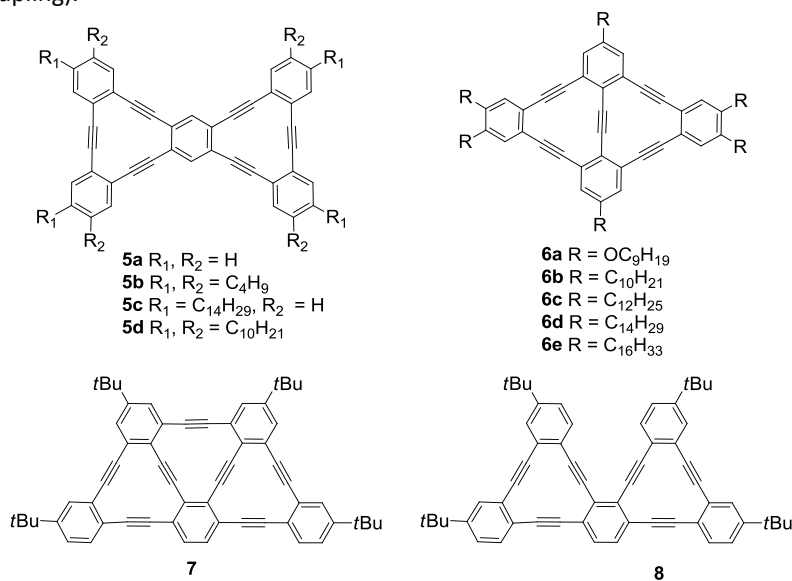

5a R$_1$, R$_2$ = H
5b R$_1$, R$_2$ = C$_4$H$_9$
5c R$_1$ = C$_{14}$H$_{29}$, R$_2$ = H
5d R$_1$, R$_2$ = C$_{10}$H$_{21}$

6a R = OC$_9$H$_{19}$
6b R = C$_{10}$H$_{21}$
6c R = C$_{12}$H$_{25}$
6d R = C$_{14}$H$_{29}$
6e R = C$_{16}$H$_{33}$

7

8

Figure 9. *Expanded dehydrobenzo[12]annulenes 5, 6, 7 and 8.*

The synthetic challenge associated with the construction of fused DBAs such as **5**, **6**, **7**, **8**, **9-T**, **9-L** and **10** has been independently addressed by the groups of Vollhardt, Tobe, Haley and Iyoda among others (Figures 9 and 10).

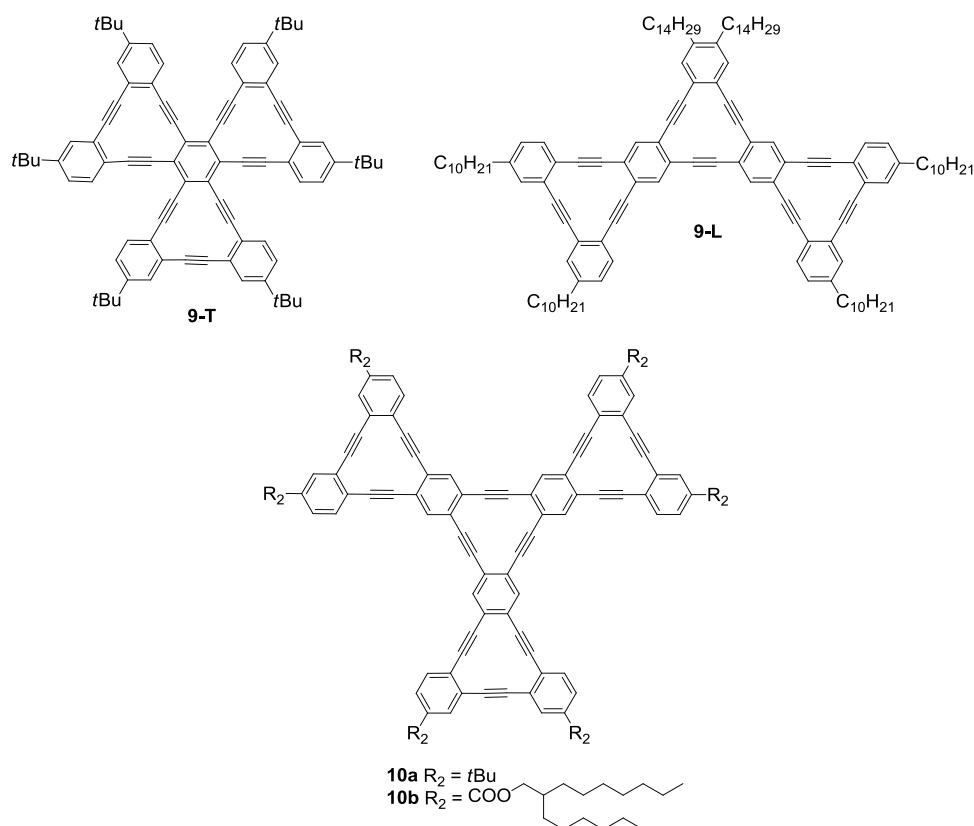[64] M. Dudič, I. Císařová, J. Michl *J. Org. Chem.* **2012**, *77*, 68–74.

Figure 10. Expanded dehydrobenzo[12]annulenes **9-T, 9-L** and **10**.

Vollhardt prepared compound **5a** in 6% yield via 6-fold intermolecular metathesis of 1,2-dipropynylbenzene and 1,2,4,5-tetrapropynylbenzene (Scheme 5).[65] However, as a consequence of solubility problems, compound **5a** was not characterized. Haley´s group addressed the stepwise route to **5a** by Sonogashira coupling and afforded an overall yield of 4.4% (11% yield for the last step).[66] In a later paper, the same group increased the global yield up to 17% over seven steps (46, 87, 91% yield for the ring closing alkyne metathesis (RCAM) step depending on the solubilizing groups and the catalyst used)[67] combining the efficiency of the more active Mo-amido catalytic system for alkyne metathesis optimized by Moore[68] with the improvement of the solubility of the products. Iyoda *et al.* also reported the formation of **5b** via intermolecular cyclization under Sonogashira conditions in <1% yield.[69]

[65] Miljanic, O.S.; Vollhardt, K.P.C.; Whitener, G.D. *SynLett* **2003**, 29-34.

[66] J. M. Kehoe, J. H. Kiley, J. J. English, C. A. Johnson, R. C. Petersen, M. M. Haley, *Org. Lett.* **2000**, *2*, 969.

[67] The structure of the catalyst used can be found in scheme 8 and in the original work: C. A. Johnson, Y. Lu, M. M. Haley, *Org. Lett.* **2007**, *9*, 3725-3728.

[68] (a) W. Zhang, S. Kraft, J. S. Moore, *J. Am. Chem. Soc.* **2004**, *126*, 329-335. (b) W. Zhang, J. S. Moore, *J. Am. Chem. Soc.* **2005**, *127*, 11863- 11870. (c) W. Zhang, S. M. Brombosz, J. L. Mendoza, J. S. Moore, *J. Org. Chem.* **2005**, *70*, 10198-10201. (d) H. M. Cho, H. Weissman, S. R. Wilson, J. S. Moore, *J. Am. Chem. Soc.* **2006**, *128*, 14742-14743. (e) W. Zhang, J. S. Moore, *Adv. Synth. Catal.* **2007**, *349*, 93-120.

[69] M. Iyoda, S. Sirinintasak, Y. Nishiyama, A. Vorasingha, F. Sultana, K. Nakao, Y. Kuwatani, H. Matsuyama, M. Yoshida, Y. Miyake *Synthesis* **2004**, *9*, 1527-1531.
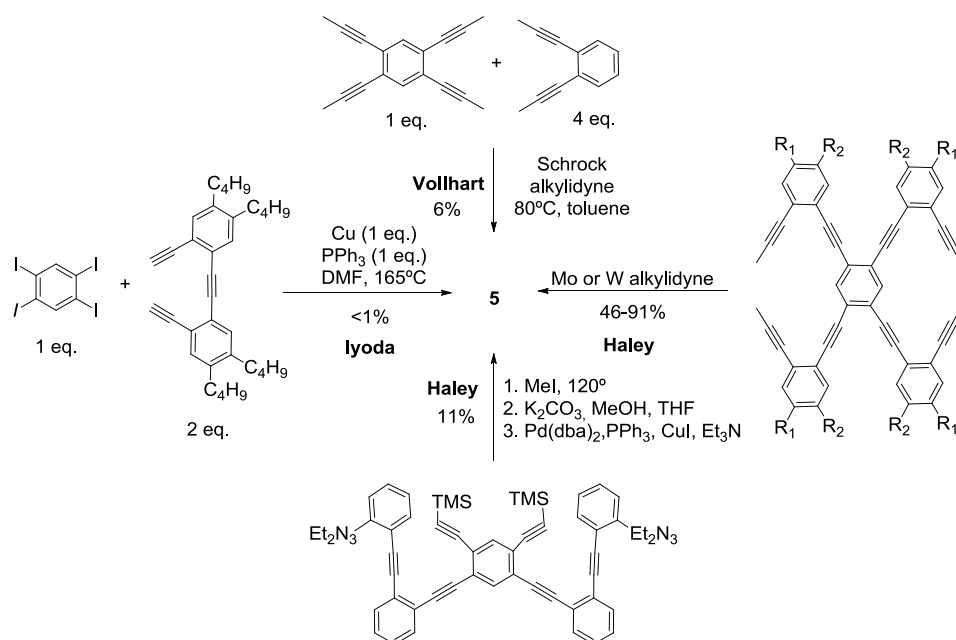
Scheme 5. *Different synthetic approaches to* ***5.***

The synthesis of the bisDBA squeleton **6** has been afforded by Haley[70] and Tobe[71] always using side chains on the periphery of the core (Scheme 6). Series of alkyl- and alkoxy-substituted rhombic-shaped bisDBA derivatives have been used by Tobe *et al.* to form porous structures at the TCB/graphite interface.[72]
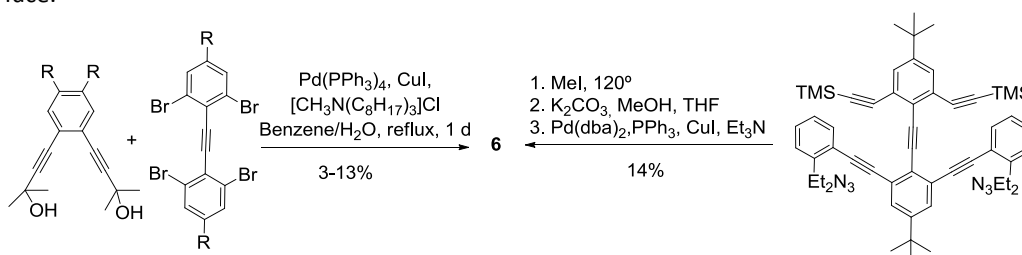
Scheme 6. *Double intermolecular coupling (left) and ring-closing (right) Sonogashira reactions to* ***6.***

Following a completely new strategy in which the peripheral triple bonds are formed by double elimination reaction from an intermediate with peripheral single bonds and appropriate leaving groups (Scheme 7), Tobe *et al.* synthesized compounds **7**, **8** and **9-T**.[73] However, the poor efficiency of this approach (<1% for the more strained compound **7**) and the major number of steps make this strategy less convenient. Interestingly, with trefoil [12]DBA **5** "in hand", this group confirmed experimentally the predicted[74] two-photon absorption (TPA) properties of **6** and **9-T**.[75]

[70] J. M. Kehoe, J. H. Kiley, J. J. English, C. A. Johnson, R. C. Petersen, M. M. Haley, *Org. Lett.* **2000**, *2*, 969.

[71] M. Sonoda, S. Yu, T. Yoshimura, Y. Tobe, K. Kamada*, Chem. Lett.* **2004**, 33(8), 972-973.

[72] K. Tahara, S. Okuhata, J. Adisoejoso, S. Lei, T. Fujita, S. De Feyter, Y. Tobe, *J. Am. Chem Soc.* **2009**, *131*, 17583–17590.

[73] (a) T. Yoshimura, A.Inaba, M. Sonoda, K. Tahara, Y. Tobe, R. V. Williams, *Org. Lett.* **2006**, *8* (14), 2933-2936; (b) K. Tahara, T. Yoshimura, M. Ohno, M Sonoda, Y. Tobe, *Chem. Lett.* **2007**, *36(7),* 838-839.

[74] Y. Zhou, S. Feng, *Solid State Commun.* **2002**, *122*, 307.

[75] K. Kamada, L. Antonov, S. Yamada, K. Ohta, T. Yoshimura, K. Tahara, A. Inaba, M. Sonoda, Y. Tobe, *ChemPhysChem* **2007**, *8*, 2671.
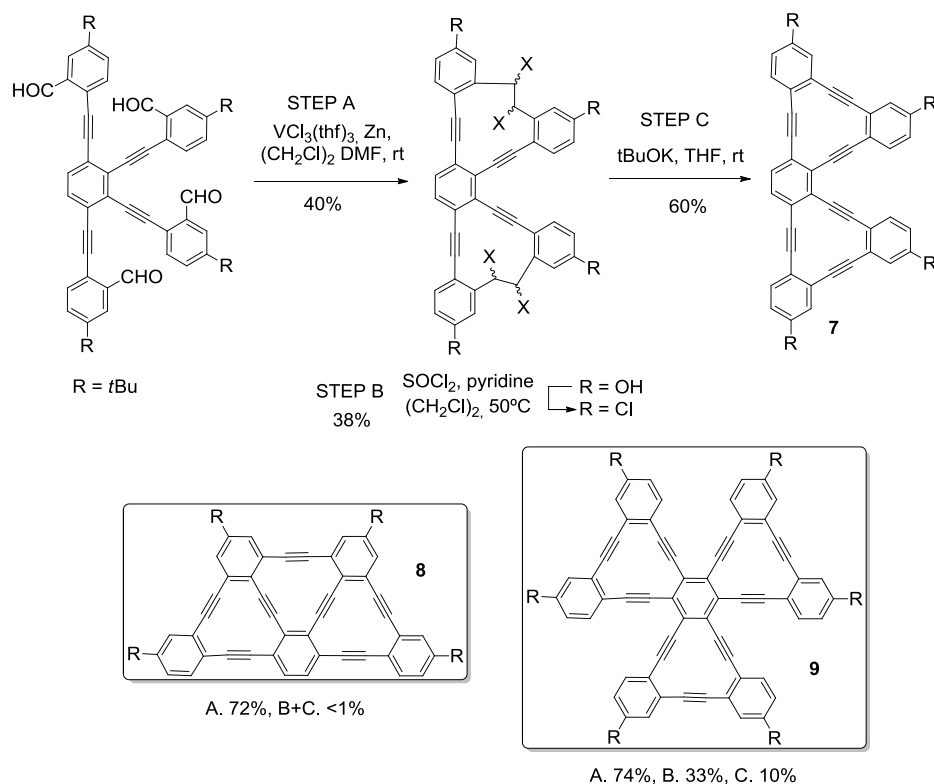
Scheme 7. *Tobe approach to 7, 8 and 9-T based on pinacol coupling, hydroxyl group substitution and double elimination of the periferial 1,2-dichlorides.*

The poly-fused [12]DBA **9-L** was synthesized by Haley *et al.* via 3-fold ring closing alkyne metathesis (RCAM) in 19 and 31% yield using W and Mo-alkylidynes catalyst respectively (Scheme 8). Although this synthetic route was quite promising, the tetrameric analog could not be isolated. Photophysical studies performed on **9-L** revealed that linear phenylacetylene conjugation length in fused dehydrobenzoannulenes dominates electronic properties over the extent of conjugation for isomeric substructures.
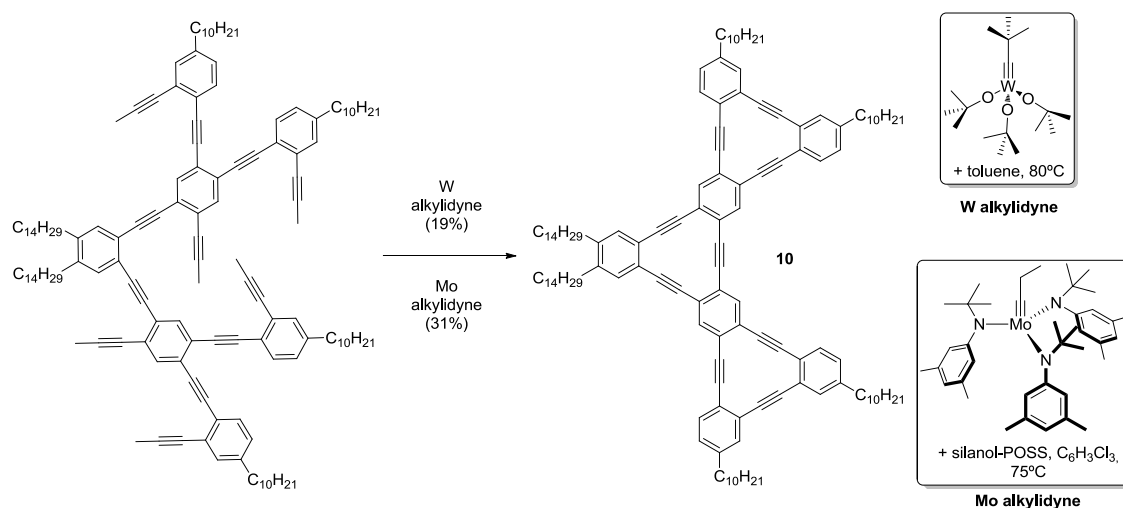
Scheme 8. *Haley approach to 9-L based on multiple RCAM.*

Finally, in July 2013, Shimizu, Seki, Kamada, Moore and Tobe *et al.* have presented the synthesis and properties of the largest graphyne fragment **10**, namely trigonally expanded

tetrakis(dehydrobenzo[12]annulene)s (tetrakis-DBAs), via intramolecular three-fold alkyne metathesis using Fürstner´s Mo nitride catalyst.[76]

a R$_1$ = Me, R$_2$ = *t*Bu
b R$_1$ = Et, R$_2$ = COO
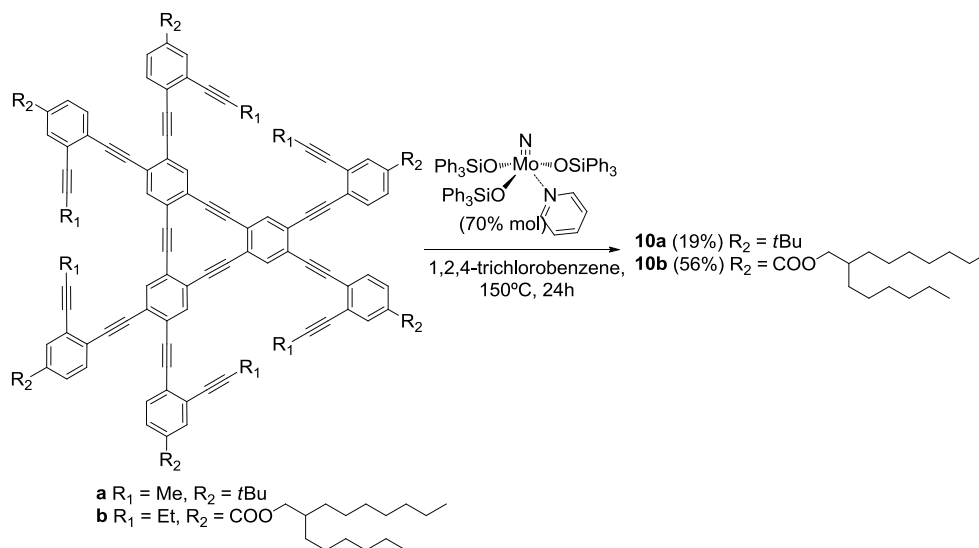
Scheme 9. *3-Fold RCAM to obtain **10**, the largest graphyne fragment synthesized to date.*

[76] K. Tahara, Y. Yamamoto, D. E. Gross, H. Kozuma, Y. Arikuma, K. Ohta, Y. Koizumi, Y. Gao, Y. Shimizu, S. Seki, K. Kamada, J. S. Moore, Y. Tobe, *Chem. Eur. J.* **2013**, doi.org/10.1002/chem.201300838.

1.2. Objective: Synthesis of anisotropic and conducting flat carbon networks based on rhomboidal tetrabenzocyclines

Molecular electronics (ME) is a branch of nanotechnology which deals with the study and application of molecular building blocks in the fabrication of electronic devices.[77] In this context, electronic transport has become a central topic for physicists and chemists who have made a great effort in theoretically modeling and experimentally testing such phenomenon.[78]

Electrical conductivity in the molecular scale is performed by the so-called *molecular wires*. From its definition, a molecular wire is a ''one dimensional molecule allowing a through-bridge exchange of an electron/hole between its remote ends/terminal groups, themselves able to exchange electrons with the outside world''.[79] Several molecular structures can be envisioned as molecular wires, but the most common types are planar π-conjugated organic molecules (Figure 11).
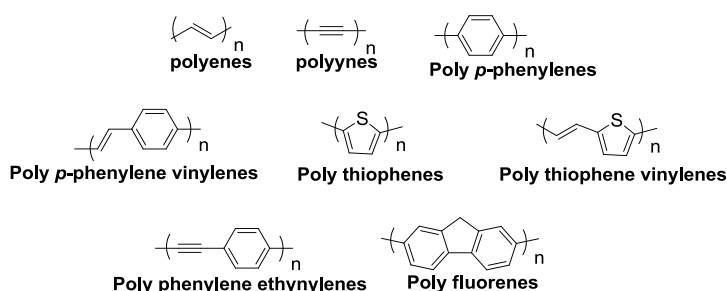
Figure 11. Building blocks of most common organic polymers consider molecular wires.

Molecular wires do not transport current at least they are connected to an electron source such as light (photo- and/or electrochemically induced electron transfer) or bulk electrodes (electron transport through a single-molecule device). Limiting the topic to single-molecule devices, a lot of knowledge about the conductance of such systems has been gained studying of molecular junctions.[80] One of the recurrent research topics has concerned the stochastic on-off switching between various conductances observed using a STM tip in contact with a self-assembled monolayer (SAM). For example, Weiss,[81] Lindsay[82] among others[83] observed conductance changes over time (called "blinking") in phenylene ethynylene-based oligomers inserted into a host SAM. Thinking in real applications, such uncontrollable variations of the conductivity could harshly affect the reliability of a molecular system.[84] Therefore, the nature and strength of the electrode–molecule contact are key points for the future development of efficient and reliable organic-based electronic nanodevices. Conspicuous works have focused on understanding the role of connecting atoms and their influence on the conductivity, charge-transport mechanism, and mechanical stability. However, experimental and theoretical approaches have been generally limited to molecules with only one connection per metal electrode.

[77] (a) K. S. Kwok, J. C. Ellenbogen, Mater. Today 2002, 5, 28–37. (b) B. A. Mantooth, P. S. Weiss, Proc. IEEE 2003, 91, 1785 – 1802.(c) C. Joachim, M. A. Ratner, Proc. Natl. Acad. Sci. USA 2005, 102, 8801 – 8808.

[78] (a) Heath, J. R.; Ratner, M. A *Phys. Today* . **2003**, *56*, 43. (b) Hutchison, G. R. *et al. Phys. Rev. B* **2003**, *68*, 035204/1. (c) Mujica, V. *et al J. Chem. Phys.* **1996**, *104*, 7296. (d) Segal, D. *et al J. Phys. Chem.B* **2000**, *104*, 2790. (e) Di Ventra, M.; Pantelides, S. T.; Lang, N. D. *Phys. Rev. Lett.* **2000**, *84*, 979.

[79] J.M. Lehn, in: Supramolecular Chemistry—Concepts and Perspectives, VCH, 1995, pp. 106, 111, 195

[80] REVIEWS
 (a) Donhauser, Z. J.; Mantooth, B. A.; Pearl, T. P.; Kelly, K. F.; Nanayakkara, S. U.; Weiss, P. S. Jpn. J. Appl. Phys., Part 1 2002, 41, 4871-4877.

[82] Ramachandran, G. K.; Hopson, T. J.; Rawlett, A. M.; Nagahara, L. A.; Primak, A.; Lindsay, S. M. Science 2003, 300, 1413-1416.

[83] (b) Wassel, R. A. *et al. Nano Lett.* **2003**, *3*, 1617.

[84] (a) Donhauser, Z. J. *et al. Science* **2001**, *292*, 2303. (b) Wassel, R. A. *et al. Nano Lett.* **2003**, *3*, 1617. (c) Ramachandran, G. K.*et al. Science* **2003**, *300*, 1413.

Intuitively, if an organic molecule were bound to a metallic electrode through more than one linking group, both an increase in the conductivity and better mechanical stability would be expected (Figure 12). Several linkers could act collectively to reduce possible molecule–electrode disconnections due to thermal or mechanical stress, and thus improve system reliability. In this sense, our group has recently demonstrated in a theoretical work that molecules with more than one connection per electrode can exhibit much better electrical efficiencies and current stabilities.[85] For these reasons, these molecules can be considered as improved candidates for the development of real nanoelectronics devices.
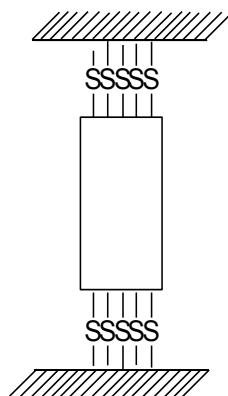
Figure 12. Cartoon of a flat conducting structure connected to two metallic electrodes by several sulfur atoms.

Concerning the internal structure of such conducting 2D molecule, work by Haley and others have shown that linear phenylacetylene conjugation length in fused dehydrobenzoannulenes dominates electronic properties over the extent of conjugation for isomeric substructures[86]. Such experimental evidence is related to the presence of both linearly-conjugated and cross-conjugated paths in the phenylene-ethynylenes (PE) core.[87] In addition, I/V measurements on single molecule electronic devices constructed by MCBJ techniques revealed that conduction is significantly by varying the position of the anchor group of the molecules to the electrodes in acyclic molecules (Figure 13).[88]
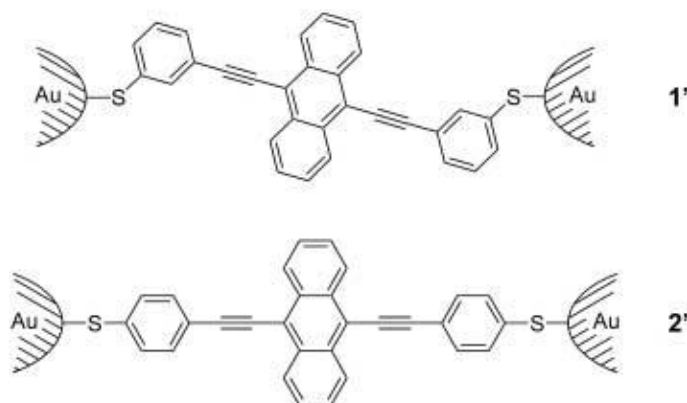

Figure 13. *Single molecule devices constructed by Mayor et al. to evaluate the influence of the anchoring group position in the electronic transport properties using the MCBJ technique.*

Inspired by all these precedents, we hypothesized that graphyne-type 2D networks comprising an anisotropic mesh which favours *para-* *vs meta*-conjugation could behave as two-dimensional anisotropic conducting polymers into which several linking groups could be introduced to improve the conducting

[85] See appendix A1.

[86] C. A. Johnson, Y. Lu, M. M. Haley, *Org. Lett.* **2007**, *9*, 3725-3728.

[87] To read about *cross*-conjugation, see e.g.: G. C. Solomon, D. Q. Andrews, R. H. Goldsmith, T. Hansen, M. R. Wasielewski, R. P. Van Duyne, M. A. Ratner, *J. Am. Chem. Soc.* **2008**, *130*, 17301–17308.

[88] M. Mayor, H. B. Weber, J. Reichert, M. Elbing, C. von Hänisch, D. Beckmann, M. Fischer, *Angew. Chem. Int. Ed*. **2003**, *42*, 5834.

properties (Figure 14). In this work, we propose that tetrabenzocycline **11** could be considered a general and adequate anisotropic building block for the preparation of covalently bound by electronically disconnected *para*-linked phenylacetylenes acting as molecular wires.
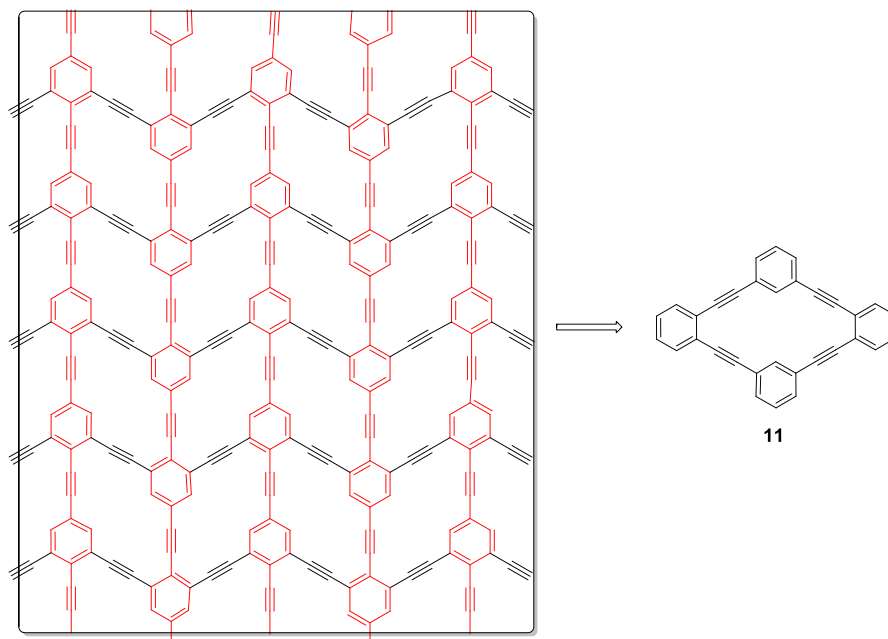

Figure 14. *Structure of the infinite anisotropic conducting flat carbon network (left) and the smallest grid subunit **11** (right).*

1.2.1. Background

Tetrabenzoannulene with rhomboidal backbone **11** has been previously synthesized by four different routes. The first synthesis was reported in 1994 by Moore *et al.* who obtained the di-tertbutyl analog **11a** in a single Sonogashira ring-closure step as an example of their convergent route to synthesize macrocycles under kinetic control (Scheme 10).[89]
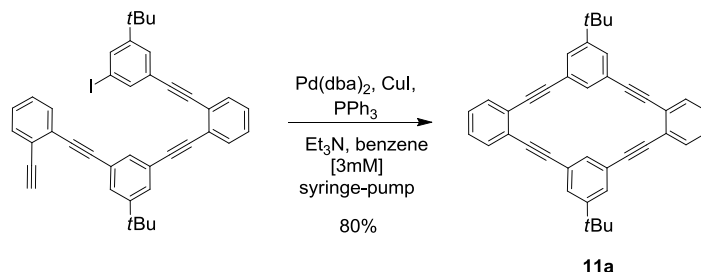
Scheme 10. *Sonogashira ring-closing macrocyclization to obtain **11a**.*

Nine years later, Vollhardt *et al.* published a pioneering approach in which they took advantage of the potential of alkyne metathesis in the construction of graphyne substructures (thermodynamic control).[90] In this work, they converted an equimolar mixture of *o*- and *m*-dipropynylbenzene into **11** by scrambling alkyne metathesis using Schrock W-alkylidyne catalyst in 19% yield (Scheme 11).
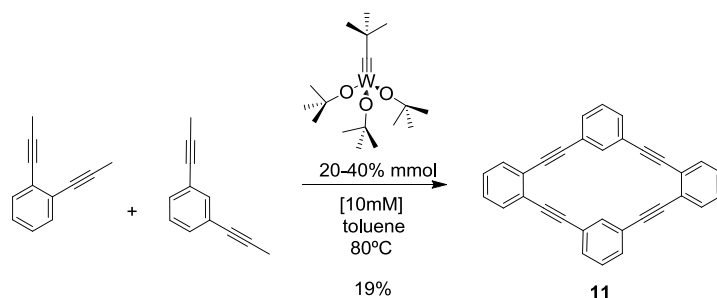
Scheme 11. *Vollhardt scrambling RCAM strategy to obtain **11**.*

Shortly after, Vollhardt reported the synthesis of a series of dodecaynes (**11b-6**) prepared by successive Sonogashira couplings following a convergent strategy similar to the one reported by Moore *et al.* (Figure 15).[91] These derivates were designed as precursor endowed with internal hydrogens for the synthesis of the circular [8]phenylene **12** also called antikekulene as potential model compound to probe the phenomenon of "superdelocalization" (following Hückel concepts).

[89] J. Zhang, J. D. Pesak, J.L. Ludwick, J.S. Moore, *J. Am. Chem. Soc.* **1994**,*116,* 4227-4239.
[90] O. S. Miljanic, K. P. C. Vollhardt, G. D. Whitener, *SynLett* **2003**, 29-34.
[91] O. S. Miljanic, D. Holmes, K. P. C. Vollhardt, *Organic Letters* **2005**, *7*, 4001-4004.
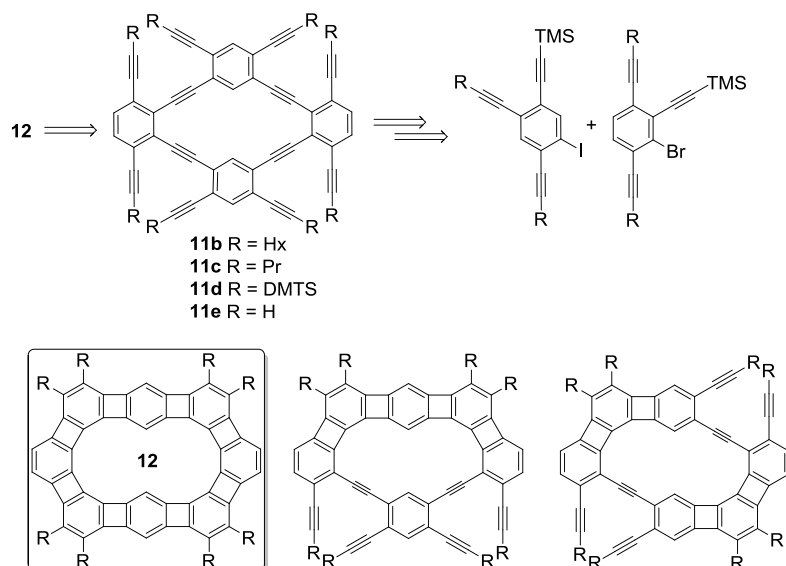
Antikekulene **12** was not obtained. The CpCo- catalyzed trimerization led to partially cyclizated products

Figure 15. *Vollhardt strategy to synthesize [8]phenylene* ***12*** *(antikekulene) via cyclotrimerization of peri-alkynylated-macrocycles* ***11b-e****.*

In the same year, the formation of **11f** was detected in a scrambling experiment monitored by FD-MS analysis (Scheme 12), in which a 1:2 mixture of the hexameric macrocycle **13** and the dehydrobenzo[12]annulene **1b** was subjected to alkyne metathesis using the molybdenum triamide alkylidyne catalyst and *p*-nitrophenol in CCl_4 at 30 °C.[92] Compound **11f** was not isolated because the objective of this experiment was just to demonstrate the reversible formation of oPE macrocycles under equilibrium conditions.
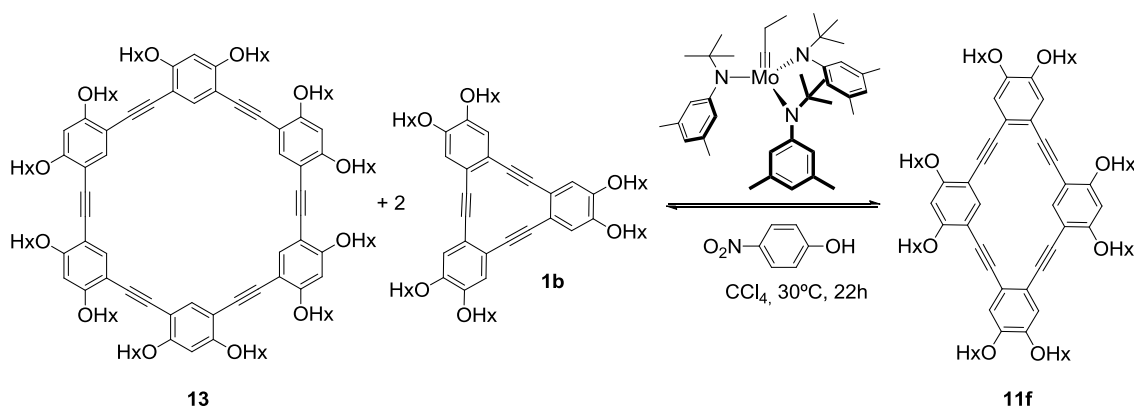
Scheme 12. *Scrambling experiment between one hexameric (**13**) and one trimeric (**1b**) PE-macrocycles to afford **11f**.*

Last year, a new synthesis appeared for push-pull macrocyles **11g-i** in which a two-component intermolecular macrocyclization was the final key step (Scheme 13).[93]

[92] W. Zhang, S. M. Brombosz, J. L. Mendoza, J. S. Moore, *J. Org. Chem.* **2005**, *70*, 10198-10201.

[93] W. C. W. Leu, A. E. Fritz, K. M. Digianantonio, C. S. Hartley, *J. Org. Chem.* **2012**, *77*, 2285–2298.
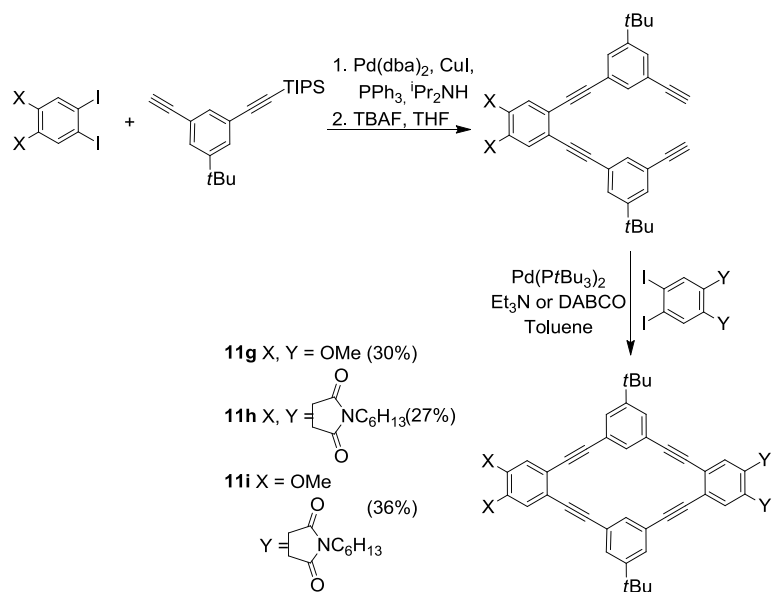
Scheme 13. *Hartley approach to push-pull macrocycles* **11g-i***.*

11g X, Y = OMe (30%)

11h X, Y =

11i X = OMe   (36%)

1.2.2. Results and discussion[94]

1.2.2.1. Synthesis and characterization of the annulene

As we have seen in the previous section, the graphyne-type annulene **11** had been previously synthesized by two different approaches: Sonogashira coupling or alkyne metathesis. Although all this mentioned examples shed light on the synthetic route to follow, neither of them would allow network growth. Hence, we planned a new combined strategy of palladium catalyzed-coupling and alkyne metathesis (Figure 16). To build and assemble the "phenylacetylene" tiles we decided to run Sonogashira reactions because this coupling is usually a pretty reliable way to make a $C(sp)$–$C(sp^2)$ bond. Moreover, the different reactivity of aryl halides allow sequential introduction of acetylenes onto a multifunctionalised benzene rings. A priori, a final alkyne metathesis might allow the closure of all the subunits in a single step.
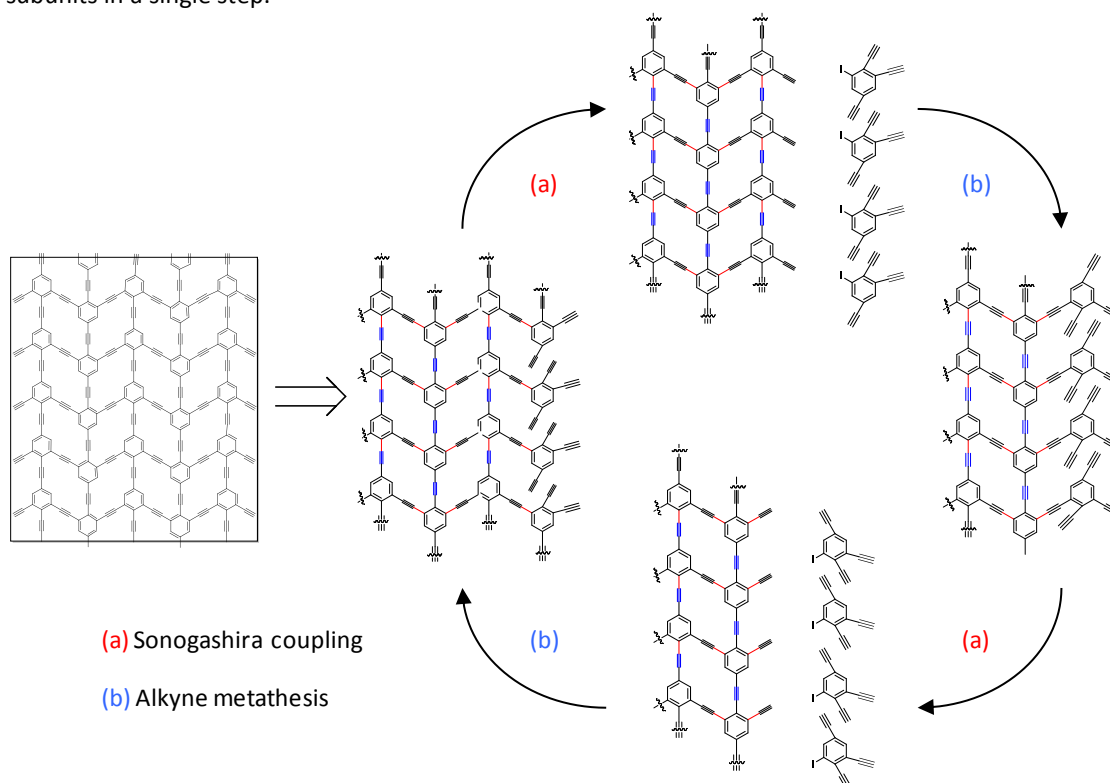

Figure 16. *General iterative strategy based on alternant Sonogashira coupling and alkyne metathesis reactions to grow the infinite anisotropic conducting flat carbon network.*

To begin, we designed a convergent modular route similar to the one described by Moore in order to obtain the smallest building block **11** (Scheme 14). Target structure **14a** beared 1-hexynyl groups to elude gas-handling. A methyl ester was located as a masked alkyne to continue with the grid-growth afterwards. Following the proposed retroanalysis, we obtain intermediate **15a** in 31% total yield after six linear steps for the longest path.
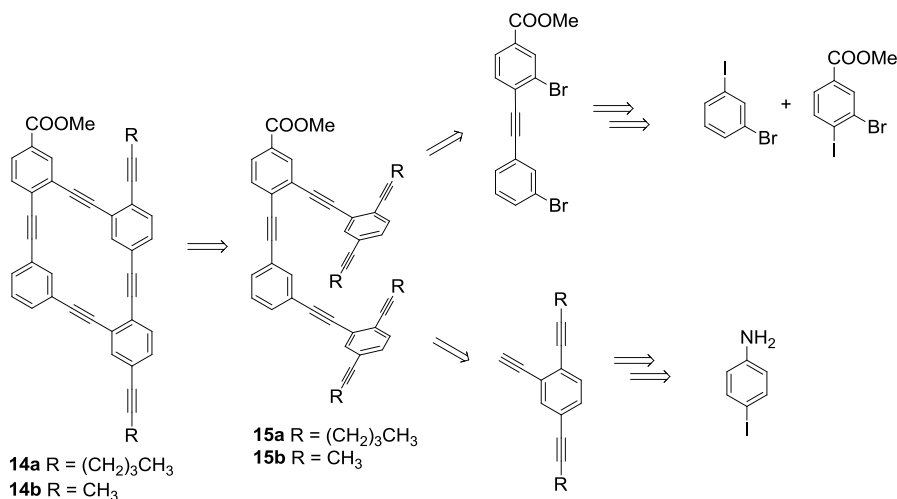
Scheme 14. *First retrosynthetic analysis to obtain **11** as **14**.*

Unfortunately, when intermediate **15a** was submitted to RCAM using either the Mortreux or Schrock catalysts the starting material was recovered (Scheme 15). After several attempts, the failure of the alkyne metathesis was attributed to the major reactivity of alkyl alkynes compared to the aryl alkynes.[95] As 5-decyne is concurrently generated with the desired macrocycle **14a**, if such internal alkyl alkyne is not removed from the reaction mixture, it keeps the catalyst busy in an independent equilibrium diminishing the catalytic proficiency.[96] The high temperatures required to remove the 5-decyne (b.p.=177-178°C) from the reaction mixture in order to shift the equilibrium, prompted us to change to 1-propynyl groups. Therefore, we synthesized the second model **15b** following the same synthetic route (22% total yield after six linear steps). Although reactions were set at high dilution conditions (>6mM), polymerization prevailed and desired macrocycle **14b** was obtained in less than 20% yield. Major byproducts were scarcely soluble oligomers and polymers that could not be purified. At this point, we decided to synthesize a third model bearing only two 1-propynyl groups.
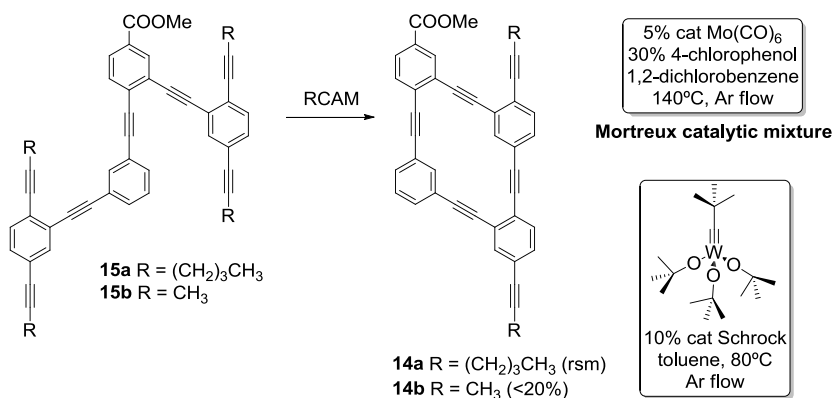

Scheme 15. *RCAM tested on **15a** and **15b** using Mortreux catalytic mixture and Schrock catalyst.*

The new target **15c** was synthesized following a different retrosynthetic analysis in which the stronger electron-widthdrawal effect of the methyl ester was used to improve the final coupling step (Scheme 16). In this approach, intermediate **14c** was obtained from two fragments **VIII** and **XII**.[97] The more electron-poor nature of the iodine **XII** combined with the major reactivity of the Pd(0) catalyst used, increased the yield of the final coupling up to 95%. However, global yield was slightly lower in this case (28% for the longest linear synthetic path: 7 steps) because some inefficient additional steps to interconvert functional groups were required.

---

[95] A. Mortreux, J.C. Delgrange, M. Blanchard, B. Lubochinsky, *J. Mol. Catal.* **1973**, *2*, 73-82.

[96] (a) W. Zhang, J. S. Moore, *JACS*, **2005**, *127*, 11863-11870; (b) A. Fürstner, *Angew. Chem. Int. Ed.* **2013**, *52*, 2794 – 2819.

[97] See experimental section for details about the syntehsis.
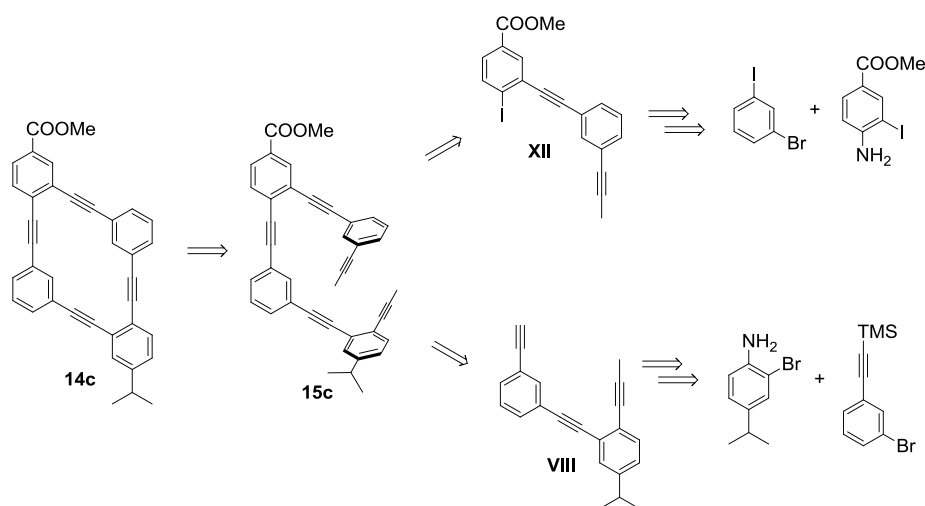
Scheme 16. *Second retroanalusis to obtain* **11** *as* **14c***.*

The RCAM using either tungsten or molybdenum alkylidynes led at last to the desired macrocycle **14c** (Scheme 17). However, repeated attempts to close **15c** with air-stable catalytic mixtures (Mortreux-type) failed. The best results were obtained using the "ate-complex" of the alkylidyne family of molybdenum complexes with ancillary silanolates developed in Fürtsner laboratory.[98]
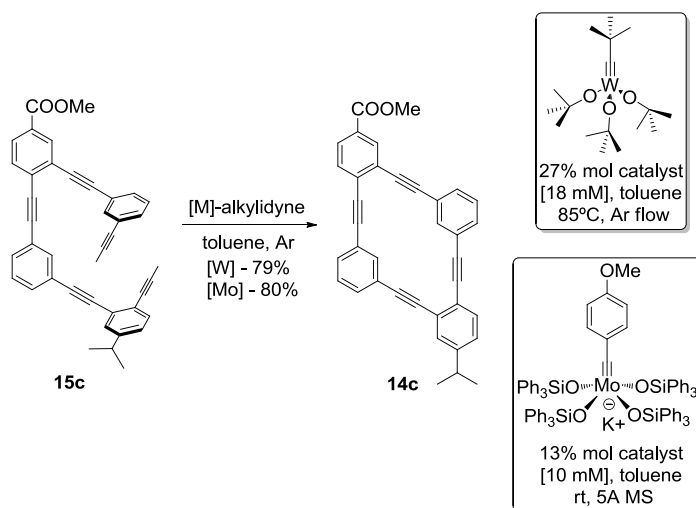
Scheme 17. *Successful RCAM of* **15c** *to obtain the smallest grid subunit* **11** *as* **14c** *using Schrock and Fürstner catalysts.*

Hydrocarbons **14c** and **15c** are stable compounds in solid state and in solution. They can be store at room temperature and exposed to sunlight and air for several weeks without any change. The ^{1}H and ^{13}C-NMR spectra of **14c** and **15c** were assigned using 2D correlation techniques.[99] Despite the inherent symmetry of the macrocycle **14c**, most of proton and carbon signals could be identified due to the different side chains. As occurred in related compounds, **14c** displayed shift of its internal hydrogen atoms to lower field (from 7.81 to 8.04 ppm for H1 and from 7.64 to 8.06 ppm for H2) which could

---

[98] (a) J. Heppekausen, R. Stade, R. Goddard, A. Fürstner, *J. Am. Chem. Soc.* **2010**, *132,* 11045–11057; (b) J.Heppekausen , R. Stade , A. Kondoh , G. Seidel , R. Goddard , A. Fürstner , *Chem. Eur. J.* **2012**, *18*, 10281–10299.

[99] ^{1}H- and ^{13}C-NMR experiments and structure of **14c** solved by Ms. Wirtz. NMR department, MPI-KOFO, Germany.

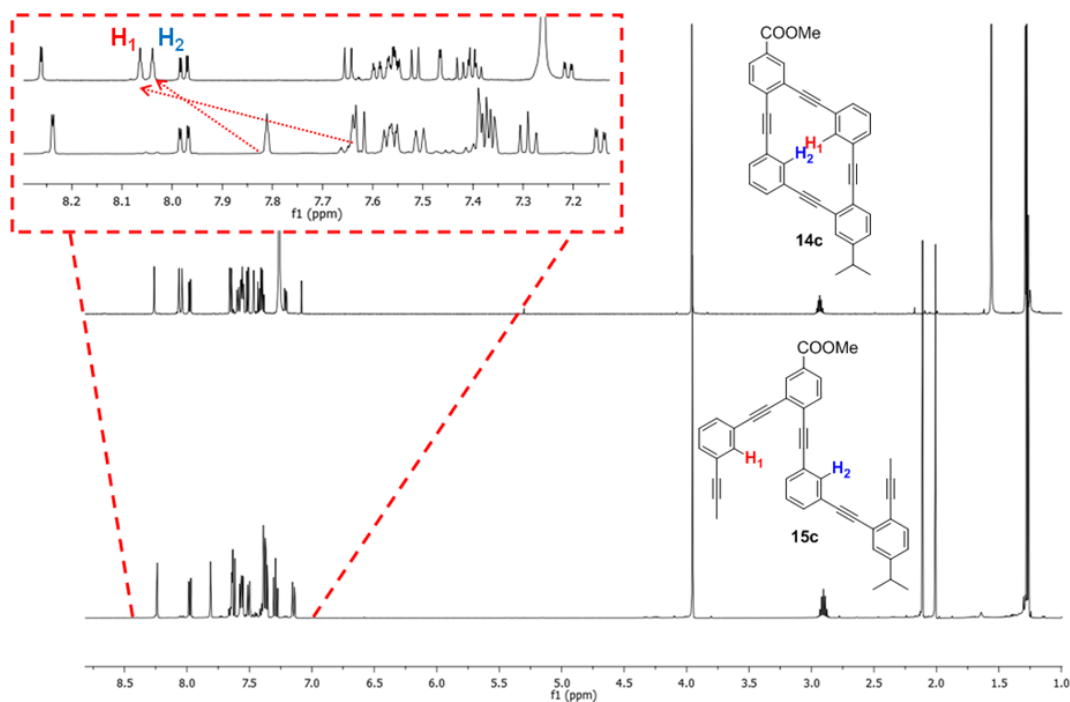indicated the weakly paratropic character of this tetrabenzocycline which is a (4n)-electron cycle (Figure 17).[100]

Figure 17. *Comparison of the ^{1}H-NMR spectra of* **14c** *and* **15c**. *The inset highlightes the aromatic region of the spectra and the shifts experienced by the inner protons H1 (red) and H2 (blue).*

Carbon nuclei of the C-C triple bonds were smoothly shielded by ca. 0.2 ppm upon cyclization except two C(sp) which were deshielded 5.15 ppm and 1.04 ppm respectively (Figure 18). Such deshielding of sp-hybridized carbon is usually caused by C-C-C angle strain as has been demonstrated convincingly by a series of cycloalkynes with decreasing ring size.[101] Hence it seems likely that strain, in adition to the local ring currents generated in the NMR experiments, also causes the deshielding of H and C nuclei in **14c**.

[100] Haigh and Mallion established a theoretical basis for relating the incidence of relatively "high" and "low" ring current intensities to the intuitive valence-bond resonance theory and the "bond fixation" in conjugated compounds. This work shows how topological arguments, combined with ring current ideas, serve to reinforce Clar's rules. See: M. Randic, *Chem. Rev.* **2003**, *103,* 3449-3605.

[101] C. Werner , H. Hopf , J. Grunenberg , L. Ernst , P. G. Jones , F. Köhler , R. Herges , *Eur. J. Org. Chem.* **2009** , 2621 –2626.
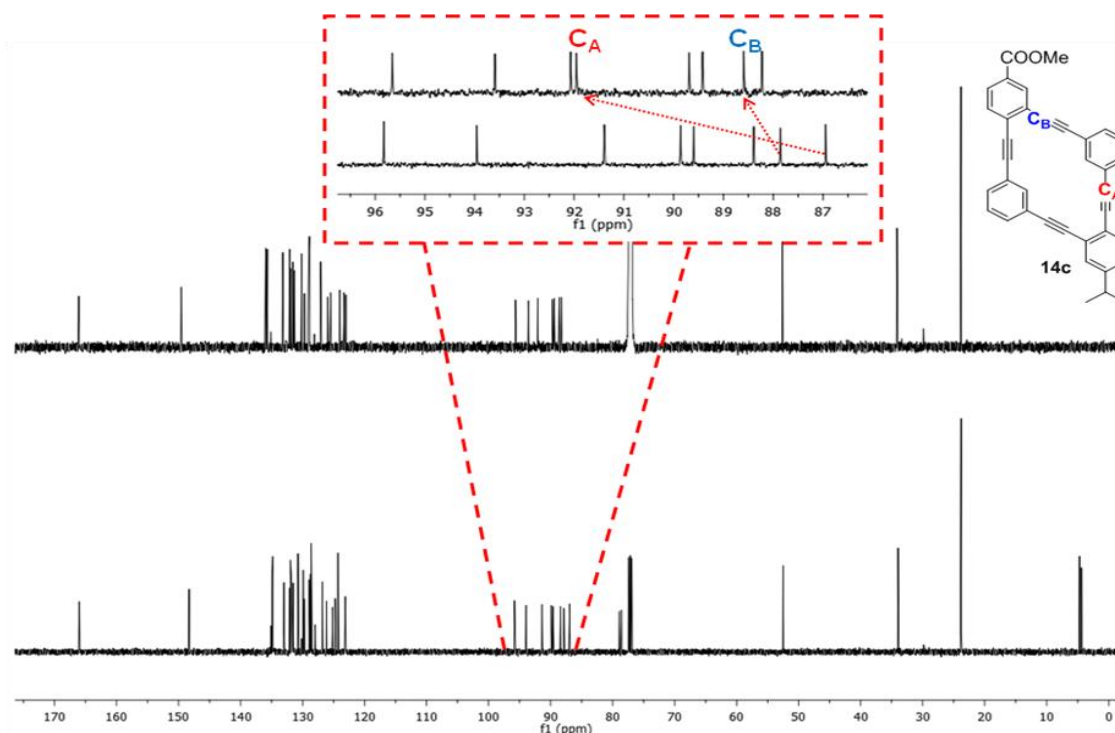
Figure 18. *Comparison of the ¹³C-NMR spectra of **14c** (top) and **15c** (bottom). The inset highlightes the aromatic region of the spectra and the larger shifts experimented by carbon nucleous CA (red) and CB (blue).*

Further insight about **14c** structure was offered by single crystal X-ray diffraction analysis.[102] Crystals of **14c** were grown in a dichlorometane saturated solution under slow evaporation at room temperature. The structure of **14c** is almost planar but exhibits larger distortions from ideal planarity compared to its non-substituted analog **11** reported by Vollhardt[103] (Figure 19). The larger distortions were derived from the more rigid and bulk *i*-propyl substituent which was partially rotated/twisted out of the plane respect to the three other rings. The ester group had an opposite effect. It provided a π-electron withdrawal stabilizing effect to the macrocyclic core and did not disrupt molecular planarity. The systematic distortion from linearity of bond angles in the ethynyl units evidenced the strain in the molecule. C(sp2)-C(sp)-C(sp) Angles were all slightly narrower that 180º (between 175-178º).
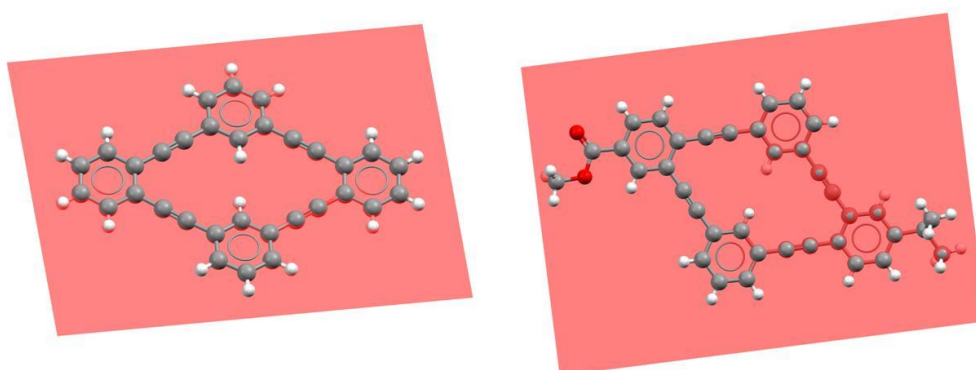

Figure 19. *X-ray structures of **11** and **14c** represented in a plane (red surface) to evidence the influence of the side-chains in the planarity of the macrocycle structure.*

---

[102] Crystallization and X-ray structure analysis performed by Dr. D. Choquesillo-Lazarte. Laboratorio de Estudios Cristalográficos IACT, CSIC- Universidad de Granada.

[103] X-ray structure of compound **11** borrowed from the CCDC, deposition number 192630.

Due to the clear influence of both side-chains so far, one would predict that the ability of such groups to interact with the annulene core should have an effect on the bond-length pattern by several resonance structures. Nevertheless, the difference is rather small. In general, bond lengths are all regarded as normal in excellent agreement with the expected values (1.40 Å for the aromatic rings, 1.43 Å for C(sp2)-C(sp) and 1.20 Å for C(sp)-C(sp) showing alternation between aromatic, single and triple bonds. This observation strongly supports the little delocalization along the annulene backbone. The distance between the intra-annular hydrogens was 2.373 Å. This value was slightly longer to the one reported for the naked **11** probably due to the distortion induced by the side chains.

In the crystal lattice, pairs of **14c** molecules related by an inversion center are formed as a consequence of π-π stacking interactions in a slightly displaced parallel-packing mode (Figure 20). The complementary electronic nature of the methyl ester and the *i*-propyl substituent is responsible of this inverse packing. The formation of similar packing structures has been ascribed to favorable quadrupole-quadrupole interactions (van der Waals) and reduction of unfavorable electrostatic repulsions (Coulombic).[104] This charge transfer interaction has been used by Tobe *et al.* for the construction of distinct supramolecular assemblies of electronically tuned [12]DBAs.[105]
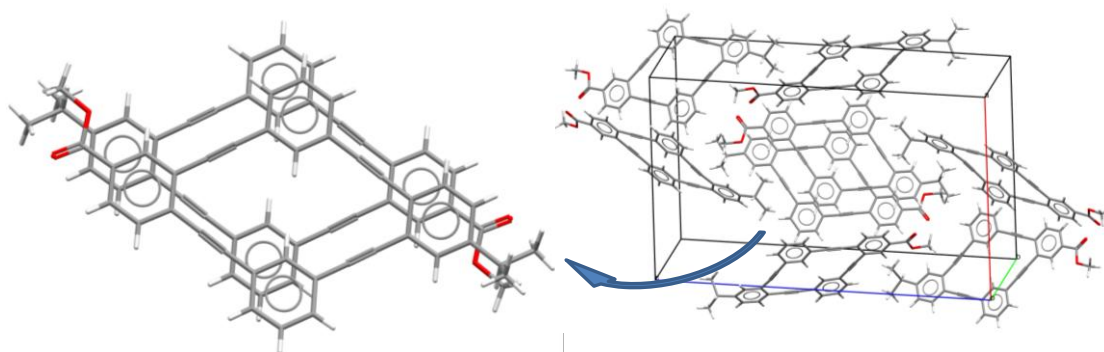

*Figure 20. Unit cell of **14c** (right) and dimers formed in solid-state (left).*

Macrocycle **14c** is separated by a mean distance of 3.55 Å with its partner and shows short distances (2.34-3.38 Å) with the neighboring molecules of the unit cell.[106] Distance between adjacent carbon atoms in the dimers are larger than the C-C distance in graphite (3.41 Å) for which semimetallic properties have been predicted along z-direction.[107] This type of crystal structure is classified as sandwich herringbone packing motif according to the Desiraju-Gavezzotti scheme for polynuclear aromatic hydrocarbons.[108]

14c crystallizes in Pbca (orthorhombic) and there are eight molecules in the unit cell (Figure 21). This crystal packing shows interesting similarities with it non-substitued analog **11**. Compound **11** crystallizes in the C2/c space group (monoclinic) with four molecules in the unit cell. The bigger unit cell for **14c** (V = 6721 Å^3) compared to **11** (V =2069 Å^3) is attributed to the side chains which play a major role in the crystal packing forces and curvature.

[104] J. H. Williams, J. K. Cockcroft, A. N. Fitch, *Angew. Chem., Int. Ed. Engl.* **1992**, *31*, 1655–1657. Y Desiraju TB!!

[105] K. Tahara, T. Fujita, M. Sonoda, M. Shiro, Y. Tobe, *J. Am. Chem. Soc.* **2008**, *130*, 14339–14345.

[106] Interlayer distance of 3.41 Å in graphyte from: *Europhys. Lett.,* **1994**, *28 (6),* 403-408.

[107] J.-H. Wong, B.-R. Wu, M.-F. Lin, *Computer Physics Communications, **2001**, 182*, 77–80

[108] G. R. Desiraju, A. J. Gavezzotti, *J. Chem. Soc., Chem. Commun.* **1989**, 621–623.
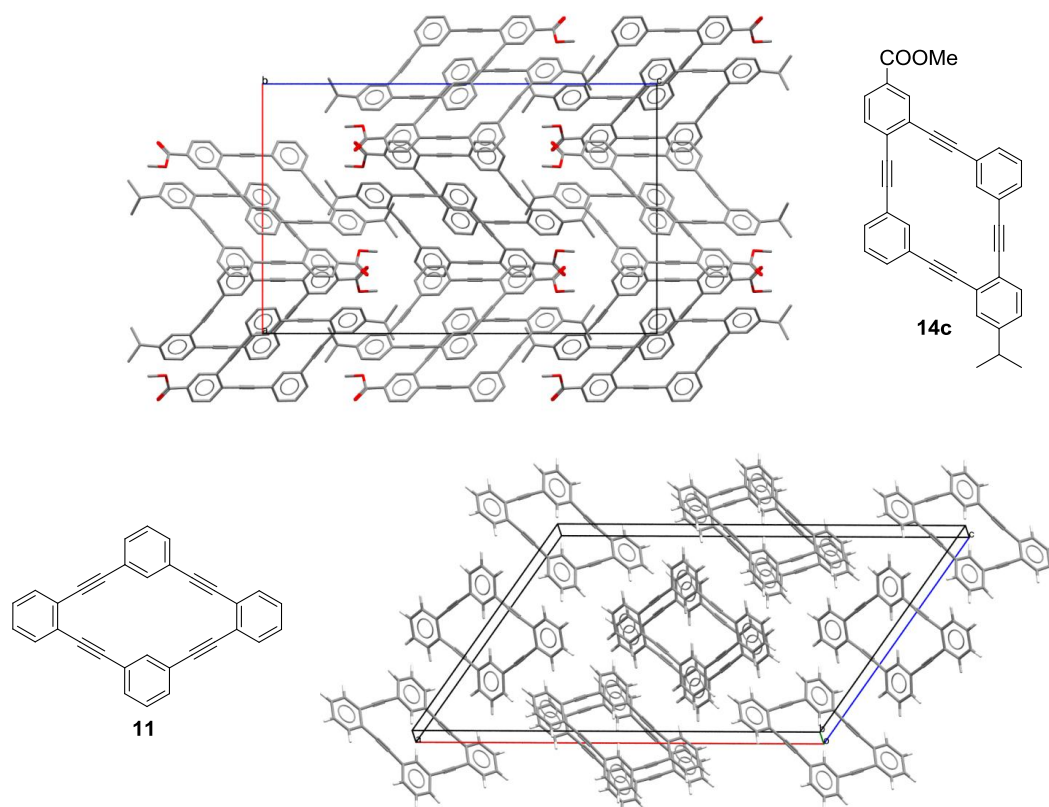
Figure 21. *Orthorhombic unit cell of **14c** (top) in the space group Pbca. Monoclinic unit cell of **11** in the C2/c space group (bottom).*

In addition to the solid-state characterization, some spectroscopic features were also studied in solution. In all cases, the shapes of the UV-vis spectra displayed a fine structure and were unchanged at different concentrations suggesting that the compounds do not aggregate in solution and all the bands can be attributed to intramolecular transitions.

The UV-vis spectra of **VIII**, **XII**, **15c** and **14c** display strong bands from 230 to 260 nm attributed to intramolecular ($\pi-\pi^*$) transitions corresponding to the phenyl rings (Figure 22). Lower-energy absorption bands above 260 nm are due to the diethynybenzene chromophores. The spectrum of **15c** has similar band to **VIII** and **XII**. However, it is not equal to the addition spectra of its fragments. Higher absorbances are related to the formation of a new phenylene-ethynylene bond. Specifically, the second pointed maximum at 287 nm ($\varepsilon = 4.08 \cdot 10^{10}$ M^{-1}cm^{-1}) is attributed to the *n-π^** transition between the ester substituted ring and the two neighbouring alkynes. An appreciable bathochromic shift ($\Delta\lambda = 30$ nm) for **15c** relative to its fragments suggests that there is still effective electronic communication through the whole backbone in solution.
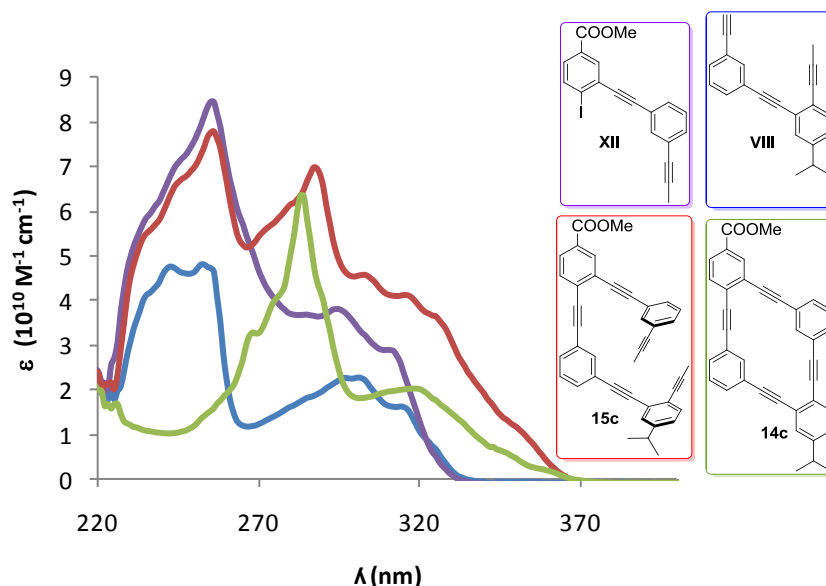
39

Figure 22. Absorption spectra of VIII, XII, 15c and 14c.

In the case of macrocycle **14c**, the absorption spectrum displays a sharp band at 283 nm (ε = 2.81·10^9 M^{-1}cm^{-1}) typical of graphyne structures such as [12]DBA.[109] It has been reported by Wirz that [12]DBA spectrum exhibits absorption/emission hallmarks owing to its unique electronic structure due to the *D*3*h* symmetry of the molecule.[110] There is a strongly allowed absorption band at around 290 nm, a weakly-allowed band at ca. 350 nm and a strongly-forbidden band at 400 nm. As occurred for [12]DBA, the spectrum of **14c** is narrow because most modes of vibration (e.g. rotations) are suppressed after cyclization. Compound **14c** exhibits a wider maximum in comparison to [12]DBA at 283 nm and a second maximum at 320 nm (ε = 5.98·10^8 M^{-1}cm^{-1}) due to the different diethynybenzene chromophores.

The profile of the fluorescence spectrum of **15c** is different from that of **14c**, with the 0-0 transition band at 380 nm as the strongest band, a typical profile for phenylacetylene derivatives (Figure 23). The fluorescence curve of **14c** exhibits a 14nm red shift relative to the 0-0 electronic transition of **15c**. Some hints of different fine structure can also be observed. However, any apparent vibrational splitting was detected for **14c** as it has been described for [12]DBA. Although quantum yield of the fluorescence were not calculated, the fluorescence intensity corrected by the molar absorptivity supported the higher intensity for the macrocycle (values 2378 vs 2456 a.u.) which is consistent with the rigid, shape-persistent nature of these compound.

[109] a) K. Kamada, L. Antonov, S. Yamada, K. Ohta, T. Yoshimura, K. Tahara, A. Inaba, M. Sonoda, and Y. Tobe, *ChemPhysChem* **2007**, *8*, 2671-2677. (b) T. Yoshimura, A. Inaba, M. Sonoda, K. Tahara, Y. Tobe, and R. V. Willians, *Org. Lett.* **2006**, *8*, 2933-2936.

[110] J. Wirz, In *Excited States in Organic Chemistry and Biology*; Pullman, B., Goldblum, N., Eds.; D. Reidal Publishing Company: Dordrecht: **1977**.
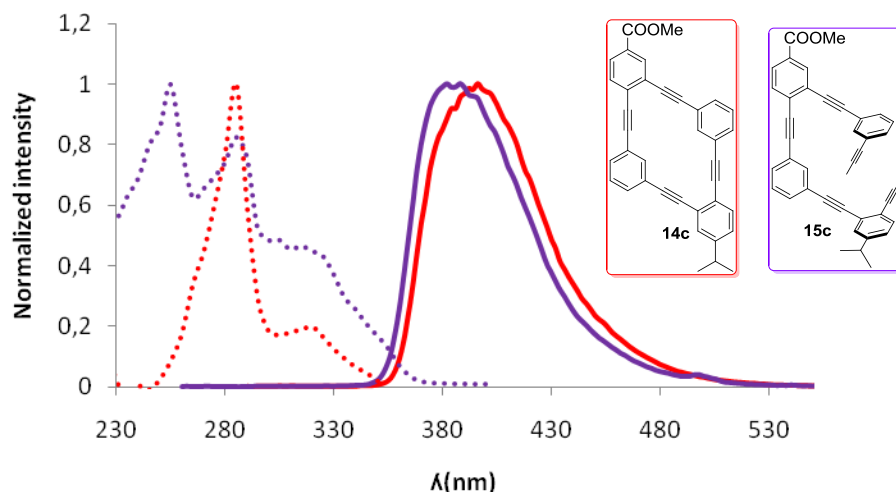
Figure 23. Comparison between the fluorescence spectra of 15c and 14c.

1.2.2.2. Synthesis and characterization of extended systems

Encouraged by these results, we planned the synthesis of bigger molecules comprising two grid subunits (Figure 24). The two new synthetic targets **16** and **17** were set in order to study the growing possibilities of our strategy and the effect of this enlargement on the optoelectronic properties and the solid state structure. As a consequence of the competing deslocalization trough the linearly conjugated *p*-phenyleneethnylene pathway, it was expected that second annulation of **16** would reduce the weakly paratropic character of the smaller [18]benzoannulene **14c** in favour of the wire segment. If our initial hypothesis were correct, compound **17** would comprise three short and "disconnected wires".
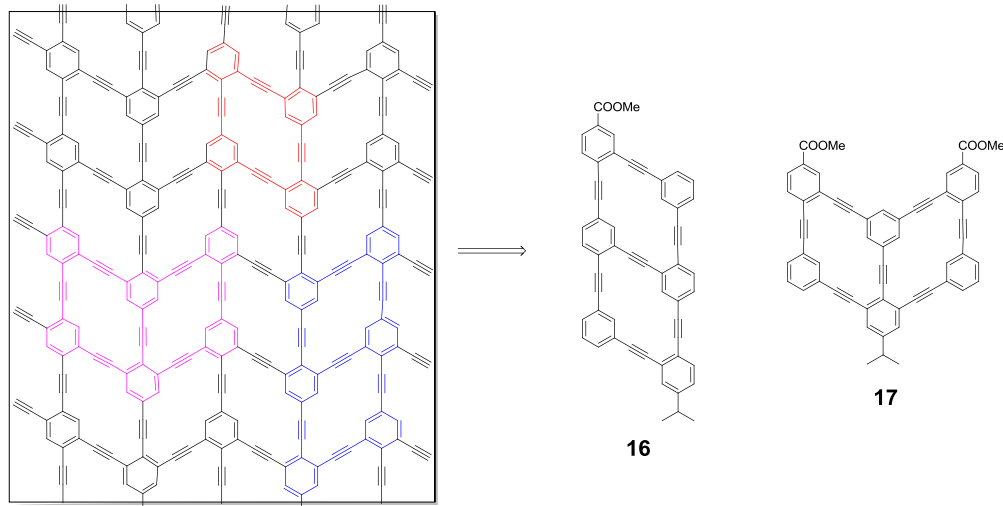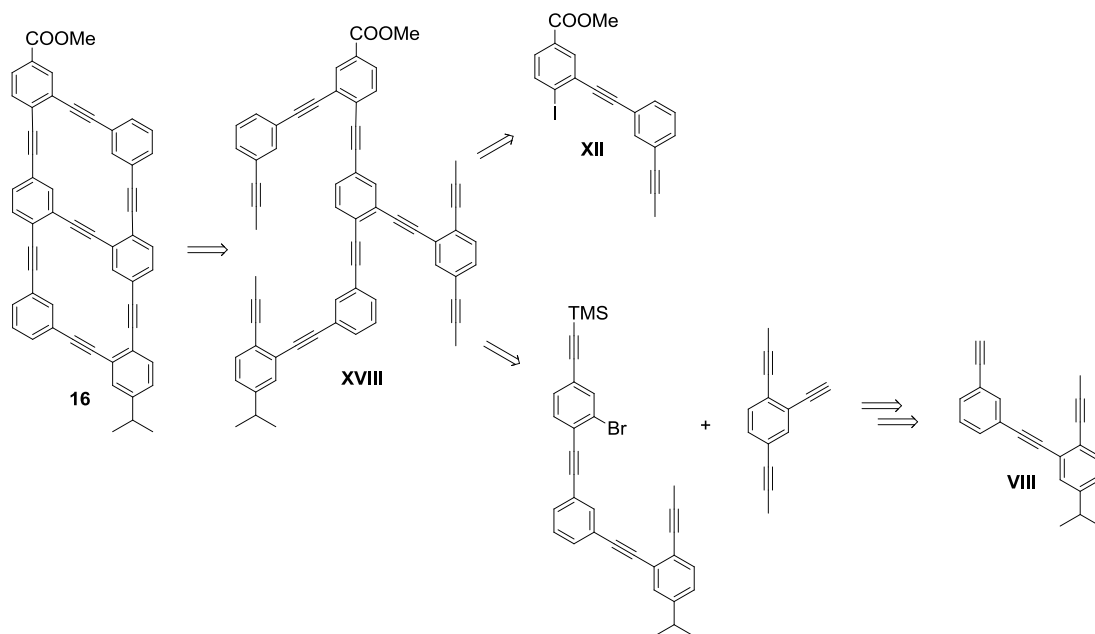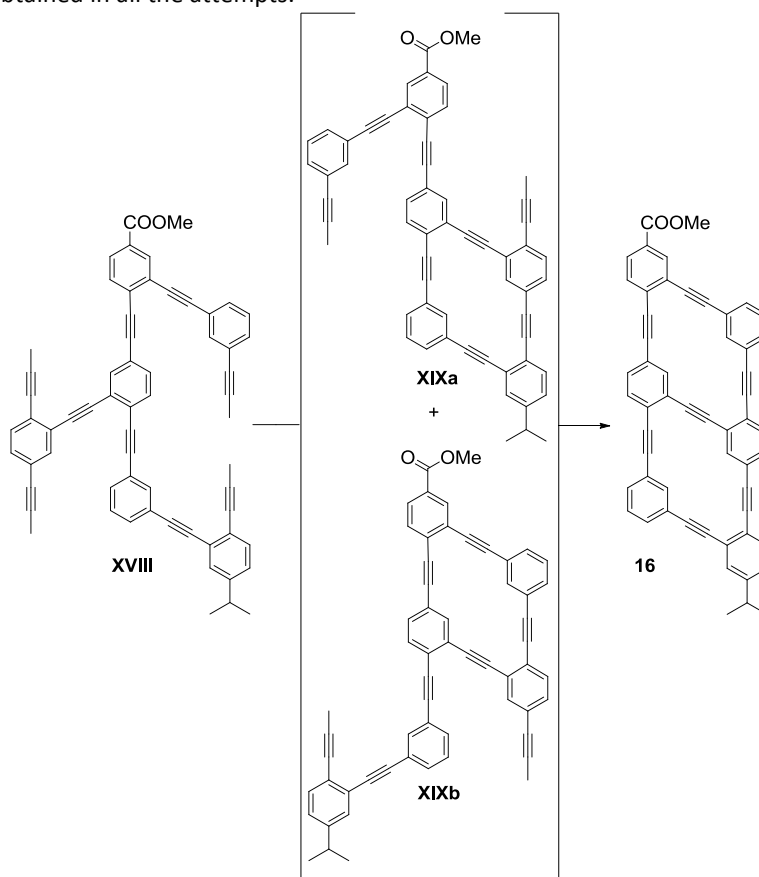

Figure 24. Target bi-fused annulenes 16 and 17.

To obtain compound **16**, intermediate **XVIII** was synthesized after four linear steps in 61% global yield calculated from **VIII** (Scheme 18).

Scheme 18. *Retroanalusis to obtain* ***16****.*

When we submitted precursor **XVIII** to RCAM (Scheme 18), a complex mixture of polymers and fragments was obtained in all the attempts.[111]

Scheme 19. *RCAM of compound* ***XVIII*** *led to the formation of two monocyclic structures* ***XIXa*** *and* ***XIXb****.*
In one of the attempts, the starting material **XVIII** was slowly (via syringe pump) added to a pre-heat solution of a Mo-alkylidyne catalyst in toluene. This reaction was monitored by APCI-LC/MS[112] analysis

---

[111] See experimental section.
[112] Analysis permormed in collaboration with Ms. Leichtweiss, MPI-KOFO, Germany.

(Figure 25). In the LC/MS chromatogram, the peak of the starting material **XVIII** came out at 8.4 minutes. During the reaction progress, two new peaks at 17.74 (peak 3) and 20.59 minutes (peak 4) both with a mass of 778 appeared and their relative abundance increased with the time (Figure 26). This m/z ratio could correspond to the desired product **16** (m/z calcd for $[C_{55}H_{30}O_2+Na^++MeOH]$: 777.86) or to the monocyclic isomers **XIXa** and **XIXb** (Scheme 18) (m/z calcd for $[C_{59}H_{36}O_2+H^+]$: 777.92).

Peak 1 SM

Figure 25. Kinetic profile: conversion of XVIII (peak 1, starting material (SM)) in XIXa and XIXb. Conditions: 1mM solution of the SM in toluene catalyzed by 100 % mol of Fürstner ate-Mo-alkylidyne complex at 80°C under Ar flow. Inset: LC/MS chromatogram shows the peak distribution after ca. 15 min.

The absorption UV/Vis spectra of both new peaks showed an increase of molar absorptivity and also bathochromic shift (λ_{max} of peak 1 = 254 nm; λ_{max} of peak 3 and 4 = 287 nm) compared to the starting material (Figure 26). These spectroscopic changes were analogous to the ones registered for **14c** and could only be consistent with the formation of a single macrocycle. Longer-wavelength absorptions are expected for more conjugated systems as **16**.[113]
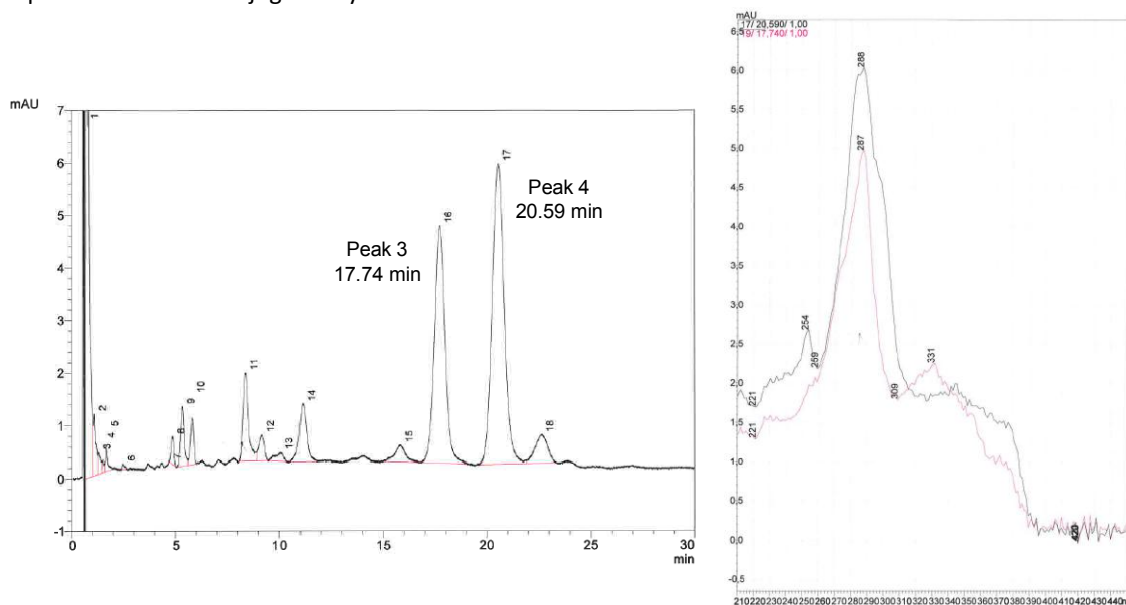

Figure 26. LC/MS chromatogram after ca. 2h reaction time (left). Absorption spectra of peak 3 (red) and peak 4 (black).

[113] (a) Marsden, J. A.; Haley, M. M. *J. Org. Chem.* **2005**, *70*, 10213; (b)Bhaskar, A.; Ramakrishna, G.; Haley, M. M.; Goodson, T., III. *J. Am. Chem.Soc.* **2006**, *128*, 13972; (c) Anand, S.; Varnavski, O.; Marsden, J. A.; Haley, M. M.; Schlegel, H. B.; Goodson, T., III. *J. Phys. Chem. A* **2006**, *110*, 1305.

In an attempt to identify the molecular structure of the two new peaks, the reaction was quenched. After recycling gel permeation chromatography (GPC),[114] peak at 20.59 min was isolated in 91% purity (measured with LC/MS) but the ^{1}H-NMR spectra in CDCl$_3$ of this sample still showed high amounts of impurities, making inconclusive the identification trials. Hence, we decided to synthesize one of the possible isomers (Scheme 20).
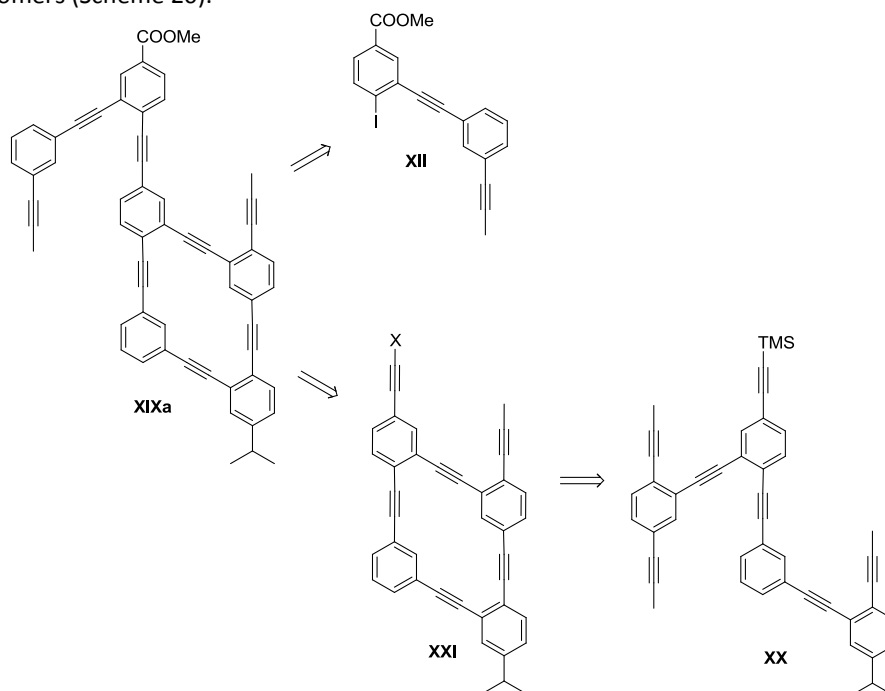
Scheme 20. *Retroanalusis followed to obtain **XIXa**.*

APCI-LC/MS analysis of the pure isolated compound **XIXa** revealed that the peak at 17.74 minutes corresponded to one of the monocyclic isomers (Figure 27). As the absorption UV/Vis spectra of the two peaks were nearly identical, hence, peak 4 was tentatively assigned to the other monocyclic isomer and the formation of the desired bis-macrocycle **16** was ruled out.
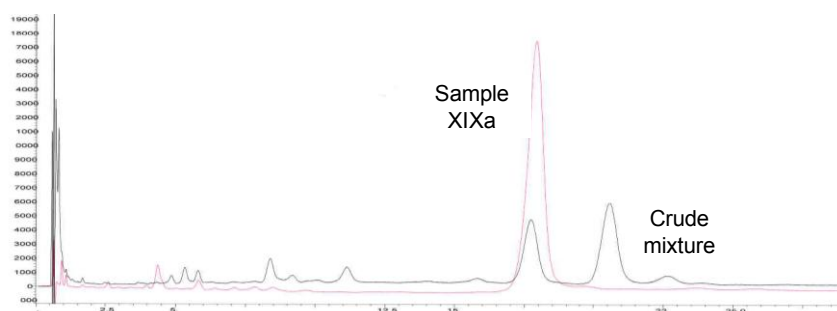

Figure 27. *LC/MS chromatogram of the crude mixture (black) overlaid by the LC/MS chromatogram of the isolated monocycle **XIXa** (red).*

When compound **XIXa** was submitted to alkyne metathesis any desired product (**16**) could be isolated. At the same time, a different route to achieve **16** which involved the simultaneous but independent closure of the macrocycles from **XXX** was also explored (Scheme 21). Unfortunately, any of the three routes drove to the desired bis-annulenes in the final RCAM.
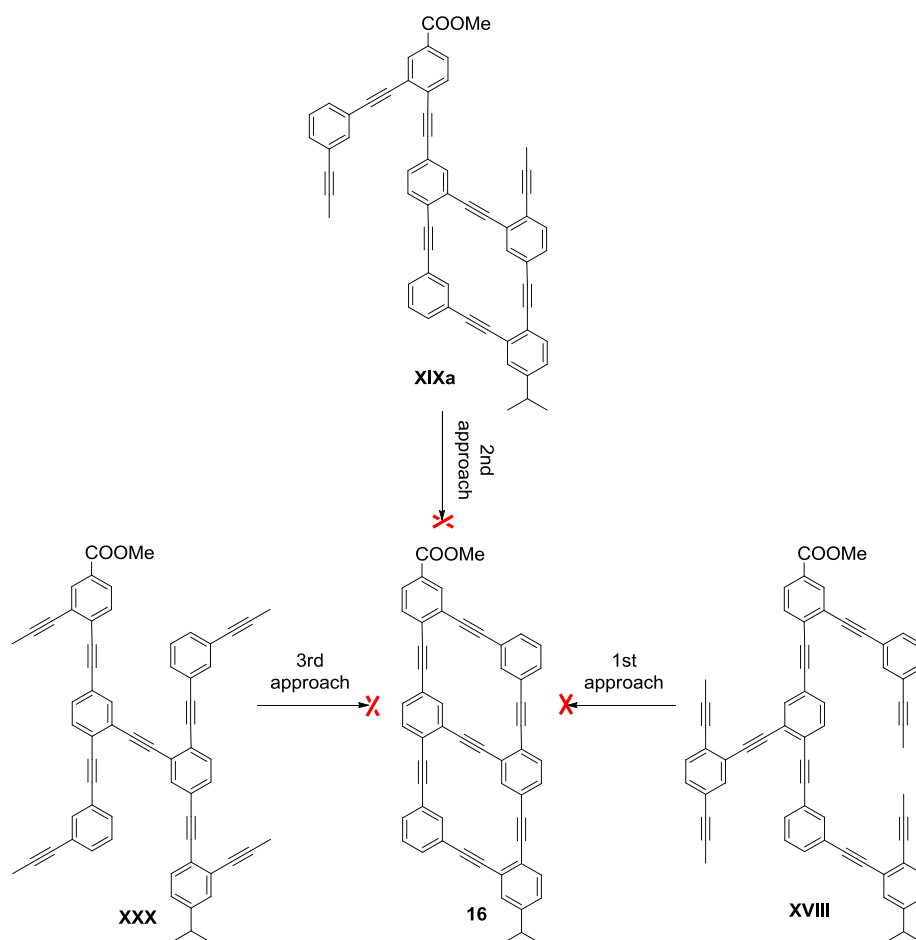
**Scheme 21.** *Summary of the unsuccessful routes explored to synthesize compound* **16.**

Compound **XXXVII** was also obtained from two independently synthesized fragments in 27 % global yield after 5 linear steps (Scheme 22). Bis-annulene **17** was neither isolated after the RCAM.
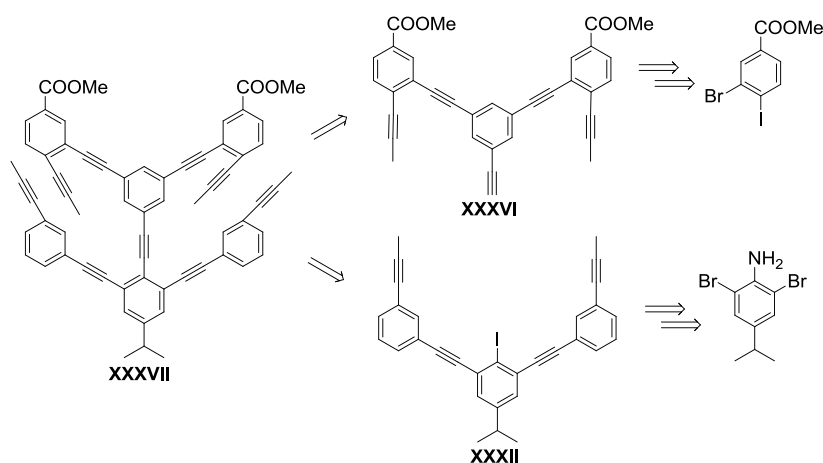
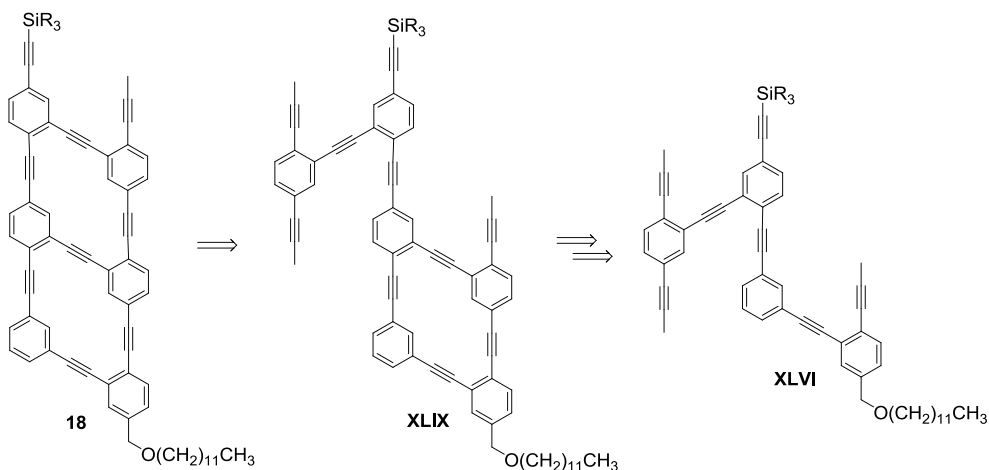**Scheme 22.** *Retroanalusis followed to obtain* **XXXVII**.

The efficiency of W/Mo alkylidyne catalysts to close one grid subunit was supported by the results obtained for **14c** and **XXI**. However, the use of RCAM to obtain bi-fused **16** and **17** structures systematically failed. The poor solubility of the final products associated with the wide planar aromatic backbone and the stiffness of the bifused structure, seemed to be the hurdles to jump over. Trying to improve the solubility of the precursor **XVIII**, a long alkyl chain was introduced by reduction of the methyl ester and nucleophilic substitution with dodecyl bromide (Scheme 23). Alkyne metathesis of **XXXVIII** yielded again to an equimolar mixture of both isomers in high yield which were separated after

column chromatography. Traces of the bi-fused cycle were detected by MALDI-HRMS analysis but any product could be isolated.
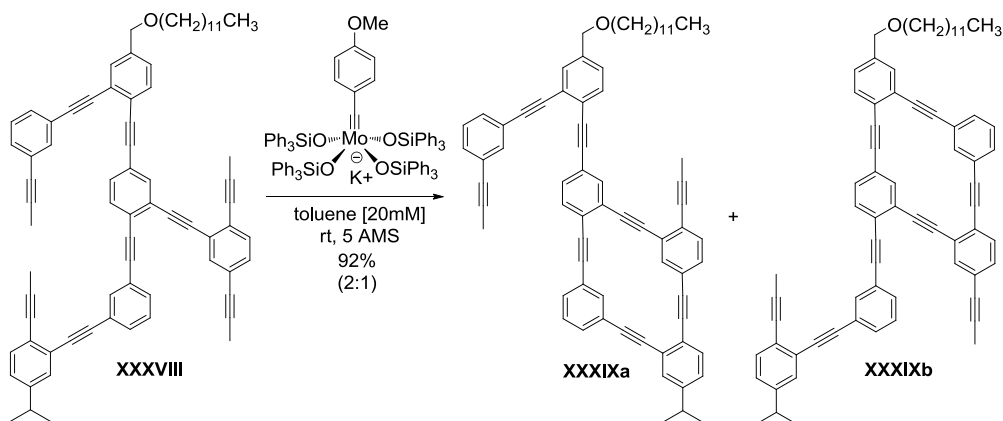

Scheme 23. *RCAM of the dodecyl-substituted compound XXXVIII also led to the formation of two monocyclic structures XXXIXa and XXXIXb*.

The stepwise approach to bi-fused compound **18** was also studied (Scheme 24). As usual, the first RCAM proceed in high yields but from the second RCAM any desired product could be recovered.

Scheme 24. *Retroanalusis followed to obtain 18*.

Despite all our efforts to grow bi-fused substructures, the formation of larger fused-macrocycles remained elusive. Taking into account the difficulty associated with the second ring-closure and the tedious and time-consuming synthesis of the RCAM precursors, we tried a last experiment in order to check if the simultaneous ring closure would yield to the less strained non-fused bis-annulene **19** (Scheme 25).
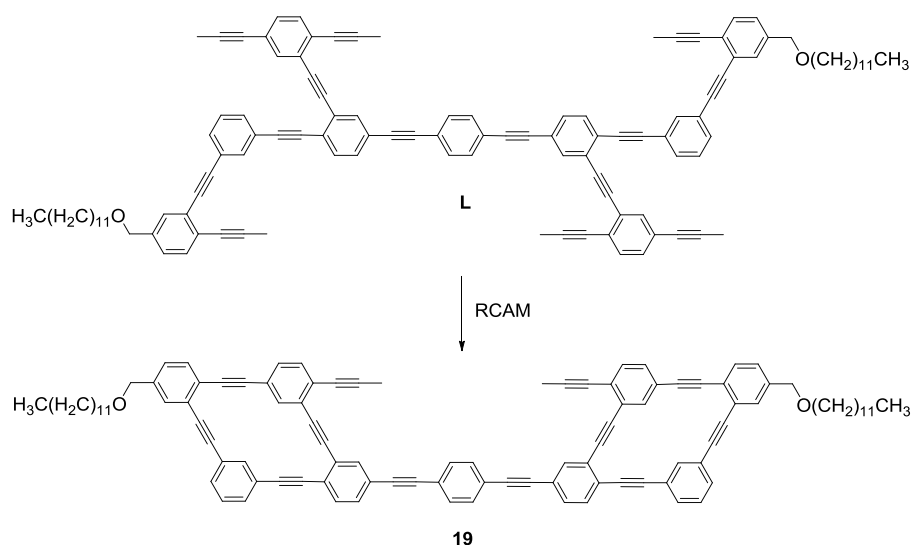
Scheme 25. *RCAM to obtain 19.*

Bis-annulene **19** was synthesized after three steps from **XLVI**. Despite its poor solubility but thanks to the reduced ring strain and planarity, the final product was obtained by double RCAM in 24% yield as a white solid after column chromatography and recrystallization in hexane/dichloromethane mixtures. Although this graphyne-cutout does not contain the original mesh of poly-fused annulenes, it includes a wire segment connected to two annulenes, thus some information about this structure on optoelectronic properties could be drawn. Moreover, we turned to the abundant library of intermediates to make a wider study.

1.2.2.3.UV-studies

Absorption curve of **XIXa** was similar to the one of **14c** but with the maximum slightly red shifted up to 295 nm (ε = 1.44·10^{10} M-^{1}cm^{-1}) which is translated in a 0.18 eV smaller optical band gap (Figure 28) and Table 1). Higher absorbances and new bands above 300 nm were consistent with the extension of the conjugation along the wire segment. The characteristic absorption bands ranging after 300 nm were nearly identical but 20 nm red-shifted to the non-annulated wire segment **XXVI**. Surprisingly, **XIXa** and **14c** exhibit almost congruent emission spectra but characterized by different fine structures.[115] All these findings suggest that the fluorescence is dominated by influence of the phenylacetylene linear segment.
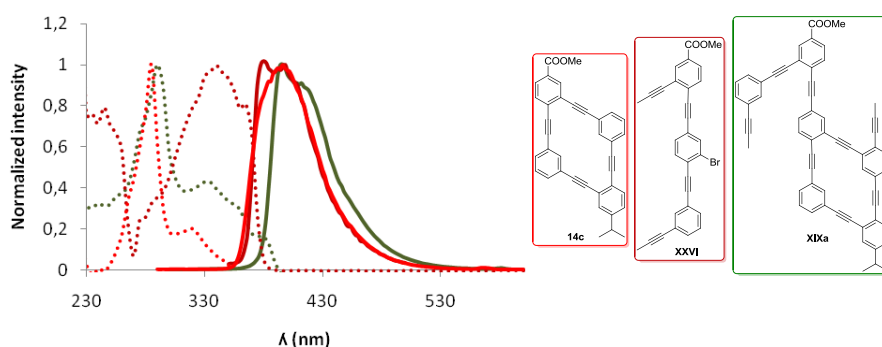

Figure 28. *Absorption (dot) and emission (line) spectra of **14c**, **XXVI** and **XIXa**.*

Compound	Λmax (nm)	ε (10^6 M-^{1}cm^{-1})	E_g^{UV} (eV)	I/ε(Λexc)

---

[115] Peaks in the UV/visible spectrum for a molecule are in fact a smeared summation of many different transitions between different vibrational and rotational substrates. In some cases, the smearing is incomplete and we can see at least hints of the individual component peaks due to individual vibronic bands called vibrational fine structure.

14c	283	$2.81 \cdot 10^3$	4.38	2456
XIXa	295	$1.44 \cdot 10^4$	4.20	2883
XXVI	340	$5.39 \cdot 10^3$	3.65	2374

Table 1

Further insight about the predominance of the linear segment on the optical properties is obtained by comparison between **XVIII** and **XXX** and their monocyclic isomer **XIXa** (Figure 29). As it could be seen in the former figure 28, the absorption profile of each compound strongly depends on the number and type of cromophores. The three isomers have very similar emissive profiles (identical for **XIXa** and **XVIII**). The less-efficient conjugation trough the meta-linkage which bounds the two independent wire segments in **XXX** is translated into a 5-nm blue-shift.
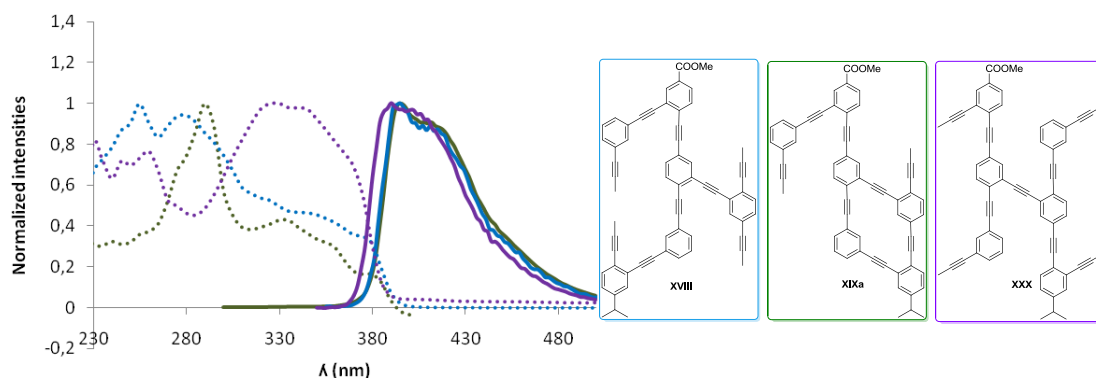

Figure 29. Absorption (dot) and emission (line) spectra of XVIII, XIXa and XXX.

Compound	Λmax (nm)	ε (10^6 M^{-1}cm^{-1})	E_g^{UV} (eV)	I/ε(Λexc)
XXX	330	$8.4 \cdot 10^4$	3.76	2766
XVIII	254	$2.1 \cdot 10^4$	4.88	5968

Table 2

In the case of intermediates **XXVI**, **XXVIII** and **XXX** all absorption/emission spectra are quite in agreement (Figure 30). The ester substituted wire **XXVI** has a 0.05 eV smaller optical band gap compared to **XXVIII** (Tables 1 and 3). In compound **XXX**, a new and longer linerly conjugated path between the four *ortho*-fused benzenes is present. Although deslocalization is thought to be weaker, ortho-fused phenylene ethynylenes can also be used as molecular wires. More interesting findings about how the *meta*-linkage and side-chain substituents affect the photoluminiscent properties were registered for **XXXVII** and its fragments.
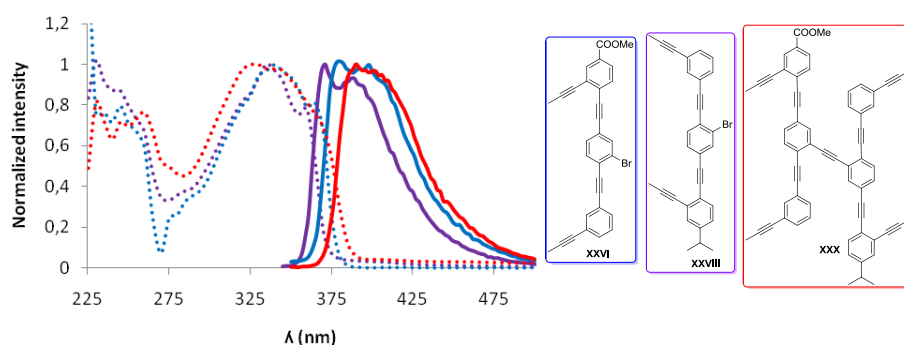

Figure 30. Absorption (dot) and emission (line) spectra of XXVI, XXVIII and XXX.

Compound	Λmax (nm)	ε (10^6 M-^{1}cm^{-1})	E_g^{UV} (eV)	I/ε(Λexc)
XXVIII	335	$1.76 \cdot 10^5$	3.70	1884

Table 3

In contrast to the UV-vis spectra, significantly different emission properties were observed for compounds **XXXII**, **XXXVI** and **XXXVII** (Figure 31 and table 3). Bathochromic shifts accompanied by the change of the vibronic fine-structure were observed for the methyl ester substituted compounds **XXXVI** and **XXXVII** in comparison to **XXXII**. To examine this effect more closely, we measured fluorescence spectra in two organic solvents with different polarity.
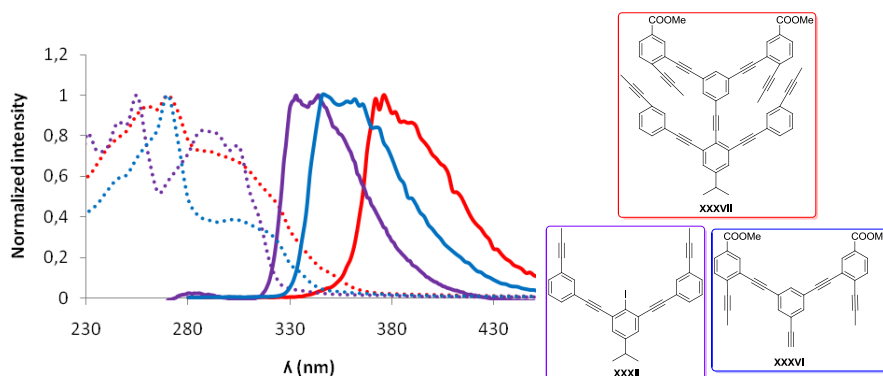

Figure 31. Absorption (dot) and emission (line) spectra of XXXII, XXXVI and XXXVII.

Compound	Λmax (nm)	ε (10^6 M^{-1}cm^{-1})	E$_g^{UV}$ (eV)	I/ε(Λexc)
XXXII	255	$4.06\cdot10^4$	4.86	1176
XXXVI	270	$7.47\cdot10^4$	4.59	7802
XXXVII	270	$8.26\cdot10^4$	4.59	1654

Table 4

The spectra of **XXXII** and **XXXVII** do not exhibit significant fluorescence solvatochromism when the solvent polarity increases from hexane to methanol, nevertheless more accused changes were observed for **XXXVI** (Figure 32). These electronic differences can be related to the induction of topological changes in the frontier orbitals due to the transformation from a phenylacetylene p–p* excitation to a ''push–pull'' n–p* transition.[116] The non-electronically-innocent esters polarize the π-electron cloud of the conjugated backbone generating fluoresce from intramolecular charge-transfer states. In general, excited-states have larger dipole moments compared to ground-states, as a result, lower-energy emissions are detected in more polar solvents. Comparison of corrected fluorescence also agreed with this hypothesis and **XXXVI** is remarkably more fluorescent (Table 4). Similar findings have been discussed for related expanded acetylenic p-systems.[117]
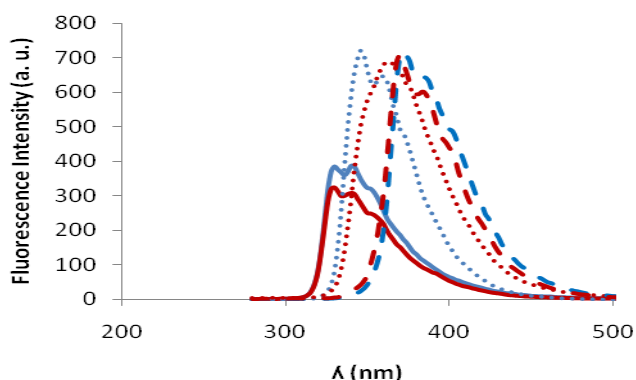
[116] (a) B. Breiten, Y.-L. Wu, P.D. Jarowski, J.-P. Gisselbrecht, C. Boudon, M. Griesser, C. Onitsch, G. Gescheidt, W. B. Schweizer, N. Langer, C. Lennartz, F. Diederich, *Chem. Sci.,* **2011**, *2*, 88; (b) L.-O. Palsson, C. Wang, A. S. Batsanov, S. M. King, A. Beeby, A. P. Monkman, M. R. Bryce, *Chem.Eur. J.,* **2010**, *16*, 1470–1479.

[117] J.-K. Fang, D.-L. An, K.Wakamatsu, T. Ishikawa, T. Iwanaga, S. Toyota, S.-I. Akita, D. Matsuo, A. Orita, J. Otera Tetrahedron, **2010**, *66*, 5479-5485.

*Figure 32. Emission spectra of **XXXVI** (dot), **XXXII** (line), **XXXVII** (dash) in hexane (red) and methanol (blue).*

Compound **XXXII** exhibits nearly identical absorption curve to **VIII** but higher molar absorption coefficients in the region of the diethynybenzene chromophores (Figure 33 and tables 4 and 5). Comparison with a series of related linear compounds provide evidence on how the growth in *para*-position has a determinant role in the sense that the HOMO–LUMO gap decreases as the length of the oligomer increases.
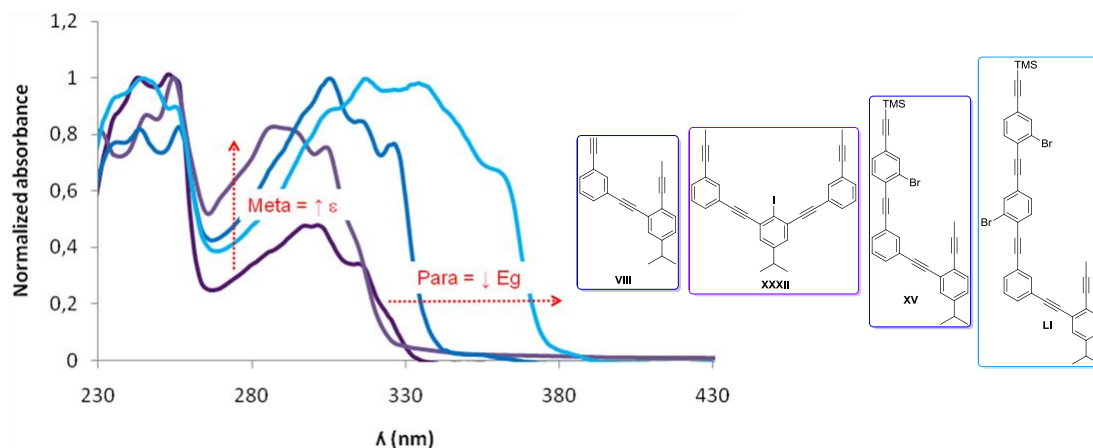

Figure 33. Influence of the connectivity between benzene rings on the absorption spectra.

Compound	Λmax (nm)	ε (10^6 M^{-1}cm^{-1})	E_g^{UV} (eV)
VIII	252	$4.81\cdot10^4$	4.92
XV	305	$4.88\cdot10^4$	4.07
LI	334	$9.38\cdot10^4$	3.71

Table 5

The good agreement of the absorption spectrum obtained by summation of the constituent **XXXII** and **XXXVI** absorptions with the actual absorption spectrum of **XXXVII** (Figure 34) supports the hypothesis that any significantly more extended chromophore is formed after coupling both fragments.
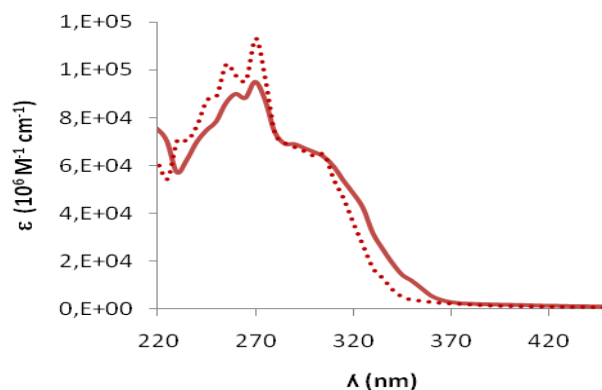

*Figure 34. Absorption spectra of **XXXII+XXXVI** (dot) in comparison to **XXXVII** (line).*

As a matter of fact related to the less conjugation through *meta*-bonds, the absorption/emission spectra of **15c** and **XXXVII** are merely comparable (Figure 35). The concordance between absorption/emission profiles shows up that the chromophores from which radiant relaxation emanates in **XXXVII** must be already present in **15c** and, therefore, the *meta*-linkages "cut in pieces" significantly the electronic communication.
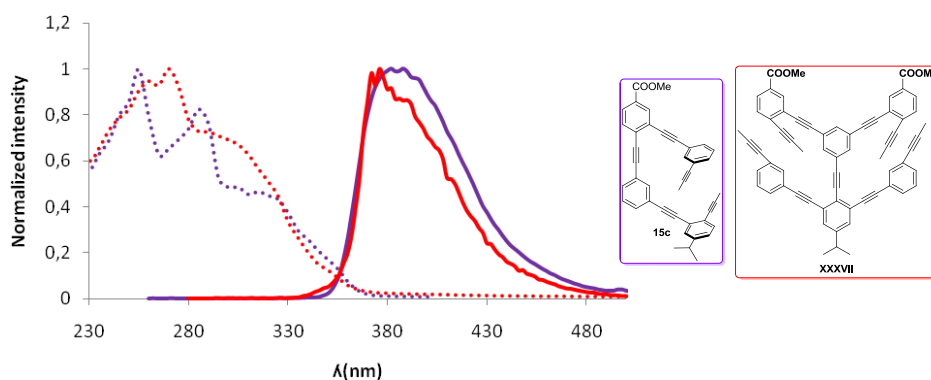
50

Figure 35. *Absorption (dot) and emission (line) spectra of **15c** and **XXXVII**.*

Finally, we studied the espectroscopic properties of compound **19** (Figure 36). Non-fused bisannulene **19** shows comparable spectroscopic curves to **15c**. It is significantly better chromophore and less fluorescent (Table 6). Fluorescence curve of **19** is characterized by a blue shifted emission probably derived from the more constrained geometry which generates less planar conformations. A wider splitting between the fluorescence bands more similar to the registered for the [12]DBA could also be detected. Although all the previous UV analysis point to the prevalence of the phenylacetylene segment over the optoelectronical properties, these last spectra raise the question whether the stiffer and 2D-larger molecules would adopt planar structures, a fundamental prerequisite for p-phenylene-ethynylene oligomers to behave as molecular wires.
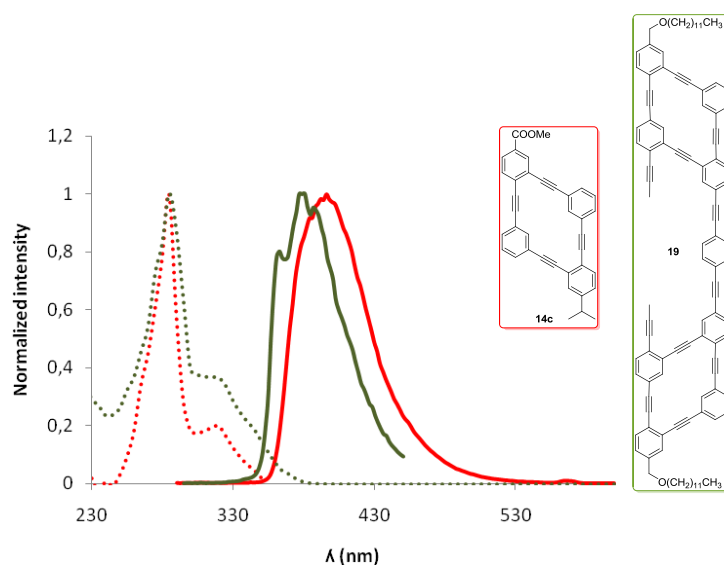

Figure 36. *Absorption (dot) and emission (line) spectra of **15c** and **19**.*

Compound	Λmax (nm)	ε (10^6 M^{-1}cm^{-1})	E_g^{UV} (eV)	I/ε(Λexc)
19	285	$4.71 \cdot 10^5$	4.35	270

Table 6

51

1.2.3. Conclusions and Outlook

The synthesis of a graphyne-type carbon network constructed by rhomboidal subunits type **11** has been studied. This graphyne-mesh has been designed in order to behave as a two-dimensional anisotropic polymer comprising covalently-bound *p*-phenylene-ethynylene molecular wires. Based on previous descriptions of quantum interferences, 2-ethylene bonds connecting neighbouring wires on *meta*-position have been proposed to hold the wires covalently bound in a single layer but acting as poor efficient bridges for electronic coupling. The bottom-up approach followed ensures molecularly-defined internal order using only two orthogonal organic transformations: Sonogashira coupling and alkyne metathesis.

Compound **14c**, the smallest unit of the infinite network, has been successfully built from a few phenyleneethynylene bricks and a final step of alkyne metathesis. The better performance of the RCAM was obtained using the new user-friendly catalysts developed by Fürstner *et al*. The synthesis of bi-fused wider compounds **16** and **17** following our initial proposal could not be accomplished albeit less strained bi-fused compound **19** was successfully isolated.

UV-vis spectroscopic analysis supports the weak electronic coupling between linear OPEs connected in meta-position by alkyne bonds in comparison to *para*- and *ortho*-connected phenyl-ethynylenes.

As we mentioned in the introduction, the final aim of this project is the synthesis of an all-carbon two-dimensional anisotropic polymer comprising two different electronic paths. Throughout this time, we become aware of the decisive role of solubility and reduced strain together with planarity to succeed in our goal and the inherent impossibility of our first mesh-design to overcome any of these drawbacks. Any future mesh-design should guarantee at least the improvement of solubility with the net growth and the coplanarity but along the wire segment and between neighbouring wires (Figure 37).[118]
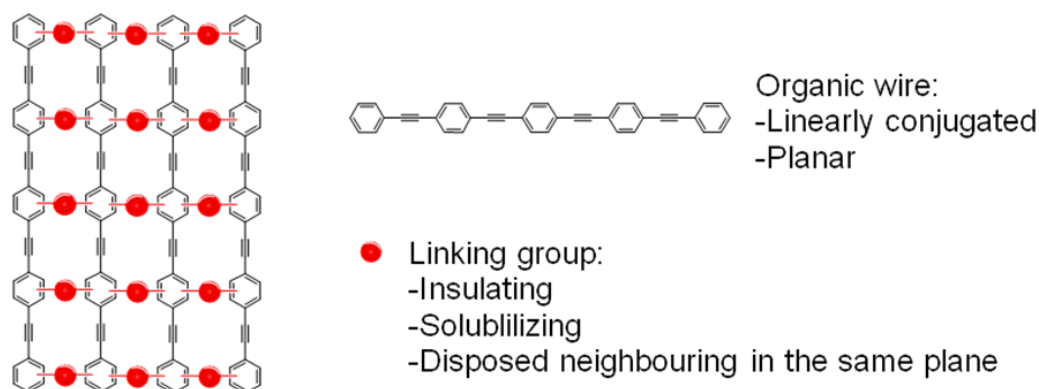

Figure 37. *General considerations to design an anisotropic 2D graphyne-substructure by organic synthesis.*

For this reason and, as future work to do, we propose a new mesh which takes into account all the aforementioned limitations (Figure 38). The new design allows the introduction of terminal linking groups such as thiols to bind it to a Au(111) surface and the organization of these rigid structures at the solid/liquid and solid/air interface would be also possible due to their extended two-dimensional structure and the ability of the long alkyl chains to interact upon van der Waals forces.[119]

---

[118] The use of shape-persistent phenylene containing oligoacenes (POAs) has been proposed in a recent work but still electronic coupling was observed. JACS swager

[119] (a) Tahara, K. *et al. J. Am. Chem. Soc.* **2006**, *128*, 16613; (b) Lei, S. *et al. J. Am. Chem. Soc.* **2008**, *130*, 7119; (c) Tahara, K. *et al. Chem. Commun.* **2010**, *46*, 8507.
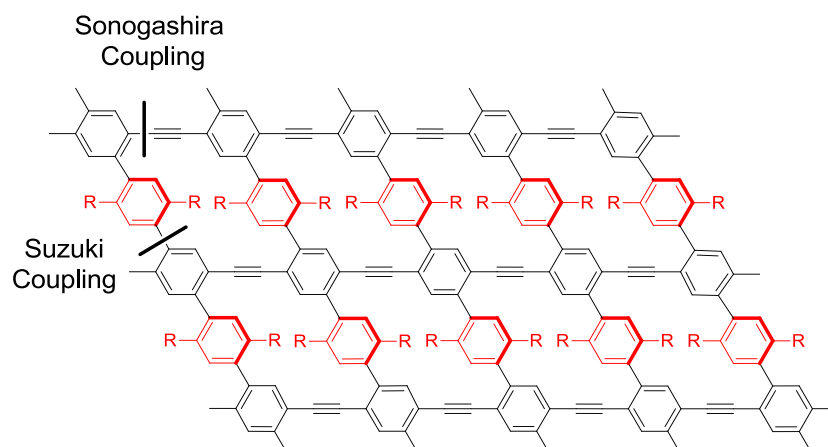
Figure 38. *New target mesh to synthesize a 2D anisotropic conduction polymer.*

Additionally, we realized that wider graphyne substructures would be more easily accessed if we focused on more symmetric cutouts like *dendrimers*. Dendrimers are repetitively branched molecules typically symmetric around a core (called focal point). Based on this concept, we have redesigned our original retrosynthetic analysis which uses Sonogashira coupling and alkyne metathesis trying to minimize the synthetic effort to reach the substrates of the final multiple-RCAM and the stiffness of the graphyne cutout. Our first generation dendrimer target would be constituted of six totally independent macrocyles (dendrons) connected to a central benzene ring (Figure 39). Moreover, changing the connectivity to the central benzene three-dimensional (propeller-shaped) morphologies could also be feasible.[120]
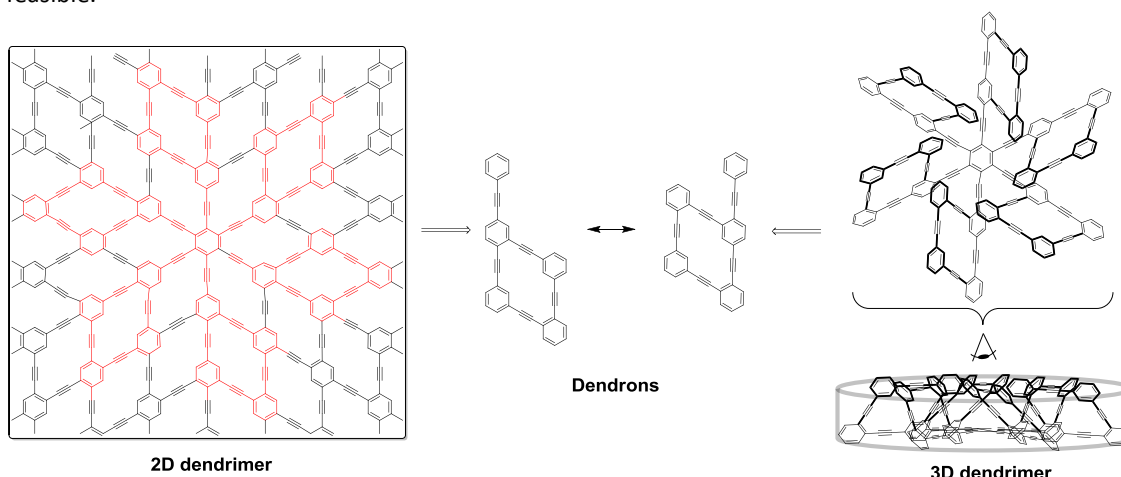

Figure 39. *Other planar and propeller-shaped graphyne substructures.*

1.2.4. Experimental section

1. General procedures: [121]

Sonogashira coupling of *aryl iodides*. **(GP1)**
A solution of the terminal alkyne (1.2 mmol) dissolved in the minimum volume of THF and with 2 mL of Et$_3$N was added dropwise to a carefully degassed solution of Pd(PPh$_3$)$_2$Cl$_2$ (5 mol%), CuI (10 mol%) and

---

[120] C. D. Simpson; G. Mattersteig; K. Martin; L. Gherghel; R. E. Bauer; H. J. Räder; K. Müllen, *J. Am. Chem. Soc.* **2004**, *126*, 3139-3147.
[121] When the alkyne used was propyne, gas flow was bubbled into the carefully degassed solution of the Pd catalyst, cooper salt and the halobenzene during 10-15 min. Then, the flask atmosphere was filled with propyne and the reaction stirred 1-3h before the quenching.

the aryl iodide (1 mmol) in 10 mL of Et$_3$N. The reaction was stirred between 3-16h at room temperature under argon atmosphere. The mixture was then diluted with EtOAc or dichloromethane, washed with saturated aq NH$_4$Cl solution, dried over anhydrous Na$_2$SO$_4$ and the solvent was removed under reduced pressure. The residue was purified by flash chromatography (EtOAc/Hexane mixtures) to give the corresponding coupling product.

Sonogashira coupling of aryl bromides. (GP2)
A solution of the terminal alkyne (1.2 mmol) dissolved in the minimum volume of THF and with 2 mL of ^{i}Pr$_2$NH was added dropwise to a carefully degassed solution of Pd(CH$_3$CN)$_2$Cl$_2$ (3 mol%), P^{t}Bu$_3$·HBF$_4$ (6 mol%), CuI (3 mol%) and the aryl bromide (1 mmol) in 10 mL of ^{i}Pr$_2$NH. The reaction was stirred between 3-16h at room temperature under argon atmosphere. The mixture was then diluted with EtOAc or dichloromethane, washed with saturated aq NH$_4$Cl solution, dried over anhydrous Na$_2$SO$_4$ and the solvent was removed under reduced pressure. The residue was purified by flash chromatography (EtOAc/Hexane mixtures) to give the corresponding coupling product.

2. *Synthesis and analytical characterization of the compounds:*
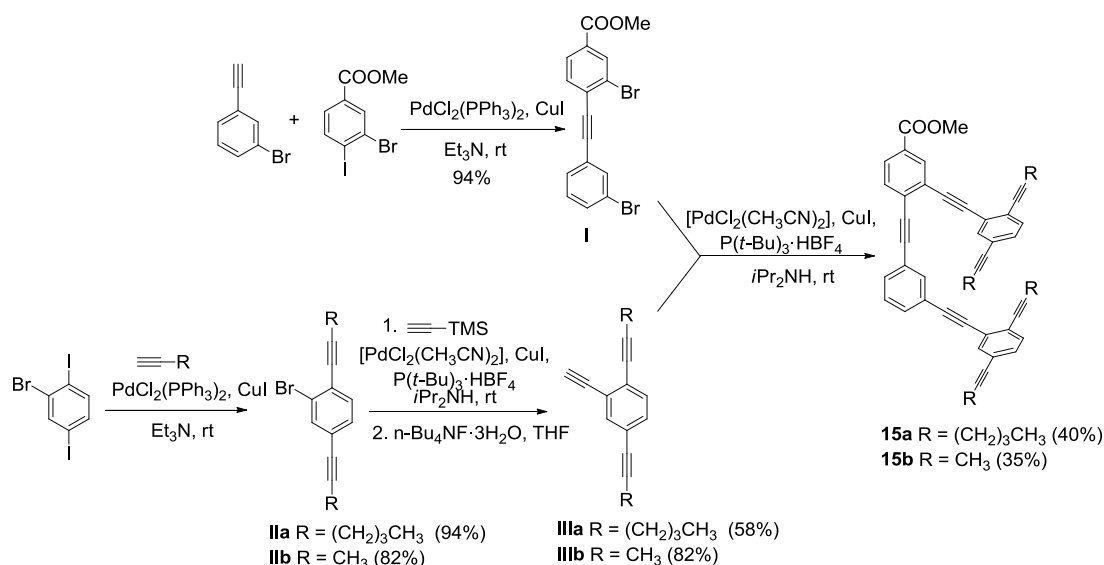
Compound I was prepared from 1-bromo-3-ethynylbenzene (169 mg, 0.93 mmol) and methyl 3-bromo-4-iodobenzoate (302 mg, 0.88 mmol) according to previously described *GP1* to give **I** in 94 % yield (191 mg) as a white solid. ^{1}H-NMR (400 MHz, CDCl$_3$): δ (ppm) = 8.31 (s, 1H), 7.98 (d, *J* = 8.1 Hz, 1H), 7.76 (s, 1H), 7.62 (d, *J* = 8.1 Hz, 1H), 7.54 (d, *J* = 8.0 Hz, 2H), 7.28 (d, *J* = 4.4 Hz, 1H), 3.96 (s, 3H); ^{13}C-NMR (101 MHz, CDCl$_3$): δ (ppm) = 165.4 (C), 134.6 (CH), 133.6 (CH), 133.2 (CH), 132.4 (CH), 131.2 (C), 130.5 (CH), 130.1 (CH), 129.4 (C), 128.2 (CH), 125.7 (C), 124.5 (C), 122.4 (C), 95.2 (C), 88.8 (C), 52.7 (CH3); EI-HRMS calculated for C$_{16}$H$_{10}$Br$_2$O$_2$: 391.9048, found: 391.9054.

Compound IIa was prepared from 1-hexyne (390 mg, 1.18 mmol) and 2-bromo-1,4-diiodobenzene (484 mg, 1.18 mmol) according to previously described *GP1* to give **IIa** in 94 % yield (337 mg) as a yellow liquid. ^{1}H-NMR (300 MHz, CDCl$_3$): δ (ppm) = 7.63 (s, 1H), 7.34 (d, *J* = 7.9 Hz, 1H), 7.25 (d, *J* = 7.9 Hz, 1H), 2.47 (dt, *J* = 20.2, 6.6 Hz, 4H), 1.74 – 1.44 (m, 8H), 0.99 (t, *J* = 5.6 Hz, 6H); ^{13}C-NMR (75 MHz, CDCl$_3$, DEPT): δ (ppm) = 135.1 (CH), 132.8 (CH), 130.0 (CH), 125.3 (C), 125.1 (C), 124.8 (C), 97.0 (C), 93.3 (C), 79.4 (C), 79.3 (C), 30.8 (CH$_2$), 30.7 (CH$_2$), 22.1 (CH$_2$), 22.1 (CH$_2$), 19.5 (CH$_2$), 19.3 (CH$_2$), 13.7 (CH$_3$); EI-HRMS calculated for C$_{18}$H$_{21}$Br: 316.0827, found: 316.0828.

Compound IIIa was prepared from compound **IIa** (484 mg, 1.53 mmol) according to previously described *GP2*. The silylated alkyne was not purified by column chromatography but redissolved in THF (0.03 M) and TBAF added (1 eq). The mixture was stirred for 5 minutes, then supported on silica gel and submitted to column chromatography (Eluent: n-hexane) to give **IIIa** in 74 % yield (296 mg) as a yellow liquid. ^{1}H-RMN (400 MHz, CDCl$_3$): δ (ppm) = 7.52 (s, 1H), 7.26 (m, 3H), 2.47 (t, 2H), 2.39 (t, 2H), 1.7-1.4 (m, 8H), 0.9 (m, 6H); ^{13}C-RMN (100 MHz, CDCl$_3$, DEPT): δ (ppm) = 135.4 (CH), 131.4 (CH), 131.3 (CH),

126.1 (C), 124.4 (C), 123.2 (C), 96.3 (C), 92.6 (C), 81.8 (C), 80.6 (C), 79.5 (C), 30.7 (CH$_2$), 22.0 (CH$_2$), 21.9 (CH$_2$), 19.3 (CH$_2$), 19.1 (CH$_2$), 13.6 (CH$_3$). EI-HRMS calculated for C$_{20}$H$_{22}$: 262.1722, found: 262.1719.

Compound **15a** was prepared from compounds **I** (154 mg, 0.39 mmol) and **IIIa** (190 mg, 0.96 mmol), according to previously described *GP2* to give **15a** in 40 % yield (148 mg) as a yellow syrup. ^{1}H NMR (400 MHz, cdcl$_3$): δ (ppm) = 8.15 (s, 1H), 7.89 (d, *J* = 8.1 Hz, 1H), 7.68 (s, 1H), 7.55 − 7.37 (m, 5H), 7.30 − 7.14 (m, 5H), 3.84 (s, 3H), 2.32 (m, 8H), 1.59 − 1.25 (m, 16H), 0.97 − 0.61 (m, 12H); ^{13}C NMR (101 MHz, CDCl$_3$, DEPT): δ (ppm) = 166.0 (C), 135.14 (CH), 135.08 (CH), 134.9 (CH), 133.3(CH), 132.0 (CH), 131.8 (CH), 131.5 (CH), 131.2 (CH), 129.9 (CH), 129.6 (C), 129.0 (C), 128.6 (CH), 126.3 (C), 125.7 (C), 125.5 (C), 125.3 (C), 123.9 (C), 123.5 (C), 123.3 (C), 123.2 (C), 96.8 (C), 96.4 (C), 95.8 (C), 93.0 (C), 92.7 (C), 92.6 (C), 92.0 (C), 90.8 (C), 88.8 (C), 88.5 (C), 79.8 (C), 79.6 (C), 79.32 (C), 79.30 (C), 52.5 (CH$_3$), 31.0 (CH$_2$), 30.84 (CH$_2$), 30.80 (CH$_2$), 30.75 (CH$_2$), 22.2 (CH$_2$), 22.13 (CH$_2$), 22.09 (CH$_2$), 19.6 (CH$_2$), 19.5 (CH$_2$), 19.3 (CH$_2$), 19.2 (CH$_2$), 13.77 (CH$_3$), 13.76 (CH$_3$), 13.74 (CH$_3$), 13.65 (CH$_3$); MALDI-HRMS calculated for C$_{56}$H$_{52}$O$_2$Na: 779.3860, found: 779.3889.

Compound **IIb** was prepared from 2-bromo-1,4-diiodobenzene (3.2 g, 8 mmol) according to previously described *GP1* to give **IIb** in 82 % yield (1.5 g) as a yellow liquid. ^{1}H NMR (500 MHz, CDCl$_3$): δ (ppm) = 7.58 (d, *J* = 1.2 Hz, 1H), 7.31 (d, *J* = 8.0 Hz, 1H), 7.22 (dd, *J* = 8.0, 1.4 Hz, 1H), 2.11 (s, 3H), 2.04 (s, 3H); ^{13}C NMR (126 MHz, CDCl$_3$, DEPT): δ (ppm) = 135.1 (CH), 133.0 (CH), 130.1 (CH), 125.3 (C), 125.0 (C), 124.8 (C), 92.4 (C), 88.8 (C), 78.5 (C), 78.4 (C), 4.8 (CH$_3$), 4.5 (CH$_3$); EI-HRMS calculated for C$_{12}$H$_9$Br: 231.9888, found: 231.9883.

Compound **IIIb** was prepared from compound **IIb** (840 mg, 3.6 mmol) according to previously described *GP2*. The silylated alkyne was not purified by column chromatography but redissolved in THF (0.03 M) and TBAF added (1 eq). The mixture was stirred for 5 minutes, then supported on silica gel and submitted to column chromatography (Eluent: n-hexane) to give **IIIb** in 82 % yield (525 mg) as a yellow liquid. ^{1}H NMR (500 MHz, CDCl$_3$): δ (ppm) = 7.48 (s, 1H), 7.30 (d, *J* = 8.1 Hz, 1H), 7.26 (d, *J* = 8.0 Hz, 2H), 3.27 (s, 1H), 2.12 (s, 3H), 2.04 (s, 3H); ^{13}C NMR (126 MHz, CDCl$_3$, DEPT): δ (ppm) = 132.1 (CH), 131.6 (CH), 126.2 (CH), 124.5 (C), 123.4 (C), 91.9 (C), 88.2 (C), 81.9 (C), 80.8 (CH), 78.8 (C), 78.2 (C), 4.8 (CH$_3$), 4.5 (CH$_3$); EI-HRMS calculated for C$_{14}$H$_{10}$: 178.0783, found: 178.0782.

Compound **15b** was prepared from compounds **I** (470 mg, 1.2 mmol) and **IIIb** (520 mg, 2.9 mmol), according to previously described *GP2* to give **15b** in 35 % yield (246 mg) as a yellow syrup. ^{1}H NMR (400 MHz, CDCl$_3$): δ (ppm) = 8.27 (d, *J* = 1.7 Hz, 1H), 8.03 − 7.95 (m, 1H), 7.83 − 7.78 (m, 1H), 7.65 (d, *J* = 8.1 Hz, 1H), 7.63 − 7.57 (m, 2H), 7.54 (d, *J* = 7.1 Hz, 2H), 7.37 (dd, *J* = 15.1, 7.9 Hz, 3H), 7.31 − 7.26 (m, 2H), 3.96 (d, *J* = 1.2 Hz, 3H), 2.12 (d, *J* = 1.2 Hz, 3H), 2.09 (d, *J* = 1.1 Hz, 3H), 2.02 (d, *J* = 1.1 Hz, 3H), 2.00 (s, 3H).
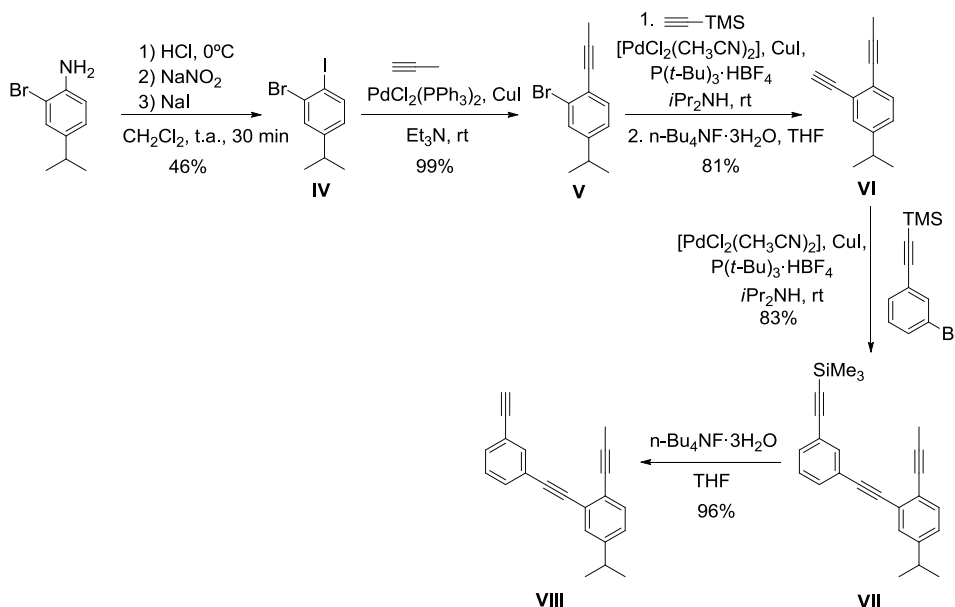
Compound IV. To a flask containing 2-bromo-4-isopropylaniline (6.8 g, 31.8 mmol), concentrated HCl was added dropwise until the formation of a white solid. Then, a solution of sodium nitrite (2.4 g, 35.0 mmol) in water (2 mL) was slowly added at 0ºC. The reaction mixture was stirred at 0ºC for an additional 30 min before adding a solution of sodium iodide (14.3 g, 95.5 mmol). After 1h stirring, the reaction mixture was diluted in dichlorometane, washed successively with brine, $Na_2S_2O_3 \cdot 5H_2O$ and water, dried over anhydrous Na_2SO_4. The crude was supported on silica gel and submitted to column chromatography (Eluent: n-hexane) to give **IV** in 46 % yield (4.6 mg) as a transparent liquid. ^{1}H NMR (401 MHz, $CDCl_3$): δ (ppm) = 7.74 (d, J = 8.1 Hz, 1H), 7.49 (d, J = 1.9 Hz, 1H), 6.87 (dd, J = 8.1, 1.9 Hz, 1H), 2.83 (hept, 7.0 Hz, 1H), 1.22 (d, J = 7.0 Hz, 6H); ^{13}C NMR (101 MHz, $CDCl_3$, DEPT): δ (ppm) = 151.1 (C), 140.2 (CH), 131.1 (CH), 129.7 (C), 127.1 (CH), 97.4 (C), 33.7 (CH), 23.8 (CH_3); EI-HRMS calculated for $C_9H_{10}BrI$: 323.9011, found: 323.9001.

Compound V was prepared from **IV** (4.6 g, 14.16 mmol) according to previously described *GP1* (see ref.1) to give **V** in 99 % yield (3.3 g) as a transparent liquid. ^{1}H NMR (500 MHz, $CDCl_3$): δ (ppm) = 7.44 (d, J = 1.4 Hz, 1H), 7.37 (d, J = 8.0 Hz, 1H), 7.11 (dd, J = 8.0, 1.5 Hz, 1H), 2.88 (hept, J = 6.9 Hz, 1H), 2.13 (s, 3H), 1.25 (d, J = 6.9 Hz, 6H); ^{13}C NMR (126 MHz, $CDCl_3$): δ (ppm) = 150.2 (C), 133.3 (CH), 130.4 (CH), 125.4 (CH), 125.3 (C), 123.4 (C), 90.0 (C), 78.6 (C), 33.9 (CH), 23.8 (CH_3), 4.7 (CH_3); EI-HRMS calculated for $C_{12}H_{13}Br$: 236.0201, found: 236.0193.

Compound VI was prepared from compound **V** (3.3 mg, 13.9 mmol) according to previously described *GP2*. The silylated alkyne was not purified by column chromatography but redissolved in THF (0.03 M) and TBAF added (1 eq). The mixture was stirred for 5 minutes, then supported on silica gel and submitted to column chromatography (Eluent: n-hexane) to give **VI** in 81 % yield (2.15 mg) as a transparent liquid. ^{1}H NMR (400 MHz, $CDCl_3$): δ (ppm) = 7.34 (s, 1H), 7.32 (d, J = 8.5 Hz, 1H), 7.13 (dd, J = 8.0, 1.8 Hz, 1H), 3.27 (s, 1H), 2.86 (hept, J = 6.9 Hz, 1H), 2.11 (s, 3H), 1.22 (d, J = 6.9 Hz, 6H); ^{13}C NMR (101 MHz, $CDCl_3$, DEPT): δ (ppm) = 148.2 (C), 132.1 (CH), 130.6 (CH), 127.0 (CH), 124.6 (C), 124.2 (C), 89.4 (C), 82.9 (C), 80.0 (CH), 78.3 (C), 33.8 (CH), 23.7 (CH_3), 4.6 (CH_3); EI-HRMS calculated for $C_{14}H_{14}$: 323.9011, found: 323.9001.

Compound VII was prepared from compound **VI** (2 g, 11 mmol) and ((3-bromophenyl)ethynyl)trimethylsilane (2.78 g, 11 mmol) according to previously described *GP2* to give **VII** in 83 % yield (3.24 g) as a pale yellow liquid. ^{1}H NMR (500 MHz, $CDCl_3$): δ (ppm) = 7.69 (s, 1H), 7.50 (d, J = 7.8 Hz, 1H), 7.44 (d, J = 7.8 Hz, 1H), 7.37 (s, 1H), 7.36 (d, J = 8.0 Hz, 1H), 7.31 (t, J = 7.8 Hz, 1H), 7.14 (dd, J = 8.0, 1.6 Hz, 1H), 2.89 (hept, 6.9 Hz, 1H), 2.17 (s, 3H), 1.26 (d, J = 6.9 Hz, 6H), 0.28 (s, 9H); ^{13}C NMR (126 MHz, $CDCl_3$, DEPT): δ (ppm) = 148.4 (C), 135.4 (CH), 132.0 (CH), 131.7 (CH), 131.6 (CH), 129.9 (CH), 128.4 (CH), 126.8 (CH), 125.3 (C), 124.3 (C), 124.0 (C), 123.6 (C), 104.4 (C), 95.0 (C), 91.6 (C), 89.5 (C), 78.6 (C), 34.0 (CH), 23.8 (CH_3), 4.8 (CH_3), 0.1 (CH_3); ESIpos-HRMS calculated for $C_{25}H_{27}Si$ [M+H^{+}]: 355.1882, found: 355.1881.

Compound VIII. The silylated alkyne **VII** (3.24 g, 9.15 mmol) was dissolved in THF (0.03 M) and TBAF added (3.5 g, 11 mmol). The mixture was stirred for 5 minutes, then supported on silica gel and submitted to column chromatography (Eluent: n-hexane) to give **VIII** in 96 % yield (2.48 mg) as a orange syrup. ^{1}H NMR (400 MHz, $CDCl_3$): δ (ppm) =7.74 (s, 1H), 7.56 (d, J = 7.8 Hz, 1H), 7.47 (d, J = 7.8 Hz, 1H), 7.42 – 7.39 (m, 1H), 7.39 (d, J = 8.1 Hz, 1H), 7.32 (t, J = 7.8 Hz, 1H), 7.14 (dd, J = 8.1, 1.8 Hz, 1H), 3.13 (s, 1H), 2.88 (hept, J = 6.9 Hz, 1H), 2.17 (s, 3H), 1.26 (d, J = 6.9 Hz, 6H); ^{13}C NMR (101 MHz, $CDCl_3$, DEPT): δ (ppm) = 148.2 (C), 135.2 (CH), 131.9 (CH), 131.7 (CH), 129.7 (CH), 128.4 (CH), 126.7 (CH), 125.1 (C), 124.2 (C), 124.0 (C), 122.5 (C), 91.4 (C), 89.8 (C), 89.5 (C), 82.9 (C), 78.6 (C), 77.8 (CH), 33.8 (CH), 23.7 (CH_3), 4.6 (CH_3); ESIpos-HRMS calculated for $C_{22}H_{19}$ [M+H^{+}]: 283.1478, found: 283.1487.
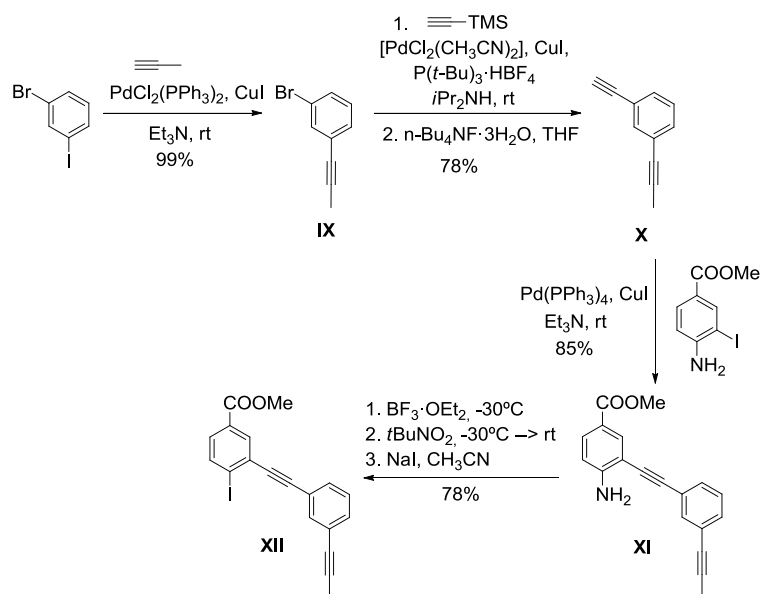
Compound IX was prepared from 1-bromo-2-iodobenzene (2 g, 7.1 mmol) according to previously described *GP1* to give **IX** in 99 % yield (1.37 g) as a transparent liquid. ^{1}H NMR (401 MHz, cdcl$_3$) δ 7.54 (s, 1H), 7.40 (d, *J* = 8.0 Hz, 1H), 7.31 (d, *J* = 7.7 Hz, 1H), 7.14 (t, *J* = 7.9 Hz, 1H), 2.05 (s, 3H); ^{13}C NMR (101 MHz, CDCl$_3$, DEPT): δ (ppm) = 134.45 (CH), 130.81 (CH), 130.18 (CH), 129.73 (CH), 126.21 (C), 122.16 (C), 87.54 (C), 78.51 (C), 4.4 (CH$_3$); EI-HRMS calculated for C$_9$H$_6$Br: 193.9731, found: 193.9726.

Compound X was prepared from **IX** (1.25 g, 6.41 mmol) according to previously described *GP2*. The silylated alkyne was not purified by column chromatography but redissolved in THF (0.03 M) and TBAF added (1 eq). The mixture was stirred for 5 minutes, then supported on silica gel and submitted to column chromatography (Eluent: n-hexane) to give **X** in 78 % yield (702 mg) as a yellow liquid. ^{1}H NMR (401 MHz, CDCl$_3$): δ (ppm) = 7.56 (s, 1H), 7.42 (d, *J* = 7.9 Hz, 1H), 7.40 (d, *J* = 8.5 Hz, 1H), 7.26 (t, *J* = 7.8 Hz, 2H), 3.11 (s, 2H), 2.07 (s, 7H); ^{13}C NMR (101 MHz, CDCl$_3$, DEPT): δ (ppm) =135.1 (CH), 131.9 (CH), 131.2 (CH), 128.4 (CH), 124.5 (C), 122.4 (C), 86.8 (C), 83.1 (C), 78.9 (C), 77.6 (C), 4.4 (CH$_3$); EI-HRMS calculated for C$_{11}$H$_8$: 139.0548, found: 139.0558.

Compound XI was prepared from **X** (600 mg, 4.28 mmol) and methyl 4-amino-3-iodobenzoate (980 g, 3.37 mmol) according to previously described *GP1* to give **XI** in 85 % yield (873 mg) as a white solid. ^{1}H NMR (400 MHz, cdcl$_3$): δ (ppm) = 8.07 (d, *J* = 1.8 Hz, 1H), 7.82 (dd, *J* = 8.5, 1.8 Hz, 1H), 7.55 (s, 1H), 7.41 (d, *J* = 7.6 Hz, 1H), 7.36 (d, *J* = 7.8 Hz, 1H), 7.27 (t, *J* = 7.6 Hz, 1H), 6.70 (d, *J* = 8.5 Hz, 1H), 4.68 (s, 2H), 3.87 (s, 3H), 2.06 (s, 3H); ^{13}C NMR (101 MHz, CDCl$_3$, DEPT): δ (ppm) =165.9 (C), 139.1 (CH), 134.6 (CH), 133.1 (CH), 132.0 (CH), 130.7 (CH), 130.2 (C), 129.8 (CH), 128.5 (CH), 124.6 (C), 122.8 (C), 107.2 (C), 93.3 (C), 91.2 (C), 86.9 (C), 79.0 (C), 52.4 (C), 4.4 (CH$_3$); EI-HRMS calculated for C$_{19}$H$_{15}$NO$_2$: 289.1103, found: 289.1112.

Compound XII. A round-bottom flask equipped with a magnetic stir bar was charged with compound **XI** (560 mg, 1.94 mmol) and dry diethyl ether (60 mL). The solution was cooled to -30 °C and boron trifluoride diethyl etherate (2.03 mL, 7.74 mmol) was added. The mixture was stirred at -30 °C for 30 min and *tert*-butyl nitrite (0.89 mL, 6.77 mmol) was added. The mixture was stirred for an additional 30 min between -20 °C and -10 °C. The white precipitate formed was collected by filtration, rinsed thoroughly with diethyl ether and dissolved in dry acetonitrile (60 mL). This solution was added to a solution of sodium iodide (1.7 g, 3.88 mmol) in acetonitrile. The resulting mixture was stirred overnight at room temperature, poured into water and extracted with dichloromethane. The combined organic layers were washed with water, dried over Na$_2$SO4, filtered and the solvent was removed under reduced pressure to give **XII** in 78 % yield (616 mg) as a white solid containing about 50% of the arylfluoride. ^{1}H NMR (400 MHz, CDCl$_3$): δ (ppm) = 8.00 (d, *J* = 2.0 Hz, 1H), 7.82 (d, *J* = 8.3 Hz, 1H), 7.52 (s, 1H), 7.49 (dd, *J* = 8.3, 2.1 Hz, 1H), 7.26 (t, *J* = 7.3 Hz, 2H), 7.17 (t, *J* = 7.6 Hz, 2H), 3.79 (s, 4H), 1.94 (s, 3H); EI-HRMS calculated for C$_{19}$H$_{13}$IO$_2$: 399.9960, found: 399.9977.
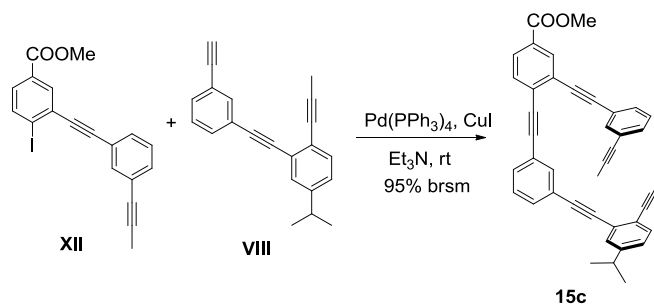
Compound 15c. A solution of the terminal alkyne **VIII** (380 mg, 1.35 mmol) dissolved in 2 mL of Et$_3$N was added dropwise to a carefully degassed solution of Pd(PPh$_3$)$_4$ (52 mg, 2 mol%), CuI (9 mg, 2 mol%) and the aryl iodide **XII** (900 mg, 2.25 mmol) in 50 mL of Et$_3$N. The reaction was stirred 16h at room temperature under argon atmosphere. Then, the crude was diluted with dichloromethane, washed with saturated aq NH$_4$Cl solution, dried over anhydrous Na$_2$SO$_4$ and filtered. The filtrate was supported on silica gel and submitted to flash chromatography (Hexane/EtOAc: 1:0 → 8:2) to give **C27** in 95 % yield based on the alkyne added (715 mg) as a orange syrup.The arylfluoride formed as a by-product in the former step was recovered unreacted. ^{1}H NMR (500 MHz, CDCl$_3$): δ (ppm) = 8.24 (d, J = 1.7 Hz, 1H), 7.98 (dd, J = 8.1, 1.7 Hz, 1H), 7.81 (s, 1H), 7.64 (s, 1H), 7.63 (d, J = 8.2 Hz, 1H), 7.59 – 7.54 (m, 2H), 7.51 (d, J = 7.6 Hz, 1H), 7.40 – 7.34 (m, 4H), 7.29 (t, J = 8.1 Hz, 1H), 7.15 (dd, J = 8.0, 1.8 Hz, 1H), 3.95 (s, 3H), 2.90 (sept, J = 6.9 Hz, 1H), 2.11 (s, 3H), 2.01 (s, 3H), 1.27 (d, J = 6.9 Hz, 6H); ^{13}C NMR (126 MHz, CDCl$_3$, DEPT): δ (ppm) = 166.0 (C), 148.3 (C), 134.9 (CH), 134.8 (CH), 133.0 (CH), 132.1 (CH), 131.0 (CH), 131.9 (CH), 131.8 (CH), 131.5 (CH), 130.7 (CH), 129.93 (C), 129.90 (CH), 129.7 (C), 129.0 (CH), 128.7 (CH), 128.6 (CH), 126.8 (CH), 126.2 (C), 125.2 (C), 124.7 (C), 124.3 (C), 123.2 (C), 123.1 (C), 95.8 (C), 94.0 (C), 91.4 (C), 89.9 (C), 89.60 (C), 88.4 (C), 87.9 (C), 87.0 (C), 78.9 (C), 78.6 (C), 52.5 (CH$_3$), 34.0 (CH), 23.8 (CH$_3$), 4.7 (CH$_3$), 4.4 (CH$_3$); ESIpos-HRMS calculated for C$_{41}$H$_{30}$O$_2$Na: 577.2138, found: 577.2144.
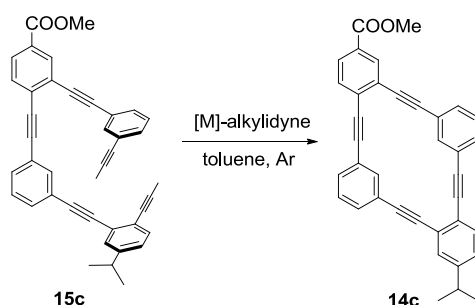
Compound 14c.

Procedure using W-alkylidyne complex **C01**: Compound **15c** (100 mg, 0.18 mmol) and (t-BuO)$_3$W≡C-t-Bu **C01** (56 mg, 60 % mol) were weighted under Ar atmosphere in a glove box and transferred into a Schlenk-flask. Dry and degassed toluene was added (10 mL, 18 mM) and the crude was stirred at 85 °C during 18h under Ar flow. Then, the solvent was evaporated under reduced pressure and residue purified using flash column chromatography (Hexane/EtOAc 8:2) to give **14c** as a white solid (57 mg, 62%).

Procedure using Mo-alkylidyne complex **C02**: A suspension containing complex **C02** (13 mol %) and dry powdered MS 5Å in toluene (0.1 M) was stirred for 10 minutes. Then a solution of the substrate **15c** in toluene (10 mg, 0.02 mmol) was added via syringe pump (0.25 mL/h) and stirred 30h at ambient temperature. The reaction crude was filtered through a short plug of silica, the filtrate evaporated and the residue purified by flash chromatography. (Hexane/EtOAc 8:2) to give **14c** as a white solid (8 mg, 80%).

Procedure using phen·Mo-alkylidyne adduct **C03**: A suspension containing complex **C03** (5 mol %), ZnCl$_2$ (10 mol %) in toluene was stirred 30 min at 80ºC. Then, the catalytic mixture was cooled to room before the product **15c** (10 mg, 0.02 mmol) and powdered MS 5Å toluene (0.07 M) were added and stirred overnight at ambient temperature. Then, the mixture was filtered through a short plug of silica. The filtrate was evaporated and the residue purified by flash chromatography (Hexane/EtOAc 8:2) to give **14c** as a white solid (5.7 mg, 63%).

C01   C02   C03
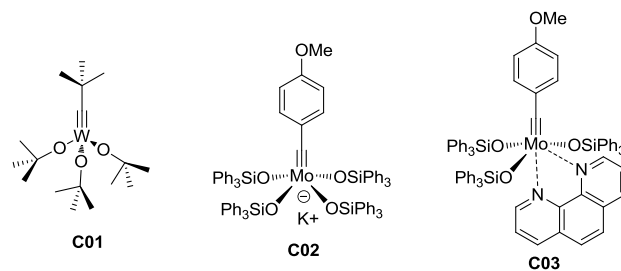
Entry	Catalyst	Loading (%mol)	Concentration (mM)	Temp. (°C)	Time (h)	Yield (%)
1	C01	60	18	85	18	62
2	C01	27	18	85	16	79
3	C01	24	9	85	43	38[a]
4	C02	13	10	Rt	30	80
5	C03	5	7	Rt	16	63

[a] Yield based on recovered starting material.

^{1}H NMR (600 MHz, CDCl$_3$):
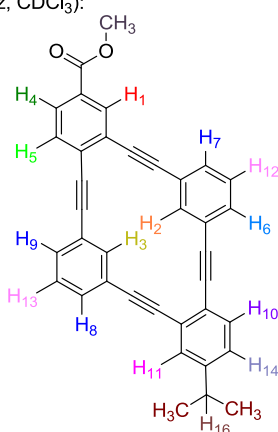
H1 - 8.26 (d, J = 1.4 Hz, 1H)
H2 - 8.06 (t, J = 1.4 Hz, 1H)
H3 - 8.04 (t, J = 1.4 Hz, 1H)
H4 - 7.98 (dd, J = 8.1, 1.7 Hz, 1H)
H5 - 7.65 (d, J = 8.1 Hz, 1H)
H6 - 7.61 - 7.58 (m, 1H)
H7,8,9 - 7.58 - 7.54 (m, 3H)
H10 - 7.52 (d, J = 8.0 Hz, 1H)
H11 - 7.47 (d, J = 1.8 Hz, 1H)
H12,13 - 7.40 (td, J = 7.7, 6.0 Hz, 2H)
H14 - 7.21 (dd, J = 8.1, 1.6 Hz, 1H)
H15 (OCH$_3$) - 3.96 (s, 3H)
H16 - 2.93 (dt, J = 13.9, 6.9 Hz, 1H)
H17 (CH$_3$) - 1.29 (s, 3H)
H18 (CH$_3$) - 1.28 (s, 3H)

^{13}C NMR (151 MHz, CDCl$_3$):

1 (CO) 166.1
2 (C)   149.6
3 (CH) 136.0
        135.7
4 (CH) 133.2
5 (CH) 132.1
        132.1
6 (CH) 131.9
        131.6
        131.5
        131.3
7 (CH) 130.2
8 (C)   129.8
        129.7
9 (CH) 129.0
10 (CH) 128.9
        128.9
11 (CH) 127.1
12 (C) 125.9
13 (C) 125.5
14 (C) 124.0
        124.0
15 (C) 123.4
        123.2
        123.0
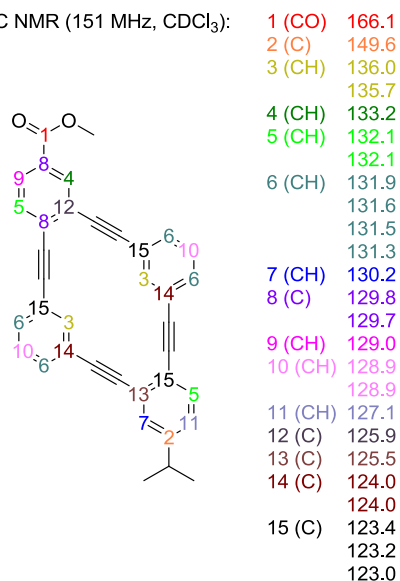
A (C) - 95.7
A (C) - 93.6
A (C) - 92.1
A (C) - 91.1
B (C) - 89.7
C (C) - 89.4
D (C) - 88.6
E (C) - 88.2
F (OCH$_3$) - 52.6
G (CH$_3$) - 34.1
H (CH$_3$) - 23.8
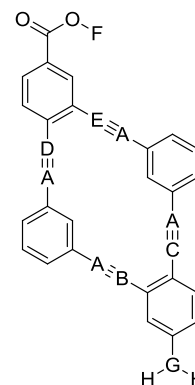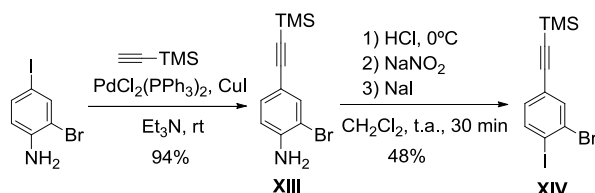
Compound XIII was prepared from 2-bromo-4-iodoaniline (4.6 g, 15.4 mmol) according to previously described *GP1* to give **XIII** in 94 % yield (3.74 g) as an orange syrup. ^{1}H NMR (401 MHz, cdcl$_3$): δ (ppm) = 7.55 (s, 1H), 7.21 (dd, *J* = 8.3, 1.3 Hz, 1H), 6.63 (d, *J* = 8.3 Hz, 1H), 4.24 (s, 2H), 0.23 (s, 9H); ^{13}C NMR (101 MHz, CDCl$_3$, DEPT): δ (ppm) = 144.6 (C), 136.2 (CH), 132.3 (CH), 115.0 (CH), 113.7 (C), 108.2 (C), 104.4 (C), 92.7 (C), 0.17 (CH$_3$); ESIpos-HRMS calculated for C$_{11}$H$_{15}$NSiBr [M+H^{+}]: 268.0157, found: 268.0155.

Compound XIV. To a flask containing **XIII** (2.5 g, 9.3 mmol), concentrated HCl was added dropwise until the formation of a pale orange solid. Then, a solution of sodium nitrite (718 mg, 10 mmol) in water (15 mL) was slowly added at 0ºC. The reaction mixture was stirred at 0ºC for an additional 30 min before adding a solution of sodium iodide (6.45 g, 46 mmol) in 10 mL water and 20 mL of dichloromethane. After stirring overnight, the reaction mixture was diluted in dichlorometane, washed successively with brine, Na$_2$S$_2$O$_3$·5H$_2$O and water, dried over anhydrous Na$_2$SO$_4$ and filtered. Then, the crude was supported on silica gel and submitted to column chromatography (Eluent: n-hexane) to give **XIV** in 70 % yield (2.9 g) as an orange syrup. ^{1}H NMR (401 MHz, CDCl$_3$): δ (ppm) = 7.78 (d, *J* = 8.0 Hz, 1H), 7.71 (s, 1H), 7.05 (dd, *J* = 8.0, 1.6 Hz, 1H), 0.24 (s, 9H); ^{13}C NMR (101 MHz, CDCl$_3$, DEPT): δ (ppm) = 140.1 (CH), 135.7 (CH), 131.6 (CH), 129.6 (C), 124.9 (C), 102.6 (C), 97.4 (C), 77.52 (C), -0.1 (CH$_3$); EI-HRMS calculated for C$_{11}$H$_{12}$BrISi: 377.8936, found: 377.8923.
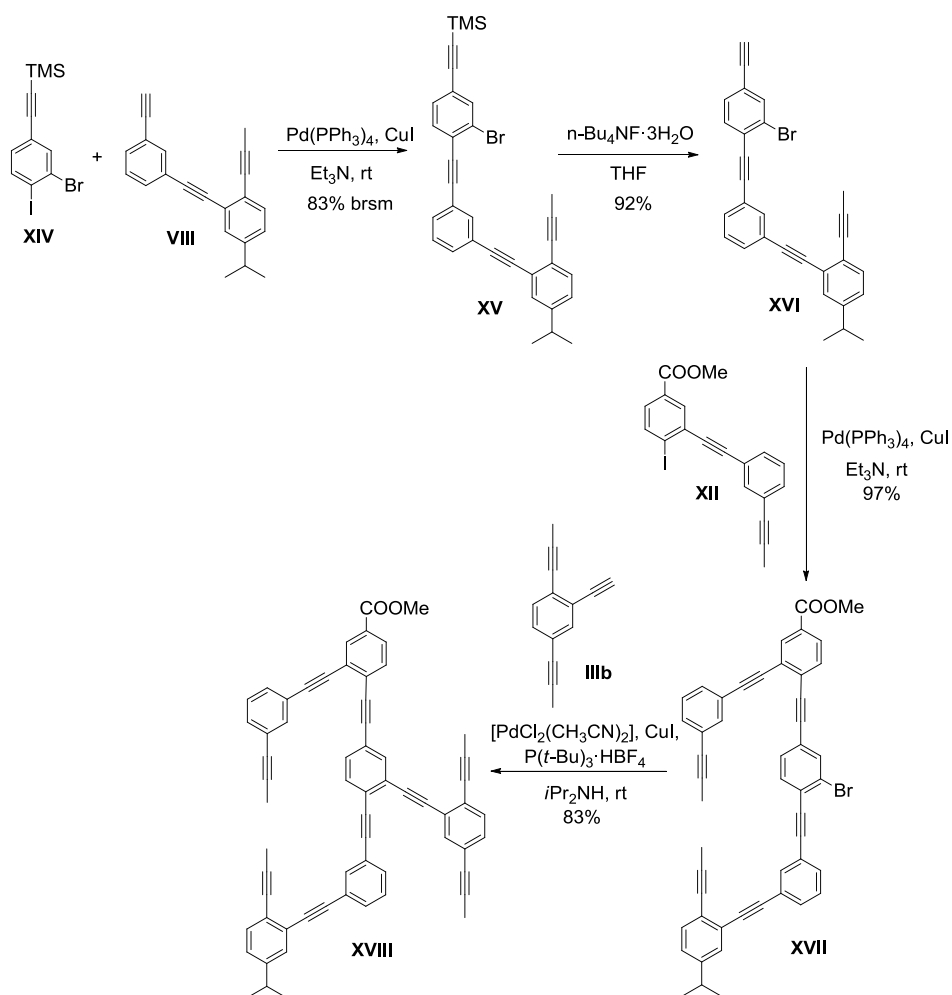
***Compound* XV**. A solution of the terminal alkyne **VIII** (670 mg, 2.43 mmol) dissolved in 2 mL of Et$_3$N was added dropwise to a carefully degassed solution of Pd(PPh$_3$)$_4$ (50 mg, 2 mol%), CuI (10 mg, 2 mol%) and the aryl iodide **XIV** (924 mg, 2.43 mmol) in 5 mL of Et$_3$N. The reaction was stirred overnight at room temperature under argon atmosphere. Then, the crude was diluted with dichloromethane, washed with saturated aq NH$_4$Cl solution, dried over anhydrous Na$_2$SO$_4$ and filtered. The filtrate was supported on silica gel and submitted to flash chromatography (Hexane/EtOAc: 1:0 → 8:2) to give **XV** in 60 % yield (774 mg, 83% brsm) as an orange syrup. ^{1}H NMR (401 MHz, CDCl$_3$): δ (ppm) = 7.85 (s, 1H), 7.80 (s, 1H), 7.64 – 7.56 (m, 2H), 7.53 (d, *J* = 8.0 Hz, 1H), 7.47 – 7.38 (m, 5H), 7.18 (d, *J* = 8.0 Hz, 1H), 2.94 (dt, 6.9 Hz, 1H), 2.23 (s, 3H), 1.31 (d, *J* = 6.9 Hz, 6H), 0.34 (s, 9H); ^{13}C NMR (101 MHz, CDCl$_3$, DEPT): δ (ppm) = 148.3 (C), 135.6 (CH), 134.9 (CH), 133.9 (CH), 132.8 (CH), 131.9 (CH), 131.3 (CH), 130.5 (CH), 129.8 (CH), 128.6 (CH), 126.8 (CH), 125.3 (C), 125.3 (C), 125.2 (C), 124.5 (C), 124.3 (C), 124.1 (C), 123.1 (C), 103.1 (C), 98.0 (C), 95.0 (C), 91.5 (C), 89.9 (C), 89.5 (C), 88.5 (C), 78.6 (C), 33.9 (CH), 23.8 (CH$_3$), 4.8 (CH$_3$), -0.1 (CH$_3$); EI-HRMS calculated for C$_{33}$H$_{29}$BrSi: 532.1222, found: 532.1246.

***Compound* XVI**. The silylated alkyne **XV** (774 g, 1.45 mmol) was dissolved in THF (0.03 M) and TBAF added (566 g, 1.79 mmol). The mixture was stirred for 5 minutes, then supported on silica gel and submitted to column chromatography (Eluent: n-hexane) to give **XVI** in 92 % yield (615 mg) as a pale orange solid. ^{1}H NMR (500 MHz, CDCl$_3$): δ (ppm) = 7.78 (s, 1H), 7.75 (d, *J* = 1.1 Hz, 1H), 7.55 (d, *J* = 7.9 Hz, 1H), 7.53 (d, *J* = 8.8 Hz, 1H), 7.49 (d, *J* = 8.0 Hz, 1H), 7.43 – 7.30 (m, 4H), 7.13 (dd, *J* = 8.0, 1.6 Hz, 1H), 3.22 (s, 1H), 2.89 (sept, *J* = 6.9 Hz, 1H), 2.17 (s, 3H), 1.26 (d, *J* = 6.9 Hz, 6H); ^{13}C NMR (126 MHz, CDCl$_3$, DEPT): δ (ppm) = 148.4 (C), 135.8 (CH), 135.0 (CH), 132.9 (CH), 132.1 (CH), 132.0 (CH), 131.4 (CH), 130.8 (CH), 129.9 (CH), 128.7 (CH), 126.9 (CH), 125.8 (C), 125.4 (C), 125.2 (C), 124.3 (C), 124.2 (C), 123.5 (C), 123.1 (C), 95.1 (C), 91.5 (C), 89.9 (C), 89.6 (C), 88.3 (C), 81.9 (C), 80.3 (CH), 78.6 (C), 34.0 (CH), 23.8 (CH$_3$), 4.8 (CH$_3$); EI-HRMS calculated for C$_{30}$H$_{21}$Br: 460.0827, found: 460.0809.

***Compound* XVII**. A solution of the terminal alkyne **XVI** (615 mg, 1.33 mmol) dissolved in 2 mL of Et$_3$N and 1 mL of THF was added dropwise to a carefully degassed solution of Pd(PPh$_3$)$_4$ (35 mg, 2 mol%), CuI (6 mg, 2 mol%) and the aryl iodide **XII** (600 mg, 1.5 mmol) in 10 mL of Et$_3$N. The reaction was stirred overnight at room temperature under argon atmosphere. Then, the crude was diluted with dichloromethane, washed with saturated aq NH$_4$Cl solution, dried over anhydrous Na$_2$SO$_4$ and filtered. The filtrate was supported on silica gel and submitted to flash chromatography (Hexane/EtOAc: 8:2) to give **XVII** in 97 % yield (952 mg) as an orange syrup. MALDI-HRMS calculated for C$_{49}$H$_{33}$BrO$_2$Ag: 839.0709, found: 839.0696.
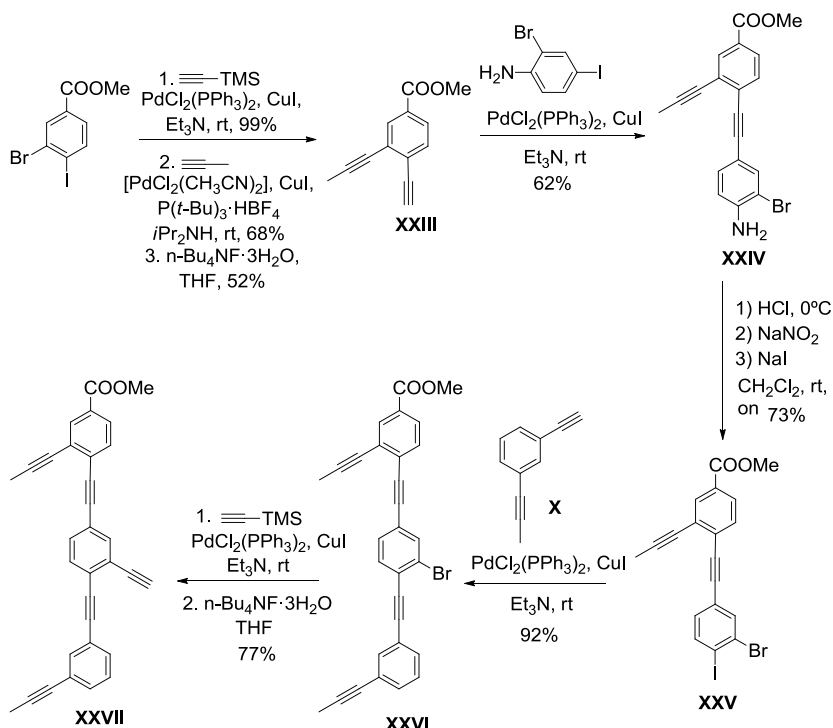
***Compound* XVIII** was prepared from **XVII** (166 g, 0.23 mmol) and **IIIb** (123 g, 0.69 mmol) according to previously described *GP2* to give **XVIII** in 83 % yield (156 mg) as a pale yellow solid. ^{1}H NMR (600 MHz, CDCl$_3$): δ (ppm) = 8.23 (d, *J* = 1.7 Hz, 1H), 7.98 (dd, *J* = 8.1, 1.7 Hz, 1H), 7.79 (dd, *J* = 1.6, 0.5 Hz, 1H), 7.78 (t, *J* = 1.3 Hz, 1H), 7.63 (d, *J* = 8.1 Hz, 1H), 7.61 (s, 1H), 7.57 (s, 1H), 7.58 (d,*J* = not measured, 1H) 7.56 (s, 1H), 7.54 – 7.51 (m, 2H), 7.48 (d, *J* = 7.7 Hz, 1H), 7.38 – 7.33 (m, 5H), 7.29 (t, *J* = 7.8 Hz, 1H), 7.27 (t, *J* = not measured, 1H), 7.13 (dd, *J* = 8.0, 1.8 Hz, 1H), 3.96 (s, 3H), 2.89 (sept, *J* = 6.9 Hz, 1H), 2.10 (s, 3H), 2.02 (s, 3H), 2.00 (s, 3H), 1.89 (s, 3H), 1.25 (d, *J* = 6.9 Hz, 6H); ^{13}C NMR (151 MHz, CDCl$_3$, DEPT): δ (ppm) = 166.1 (C), 148.4 (C), 135.4 (CH), 135.3 (CH), 135.0 (CH), 134.9 (CH), 133.1 (CH), 132.2 (CH), 132.1 (CH), 132.00 (CH), 131.95 (CH), 131.9 (CH), 131.7 (CH), 131.37 (CH), 131.35 (CH), 130.7 (CH), 129.94 (CH), 129.92 (C), 129.8 (C), 129.0 (CH), 128.7 (CH), 128.6 (CH), 126.9 (CH), 126.4 (C), 126.3 (C), 125.9 (C), 125.7 (C), 125.4 (C), 125.2 (C), 124.8 (C), 124.2 (C), 124.1 (C), 123.5 (C), 123.4 (C), 123.0 (C), 122.7 (C), 95.5 (C), 95.0 (C), 94.1 (C), 92.8 (C), 92.4 (C), 91.5 (C), 90.8 (C), 90.1 (C), 89.7 (C), 89.6 (C), 88.7 (C), 88.2 (C), 87.8 (C), 87.1 (C), 78.9 (C), 78.8 (C), 78.6 (C), 78.4 (C), 52.6 (CH3), 34.0 (CH), 23.8 (CH3x2), 4.8 (CH3x2), 4.53 (CH3), 4.48 (CH3). One CH carbon is missing; EI-HRMS calculated for C$_{63}$H$_{42}$O$_2$Na: 853.3077, found: 853.3088.

C01

C02

C03
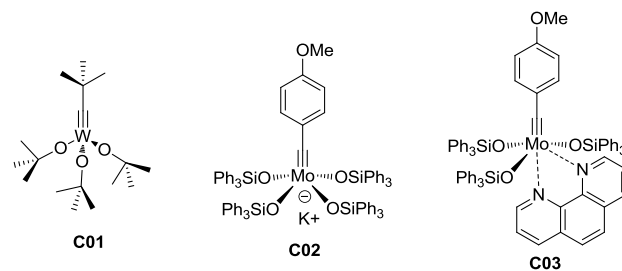
Entry	Catalyst	Loading (%mol)	Concentration (mM)	Addition rate (mL/h)	Temp. (°C)	Time (h)	Yield (%)
1	C02	9	10	0.5	40	30	Polimer
2	C02	10	6	-	Rt	3	Semiprep-HPLC
3	C02	50	2	2.6	80	40	Polimer
4	C02	50	4	0.8	110	148	SM and fragmentation products
5	C01	62	3	5	80	16	Polimer
6	C02	100	1	6	80	144	Semiprep-HPLC

XV

IIb

[PdCl$_2$(CH$_3$CN)$_2$], CuI,
P(t-Bu)$_3$·HBF$_4$,
iPr$_2$NH, rt
70%

XX

Ph$_3$SiO, Mo, OSiPh$_3$
Ph$_3$SiO, K+, OSiPh$_3$
toluene [20mM]
rt, 5 AMS

n-Bu$_4$NF·3H$_2$O
THF
R = H **XXI** (97%brsm)
R = TMS **XXII** (99%)

Pd(PPh$_3$)$_4$, CuI
Et$_3$N, rt
40%brsm

XII

XIXa
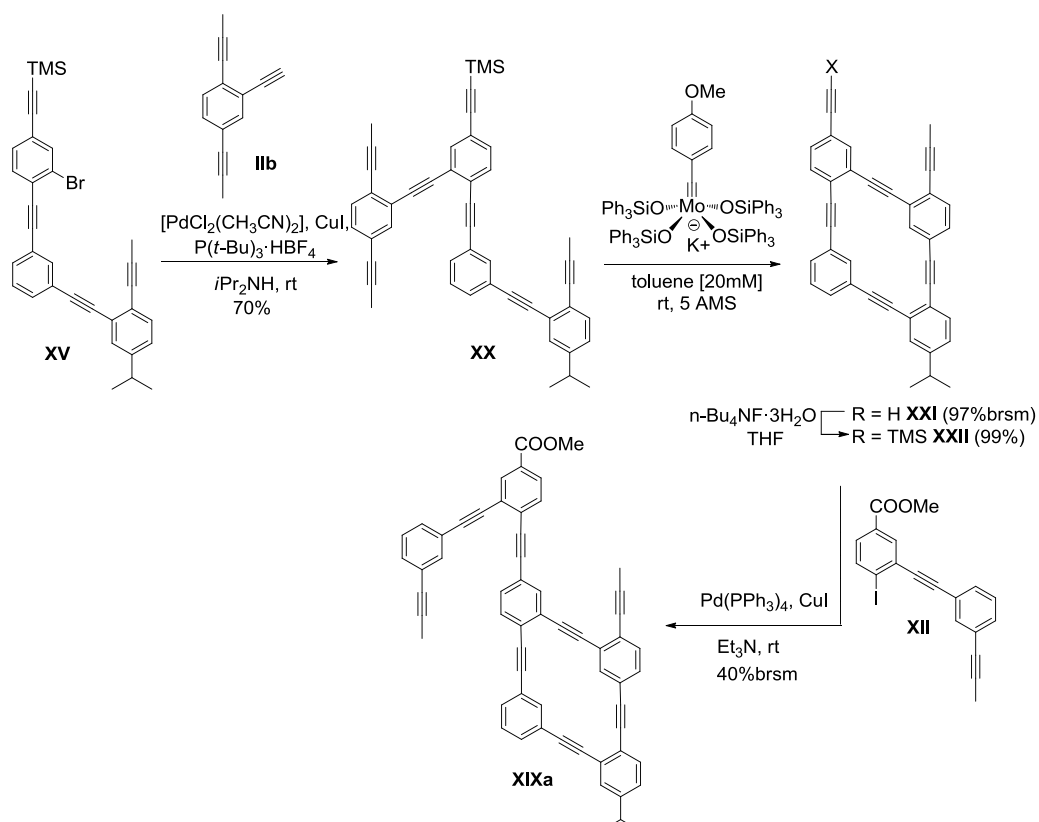
Compound **XX** was prepared from **XV** (846 mg, 1.58 mmol) and **IIIb** (338 g, 1.9 mmol) according to the previously described *GP2* to give **XX** in 70 % yield (689 mg) as an orange syrup. ^{1}H NMR (401 MHz, CDCl$_3$) δ 7.88 (s, 1H), 7.77 (d, *J* = 1.3 Hz, 1H), 7.67 (d, *J* = 1.3 Hz, 1H), 7.63 (d, *J* = 7.8 Hz, 1H), 7.60 (d, *J* = 7.8 Hz, 1H), 7.57 (d, *J* = 8.1 Hz, 1H), 7.48 − 7.37 (m, 5H), 7.32 (dd, *J* = 8.1, 1.3 Hz, 1H), 7.18 (dd, *J* = 8.1, 1.3 Hz, 1H), 2.94 (sept, *J* = 6.9 Hz, 1H), 2.17 (s, 3H), 2.07 (s, 3H), 2.03 (s, 3H), 1.31 (d, *J* = 6.9 Hz, 6H), 0.35 (s, 9H); ^{13}C NMR (100 MHz, CDCl$_3$; DEPT): δ (ppm) = 148.2 (C), 135.6 (CH), 135.0 (CH), 134.8 (CH), 132.0 (CH),

131.9 (CH), 131.8 (CH), 131.7 (CH), 131.6 (CH), 131.34 (CH), 131.25 (CH), 129.8 (CH), 128.5 (CH), 126.7 (CH), 126.1 (C), 125.6 (C), 125.42 (C), 125.40 (C), 125.2 (C), 124.3 (C), 124.1 (C), 123.5 (C), 123.4 (C), 123.2 (C), 103.9 (C), 97.0 (C), 94.6 (C), 92.7 (C), 92.1 (C), 91.5 (C), 91.0 (C), 89.7 (C), 89.5 (C), 88.7 (C), 88.1 (C), 78.8 (C), 78.6 (C), 78.4 (C), 33.9 (CH), 23.7 (CH_3), 4.6 (CH_3), 4.5 (CH_3), 4.3 (CH_3), -0.1 (CH_3); MALDI-HRMS calculated for $C_{47}H_{38}SiAg$: 737.1788, found: 737.1760.

***Compound* XXI**. A suspension containing -alkylidyne complex **C02** (10 mol %) and dry powdered MS 5Å in toluene (1 mL) was stirred for 10 minutes. Then, a solution of the substrate **XX** (414 mg, 0.66 mmol) in toluene (20mM) was added and stirred 24h at ambient temperature. The reaction crude was filtered through a short plug of silica, the filtrate evaporated and the residue purified by flash chromatography. (Hexane/EtOAc= 10:0 → 8:2) to give **XXI** in 71% (97% brsm) as a pale yellow solid (270 mg). ^{1}H NMR (500 MHz, $CDCl_3$): δ (ppm) = 7.99 (d, *J* = 1.4 Hz, 1H), 7.96 (d, *J* = 0.8 Hz, 1H), 7.64 (d, *J* = 1.4 Hz, 1H), 7.57 − 7.35 (m, 9H), 7.19 (dd, *J* = 8.1, 1.7 Hz, 1H), 2.93 (sept, *J* = 6.9 Hz, 1H), 2.24 (s, 1H), 1.28 (d, *J* = 6.9 Hz, 6H), 0.27 (s, 9H); ^{13}C NMR (126 MHz, $CDCl_3$; DEPT): δ (ppm) = 149.6 (C), 135.8 (CH), 135.75 (CH), 135.71 (CH), 135.68 (CH), 132.2 (CH), 132.1 (CH), 131.8 (CH), 131.59 (CH), 131.55 (CH), 131.3 (CH), 131.0 (CH), 130.2 (CH), 128.8 (CH), 127.0 (CH), 126.4 (C), 126.1 (C), 125.8 (C), 125.6 (C), 125.5 (C), 124.0 (C), 123.6 (C), 123.2 (C), 123.1 (C), 122.8 (C), 104.1 (C), 97.2 (C), 94.7 (C), 92.7 (C), 92.5 (C), 92.3 (C), 91.9 (C), 91.5 (C), 90.6 (C), 89.6 (C), 89.0 (C), 78.6 (C), 34.0 (CH), 23.8 (CH_3), 4.9 (CH_3), 0.0 (CH_3); ESIpos-HRMS calculated for $C_{43}H_{32}Si$: 576.2273, found: 576.2248.

***Compound* XXII**. The silylated alkyne **XXI** (270 mg, 0.48 mmol) was dissolved in THF (0.03 M) and TBAF added (184 mg, 0.58 mmol). The mixture was stirred for 5 minutes, then supported on silica gel and submitted to column chromatography (Hexane/EtOAc= 10:0 → 6:4) to give **XXII** in 99 % yield (236 mg) as a white solid. ^{1}H NMR (500 MHz, $CDCl_3$): δ (ppm) = 8.00 (bs, 1H), 7.98 (s, 1H), 7.66 (d, *J* = 1.3 Hz, 1H), 7.57 - 7.52 (m, 3H), 7.49 (d, *J* = 8.0 Hz, 2H), 745 − 7.36 (m, 4H), 7.20 (d, *J* = 8.1, 1H), 3.20 (s, 1H), 2.93 (sept, *J* = 6.9 Hz, 1H), 2.24 (s, 3H), 1.28 (d, *J* = 6.9 Hz, 6H); ^{13}C NMR (126 MHz, $CDCl_3$, DEPT): δ (ppm) = 149.6 (C), 135.84 (CH), 135.79 (CH), 135.7 (CH), 132.2 (CH), 132.1 (CH), 131.9 (CH), 131.8 (CH), 131.7 (CH), 131.4 (CH), 131.1 (CH), 130.2 (CH), 128.9 (CH), 127.0 (CH), 126.4 (C), 126.2 (C), 125.9 (C), 125.7 (C), 125.5 (C), 124.0 (C), 123.5 (C), 123.0 (C), 122.8 (C), 122.2 (C), 94.7 (C), 92.7 (C), 92.6 (C), 92.2 (C), 91.9 (C), 91.3 (C), 90.7 (C), 89.6 (C), 88.8 (C), 82.7 (C), 79.6 (C), 78.5 (C), 34.2 (CH), 23.8 (CH_3), 5.0 (CH_3); ESIpos-HRMS calculated for $C_{40}H_{24}$: 504.1878, found: 504.1878.

***Compound* XIXa**. A solution of the terminal alkyne **XXII** (205 mg, 0.33 mmol) dissolved in 2 mL of Et_3N and 2 mL of THF was added dropwise to a carefully degassed solution of $Pd(PPh_3)_4$ (38 mg, 10 mol%), CuI (13 mg, 10 mol%) and the aryl iodide **XII** (260 mg, 0.65 mmol) in 4 mL of Et_3N and 4 mL of THF. The reaction was stirred overnight at room temperature under argon atmosphere. Then, the crude was diluted with dichloromethane, washed with saturated aq NH_4Cl solution, dried over anhydrous Na_2SO_4 and filtered. The filtrate was supported on silica gel and submitted to flash chromatography (Hexane/EtOAc: 1:0 → 1:1) to give **XIXa** in 31 % yield (75 mg, 40% brsm) as a white solid. ^{1}H NMR (500 MHz, $CDCl_3$): δ (ppm) = 8.22 (s, 1H), 7.99 (s, 1H), 7.96 (m, 2H), 7.76 (s, 1H), 7.63 − 7.58 (m, 2H), 7.56 (d, *J* = 8.0 Hz, 2H), 7.44 (m, 9H), 7.29 (t, *J* = 7.7 Hz, 1H), 7.19 (dd, *J* = 8.1, 1.3 Hz, 1H), 3.94 (s, 3H), 2.93 (sept, *J* = 6.9 Hz, 1H), 2.03 (s, 3H), 2.01 (s, 3H), 1.28 (d, *J* = 6.9 Hz, 6H); ^{13}C NMR (126 MHz, $CDCl_3$, DEPT): δ (ppm) = 166.0 (C), 149.6 (C), 135.8 (CH), 135.6 (CH), 135.2 (CH), 134.9 (CH), 133.1 (CH), 132.2 (CH), 132.2 (CH), 132.1 (CH), 132.0 (CH), 132.0 (CH), 131.6 (CH), 131.5 (CH), 131.3 (CH), 131.1 (CH), 130.7 (CH), 130.2 (CH), 130.0 (C), 129.7 (C), 129.0 (CH), 128.8 (CH), 128.7 (CH), 127.0 (CH), 126.5 (C), 126.4 (C), 126.3 (C), 125.9 (C), 125.7 (C), 125.5 (C), 124.9 (C), 124.0 (C), 123.5 (C), 123.0 (C), 122.8 (C), 122.7 (C), 95.5 (C), 94.9 (C), 94.2 (C), 92.9 (C), 92.7 (C), 92.2 (C), 91.9 (C), 91.3 (C), 90.6 (C), 90.2 (C), 89.6 (C), 89.0 (C), 87.8 (C), 87.1 (C), 78.9 (C), 78.5 (C), 52.6 (CH3), 34.1 (CH), 23.8 (CH_3), 4.8 (CH_3), 4.5 (CH_3); MALDI-HRMS calculated for $C_{59}H_{36}O_2Na$: 799.2608, found: 799.2614.

COOMe

1. ≡—TMS
PdCl₂(PPh₃)₂, CuI,
Et₃N, rt, 99%

2. ≡
[PdCl₂(CH₃CN)₂], CuI,
P(t-Bu)₃·HBF₄
iPr₂NH, rt, 68%
3. n-Bu₄NF·3H₂O,
THF, 52%

XXIII

Br
H₂N—I

PdCl₂(PPh₃)₂, CuI

Et₃N, rt
62%

COOMe

Br
NH₂

XXIV

1) HCl, 0°C
2) NaNO₂
3) NaI
CH₂Cl₂, rt,
on 73%

COOMe

Br
I

XXV

X

PdCl₂(PPh₃)₂, CuI

Et₃N, rt
92%

COOMe

Br

XXVI

1. ≡—TMS
PdCl₂(PPh₃)₂, CuI
Et₃N, rt

2. n-Bu₄NF·3H₂O
THF
77%

COOMe

XXVII

Compound XXIII was prepared from methyl 3-bromo-4-iodobenzoate (3.6 g, 10.6 mmol) according to previously described *GP1* to give the silylated intermediate in 99 % yield (3.27 g) as a pale yellow liquid. Methyl 3-bromo-4-((trimethylsilyl)ethynyl)benzoate (3.1 g, 9.97 mmol) was transformed into methyl 3-(prop-1-yn-1-yl)-4-((trimethylsilyl)ethynyl)benzoate according to previously described *GP2* in 68 % yield (1.82 g) as a orange liquid. This propynyl-silylated intermediate (1.82 g, 6.74 mmol) was dissolved in THF (0.03 M) and TBAF added (2.57 g, 8.1 mmol). The mixture was stirred for 5 minutes, then supported on silica gel and submitted to column chromatography (Hexane/EtOAc= 8:2) to give **XXIII** in 52 % yield (694 mg) as a yellow solid. ^{1}H NMR (400 MHz, CDCl₃): δ (ppm) = 7.93 (s, 1H), 7.72 (dd, J = 8.1, 1.5 Hz, 2H), 7.40 (d, J = 8.1 Hz, 1H), 3.78 (s, 3H), 3.43 (s, 1H), 2.01 (s, 3H). EI-HRMS calculated for $C_{13}H_{10}O_2$: 198.0681, found: 198.0676.

Compound XXIV was prepared from **XXIII** (690 mg, 3.48 mmol) and 2-bromo-4-iodoaniline (1.04 g, 3.48 mmol) according to previously described *GP1* to give **XXIV** in 62 % yield (792 mg) as a pale yellow solid. ^{1}H NMR (401 MHz, CDCl₃): δ (ppm) = 8.08 (d, J = 1.3 Hz, 1H), 7.87 (dd, J = 8.1, 1.7 Hz, 1H), 7.64 (d, J = 1.7 Hz, 1H), 7.49 (d, J = 8.2 Hz, 1H), 7.31 (d, J = 1.7 Hz, 1H), 6.72 (d, J = 8.3 Hz, 1H), 4.32 (bs, 2H), 3.91 (s, 3H), 2.17 (s, 3H); ^{13}C NMR (101 MHz, CDCl₃, DEPT): δ (ppm) = 166.3 (C), 145.0 (C), 136.2 (CH), 133.1 (CH), 132.3 (CH), 131.4 (CH), 130.4 (C), 129.1 (C), 128.2 (CH), 126.6 (C), 115.2 (CH), 113.5 (C), 108.5 (C), 95.6 (C), 91.2 (C), 87.2 (C), 78.1 (C), 52.4 (CH₃), 4.8 (CH₃); EI-HRMS calculated for $C_{19}H_{14}BrNO_2$: 367.0208, found: 367.0197.

Compound XXV. To a flask containing **XXIV** (780 mg, 2.12 mmol), concentrated HCl was added dropwise until the formation of a pale orange solid. Then, a solution of sodium nitrite (159 mg, 2.33 mmol) in water (7 mL) was slowly added at 0ªC. The reaction mixture was stirred at 0ºC for an additional 30 min before adding a solution of potassium iodide (1.8 g, 10.6 mmol) in 7 mL water. After 15 min, 20 mL of dichloromethane were added and the mixture vigorously stirred overnight. The reaction mixture was diluted in dichlorometane, washed successively with brine, Na₂S₂O₃·5H₂O and water, dried over anhydrous Na₂SO₄ and filtered. Then, the crude was supported on silica gel and submitted to flash chromatography (Hexane/EtOAc = 8:2) to give **XXV** in 73 % yield (741 mg) as a pale orange solid. ^{1}H NMR (401 MHz, CDCl₃): δ (ppm) =8.10 (s, 1H), 7.90 (d, J = 8.2 Hz, 1H), 7.86 (d, J = 8.2 Hz, 1H), 7.80 (d, J = 1.6 Hz, 1H), 7.53 (d, J = 8.1 Hz, 1H), 7.15 (dd, J = 8.2, 1.8 Hz, 1H), 3.92 (s, 3H), 2.16 (s, 3H); ^{13}C NMR (101 MHz, CDCl₃, DEPT): δ (ppm) = 166.1 (C), 140.3 (CH), 135.5 (CH), 134.8 (C), 133.2 (CH), 131.8 (CH), 131.3 (CH), 130.1 (C), 129.2 (C), 128.3 (CH), 127.2 (C), 124.7 (C), 101.9 (C), 93.4 (C), 91.8 (C), 90.4 (C), 77.9 (C), 52.5 (CH₃), 4.8 (CH₃); EI-HRMS calculated for $C_{19}H_{12}BrIO_2$: 477.9065, found: 477.9067.

Compound **XXVI** was prepared from **XXV** (780 mg, 2.12 mmol) and **X** (245 mg, 1.75 mmol) according to previously described *GP1* to give **XXVI** in 92 % yield (650 mg) as an orange solid. ^{1}H NMR (401 MHz, CDCl$_3$) δ 8.11 (d, *J* = 1.5 Hz, 1H), 7.90 (dd, *J* = 8.1, 1.5 Hz, 1H), 7.81 (d, *J* = 1.3 Hz, 1H), 7.61 (s, 1H), 7.54 (d, *J* = 8.5 Hz, 1H), 7.52 (d, *J* = 8.3 Hz, 1H), 7.47 (dd, *J* = 8.1, 1.5 Hz, 1H), 7.45 (dd, *J* = 8.1, 1.5 Hz, 1H), 7.38 (d, *J* = 7.8 Hz, 1H), 7.28 (t, *J* = 7.8 Hz, 1H), 3.92 (s, 3H), 2.18 (s, 3H), 2.06 (s, 3H); ^{13}C NMR (101 MHz, CDCl$_3$, DEPT): δ (ppm) = 166.1 (C), 135.6 (CH), 134.8 (CH), 133.2 (CH), 133.0 (CH), 132.1 (CH), 131.8 (CH), 130.8 (CH), 130.4 (CH), 130.0 (C), 129.3 (C), 128.6 (CH), 128.3 (CH), 127.2 (C), 125.7 (C), 125.5 (C), 124.7 (C), 124.3 (C), 123.0 (C), 95.5 (C), 94.0 (C), 91.8 (C), 91.0 (C), 88.3 (C), 87.0 (C), 79.0 (C), 77.9 (C), 52.5 (CH$_3$), 4.8 (CH$_3$), 4.5 (CH$_3$); EI-HRMS calculated for C$_{30}$H$_{19}$BrO$_2$: 490.0568, found: 490.0562.

Compound **XXVII** was prepared from **XXVI** (300 mg, 0.61 mmol) according to previously described *GP2*. The silylated alkyne was not purified by column chromatography but redissolved in THF (0.03 M) and TBAF added (1 eq). The mixture was stirred for 5 minutes, then supported on silica gel and submitted to column chromatography (Eluent: n-hexane) to give **XXVII** in 77 % yield (204 mg) as a pale yellow solid. ^{1}H NMR (401 MHz, CDCl$_3$): δ (ppm) = 8.10 (s, 1H), 7.89 (dd, *J* = 8.1, 1.5 Hz, 1H), 7.71 (s, 1H), 7.59 (s, 1H), 7.57 – 7.42 (m, 4H), 7.37 (d, *J* = 7.8 Hz, 1H), 7.27 (t, *J* = 7.8 Hz, 1H), 3.91 (s, 3H), 3.41 (s, 1H), 2.17 (s, 3H), 2.05 (s, 3H); ^{13}C NMR (101 MHz, CDCl$_3$, DEPT): δ (ppm) = 166.1 (C), 135.9 (CH), 134.8 (CH), 133.2 (CH), 132.0 (CH), 131.9 (CH), 131.8 (CH), 131.7 (CH), 130.9 (CH), 129.9 (C), 129.4 (C), 128.5 (CH), 128.2 (CH), 127.2 (C), 126.4 (C), 125.12 (C), 124.6 (C), 123.2 (C), 123.0 (C), 95.1 (C), 94.5 (C), 91.7 (C), 90.5 (C), 88.1 (C), 86.9 (C), 82.0 (CH), 81.4 (C), 79.2 (C), 77.9 (C), 52.4 (CH$_3$), 4.7 (CH$_3$), 4.4 (CH$_3$); EI-HRMS calculated for C$_{32}$H$_{20}$O$_2$: 436.1463, found: 436.1460.
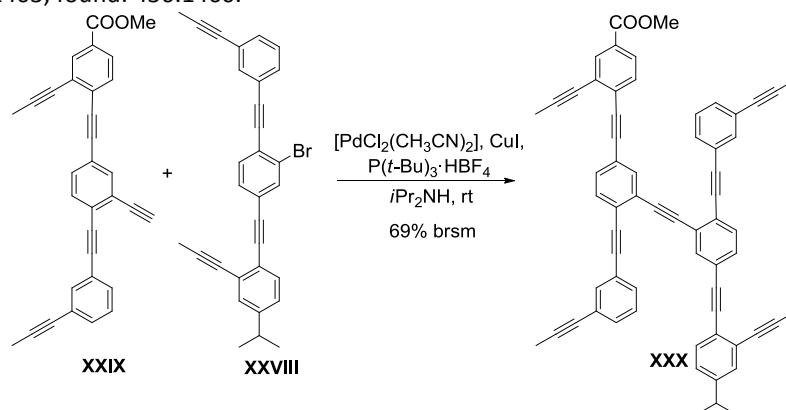
Compound **XXVIII** was prepared from **IV** following the same synthetic route depicted above for **XXVII**. ^{1}H NMR (401 MHz, cdcl$_3$) δ 7.79 (d, *J* = 1.3 Hz, 1H), 7.62 (s, 1H), 7.50 (d, *J* = 8.0 Hz, 1H), 7.47 (d, *J* = 7.7 Hz, 1H), 7.43 (dd, *J* = 7.9, 1.6 Hz, 1H), 7.41 (d, *J* = 7.7 Hz, 1H), 7.38 (d, *J* = 7.8 Hz, 1H), 7.32 (d, *J* = 1.3 Hz, 1H), 7.27 (d, *J* = 7.9 Hz, 1H), 7.12 (dd, *J* = 8.1, 1.6 Hz, 1H), 2.88 (sept, *J* = 6.9 Hz, 1H), 2.17 (s, 3H), 2.06 (s, 3H), 1.24 (d, *J* = 6.9 Hz, 6H); ^{13}C NMR (101 MHz, cdcl$_3$) δ 149.8 (C), 135.4 (CH), 134.8 (CH), 132.9 (CH), 131.92 (CH), 131.90 (CH), 130.8 (CH), 130.2 (CH), 130.1 (CH), 128.5 (CH), 126.9 (C), 126.1 (CH), 125.4 (C), 125.2 (C), 124.9 (C), 124.7 (C), 123.1 (C), 122.4 (C), 95.0 (C), 92.1 (C), 90.6 (C), 90.1 (C), 88.5 (C), 86.9 (C), 79.0 (C), 78.8 (C), 34.1 (CH), 23.7 (CH3), 4.7 (CH3), 4.5 (CH3); EI-HRMS calculated for C31H23Br: 474.0983, found: 474.0992.

Compound **XXX** was prepared from **XXVIII** (150 mg, 0.32 mmol) and **XXIX** (138 mg, 0.32 mmol) according to previously described *GP2* to give **XXX** in 34 % yield (88 mg, 69% brsm) as a pale yellow solid. ^{1}H NMR (401 MHz, CDCl$_3$): δ (ppm) = 8.10 (s, 1H), 7.91 (d, *J* = 8.1 Hz, 1H), 7.80 (s, 1H), 7.79 (s, 1H), 7.57 - 7.48 (m, 7H), 7.43 -7.40 (m, 3H), 7.33 – 7.25 (m, 3H), 7.22 - 7.16 (m, 2H), 7.13 (d, *J* = 7.9 Hz, 1H), 3.92 (s, 3H), 2.88 (sept, *J* = 6.7 Hz, 1H), 2.10 (s, 3H), 2.09 (s, 3H), 1.98 (s, 3H), 1.97 (s, 3H), 1.25 (d, *J* = 6.7 Hz, 6H); ^{13}C NMR (101 MHz, CDCl$_3$, DEPT): δ (ppm) = 166.2 (C), 149.6 (C), 135.4(CH), 135.1 (CH), 134.9 (CH), 134.8 (CH), 133.1 (CH), 132.1 (C), 132.0 (CH), 132.0 (CH), 131.9 (CH), 131.8 (CH), 131.7 (CH), 131.5 (CH), 130.9 (CH), 130.8 (CH), 130.1 (CH), 129.8 (C), 129.6 (C), 128.5 (CH), 128.4 (CH), 128.2 (CH), 127.2 (C), 126.8 (C), 126.2 (CH), 126.04 (C), 126.00 (CH), 125.9 (C), 125.4 (C), 124.6 (C), 123.9 (C), 123.2 (C), 123.10 (C), 123.05 (C), 122.7 (CH), 95.5 (C), 95.1 (C), 94.7 (C), 92.4 (C), 91.9 (C), 91.8 (C), 91.4 (C), 91.2 (C), 90.4 (C), 90.2 (C), 88.6 (C), 88.4 (C), 86.8 (C), 86.7 (C), 79.04 (C), 79.03 (C), 78.9 (C), 77.9 (C), 52.4 (CH$_3$), 34.2 (CH), 23.6 (CH$_3$), 4.9 (CH$_3$), 4.4 (CH$_3$); MALDI-HRMS calculated for C$_{63}$H$_{42}$O$_2$Na: 853.3070, found: 830.3077.

X

[PdCl$_2$(CH$_3$CN)$_2$], CuI,
P(*t*-Bu)$_3$·HBF$_4$

*i*Pr$_2$NH, rt

97%

1) HCl, 0 °C
2) NaNO$_2$
3) NaI

CH$_2$Cl$_2$, rt, on

49%
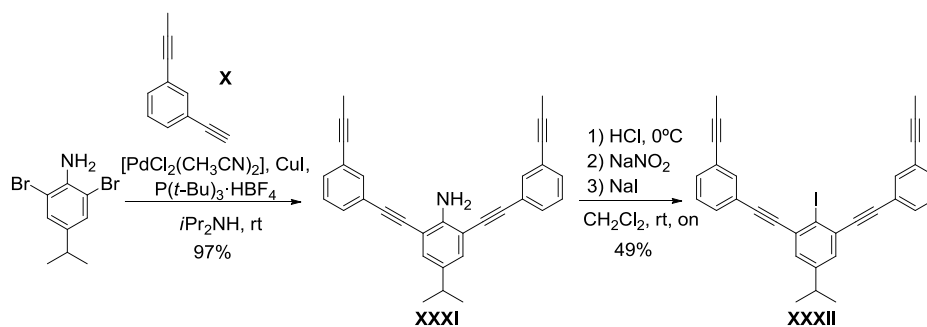
XXXI

XXXII

Compound **XXXI** was prepared from 2,6-dibromo-4-isopropylaniline (1.07 g, 3.4 mmol) and **X** (1.15 g, 8.2 mmol) according to previously described *GP2* to give **XXXI** in 97 % yield (1.38 g) as a orange liquid. ^{1}H NMR (401 MHz, CDCl$_3$): δ (ppm) = 7.54 (s, 2H), 7.41 (dd, *J* = 7.8, 1.2 Hz, 2H), 7.38 (d, *J* = 7.8 Hz, 2H), 7.25 (t, *J* = 7.8 Hz, 1H), 7.23 (s, 1H), 4.39 (bs, 2H), 2.76 (sept, *J* = 6.9 Hz, 1H), 2.05 (s, 6H), 1.19 (d, *J* = 6.9 Hz, 6H); ^{13}C NMR (101 MHz, CDCl$_3$, DEPT): δ (ppm) = 140.8 (C), 139.9 (C), 135.5 (CH), 132.4 (CH), 131.6 (CH), 129.9 (CH), 128.6 (CH), 124.8 (C), 122.0 (C), 109.0 (C), 87.2 (C), 81.1 (C), 78.8 (C), 74.3 (C), 33.1 (CH), 24.1 (CH$_3$), 4.5 (CH$_3$).

Compound **XXXII**. A round-bottom flask equipped with a magnetic stir bar was charged with compound **XXXI** (1.38 g, 3.35 mmol) and dry diethyl ether (40 mL). The solution was cooled to -30 °C and boron trifluoride diethyl etherate (3.5 mL, 13. 4 mmol) was added. The mixture was stirred at -30 °C for 30 min and *tert*-butyl nitrite (1.34 mL, 11.73 mmol) was added. The mixture was stirred for an additional 30 min between -20 °C and -10 °C. The white precipitate formed was collected by filtration, rinsed thoroughly with diethyl ether and dissolved in dry acetonitrile (40 mL). This solution was added to a solution of sodium iodide (1.4 g, 9 mmol) in acetonitrile (40 mL). The resulting mixture was stirred 1h at room temperature, poured into water and extracted with dichloromethane. The combined organic layers were washed with water, dried over Na$_2$SO$_4$, filtered, supported on silica gel and submitted to column chromatography (Eluent: n-hexane) to give **XXXII** in 49 % yield (862 mg) as a orange solid containing about 30% of the arylfluoride. ^{1}H NMR (500 MHz, CDCl$_3$): δ (ppm) = 7.67 (s, 2H), 7.59 (s, 2H), 7.52 (d, *J* = 7.8 Hz, 2H), 7.44 (d, *J* = 7.7 Hz, 2H), 7.30 (t, *J* = 7.8 Hz, 2H), 2.87 (sept, *J* = 6.9 Hz, 1H), 2.07 (s, 6H), 1.28 (d, *J* = 6.8 Hz, 6H); ^{13}C NMR (126 MHz, CDCl$_3$, DEPT): δ (ppm) = 149.4 (C), 148.9 (C), 134.7 (CH), 131.8 (CH), 130.8 (CH), 130.0 (CH), 128.5 (CH), 124.5 (C), 123.4 (C), 104.2 (C), 92.6 (C), 89.3 (C), 86.8 (C), 79.1 (C), 34.0 (CH), 23.9 (CH$_3$), 4.5 (CH$_3$); EI-HRMS calculated for C$_{31}$H$_{23}$I: 522.0845, found: 522.0852.

1. ≡—TMS
[PdCl$_2$(CH$_3$CN)$_2$], CuI,
P(*t*-Bu)$_3$·HBF$_4$

*i*Pr$_2$NH, rt

2. n-Bu$_4$NF·3H$_2$O
THF

39%

PdCl$_2$(PPh$_3$)$_2$, CuI

Et$_3$N, rt

99%

XXXIII

XXXIV

[PdCl$_2$(CH$_3$CN)$_2$], CuI,
P(*t*-Bu)$_3$·HBF$_4$
*i*Pr$_2$NH, rt

91%

K$_2$CO$_3$, MeOH,
rt., 24h

78%

XXXVI

XXXV
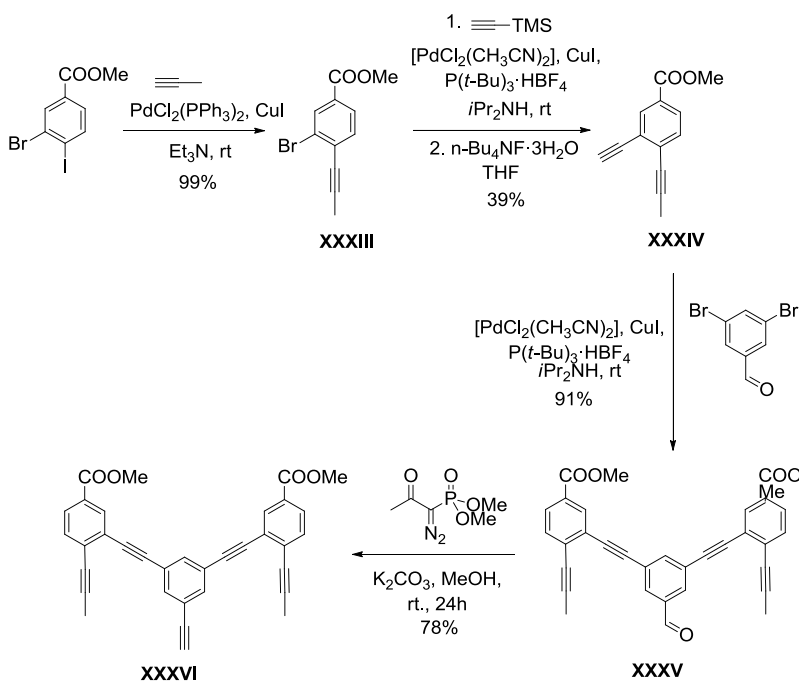
Compound **XXXIII** was prepared from methyl 3-bromo-4-iodobenzoate (4.3 g, 12.6 mmol) according to previously described *GP1* to give **XXXIII** in 99 % yield (3.19 g) as a pale yellow liquid. ^{1}H NMR (500 MHz,

CDCl$_3$): δ (ppm) = 8.21 (d, J = 1.6 Hz, 1H), 7.87 (dd, J = 8.1, 1.7 Hz, 1H), 7.46 (d, J = 8.1 Hz, 1H), 3.90 (s, 3H), 2.13 (s, 3H); ^{13}C NMR (126 MHz, CDCl$_3$, DEPT): δ (ppm) = 165.5 (C), 133.4 (CH), 133.3 (CH), 130.7 (C), 130.3 (C), 128.0 (CH), 125.3 (C), 94.7 (C), 78.4 (C), 52.5 (CH$_3$), 4.9 (CH$_3$); EI-HRMS calculated for C$_{11}$H$_9$BrO$_2$: 251.9786, found: 251.9777.

Compound XXXIV was prepared from **XXXV** (3.2 g, 12.7 mmol) according to previously described *GP2*. The silylated alkyne was not purified by column chromatography but redissolved in THF (0.03 M) and TBAF added (1 eq). The mixture was stirred for 5 minutes, then supported on silica gel and submitted to column chromatography (Hexane/EtOAc: 1:0 → 8:2) to give **XXXIV** in 39 % yield (970 mg) as a pale yellow solid. ^{1}H NMR (500 MHz, CDCl$_3$): δ (ppm) = 8.14 (d, J = 1.7 Hz, 1H), 7.91 (dd, J = 8.2, 1.8 Hz, 1H), 7.46 (d, J = 8.2 Hz, 1H), 3.91 (s, 3H), 3.32 (s, 1H), 2.14 (s, 3H); ^{13}C NMR (126 MHz, CDCl$_3$, DEPT): δ (ppm) = 165.9 (C), 133.7 (CH), 132.0 (CH), 131.4 (C), 131.4 (C), 129.2 (CH), 124.6 (C), 93.9 (C), 81.5 (C), 81.2 (CH), 77.9 (C), 52.3 (CH$_3$), 4.7 (CH$_3$); EI-HRMS calculated for C$_{13}$H$_{10}$O$_2$: 198.0681, found: 198.0690.

Compound XXXV was prepared from 3,5-dibromobenzaldehyde (533 mg, 2.02 mmol) and **XXXIV** (800 mg, 4.32 mmol) according to previously described *GP2* to give **XXXV** in 91 % yield (753 mg) as a pale yellow solid. ^{1}H NMR (401 MHz, CDCl$_3$): δ (ppm) = 10.04 (s, 1H), 8.19 (s, 2H), 8.01 (d, J = 1.0 Hz, 2H), 7.94 (dd, J = 13.9, 1.4 Hz, 2H), 7.94 (s, 1H), 7.51 (d, J = 8.1 Hz, 2H), 3.94 (s, 6H), 2.22 (s, 6H); ^{13}C NMR (101 MHz, CDCl$_3$, DEPT): δ (ppm) = 190.7 (CH), 166.1 (C), 139.7 (CH), 136.9 (C), 133.2 (CH), 132.5 (CH), 132.3 (CH), 131.3 (C), 129.5 (CH), 129.2 (C), 125.2 (C), 125.0 (C), 94.4 (C), 91.3 (C), 90.0 (C), 78.3 (C), 52.5 (CH$_3$), 5.0 (CH$_3$); EI-HRMS calculated for C$_{33}$H$_{22}$O$_5$Na: 521.1359, found: 521.1377.

Compound XXXVI. Ohira-Bestmann reagent (457 mg, 2.38 mmol) and K$_2$CO$_3$ (493 mg, 3.57 mmol) were added to a solution of the aldehyde **XXXV** (490 mg, 1.19 mmol) in dry MeOH and the resulting mixture was stirred overnight. Afterwards, the solvent was evaporated and the crude partitioned between EtOAc and saturated aq NH$_4$Cl solution. The combined organic layers were dried over Na$_2$SO$_4$, filtered, supported on silica gel and submitted to column chromatography (Hexane/EtOAc= 7:3) to give **XXXVI** in 78 % yield (376 mg) as a pale yellow solid. ^{1}H NMR (401 MHz, CDCl$_3$): δ (ppm) = 8.15 (d, J = 1.7 Hz, 2H), 7.90 (dd, J = 8.1, 1.7 Hz, 2H), 7.67 (d, J = 1.4 Hz, 1H), 7.62 (d, J = 1.5 Hz, 2H), 7.48 (d, J = 8.2 Hz, 2H), 3.92 (s, 6H), 3.14 (s, 1H), 2.19 (s, 6H); ^{13}C NMR (101 MHz, CDCl$_3$, DEPT): δ (ppm) = 166.0 (C), 135.1 (CH), 134.9 (CH), 133.1 (CH), 132.1 (CH), 131.2 (C), 129.2 (CH), 129.1 (C), 125.4 (C), 124.1 (C), 123.2 (C), 94.2 (C), 91.8 (C), 89.1 (C), 82.1 (C), 78.7 (CH), 78.3 (C), 52.4 (CH$_3$), 4.9 (CH$_3$); EI-HRMS calculated for C$_{34}$H$_{22}$O$_4$: 494.1518, found: 494.1534.
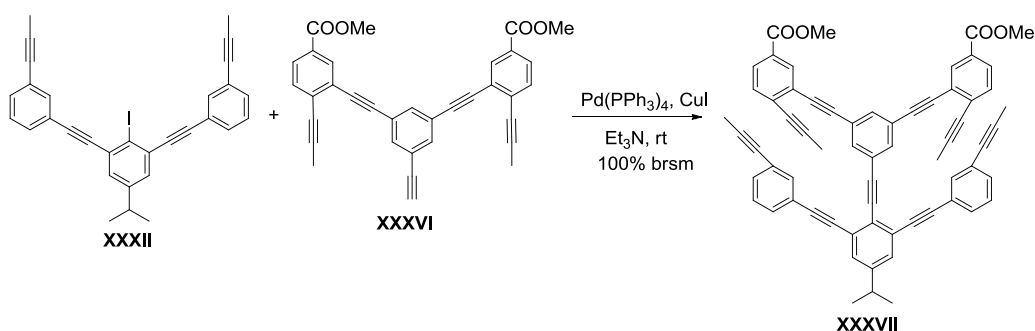
Compound XXXVII. A solution of the terminal alkyne **XXXVI** (430 mg, 1.05 mmol) dissolved in 5 mL of Et$_3$N and 5 mL of THF was added dropwise to a carefully degassed solution of Pd(PPh$_3$)$_4$ (40 mg, 4 mol%), CuI (20 mg, 10 mol%) and the aryl iodide **XXXII** (473 mg, 0.01 mmol) in 5 mL of Et$_3$N. The reaction was stirred overnight at room temperature under argon atmosphere. Then, the crude was diluted with EtOAc, washed with saturated aq NH$_4$Cl solution, dried over anhydrous Na$_2$SO$_4$ and filtered. The filtrate was supported on silica gel and submitted to flash chromatography (Hexane/EtOAc: 1:0 → 1:1) to give **XXXVII** in 30 % yield (220 mg, 100% brsm) as a white solid. ^{1}H NMR (500 MHz, CDCl$_3$): δ (ppm) = 8.17 (d, J = 1.6 Hz, 2H), 7.92 (dd, J = 8.1, 1.5 Hz, 2H), 7.78 (d, J = 1.5 Hz, 2H), 7.70 (t, J = 1.5 Hz, 2H), 7.65 (s, 2H), 7.54 (d, J = 7.5 Hz, 2H), 7.49 (d, J = 8.1 Hz, 2H), 7.42 (s, 2H), 7.35 (dt, J = 7.6, 1.3 Hz, 2H), 7.30 (t, J = 7.7 Hz, 2H), 3.94 (s, 6H), 2.89 (sept, J = 6.9 Hz, 1H), 2.07 (s, 6H), 1.95 (s, 6H), 1.30 (d, J = 6.9 Hz, 6H); ^{13}C NMR (126 MHz, CDCl$_3$, DEPT): δ (ppm) = 166.0 (C), 149.3 (C), 134.7 (CH), 134.6 (CH), 134.4 (CH), 133.0 (CH), 132.0 (CH), 131.8 (CH), 131.2 (C), 130.7 (CH), 130.0 (CH), 129.1 (CH), 128.9 (C), 128.6 (CH), 126.2 (C), 125.5 (C), 125.2 (C), 124.8 (C), 124.5 (C), 124.2 (C), 123.2 (C), 119.1 (C), 94.3 (C), 93.1 (C), 92.0 (C), 89.0

(C), 88.5 (C), 86.9 (C), 79.0 (C), 78.3 (C), 52.4 (CH$_3$), 34.0 (CH), 23.6 (CH$_3$), 4.7 (CH$_3$), 4.3 (CH$_3$); MALDI-HRMS calculated for C$_{65}$H$_{44}$O$_4$Na: 911.3140, found: 911.3132.
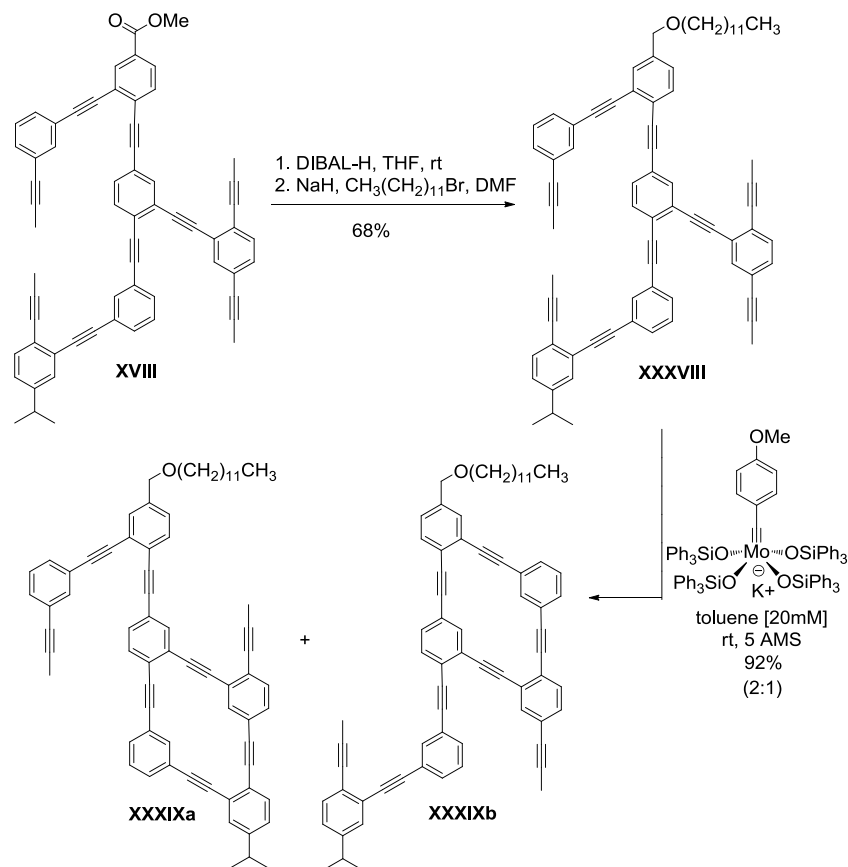
Compound XXXVIII. DIBAL (0.22 mL, 1M solution in CH2Cl$_2$) was added to a solution of the compound **XVIII** (62.5 mg, 0.075 mmol) in dry THF (5 mL) at 0ªC under Ar. The reaction was gradually warmed up to room temperature and stirred overnight. Then, the crude was diluted with DCM, washed with a 15% aqueous solution of citric acid and brine, dried over anhydrous Na$_2$SO$_4$ and the solvent removed under reduced pressure. The alcohol was dissolved in dry DMF under Ar. NaH (3 mg, 0.13 mmol) and dodecylbromide (0.1 mL, 0.4 mmol) were successively added and the reaction stirred overnight. The crude was diluted in EtOAc, washed twice with aq HCl solution (10%) and brine, dried over anhydrous Na$_2$SO$_4$ and filtered. The filtrate was supported on silica gel and submitted to flash chromatography (Hexane/EtOAc: 1:0 → 1:1) to give **XXXVIII** in 68 % yield (49.6 mg) as a white solid. ^{1}H NMR (600 MHz, CDCl$_3$): δ (ppm) = 7.78 (bs, 2H), 7.61 (s, 1H), 7.57 (s, 1H), 7.56 - 7.49 (m, 6H), 7.48 (d, J = 7.6 Hz, 1H), 7.39 − 7.23 (m, 8H), 7.13 (d, J = 8.0 Hz, 1H), 4.51 (s, 2H), 3.49 (t, J = 6.6 Hz, 2H), 2.89 (sept, J = 6.9 Hz, 1H), 2.11 (s, 3H), 2.02 (s, 3H), 2.00 (s, 3H), 1.90 (s, 3H), 1.68 − 1.60 (m, 2H), 1.41 − 1.34 (m, 18H), 1.27 (dd, J = 6.9 Hz, 6H), 0.87 (t, J = 8.1 Hz, 3H); ^{13}C NMR (151 MHz, cdcl$_3$) δ 148.3 (C), 139.7 (C), 135.3 (CH), 135.3 (CH), 135.0 (CH), 134.8 (CH), 132.1 (CH), 132.0 (CH), 132.0 (CH), 131.9 (CH), 131.8 (CH), 131.7 (CH), 131.3 (CH), 131.3 (CH), 130.8 (CH), 130. (CH), 129.9 (CH), 128.6 (CH), 128.6 (CH), 127.4 (CH), 126.8 (CH), 126.4 (C), 126.0 (C), 125.8 (C), 125.6 (C), 125.4 (C), 125.3 (C), 124.7 (C), 124.6 (C), 124.3 (C), 124.1 (C), 123.6 (C), 123.5 (C), 123.5 (C), 123.4 (C), 94.7 (C), 93.3 (C), 92.7 (C), 92.6 (C), 92.4 (C), 91.6 (C), 91.0 (C), 90.8 (C), 89.7 (C), 89.6 (C), 88.9 (C), 88.7 (C), 88.1 (C), 86.9 (C), 79.0 (C), 78.9 (C), 78.6 (C), 78.4 (C), 72.2 (CH2), 71.0 (CH2), 34.0 (CH), 32.1 (CH$_2$), 29.9 (CH$_2$), 29.83 (CH$_2$), 29.80 (CH$_2$), 29.78 (CH$_2$), 29.77 (CH$_2$), 29.6 (CH$_2$), 29.5 (CH$_2$), 26.3 (CH$_2$), 23.8 (CH$_3$), 22.9 (CH$_2$), 14.3 (CH$_3$), 4.73 (CH$_3$), 4.72 (CH$_3$), 4.50 (CH$_3$), 4.45 (CH$_3$).

Compounds XXXIXa and **b**. A suspension containing -alkylidyne complex **C02** (5 mg, 10 mol %) and dry powdered MS 5Å in toluene (1 mL) was stirred for 10 minutes. Then, a solution of the substrate **XXXVIII** (37.8 mg, 0.04 mmol) in toluene (20mM) was added and stirred 24h at ambient temperature. The reaction crude was filtered through a short plug of silica, the filtrate evaporated and the residue purified

by flash chromatography (Hexane/EtOAc= 10:0 → 8:2) to give **XXXIXa** (21 mg) and **XXXIXb** (10 mg) in 92% as white solids.

Compound XXXIXa: ^{1}H NMR (600 MHz, cdcl$_3$) δ 8.02 (s, 1H), 7.99 (d, *J* = 1.4 Hz, 1H), 7.77 (d, *J* = 1.5 Hz, 1H), 7.60 − 7.26 (m, 16H), 7.20 (dd, *J* = 8.1, 1.7 Hz, 1H), 4.52 (s, 2H), 3.49 (t, *J* = 6.6 Hz, 2H), 2.03 (s, 3H), 2.01 (s, 3H), 1.27 (m, 26H), 0.92 (t, *J* = 6.8 Hz, 3H); ^{13}C NMR (151 MHz, CDCl$_3$, DEPT): δ (ppm) = 149.6 (C), 139.7 (C), 135.8 (CH), 135.7 (CH), 135.2 (CH), 134.8 (CH), 132.2 (CH), 132.1 (CH), 132.0 (CH), 131.7 (CH), 131.5 (CH), 131.3 (CH), 131.1 (CH), 131.0 (CH), 130.8 (CH), 130.7 (CH), 130.2 (CH), 129.0 (CH), 128.9 (CH), 128.7 (CH), 127.4 (CH), 127.0 (CH), 126.5 (C), 126.3 (C), 126.0 (C), 125.8 (C), 125.5 (C), 125.4 (C), 124.8 (C), 124.6 (C), 124.0 (C), 123.6 (C), 123.5 (C), 123.3 (C), 123.0 (C), 122.7 (C), 94.6 (C), 93.3 (C), 93.0 (C), 92.6 (C), 92.5 (C), 92.3 (C), 91.9 (C), 91.5 (C), 90.8 (C), 90.6 (C), 89.6 (C), 89.1 (C), 88.6 (C), 87.0 (C), 79.0 (C), 78.5 (C), 72.2 (CH$_2$), 71.0 (CH$_2$), 34.2 (CH), 32.1 (CH$_2$), 29.9 (CH$_2$), 29.83 (CH$_2$), 29.81 (CH$_2$), 29.79 (CH$_2$), 29.7 (CH$_2$), 29.5 (CH$_2$), 29.2 (CH$_2$), 26.3 (CH$_2$), 23.8 (CH$_3$), 22.9 (CH$_2$), 14.3 (CH$_3$), 4.8 (CH$_3$), 4.5 (CH$_3$).

Compound XXXIXb: ^{1}H NMR (600 MHz, CDCl$_3$): δ (ppm) = 8.05 (d, *J* = 1.4 Hz, 1H), 8.02 (s, 1H), 7.85 (s, 1H), 7.65 − 7.29 (m, 16H), 7.13 (dd, *J* = 8.0, 1.8 Hz, 1H), 4.52 (s, 2H), 3.52 − 3.46 (m, 2H), 2.93 − 2.85 (m, 1H), 2.11 (s, 3H), 1.90 (s, 3H), 1.26 (m, 26H), 0.92 (t, *J* = 6.8 Hz, 3H); ^{13}C NMR (151 MHz, CDCl$_3$, DEPT): δ (ppm) = 148.3 (C), 139.7 (C), 135.9 (CH), 135.7 (CH), 135.4 (CH), 134.8 (CH), 132.2 (CH), 132.1 (CH), 131.9 (CH), 131.9 (CH), 131.7 (CH), 131.6 (CH), 131.5 (CH), 131.4 (CH), 131.1 (CH), 131.0 (CH), 130.8 (CH), 130.7 (CH), 130.0 (CH), 128.9 (CH), 128.7 (CH), 127.5 (CH), 126.8 (C), 126.2 (C), 126.0 (C), 125.9 (C), 125.8 (C), 125.4 (C), 125.3 (C), 124.7 (C), 124.4 (C), 124.4 (C), 124.3 (C), 123.8 (C), 123.7 (C), 123.6 (C), 123.5 (C), 94.9 (C), 94.1 (C), 92.8 (C), 92.6 (C), 92.5 (C), 91.9 (C), 91.6 (C), 91.0 (C), 89.8 (C), 89.6 (C), 89.2 (C), 89.1 (C), 89.1 (C), 88.8 (C), 78.8 (C), 78.7 (C), 72.2 (CH2), 71.0 (CH$_2$), 36.2 (CH), 34.8 (CH$_2$), 32.1 (CH$_2$), 29.9 (CH$_2$), 29.9 (CH$_2$), 29.8 (CH$_2$), 29.8 (CH$_2$), 29.7 (CH$_2$), 29.5 (CH$_2$), 29.2 (CH$_2$), 26.4 (CH$_2$), 23.8 (CH$_3$), 14.3 (CH$_3$), 4.8 (CH$_3$), 4.4 (CH$_3$).

MALDI-HRMS calculated for C$_{70}$H$_{60}$O: 916.4639, found: 916.4655.

The signal corresponding to the bi-fused annulene was also detected in the MALDI-HRMS but this product could not be isolated from the crude mixture. MALDI-HRMS calculated for C$_{66}$H$_{54}$O: 862.4169, found: 862.4160.
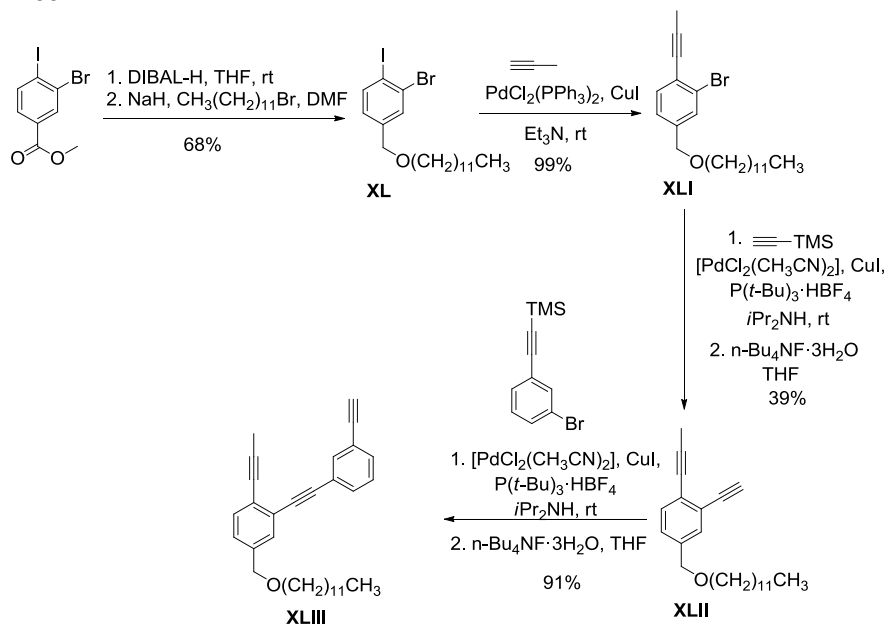
Compound XL. DIBAL (15 mL, 1M solution in CH$_2$Cl$_2$) was added to a solution of methyl 3-bromo-4-iodobenzoate (2 g, 6.39 mmol) in dry THF (10 mL) at 0ªC under Ar. The reaction was gradually warmed up to room temperature and stirred overnight. Then, the crude was diluted with DCM, washed with a 15% aqueous solution of citric acid and brine, dried over anhydrous Na$_2$SO$_4$ and the solvent removed under reduced pressure. The alcohol was dissolved in dry DMF under Ar before NaH (380 mg, 9.49 mmol) and dodecylbromide (2.8 mL, 9.54 mmol) were successively added. After stirring overnight, the crude was diluted in EtOAc, washed twice with aq HCl solution (10%) and brine, dried over anhydrous Na$_2$SO$_4$ and filtered. The filtrate was supported on silica gel and submitted to flash chromatography (Hexane/EtOAc: 1:0 → 1:1) to give **XL** in 70 % yield (2.17 g) as an off-white solid. ^{1}H NMR (401 MHz CDCl$_3$): δ (ppm) = 7.83 (d, *J* = 8.1 Hz, 1H), 7.63 (d, *J* = 1.9 Hz, 1H), 6.99 (dd, *J* = 8.1, 1.9 Hz, 1H), 4.44 (s, 2H), 3.48 (t, *J* = 6.6 Hz, 2H), 1.71 − 1.54 (m, 2H), 1.30 (m, 16H), 0.92 (t, *J* = 6.8 Hz, 3H); ^{13}C NMR (101

MHz, CDCl$_3$, DEPT): δ (ppm) = 141.1 (C), 140.2 (CH), 131.6 (CH), 129.8 (C), 127.5 (CH), 99.5 (C), 71.5 (CH2), 71.0 (CH2), 32.1 (CH2), 32.0 (CH2), 29.8 (CH2), 29.8 (CH2), 29.8 (CH2), 29.7 (CH2), 29.7 (CH2), 29.6 (CH2), 29.5 (CH2), 26.3 (CH2), 22.8 (CH2), 14.5 (CH3); EI-HRMS calculated for C$_{19}$H$_{30}$BrIO: 480.0525, found: 480.0517.

Compound XLI was prepared from **XL** (2.17 g, 4.5 mmol) according to previously described *GP1* (See ref.1) to give **XLI** in 89 % yield (1.57 g) as a pale yellow wax. ^{1}H NMR (401 MHz, CDCl$_3$): δ (ppm) =7.54 (s, 1H), 7.38 (d, *J* = 7.9 Hz, 1H), 7.17 (dd, *J* = 7.8, 0.6 Hz, 1H), 4.43 (s, 2H), 3.44 (t, *J* = 6.6 Hz, 2H), 2.10 (s, 3H), 1.69-1.53 (m, 2H), 1.27 (s, 16H), 0.89 (t, *J* = 6.7 Hz, 3H); ^{13}C NMR (101 MHz, CDCl$_3$, DEPT): δ (ppm) = 140.1 (C), 133.3 (CH), 131.2 (CH), 126.0 (CH), 125.4 (C), 125.1 (C), 90.7 (C), 78.5 (C), 71.8 (CH$_2$), 70.9 (CH$_2$), 32.1 (CH$_2$), 29.84 (CH$_2$), 29.81 (CH$_2$), 29.78 (CH$_2$), 29.75 (CH$_2$), 29.7 (CH$_2$), 29.6 (CH$_2$), 29.5 (CH$_2$), 26.3 (CH$_2$), 22.8 (CH$_2$), 14.3 (CH$_3$), 4.7 (CH$_3$).

Compound XLII was prepared from **XLI** (1.57 g, 3.99 mmol) according to previously described *GP2*. The silylated alkyne was not purified by column chromatography but redissolved in THF (0.03 M) and TBAF added (1 eq). The mixture was stirred for 5 minutes, then supported on silica gel and submitted to column chromatography (Hexane/EtOAc: 1:0 → 8:2) to give **XLII** in 79 % yield (1.06 g) as a transparent wax. ^{1}H NMR (300 MHz, CDCl$_3$): δ (ppm) = 7.48 (s, 1H), 7.41 (d, *J* = 8.0 Hz, 1H), 7.27 (d, *J* = 8.1 Hz, 1H), 4.47 (d, *J* = 2.3 Hz, 2H), 3.48 (t, *J* = 6.6 Hz, 2H), 3.31 (s, 1H), 2.15 (s, 3H), 1.69 – 1.53 (m, 2H), 1.29 (s, 18H), 0.92 (t, *J* = 6.7 Hz, 3H); ^{13}C NMR (101 MHz, CDCl$_3$, DEPT): δ (ppm) = 138.3 (C), 132.2 (CH), 131.6 (CH), 127.8 (CH), 126.2 (C), 124.4 (C), 90.3 (C), 82.6 (C), 80.4 (CH), 78.2 (C), 72.1 (CH$_2$), 70.9 (CH$_2$), 32.1 (CH$_2$), 29.9 (CH$_2$), 29.82 (CH$_2$), 29.79 (CH$_2$), 29.76 (CH$_2$), 29.75 (CH$_2$), 29.6 (CH$_2$), 29.5 (CH$_2$), 26.3 (CH$_2$), 22.8 (CH$_2$), 14.3 (CH$_3$), 4.8 (CH$_3$); EI-HRMS calculated for C$_{24}$H$_{34}$O: 338.2610, found: 338.2610.

Compound XLIII was prepared from **XLII** (1.06 g, 3.13 mmol) according to previously described *GP2* to give the silylated alkyne in 88% (1.42 g). Subsequently, the silylated alkyne (930 mg, 1.82 mmol) was dissolved in THF (0.03 M) and TBAF added (1 eq). The mixture was stirred for 5 minutes, then supported on silica gel and submitted to column chromatography (Hexane/EtOAc: 1:0 → 8:2) to give **XLIII** in 45 % yield (362 mg) as a white wax. ^{1}H NMR (401 MHz, CDCl$_3$): δ (ppm) =7.67 (s, 1H), 7.52 (d, *J* = 7.8 Hz, 1H), 7.47 (s, 1H), 7.45 (d, *J* = 7.8 Hz, 1H), 7.40 (d, *J* = 8.0 Hz, 1H), 7.31 (t, *J* = 7.8 Hz, 1H), 7.23 (d, *J* = 8.0 Hz, 1H), 4.47 (s, 2H), 3.46 (t, *J* = 6.6 Hz, 2H), 3.10 (s, 1H), 2.16 (s, 3H), 1.65 – 1.55 (m, 2H), 1.39 – 1.20 (m, 18H), 0.88 (t, *J* = 6.8 Hz, 3H); ^{13}C NMR (101 MHz, CDCl$_3$, DEPT): δ (ppm) = 138.4 (C), 135.4 (CH), 132.1 (CH), 132.04 (CH), 131.96 (CH), 130.8 (CH), 128.6 (CH), 127.5 (CH), 125.9 (C), 125.4 (C), 124.0 (C), 122.6 (C), 91.9 (C), 90.4 (C), 89.4 (C), 83.0 (C), 78.5 (C), 77.9 (CH), 72.2 (CH$_2$), 70.9 (CH$_2$), 32.1 (CH$_2$), 29.9 (CH$_2$), 29.82 (CH$_2$), 29.79 (CH$_2$), 29.77 (CH$_2$), 29.76 (CH$_2$), 29.6 (CH$_2$), 29.5 (CH$_2$), 26.3 (CH$_2$), 22.8 (CH$_2$), 14.3 (CH$_3$), 4.8 (CH$_3$); EI-HRMS calculated for C$_{32}$H$_{38}$O: 438.2923, found: 438.2943.
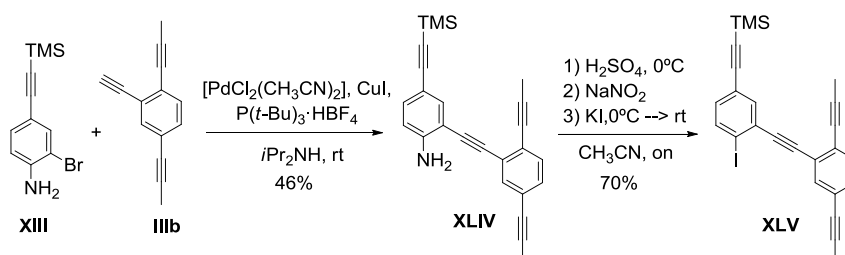
Compound XLIV was prepared from **XIII** (1 g, 3.72 mmol) and **IIIb** (728 mg, 4.1 mmol) according to previously described *GP2* to give **XLIV** in 46 % yield (628 mg) as an orange syrup. ^{1}H NMR (401 MHz, CDCl$_3$): δ (ppm) =7.50 (m, 2H), 7.33 (d, *J* = 8.0 Hz, 1H), 7.26 – 7.21 (m, 2H), 6.60 (d, *J* = 8.4 Hz, 1H), 4.71 (bs, 2H), 2.09 (s, 3H), 2.05 (s, 3H), 0.25 (s, 9H); ^{13}C NMR (101 MHz, CDCl$_3$, DEPT): δ (ppm) = 148.4 (C), 135.7 (CH), 134.1 (CH), 133.7 (CH), 132.0 (CH), 130.9 (CH), 125.4 (C), 124.9 (C), 123.6 (C), 113.9 (CH), 112.0 (C), 107.5 (C), 105.3 (C), 93.7 (C), 91.8 (C), 91.4 (C), 89.0 (C), 88.3 (C), 79.3 (CH), 78.9 (C), 4.8 (CH$_3$), 4.5 (CH$_3$), 0.2 (CH$_3$).

Compound XLV[122] A 250-mL three-necked round-bottom flask was charged with ice (3 g) and concentrated sulfuric acid (3 mL). To the stirred solution at 0 °C, a solution of **XLIV** (435 mg, 1.19 mmol)

---

[122] Procedure from: K. Yamada, T. Kurokawa, H. Tokuyama, T. Fukuyama, *J. Am. Chem. Soc.*, **2003**, *125*, 6630–6631.

in acetonitrile was added (4 mL) slowly *via* dropping-funnel over 20 min. Then, sodium nitrite (148 mg, 2.15 mmol) in cold water (2 mL) was added dropwise *via* dropping-funnel to the slurry crude over 20 min. The resulting solution was poured into a solution of potassium iodide (700 mg, 4.22 mmol) in water (2 mL). After the resulting mixture was stirred vigorously for 1h, the reaction mixture was diluted with dichloromethane and washed with saturated aq. Na_2CO_3, saturated aq. $Na_2S_2O_3 \cdot 5H_2O$ and brine, dried over anhydrous Na_2SO_4 and filtered. Then, the crude was supported on silica gel and submitted to flash chromatography (Hexane/EtOAc = 1:0 → 8:2) to give **XLV** in 70 % yield (396 mg) as a pale orange solid. ^{1}H NMR (401 MHz, $CDCl_3$): δ (ppm) = 7.80 (d, *J* = 8.3 Hz, 1H), 7.68 – 7.57 (m, 2H), 7.34 (d, *J* = 8.1 Hz, 1H), 7.28 (s, 1H), 7.07 (d, *J* = 8.3 Hz, 1H), 2.15 (s, 3H), 2.05 (s, 3H), 0.26 (s, 9H); ^{13}C NMR (101 MHz, $CDCl_3$, DEPT): δ (ppm) = 138.8 (CH), 136.1 (CH), 135.0 (CH), 132.4 (CH), 132.0 (CH), 131.5 (CH), 130.2 (C), 125.6 (C), 125.0 (C), 123.4 (C), 123.2 (C), 103.4 (C), 100.6 (C), 96.5 (C), 94.0 (C), 92.1 (C), 92.1 (C), 88.2 (C), 78.9 (C), 78.5 (C), 5.3 (CH_3), 4.6 (CH_3), 0.1 (CH_3), One quaternary carbon is missing; EI-HRMS calculated for $C_{25}H_{21}SiI$: 476.0457, found: 476.0462
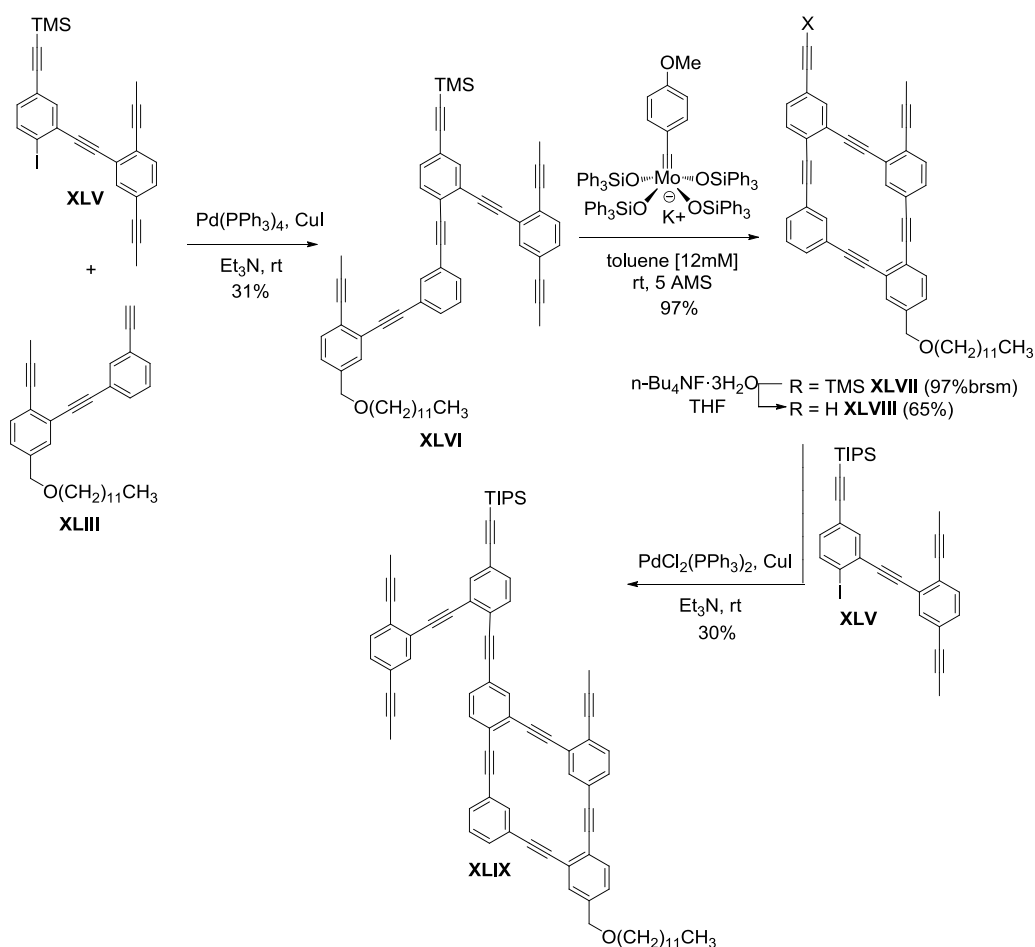
***Compound* XLVI**. A solution of the terminal alkyne **XLIII** (344 mg, 0.78 mmol) dissolved in 5 mL of Et_3N was added dropwise to a carefully degassed solution of $Pd(PPh_3)_4$ (100 mg, 10 mol%), CuI (40 mg, 10 mol%) and the aryl iodide **XLV** (410 mg, 0.86 mmol) in 5 mL of Et_3N. The reaction was stirred overnight at room temperature under argon atmosphere. Then, the crude was diluted with EtOAc, washed with saturated aq NH_4Cl solution, dried over anhydrous Na_2SO_4 and filtered. The filtrate was supported on silica gel and submitted to flash chromatography (Hexane/EtOAc: 1:0 → 1:1) to give **XLVI** in 31 % yield (189 mg) as an orange syrup. ^{1}H NMR (500 MHz, $CDCl_3$): δ (ppm) = 7.79 (s, 1H), 7.70 (d, *J* = 1.5 Hz, 1H), 7.58 (d, *J* = 1.6 Hz, 1H), 7.57 (dd, *J* = 7.8, 1.3 Hz, 1H), 7.52 (d, *J* = 8.4 Hz, 1H), 7.51 (d, *J* = 8.2 Hz, 1H), 7.48 (s, 1H), 7.41 (dd, *J* = 8.1, 1.7 Hz, 1H), 7.41 (d, *J* = 8.0 Hz, 1H), 7.36 (d, *J* = 8.1 Hz, 2H), 7.34 (t, *J* = 7.8 Hz, 1H), 7.26 (dd, *J* = 8.2, 1.8 Hz, 1H), 7.25 (dd, *J* = 8.0, 1.6 Hz, 1H), 4.48 (s, 2H), 3.48 (t, *J* = 6.7 Hz, 2H), 2.12 (s, 3H), 2.00 (s, 3H), 2.00 (s, 3H), 1.63 (m, 2H), 1.46 – 1.22 (m, 18H), 0.90 (t, *J* = 6.8 Hz, 3H), 0.28 (s, 9H); ^{13}C NMR (126 MHz, $CDCl_3$, DEPT): δ (ppm) = 138.3 (C), 135.7 (CH), 135.2 (CH), 135.0 (CH), 132.1 (CH), 132.0 (CH), 131.9 (CH), 131.81 (CH), 131.79 (CH), 131.4 (CH), 131.3 (CH), 130.9 (CH), 128.6 (CH), 127.4 (CH), 126.2 (C), 125.9 (C), 125.7 (C), 125.5 (C), 125.5 (C), 125.5 (C), 124.0 (C), 123.5 (C), 123.5 (C), 123.2

(C), 103.9 (C), 97.1 (C), 94.6 (C), 92.7 (C), 92.2 (C), 92.0 (C), 91.0 (C), 90.4 (C), 89.4 (C), 88.7 (C), 88.1 (C), 78.9 (C), 78.51 (C), 78.45 (C), 72.2 (CH$_2$), 70.9 (CH$_2$), 32.1 (CH$_2$), 29.9 (CH$_2$), 29.82 (CH$_2$), 29.79 (CH$_2$), 29.78 (CH$_2$), 29.76 (CH$_2$), 29.6 (CH$_2$), 29.5 (CH$_2$), 26.3 (CH$_2$), 22.8 (CH$_2$), 14.3 (CH$_3$), 4.8 (CH$_3$), 4.7 (CH$_3$), 4.5 (CH$_3$), 0.0 (CH$_3$); MALDI-HRMS calculated for C$_{57}$H$_{58}$OSiNa: 809.4149, found: 809.4122.

***Compound* XLVII.** A suspension containing -alkylidyne complex **C02** (24 mg, 7 mol %) and dry powdered MS 5Å in toluene (1 mL) was stirred for 10 minutes. Then, a solution of the substrate **XLVI** (188 mg, 0.24 mmol) in toluene (12mM) was added and stirred 24h at ambient temperature. The reaction crude was filtered through a short plug of silica, the filtrate evaporated and the residue purified by flash chromatography (Hexane/EtOAc= 10:0 → 8:2) to give **XLVII** (170 mg) in 97% as pale yellow solid. ^{1}H NMR (401 MHz, CDCl$_3$): δ (ppm) = 7.98 (s, 1H), 7.96 (s, 1H), 7.63 (d, *J* = 1.2 Hz, 1H), 7.57 − 7.47 (m, 5H), 7.44 − 7.35 (m, 4H), 7.29 (d, *J* = 8.0 Hz, 1H), 4.50 (s, 2H), 3.49 (t, *J* = 6.6 Hz, 2H), 2.24 (s, 3H), 1.71 − 1.60 (m, 2H), 1.49 − 1.17 (m, 18H), 0.89 (t, *J* = 13.1 Hz, 3H), 0.27 (s, 9H); ^{13}C NMR (101 MHz, CDCl$_3$, DEPT): δ (ppm) = 139.5 (C), 135.8 (CH), 132.2 (CH), 132.1 (CH), 131.8 (CH), 131.6 (CH), 131.4 (CH), 131.04 (CH), 131.01 (CH), 131.0 (CH), 128.9 (CH), 128.8 (CH), 127.5 (CH), 126.5 (C), 126.1 (C), 125.8 (C), 125.7 (C), 125.6 (C), 124.6 (C), 123.8 (C), 123.6 (C), 123.3 (C), 122.6 (C), 104.0 (C), 97.2 (C), 94.6 (C), 92.8 (C), 92.7 (C), 92.5 (C), 92.4 (C), 91.5 (C), 90.4 (C), 89.3 (C), 89.0 (C), 78.6 (C), 77.5 (C), 72.2 (CH$_2$), 71.0 (CH$_2$), 32.1 (CH$_2$), 29.9 (CH$_2$), 29.84 (CH$_2$), 29.81 (CH$_2$), 29.79 (CH$_2$), 29.78 (CH$_2$), 29.5 (CH$_2$), 22.9 (CH$_2$), 14.3 (CH$_3$), 0.0 (CH$_3$).

***Compound* XLIX.** The silylated alkyne **XLVII** (120 mg, 0.164 mmol) was dissolved in THF (0.03 M) and TBAF added (98 g, 0.31 mmol). The mixture was stirred for 5 minutes, then supported on silica gel and submitted to column chromatography (Hexane/EtOAc= 10:0 → 8:2) to give **XLVIII** in 65 % yield (70 mg) as a yellow solid. A solution of this terminal alkyne (70 mg, 0.112 mmol) dissolved in the 0.5 mL of THF and with 2 mL of Et$_3$N was added dropwise to a carefully degassed solution of Pd(PPh$_3$)$_2$Cl$_2$ (20 mg, 25 mol%), CuI (10 mg, 50 mol%) and the aryl iodide **XLV** (226 mg, 0.4 mmol) in 5 mL of Et$_3$N. The reaction was stirred overnight at room temperature under argon atmosphere. The mixture was then diluted with dichloromethane, washed with saturated aq NH$_4$Cl solution, dried over anhydrous Na$_2$SO$_4$ and the solvent was removed under reduced pressure. The residue was purified by flash chromatography (EtOAc/Hexane = 0:1 → 1:1) and recrystallization in hexane/dichloromethane to give **XLIX** in 30% (36 mg) as pale yellow solid. ^{1}H NMR (401 MHz, CDCl$_3$): δ (ppm) = 7.98 (s, 3H), 7.58 − 7.29 (m, 16H), 4.51 (s, 2H), 3.49 (t, *J* = 6.6 Hz, 2H), 2.24 (s, 3H), 2.23 (s, 3H), 2.09 (s, 3H), 1.62 − 1.64 (m, 2H), 1.26 (m, 20H), 1.13 (m, 10H), 0.87 (t, *J* = 5.8 Hz, 3H).
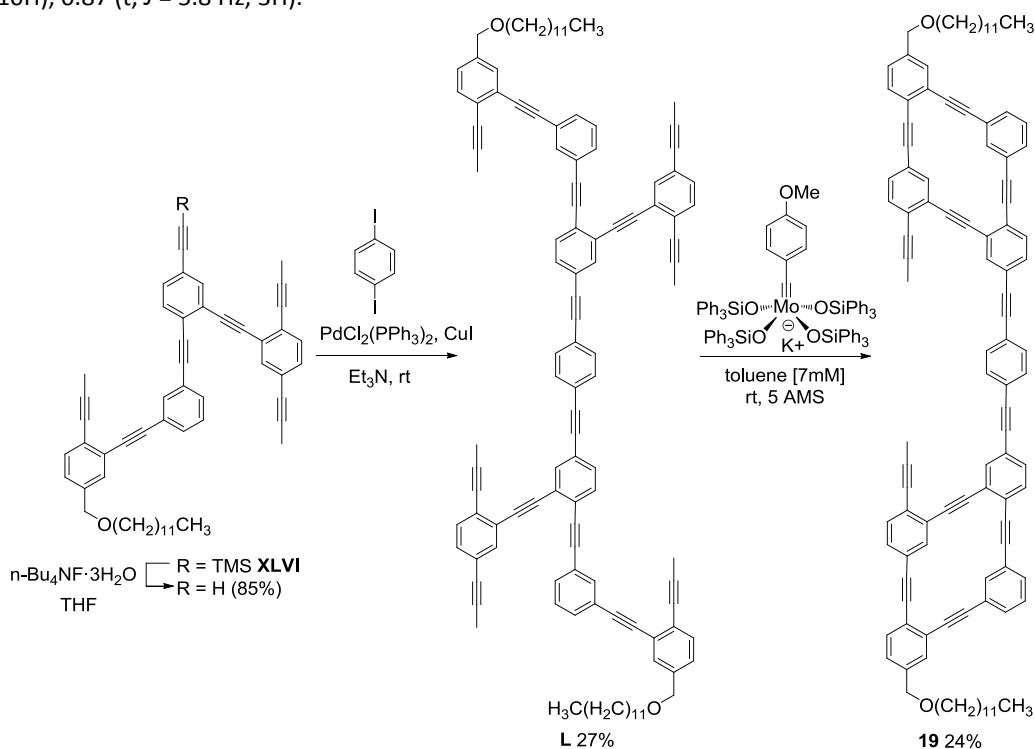
***Compound* L**. The silylated alkyne **XLVI** (600 mg, 0.76 mmol) was dissolved in THF (0.03 M) and TBAF added (240 mg, 0.76 mmol). The mixture was stirred for 5 minutes, then supported on silica gel and submitted to column chromatography (Hexane/EtOAc= 1:0 → 8:2) to give the terminal alkyne in 74 % yield (400 mg) as a yellow solid. A solution of this terminal alkyne (400 mg, 0.59 mmol) dissolved in the 3 mL of THF and with 5 mL of Et$_3$N was added dropwise to a carefully degassed solution of Pd(PPh$_3$)$_2$Cl$_2$ (60 mg, 14 mol%), CuI (40 mg, 35 mol%) and the aryl iodide (180 mg, 0.55 mmol) in 10 mL of Et$_3$N. The reaction was stirred overnight at room temperature under argon atmosphere. The mixture was then diluted with dichloromethane, washed with saturated aq NH$_4$Cl solution, dried over anhydrous Na$_2$SO$_4$ and the solvent was removed under reduced pressure. The residue was purified by flash chromatography (EtOAc/Hexane = 0:1 → 1:1) and recrystallization in hexane/dichloromethane to give **L** in 27% yield (162 mg) and the monocoupled product in 65% yield (337 mg) as orange solids.

***Compound* 19.** A suspension containing -alkylidyne complex **C02** (21 mg, 10 mol %) and dry powdered MS 5Å in toluene (1 mL) was stirred for 10 minutes. Then, a solution of the substrate **L** (160 mg, 0.11 mmol) in toluene (7mM) was added and stirred 24h at ambient temperature. The reaction crude was filtered through a short plug of silica, the filtrate evaporated and the residue purified by flash chromatography (Hexane/EtOAc= 10:0 → 1:1) and recrystallization in hexane/dichloromethane to give **19** (35 mg) in 24% as pale yellow solid. ^{1}H NMR (500 MHz, cdcl$_3$) δ 8.03 (s, 2H), 7.60 (s, 1H), 7.58 – 7.50 (m, 7H), 7.49 (d, *J* = 8.0 Hz, 1H), 7.40 – 7.35 (m, 3H), 7.31 (m, 2H), 4.51 (s, 2H), 3.49 (t, *J* = 6.6 Hz, 2H), 1.27 (bs, 20H), 0.89 (t, *J* = 6.7 Hz, 3H); ^{13}C NMR (126 MHz, cdcl$_3$) δ 173.7 (C), 139.4 (C), 135.7 (CHx2), 135.0 (CH), 132.1 (CH), 131.9 (CH), 131.5 (CH), 131.5 (CH) 131.4 (CH), 131.4 (CH), 131.2 (CH), 130.9 (CH), 128.8 (CHx4), 127.5 (CH), 125.8 (C), 125.7 (C), 124.7 (C), 124.6 (C), 124.4 (C), 123.9 (C), 123.8 (C), 123.7 (C), 123.6 (C), 94.0 (C), 93.0 (C), 92.7 (C), 92.6 (C), 89.24 (C), 89.21 (C), 89.1 (C), 88.8 (C), 88.5 (C), 79.0 (C), 72.2 (CH$_2$), 71.0 (CH$_2$), 32.1 (CH$_2$), 29.9 (CH$_2$), 29.84 (CH$_2$), 29.80 (CH$_2$), 29.79 (CH$_2$), 29.78 (CH$_2$), 29.6 (CH$_2$), 29.5 (CH$_2$), 26.4 (CH$_2$), 22.9 (CH$_2$), 14.3 (CH$_3$).

1.3. Objetive: Supramolecular approach to carbon networks based on base-pairing

Given the unavoidable increase in the insolubility concomitant to planarization of the 2D-polymers, at first glance a self-assembly approach could be an attractive alternative. For this reason, we started to explore the assembly capabilities of supramolecular cross-linked polymer networks. In this case, *para*-poly-phenylenes (*p*PPs) were chosen to behave as efficient conducts for long range energy transfer (molecular wires).[123] In the current approach, covalent polymeric backbones of PPPs could be tied together by nucleobase-pairing dictated by specific hydrogen bonding patterns (Figure 40).
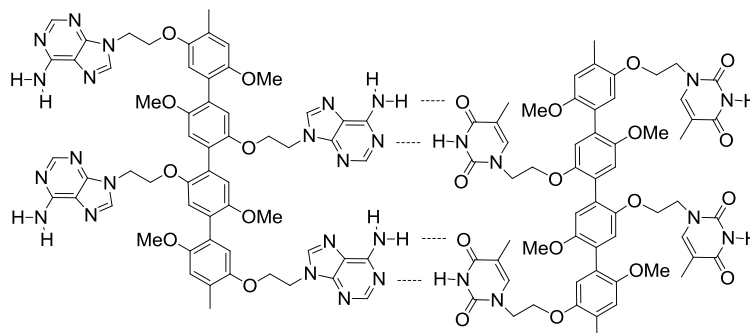
Figure 40. *Structure carbon network formed by wires of pPPs assembled by adenine-thymine interactions.*

The synthetic plan was organized in three different stages: 1) check the assembly of some model systems, 2) build a nucleobase-containing conjugated polymer generated by solid-phase methods with a defined length and 3) study the assembling phenomenon of these strands into a surface and the properties of the two-dimensional polymer generated by scanning probe microscopy. The following section shows only our first efforts to deal with this supramolecular approach. Further synthetic progress is ongoing in our laboratory.

---

[123] M. Banerjee, R. Shukla, R. Rathore, *J. Am. Chem. Soc.* **2009**, *131*, 1780–1786.

1.3.1. Background

Molecular self-assembly can be described as the thermodynamically controlled association of molecules into structurally well defined, stable aggregates through noncovalent interactions.[124] Hydrogen bonding between complementary bases of nucleic acids plays a key role in self-aggregation processes and the spatial arrangement of biological macromolecules such as DNA or RNA.[125] This unique supramolecular performance of nucleic acids has stimulated chemists to explore the possibilities of utilizing these features for the development of artificial polymers bearing nucleobases moieties in molecular nanotechnology and biotechnology.[126]

Contemporaneous with the above mentioned research, non-classical base-pairing patterns to the four elucidated by Watson and Crick have been deeply studied specially by Hoogsteen[127] and Sessler.[128] The interaction between two DNA strands is primarily mediated by four nucleobases adenine (A), thymine (T) – or uracil (U)-, guanine (G) and cytosine (C) (Figure 41). The two anti-parallel strands of DNA are held together by A–T and C–G base pairs to form the famous double helix. While the selectivity of these base-pair interactions is controlled mainly by hydrogen bonding, both π-π stacking and hydrophobic effects also play a role in stabilizing the resulting structure.
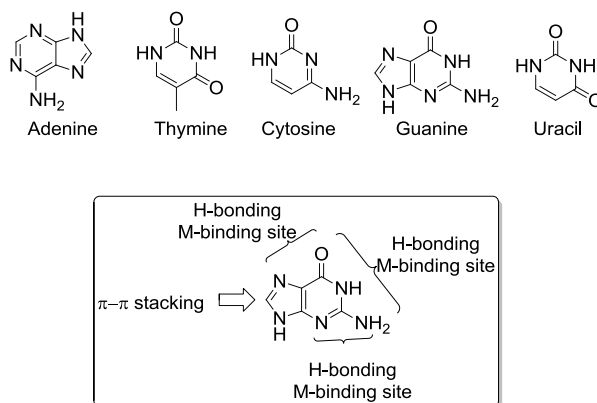
Figure 41. *Structure of the natural nucleobases and their potential binding sites. [From ref. 136]*

Utilization of the common nucleobases in supramolecular chemistry offers the flexibility of exploiting four different binding units A, C, G, and T (or U), all of which offer different binding characteristics. Other dimeric binding modes are also possible due to tautomerism and ionization of nucleobases. In addition to base dimerization, individual nucleobases can also form trimers and other higher order oligomers. Among the five nucleobases, guanine has the most diverse supramolecular chemistry, as it can self-assemble into discrete dimers and tetramers, or extended ribbon- and helix-shaped structures (Figure 42).[129] Despite far from our synthetic interests, guanine quartets' symmetry, convergent geometry, and ability to complex cations make it a versatile and often used component of functional supramolecular assemblies, including ion transporters, gelators, liquid crystals, drug-delivery vehicles, and DNA-based molecular machines.[130]

[124] G. M. Whitesides, J. P. Mathias, C. T. Seto, *Science* **1991**, *254*, 1312.

[125] G. A Jeffrey, W. Saenger, *Hydrogen Bonding in Biological Structures*; Springer: Berlin, **1991**.

[126] R. McHale, R. K. O'Reilly, *Macromolecules* **2012**, *45*, 7665–7675.

[127] (a) K. Hoogsteen, *Acta Crystallogr.,* **1963**, *16*, 907; (b) K. Hoogsteen, *Acta Crystallogr.,* **1959**, *12*, 822.

[128] (a) J. L. Sessler, D. J. Magda and H. Furuta, *J. Org. Chem.,* **1992**, *57*, 818; (b) J. L. Sessler and R. Wang, *J. Am. Chem. Soc.,* **1996**, *118*, 9808; (c) J. L. Sessler and R. Wang, *J. Org. Chem.,* **1998**, *63*, 4079.

[129] S. L. Forman, J. C. Fettinger, S. Pieraccini, G. Gottarelli, J. T. Davis, *J. Am. Chem. Soc.,* **2000**, *122*, 4060.

[130] S. Sivakova, S. J. Rowan, *Chem. Soc. Rev.* **2005**, *34*, 9–21.
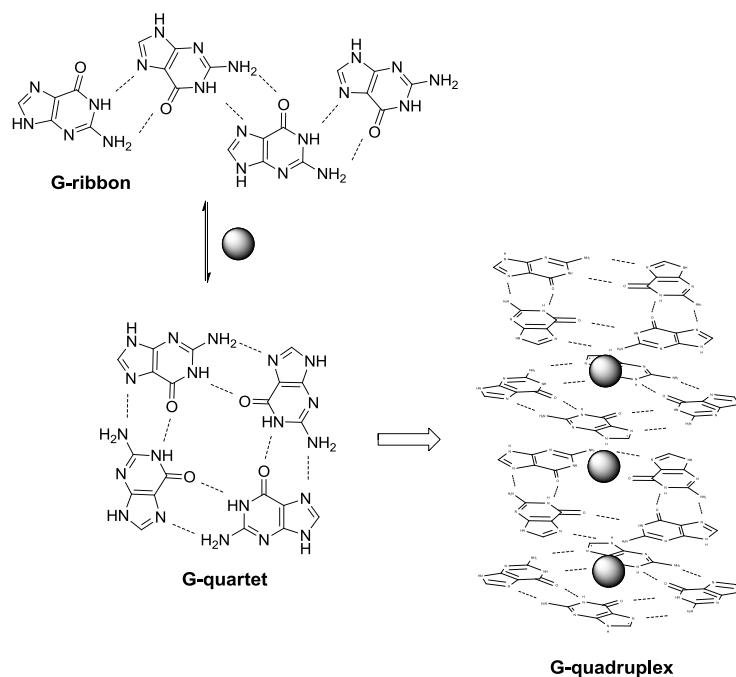
Figure 42. *Self-assembly of guanine derivatives into G-ribbon, G-quartet and G-quadruplex formed by stacking of G-quartets around a column of cations. [From ref. 136]*

Going back to the non-natural polymers, the main pioneers in the crossovers between synthetic self-assembly and nucleobase containing polymers have been Rotello and Sleiman groups. The first work from the Rotello group into this field involved the incorporation of side-chain functionalities such as diaminotriazine[131] or diaminopyridine[132] onto polystyrene-based polymers and the elegant demonstration of the assembly of individual chains with a thymine-based polymer via intramolecular H-bonding interactions (Figure 43).[133] Rotello group has also taken advantage of this polymer-mediated self-assembly to organize gold nanoparticles into highly ordered spherical arrays[134] and complementary polymer strands into giant vesicles.[135]

---

[131] (a) T. H. Galow, F. Ilhan, G. Cooke, V. M. Rotello, *J. Am. Chem. Soc.* **2000**, *122*, 3595-3598

[132] (b) F, Ilhan, T. H. Galow, M. Gray, G. Clavier, V. M. Rotello* *J. Am. Chem. Soc.* **2000,** *122,* 5895-5896

[133] (a) T. H. Galow, F. Ilhan, G. Cooke, V. M. Rotello, *J. Am. Chem. Soc.* **2000**, *122*, 3595-3598; (b) F, Ilhan, T. H. Galow, M. Gray, G. Clavier, V. M. Rotello* *J. Am. Chem. Soc.* **2000,** *122,* 5895-5896; (c) Ilhan, F.; Gray, M.; Blanchette, K.; Rotello, V. *Macromolecules* **1999**, *32*, 6159.

[134] Boal, A. K.; Ilhan, F.; DeRouchey, J. E.; Thurn-Albrecht, T.; Russell, T. P.; Rotello, V. M. Nature 2000, 404, 746–748.

[135] (a) Boal, A. K.; Ilhan, F.; DeRouchey, J. E.; Thurn-Albrecht, T.; Russell, T. P.; Rotello, V. M. Nature 2000, 404, 746–748, (b) Thibault, R. J.; Galow, T. H.; Turnberg, E. J.; Gray, M.; Hotchkiss, P. J.; Rotello, V. M. J. Am. Chem. Soc. 2002, 124, 15249– 15254.
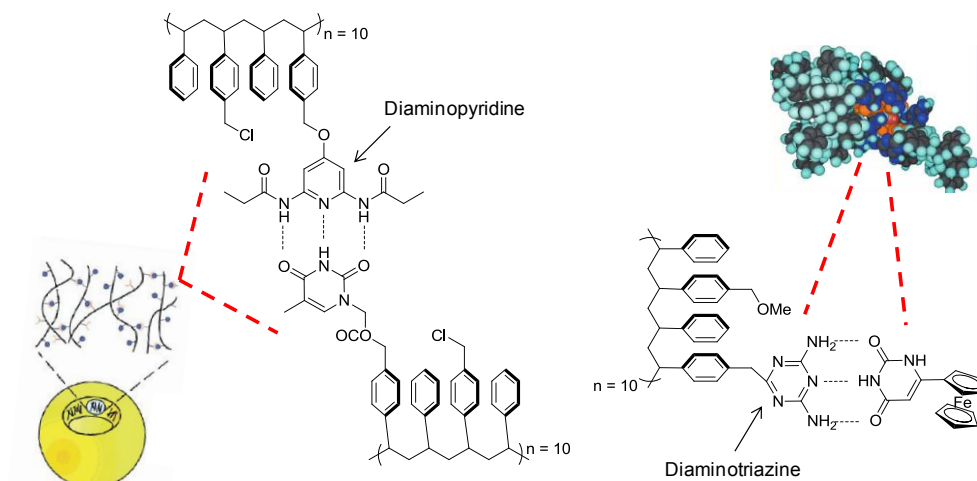
Figure 43. *Two polystyrene-based polymers functionalized with side-chains able to assemble in three dimensional vesicles. [From ref. 133 and ref. 137]*

Sleiman group has also intensively investigated about self-assembly and synthetic nucleobase systems with an emphasis on ring-opening metathesis polymerizations (ROMP). This group work, focused on template polymerization, is arguably the most fundamental and synthetically rewarding goal in the field of nucleobase containing polymers in the last years. Recently they reported a particularly attractive methodology to synthesize PPE polymers in solution inspired by the precise copying of the sequence and length of a DNA or RNA strand into a daughter polymer (Figure 44).[136] The use a thymine-substituted-polymer generated by living ring-opening metathesis polymerization[137] as the template strand ("primer") allowed the faithful transfer of chain length and polydispersity to a second adenine-PPE polymer daughter strand synthesized by nucleobase-templated Sonogashira polymerization.
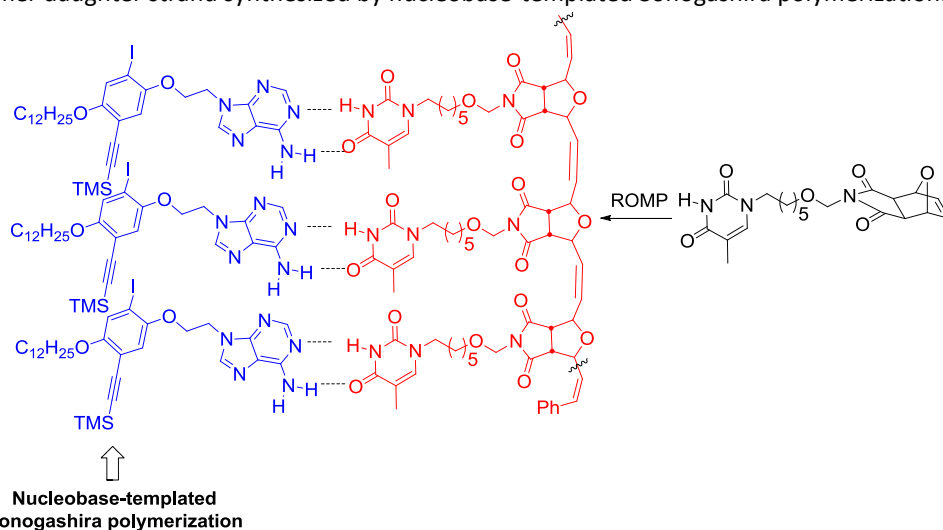
Figure 44. *Sleiman strategy to cop the chain length and polydispersity of living polymers into conjugated polymers. [From ref. 143]*

van Hest, Lutz and Gross laboratories have also explored the controlled polymerization of nucleobase containing monomers. Initially concentrating on the atom transfer radical polymerization (ATRP) methodology described by Haddleton *et al.*,[138] van Hest group demonstrated that Cu(I)-ATRP can also be used to polymerize protected all four nucleobase methacrylate monomers in a controlled fashion

---

[136] P. K. Lo, H. F. Sleiman, *J. Am. Chem. Soc.* **2009**, *131*, 4182–4183.

[137] B. Chen, K. Metera, H. F. Sleiman, *Macromolecules*, **2005**, *38*, 1084-1090.

[138] (a) Khan, A.; Haddleton, D. M.; Hannon, M. J.; Kukulj, D.; Marsh, A. *Macromolecules* **1999**, *32*, 6560, (b) Marsh, A.; Khan, A.; Haddleton, D. M.; Hannon, M. J. *Macromolecules* **1999**, *32*, 8725.

(Scheme 26).[139] Lutz *et al.* started their contributions to the field preparing nucleobase functionalized styrene-like copolymers via ARTP and demonstrating the DNA-like melting behavior in nonpolar solvents.[140] Gross *et al.* polymerized with ATRP unprotected adenine- and thymine-based monomers using polyethylene glycol macroinitiators in order to obtain amphiphilic block copolymers.[141] These diblock copolymers showed an assembly behavior that was affected by the presence of the complementary nucleobases.

Scheme 26. *van Hest Cu(I)-ATRP.*
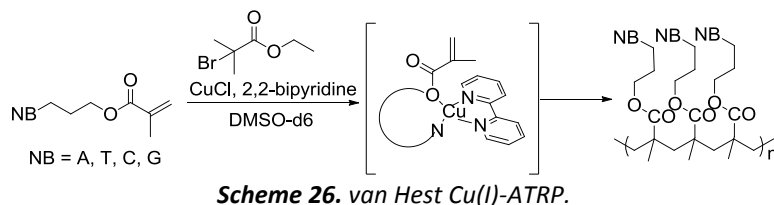
The nucleobase derivatives T and A, have also been attached to a bis(4-alkoxy)-substituted bis(phenylethynyl)benzene core to obtain a supramolecular, liquid crystalline, fluorescent polymeric material by Rowan *et al.* (Figure 45).[142]
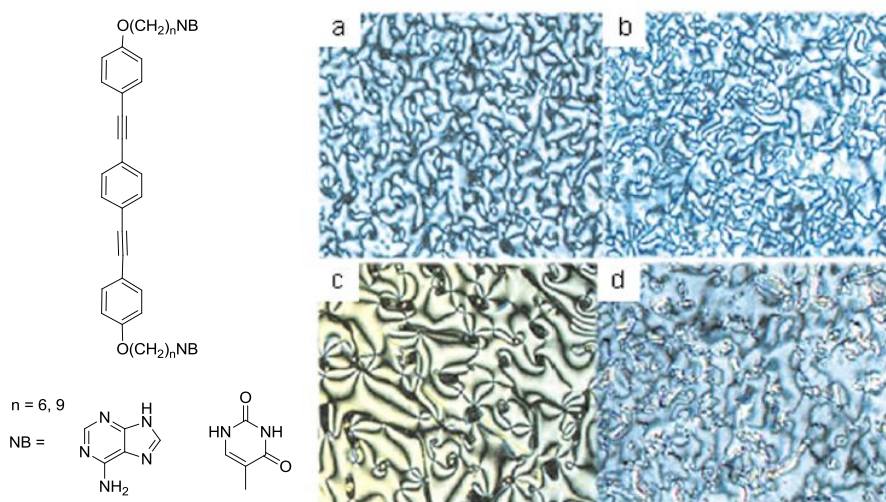
Figure 45. *LC formation of nucleobase-terminated pPE rods (left). Polarized optical micrographs of bifringent textures observed (right). [From ref. 149a]*

[139] H. J. Spijker, F- L. van Delft, J. C. M. van Hest, *Macromolecules,* **2007**, *40*, 12–18.

[140] J.-F. Lutz, A. F. Thünemann, K. Rurack, *Macromolecules*, **2005**, *38*, 8124−8126.

[141] T. Glauser, M. Ranger, B. Kalra, W. Gao, J. Hedrick, R. A. Gross, *Polym. Prepr. (Am. Chem. Soc., DiV. Polym. Chem.)* **2003**, *44*, 624.

[142] (a) S. Sivakova and S. J. Rowan, *Chem. Commun.* **2003**, 2428-2429; (b) S. Sivakova, J. Wu, C. J. Campo, P. T. Mather, S. J. Rowan, *Chem. Eur. J.* **2006**, *12*, 446.

1.3.2. Results and discussion

Initial work was focused on the synthesis of monomers **20**-**25**, containing adenine and thymine units connected to different conjugated backbones (Figure 46).
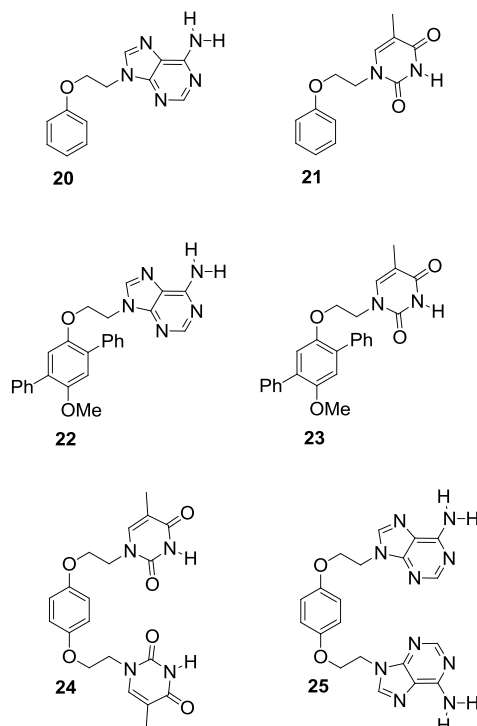
Figure 46. *Model structures **20**-**25** to check the assembly.*

Both phenoxy-ethyl-pyrimidine **20** and purine **21** were obtained by direct alkylation of the corresponding nitrogenous base (2-iodoethoxy)benzene in moderate yields.[143] The formation of base pairs between both compounds was then examined by ¹H-NMR. Intermolecular hydrogen-bonding was confirmed with downfield shifts of the NH resonances of adenine **20** from 5.82 to 6.24 ppm, and of thymine **21** from 8.65 to 10.47 ppm (Figure 47).

---

[143] See experimental section.
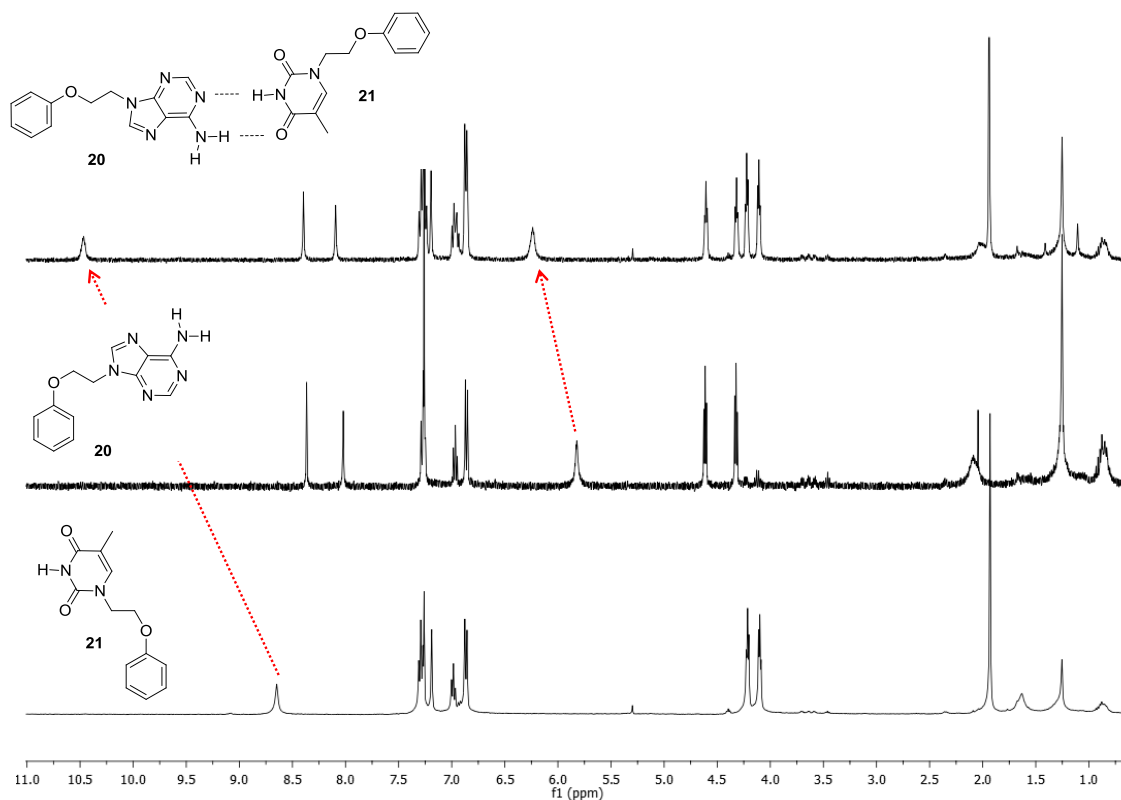
Figure 47. ^{1}H-NMR spectra in CDCl₃ of **21** and **22** (bottom) and ^{1}H-NMR nucleobase-assembly experiment (top).

In order to check if this assembling phenomenon could be efficiently translated into a two-dimensional network, we obtained the bis-functionalized analogs **24** and **25** from hydroquinone.[144] However both products resulted to be quite insoluble and we could not obtain any proper spectra of their assembly in solution. Only a weak hint of binding could be observed when we mixed compound **25** with **20** (Figure 48).[145]

---

[144] See experimental section.

[145] Due to the low solubility of compound **24** in CDCl₃, the spectra was recorded in MeOH-d4 and the labile NH-6 of the purine dissapeared as a consequence of the exchange of this proton with the acidic deuterium ion of the solvent. The red arrow indicates the change from the chemical shift for this proton assuming that it appeares at a similar value that the one registered for its shorther analog **21**.
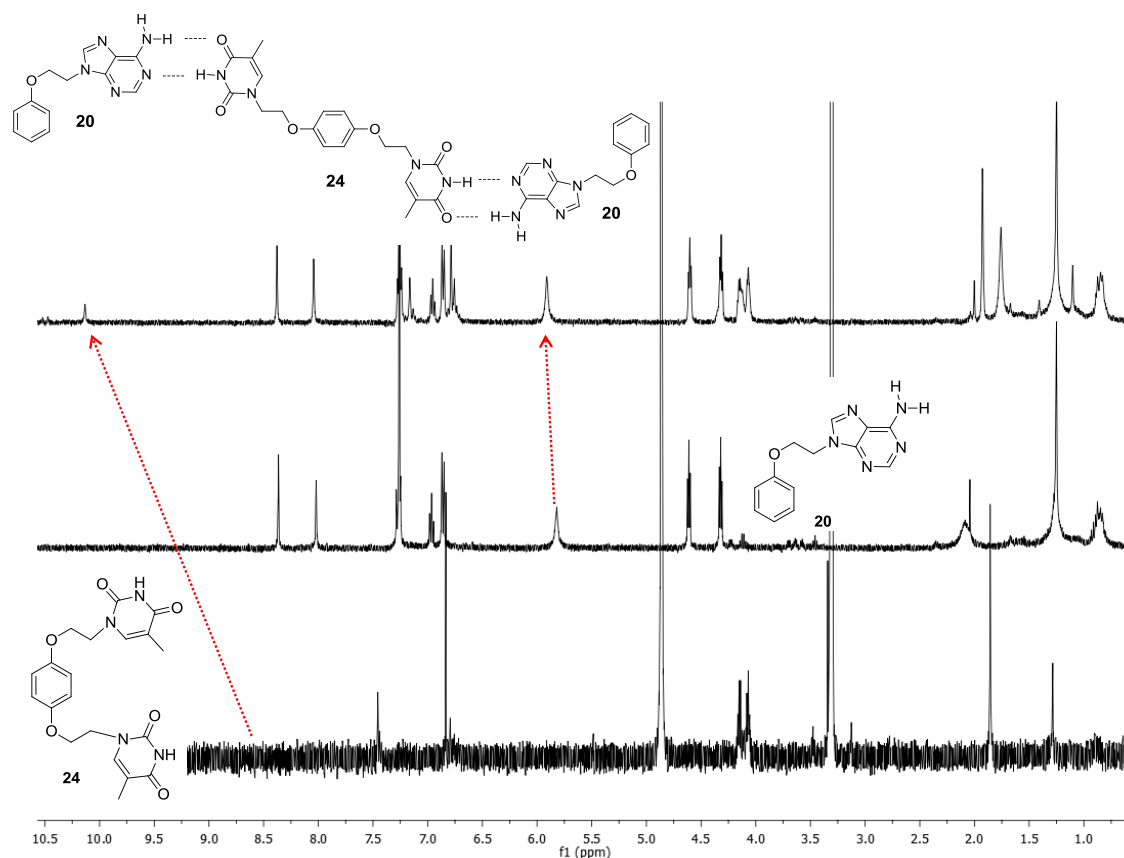
Figure 48. ^{1}H-NMR spectra of **24** in CD$_3$OD and of **20** in CDCl$_3$ (bottom) and ^{1}H-NMR nucleobase-assembly experiment (top).

Finally, we synthesized the mono-functionalized compounds **22** and **23** as the shortest *p*PP mimics. The assembly of both fragments was also supported by the changes observed in the NH-6 of the thymine but the peak corresponding to the adenine-NH$_2$ could not be detected (Figure 49).
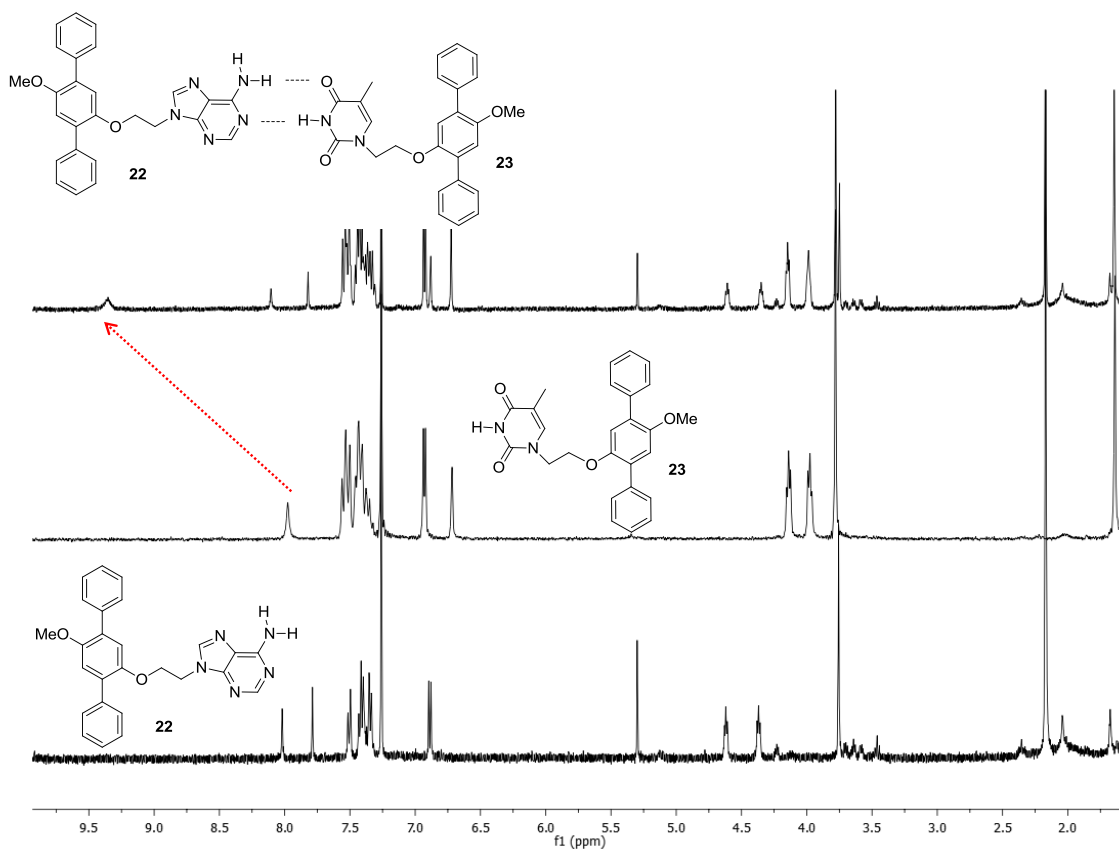
Figure 49. ^{1}H-NMR spectra of **22** and **23** in CDCl$_3$ (bottom) and ^{1}H-NMR nucleobase-assembly experiment (top).

1.3.3. Conclusions and outlook

We have synthesized the adenine-functionalized monomers **20-22-24** and their thymine-counterparts **21-23-25.** Complementary monomers **20** and **21** self-assemble into supramolecular aggregates in aprotic solvents. However, in other systems the self-assembly was not so clear.

As future work, we are interested in exploring the responses of related oligomers with longer polar side chains in order to enhance the solubility of these products. On the other hand, other threefold hydrogen bonding motifs for which higher association constants have been reported (Figure 50), are attractive alternatives to improve the self-assembly.[146]
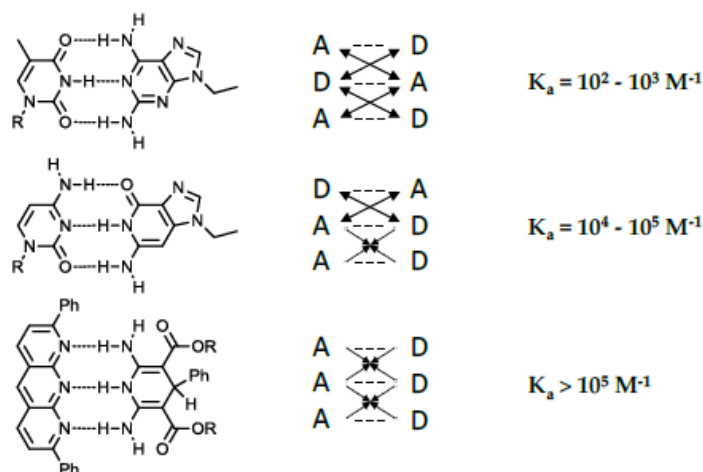
Figure 50. *Other complexes with threefold hydrogen bonding motifs (left) and their binding constants measured in chloroform (right). [From ref. 153b]*

1.3.4. Experimental section

1. General procedures:

Alkylation of adenine. (GP3)
The iodide derivate (1 mmol) was added to a stirred solution of adenine (2.5 mmol), sodium hydride (3.5 mmol) in DMF under Ar. The reaction mixture was heated to 60 °C overnight under Ar. After cooling to room temperature, the DMF was evaporated under reduced pressure. The remaining syrup was diluted with EtOAc (3x50 mL) and washed with water six times, dried over anhydrous Na_2SO_4, filtrated and evaporated to dryness. The pure product was isolated through a silica-gel column chromatography using CH_2Cl_2: MeOH mixtures and a subsequent recrystallization.

Alkylation of timine. (GP4)
The iodide derivate (1 mmol) was added to a stirred solution of thymine (3 mmol), potassium carbonate (3.5 mmol) in DMF under Ar. The reaction mixture was heated to 60 °C overnight under Ar. After cooling to room temperature, the reaction mixture was extracted with EtOAc (3×50 mL). The combined organic layers were washed with water six times, dried over anhydrous Na_2SO_4, filtrated and evaporated to dryness. The pure product was isolated through a silica-gel column chromatography using CH_2Cl_2: MeOH mixtures and a subsequent recrystallization.

2. Synthesis and analytical characterization of the compounds:

---

[146] (a) H. Zeng, H. Ickes, R. A. Flowers, B. Gong, *J. Org. Chem.* **2001**, *66*, 3574; (b) P. S. Corbin, S. C. Zimmerman, *J. Am. Chem. Soc.* **2000**, *122*, 3779; (c) W. L. Jorgensen, J. Pranata, *J. Am. Chem. Soc.* **1990**, *112*, 2008; (d) Pranata, S. G. Wierschke, W. L. Jorgensen, *J. Am. Chem. Soc.* **1991**, *113*, 2810; (e) T. J. Murray, S. C. Zimmerman, *J. Am. Chem. Soc.* **1992**, *114*, 4010; (f) J. Sartorius, H.-J. Schhneider, *Chem. Eur. J.* **1996**, *2*, 1446.
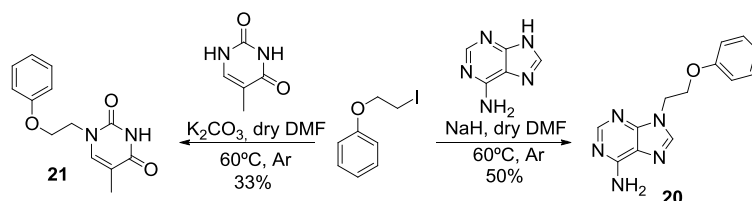
Compound 20 was prepared from 1-Iodo-2-phenoxyethane[147] (184 mg, 0.74 mmol) and adenine (200 mg, 1.44 mmol) according to previously described **GP3** to give **20** in 50 % yield (95 mg) as a white solid. ^{1}H NMR (400 MHz, CDCl$_3$): δ (ppm) = 8.36 (s, 1H, purine H-2), 8.02 (s, 1H, purine H-8), 7.29 − 7.24 (m, 2H), 6.96 (t, *J* = 7.4 Hz, 1H), 6.86 (d, *J* = 7.9 Hz, 2H), 5.82 (bs, 2H, purine NH$_2$), 4.61 (t, *J* = 4.9 Hz, 2H), 4.32 (t, *J* = 4.9 Hz, 2H).

Compound 21 was prepared from 1-Iodo-2-phenoxyethane (144 mg, 0.58 mmol) and thymine (220 mg, 1.74 mmol) according to previously described **GP4** to give **21** in 33 % yield (47 mg) as a white solid. ^{1}H NMR (600 MHz, CDCl$_3$): δ (ppm) = 9.14 (bs, 1H, pyrimidine NH), 7.29 (t, *J* = 7.9 Hz, 2H), 7.19 (s, 1H, pyrimidine H-6), 6.98 (t, *J* = 7.3 Hz, 1H), 6.86 (d, *J* = 8.1 Hz, 2H), 4.21 (t, *J* = 4.8 Hz, 2H), 4.10 (t, *J* = 4.8 Hz, 2H), 1.93 (s, 3H); ^{13}C NMR (151 MHz, CDCl$_3$, DEPT): δ (ppm) = 164.4 (C), 158.0 (C), 151.1 (C), 141.7 (CH), 129.8 (CH), 121.7 (CH), 114.6 (CH), 110.3 (C), 65.8 (CH$_2$), 48.2 (CH$_2$).
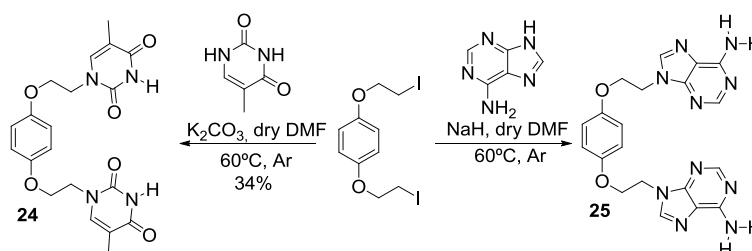
Compound 24 was prepared from 1,4-bis(2-iodoethoxy)benzene (330 mg, 2.39 mmol) and thymine (300 mg, 2.39 mmol) according to previously described **GP4** to give **24** in 34 % yield (47 mg) as a white solid. ^{1}H NMR (400 MHz, CD$_3$OD): δ (ppm) = 7.46 (s, 2H), 6.83 (s, 2H), 4.15 (d, *J* = 4.9 Hz, 4H), 4.07 (d, *J* = 4.9 Hz, 4H), 1.86 (s, 6H).

Compound 25 was prepared from 1,4-bis(2-iodoethoxy)benzene[148] and adenine according to previously described **GP3** to give **25** as a brick-stone-like insoluble white solid.
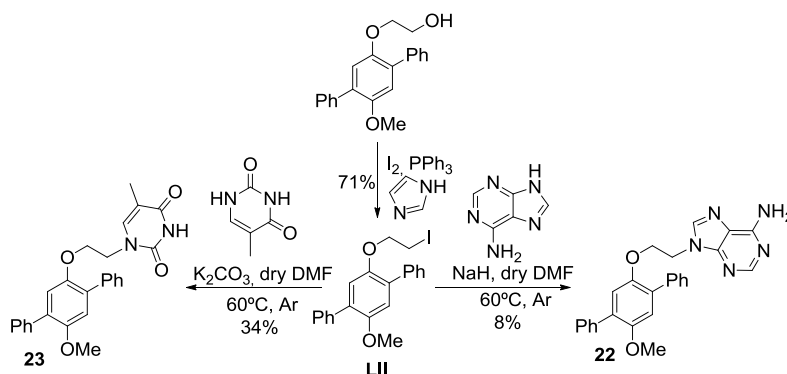
Compound LII. To a solution of I$_2$ (214 mg, 0.84 mmol) in dry CH$_2$Cl$_2$ (20 mL) was added the PPh$_3$ (220 mg, 0.84 mmol), giving the solution a brown-yellow color. Then, imidazole (122 mg, 2.1 mmol) was

[147] G. Cahiez, O. Gager, A. Moyeux, T. Delacroix, *Adv. Synth. & Catal.,* **2012**, *354*, 1519–1528.
[148] H. Ito, Y. Ishida, K. Saigo, *Tetrahedron Letters*, **2006**, *47*, 3095–3098.

added, changing the color to light yellow. Subsequently, a solution of the alcohol[149] (270 mg, 0.84 mmol) in dry CH_2Cl_2 was added and the solution was stirred for 15 min at room temperature. After that time, the completely consumption of the starting material was checked by TLC, hence the crude was diluted in CH_2Cl_2, washed with water, dried over anhydride Na_2SO_4 and the solvent removed. The residue was submitted to flash chromatography (EtOAc/hexane = 9:1 → 7:3) to give **LII** in 71 % yield (257 mg) as a pale yellow solid. ^{1}H NMR (400 MHz, CDCl_3): δ (ppm) = 7.65 (d, *J* = 7.6 Hz, 2H), 7.58 (d, *J* = 7.6 Hz, 2H), 7.48 – 7.41 (m, 4H), 7.39 – 7.33 (m, 2H), 6.99 (s, 2H), 4.16 (t, *J* = 6.8 Hz, 2H), 3.80 (s, 3H), 3.29 (t, *J* = 6.8 Hz, 2H).

Compound **22** was prepared from **LII** (100 mg, 0.23 mmol) and adenine (77 mg, 0.57 mmol) according to previously described *GP3* to give **22** in 8 % yield (10 mg) as a white solid. ^{1}H NMR (400 MHz, CDCl_3): δ (ppm) = 8.02 (s, 1H, purine H-2), 7.79 (s, 1H, purine H-8), 7.51 (d, *J* = 7.6 Hz, 2H), 7.51-7.34 (m, 8H), 6.90 (s, 1H), 6.88 (s, 1H), 5.30 (s, 2H), 4.62 (t, *J* = 4.6 Hz, 1H), 4.37 (t, *J* = 4.5 Hz, 2H), 3.76 (s, 3H); ^{13}C NMR (151 MHz, CDCl_3, DEPT): δ (ppm) = 155.4 (C), 153.0 (C), 151.4 (C), 149.1 (C), 138.0 (C), 131.3 (C), 130.7 (C), 129.5 (CH), 128.3 (C), 127.5 (CH), 127.4 (CH), 116.4 (CH), 114.7 (CH), 67.7 (CH_3), 56.5 (CH_2), 43.6 (CH_2).

Compound **23** was prepared from **LII** (100 mg, 0.23 mmol) and thymine (88 mg, 0.7 mmol) according to previously described *GP4* to give **23** in 34 % yield (33 mg) as a white solid. ^{1}H NMR (600 MHz, CDCl_3): δ (ppm) = 8.78 (bs, 1H, pyrimidine NH), 7.55 (d, *J* = 7.6 Hz, 2H), 7.51 (d, *J* = 7.5 Hz, 2H), 7.45-7.41 (m, 4H), 7.38(t, *J* = 7.2 Hz, 1H), 7.35 (t, *J* = 7.2 Hz, 1H), 6.93 (s, 1H), 6.92 (s, 1H), 6.71 (s, 1H, pyrimidine H-6), 4.20 – 4.09 (m, 2H), 4.05 – 3.92 (m, 2H), 3.78 (s, 3H), 1.63 (s, 3H); ^{13}C NMR (151 MHz, CDCl_3, DEPT): δ (ppm) = 164.2 (C), 151.3 (C), 150.9 (C), 149.0 (C), 141.9 (CH), 138.4 (C), 138.0 (C), 130.9 (C), 130.8 (C), 129.52 (CH), 129.50 (CH), 128.3 (CH), 128.3 (CH), 127.5 (CH), 127.4 (CH), 115.8 (CH), 114.9 (CH), 110.0 (C), 67.4 (CH_3), 56.5 (CH_2), 48.3 (CH_2).

3. ^{1}H-NMR nucleobase-assembly experiments (representative example):

Compound **21** (10 mg, 0.041 mmol) was dissolved in 0.5 mL CDCl_3 (82 mM), transferred into a NMR-tube and the ^{1}H-NMR spectrum registered. Then, this solution was added into a vial with compound **20** (10.37 mg, 0.041 mmol). The suspension was mixed using a Pasteur pipette until the solid was completely dissolved. The ^{1}H-NMR spectrum of the mixture showed the downfield shift of both NH-protons (Δδ (Adenine) = 0.42 ppm, Δδ (Thymine) = 1.82 ppm) which evidenced the formation of the nucleobase-pairing.

---

[149] N. Fuentes, L. Álvarez de Cienfuegos, A. Parra, D. Choquesillo-Lazarte, J. M. García-Ruiz, M. L. Marcos, E. Buñuel, M. Ribagorda, M. C. Carreño, D. J. Cárdenas, J. M. Cuerva, Chem. Commun*., ***2011**,*47*, 1586-1588.

CHAPER II. Synthesis and characterization of graphyne-based helical scaffolds.

2.1. Introduction

The functionality of biomacromolecules is embedded into their three dimensional structure. For example, proteins fold by precise controlling non-covalent interactions such as hydrogen bonds, π-stacking, electrostatics and solvophobics, consequently creating binding sites with proper functional groups that efficiently recognize substrates.[150]

From an organic chemist´s perspective, strategies to construct molecular entities with defined 3D dimension, shape and functionality frequently belong to the realm of synthesis and supramolecular chemistry. Using guidelines from nature and the molecular construction kit developed by the scientific community, a diverse set of functional entities appeared in the last decades. Among the vast variety of functional nanostructures, helices are probably the most abundant motifs.[151]

Limiting the topic to unnatural polymers and concerning the strategies to generate synthetic macromolecules with orientational-spatial (3D) control, the more succeful progress has been provided by the *foldamer* concept.[152] A *foldamer* is defined as a synthetic chain molecule or oligomer that adopts a conformationally ordered state in solution by a collection of non-covalent interactions between non-adjacent monomer units.[153] For certain applications, structural robustness of helical structures is demanded and some methodologies to covalently lock such supramolecular arrangement have been developed.

2.1.1.Strategies to induce the helical arrangement

2.1.1.1.Non-specific supramolecular forces

Non-specific supramolecular forces such as solvophobic interactions and π-stacking of aromatic units have been the more recurrent tools to stabilize the secondary structure. For a variety of synthetic backbones, cooperative collapse of random-coil into a compact helix has been experimentally performed using solvent mixtures or temperature.[154] The underlying phenomena can be easily understood thinking in a specific case. For example, according to a two state transition model, the energy associated with the helix formation involves an entalphic stabilization derived from monomer-monomer interactions in poorly solubilising media which outweights entropy penalty to restrict the conformation (Figure 51). Thus, if the solvent composition is gradually changed from a pure "denaturant" solvent to a poor solvent, a cooperative behaviour consistent with helix formation can be monitored using several techniques.

[150] H. Juwarker, J.-M. Suk, K.-S. Jeong, *Chem. Soc. Rev.* **2009**, *38*, 3316-3325.

[151] O. Vogl, D. Jaycox, *Polymer*, **1987**, *28* (13), 2179–2182.

[152] V. Dehm, M. Büchner, J. Seibt, V. Engel, F. Würthner, *Chem. Sci.*, **2011**, 2, 2094.

[153] (a) D. J. Hill ,M. J. Mio, R. B. Prince, T. S. Hughes, J. S. Moore, *Chem. Rev.* **2001,** *101,* 3893-4011; (b) H. Juwarker, J. Suk, K. Jeong, *Chem. Soc. Rev.*, **2009**, *38*, 3316-3325.

[154] D. J. Hill ,M. J. Mio, R. B. Prince, T. S. Hughes, J. S. Moore, *Chem. Rev.* **2001,** *101,* 3893-4011.
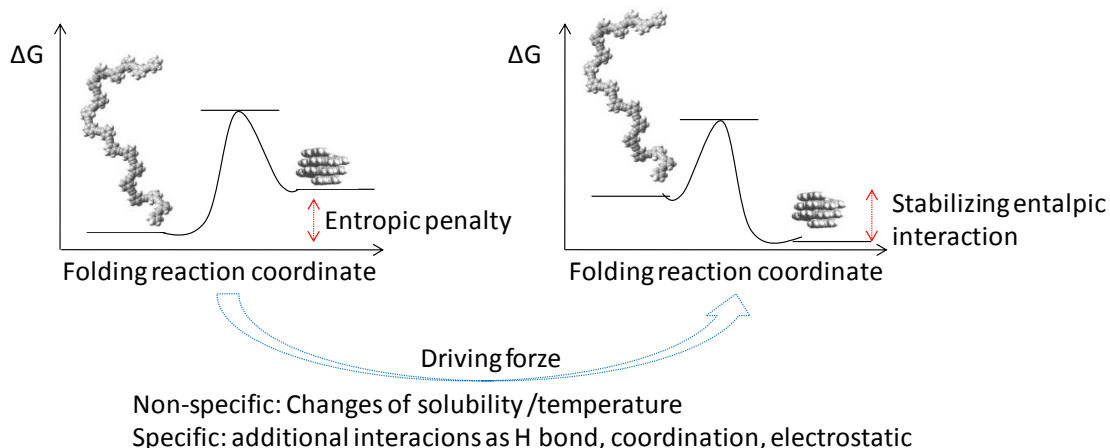
Figure 51. *Schematic representation of how stabilizing driving forzes transform the fonding in a "spontaneous" process.*

The first application of such solvophobically driven strategy in all-carbon foldamers was reported in 1997 by Moore *et al.*[155] The model system developed by this group consisted on polar side chains (Tg= triethylene glycol) connected to a mPEOs backbone through ester groups. Preparing a collection of solutions of this oligomer in solvents mixtures going from 100% chloroform ("denaturant" solvent) to 100% acetonitrile ("naturant" solvent), spectroscopic properties were recorded. In this system *transoid* to *cisoid* conformations display different spectroscopic features being an excellent track to follow the folding phenomemon.[156] For example, isolated and stacked cross-conjugated monomer units show direct and excimer-like emission respectively (Figure 52 right). Analysis of the titration data to obtain the thermodynamic constant of the folding is made by plotting the normalized fluorescence intensity at the helix Λ_{max} against the amount of "naturant" solvent (Figure 52 left). Similar procedures involving changes on temperature and other techniques as UV-vis absorption and CD spectroscopy[157] has also been used to study this phenomenon.
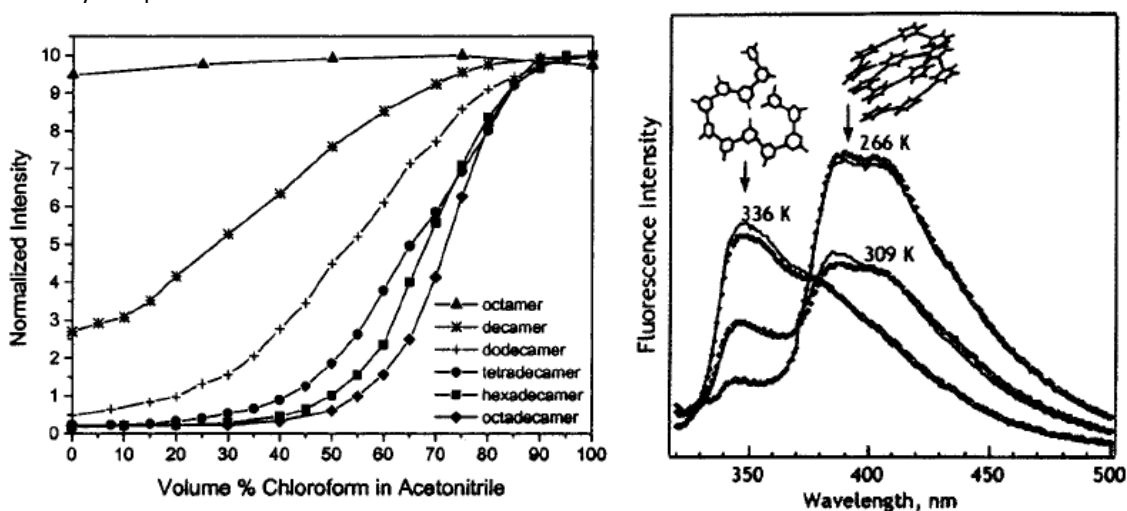
Figure 52. *Schematic representation of how stabilizing driving forzes transform the fonding in a "spontaneous" process.*

During the last decade, uncountable solvophobically driven folding into helical structures have been reported with an aromatic backbone. In particular, polar,[158] amphyphilic[159] and apolar oPEOs up to nine

---

[155] J. C. Nelson, J. G. Saven, J. S. Moore, P. G. Wolynes, *Science*, **1997,** *277,* 1793-1796.

[156] W. Y. Yang, R. B. Prince, J. Sabelko, J. S. Moore, M. Gruebele, *J. Am. Chem. Soc.* **2000**, *122*, 3248-3249.

[157] See for example: R. B. Prince, J. S. Moore, L. Brunsveld, E. W. Meijer, *Chem.Eur. J.* **2001**, *7*, 4150-4154.

[158] M. P. Patel, W. Liu, J. West, D. P. Tew, T. D. Meek, S. H. Thrall, *JACS*, **2005,** *44 (50)*, 6753–16765.

[159] T. Helgaker, W. Klopper, D. P. Tew, *N J Chem*, **2008**, *106,* 2107-2143.

benzene rings[160] have been experimentally and theoretically[161] studied by Tew group following the original concept developed by Moore for mPEOs (Figure 53).
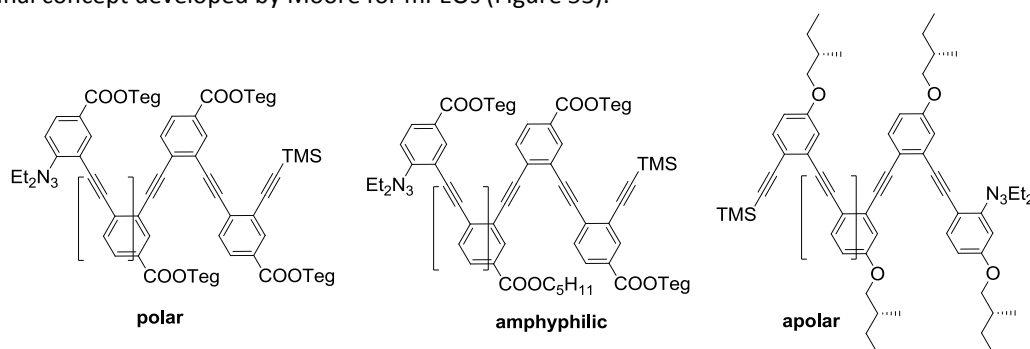
Figure 53. *Types of oPE foldamers developed by Tew et al.*

o-Phenylenes have recently received increasing attention because they exhibit weak delocalization quite sensitive to substituent effects and short o-phenylene oligomers are strongly predisposed to folding into well-defined helical conformations in solution (Figure 54).[162] In this context, Fukushima and Aida *et al.* have reported a remarkable helical o-phenylene oligomer that spontaneously resolves in the solid state and undergoes a large decrease of its racemization rate on oxidation.[163] More recently, they have demonstrated a solvent effect whereby acetonitrile appears to uniquely promote the folding of theirmethoxy-functionalized o-phenylene oligomers into "perfect" helices as occurred for its expanded o- and mPE analogs.[164]
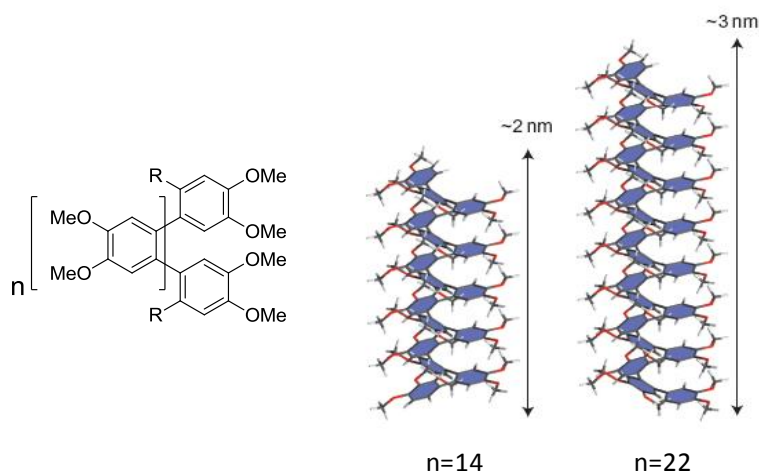
Figure 54. *Chemical structure of o*-phenylenes *substituted with methoxy groups (left). Schematic structure of the helical configuration reported by Aida et al. [From ref. 172]*

2.1.1.1.Specific supramolecular forces

A proper understanding of specific (directionals) non-covalent such as hydrogen bonds and host-guest interactions has also opened the door to a new variety of foldable molecular oligomers. Much emphasis has been placed on the role of hydrogen bonds in stabilizing secondary structure. In 1994, Hamilton and co-workers reported the first generation of helices based on aromatic amide foldamers.[165] In this

[160] J. Jiang, M. M. Slutsky, T. V. Jones, G. N. Tew, *New J. Chem.* **2010**, *34*, 307.

[161] R. A. Blatchly, G. N. Tew, *JOC,* **2003**, *68*, 8780-8785.

[162] S. M. Mathew, J. T. Engle, C. J. Ziegler, C. S. Hartley, *J. Am. Chem. Soc.* **2013**, *135*, 6714−6722.

[163] E. Ohta, H. Sato, S. Ando, A. Kosaka, T. Fukushima, D. Hashizume, M. Yamasaki, K. Hasegawa, A. Muraoka, H. Ushiyama, K. Yamashita, T. Aida, *Nat. Chem.* **2011**, *3*, 68−73.

[164] S. Ando, E. Ohta, A. Kosaka, D. Hashizume, H. Koshino, T. Fukushima, T. Aida, *J. Am. Chem. Soc.* **2012**, *134*, 11084−11087.

[165] Y. Hamuro, S. J. Geib, A. D. Hamilton, *Angew. Chem.* **1994**, 446-448.

seminal paper, two compact structures were described. An extended sheet conformation stabilized by six membered NH····O=C hydrogen bonding between 2-substituted antranilamide units, and a helical conformation resulted from intramolecular H bonding in a oligomer composed by 2,6-pyridinedicarboxamide rings (Figure 55). Several works from Huc[166] and Lehn[167] *inter alia* have carried out detailed studies on such bis-*meta*-substitued pyridines in which interconnected amide groups favoured kinked conformations. Related oligomers composed by alternating pyridine-pyrimidine,[168] pyridine-pyridazine[169] and naphthyridine-pyrimidine[170] units have been synthesized and shown to adopt helical conformations by hydrogen bonding or metal coordination.

2-substituted antranilamide   **2,6-pyridinedicarboxamide**   **pyridine-pyrimidine oligomers**

pyridine-pyridazine oligomers   **naphthyridine-pyrimidine oligomers**
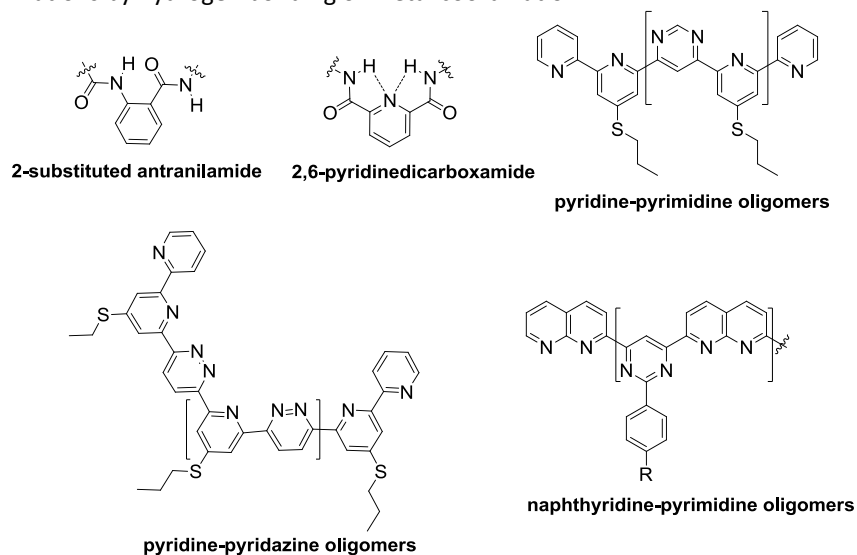
Figure 55. *Some N-funtionalized oligomers which adopt folded conformations by* hydrogen bonding or metal coordination

At the same time, a significant amount of work has been conducted on chain molecules that fold upon binding ionic species. The term *helicate* coined by Lehn *et al.* in 1987, refers specifically to those formed by metal ion coordination.[171] In this family of oligomers, the folding reaction of these backbones is coupled to the assembly-disassembly process of metal coordination.[172] Pyrroles, pyridines and imines and other Lewis basic functionalities have been incorporated into single-stranded oligomers to bind a variety of metal ions in different stoichiometries and with predictable geometries due to their substitution patterns along the aromatic rings.

Oligopyridines are probably the most thoroughly studied poly-heterocyclic ligands and helicates based on *c*oordination to a lot of different transition-metal ions including Co(II),[173] Co(III),[174] Cu(II), Ni(II),[175] Pd(II),[176] Cr(III),[177] Y(III),[178] Ag(I)[179] and Cu(I)[180] and have been pusblished. For example, different helical

[166] See e.g.: H. Jiang, J. Léger, I. Huc, *J. Am. Chem. Soc.,* **2003**, *125*, 3448.

[167] See e.g.: Lehn, J.-M. et al. *ACIE,* **1997**, *36*, 1845.

[168] G. S. Hanan, J. Lehn, N. Kyritsakas, J. Fischer, *J. Chem. Soc., Chem. Commun.*, **1995**, *765*.

[169] D. P. Funeriu, K. Rissanen, J.-M. P. Lehn, *ACIE*, **2000**, *39*, 233.

[170] A.-M. Stadler, N. Kyritsakasb, J.-M. Lehn, *ACIE* **2002**, *41*, 1195.

[171] J. M. Lehn, A, Rigault, J. Siegel, J. Harrowfield, B. Chevrier, D. Moras, *Proc. Natl. Acad. Sci. U. S. A.* **1987,** *84*, 2565-2569.

[172] For a in depth review: H. Miyake, H. Tsukube, *Chem. Soc. Rev.,* **2012**, *41*, 6977-6991.

[173] W. Von Henke, S. Kremer, D. Z. Reinen, *Anorg. Allg. Chem,* **1982**, *491*, 124-136.

[174] E. N. Maslen, C. L. Raston, A. H. White, *J. Chem. Soc., Dalton Trans.* **1975**, 323-326.

[175] E. C. Constable, S. M. Elder, J. Healey, D. A. Tocher, *J. Chem. Soc., Dalton Trans.* **1990**, 1669-1674.

[176] (a) E. C. Constable, S. M. Elder, J. Healy, M. D. Ward, D. A. Tocher, *J. Am. Chem. Soc.* **1990**, *112*, 4590-4592, (b) M. T. Stone, J. S. Moore, *J. Am. Chem. Soc.* **2005**, *127*, 5928-5935.

[177] E. C. Constable, S. M. Elder, D. A. Tocher, *Polyhedron* **1992**, *11*, 1337-1342.

[178] E. C. Constable, S. M. Elder, D. A. Tocher, *Polyhedron* **1992**, *11*, 2599-2604.

[179] Q. Ren, C. G. Reedy, E. A. Terrell, J. M. Wieting, R. W. Wagie, J. P. Asplin, L. M. Doyle, S. L. Long, M. T. Everard, J. S. Sauer, C. E. Baumgart, J. S. D´Acchioli, N. P. Bowling, *J. Org. Chem*. **2012**, *77*, 2571-2577.

conformations in solid-state and solution occurs upon coordination a quinquepyridine to Re(I) or Re(III) (Figure 56). When Re(I) is added, a dinuclear helicate where the metal ions partition the oligomer into two bipy segments leaving the central pyridine uncoordinated was isolated while a mononuclear helicate occurs by interannular twists in the hole backbone in the presence of Re(III) ions.[181]
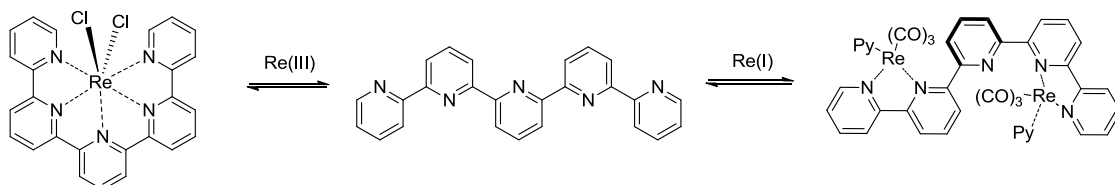
Figure 56. *Example of diferent helical conformations adopted by the same quinquepyridine upon coordination to Re(I) or Re(III).*

Oligopyridines can also adopt double-stranded helical conformations depending on the coordination metal ion employed. Crystal structures of sexipyridine complexes revealed a binuclear double-helix with Cd(II) but a trinuclear double helicate with Cu(II).[182] In these cases, multiple-helical conformations are a result of the system maximizing coordination bonds and aromatic-aromatic stacking while minimizing the number of components in the assembly.[183]

Helicates incorporating symmetric oligomers do not possess strand directionality. Incorporation of chiral fused or side chain moieties has been explored in a similar way that has been traditionally done for helicenes[184] to induce chiral bias. For example, strands incorporating fused chiral (1S)-(-)-R-pinene end groups formed *P* helical complexes with Ag(I) while the (1R,1R)-(+)-R-pinene-terminated strand led to the *M* helicate (Figure 57).[185]

(1S,1S)-(+)-L

[Ag$_2${(1S,1S)-L}$_2$] [PF$_6$]
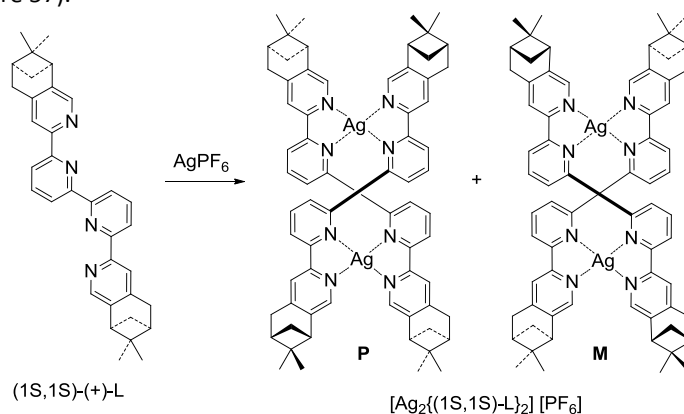
Figure 57. *Chiral (1S)-(-)-R-pinene end groups induce the preferential formation of a P double-stranded helical complex with Ag(I).*

The origin of selectivity arose from interactions of the pinene end groups with the pyridine ligands in the backbone. Such chiral oligopyridine backbones have also been incorporated into Dutch-door-like aryl-

---

[180] A. Orita, T. Nakano, D. L. An, K. Tanikawa, K. Wakamatsu, J. Otera, *J. Am. Chem. Soc.* **2004**, *126*, 10389-10396.

[181] P. K. Ho, K.-K. Cheung, S.-M. Peng, C.-M Che, *J. Chem. Soc., Dalton Trans.* **1996**, 1411-1417.

[182] E. C. Constable, S. M. Elder, J. Healy, M. D. Ward, D. A. Tocher, *J. Am. Chem. Soc.* **1990**, *112*, 4590-4592.

[183] A wider overview about multiple-stranded helices: E. Yashima, K. Maeda, Y. Furusho, *Accounts of chemical research*, **2008**, *41*, 1166-1180.

[184] Y. Shen, C.-F. Chen, *Chem. Rev.* **2012**, *112*, 1463.

[185] (a) G. Baum, E. C. Constable, D. Fenske, T. Kulke, *Chem. Commun.* **1997**, 2043-2044; (b) E. C. Constable, T. Kulke, M. Neuburger, M. Zehnder, *Chem. Commun.* **1997**, 489-490; (c) G. Baum, E. C. Constable, D. Fenske, C. E. Housecroft, T. Kulke, *Chem. Eur. J.* **1999**, *5*, 1862-1873.

ethynyl foldamers to restricte the rotation around the biaryl-axel into a chiral helicate by coordination with Zn(II) (Figure 58).[186]
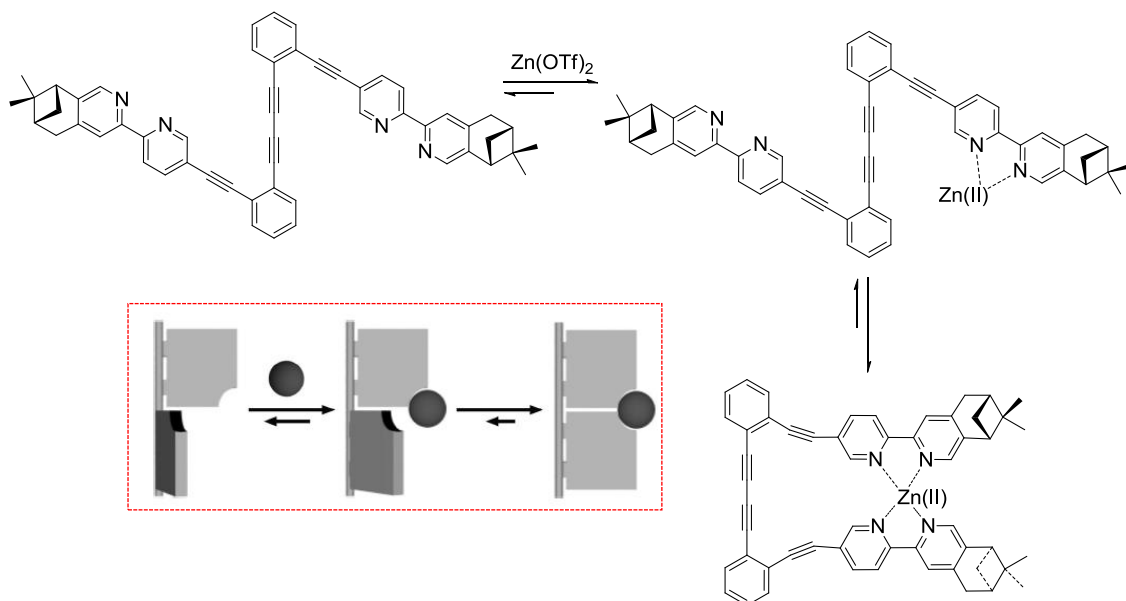
Figure 58. Chiral Dutch-door-like aryl-ethynyl foldamers formed by Zn(II) chelation.

The success of both the above mentioned metal-template approaches are based on the superior coordination capabilities of the heteroatoms towards those metals. A modification of the tubular cavity of a mPEO decorated with nitrile functionalities led to the first example of mPEO whose secondary structure could be controlled by both nonspecific (solvophobic) and specific (metal-coordination) interactions.[187] Since the coordinating group was introduced every two building blocks, three nitriles per turn formed a trigonal planar complex (Figure 59).
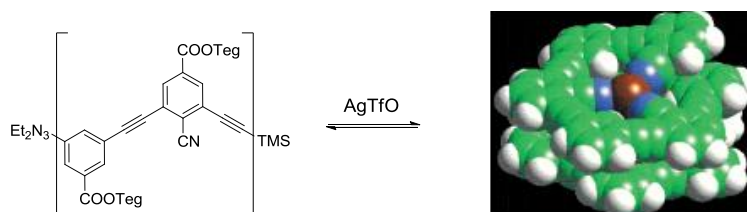
Figure 59. Moore Ag(I)-mPE helicate.

Similarly to oligopyridines, Mitzunati group reported the folding of acyclic porphyrin derivatives known as bilinones into helical conformations in the presence of Zn(II) (Figure 60 left).[188] Together with the metal-template folding strategy briefly depicted above, there is vast literature concerning other host-guest interactions which promote folding into helical arrangements. Compared to their cation-binding analogues, anion-binding helical foldamers are far less common due to the lack of discrete denticity in anion coordination chemistry. For example, Sessler *et al.* reported that a discrete "S"-shaped conformation in solution and in the solid state is adopted by 5,15,25-tris-nor-hexapyrrins with chloride ions while the fully conjugated hexapyrrin adopted a completely planar conformation in which one chloride ion rests in each of the two clefts generated in the "S" (Figure 60 right). [189]

[186] J. Jung, J. Jo, M. Laskar, D. Lee, *Chem Eur J.* **2013**, *19*, 5156-5168.

[187] R.B. Prince, T. Okada, J. S. Moore, *Angew. Chem*., **1999**, *38*, 233-236.

[188] T. Mizutani, S. Yagi, T. Morinaga, T. Nomura, T. Takagishi, S. Kitagawa, H. Ogoshi, *J. Am. Chem. Soc.* **1999**, *121*, 754-759.

[189] J. L. Sessler, S. J. Weghorn, V. Lynch, K. Fransson, *J. Chem. Soc., Chem. Commun.* **1994**, 1289-1290.
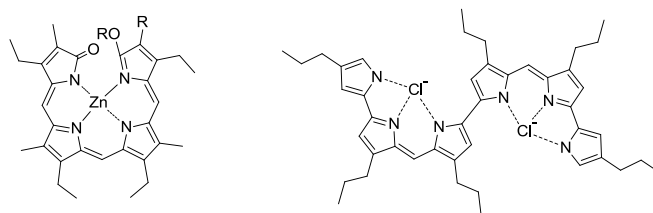
Figure 60. *Cation-binding and anion-binding motifs in acyclic porphyrin derivates.*

A more promising field in anion-templated folding has been investigated by Jeong *et al.*[190] This group has recently reported several works on oligoindoles,[191] indolocarbazoles[192] and diphenylureas[193] linked by ethylene units as anion receptors. Three different anions, chloride, sulfate and (R)-10-camphorolsulfonate, have successfully led to these oligomeric backbones to fold into compact helical structures (Figure 62).
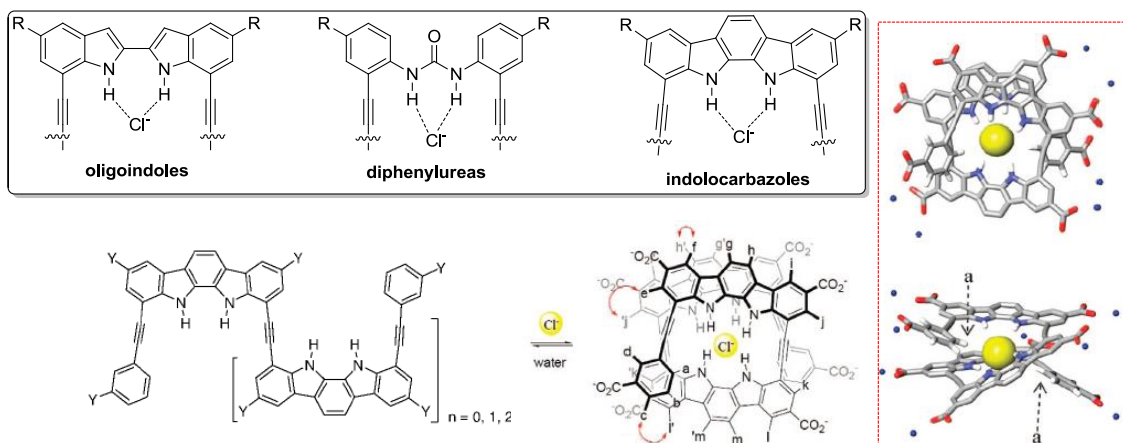
Figure 61. *Different anion-binding helicates developed by Jeong et al. [From ref.202]*

2.1.2. Potential applications of unnatural helices

Potential applications of helical polymers related to chemistry fundamentally involve catalysis, chemical sensing and substrate-carries which it is frequently translated as enzyme mimicking with biotechnological applications. Beyond chemistry and biology, other cutting-edge fields in which structure-function relationship occupies a central role are nanotechnology and material science. These sciences focus on the creation and miniaturization of materials with tunable topologies which lead to controllable micro- and nanosized features.

2.1.2.1. Helical polymers as enantioselective catalysts

Successful examples of single stranded helices able to act as asymmetric catalyst are still rare. However, Yashima *et al.*have reported a work a in which a metal-directed doublestranded helicate is able to catalyze an asymmetric cyclopropanation reaction of styrene with ethyl diazoacetate (Scheme 27).[194] Their results suggest that the alkynyl units oh the Pt-helicate accommodate Cu(I) ions in a tweezer-like fashion. The chiral space generated by the double helix is effective and indispensable for the high enatioselectivity, thus providing a promising and conceptually new strategy in the field of supramolecular catalysis.[195]

[190] K.-J. Chang , B.-N. Kang , M.-H. Lee, K.-S. Jeong, *J. Am. Chem. Soc.* **2005**, *127*, 12214.

[191] CEJ 2008, 14, 11406.

[192] J.-M. Suk , K.-S. Jeong, *J. Am. Chem. Soc.* **2008**, *130*, 11868.

[193] M. J. Kim,H.-W. Lee,D. Moon,K.-S. Jeong *Org. Lett,* **2012**, *14 (19)*, 5042-5045.

[194] T. Hasegawa, Y. Furusho, H. Katagiri, E. Yashima, *Angew. Chem., Int. Ed.* **2007**, *46*, 5885–5888.

[195] E. Yashima, K. Maeda, Y. Furusho, *Accounts of chemical research*, **2008**, *41*, 1166-1180.
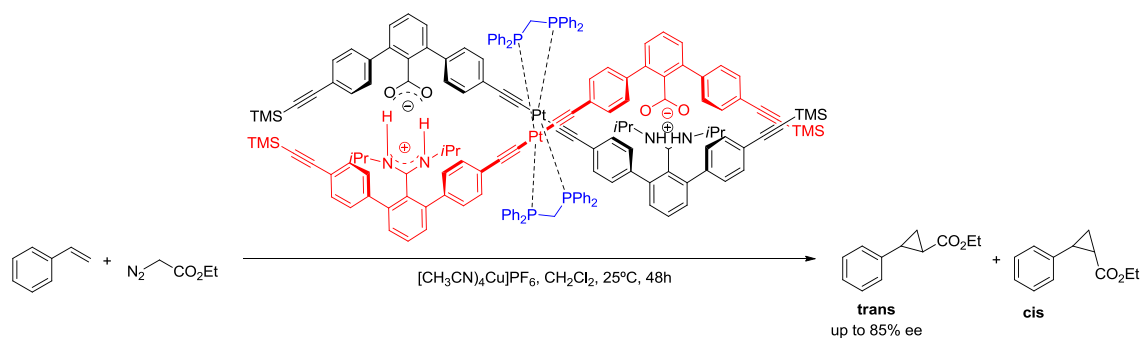
Scheme 27. *Double-helicate which catalyzes asymmetric cyclopropanation.*

2.1.2.2. Unnatural helices as enzyme mimics: recognition and reactivity

Several ground-breaking works reported by Moore *et al.* have paved the way to use this foldamer as enzyme mimics. For example, sulfonates have been used as substrates of artificial enzymes emulated by pyridine-containing mPEOs (Figure 62). Monitoring the progress of methylation the mPEOs (enzyme) by different size methyl sulfonate esters (substrates), this group has ventured down the path in developing foldamers that can perform chemical transformations.[196] Other enzyme functions such as recognition phenomena of small terpenes[197] and sugars[198] have also been developed.
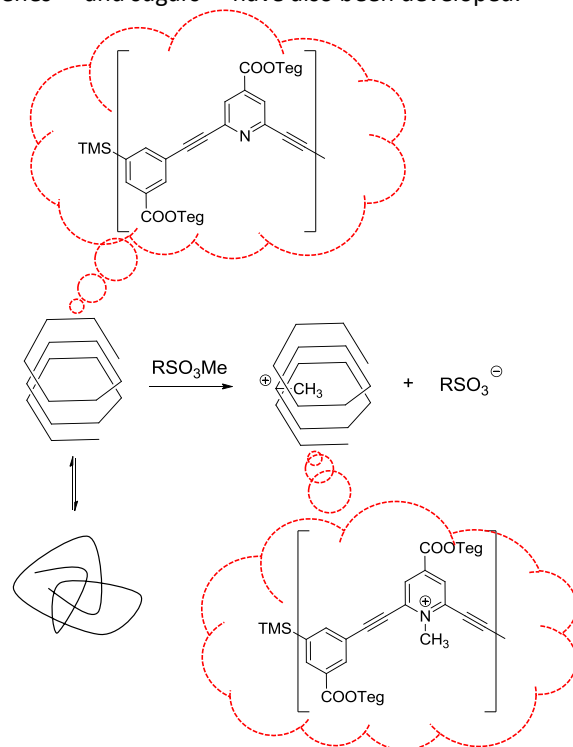
Figure 62. *Schematic representation of one enzyme mimic reported by Moore.*

2.1.2.3. All-carbon helices as solenoids: helical structure and electronic function

Solenoids offer two nice examples of how chemical research looks for applications in nanotechnology and material science. In 1990, Motojima *et al.* developed a synthetic method to produce regular helical carbon coils (CNCs) with high productivity and duplicability (Figure 63).[199] Among the various properties

---

[196] R. A. Smaldone, J. S. Moore, *JACS*, **2007**, *129*, 5444-5450.

[197] R. B. Prince, S. A. Barnes, J. S. Moore, *JACS,* **2000**, *122*, 2758.

[198] M. Inouye, M. Waki, H. Abe, *JACS*, **2004**, *126*, 2022 (b) H. Abe, Y. Ohishi, M. Inouye, *JOC*, **2012**, *77*, 5209.

[199] (a) S. Motojima, M. Kawaguchi, K. Nozaki, H. Iwanaga, *Appl. Phys. Lett.* **1990**, *56,* 321; (b) X. Chen, S. Motojima, H. Iwanaga, *Carbon*, **1999**, *37*, 1817-1823.

studies for such material, they observed using a transmission electron microscope coupled to a focused ion beam (FIB) system, that when a direct current passes through a carbon coil, a micro-magnetic field is generated from the coil.[200] This magnetic field is easily controlled by changing the current, thus, mimicking the behavior of a micro-solenoid.
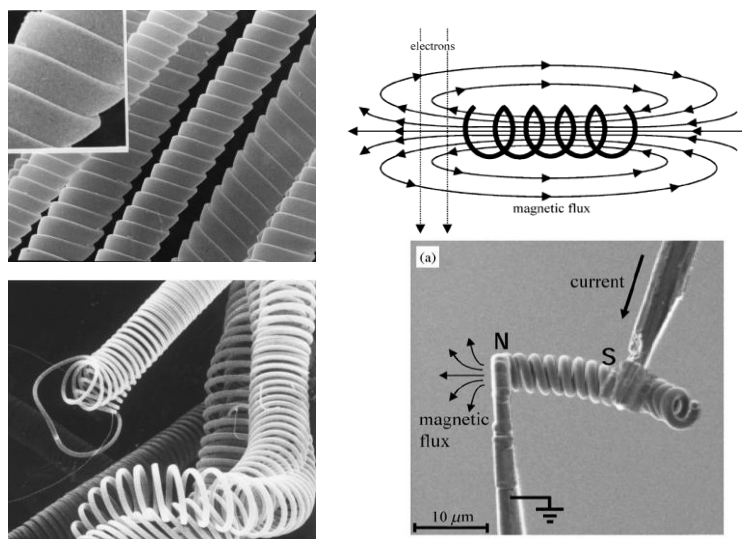
Figure 63. *Representative SEM images of the flat (top left side) and circular (bottom left side) carbon coils. llustration of magnetic field generated from a coil (top right side). Scanning ion electron microscopy (SIM) image of a single carbon coil connected to two electrodes (bottom right side). [From ref. 209b and 210]*

A completely different approach to fabricate nanosolenoids has been recently reported by Li *et al.* (Figure 64). Taking advantage of the self-assembly of oligomeric sequences of perylene diimides (PDIs) able to give strong intermolecular π-π* electronic transitions, Li *et al.* experimentally elucidated using NMR spectroscopy and theoretical calculation that such macromolecules exhibit a great ring-current effect consistent with a nanosolenoidal shielding caused by a reinforcement of the magnetic field.[201]
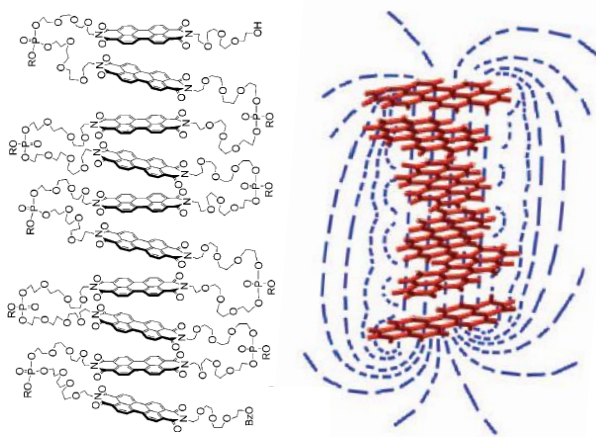
Figure 64. *Chemical structure of a PDI foldamer (left). Schematic representation of how PDI stacks form a nanosolenoid responsible for the reinforcing ring-current effect in NMR experiments (right). [From ref. 211]*

[200] K. Yamamoto, T. Hirayama, M. Kusunoki, S. Yang and S. Motojima, *Ultramicroscopy* **2006**, *106*, 314-319.

[201] A. D. Shaller, W. Wang, A. Li, G. Moyna, J. J. Han, G. L. Helms, *A. D. Q. Li. CEJ*, **2011**, *17*, 8350-8362.

2.2. Objetive: A Versatile Bottom-up Approach to Stapled *o*-Phenylene Ethynylene Oligomers[202]

As benzocyclines, phenylene-ethynylene oligomers can be considered cutouts of graphyne (Figure 65). While *para*-phenylene-ethynylene oligomers have been extensively studied as molecular wires, *ortho*- and *meta*-connected oligomers have received less attention.
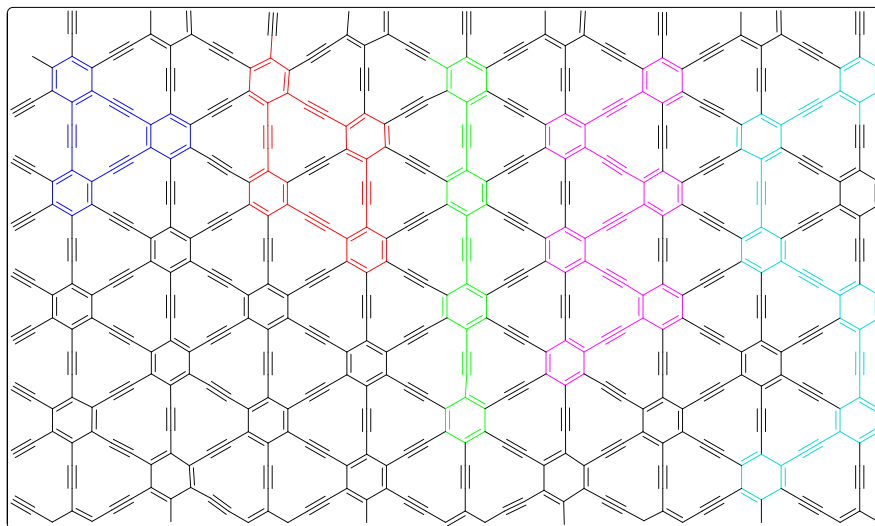
Figure 65. *[12]DBA **1** (dark blue), tetrabenzocycline **11** (red) and para- (green), ortho- (pink) and meta- (pale blue) phenylene-ethynylene oligomers depicted as graphyne fragments.*

As we have seen in the introduction, oligomers of phenylacetylene can fold into helical structures due to the conformational freedom of their backbones. Looking for new applications of such conducting molecules, we hypothesized that restricting the conformational flexibility of *o*-phenylene-ethynylene oligomers which feature a full linearly conjugated backbone, we could fabricate helical wires (Figure 66). Thinking in the potential applications, if the the *covalent stapling*[203] of conformationally dynamic *o*-PEOs would be made by insulating spacers which would impose a distance between superposed rings longer than the well-stablished distance for π-π stacking interactions, these helices could emulate at the nanoscale the behaviour of a macroscopic solenoid. Moreover, if the oligomer flexibility were maintained after the *stapling*, these helices could also behave as molecular-springs under tensile loading.

---
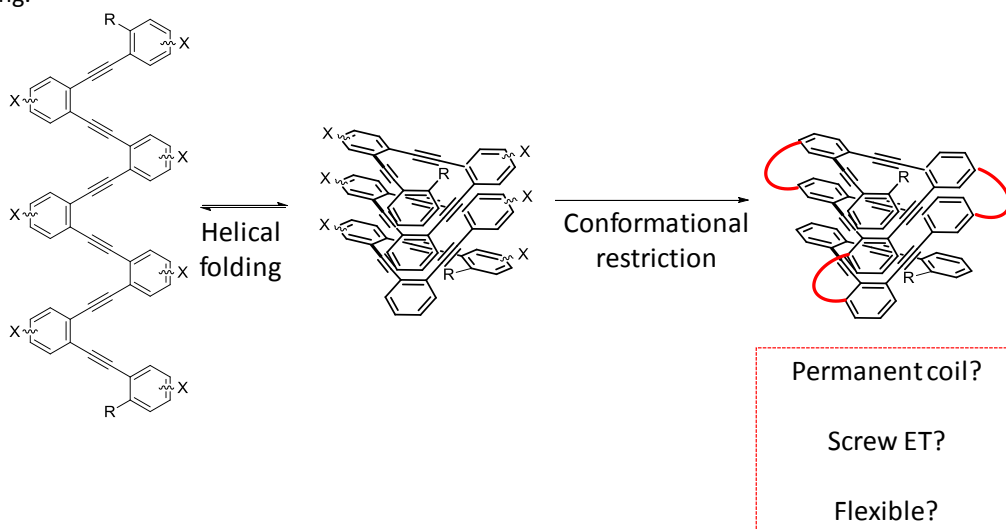
[202] This section has been developed in collaboration with Dr. Fuentes. Part of this work has been developed in Prof. Carreño laboratory. Universidad Autónoma de Madrid (UAM). Madrid, Spain..

[203] E. Yashima, K. Maeda, H. Iida, Y. Furusho, K. Nagai, *Chem. Rev.* **2009**, *109*, 6102-6211.

95

Figure 66. Working hypothesis towards the synthesis of stapled molecular helices with potential applications as molecular solenoids and molecular springs.

In the following pages, we will show the synthesis and characterizacion of the smallest mimick of such potential helical wire (Figure 67).
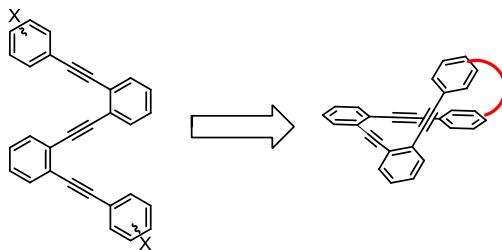
Figure 67. Schematic representation of the approach developed in section 2.2.

2.2.1.Background: Covalent stabilization of the helical arrangement by intramolecular crosslinking

Covalent stapling as a strategy to enforce the helical structure of peptides has been independently reported by Verdine[204] and Grubbs.[205] For example, Verdine utilized ruthenium-catalyzed ring closing alkene metathesis (RCM) to cross-link two unnatural amino acids located on adjacent helical turns (Figure 68). This modification was proved to enhance the helicity and thereby the metabolic stability (increased resistance to proteolysis) of these peptides compared to their natural analogs.[206]
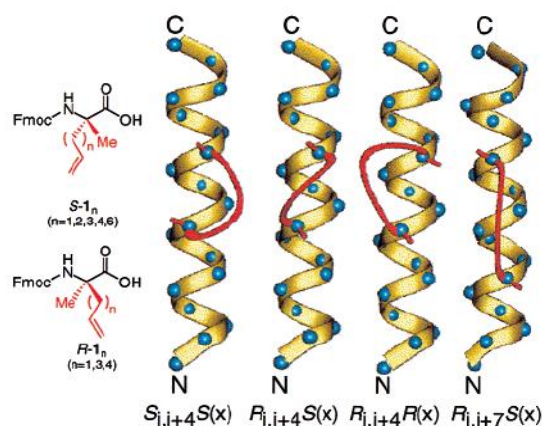
Figure 68. *Structures of the two enantiomeric unnatural aminoacids used by Verdine et al. to stabilize α-peptidic-helices via ring-closing olefin metathesis [From ref. 216]*

In the field of unnatural oligomers, *meta*-phenylene-ethynylenes have been covalently crosslinked by Hecht[207] and Moore. Hecht and Khan introduced reactive cinnamate functional groups, able to suffer [2+2] photodimerization, to a *m*PE polymeric backbone (Figure 69). When polymer was irradiated under high dilution conditions in a folding-promoting solvent such as acetonitrile, the helical structure was transformed into an organic nanotube.[208]
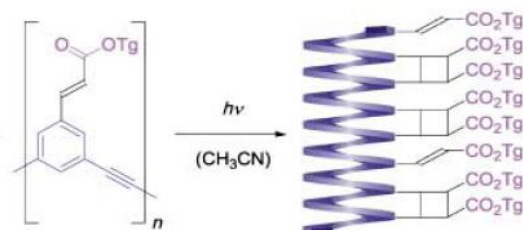
Figure 69. *Hecht and Khan´s strategy to develop organic carbon nanotubes by [2+2] photodimerization of the cinnamate side-chains. [From ref. 219]*

Using a reductive amination-based methodology, Moore´s group has restricted the unfolding of mPE backbones in which aldehyde moieties were placed.[209] A three carbon diamine spacer (1,3-diamino-2,2-dimethylpropane) was the best length to bridge a single turn of the helix (Figure 70).[210]

[204] Y.-K. Kim, P. S. Kutchukian, G. L. Verdine, *Org. Lett.,* **2010**, *12,* 3046-3049.

[205] See e. g.: H. E. Blackwell, R. H. Grubbs, *Angew. Chem., Int. Ed.* **1998**, *37*, 3281-3284.

[206] See e.g.: C. E. Schafmeister, J. Po, G. L. Verdine, *J. Am. Chem. Soc.* **2000**, *122*, 5891–5892.

[207] M. A. Balbo Block, C. Kaiser, A. Khan, S. Hecht, *Top. Curr. CHem*. **2005**, *245*, 89-150.

[208] S. Hecht, A. Khan, *Angew. Chem*. *Int. Ed.* **2003**, *42*, 6021–6024.

[209] R. A. Smaldone, E.-C. Lin, J. S. Moore, *J. Pol. Sci., Part A: Pol. Chem.* **2010**, *48(4)*, 927-935.

[210] The reductive amination strategy proceeded in ca. 20% yield.
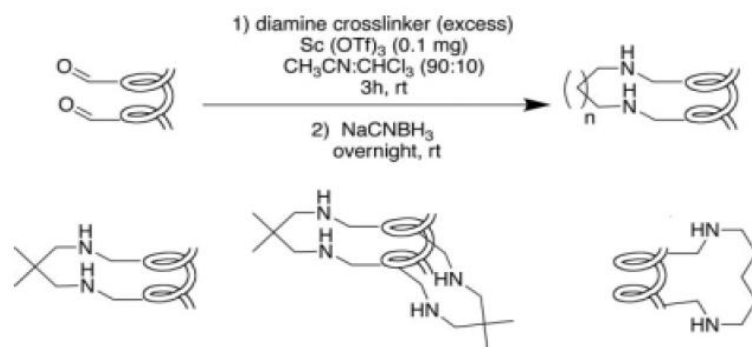
Figure 70. *Moore et al. reductive amination strategy to lock the helical conformation of mPE foldamers (top). Three different foldamers with crosslinks placed at different locations in the backbone (bottom).*

2.2.2. Results and discussion

2.2.2.1.Conformational restriction (macrociclization) of *o*PE tetramers by double esterification

Firstly, we prepared four different *o*-phenylene ethynylene (*o*PE) tetramers using Sonogashira coupling of the corresponding bromo and iodo derivatives to assemble the carbon skeleton (Scheme 28). Compound **26** was submitted to direct lactamization through the activation of the acid group with dicyclohexylcarbodiimide (DCC) and dimethylamino-pyridine (DMAP) in dichlorometane. Disappointingly, this methodology led to the unreactive N-acyl urea intermediate.[211] Then, we attempted to perform the macrocyclization using malonyl chloride and DMAP in dry dichloromethane of compounds **27**, **28** and **29**. Despite compound **27** led to a complex mixture of polymers, we obtained cyclic products from **28** and **29**.
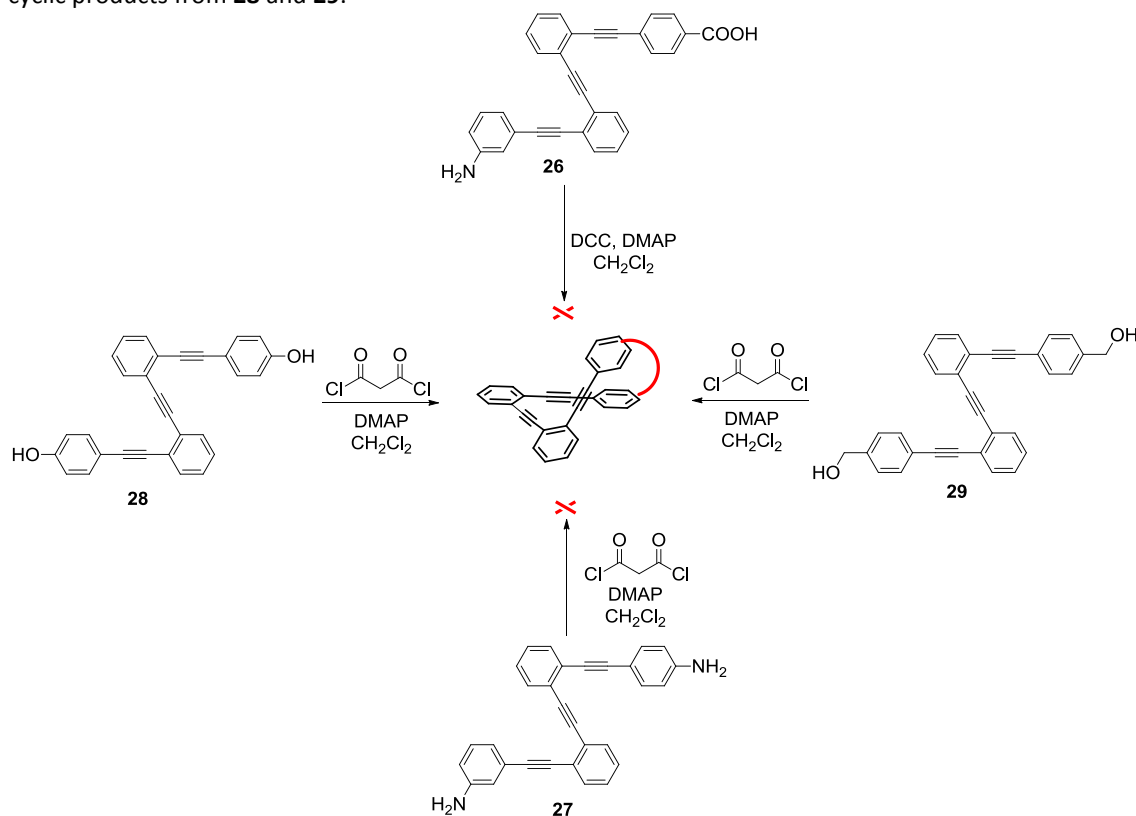
Scheme 28. *Initial screening for restricting the random coil oPE conformation into a permanent helix.*

After NMR and X-ray characterization, we realized that the two cyclic products obtained from **28** and **29** were the single coil **30** (25-membered macrocycle) for the benzyl derivate **29** and the macrocycle formed by dimerization of two *o*PE tetramers (50-membered macrocycle) **28a** for the phenyl derivate **28** (Figure 71).

---

[211] Fuentes, Noelia. *PhD Thesis*, **2011**, UGR.
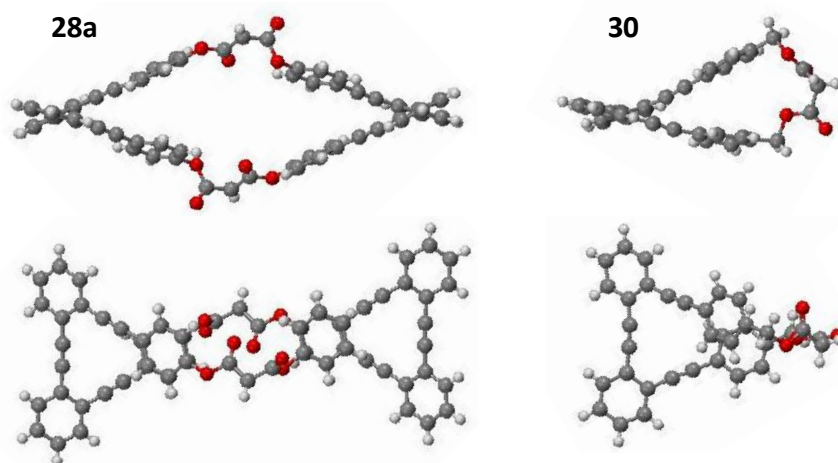
*Figure 71. X-ray structures of **28a** and **30**, top and side views.*

It has been argued for similar macrocyclization of peptides that the success or failure of macrocyclization relies on the ability of a linear precursor to conformationally pre-organize its reactive ends in close spatial proximity before ring closure. Molecular mechanic calculations of the best linear precursor in the synthesis of cyclotetrapeptides revealed that the ring-closure process is favoured when the various structural elements of the linear precursor can accommodate the angular requirements for both termini in the transition state with the least amount of strain.[212] This work prompted us to theoretically study the folding event and the facts that influence the formation of each cycle our case.

DFT calculation[213] revealed that in **28** and the unsubstituted analog **31**, the free energy values stem from π-stacking stabilization (Figure 72). However, in compound **29** an intramolecular hydrogen bond formed between the two benzyl alcohol groups additionally stabilizes the folded conformation.

	28	**29**	**31**
ΔH (Kcal/mol)	-3.6	-10.8	-2.5
ΔS (Kcal/mol)	-3.9	-11.5	-2.1
ΔG (Kcal/mol)	-1	-5.7	-0.1
kfolding	5	15144	1
[folded]:[unfolded]	85 : 15	99.99 : 0.01	54 : 46
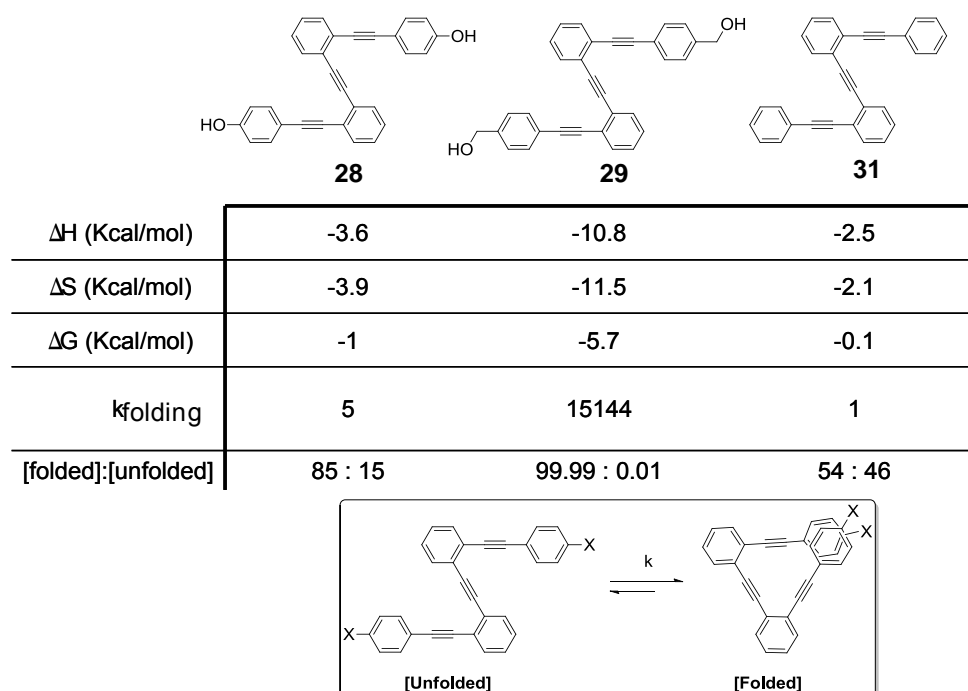
*Figure 72. Summary of the folding thermodynamic parameter calculated for **28**, **29** and **31**.*

Further theoretical analysis suggested that this macrocyclization is a two step thermodynamically favoured process in which the formation of intermediate **A** stabilized by hydrogen-bong is the driving

---

[212] F. Cavelier-Frontin, G. Pèpe, J. Verducci, D. Siri, R. Jacquier, *J. Am. Chem. Soc.* **1992**, *114*, 8885–8890.

[213] Performed by Dr. Mota. Departamento de Química Inorgánica, Universidad de Granada, Spain.

force behind (Figure 73). The energy gained from this template alleviates the entropic penalty of folding the rigid backbone to approximate the side chains. Great success in contemporary peptides ligation strategies under mild conditions rely on a similar capture/rearrangement mechanisms.[214]

ΔG = -17.5 Kcal/mol

ΔG = -16.4 Kcal/mol

ΔG = -33.9 Kcal/mol
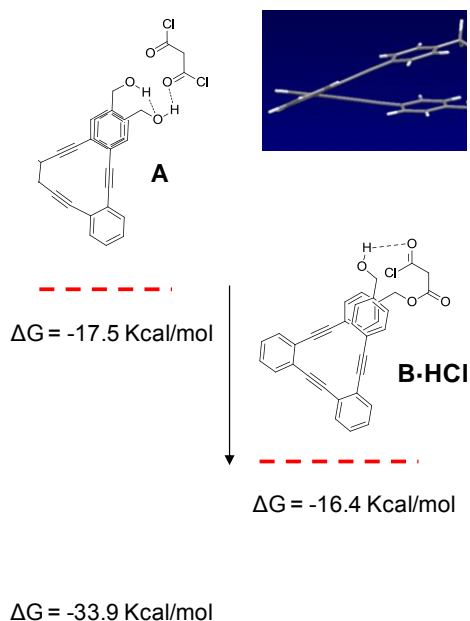
Figure 73. Thermodynamic of the macrocyclization of 29 with manonyl chloride.

^{1}H-NMR experiments performed on **29** and their mono- and di- acetylated non-cyclic analogs gave experimental evidences of the intramolecular hydrogen-bond on compound **28** supporting the calculation guidelines. Under the light of these results, the success and the stoichiometry of this macrocyclization depended on a subtle balance between the unfavorable π-repulsions, the flexibility of the backbone and the preorganization of compound **29**. The few flexibility and length of the stapling group could also prevent the appropriate gathering of the remaining hydroxyl group and the second acid group after the first condensation reaction step.

<u>2.2.2.2.Changing the staple length and the hydroxybenzyl groups location</u>

Using compound **29** as model, we screened different alkyl diacid chlorides (Scheme 29).[215] Compound **29**[216] gave stapled products with diacids from 3 (malonyl) to 6 (glutaryl) carbon atoms in moderate yields.[217] More rigid *staples* with four (phtaloyl), five (*iso*-phthaloyl) and six (*tert*-phthaloyl) carbon atoms aromatic linkers were also tested but only the reaction using iso-phthaloyl chloride yielded to the desired product.

---

[214] C. J. White, A. K. Yudin, *Nat. Chem.* **2011**, *3*, 509–524.

[215] A minor compound (13 mg, 8%) assigned to the 52-membered macrocycle was also obtained when we repetead the reaction of **29** with malonyl chloride. ^{1}H-NMR (600 MHz, CDCl3) δ (ppm): 7.53 − 7.46 (m, 8H), 7.37 (d, J = 8.1 Hz, 8H), 7.23–7.18 (m, 8H), 7.08 (d, J = 8.1 Hz, 8H), 5.08 (s, 8H), 3.50 (s, 4H). 13C NMR (151 MHz, CDCl3; DEPT) δ (ppm): 168.7 (C), 137.5 (C), 134.7 (CH), 134.5 (CH), 134.5 (CH), 130.6 (CH), 130.5 (CH), 128.5 (C), 128.1 (C), 126.1 (C), 95.7 (C), 94.8 (C), 91.6 (C), 69.5 (CH2), 44.4 (CH2).

[216] Macrocyclization of compound **28** with succinyl and adipoyl chloride were also tested but starting material or polymers were obtained from all the trials.

[217] The sterification with phosgene and oxalyl chloride were also tested but in any case the macrocycle was obtained.
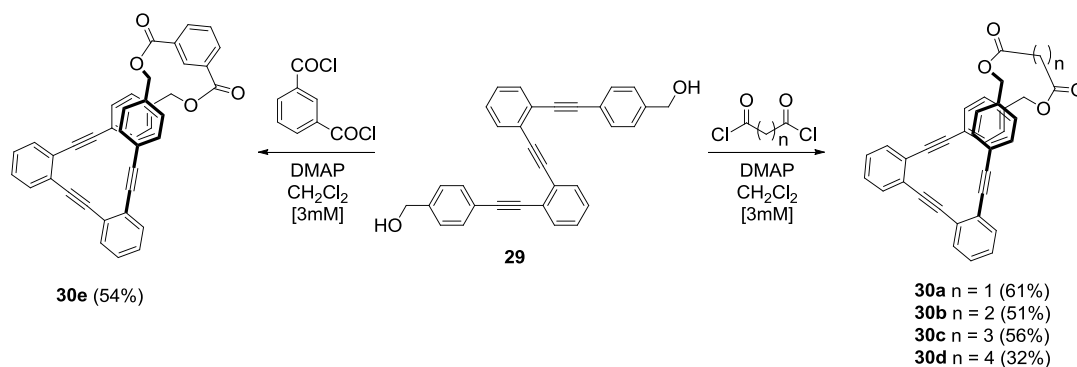
Scheme 29. *Synthesis of new helices with different staples. Changing staple length and flexibility.*

30e (54%)

30a n = 1 (61%)
30b n = 2 (51%)
30c n = 3 (56%)
30d n = 4 (32%)

To test if the linking points placement had any consequence on the stapling efficiency, we also prepared *meta-para* and *meta-meta* hydroxybenzyl analogs **32** and **33**. Interestingly, **30a** isomers (compounds **34** and **35**) were obtained in higher yields (Scheme 30).

34 *meta, para* (81%)
35 *meta, meta* (86%)
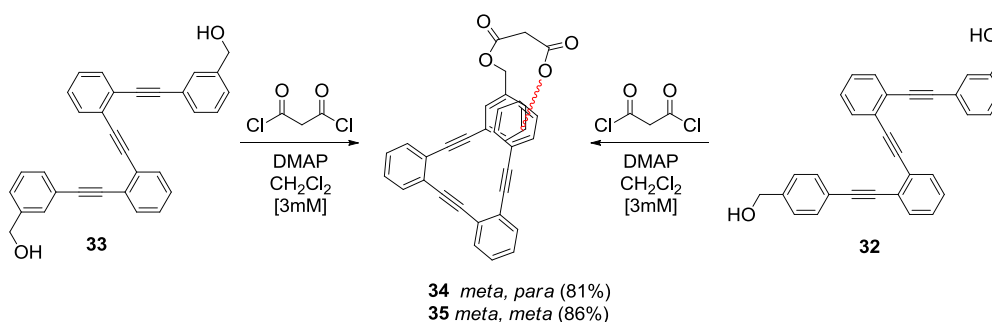
Scheme 30. *Synthesis of new helices. Changing cross-linking groups location on the oPE backbone.*

Alkene metathesis was also found as an excellent stapling reaction when 1st generation Grubbs´ catalyst was used. For such reaction, the *o*-allyl ether of benzyloxy and phenoxy tetramers (compounds **36** and **37**) were successfully transformed into the helical products **38** and **39** with moderate good to excellent yields and modest E:Z ratio (Scheme 31).

38 (56%)
(E:Z = 2:1)

39 (91%)
(E:Z = 2:1)
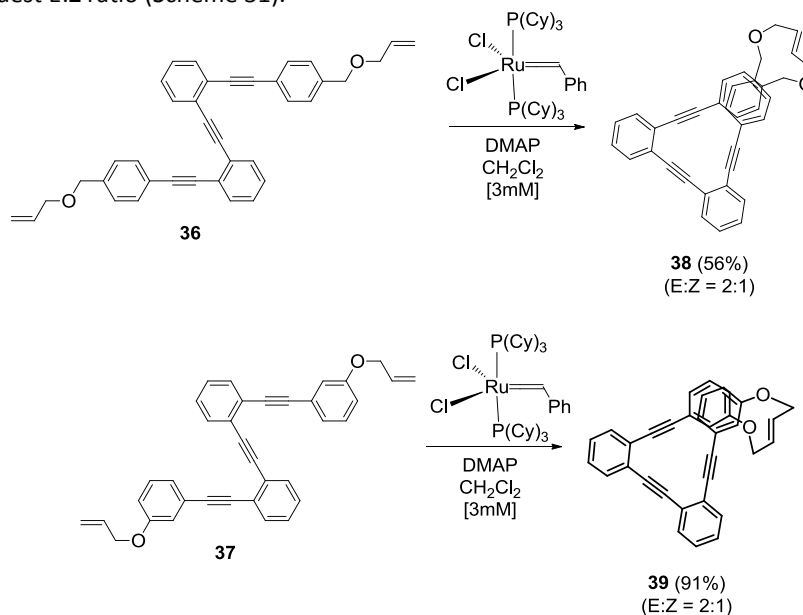
Scheme 31. *Synthesis of new helices. RCM as stapling reaction.*

102

Further insight about the structure of these macrocycles[219] was offered by single crystal X-ray diffraction analysis. Most of the compounds crystallized with the expected helical arrangement except compound **30e** bearing the aromatic *i*-phtaloyl linker (Figure 74). Compound **30e** adopted a nearly a planar conformation (only 1⁰ out of the plane) distorting the alkynyl rods 10⁰ far from lineality. This structure was non-merohedrally twinned in the crystal cell, what brought to out mind the crystal structure obtained for the rhomboidal tetrabenzocycline **14c** isolated in the previous chapter (Figure 20).
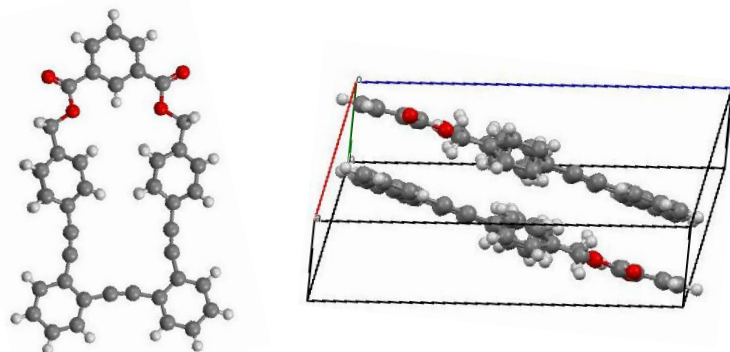
Figure 74. Top view of the solid-state structure of 30e and the dimer formed in the unit cell.

Attending to the relative arrangement in solid-state of all the rest macrocycles, we found that not only the staple and flexibility of the backbone were determinant for the helical structural features of the loops but also the relative localization (*ortho, meta, para*) of the functional group in the terminal benzenes. Measuring the torsion angle formed by the macrocycles squeleton (Figure 75), we detected that the staple length had little influence on the distance between the two superimposed benzenes (ca. 47⁰ which corresponded to a mean distance of 5.4 Å). Even the dimeric macrocycle **29**, which crystallized with two dichloromethane molecules in its unit cell, was characterized by a similar torsion angle. After some discussion, we concluded that the fact that more significantly influenced the helical conformation was the location of the *staple*.
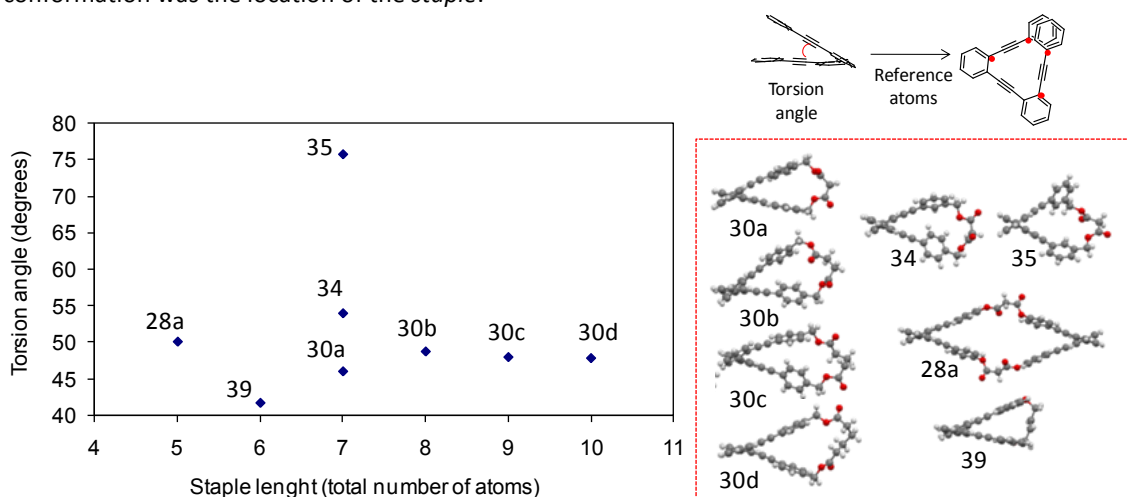
Figure 75. Torsion angle measured in the crystal structures of 28a, 30a-d, 34, 35 and 39.

As a matter of fact, compound **35**, which was characterized by the largest torsion angle by far, did not really adopted an helical conformation but it exhibited a shell-like structure with several crystal features

---

[218] Crystallization and X-ray structure analysis performed by Dr. Choquesillo-Lazarte. Laboratorio de Estudios Cristalográficos IACT, CSIC- Universidad de Granada.

[219] The open oPE tetramers were also crystallized. They exhibited an unfolded structure in solid state and hydrogen bonds were observed between the hydroxyl groups of neibouring compounds.

in common with the non planar tetrabenzocycline **2**[220] (Figure 76). The shortest torsion angle was observed in compound **39** closed by an olefin bridge but in all cases the distance between final benzenes was longer than the typical π-stacking distance (3.5-3.8 Å).

2

35
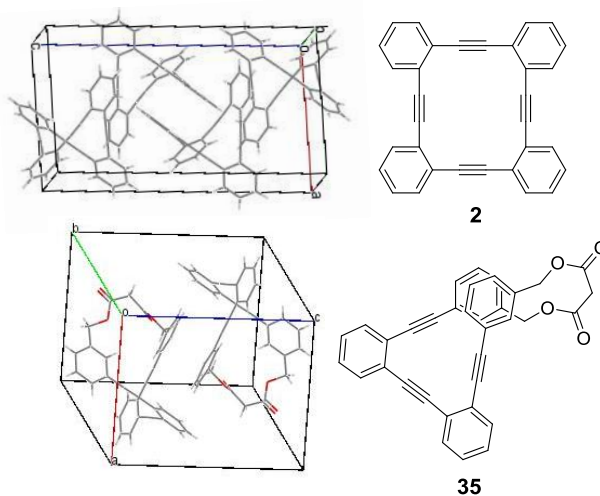
*Figure 76. Unit cells of TBC **2** and macrocycle **35**.*

Another interesting observation was that, when the structure constraints allowed it (compounds **30b**, **30c**, **34** and **35**), the two final benzene rings adopted a preferred edge-to-face (also called T-shaped) geometry.[221] The expected nearly sandwich-type or parallel-displaced configurations were only adopted by **30a**, **30d**, **28a** and **39**.

2.2.2.4.UV-vis spectroscopic features

UV-vis measurements of open precursors and macrocycles in dichloromethane reflected the different electronic transitions in the conformationally-restricted *o*PEs. Open tetramers displayed their absorption maximum around 270 nm while the related macrocycles maxima appeared around 300 nm (Figure 77).
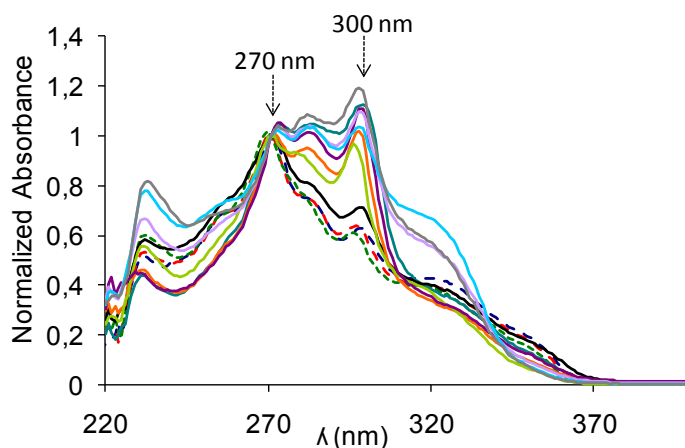
Figure 77. Normalized absorption spectra of open oPE tetramers (dashed) and macrocycles (line).

---

[220] X-ray structure of compound **11** borrowed from the CCDC, deposition number 192630.

[221] This T-shaped configuration enjoys favorable quadrupole/quadrupole interactions, as the positive quadrupole of one benzene ring interacts with the negative quadrupole of the other. The benzene rings are furthest apart in this configuration, so the favorable quadrupole/quadrupole interactions evidently compensate for diminished dispersion forces.

Despite there was no precedent in literature of covalently locked *o*PEs, a related cyclophane-based structure **40**[222] and the [12]DBA **1** also enxhibit a strong absorption band around 300 nm. In analogy to the observations made in *m*PEOs (Figure 78),[223] this coincidence between the three macrocycles suggested that the new band can be related with the *cisoid* conformation of the bis-phenylene-ethylene chromophores, which is associated with the helix conformation (Figure 79).[224]
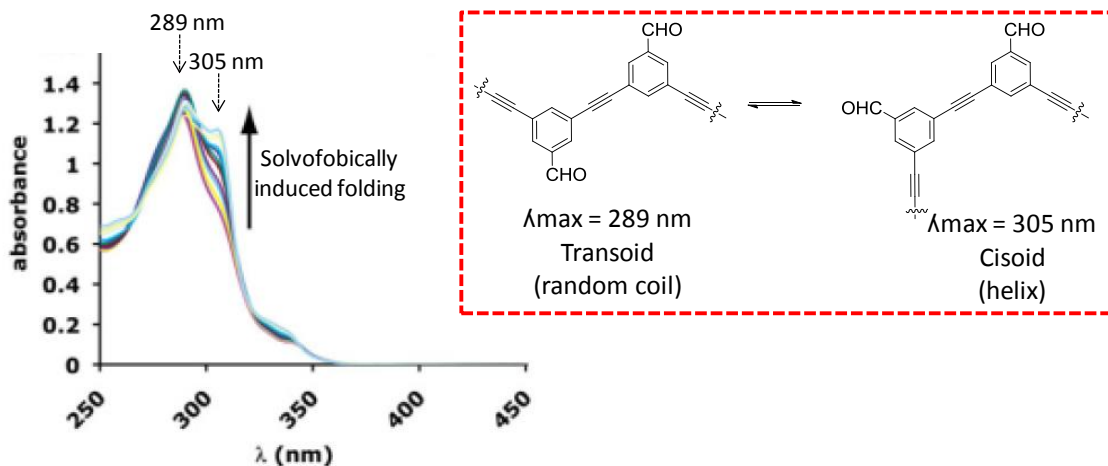
Figure 78. *UV–vis solvent denaturation titration (left) for a mPEs oligomer bearing aldehyde side chains. [From ref. 220] Cisoid-transoid exchange of the bis-phenylene-ethylene chromophores related with the two characteristic absorption maxima (right).*
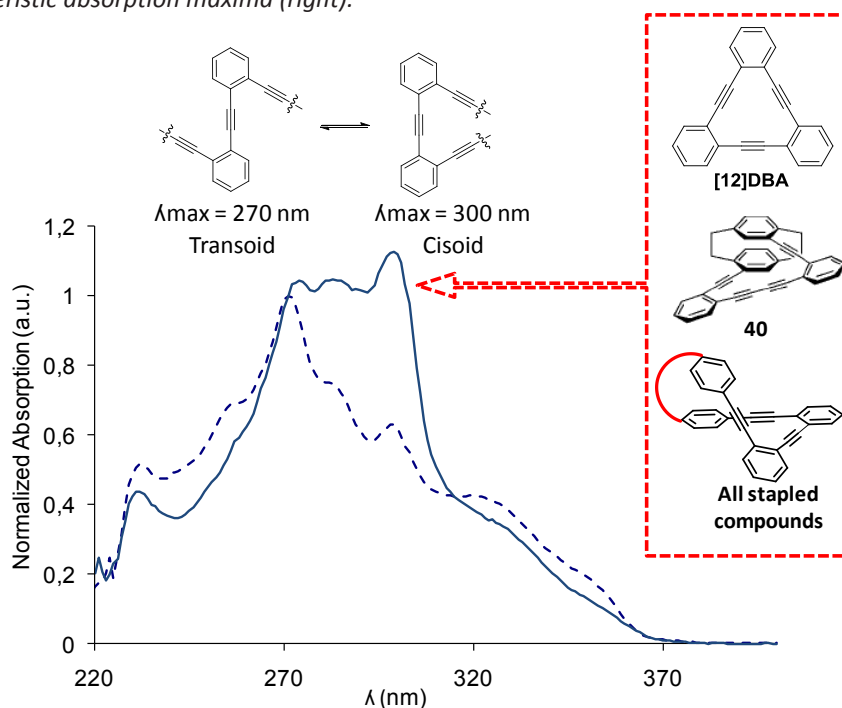
Figure 79. *UV–vis spectra of **29** and **30a**. Inferred relation between the UV-vis absorption maxima and the cisoid-transoid conformation of ortho-phenylene ethynylene chromophores.*

[222] A. J. Boydston, L. Bondarenko, I. Dix, T. J. R. Weakley, H. Hopf, M. M. Haley, *Angew. Chem. Int. Ed.* **2001**, *40*, 2986-2989.

[223] In mPEOs *transoid* to cisoid conformations display different absorption spectroscopic features. The random coil conformation (transoid) shows an absorption maximum ca. 279 nm while the helix maximum appears ca. 307 nm. See the original work: e.g.: Science 1997 Moore

[224] Despite this assertion seems quite reasonable, it has been previously rejected in related oPEOs folded by solvophobic interactions. See: . See: J. Jiang, M. M. Slutsky, T. V. Jones, G. N. Tew, *New J. Chem.* **2010**, *34*, 307.

The ratio between the two characteristic absorption maxima between the folded and unfolded configurations has been previously calculated as an estimation of the population of the fully helical state for solvophobically-folded *m*PEs, but in our case, the two bands presented the same relative intensity regardless the staple features. Additionally, similar absorption cut-offs and broad spectra were registered for open and stapled products what is consistent with the still quite flexible backbones of the macrocycles.[225]

2.2.2.5.Teoretical studies about the mechanical properties[226]

Trying to gain an overview about the mechanical properties of these new coiled macrocycles, we turned to theoretical calculations. Choosing compound **30a** as a model, we submitted it to mechanical stress and monitored the changes caused in its potential energy (Figure80). DFT calculations revealed two different regimes for the compression and the lengthening. An almost quadratic behaviour was observed at low elongations (±0.2 Å) with an estimated *Hook force constant* of 20.2 Kcal Å^{-2} mol^{-1}.[4] Beyond 0.2 Å in the compression regime, the behaviour was dominated by repulsion between the aromatic rings. In the lengthening regime, except for small elongations, the system dependence was practically linear and elongations up to 2 Å (55% longer) were accessible with low energetic requirements (< 3 Kcal mol^{-1}). Similar pseudoelastic behaviours are typical of micrometric CNCs.[227]
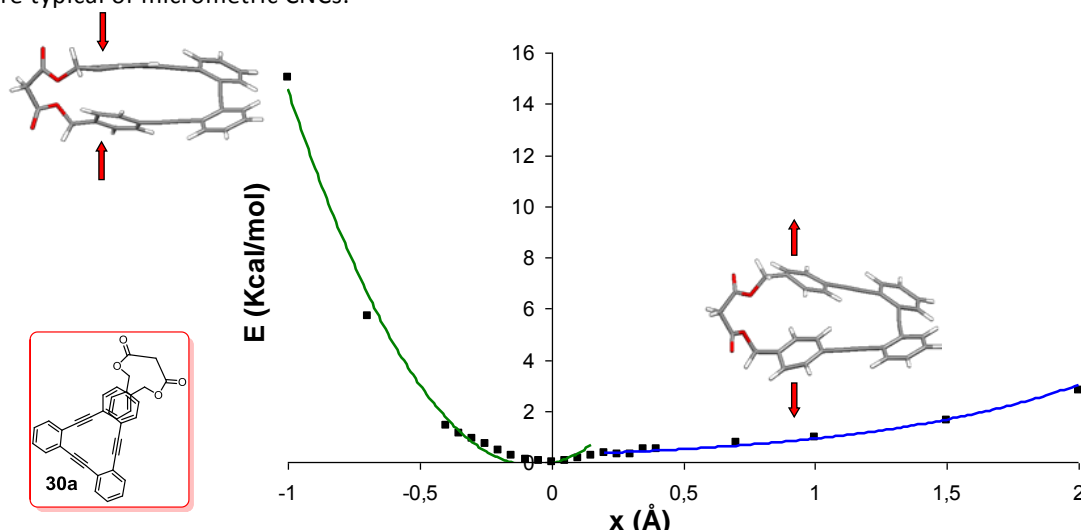
Figure 80. *Potential energy profile of compound **30a** toward elongation and compression.*

2.2.2.6. Inducing chiral bias

Once we had completely characterized the first generation of coils, we decided to go beyond inducing chiral bias into the foldamer structure through the incorporation of a chiral linker. A tartrate-derived flexible tether had been previously used by Moore *et al.* to favour the formation of only one helical twist sense on related helical compounds.[228] Thus, after some screening for the optimal esterification methodology, compounds **41**, **42** and **43** were successfully synthesized from a (-)-*O,O´*-di-pivaloyl-L-tartrate acid using a mild method based on the Garegg-Samuelsson reaction developped in our lab[229] (Scheme 32).

[225] In [12]DBAs and **14c**, narrower absorption spectra are observed due to the restriction of some vibration modes (e.g. rotations).

[226] Performed by Dr. Mota. Departamento de Química Inorgánica, Universidad de Granada, Spain.

[227] X. Chen, S. Zhang, D. A. Dikin, W. Ding, R. S. Ruoff, L. Pan and Y. Nakayama, *Nanolett.* **2003**, *3*, 1299-1304.

[228] M. S. Gin, J. S. Moore, *Org. Lett.* **2000**, *2*, 135-138.

[229] S. Morcillo, L. Álvarez de Cienfuegos, A. J. Mota, J. Justicia, and R. Robles *J. Org. Chem.* **2011**, *76*, 2277-2281.
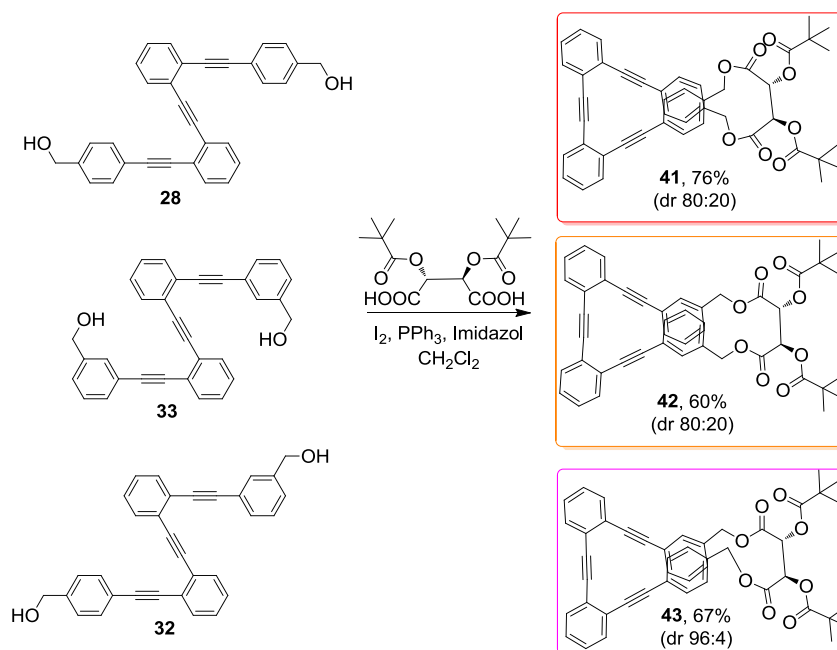
Scheme 32. *Synthesis of chiral helices.*

Althought crystals of compound **41** were obtained as a racemic,[230] chiral HPLC studies[231] revealed that the three products were diastereomerically enriched samples (Scheme 32, see *dr* ratio) evidencing the presence of two chiral elements in the structures: the stereogenic centers of the *L*-tartrate unit and a new chiral helix induced in the macrocyclization.[232]

Taking into account the presence of both *M* and *P*-helical diastereomers in these derivatives, the chiroptical responses measured were noteworthy (Figure 81).[233] CD absorptions of the tartrate moiety overlapped with bands corresponding to the aromatic framework in the region of $\lambda < 270$ nm. As the *R,R* configuration of the stereogenic carbons of the tartrate was the same in all cases, the presence in this region of positive and negative bands indicated a significant contribution of the aromatic chiral helical framework to the absorption. More intense and also of opposite sign CD bands appeared above 270 nm. The *p*-substituted mono *stapled* tartrate **41** gave a chiroptical response which was much more intense ($\Delta\varepsilon = 47.35$) and pseudoenantiomeric to that of the *meta-meta-* and *meta-para-* substituted analogues **42** ($\Delta\varepsilon = -5.07$) and **43** ($\Delta\varepsilon = -10.23$). Thus, the same chiral *L*-tartrate unit was able to induce a helix of different configuration depending on the relative *meta* or *para* positions of the benzyl alcohols in the initial *o*PE precursors. Moreover, the intensity of these bands was significantly different.

---

[230] Interestingly, the mayor rigidity imposed by this staple reduced the torsion angle of **41** in comparison to it succinyl analog **30b**. I.e. the internal void of macrocycle **41** is significantly smaller. See experimental section.

[231] Chiral HPLC experiments performed in Prof. Carreño laboratory (UAM).

[232] This phenomenon is known as intramolecular central-to-helix chirality transfer.

[233] CD experiments performed in Prof. Carreño laboratory (UAM) and in the Department of Physical Chemistry (UGR).
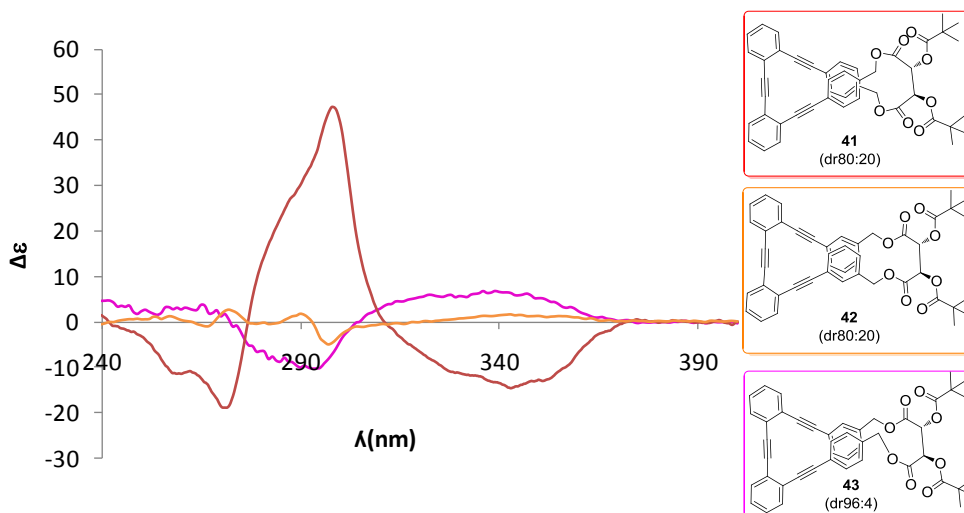
Figure 81. CD spectra of monostapled derivates 41, 42 and 43.

Pure (*R,R,M*)-**41** (Figure 82, blue) and (*R,R,P*)-**41** (Figure 82, pale blue) diastereomers could be independently measured after separation by chiral HPLC from the 80:20 initial mixture (Figure 82, green). Pseudoenantiomeric CD bands were obtained for each diastereomer. The CD bands of the 80:20 mixture of **41** were very similar to those of the expected (*R,R,M*)-**41** diastereomer.
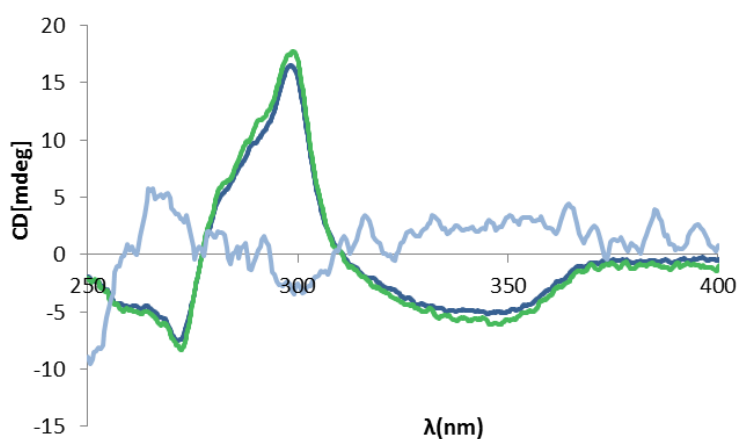
Figure 82. CD spectra of the diateromeric mixture of 41 (green) and pure diastereomers (M,R,R)-41 (dark blue) and (P,R,R)-41 (pale blue).

The theoretical simulation of the ECD spectra using *ab initio* techniques (TD-DFT)[234] of the two possible (*M,R,R*) and (*P,R,R*) helical structures of **41** as well as that of the 80:20 and 20:80 mixtures of both diastereomers, allowed the identification of the absolute configuration of the species contributing to a major extent to the 80:20 mixture of **41**, experimentally obtained (Figure 83).

ECD Spectrum TD-B3LYP/6-31g*   Gauss=10   Shift= -15 nm
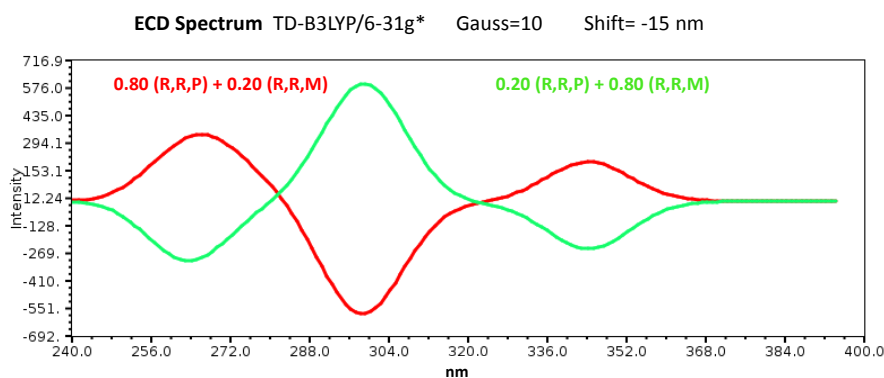
Figure 83. *TD-PBE0/6-31G* spectra of* **41** *[80:20, (M,R,R)-3: (P,R,R)-3] (green) and* **41** *[80:20, (P,R,R)-3: (M,R,R)-3] (red).*

Looking for an opportunity to lock in a single *M* or *P* stereochemistry the original *o*PE tetramers, we decided to synthesize tetrafunctionalized *o*PE oligomers **44** and **45** bearing the potential cross-linking groups (Scheme 33). Three new compounds were obtained from these tetrafunctionalized *o*PEs. A double esterification with the *L*-tartaric acid derivative transformed compound **44** into **46** as a 94:6 mixture. Esterification of **45** led the intermediate **47** (93:7 mixture) and subsequent alkene metathesis gave compound **48** as a single chiral loop.
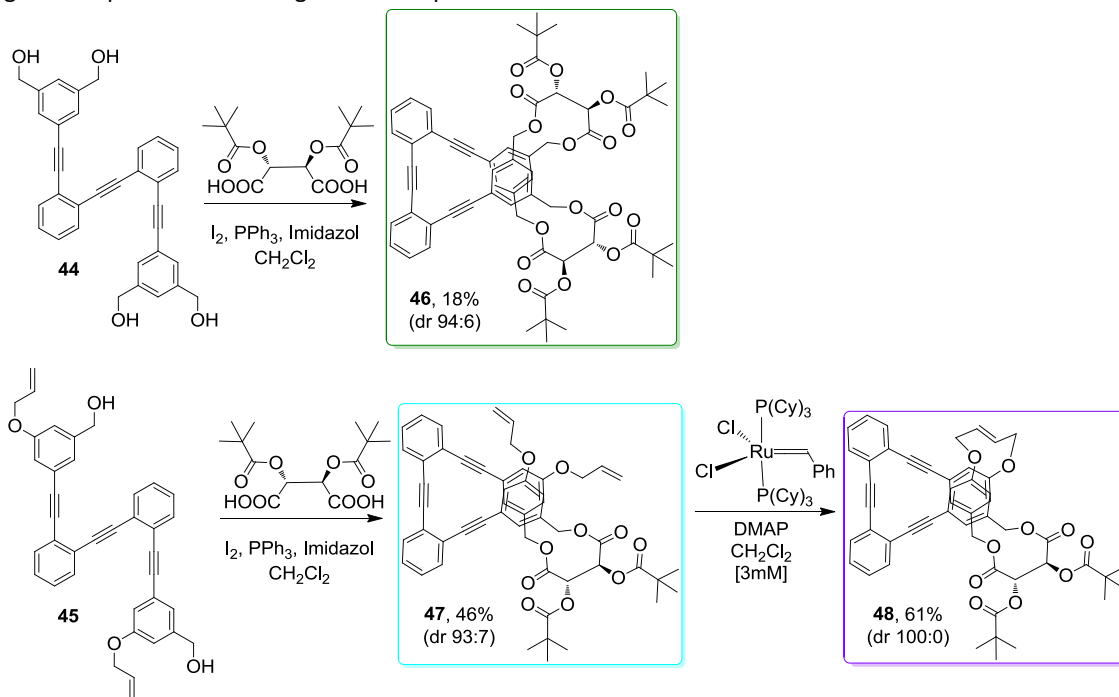
Scheme 33. *Synthesis of bis-stapled chiral helices.*

The CD spectra of mono-stapled compound **47** gave a chiroptical response quite similar but slightly more intense (Δε = -12.21) to that of the *meta*-substituted analogues **42** and **43** (Figure 84). Compound **46** closed by two tartrate moieties, gave the strongest CD response (Δε (292nm) = 35.02) with the same sign to the others meta substituted macrocycles. Surprisingly, a negative broad band was registered for the single helix **48**. In a similar way, the configuration of the diastereomeric mixtures for **46** and **47** and the single helix **48** were assigned as (*P,R,R*)-**46**, (*P,R,R*)-**47** and (*M,R,R*)-**48**.
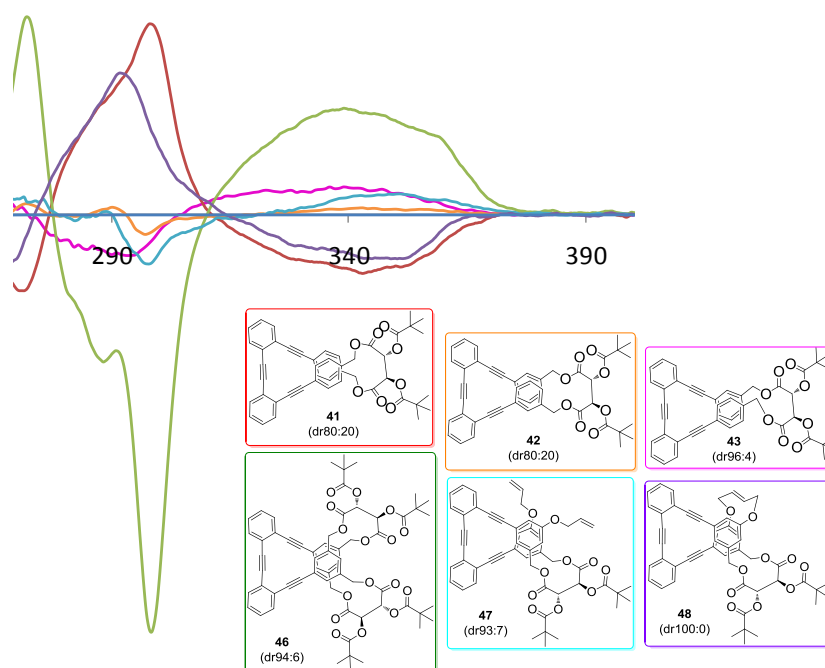
Figure 84. *CD spectra of all chiral products **41**, **42**, **43**, **46**, **47** and **48**.*

2.2.2.7.Extending this methodology to other geometries and larger oPEs

At this point, we tried to extend the helix length to more than one single loop, fused-single loops and to different geometries (Figure 85). Compounds **49**[235] and **52**[236] were successfully synthesized with a succinyl and tartrate moiety respectively. However, poly-hydroxylated backbones such as **50** turn out to be quite challenging because of the insolubility of the products and the competing polymerizations in the macrocyclization step.[237] Allyl-derivates resulted to be much more soluble and the stapling more straightforward,[238] thus a new approach in which the chirality is introduced after cyclization by asymmetric hydroxylation is underway.

---

[235] Morcillo, Sara. *PhD Thesis* underway.

[236] See experimental section.

[237] The synthesis of compound **50** was attempted several times following different approaches, and changing the location and number of side chains. The synthesis was also faced using the TBDMS-protected alcohols. Unfortunately, the final product was obtained impurified with some impurities (i.e. the mono-coupled products and dimers).

[238] Using alkene metathesis, a new type of helices with a carbazole squeleton has been successfully developed. Jurado, Rocío. *Master Thesis*, **2013**, UGR.
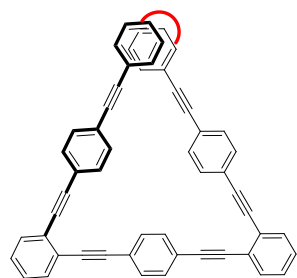
49
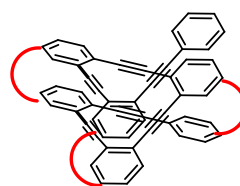
50
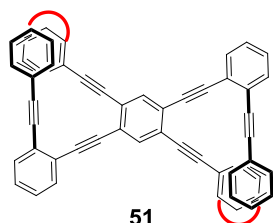
51
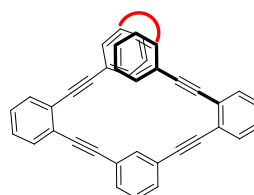
52

Figure 85. *Target compounds to test the stapling.*

2.2.3. Conclusions and outlook

We have developed a versatile methodology to synthesize flexible π-conjugated helices from open oPE tetramers bearing hydroximethyl side chains. The flexibility of the oPE foldamers has been restricted in a simple esterification step using different diacid derivatives. Single coils were able to efficiently accommodate diesters derived from malonate, succinate, glutarate, adipoate and isophtalate. Alkene metathesis using 1st generation Grubbs catalyst has also been used as an efficient stapling reaction.

Analysis of the solid state structures confirmed the helical arrangement of most of the products and shed light on the different factors which determine this "secondary structure". Surprisingly, a major influence of the crosslining points in comparison to the staple length was observed. The formation of flexible helical macrocycles was also supported by UV-vis studies. Open tetramers displayed their absorption maximum around 270 nm while all the macrocycles maxima appeared around 300 nm. In analogy to the reported absorption features for the transoid-cisoid isomerization of mPEOs, we propose that such UV-bands can be also related to the transoid and cisoid conformations of the o-diethynylbenzene chromophores, and, hence to the random coil/helix transition.

Additionally, we were able to induce a chiral bias to obtain homochiral loops using a L-pivaloyl-protected tartaric acid. The induced intramolecular central-to-helix chirality transfer was supported by CD and chiral HPLC studies. Results derived from such studies evidenced that the same chiral unit is able to induce opposite *P* or *M* configurations in the helical systems according to the relative position of the tartrate in the terminal benzenes. The combination of both stapling reactions (alkene metathesis and the intramolecular esterification) allowed the formation of asymmetrically bis-stapled compound **48** which was isolated as a single (*M,R,R*)-diasteromer.

DFT calculations revealed the primary role of an intramolecular hydrogen-bond in the macrocyclization and the pseudoelastic properties of compound **30a** under compression/tensile loading. UV-vis results and DFT simulation strongly support our initial hypothesis about the potential use of these products as molecular springs. Xray structures and UV studies also support the absence of axial electronic connection between superposed rings what would allow the used of such macrocycles as conducting helical wires.

Current work in our laboratory involves increasing the number of loops to have longer coils and we are trying to extend this permanent helical arrangement into other geometries. Our first efforts to synthesize larger systems using the sterification strategy led to modest success. However, allyl-derivates resulted to be much more soluble and the stapling more straightforward. Hence, a new approach in which the chirality is introduced after cyclization by asymmetric hydroxylation is underway.

2.2.4. Experimental section[239]

1. *General procedures:*[240]

*Representative protocol for the esterification with diacid chlorides. **(GP5)***
The corresponding diacid chloride (1 mmol) was added dropwise and gradually during one hour at room temperature to a solution of the starting *o*-OPE (1 mmol), DMAP (2 mmol) and 4 Å molecular sieves (activated powder) in dry CH_2Cl_2 (10^{-3} M),. When the macrocycle was formed a new spot visible under *UV* light appeared on the TLC plate (*Rf* 0.6, EtOAc/Hexane, 4:6, v/v).[241] The solvent was then removed under reduced pressure and the residue was purified by flash chromatography (EtOAc/Hexane mixtures) to give the corresponding *stapled* product.

*Representative protocol for the esterification with (–)-O,O'-di-pivaloyl-L-tartaric acid. **(GP6)**[242]*
To a stirred solution of I_2 (3 mmol) in dry CH_2Cl_2 (10^{-3} M), PPh_3 (3 mmol), imidazole (3 mmol) and (–)-O,O'-di-pivaloyl-L-tartaric acid (1 mmol) were sequentially added. After 5 min, a solution of the alcohol (1 mmol) in dry CH_2Cl_2 (10^{-2} M) was added. The mixture was stirred during 12 h at room temperature. Then, the solution was washed with water, dried over anhydrous Na_2SO_4 and the solvent was removed under reduced pressure. The residue was purified by flash chromatography (EtOAc/Hexane mixtures) to give the corresponding *stapled* product.

*Representative protocol for the metathesis reaction. **(GP7)***
A solution of the corresponding starting *o*-OPE in dry deoxygenated CH_2Cl_2 (1 mmol) was added dropwise at room temperature to a solution of Grubbs´ first generation catalyst (0.1 mmol) in dry deoxygenated CH_2Cl_2 (10^{-3} M). The reaction was stirred during 2 h at 50 ºC under argon atmosphere. The solvent was then removed under reduced pressure and the residue was purified by flash chromatography (EtOAc/Hexane mixtures) to give the corresponding *stapled* product.

2. *Synthesis and analytical characterization of the compounds.*

---

[239] A more detailed experimental section about UV, CD, HPLC, ECD, Xray studies and theoretical calculations can be found in *Angew. Chem. Int. Ed.* **2012**, *51*, 1-6.

[240] For general procedures of the Sonogashira reaction (GP1 and GP2), see experimental section chapter 1 objective 1.

[241] If the reaction was too concentrated, polymerization products appeared at the bottom of the TLC plate. Starting compounds were easily recovered using K_2CO_3 in MeOH.

[242] S. Morcillo, L. Álvarez de Cienfuegos, A. J. Mota, J. Justicia, and R. Robles *J. Org. Chem.* **2011**, *76*, 2277-2281.
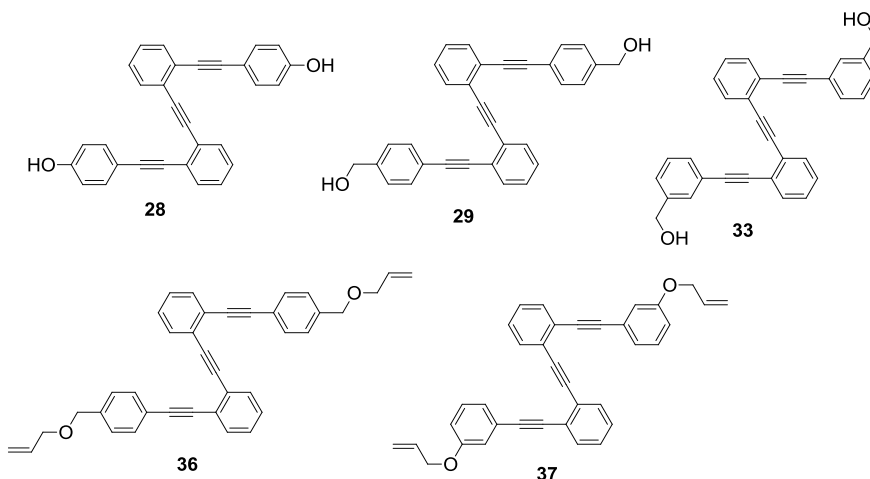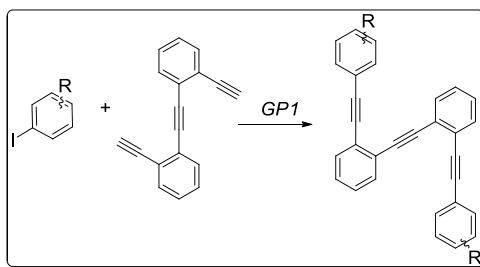
Compound 28 was prepared from 4-iodophenol (127.4 mg, 0.88 mmol) and 2,2'-bis(ethynyl)diphenylacetylene[243] (100 mg, 0.44 mmol) according to previously described *GP1* to give **28** in a 88 % yield (160 mg) as a white solid. ^{1}H RMN (400 MHz, CDCl$_3$): δ (ppm) = 7.63 (dd, *J* = 7.4, 1.0 Hz, 2H), 7.59 (dd, *J* = 7.4, 1.0 Hz, 2H), 7.47 (d, *J* = 8.6 Hz, 4H), 7.37 – 7.26 (m, 4H), 6.83 (d, *J* = 8.7 Hz, 4H); ^{13}C RMN (126 MHz, CDCl$_3$, DEPT): δ (ppm) = 155.8 (C), 133.4 (CH), 132.0 (CH), 131.6 (CH), 128.0 (CH), 127.5 (CH), 126.1 (C), 125.8 (C), 115.6 (C), 115.4 (CH), 93.8 (C), 92.3 (C), 87.0 (C); EI-HRMS calculated for C$_{30}$H$_{18}$O$_2$: 410.1307 found: 410.1312.

Compound 28 was prepared from 4-iodobenzyl alcohol (270 mg, 1.15 mmol) and 2,2'-bis(ethynyl)diphenylacetylene (130 mg, 0.58 mmol) according to previously described *GP1* to give **28** in 88 % yield (223 mg) as a pale yellow solid. ^{1}H NMR (500 MHz, CDCl$_3$): δ (ppm) = 7.64 – 7.56 (m, 4H), 7.49 (d, *J* = 8.2 Hz, 4H), 7.32 (dq, *J* = 7.5, 5.9 Hz, 4H), 7.23 (d, *J* = 8.2 Hz, 4H), 4.66 (s, 4H); ^{13}C NMR (126 MHz, CDCl$_3$, DEPT): δ (ppm) = 140.96 (C), 132.24 (CH), 131.97 (CH), 131.95 (CH), 128.20 (CH), 127.98 (CH), 126.72 (CH), 125.83 (C), 125.76 (C), 122.53 (C), 93.67 (C), 92.34 (C), 88.41 (C), 65.02 (CH$_2$); EI-HRMS calculated for C$_{32}$H$_{22}$O$_2$: 438.1620 found: 438.1619.

Compound 33 was prepared from 3-iodobenzyl alcohol (100 mg, 0.43 mmol) and 2,2'-bis(ethynyl)diphenylacetylene (193 mg, 0.85 mmol) according to previously described *GP1* to give **33** in 53 % yield (98 mg) as a pale yellow solid. ^{1}H NMR (500 MHz, CDCl$_3$): δ (ppm) = 7.64 – 7.62 (m, 2H), 7.60 – 7.57 (m, 2H), 7.45 – 7.44 (m, 2H), 7.42 – 7.39 (m, 2H), 7.35 – 7.31 (m, 4H), 7.25 – 7.23 (m, 4H), 4.57 (s, 4H); ^{13}C NMR (126 MHz, CDCl$_3$, CDCl$_3$, DEPT): δ (ppm) = 140.9 (C), 132.2 (CH), 131.9 (CH), 130.9 (CH), 130.3 (CH), 128.4 (CH), 128.2 (CH), 128.0 (CH), 126.9 (CH), 125.9 (C), 125.7 (C), 123.4 (C), 93.7 (C), 92.3 (C), 88.5 (C), 64.9 (CH$_2$); EI-HRMS calculated for C$_{32}$H$_{22}$O$_2$: 438.1620 found: 438.1626.

Compound 36 was prepared from 1-(allyloxymethyl)-4-iodobenzene (322 mg, 1.21 mmol) and 2,2'-bis(ethynyl)diphenylacetylene (137 mg, 0.60 mmol) according to previously described *GP1* to give **36** in 95 % yield (300 mg) as a brown solid. ^{1}H NMR (400 MHz, CDCl$_3$): δ (ppm) = 7.62 – 7.57 (m, 4H), 7.53-7.50 (m, 4H), 7.34–7.25 (m, 8H), 6.00–5.90 (m, 2H), 5.33–5.28 (m, 2H), 5.23–5.19 (m, 2H), 4.50 (s, 4H), 4.02–4.00 (m, 4H); ^{13}C NMR (100 MHz, CDCl$_3$, DEPT): δ (ppm) = 138.7 (C), 134.7 (CH), 132.1 (CH), 131.9 (CH),

[243] I. V. Alabugin, K. Gilmore, S. Patil, M. Manoharan, S. V. Kovalenko, R. J. Clark, I. Ghiviriga, *J. Am. Chem. Soc.* **2008**, *130*, 11535-11545.

131.8 (CH), 128.3 (CH), 128.0 (CH), 127.5 (CH), 125.9 (C), 125.8 (C), 122.5 (C), 117.4 (CH$_2$), 93.8 (C), 92.4 (C), 88.4 (C), 71.8 (CH$_2$), 71.3 (CH$_2$); MALDI-HRMS calculated for C$_{38}$H$_{30}$O$_2$Na [M+Na]$^+$: 541.2143, found: 541.2157.

Compound 37 was prepared from 1-(allyloxy)-3-iodobenzene (230 mg, 0.88 mmol) and 2,2'-bis(ethynyl)diphenylacetylene (100 mg, 0.44 mmol) according to previously described *GP1* to give **37** in 60 % yield (130 mg) as a brown solid. ^{1}H NMR (400 MHz, CDCl$_3$): δ (ppm) = 7.64–7.57 (m, 4H), 7.36–7.28 (m, 4H), 7.21–7.11 (m, 4H), 7.08 (bs, 2H), 6.89–6.86 (m, 2H), 6.05-5.96 (m, 2H), 5.37 (dd, *J* = 17.3, 1.5 Hz, 2H), 5.31–5.21 (m, 2H), 4.41 (d, *J* = 5.2 Hz, 4H); ^{13}C NMR (100 MHz, CDCl$_3$, DEPT): δ (ppm) = 158.4 (C), 133.1 (CH), 132.1 (CH), 131.8 (CH), 129.4 (CH), 128.3 (CH), 128.1 (CH), 126.0 (C), 125.9 (C), 124.5 (CH), 124.3 (C), 117.8 (CH$_2$), 116.9 (CH), 116.4 (CH), 94.0 (C), 92.3 (C), 88.2 (C), 68.8 (CH$_2$); ESIpos-HRMS calculated for C$_{36}$H$_{27}$O$_2$ [M+H]$^+$: 491.2005, found: 491.2008.
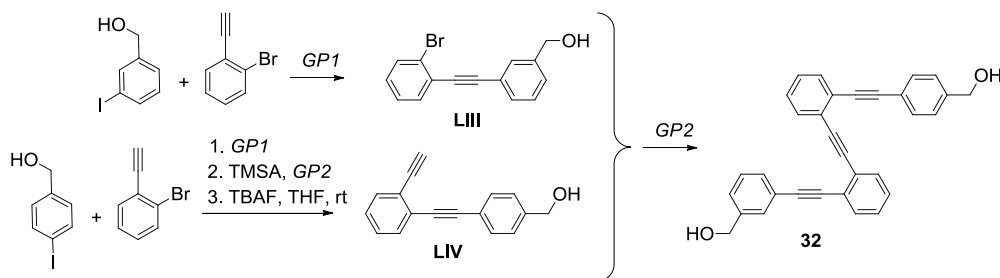
Compound LIII was prepared from 3-iodobenzyl alcohol (500 mg, 2.14 mmol) and 2-bromo-1-ethynylbenzene (0.17 mL, 2.14 mmol) according to previously described *GP1* to give **LIII** in 74 % yield (300 mg) as a pale orange solid. ^{1}H NMR (400 MHz, CDCl$_3$): δ (ppm) = 7.62 (d, *J* = 7.9 Hz, 1H), 7.60 (s, 1H), 7.56 (t, *J* = 7.6 Hz, 1H), 7.51 (d, *J* = 3.8 Hz, 1H), 7.37 (d, *J* = 5.2 Hz, 2H), 7.30 (t, *J* = 7.6 Hz, 1H), 7.19 (t, *J* = 10.9, 4.6 Hz, 1H), 4.72 (s, 2H); ^{13}C NMR (75 MHz, CDCl$_3$, DEPT): δ (ppm) = 141.43 (C), 133.54 (CH), 132.73 (CH), 131.11 (CH), 130.32 (CH), 129.73 (CH), 128.90 (CH), 127.51 (CH), 127.35 (CH), 125.91 (C), 125.59 (C), 123.3 (C), 94.11 (C), 88.44 (C), 64.93 (CH$_2$); EI-HRMS calculated for C$_{15}$H$_{11}$BrO: 285.9993, found: 285.9996.

Compound LIV was prepared from 4-iodobenzyl alcohol (500 mg, 2.14 mmol) and 2-bromo-1-ethynylbenzene (0.17 mL, 2.14 mmol) according to previously described *GP1* to give a brown syrup which was used in the next step without further purification. Trimethylsilylacetylene (0.4 mL, 2.98 mmol) was added to the reaction mixture following *GP2*. This residue was again evaporated under reduced pressure to give a black syrup which was diluted in THF (200 mL) and tetra-*n*-butylammonium fluoride (1.06 g, 2.57 mmol) was added. The mixture was stirred overnight, then evaporated under reduced pressure and finally purified by flash chromatography (EtOAc/Hexane mixtures) to give **LIV** in 40 % yield (200 mg) as a pale orange solid. ^{1}H NMR (400 MHz, CDCl$_3$): δ (ppm) = 7.46 (m, 4H), 7.26 (d, *J* = 8.0 Hz, 2H), 7.24 – 7.16 (m, 2H), 4.62 (s, 2H), 3.29 (s, 1H); ^{13}C NMR (101 MHz, CDCl$_3$, DEPT): δ (ppm) = 141.29 (C), 132.57 (CH), 131.91 (CH), 131.74 (CH), 128.54 (CH), 127.92 (CH), 126.77 (CH), 126.24 (C), 124.58 (C), 122.32 (C), 93.38 (C), 87.91 (C), 82.19 (C), 81.16 (CH), 64.89 (CH$_2$); EI-HRMS calculated for C$_{17}$H$_{12}$O: 232.0888, found: 232.0886.

Compound 32 was prepared from aryl bromide **LIII** (60 mg, 0.21 mmol) and ethynylbenzene **LIV** (50 mg, 0.21 mmol) according to previously described *GP2* to give **32** in 74 % yield (60 mg) as a pale yellow solid. ^{1}H NMR (500 MHz, CDCl$_3$): δ (ppm) = 7.64 – 7.56 (m, 4H), 7.49 (d, *J* = 8.2 Hz, 4H), 7.32 (dq, *J* = 7.5, 5.9 Hz, 4H), 7.23 (d, *J* = 8.2 Hz, 4H), 4.66 (s, 4H); ^{13}C NMR (126 MHz, CDCl$_3$, DEPT): δ (ppm) = 140.96 (C), 132.24 (CH), 131.97 (CH), 131.95 (CH), 128.20 (CH), 127.98 (CH), 126.72 (CH), 125.83 (C), 125.76 (C), 122.53 (C), 93.67 (C), 92.34 (C), 88.41 (C), 65.02 (CH2); EI-HRMS calculated for C$_{32}$H$_{22}$O$_2$: 438.1620, found: 438.1619.
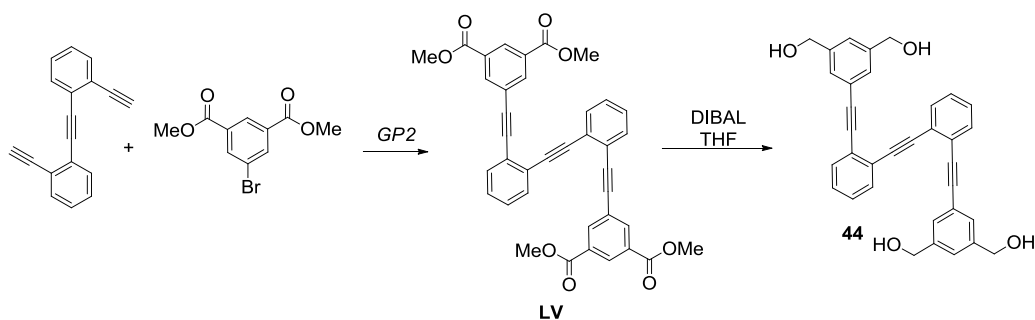
Compound LV was prepared from dimethyl 5-bromoisophthalate (370 mg, 1.36 mmol) and 2,2'-bis(ethynyl)diphenylacetylene (153 mg, 0.68 mmol) according to previously described *GP2* to give **LV** in 55 % yield (228 mg) as a brown solid. ^{1}H NMR (400 MHz, CDCl$_3$): δ (ppm) = 8.52 (s, 2H), 8.23 (s, 4H), 7.70-7.66 (m, 2H), 7.62-7.58 (m, 2H), 7.40-7.35 (m, 4H), 3.91 (s, 12H); ^{13}C NMR (100 MHz, CDCl$_3$, DEPT): δ (ppm) = 165.6 (C), 136.6 (CH), 132.4 (CH), 132.2 (CH), 130.8 (C), 130.2 (CH), 128.8 (CH), 128.5 (CH), 126.1 (C), 125.2 (C), 124.3 (C), 92.4 (C), 91.6 (C), 90.3 (C), 52.6 (CH$_3$); ESIpos-HRMS calculated for C$_{38}$H$_{26}$O$_8$Na [M+Na]$^+$: 633.1519, found 633.1493.

Compound 44. DIBAL-H (274 mg, 1.89 mmol) was added dropwise to a deoxygenated solution of **LV** (96 mg, 0.16 mmol) in THF (25 mL) under argon at 0 ºC. The mixture was stirred at room temperature for 2 h and, then, diluted with EtOAc, washed with brine, dried over anhydrous Na$_2$SO$_4$, and the solvent removed. The residue was submitted to flash chromatography (CH$_2$Cl$_2$/MeOH: 9/1) to give **44** (51 mg, 65 %) as a white solid. ^{1}H NMR (400 MHz, Acetone-d_6): δ (ppm) = 7.74 (dd, J = 5.6, 3.3 Hz, 2H), 7.64 (dd, J = 5.5, 3.4 Hz, 2H), 7.49 – 7.40 (m, 8H), 7.36 (s, 2H), 4.61 (s, 8H); ^{13}C NMR (100 MHz, Acetone-d_6, DEPT): δ (ppm) = 143.7 (C), 133.0 (CH), 132.6 (CH), 129.6 (CH), 129.3 (CH), 128.9 (CH), 126.5 (C), 126.3 (C), 125.9 (CH), 123.4 (C), 95.0 (C), 93.0 (C), 88.4 (C), 64.2 (CH$_2$); MALDI-HRMS calculated for C$_{34}$H$_{26}$O$_4$Na: 521.1723, found: 521.1745.
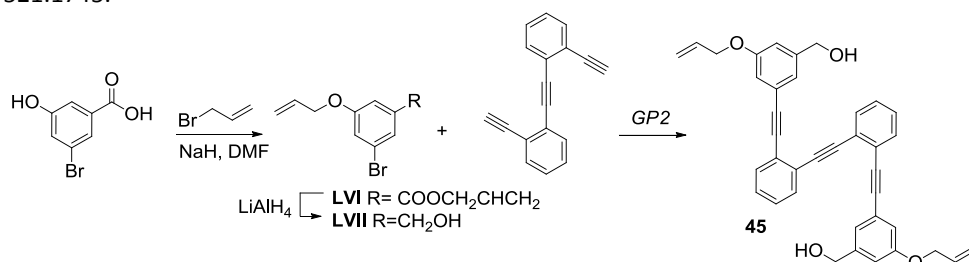
Compound LVI. Allyl bromide (1672 mg, 13.8 mmol) was added to a mixture of NaH (553 mg, 13.8 mmol) and 3-bromo-5-hydroxybenzoic acid (500 mg, 2.35 mmol) in DMF (30mL). This solution was stirred at room temperature for 6 h and then diluted with AcOEt, washed with 10% aqueous HCl and dried with anhydrous Na$_2$SO$_4$, and the solvent was removed. The residue was submitted to flash chromatography (EtOAc/Hexane,1/9) to give **LVI** (706 mg, 100 %) as a colourless oil; ^{1}H NMR (400 MHz, CDCl$_3$): δ (ppm) = 7.78 (s, 1H), 7.52 (s, 1H), 7.26 (s, 1H), 6.01-5.97 (m, 2H), 5.42 (dd, J = 16.0, 1.6 Hz, 1H), 5.39 (dd, J = 16.0, 1.6 Hz, 1H), 5.31 (dd, J = 10.5, 1.6 Hz, 1H), 5.29 (dd, J = 10.5, 1.6 Hz, 1H), 4.81 (d, J = 5.7 Hz, 2H), 4.57 (d, J = 5.2 Hz, 2H); ^{13}C NMR (100 MHz, CDCl$_3$, DEPT): δ (ppm) = 164.9 (C), 159.3 (C), 132.8 (C), 132.4 (CH), 132.0 (CH), 125.2 (CH), 123.0 (CH), 122.8 (C), 118.8 (CH$_2$), 118.4 (CH$_2$), 114.5 (CH), 69.4 (CH$_2$), 66.1 (CH$_2$); GC-EI-HRMS calculated for C$_{13}$H$_{13}$BrO$_3$: 296.0048, found: 296.0045.

Compound LVII. A solution of **LVI** (726 mg, 2.44 mmol) in deoxygenated THF (10 mL) was added dropwise to a deoxygenated solution of LiAlH$_4$ (120 mg, 3.18 mmol) in deoxygenated THF (40 mL) under argon at 0ºC. The mixture was stirred at room temperature for 2 h and, then, HCl 2 M was added until neutral pH. Then the crude was removed, and the residue was diluted with brine, extracted with CH$_2$Cl$_2$, dried over anhydrous Na$_2$SO$_4$, and the solvent removed. The residue was submitted to flash chromatography (AcOEt/Hexane: 3/7) to give **LVII** (426 mg, 72 %) as a yellow oil. ^{1}H NMR (400 MHz, CDCl$_3$): δ (ppm) =7.08 (s, 1H), 6.95 (s, 1H), 6.84 (s, 1H), 6.02 (m, 1H), 5.40 (dd, J = 17.3, 1.3 Hz, 1H), 5.31 (dd, J = 10.5, 1.3 Hz, 1H), 4.62 (s, 2H), 4.51 (d, J = 5.2 Hz, 2H); ^{13}C NMR (100 MHz, CDCl$_3$, DEPT): δ (ppm) = 159.6 (C), 144.2 (C), 132.7 (CH), 122.9 (C), 122.3 (CH), 118.1 (CH$_2$), 117.1 (CH), 112.1 (CH), 69.1 (CH$_2$), 64.5 (CH$_2$); GC-EI-HRMS calculated for C$_{10}$H$_{11}$BrO$_2$: 241.9922, found: 241.9932.

Compound **45** was prepared from compound **LVII** (215 mg, 0.88 mmol) and 2,2'-bis(ethynyl)diphenylacetylene (100 mg, 0.44 mmol) according to previously described *GP2* to give **45** in 38 % yield (92 mg) as a brown solid. ^{1}H NMR (500 MHz, CDCl$_3$): δ (ppm) = 7.64–7.62 (m, 2H), 7.56–7.55 (m, 2H), 7.35–7.32 (m, 4H), 7.00 (s, 2H), 6.91 (s, 2H), 6.83 (s, 2H), 5.98 (ddd, *J* = 17.2, 10.5, 5.3 Hz, 2H), 5.34 (dd, *J* = 17.2, 1.5 Hz, 2H), 5.24 (dd, *J* = 10.5, 1.3 Hz, 2H), 4.52 (s, 4H), 4.40 (d, *J* = 5.2 Hz, 4H); ^{13}C NMR (125 MHz, CDCl$_3$, DEPT): δ (ppm) =158.4 (C), 142.4 (C), 133.0 (CH), 132.2 (CH), 131.8 (CH), 128.3 (CH), 128.1 (CH), 126.0 (C), 125.7 (C), 124.2 (C), 122.9 (CH), 117.7 (CH$_2$), 116.2 (CH), 114.6 (CH), 93.9 (C), 92.2 (C), 88.2 (C), 68.8 (CH$_2$), 64.7 (CH$_2$); ESIpos-HRMS calculated for C$_{38}$H$_{30}$O$_4$Na*: 573.2036, found: 573.2045.
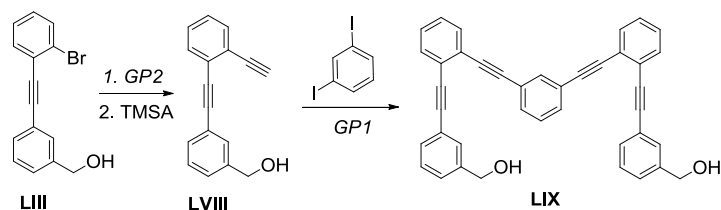
Compound **LVIII** was prepared from intermediate **LIII** (850 mg, 3.24 mmol) and trimethylsilylacetylene (0.7 mL, 4.87 mmol) according to previously described *GP2* to give a brownish syrup which was diluted in THF (110 mL) and tetra-*n*-butylammonium fluoride (1.5 g, 4.76 mmol) was added. The mixture was stirred five minutes, then evaporated under reduced pressure and finally purified by flash chromatography (EtOAc/Hexane: 8/2) to give **LVIII** in 97 % yield (874 mg) as a pale orange syrup. ^{1}H NMR (401 MHz, CDCl$_3$): δ (ppm) = 7.59 – 7.52 (m, 3H), 7.52 – 7.47 (m, 1H), 7.37 – 7.25 (m, 4H), 4.67 (s, 2H), 3.39 (s, 1H); ^{13}C NMR (101 MHz, CDCl$_3$, DEPT): δ (ppm) = 141.2 (C), 132.7 (CH), 131.9 (CH), 131.0 (CH), 130.2 (CH), 128.7 (CH), 128.7 (CH), 128.1 (CH), 127.2 (CH), 126.3 (C), 124.7 (C), 123.4 (C), 93.5 (C), 88.01 (C) 82.3 (C), 81.4 (CH), 64.9 (CH$_2$); EI-HRMS calculated for C$_{17}$H$_{12}$O: 232.0888, found: 232.0893.

Compound **LIX** was prepared from intermediate **LVIII** (138 mg, 0.59 mmol) and 1,3-diiodobenzene (258 mg, 0.59 mmol) according to previously described *GP1* to give **LIX** in 82 % yield (262 mg) as a white solid. ^{1}H NMR (401 MHz, CDCl$_3$): δ (ppm) =7.81 (s, 1H), 7.56 – 7.48 (m, 6H), 7.47 (s, 2H), 7.39 (d, *J* = 7.1 Hz, 2H), 7.35-7.27 (m, 5H), 7.22 (dd, *J* = 8.2, 5.3 Hz, 4H), 4.56 (s, 4H); ^{13}C NMR (101 MHz, CDCl$_3$, DEPT): δ (ppm) = 141.4 (C), 134.8 (C), 131.9 (CH), 131.8 (CH), 131.7 (CH), 130.7 (CH), 130.1 (CH), 128.8 (CH), 128.7 (CH), 128.5 (CH), 128.2 (CH), 127.1 (CH), 126.1 (C), 125.7 (C), 123.8 (C), 123.3 (C), 94.0 (C), 92.9 (C), 89.2 (C), 88.4 (C), 64.8 (CH$_2$); ESIpos-HRMS calculated for C$_{40}$H$_{26}$O$_2$Na: 561.1822, found: 561.1825.

3. *Synthesis and analytical characterization of the stapled-compounds*
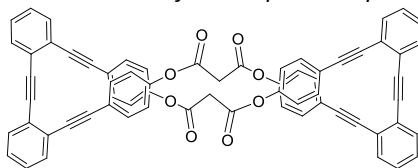
Compound **28a** was prepared from **28** (70 mg, 0.17 mmol) according to previously described *GP3* to give **28a** in a 55 % yield (86 % bsmr, 46 mg) as a white solid. ^{1}H RMN (500 MHz, CDCl$_3$): δ (ppm) =7.64 (dd, *J* = 5.8, 3.2 Hz, 4H), 7.58 (dd, *J* = 5.9, 3.2 Hz, 4H), 7.35 (dd, *J* = 5.8, 3.3 Hz, 8H), 7.29 (d, *J* = 8.7 Hz, 8H), 6.91 (d, *J* = 8.7 Hz, 8H), 3.79 (s, 4H); ^{13}C RMN (125 MHz, CDCl$_3$, DEPT): δ (ppm) = 164.5 (C), 150.0 (C), 133.2 (CH), 132.5 (CH), 132.3 (CH), 128.3 (CH), 128.1 (CH), 125.8 (C), 125.7 (C), 121.4 (C), 121.1 (CH), 93.1 (C), 92.1 (C), 88.4 (C), 41.9 (CH$_2$). MALDI-HRMS calculated for C$_{66}$H$_{36}$O$_8$ [M+Na]$^+$: 979.2326, found 979.2280.

30a **30b** **30c** **30d** **30e**

34 **35** **38** **39**
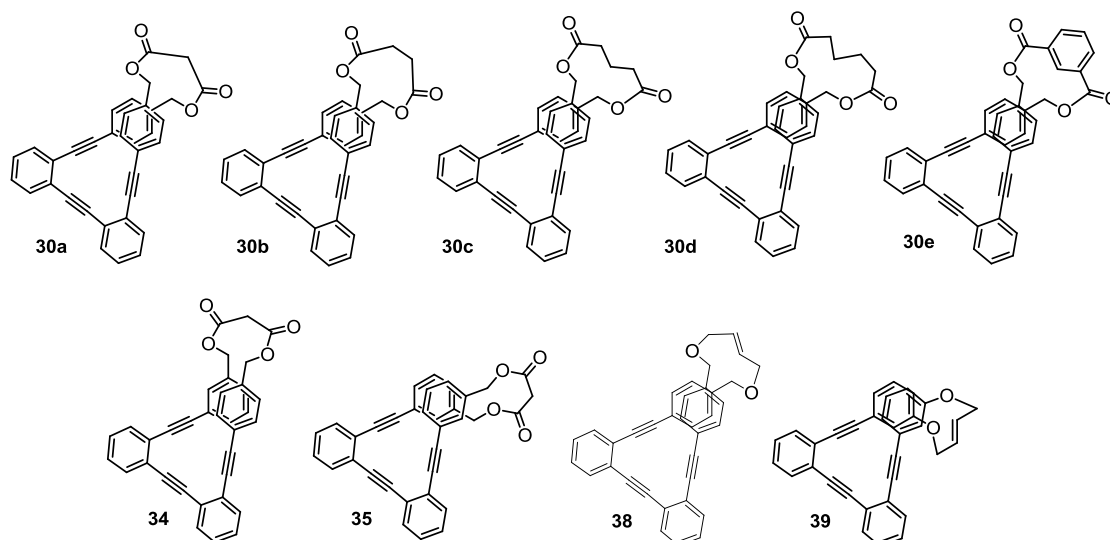
Compound **30a** was prepared from **29** (150 mg, 0.34 mmol) according to previously described *GP3* to give **30a** in 61 % yield (106 mg) as a white solid. ^{1}H NMR (500 MHz, CDCl$_3$): δ (ppm) =7.66-7.63 (m, 4H), 7.42–7.27 (m, 8H), 6.99 (d, *J* = 8.1 Hz, 4H), 5.00 (s, 4H), 3.44 (s, 2H); ^{13}C NMR (126 MHz, CDCl$_3$, DEPT): δ (ppm) = 165.8 (C), 135.0 (C), 133.4 (CH), 133.0 (CH), 132.2 (CH), 128.9 (CH), 128.4 (CH), 128.2 (CH), 125.4 (C), 125.2 (C), 123.5 (C), 93.5 (C), 92.3 (C), 89.3 (C), 66.7 (CH$_2$), 42.4 (CH$_2$); EI-HRMS calculated for C$_{35}$H$_{22}$O$_4$: 506.1518, found 506.1517.

Compound **30b** was prepared from **29** (50 mg, 0.12 mmol) according to previously described *GP3* to give **30b** in 51 % yield (32 mg) as a white solid. ^{1}H NMR (500 MHz, CDCl$_3$) δ (ppm): 7.67–7.58 (m, 4H), 7.36–7.29 (m, 8H), 6.98 (d, *J* = 8.3 Hz, 4H), 4.98 (s, 4H), 2.70 (s, 4H); ^{13}C NMR (126 MHz, CDCl$_3$; DEPT) δ (ppm): 170.5 (C), 135.6 (C), 132.8 (CH), 132.5 (CH), 131.9 (CH), 128.2 (CH), 127.9 (CH), 127.3 (CH), 125.3 (C), 122.7 (C), 93.6 (C), 92.0 (C), 88.5 (C), 65.7 (CH$_2$), 29.5 (CH$_2$), (one carbon signal was not observed); EI-HRMS calculated for C$_{36}$H$_{24}$O$_4$: 520.1675, found 520.1685.

Compound **30c** was prepared from **29** (50 mg, 0.12 mmol) according to previously described *GP3* to give **30c** in 56 % yield (34 mg) as a white solid. ^{1}H NMR (500 MHz, CDCl$_3$) δ (ppm): 7.67 – 7.59 (m, 4H), 7.40 – 7.29 (m, 8H), 7.07 (d, *J* = 8.0 Hz, 4H), 5.01 (s, 4H), 2.38 (t, *J* = 6.7 Hz, 4H), 2.01 – 1.92 (m, 2H); ^{13}C NMR (126 MHz, CDCl$_3$; DEPT) δ (ppm): 172.4 (C), 135.7 (C), 132.8 (CH), 132.5 (CH), 132.0 (CH), 128.2 (CH), 128.1 (CH), 127.9 (CH), 125.4 (C), 125.3 (C), 123.1 (C), 93.3 (C), 91.9 (C), 88.7 (C), 65.7 (CH$_2$), 32.7 (CH$_2$), 20.5 (CH$_2$); EI-HRMS calculated for C$_{37}$H$_{26}$O$_4$: 534.1831, found: 534.1830.

Compound **30d** was prepared from **29** (100 mg, 0.22 mmol) according to previously described *GP3* to give **30d** in a 32 % yield (40mg) as a white solid. ^{1}H NMR (400 MHz, CDCl$_3$) δ (ppm): 7.65–7.57 (m, 4H), 7.37–7.30 (m, 8H), 7.09 (d, *J* = 8.0 Hz, 4H), 5.03 (s, 4H), 2.35 (m, 4H), 1.65 (m, 4H); ^{13}C NMR (101 MHz, CDCl$_3$; DEPT) δ (ppm): 172.8 (C), 135.8 (C), 132.5 (CH), 132.2 (CH), 132.0 (CH), 128.2 (CH), 127.9 (CH), 127.5 (CH), 125.5 (C), 125.5 (C), 122.9 (C), 93.4 (C), 91.8 (C), 88.5 (C), 65.7 (CH$_2$), 34.2 (CH$_2$), 24.6 (CH$_2$); EI-HRMS calculated for C$_{38}$H$_{28}$O$_4$: 548.1988, found: 548.1989.

Compound **30e** was prepared from **29** (50 mg, 0.12 mmol) according to previously described *GP3* to give **30e** in a 54 % yield (34 mg) as a white solid. ^{1}H NMR (500 MHz, CDCl$_3$) δ (ppm): 8.41 (s, 1H), 8.24 (d, *J* = 7.8, 2H), 7.66 – 7.62 (m, 4H), 7.60 – 7.56 (m, 4H), 7.38 – 7.33 (m, 4H), 7.28 – 7.24 (m, 5H), 5.19 (s, 4H); ^{13}C NMR (126 MHz, CDCl$_3$; DEPT) δ (ppm): 164.9 (C), 135.3 (C), 133.8 (CH), 132.9 (CH), 132.8 (CH), 132.2 (CH), 131.4 (CH), 130.4 (C), 128.9 (CH), 128.9 (CH), 128.2 (CH), 128.1 (CH), 125.3 (C), 125.2 (C), 123.6 (C), 92.9 (C), 91.8 (C), 89.1 (C), 67.1 (CH$_2$); EI-HRMS calculated for C$_{40}$H$_{24}$O$_4$: 568.1675, found: 568.1678.

Compound **34** was prepared from **32** (30 mg, 0.07 mmol) according to previously described *GP3* to give **34** in 81 % yield (28 mg) as a white solid. ^{1}H NMR (300 MHz, CDCl$_3$) δ (ppm): 7.67–7.63 (m, 4H), 7.39 - 7.36 (m, 4H), 7.33 – 7.24 (m, 3H), 7.22 (s, 1H), 7.11 - 7.03 (m, 4H), 5.06 (s, 2H), 5.01 (s, 2H), 3.49 (s, 2H); ^{13}C NMR (75 MHz, CDCl$_3$; DEPT) δ (ppm): 166.1 (C), 166.0 (C), 134.9 (C), 134.5 (C), 133.2 (CH), 132.8 (CH), 132.7 (CH), 132.5 (CH), 132.3 (CH), 132.2 (CH), 132.2 (CH), 132.0 (CH), 129.1 (CH), 128.5 (CH), 128.4 (CH),

128.4 (CH), 128.3, (CH) 128.2 (CH), 128.2 (CH), 123.7 (C), 123.4 (C), 121.4 (C), 96.2 (C), 94.1 (C), 92.3 (C), 67.2 (CH$_2$), 66.9 (CH$_2$), 42.3 (CH$_2$); EI-HRMS calculated for C$_{35}$H$_{22}$O$_4$: 506.1518, found 506.1522.

Compound 35 was prepared from **33** (50 mg, 0.12 mmol) according to previously described *GP3* to give 3**5** in 83 % yield (48 mg) as a white solid. ^{1}H NMR (300 MHz, CDCl$_3$) δ (ppm): 7.63-7.60 (m, 4H), 7.44–7.32 (m, 8H), 7.11 (m, 4H), 5.02 (s, 4H), 3.47 (s, 2H); ^{13}C NMR (75 MHz, CDCl$_3$; DEPT) δ (ppm): 166.1 (C), 135.0 (C), 132.7 (CH), 132.6 8 (CH), 132.3 (CH), 132.0 (CH), 129.0 (CH), 128.5 (CH), 128.4 (CH), 128.3 (CH), 125.9 (C), 125.8 (C), 123.6 (C), 93.7 (C), 92.3 (C), 91.2 (C), 66.8 (CH2), 38.9 (CH2); EI-HRMS calculated for C$_{35}$H$_{22}$O$_4$: 506.1518, found 506.1519.

Compound 38 was prepared from **36** (102 mg, 0.19 mmol) according to previously described *GP5* to give 3**8** (2:1 mixture of *E:Z* stereisomers) in 56 % yield (52 mg) as a white solid.
E stereisomer: ^{1}H NMR (500 MHz, CDCl$_3$) δ (ppm): 7.71–7.60 (m, 4H), 7.46 (d, *J* = 8.1 Hz, 4H), 7.42–7.29 (m, 4H), 7.01 (d, *J* = 8.1 Hz, 4H), 5.79-5.77 (m, 2H), 4.37 (s, 4H), 3.55 (d, *J* = 5.2 Hz, 4H). ^{13}C NMR (100 MHz, CDCl$_3$; DEPT) δ (ppm): 138.0 (C), 133.0 (CH), 132.6 (CH), 132.4 (CH), 130.0 (CH), 128.3 (CH), 128.0 (CH), 127.7 (CH), 125.56 (C), 125.52 (C), 122.6 (C), 93.9 (C), 92.1 (C), 88.7 (C), 71.2 (CH$_2$), 63.3 (CH$_2$). IR (cm^{-1}): υ(C=C trans): 973.
Z stereisomer: ^{1}H NMR (500 MHz, CDCl$_3$) δ (ppm): 7.64-7.61 (m, 4H), 7.44 (d, *J* = 8.1 Hz, 4H), 7.38 – 7.29 (m, 4H), 7.05 (d, *J* = 8.1 Hz, 4H), 5.43-5.42 (m, 2H), 4.43 (s, 4H), 3.95 – 3.86 (m, 4H). ^{13}C NMR (125 MHz, CDCl$_3$; DEPT) δ (ppm): 139.5 (C), 133.0 (CH), 132.8 (CH), 132.1 (CH), 129.6 (CH), 128.3 (CH), 128.0 (CH), 127. 3 (CH), 125.4 (C), 125.4 (C), 122.2 (C), 93.9 (C), 92.2 (C), 88.7 (C), 71.8 (CH$_2$), 70.1 (CH$_2$). MALDI-HRMS calculated for C$_{36}$H$_{26}$O$_2$Na [M+Na]$^+$: 513.1830 found: 513.1825.

Compound 39 was prepared from **37** (69 mg, 0.14 mmol) according to previously described *GP5* to give 3**9** (2:1 mixture of *E:Z* stereisomers) in 91 % yield (59 mg) as a white solid.
Z stereisomer: ^{1}H NMR (500 MHz, CDCl$_3$) δ (ppm): 7.61-7.59 (m, 2H), 7.55 – 7.52 (m, 2H), 7.33-7.30 (m, 4H), 7.12 – 7.06 (m, 4H), 6.79-6.75 (m, 4H), 5.93-5.91 (m, 2H), 4.62 (d, *J* = 4.0 Hz, 4H). ^{13}C NMR (125 MHz, DEPT) δ (ppm): 158.2 (C), 132.6 (CH), 132.4 (CH), 129.1 (CH), 129.0 (CH), 128.2 (CH), 128.0 (CH), 125.8 (C), 125.7 (C), 125.6 (CH), 124.4 (C), 119.0 (CH), 115.9 (CH), 93.5 (C), 92.0 (C), 88.0 (C), 65.6 (CH$_2$). IR (cm^{-1}): υ(C=C cis): 683.
E stereisomer: ^{1}H NMR (500 MHz, CDCl$_3$) δ (ppm): 7.64-7.60 (m, 2H), 7.57-7.53 (m, 2H), 7.35–7.32 (m, 4H), 7.03-6.97 (m, 4H), 6.77-6.75 (m, 2H), 6.64–6.63 (m, 2H), 5.73-7.72 (m, 2H), 4.63-4.62 (m, 4H). ^{13}C NMR (125 MHz, DEPT) δ (ppm): 156.5 (C), 132.1(CH), 132.0 (CH), 129.6 (CH), 128.7 (CH), 128.2 (CH), 127.9 (CH), 126.4 (CH), 126.1 (C), 125.9 (C), 124.2 (C), 118.9 (CH), 117.2 (CH), 94.3 (C), 92.3 (C), 88.1 (C), 67.4 (CH$_2$). MALDI-HRMS calculated for C$_{34}$H$_{22}$O$_2$Na [M+Na]$^+$: 485.1512, found: 485.1528.

41 **42** **43**

46 **47** **48**
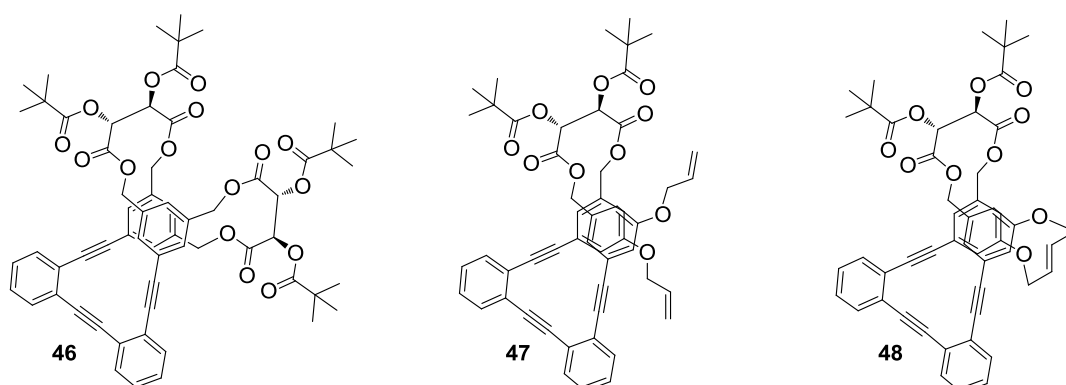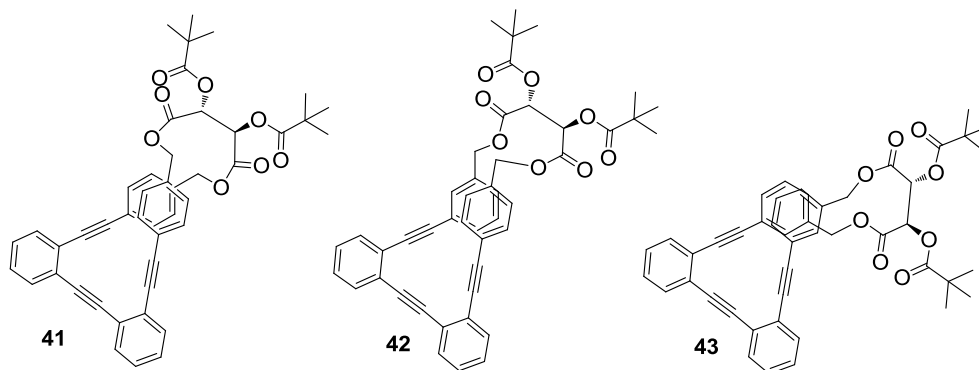
Compound **(-)-41** was prepared from **28** (50 mg, 0.12 mmol) according to previously described *GP4* to give (-)-**41** in 48 % yield (76 % bsrm, 38 mg) as a white solid. $[\alpha]_D^{20}$ = −30 (*c*= 0.33, CHCl$_3$). ^{1}H NMR (500 MHz, CDCl$_3$) δ (ppm): 7.66 − 7.64 (m, 2H), 7.63 − 7.60 (m, 2H), 7.36 − 7.34 (m, 4H), 7.27 (d, *J* = 8.2 Hz, 4H), 6.94 (d, *J* = 8.2 Hz, 4H), 5.40 (s, 2H), 5.08 (d, *J* = 12.7 Hz, 2H), 5.00 (d, *J* = 12.7 Hz, 2H), 1.28 (s, 18H); ^{13}C NMR (125 MHz, CDCl$_3$; DEPT) δ (ppm): 177.2 (C), 166.0 (C), 134.4 (C), 133.1 (CH), 132.7 (CH), 132.0 (CH), 128.3 (CH), 128.1 (CH), 127.2 (CH), 125.5 (C), 125.3 (C), 123.1 (C), 93.6 (C), 92.2 (C), 88.8 (C), 71.1 (CH), 67.0 (CH$_2$), 38.9 (C), 27.1 (CH$_3$). A good quality HRMS for this compound could not be obtained. Instead, we could obtain a X-Ray structure (see below).

Compound **(+)-42** was prepared from **33** (40 mg, 0.09 mmol) according to previously described *GP4* to give **42** in 30 % yield (60% brsm, 20 mg) as a colourless oil. $[\alpha]_D^{20}$ = +29 (*c*= 0.002, CHCl$_3$).^{1}H NMR (500 MHz, CDCl$_3$) δ (ppm): 7.65 − 7.60 (m, 4H), 7.40 − 7.37 (m, 2H), 7.37 − 7.34 (m, 4H), 7.29 (d, *J* = 1.3 Hz, 2H), 7.14 − 7.11 (m, 4H), 5.34 (s, 2H), 5.03 − 4.89 (m, 4H), 1.24 (s, 18H); ^{13}C NMR (126 MHz, CDCl$_3$; DEPT) δ (ppm): 177.3 (C), 166.2 (C), 134.5 (C), 132.7 (CH), 132.4 (CH), 132.2 (CH), 131.6 (CH), 128.4 (CH), 128.4 (CH), 128.2 (CH), 127.9 (CH), 125.8 (C), 125.5 (C), 123.4 (C), 93.3 (C), 92.1 (C), 88.9 (C), 71.6 (CH), 67.1 (CH2), 38.9 (C), 27.1 (CH$_3$); MALDI-HRMS calculated for C$_{46}$H$_{40}$O$_8$Na [M+Na]$^+$: 743.2621, found: 746.2615.

Compound **(+)-43** was prepared from **32** (48 mg, 0.11 mmol) according to previously described *GP4* to give **43** in 29 % yield (67% brsm, 22 mg) as a colourless oil. ^{1}H NMR (500 MHz, CDCl$_3$) δ (ppm): 7.65 − 7.60 (m, 4H), 7.40 − 7.37 (m, 2H), 7.37 − 7.34 (m, 4H), 7.29 (d, *J* = 1.3 Hz, 2H), 7.14 − 7.11 (m, 4H), 5.34 (s, 2H), 5.03 − 4.89 (m, 4H), 1.24 (s, 18H); ^{13}C NMR (126 MHz, CDCl$_3$; DEPT) δ (ppm): 177.3 (C), 166.2 (C), 134.5 (C), 132.7 (CH), 132.4 (CH), 132.2 (CH), 131.6 (CH), 128.4 (CH), 128.4 (CH), 128.2 (CH), 127.9 (CH), 125.8 (C), 125.5 (C), 123.4 (C), 93.3 (C), 92.1 (C), 88.9 (C), 71.6 (CH), 67.1 (CH2), 38.9 (C), 27.1 (CH$_3$).

Compound **(+)-46** was prepared from **44** (89 mg, 0.18 mmol) according to previously described *GP4* to give **(+)-46** in 18 % yield (18 % bsrm, 22 mg) as a colourless oil. $[\alpha]_D^{20}$ = +88 (*c*= 0.04, CHCl$_3$). ^{1}H NMR (500 MHz, CDCl$_3$) δ (ppm): 7.71 − 7.68 (m, 2H), 7.67 − 7.65 (m, 2H), 7.41 − 7.35 (m, 4H), 7.29 (s, 2H), 7.15 (s, 2H), 6.95 (s, 2H), 5.47 (d, *J* = 8.2 Hz, 2H), 5.43 (d, *J* = 8.2 Hz, 2H), 5.18 (d, *J* = 13.5 Hz, 2H), 5.13 (d, *J* = 12.8 Hz, 2H), 5.04 (d, *J* = 12.8 Hz, 2H), 4.70 (d, *J* = 13.5 Hz, 2H), 1.31 (s, 18H), 1.30 (s, 18H). ^{13}C NMR (125 MHz, CDCl$_3$; DEPT) δ (ppm): 177.2 (C), 177.2 (C), 166.3 (C), 166.1 (C), 135.4 (C), 135.0 (C), 134.9 (C), 132.9 (CH), 132.8 (CH), 130.6 (CH), 130.4 (CH), 128.5 (CH), 128.3 (CH), 127.8 (C), 125.6 (C), 125.3 (CH), 125.1 (C), 123.3 (C), 92.9 (C), 92.3 (C), 89.5 (C), 71.31 (CH), 71.30 (CH), 66.7 (CH$_2$), 65.8 (CH$_2$), 39.0 (C), 38.9 (C),

27.2 (CH$_3$), 27.1 (CH$_3$). Some carbon signals were not observed; MALDI-HRMS calculated for C$_{62}$H$_{62}$O$_{16}$Na [M+Na]$^+$: 1085.3936, found: 1085.3953.

Compound (+)-47 was prepared from **45** (79 mg, 0.14 mmol) according to previously described *GP4* to give **(+)-47** in 24 % yield (46 % bsmr, 28 mg) as a colorless oil. [α]$_D^{20}$ = +8 (*c*= 0.12, CHCl$_3$).^{1}H NMR (500 MHz, CDCl$_3$) δ (ppm): 7.65–7.62 (m, 2H), 7.60–7.56 (m, 2H), 7.37–7.33 (m, 4H), 6.91 (bs, 2H), 6.89 (s, 2H), 6.71 (s, 2H), 5.94 (ddt, *J* = 17.2, 10.5, 5.2 Hz, 2H), 5.33 (s, 2H), 5.31 (dd, *J* = 17.4, 1.5 Hz, 2H), 5.24 (dd, *J* = 11.9, 1.5 Hz, 2H), 4.97 (d, *J* = 12.4 Hz, 2H), 4.90 (d, *J* = 12.4 Hz, 2H), 4.38 (d, *J* = 5.0 Hz, 4H), 1.25 (s, 18H); ^{13}C NMR (125 MHz, CDCl$_3$; DEPT) δ (ppm): 177.3 (C), 166.1 (C), 158.3 (C), 135.8 (C), 133.1 (CH), 132.7 (CH), 132.2 (CH), 128.4 (CH), 128.2 (CH), 125.8 (C), 125.4 (C), 124.2 (C), 117.7 (CH$_2$), 117.5 (CH), 115.7 (CH), 93.6 (C), 92.1 (C), 88.7 (C), 71.6 (CH), 68.9 (CH$_2$), 67.0 (CH$_2$), 38.9 (C), 27.1 (CH$_3$). One carbon signal was not observed; MALDI-HRMS calculated for C$_{52}$H$_{48}$O$_{10}$Na [M+Na]$^+$: 855.3145, found: 855.3164.

Compound (-)-48. It was prepared from **(+)-47** (28 mg, 0.03 mmol) according to previously described *GP5* to give **(-)-48** in 61 % yield (14 mg) as a white solid. [α]$_D^{20}$ = -7 (*c*= 0.3, CHCl$_3$). ^{1}H NMR (500 MHz, CDCl$_3$) δ (ppm): 7.67 – 7.63 (m, 4H), 7.38-7.33 (m, 4H), 6.95 (s,1H), 6.93 (s, 1H), 6.73 (s, 1H), 6.67 (s, 1H), 6.63 (s, 1H), 6.58 (s, 1H), 5.76-5.73 (m, 2H), 5.47 (d, *J* = 7.7 Hz, 1H), 5.40 (d, *J* = 7.7 Hz, 1H), 5.29 (d, *J* = 13.2 Hz, 1H), 4.99 (d, *J* = 12.9 Hz, 1H), 4.93 (d, *J* = 12.9 Hz, 1H), 4.84 (d, *J* = 13.2 Hz, 1H), 4.68 – 4.64 (m, 2H), 4.60 – 4.55 (m, 2H), 1.31 (s, 9H), 1.29 (s, 9H). ^{13}C NMR (125 MHz, CDCl$_3$, DEPT) δ (ppm): 177.4 (C), 177.3 (C),166.1 (C), 166.0 (C), 156.2 (C), 156.0 (C), 135.9 (C), 135.0 (C), 133.0 (CH), 132.9 (CH), 132.8 (CH), 130.9 (CH), 130.7 (C), 128.4 (CH), 128.3 (CH), 128.1 (CH), 125.5 (C), 125.4 (C), 125.3 (C), 124.8 (CH), 124.3 (C), 123.7 (CH), 119.8 (CH), 119.0 (CH), 115.1 (CH), 114.9 (CH), 93.3 (C), 92.2 (C), 92.1 (C), 88.6 (C), 88.5 (C), 71.8 (CH), 71.5 (CH), 66.9 (CH$_2$), 66.4 (CH$_2$), 66.3 (CH$_2$), 66.2 (CH$_2$), 39.0 (C), 38.9 (C), 27.2 (CH$_3$), 27.1 (CH$_3$). Some carbon signals were not observed; MALDI-HRMS calculated for C$_{50}$H$_{44}$O$_{10}$Na [M+Na]$^+$: 827.2832, found: 827.2827.
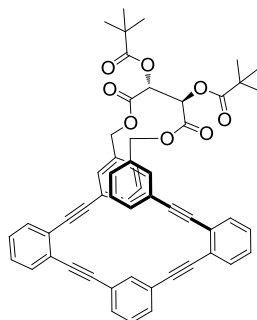
Compound 52 was prepared from **LIX** (176 mg, 0.33 mmol) according to previously described *GP4* to give **52** in 23 % yield (62 mg) as a colourless oil. ^{1}H NMR (500 MHz, CDCl$_3$) δ (ppm): 7.74 (s, 1H), 7.60 – 7.49 (m, 21H), 7.33 (ddt, *J* = 11.2, 7.8, 3.4 Hz, 16H), 5.54 (s, 3H), 5.06 (s, 6H), 1.13 (s, 29H); ^{13}C NMR (126 MHz, CDCl$_3$, DEPT) δ (ppm): 177.0 (CO), 165.9 (CO), 134.9 (C), 134.0 (CH), 132.4 (CH), 132.2 (CH), 132.1 (CH), 131.9(CH), 131.8 (CH), 129.5 (CH), 128.9 (CH), 128.7 (C), 128.3 (CH), 128.3 (CH), 126.0 (C), 125.9 (C), 123.9 (C), 123.7 (C), 93.1 (C), 93.1 (C), 89.0 (C), 88.8 (C), 70.8 (CH), 67.5 (CH2), 38.8 (C), 26.9 (CH3).

4. *UV-vis studies.*

UV-visible normalized absorption spectra of all open *o*-OPEs and related macrocycles were registered at 10^{-5}M in CH$_2$Cl$_2$ at room temperature. The reported structures showed two characteristic UV-vis absorptions at around 270 and 300 nm.

5. *CD studies.*

CD spectra of the all the chiral compounds were registered at 10^{-5} M in CH$_2$Cl$_2$ at room temperature. The concentration of the compound (*P,R,R*)-**XXX** could not be determined due to the small amount of product obtained after semipreparative HPLC. In this case, the value of CD signal registered was multiplied by five.

6. *HPLC studies.*

We obtained the two diastereisomers of compound **3** through analytical separation using a Chiralpack IC column, with hexane/*i*PrOH (90/10) as eluent, and a flow of 0.5 mL min^{-1}.

7. *ECD calculations.*

The geometries of the *(M,R,R)*-**3** and *(P,R,R)*-**3** compounds as extracted from X-Ray diffractrometry studies were taken as suitable structures to model their UV and ECD spectra. All the parameters for the two stereoisomers were computed using the very popular TD-B3LYP/6-31G*. The importance of bulk CH_2Cl_2 effects in the ECD spectra was assessed considering the polarized continuum model PCM. A total of 100 excited states were computed in order to completely cover the wavelength interval of the experimental ECD spectra. The simulation of the ECD spectra was achieved through the overlap of Gaussian shaped functions centered at each electronic transition assuming an exponential half-width of 20 eV, unless otherwise specified. All linear response theory calculations were carried out with the commercial version of Gaussian 09 quantum chemistry software. All the simulated ECD spectra were obtained with the 1.53 version of the SpecDis program.

8. *Computatinal details for geometries optimization, thermodynamics and spring behaviour.*

All theoretical calculations were carried out at the DFT level of theory using the hybrid M06 exchange-correlation functional proposed by Truhlar and Zhao[244], as implemented in the Gaussian 09 program. The Pople standard 6-31G* basis set[245] has been used in all cases. Enthalpies and free energies, where necessary, were determined by the corresponding frequency calculation on each optimized structure.

9. *X-ray structure determinations.*

Crystals were grown from methyl acetate, acetone, diethyl ether, acetonitrile or ethyl acetate saturated solutions under slow evaporation at room temperature. Measured crystals were prepared under inert conditions immersed in perfluoropolyether as protecting oil for manipulation. Suitable crystals were mounted on MiTeGen MicromountsTM and these samples were used for data collection. Data were collected with Bruker X8 Proteum and Bruker SMART APEX diffractometers at beamline BM16 (ESRF synchrotron, Grenoble, France) and at beamline I19 (Diamond, UK). The data were processed with APEX2 program. The structures were solved by direct methods. CELL_NOW was used to determined the orientation matrices and the domains were related by a 180 deg rotation around the recipocal axis 0 0 1. Crystallographic data (excluding structure factors) reported in this paper have been deposited with the Cambridge Crystallographic Data Center: http://www.ccdc.cam.ac.uk/products/csd/request/.

---

[244] Y. Zhao, D. G. Truhlar, *Acc. Chem. Res.* **2008**, *41*, 157-167.

[245] V. A. Rassolov, M. A. Ratner, J. A. Pople, P. C. Redfern, L. A. Curtiss, *J. Comp Chem.* **2001**, *22*, 976-984.

2.3. Novel *o*-PE-based helicates by Ag(I) templating

The strategy to covalently lock flexible *o*PEOs into well define macrocycles exposed in the previous chapter, provided us a wide variety of ready-available free *molecular pockets*. Integration of transition metals within the cavity of a molecular sieve is one objective that several laboratories in the word pursuit to develop molecular catalysts.[246] Some precedent related to the ability of tribenzocyclines **1** and **2** to act as a versatile ligand to Ni(0), Cu(I), Co(0), Ag(I) and Pt(II),[247] awaked our interest in screening the potential features as metal ligands of the new family of macrocycles developed in our laboratory. Moreover, π-prismands mainly developed by *Gleiter et al.* are also able to complex Li(I), Na(I), Cd(II), Cu(I) and Ag(I).[248]

On the other hand, defining the secondary structure of a chain molecule based on the ability of metal ions to selectively coordinate to preferred segments within its backbone, has been restricted to the superior coordination capabilities of heteroatoms towards metals. As a consequence of some unexpected but promising results obtained in the beginning of the above-mentioned purpose, we also started an experimental and theoretical study to develop *ortho*-phenylene-ethynylene helicates on metal-templated folding. To the best of our knowledge, the coordination capability of alkynes towards carbophilic metals to induce helical folding has not been explored to date.
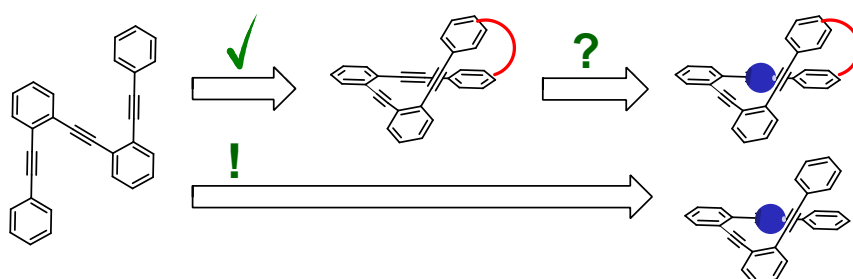
Figure 86. *Schematic summary of the hypothesis and results of this section.*

[246] W. Zhang, J. S. Moore, *J. Am. Chem. Soc.* **2005**, *127*, 11863- 11870.

[247] J. L. Kendall, D. A. Canelas, J. L. Young, J. M. De Simone, *Chem. Rev.* **1999**, *99*, 543-563.

[248] A. Kunze, F. Rominger, R. Gleiter, *Eur. J. Inorg. Chem.* **2006**, 621–627.

2.3.1. Background

In coordination chemistry a *ligand* is an ion or a molecule that binds to a central atom to form a coordination complex.[249] The coordination phenomenon is determined not only by the features of the interaction but also by the coordination possibilities which stem from the number (denticity) and allocation of the binding sites in the ligand. In the specific case of multidentated ligands, the flexibility of the ligand backbone also plays a role.

Nowadays, one of the more active research fields deal with chain and cyclic molecules bearing sereral π-donor groups able to form complexes with metal ions by carbon metal interactions. For example, coinage metal (Cu, Ag, Au) ions are some of the best reagents to activate and mediate reactions involving alkynes.[250] Most of these processes are known to start by the coordination of only one of the π-bonds to the catalytically active metal center.[251] Therefore, study such coordination event is of considerable interest. Despite the literature involving one M-alkyne bond is quite vast, structurally characterize complexes with more than one alkyne moiety bounded to the same metal center are scarce. To the best of our knowledge, only the works from Young, Dias and Gleiter have been focused on describing such binding interaction.

Young *et al.* have exhaustively studied the nature of the alkyne-metal bond in planar metallocyclynes. In contrast to other planar ligands such as porphyrins and phtalocyanines which bind the metal through relatively hard nitrogen atoms leading to formal negatively charged complex, cyclotriynes are neutral and bind a metals via a three soft, polarizable alkyne donors. By combination of different substituted and unsubstituted [12]DBAs and related cyclynes with Ni(0), Cu(I), Co(0) and Ag(I), several metallocyclynes have been isolated in solid state. Analysis of the crystal structures have shown that only Co, Ni, and Cu are small enough to bind with in the cavity of a trynezocycline derivate (Figure 87).
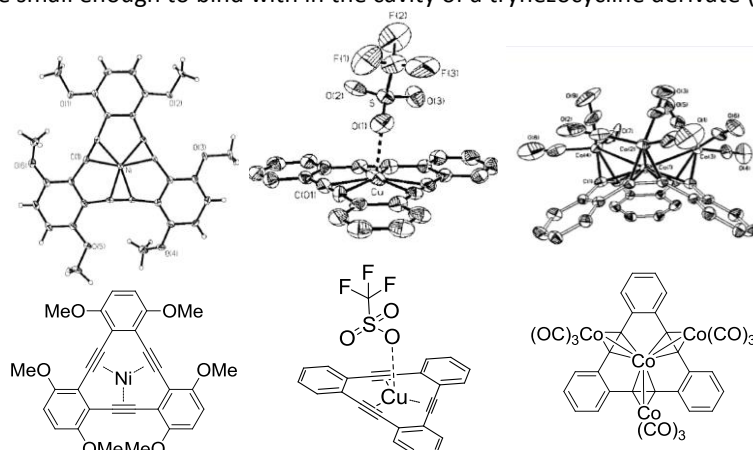
Figure 87. *Crystal structures of metallocyclines formed by a [12]DBA ligand and Ni(0), Cu(I) and Co(0) metals coordinated to the three alkynes. [From ref. 46]*

With larger metals as Ag(I), sandwich systems are formed and both staggered and eclipsed conformations have been detected in the same unit cell (Figure 88).[252]

[249] "Ligand", IUPAC Gold Book Electronic version, http://goldbook.iupac.org.
[250] A. Das, C. Dash,M. A. Celik,M. Yousufuddin,G. Frenking, H. V. R. Dias, *Organometallics,* **2013**, *32*, 3135–3144.
[251] S. Flügge, A. Anoop, R. Goddard, W. Thiel, A. Fürstner, *CEJ*, **2009**, *15*, 8558-8565.
[252] (a) Ferrara, J. D.; Djebli, A.; Tessier-Youngs, C.; Youngs, W. J. *J.Am. Chem. Soc.* **1988**, *110*, 647-649; (b) Dunbar, R. C.; Solooki, D.; Tessier, C. A.; Youngs, W. J.; Asamoto, B. *Organometallics* **1991**, *10*, 52-54.
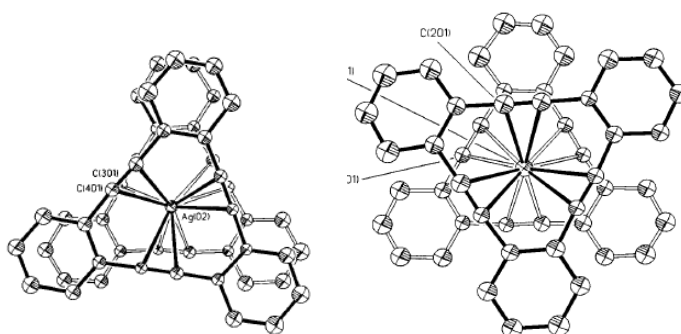
Figure 88. Eclipsed and staggered conformations observed in the crystal structure of a [12]DBA·Ag(I) complex.[From ref. 46]

Interestingly, Komatsu *et al.* reported that the related tetrabenzocycline **2** forms a planar complex with the silver[253] which demonstrates that more flexible ligands (or ligands with larger cavities) are able to incorporate the second row transition metals (Figure 89 right). Reaction of TBC **2** with dicobalt octacarbonyl produced a non-planar stable complex in which two of the four alkynes are bound to $Co_2(CO)_6$ moeties in a linear fashion reducing the volume of the central pocket (Figure 89 left).[254]
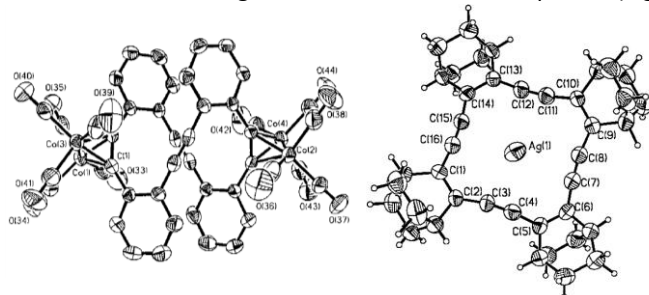
Figure 89. Crystal structures of organometallic complexes formed between non-planar tetrabenzocyclines and Co(0) (left) and Ag(I) atoms. [From ref. 46]

Gleiter *et al.* have also reported flexible cage structures called π-prismand (Figure 90) with the *in/in* conformation of the N-bridgehead lone-pairs. This lone pairs and the triple bonds in the bridges are responsible for including Cu(I) and Ag(I) ions inside the cage.[255]
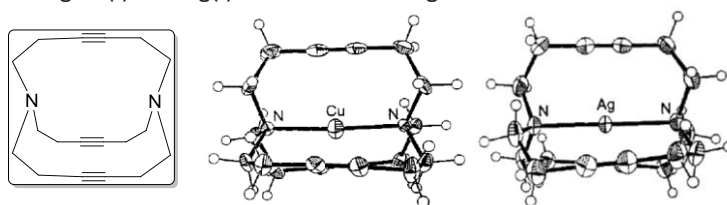
Figure 90. Chemical structure of 1,8-diazabicyclo[6.6.6]eicosa-4,11,17-triyne (left). Crystal structures of the organometallic complexes formed with Ag(I) and Cu(I). [From ref. 268]

The replacement of one 3-hexyne unit in such cavitant by a the 3,6-dioxaoctane unit have widen the resulting π-prismand complex family to other metals centers such as Li, Na and Cd (Figure 91).[256]

[253] T. Nishinaga, T. Kawamura, K. Komatsu, *J. Chem. Soc., Chem. Commun.* **1998**, 2263-2264.

[254] R. S. Dickson, P. Fraser, J. *Adv. Organomet. Chem.* **1974**, *12*, 323-377.

[255] (a) V. Wolfart, R. Gleiter, H. Irngartinger, T. Oeser, C. Krieger, *Eur. J. Org. Chem.* **1998**, 2803–2809; (b) A. Kunze, R. Gleiter, F. Rominger, *Chem. Commun.* **1999**, 171–172.

[256] A. Kunze, F. Rominger, R. Gleiter, *Eur. J. Inorg. Chem*. **2006**, 621–627.
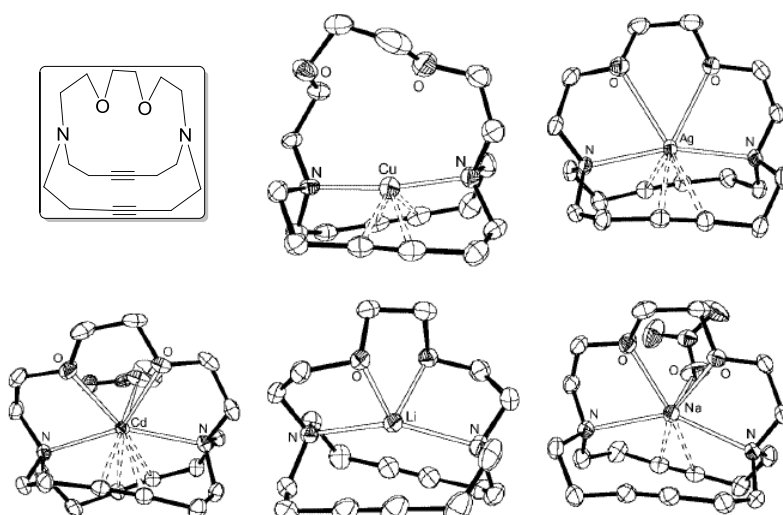
Figure 91. *Chemical structure of 4,7-dioxa-1,10-diazabicyclo[8.6.6]docosa-13,19-diyne (left). Crystal structures of the organometallic complexes formed with Ag(I), Cu(I), Li(I), Na(I) and Cd(II). [From ref. 269]*

Additionally, Gleiter´s group has also replaced one, two and tree of the alkynes by other π-donors as benzene rings (Figure 92). Again, metal complexes with Cu(I) and Ag(I) salts have been obtained for the six ligands but when the three π-donors are benzenes only one N was found to bind the metal center.[257]
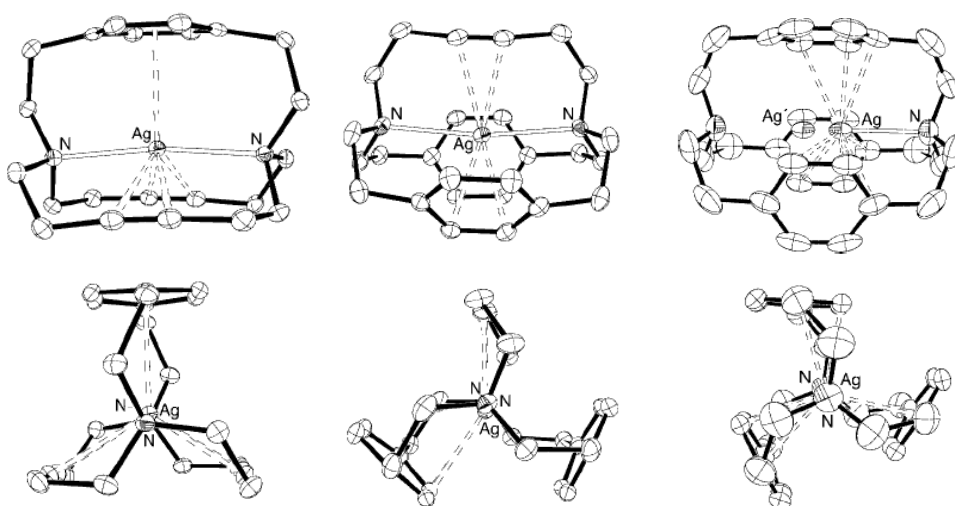
Figure 92. *Crystal structures of the Ag(I) organometallic complexes with alkyne and benzene π-donors developed by Gleiter et al. [From ref. 270]*

Unlike in the above-mentioned examples, Dias *et al.* work has been focused on "series of well-authenticated, isoleptic[258] coinage metal alkynes complexes."[259] In particular, they have recently reported monomeric coinage metal complexes including two or three triple bonds coming from independent but identical ligands. To obtain bis- and tris(alkyne) adducts in neutral and cationic forms, the ligands of choice has been cyclooctyne.[260] Other structurally authenticated coinage metal bis- and tris(alkyne) adducts based on regular monoalkyne hydrocarbon donors including

---

[257] A. Kunze, S. Balalaie, R. Gleiter, F. Rominger, *Eur. J. Org. Chem.* **2006**, 2942–2955.

[258] Isoleptic (also called homoleptic) metal adducts are those with the same ligand set. See: (a) Davidson, P. J.; Lappert, M. F.; Pearce, R. *Acc. Chem. Res.* **1974**, *7*, 209–217; (b) Davidson, P. J.; Lappert, M. F.; Pearce, R. *Chem. Rev.* **1976**, *76*, 219–242.

[259] H. V. R. Dias, J. A. Flores, J. Wu, P. Kroll, *J. Am. Chem. Soc.* **2009**, *131*, 11249−11255.

[260] A. Das, C. Dash, M. A. Celik, M. Yousufuddin, G. Frenking, H. V. R. Dias, *Organometallics,* **2013**, *32*, 3135−3144.

[Ag(C$_2$H$_2$)$_3$][Al{OC(CF$_3$)$_3$}$_4$][261] and [M(L)(OTf)]$_n$ (M = Cu, Ag; L= 1,6-cyclodecadiyne, 1,7-cyclododecadiyne, 1,8-cyclotetradecadiyne) [262] have been reported in advance by other groups.

In the last work from Dias´ group, the treatment of, CuSbF$_6$, AgSbF$_6$ and AuSbF$_6$ (Cu and Au salts prepared in situ from CuBr and AuCl with AgSbF$_6$ respectively) with slightly more than four equivalents of cyclooctyne in dichloromethane at -10°C under nitrogen led to the tris(alkyne) adducts in 51, 54 and 60% yield respectively (Scheme 34 right). The copper and silver adducts are moderately air and thermal stable compounds in comparison to the gold adduct. Treatment of AuCl with about 5 equiv of cyclooctyne in dichloromethane led to [Au(L)$_2$Cl] in 52% yield (Scheme 34 left).The cationic complex was obtained by adding one equivalent of AgSbF$_6$.
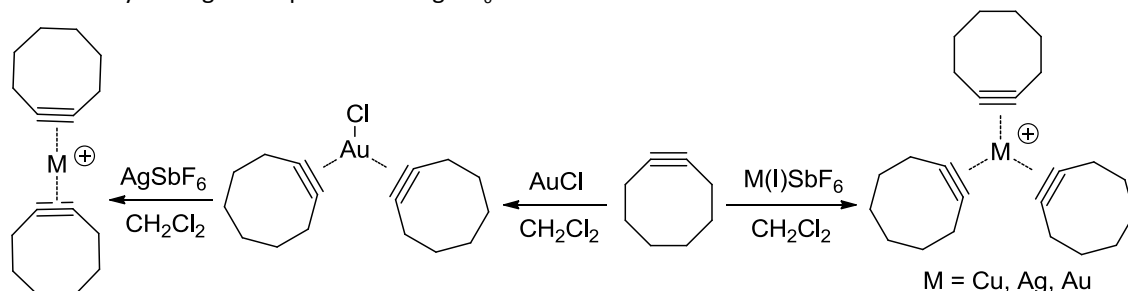
Scheme 34. *Tris(alkyne) and bis(alkyne) complexes of coinage metals reported by Dias.*

Together with the NMR, X-ray and IR analysis of the complexes, a detailed theoretical analysis of the M–alkyne bonding interactions have also been presented by Dias group, thus providing useful information on preferred coordination modes/geometry and the effects of a π-bound coinage metal on an alkyne moiety. Despite the breakdown of ΔEorb into contributions of orbitals that have different symmetry for the metal-alkyne bond, depends on each specific case, it is well-worth to mention that its generally studied based on four components: alkyne-M σ-donation (Figure 93, (1)), in-plane M-alkyne backdonation (Figure 93, (2)), out-of-plane alkyne-M π-donation (Figure 93, (3)) and a general term than include small contributions from-lower lying orbitals (Figure 93, (4)). Among them, alkyne-M σ-donationis the largest component for the more strongly bonded ligands while higher back donation contributions are typical of less strongly bonded ligands.
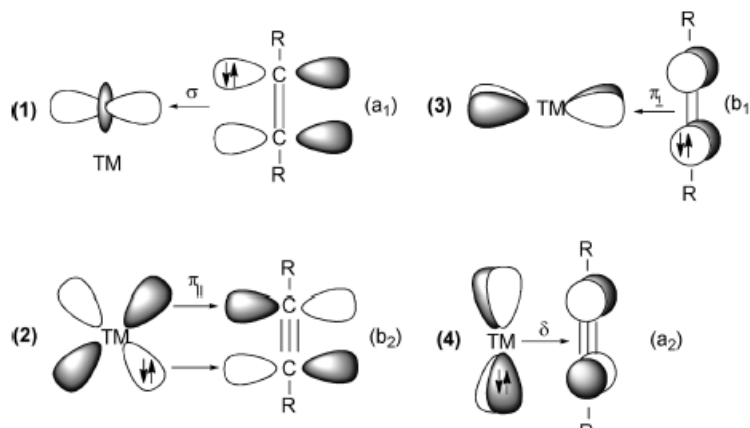
Figure 93. *General scheme for orbital interactions between a transition metal atom (TM) and an alkyne moiety. [From ref.273]*

Concerning the different coordination modes of M-alkyne bonds depending on the nature of the non terminal alkyne, some related disubstituted acetilydes and organometallic bridged 1,4-diynes, an in-depth study has been review by Lang *et al.*[263]

---

[261] A. Reisinger, N. Trapp, I. Krossing, S. Altmannshofer, V. Herz, M. Presnitz, W. Scherer, *Angew. Chem., Int. Ed.* **2007**, *46*, 8295-8298.

[262] Note that the cited cyclodialkynes serve as monoalkynes ligands for a given metal leading to multinuclear species in the solid-state. The first reported example can be found in: Gleiter, R.; Karcher, M.; Kratz, D.; Ziegler, M. L.; Nuber, B. *Chem. Ber.* **1990**, *123*, 1461–1468.

2.3.2. Results and discussion

2.3.2.1.Initial screening

Our initial efforts to screen the capability of the macrocyclic compounds developed in the former section to act as ligand, dealed with small selection of commertial metal salts (NaBF$_4$, LiBF$_4$, ZnBF$_4$ and AgBF$_4$) bearing the weakly coordinating counterion BF$_4^-$.[264] For that, we treated several macrocycles **30a**, **35**, **30e** with an excess of the metal salts and the corresponding samples were analyzed by ^{1}H-NMR. Although Na, Li and Zn did not induce any appreciable change in the proton spectra, the samples treated with silver exhibited changes in the aromatic region. To continue with the study, we selected compound **30a** as a model. The formation of a discrete complex was confirmed in a second experiment upon addition of a controlled excess (15 equivalents) of AgBF$_4$ to a solution of compound **30a** in CD$_2$Cl$_2$ (Figure 94). Due to the versatility of the Ag(I) ions to coordinate to n-donors as carbonyl groups and π-donors as aromatic rings as alkynes, a wide range of host-guest complexes featuring one or more silver atoms and **30a** could be imagined for such changes. To further investigate the above-mentioned silver incorporation, we decided to make some control experiments with the related compounds **29** and **31**.
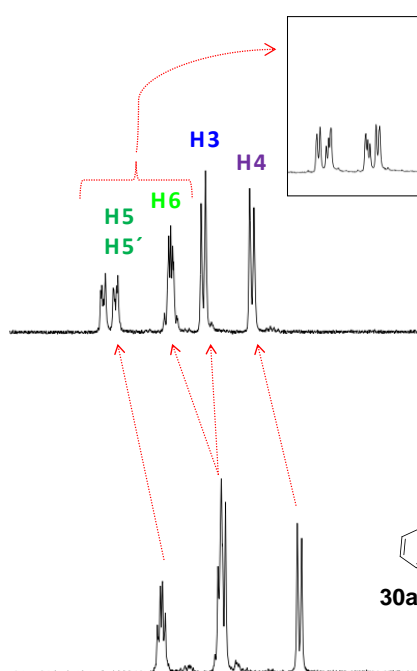
Figure 94. *Changes observed by ^{1}H-NMR after adding AgBF$_4$ to a solution of **30a** in CH$_2$Cl$_2$.*

Interestingly, the ^{1}H-NMR spectra registered after adding an excess of AgBF$_4$ to **29** (Figure 95) and **31** (Figure 96) resulted in a very similar chemical shift pattern. The most noteworthy change in the three samples tested was the distinctive deshielding of the aromatic protons of the inner benzenes (See inset in figure 8 94).

---

[263] H. Lang, K. Köhler, S. Blau, *Coordination Chemistry Reviews*, **1995**, *143*, 113-168.
[264] Au(I) was also tested and the formation of a new complex was also observed. Additional information about this experiments can be found in the experimental section. Further studies on Au(I) complex are underway in collaboration with Alice Johnson and Prof. Echavarren. Institute of Chemical Research of Catalonia (ICIQ), Tarragona, Spain.
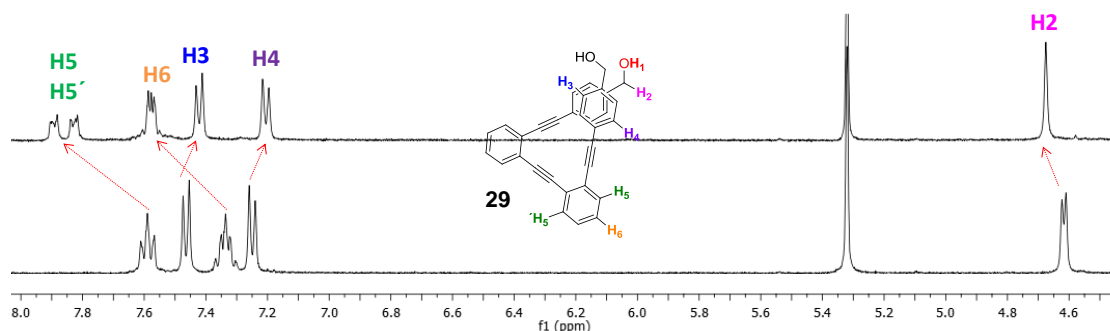
Figure 95. Changes observed by ^{1}H-NMR after adding AgBF$_4$ to a solution of **29** in CH$_2$Cl$_2$.
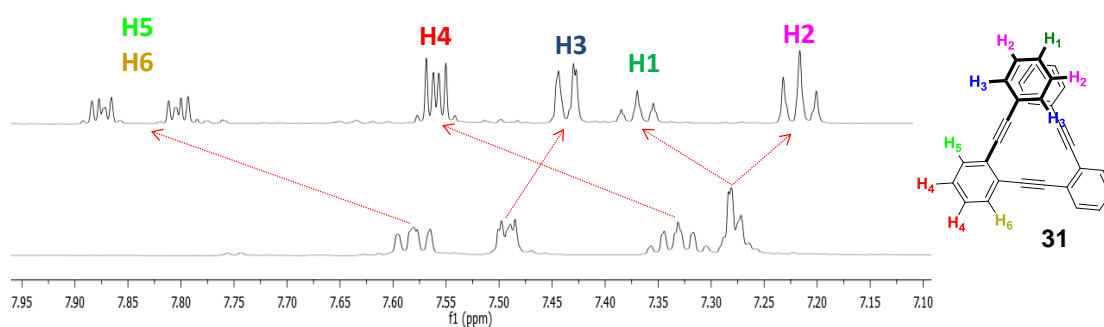
Figure 96. Changes observed by ^{1}H-NMR after adding AgBF$_4$ to a solution of **31** in CH$_2$Cl$_2$.

A possible coordination interaction involving dimeric cation-π complexes with the terminal benzenes of **30a**, **29** and **31** could give similar observations.[265] To evaluate the influence of the silver on each part of the molecule, changes on the ^{13}C-NMR spectra between the free and the coordinated compound were used. For that, the chemical shift of each nucleus was averaged[266] for the terminal benzenes, the inner benzenes and the alkynes (Figure 97).[267] In all the cases, stronger deshielding was observed for the inner benzenes and for this reason the possible cation-π coordination motif was rejected.
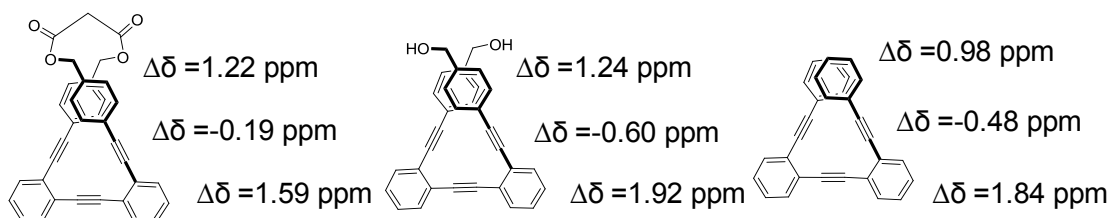
Figure 97. Averaged changes on the ligands observed by ^{13}C-NMR after adding AgBF$_4$.

Additionally, a mechanistic study on Ag/Pd-catalyzed sp-sp^2 cross-coupling reaction reported by Pale *et al.* provided several data to contrast our findings. In this work, the authors used ^{1}H, ^{13}C and ^{109}Ag-NMR to evidence the *in situ* formation of 1-alkynyl and a silver π-complex from alkynes and silver salts.[268] Despite ^{109}Ag-NMR proved to be helpful, the more revealing observations which supported the formation of a silver π-complex between the silver cation and 1-hexyne were extracted from the ^{1}H- and ^{13}C-NMR data. These observations were: 1) a decrease on the coupling constant $^4J\{^1H,^1H\}$ of the

---

[265] Sandwiching of metal ions between planar aromatic structures is a frequent motif in organometallic chemistry.

[266] This simplification of the NMR changes have been previously used by Tew. See for example: *N J Chem.* **2008**.

[267] Despite this approximation is quite representative of the net influence of the Ag(I) on the benzene rings, it does not account for the alkynes. The alkyne carbon atoms experiment different shifts (upfield and downfield) on the 13C resonances probably due to the different contributions of each nucleous to the coordination bond with the silver.

[268] U. Létinois-Halbes, P. Pale, S. Berger, *J. Org. Chem.* **2005**, *70*, 9185-9190.

neighboring protons which indicated a loss of electron density of the triple bond, 2) the deshielding of the alkyne neighboring protons and 3) the deshielding of the internal sp carbon (from 87.0 to 83.9 ppm) which was accompanied by a shielding of the terminal carbon (from 66.2 to 68.2 ppm). Interestingly, analogous hints of coordination were recorded in our case (Table 7).

	$^4\Delta J^a$	$\Delta\delta(^1H)$ (ppm)^a	$\Delta\delta(^{13}C)$ (ppm) of the alkynes ^{b}
209	-1.4	0.25	93.88, 92.55, 89.44 → 96.50, 93.56, 85.61
208	-1.6	0.27	94.17, 92.71, 88.63 → 96.07, 92.95, 84.91
256	-1.3	0.35	94.15, 92.63, 88.57 → 95.95, 92.63, 85.31

^{a}Coupling constants and shifts of H5 protons (see figures 89, 90 and 91). ^{b}See experimental section.

Table 7

All these evidences led us to bestow that the Ag(I) was able to bind the three alkynes of **30a** which were already forming a molecular pocket optimal to allocate carbophylic metals giving a new type of metallocavitand.[269] Moreover, the analogous observations made on **28** and **31** strongly suggested that the Ag(I) was inducing a helical conformation by coordination with the alkynes. As it can be read in the introduction to this section, the formation of coinage-metal alkyne complexes was previously known however this interaction has never been used as driving force for the folding of *o*PEs.

Under the light of these results, we decided to study the stability of the Ag(I)-alkyne interaction with the three above-mentioned compounds.[270] For that, ^{1}H-NMR titrations were performed in CD_2Cl_2:Acetone (9:1) solvent mixtures to facilitate the solubility of the metal salt. Upon stepwise additions of $AgBF_4$ to a solution of **28**, homogeneous changes on all the aromatic signals revealed a nice binding phenomenon.[271] Characteristic deshielding of the aromatic protons attributed to the Ag-alkyne interaction could be unambiguously identified and only one set of signals was observed in all spectra suggesting stable complexation under fast exchange conditions (Figure 98).[272] Synergetic contributions of the free alcohols to fold compound **28** was reflected by the impressive high value of the binding constant (K_{eq}= 769 ± 108 M^{-1}) in comparison to its unsubstituted analog **31** (K_{eq}= 50 ± 2 M^{-1}, Figure 99).[273]
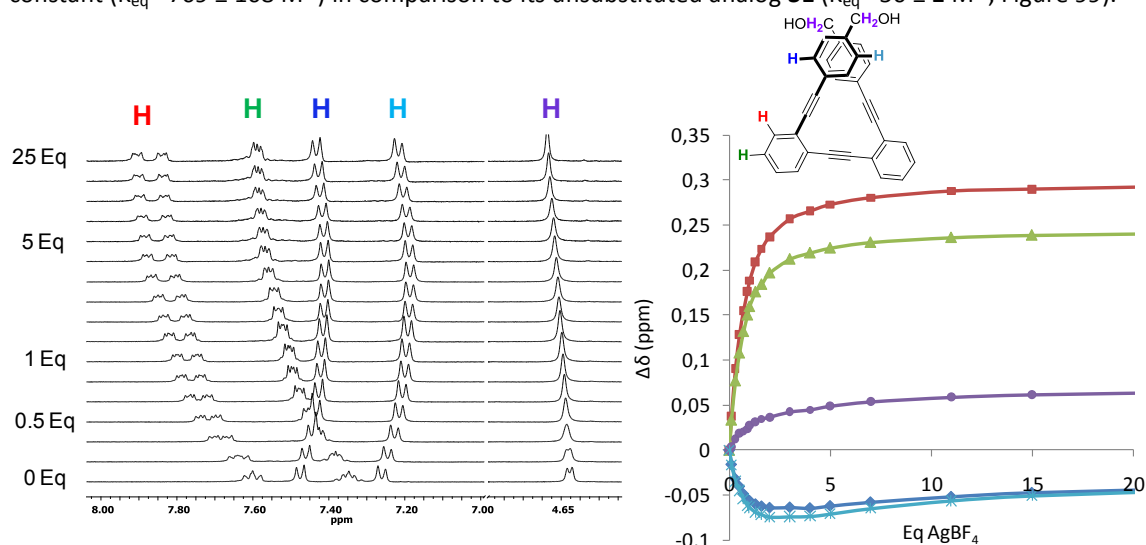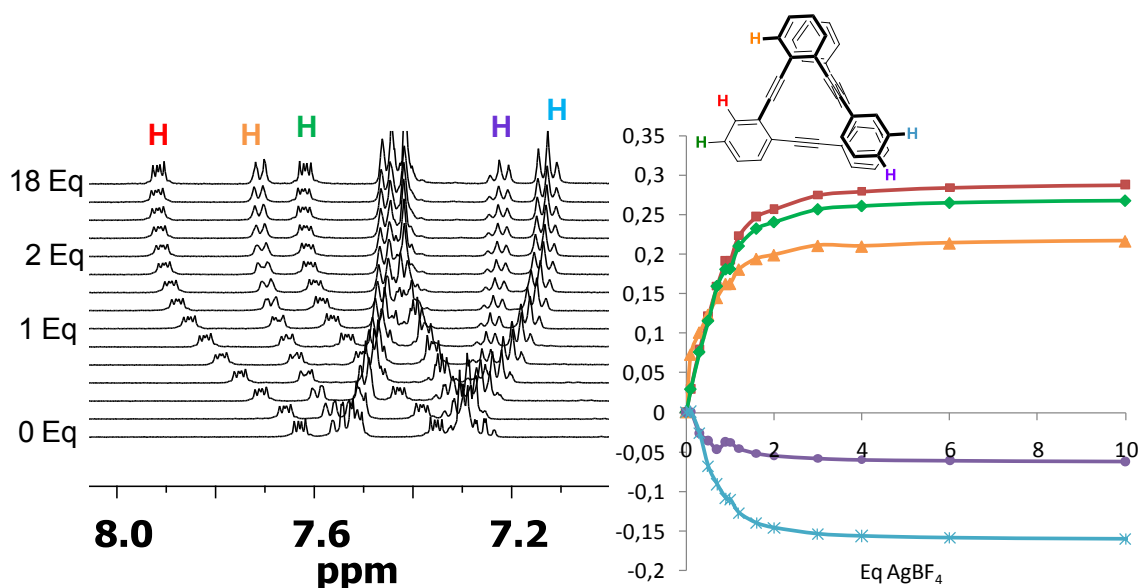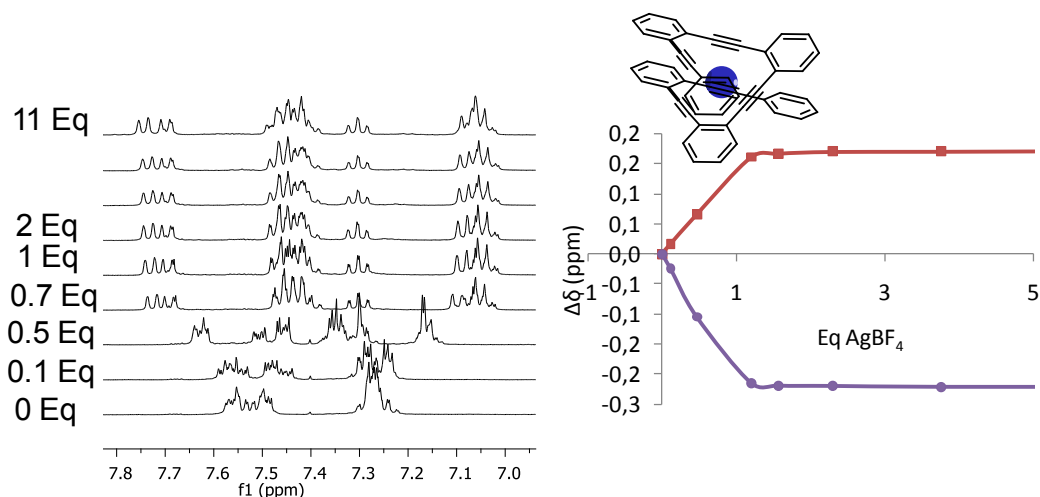

Figure 98. *^{1}H-NMR spectra of **29** by stepwise addition of $AgBF_4$ (left) and titration curves obtained from the experimental data (right).*

[269] P. D. Frischmann, M. J. MacLachlan, *Chem. Soc. Rev.* **2013,** *42*, 871-890.

[270] The metallo-induced folding of unsubstituted oPEs would be further studied in the following section.

[271] This experiment was repeated several times at different concentrations an the same titration curve has been obtained in all the cases. When pure CD_2Cl_2 was used as solvent, a different behaviour was observed for **29**. See experimental section for details.

[272] When fast-exchange conditions apply, the chemical shift is a weighted average of chemical shifts of all microscopic states of the given nucleus.

[273] As we discussed in the former chapter, compound **29** is probably partially preorganized in solution due to the energetically favoured formation of an intramolecular hydrogen bond.
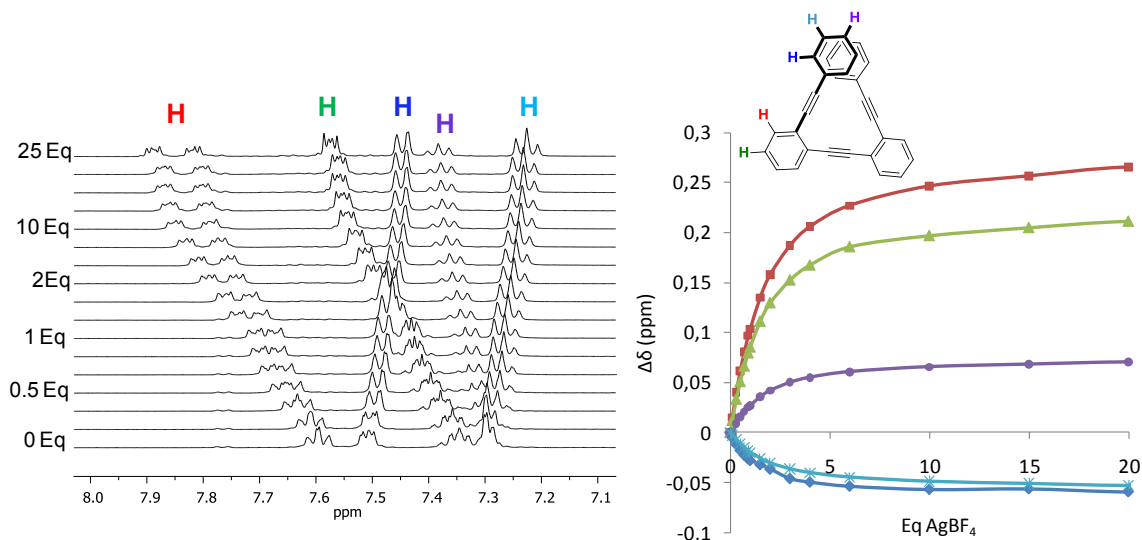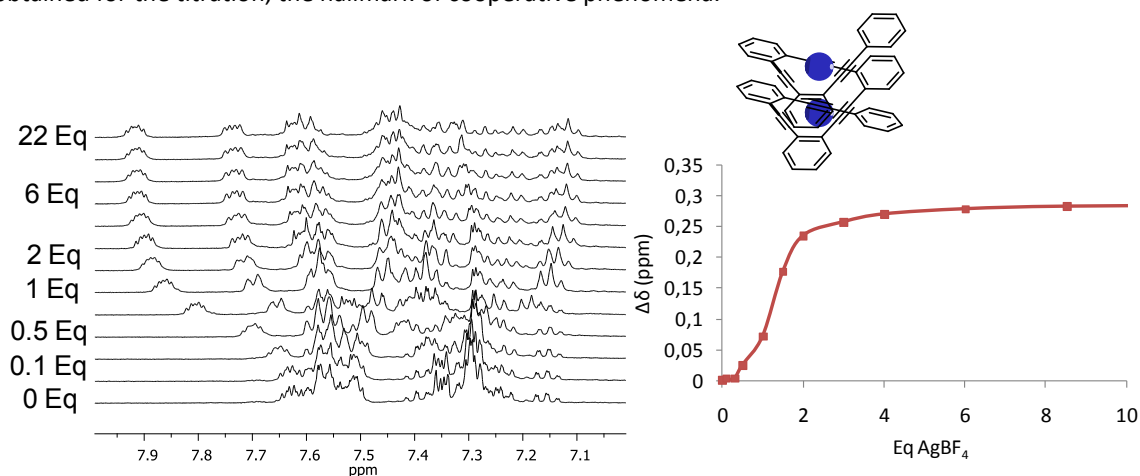
Figure 99. *^{1}H-NMR spectra of **31** by stepwise addition of AgBF$_4$ (left) and titration curves obtained from the experimental data (right).*

For compound **30a**, all the signals changed to lower fields but the coordination of the Ag(I) to the malonyl group (*exo*-coordination) was rejected after comparing the ^{13}C-NMR spectra (Figure 100).[274]
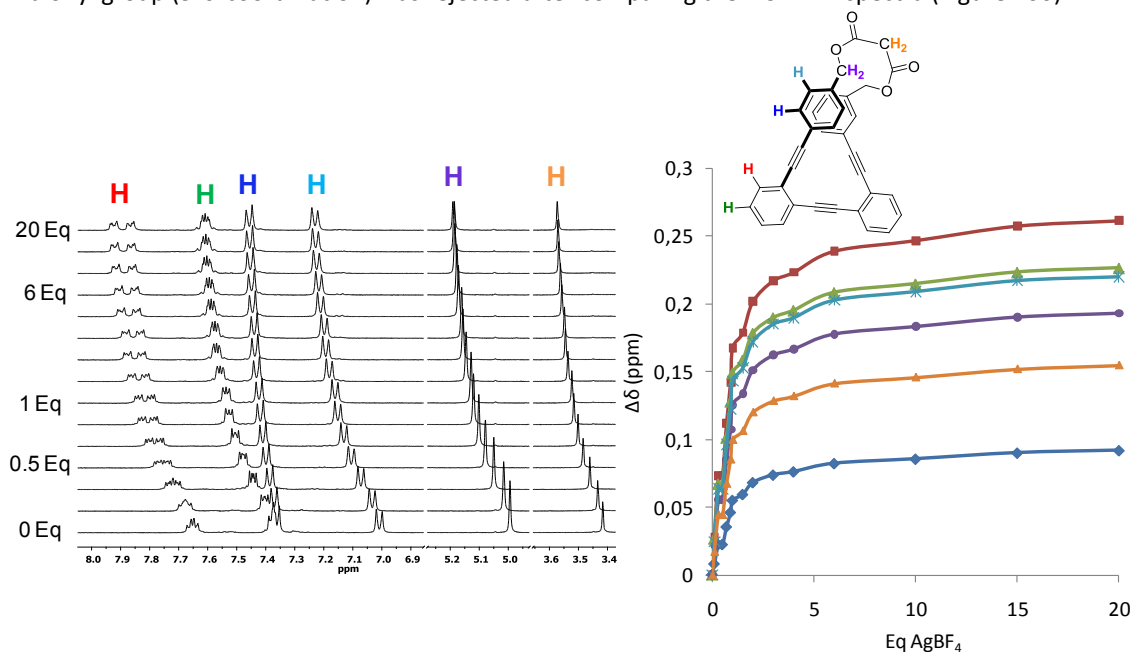
Figure 100. *^{1}H-NMR spectra of **30a** by stepwise addition of AgBF$_4$ (left) and titration curves obtained from the experimental data (right).*

Fortunately, we were able to obtain a suitable X-ray structure of the silver complex of **30a**.[275] This complex was comprised by one silver ion simultaneously coordinated to the three alkynes from the same ligand and one oxygen atom from the malonyl group of a neighboring complex in apical position. The charge was neutralized by a BF$_4^-$ anion located in the free face of the complex. This arrangement leads to a distorted trigonal-bipyramidal geometry around the silver ion provided by the planarization of the ligand (Figure 101).

---

[274] Similar small changes for the terminal benzenes and for the covalent crosslinker have been detected in low temperature NMR experiments what suggested that this changes are due to the more compact and conformational restricted conformation. Any change was observed for the inner benzenes.

[275] Crystallization and X-ray structure determination performed by Alice Johnson, PhD student in Prof. Echavarren Group. Institute of Chemical Research of Catalonia (ICIQ), Tarragona, Spain.
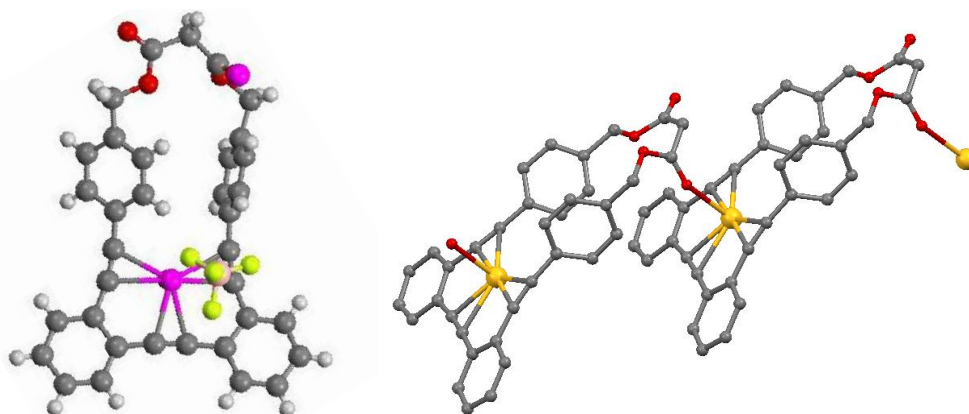
Figure 101. Crystal structure of the complex [30a·Ag(I)]BF₄.

Notably, the major distance imposed by the Ag(I) between the final benzene rings suggested a diminished π-π stacking interaction consistent with the upfield shift observed for such protons by NMR (Figure 100).

In order to obtain a wider view about the binding ability of such oPEs to Ag(I), some related products were synthesized and titrated. Mono-hydroxylated compound **53** (Figure 102) and bis-acetylated compound **54** (Figure 103) gave K values closer to the ones obtained for **31** (K_{eq}= 17 ± 5 M^{-1} and K_{eq}= 71 ±5 M^{-1} respectively) which supported the hypothesis that the exceptionally high binding affinity of **28** stems from the intramolecular hydrogen bond. Succinyl macrocycle **30b** (Figure 104) gave a slightly higher value to the one obtained for **30a** (K_{eq}= 1051 ± 357 M^{-1}).
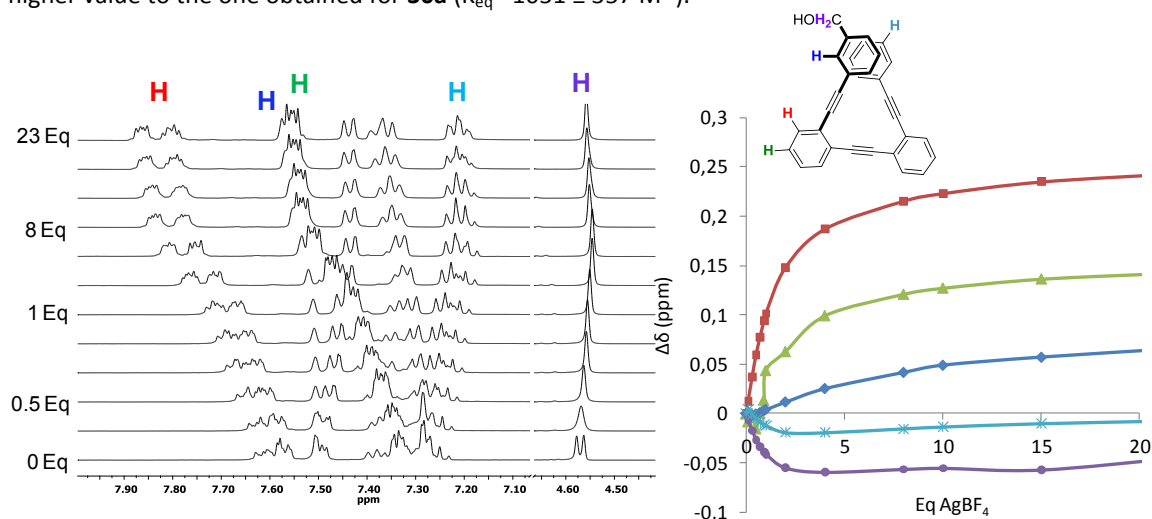
Figure 102. ¹H-NMR spectra of **53** by stepwise addition of AgBF₄ (left) and titration curves obtained from the experimental data (right).
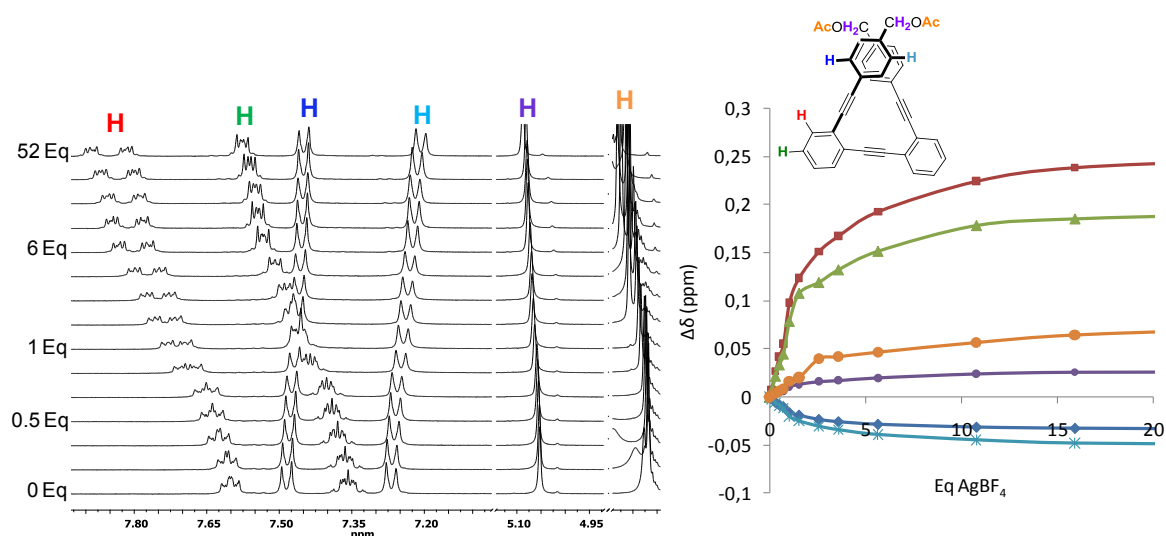
Figure 103. ^{1}H-NMR spectra of **54** by stepwise addition of AgBF$_4$ (left) and titration curves obtained from the experimental data (right).
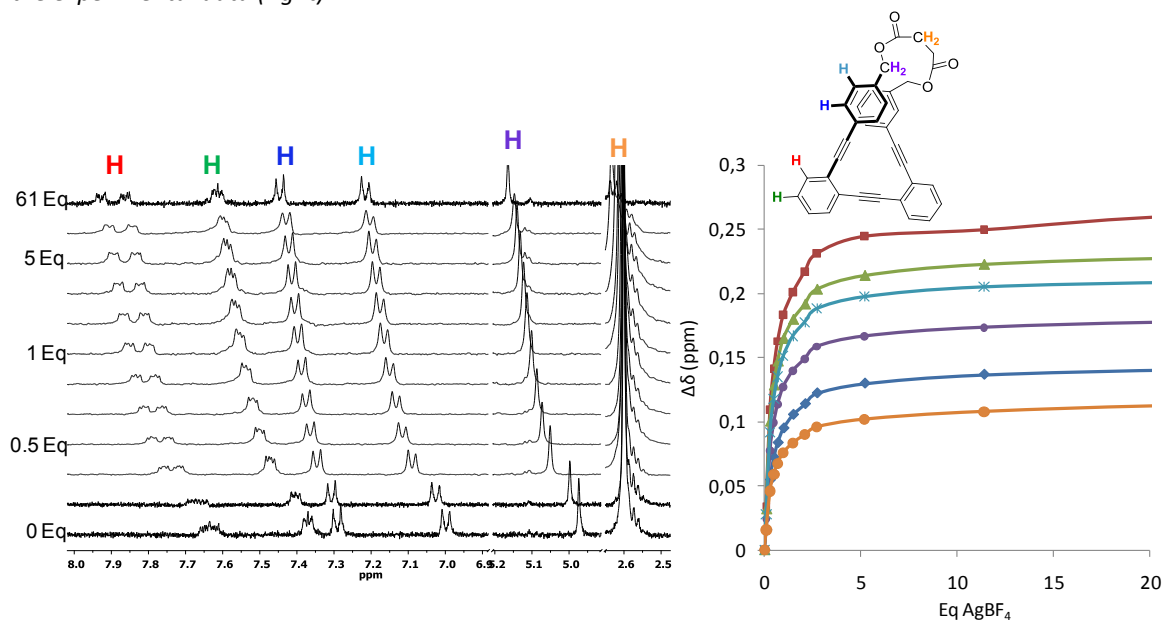
Figure 104. ^{1}H-NMR spectra of **30b** by stepwise addition of AgBF$_4$ (left) and titration curves obtained from the experimental data (right).

The *meta,meta*-substituted tartrate derivate **42** was also titrated but small changes were detected along the range studied in comparison to the other macrocycles (Figure 105). The low binding affinity detected (K_{eq}= 6.6 ± 0.7 M^{-1}) could be related to the major rigidity imposed the staple and/or a disfavorable conformation of the alkynes for the coordination.
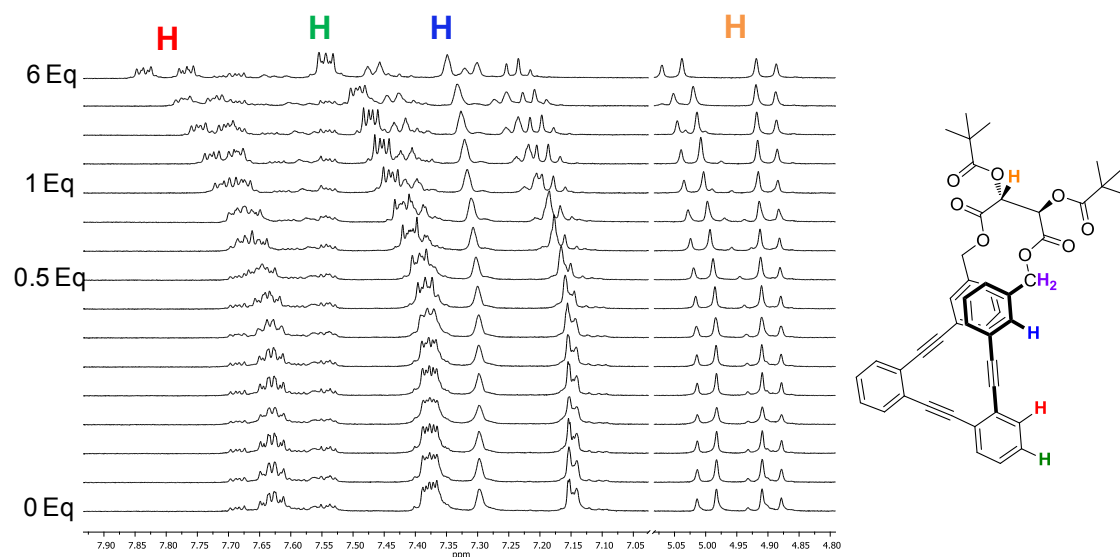
Figure 105. ^{1}H-NMR changes of **42** when AgBF$_4$ is added.

As the chiral loops exhibited characteristic and stronger CD signals, we decided to study the evolution of the helicity as a function of the metal loading using CD spectroscopy for these samples. Surprisingly, different behaviours were observed for **41** (Figure 106 right) and **43** (Figure 106 left) but in both cases the appreciable changes came after adding more then five equivalents (Figure 101, pale blue lines). Titration of compound **43** led to an increase of the intensity of the CD signals at ca. 300 nm and in the 330-400 nm spectral region while compound **41** displayed an opposite response.[276] The different responses observed could be argued if the coordination of the silver could facilitate the racemization for the more flexible binding sites (decreasing the CD signal) or could form more compact complexes (and therefore, increase the CD signal)[277] if the size[277] and shape[278] of the binding pocket were appropriate.[279] Additional efforts to transfer chirality from analogous ligands to metal centers[280] and their uses as supramolecular catalysis are underway.
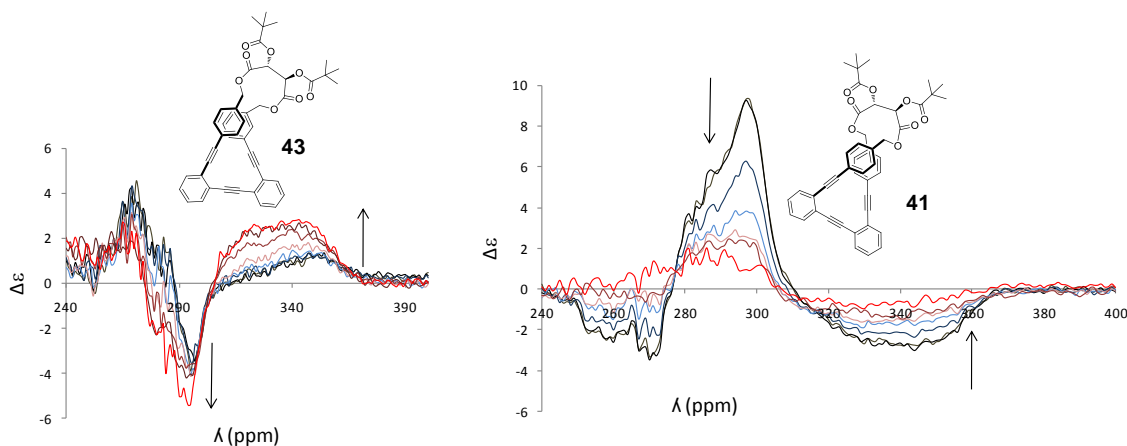
Figure 106. CD changes observed when AgBF$_4$ is added to a solution of **41** (right) and **43** (left) in CH$_2$Cl$_2$.

[276] Similar apparently contradictory phenomenon have been observed for mPEOs and Cu(I) salts: (a) *Chem Commun,* **2012**, *48*, 3330.3332; (b) JOC **2012**, *77*, 5209.

[277] B. Paredes, R. V. Griekena, A. Carrerob, J. Morenoa, A. Moral, *Cej*, **1998**, *4*, 1016.

[278] R. A. Smaldone, J. S. Moore, *JACS*, **2007**, *129*, 5444.

[279] As the Xray structures and the CD analysis discussed in the former section revealed that the structural characteristics of the cavity of these stapled-oPEOs are highly dependent of the location of the side-chains and the nature of the crosslinker.

[280] V. Kumar, T. Endoh, K. Murakami, N. Sugimoto, *Chem Commun*, **2012**, *48*, 9684.

2.3.2.2.Novel oPE-based helicates by Ag(I)-templating

2.3.2.2.1.[1]H-MNR titrations

Returning to the previous experimental observations that strongly suggested that a helical conformation is solution was stabilized for **31** by coordination of a Ag(I) ion into the oPEO cavity, we decided to start an in-depth study. Additional insights into the binding energy of the alkyne-Ag(I) interaction, chain-length dependence of the conformational transition, solvent effects and ion-binding modes of the Ag(I) to several OPE ligands was gained by comparison of the behavior of a collection of potential ligands **55**, **56**, **57**, **58**, **59** and **60** (Figure 107) in solution.
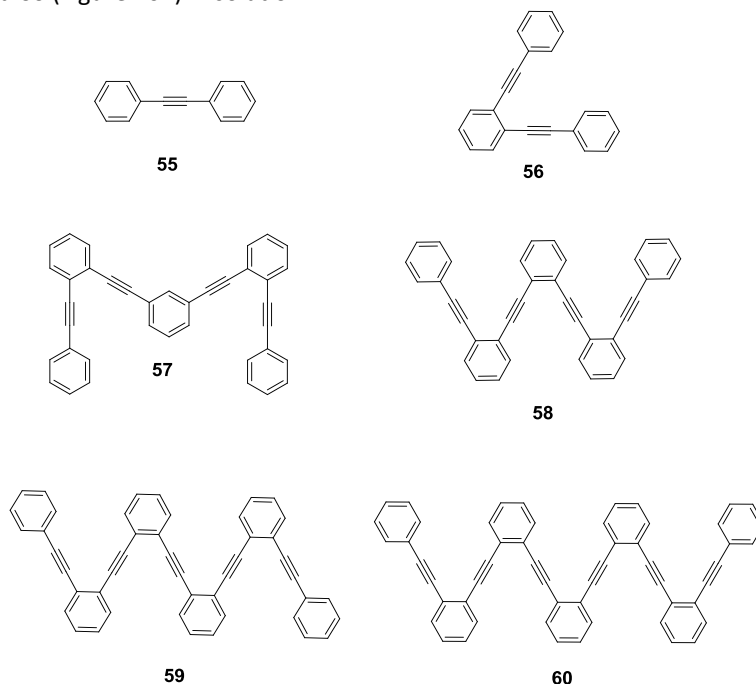
Figure 107. *Model structures **55**-**60** to check the Ag(I)-induced assembly.*

For all these unsubstituted compounds, ^{1}H-NMR titrations evidenced the characteristic deshielding of the aromatic protons attributed to the Ag(I)-alkyne interaction. Such upfield shift could be detected even in mono- and bis-alkynyl compounds **55** and **56** indicating that Ag(I)-alkyne coordination is preferred in such conditions (Figures 108 and 109).[281] The titration curves of the shortest ligand **55** showed no clear break point over the range investigated, suggesting the coexistence of several complexes with different stoichiometries in solution.
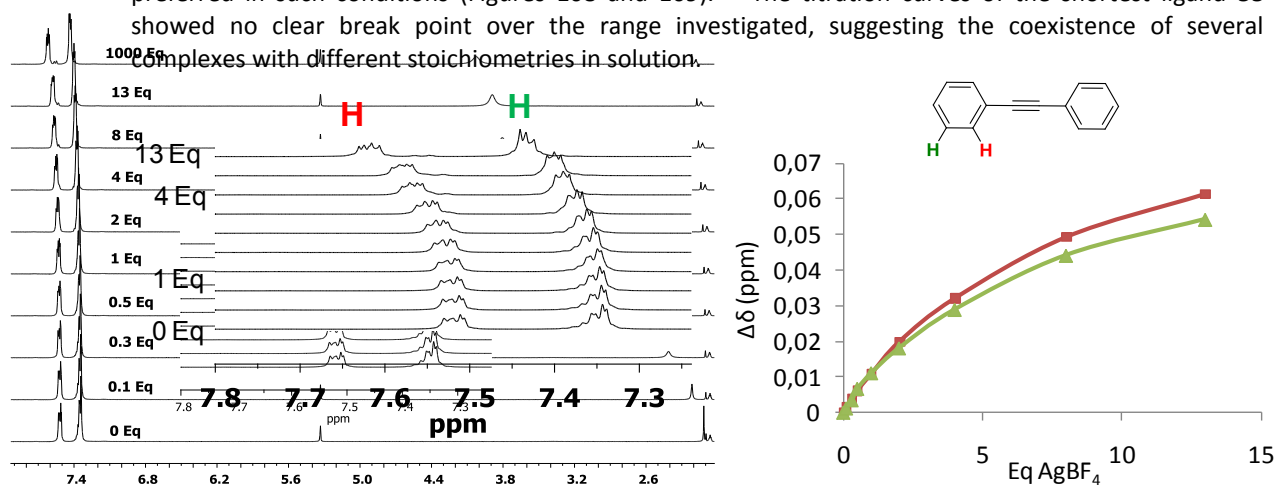
Figure 108. *^{1}H-NMR spectra of **55** by stepwise addition of AgBF$_4$ (left) and titration curves obtained from the experimental data (right).*

---

[281] Because of the weak nature of the Ag(I)-alkyne bond, the competing coordination of the polar aprotic solvent acetone could potentially minimize the desired chelation.

From the NMR data of compound **56**[282] (Fogure 109) and **57** (Figure 110), low thermodynamic constants were obtained (K_{eq}= 6.7 ± 0.6 M^{-1} and K_{eq}= 3.4 ± 0.6 M^{-1}). As it could be intuitively suspected, these values in comparison to the one obtained for **31** revealed that the binding energy of the alkyne-Ag(I) interaction was quite weak in terms of energy and that at the least three alkynes located in *ortho* position (adjacent coordination sites) were required to detected the template effect of the folding.
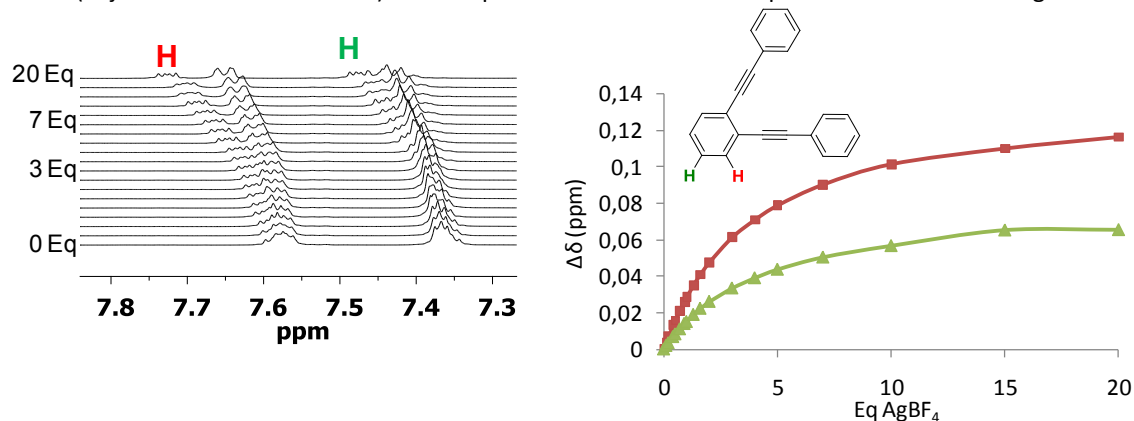
Figure 109. ^{1}H-NMR spectra of **56** by stepwise addition of AgBF$_4$ (left) and titration curves obtained from the experimental data (right).
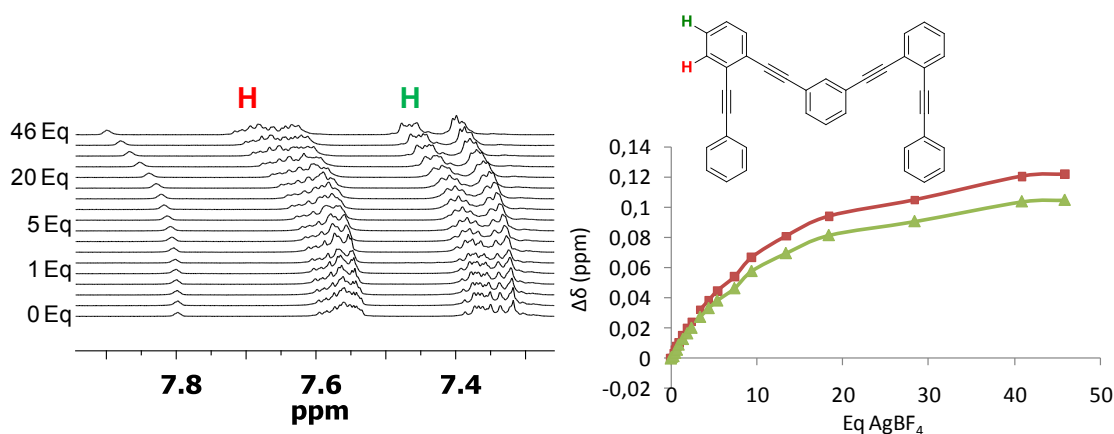
Figure 110. ^{1}H-NMR spectra of **57** by stepwise addition of AgBF$_4$ (left) and titration curves obtained from the experimental data (right).

Analogous changes to the one observed for **31** (Figure 99) were detected during the titration of **58** (Figure 111). Together with the already recognizable ortho protons of the inner benzenes (red and green), a new upfield-shifted doublet (orange) was assigned to one of the protons located in ortho position to the stacked benzenes. A group of signals located between 7.40-7.50 ppm corresponding to ten hydrogen atoms which were upfield and downfield shifted converged when 1 equivalent of silver was added, making impossible their identification. The equilibrium constant was calculated from the five distinguishable peaks (K_{eq}= 697 ± 250 M^{-1}).

---

[282] Although in the majority of the complexes tested could be stored several days without any appreciable decomposition of the final complexes, this was not the case for compound **56**. A complex mixture of aromatic signals on the ^{1}H and ^{13}C spectra suggested that some cyclization happened. A similar [2+2+2] cycloaddition (cyclotrimerization) has been observed in [(cyclooctyne)$_3$Au]SbF$_6$ complexes. See: A. Das, C. Dash, M. Yousufuddin, M. A. Celik, G. Frenking, H. V. R. Dias, *Angew. Chem. Int. Ed.* **2012**, *51*, 3940 –3943.

Figure 111. ^{1}H-NMR spectra of **58** by stepwise addition of AgBF$_4$ (left) and titration curves obtained from the experimental data (right).

The comparison of the K$_{eq}$ values obtained for 1:1 complexes of **31** (K$_{eq}$= 50 ± 2 M^{-1}) and **58** (K$_{eq}$= 697 ± 250 M^{-1}) revealed that the capability of the alkynes to roll-around the metal was again modest in terms of free energy (-2.3 Kcal/mol and -3.8 Kcal/mol respectively) but it increases significantly with the number of alkynes. Interestingly, when longer oligomers **59** and **60** were also tested, some additional phenomena appeared.

Titration of compound **59** showed sharp different spectra for 0.5, 0.7 and 1 equivalents of Ag(I) (Figure 112). After adding one equivalent, any detectable change could be observed on the chemical shift pattern sugegesting that the saturation *plateau* was alredy reached which was associated to a significant increase in terms of binding energy. The explanation for such behavior was found in the review reported by Young *et al.*[283] Based on the 2:1 metallacycles formed between [12]DBA and Ag(I) in which the metals is coordinated to six alkynes, we reasoned that around 0.5 equivalents of Ag(I), i.e. 2:1 ratio, the five alkynes of **59** would probably be simultaneously bound to the silver atom, maximizing the stabilizing entalphyc interaction. However, the minimal alteration of such ratio immediately evolves to the formation of a different coordination mode probably including both 1:1 and 2:1 complexes. The better curve fitting for the obtained data suggested a bimolecular process for which the value of the calculated thermodynamic constant was K$_{eq}$=3779 ± 1700 M^{-1}.

---

[283] W. J. Youngs, C. A. Tessier, J. D. Bradshaw, *Chem. Rev.* **1999**, *99 (11)*, 3153.

Figure 112. [1]*H-NMR spectra of **59** by stepwise addition of AgBF₄ (left) and titration curves obtained from the experimental data (right).*

Finally, we studied the binding behavior of compound **60** which exhibited a remarkably genuine titration curve too (Figure 113). The double-doublets at δ≈7.9 and 7.7 ppm diagnostic of the coordination to the silver revealed that the saturation was obtained at 2 equivalents. Furthermore, a cooperative folding could be guess at first glance.[284] This hypothesis was confirmed afterwards by the sigmoidal curve obtained for the titration, the hallmark of cooperative phenomena.[285]
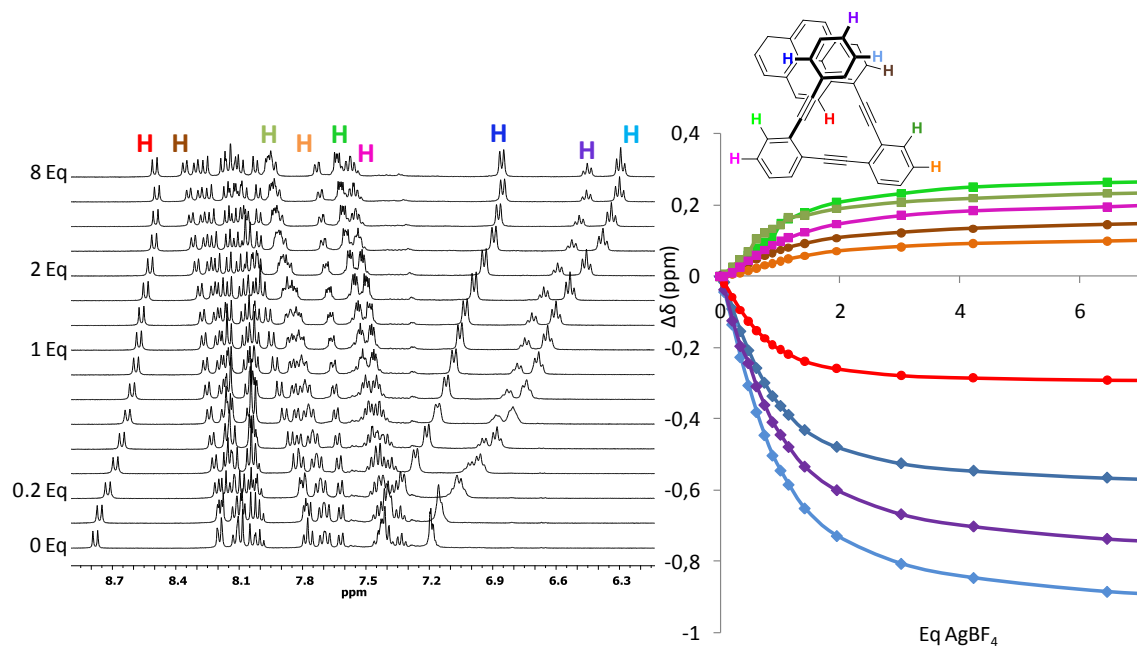

Figure 113. [1]*H-NMR spectra of **60** by stepwise addition of AgBF₄ (left) and titration curves obtained from the experimental data (right).*

Using a trimolecular model, values higher that 10^5 M^{-1} were obtained with good fitting parameter for the thermodynamic constant of **60**. Although modern NMR instruments can register good quality spectra with sub-millimolar concentrations and therefore NMR might be suitable for measuring association constants up to and even above 10^6 M^{-1}, many literature references will state that 10^5 M^{-1} is the limit for NMR titration experiments. For this reason, UV/vis fluorescence titrations were conducted to further explore the thermodynamic driving forces of compound **58** and **60**.

2.3.2.2.2. Fluorescence titrations

---

[284] The statistical thermodynamic analysis of the coil-helix transition has been provided by Zimm and Bragg, see: B. H. Zimm, J. K. Bragg, *J. Chem. Phys.* **1959**, *31*, 526-533. The important findings from their equations are that with increasing chain length the helix stability increase linearly and the cooperativity of the folding transition is enhanced.

[285] Within the context of M-L coordination a quelation effect could be analogous to positive cooperativity.

Substantial fluorescence quenching was observed in the titration of **58** (Figure 114, left) and **60** (Figure 115, left).[286] Normalizing the spectra, any change between the different samples measured was observed for **58** (Figure 114, right).[287] However, a 3.8 nm red-shift of the emission maximum and a different I_{371}/I_{387} ratio became evident when more that 20 equivalents of Ag(I) were added to the solution of **60** (Figure 115, right). From 50 equivalents onwards, any further intensity decrease was observed but the red-shift of the emission maximum and the I_{371}/I_{387} ratio continued changing.
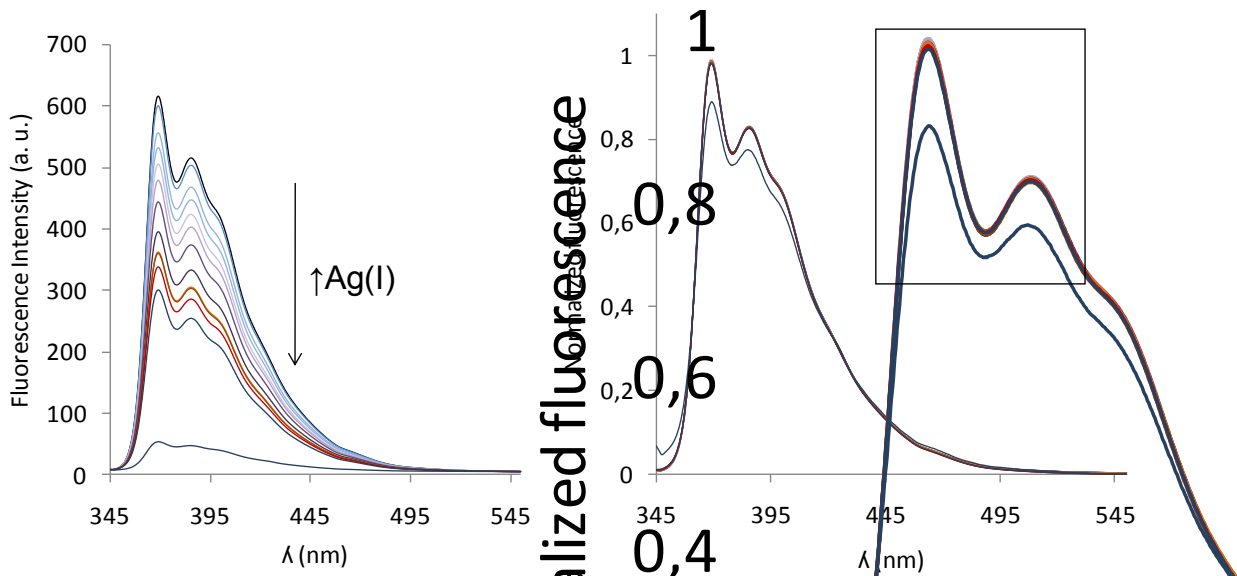
Figure 114. *Fluorescence quenching registered when* [...] *spectra of the titration (right).*
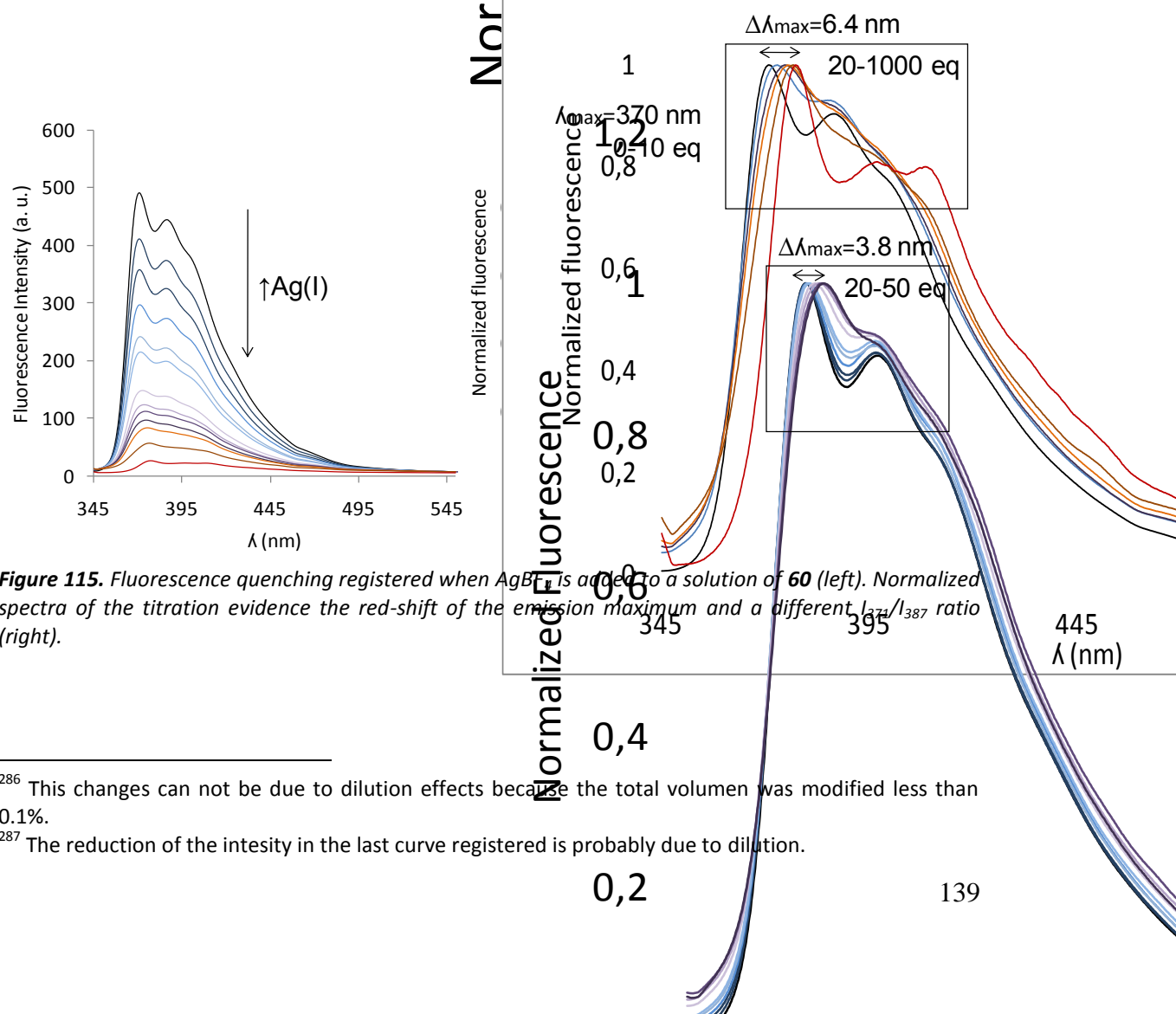
Figure 115. *Fluorescence quenching registered when AgBF is added to a solution of **60** (left). Normalized spectra of the titration evidence the red-shift of the emission maximum and a different I_{371}/I_{387} ratio (right).*

---

[286] This changes can not be due to dilution effects because the total volumen was modified less than 0.1%.

[287] The reduction of the intesity in the last curve registered is probably due to dilution.

Similar observations have been made in solvent titration experiments of *m*PEs. Initial emission quenching has been attributed to the diminished π-π overlap resulting from a considerable tilted angle and the less exposure of the chomophores consistent with the metallo-induced folding.[288] On the other hand, the non-linear progression of the S0→S1 transition and the changes on the I_{371}/I_{387} ratio must derive from different phenomena.[289] It seems reasonable that two oligomers with coordinating end-groups such as **60** could be joint with another Ag(I) to form a larger complex that is constituted of individual strands of **60** (Figure 116). In contrast to traditional coordination complexes that are only stabilized by M-L interactions, **60** gain stability of two coupled events. Once all the "intramolecular" binding sites of **60** are saturated, interhelical complex-complex interactions should shame some of the entropic costs due to their common lost of translational degrees of freedom. Thus, the formation of higher ordered aggregates could be responsible of the progression of the S0→S1 transition.[290]
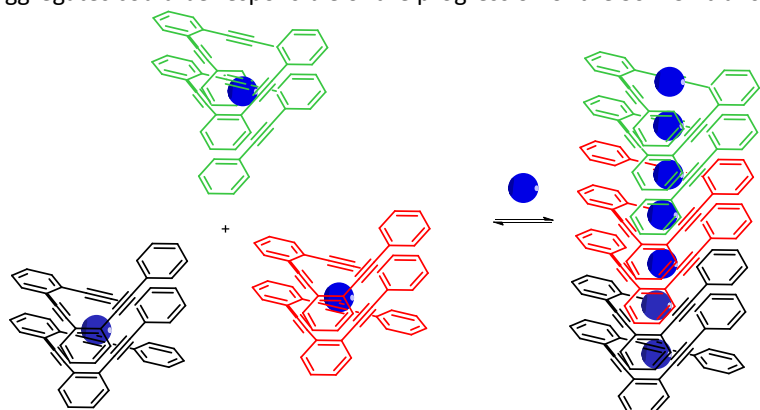
Figure 116. *Schematic representation of one plausible phenomenon associated to the red-shift of the emission maximum during the emission titration of* **60**.

2.3.2.2.3. Theoretical studies[291]

In general, all the collected data for the family of unsubstituted oPEs have pointed out the ability of the Ag(I) π-bond to induce the folding of the flexible oPE backbones into thermodynamically favored helicates with at least three alkynes suggesting that the enthalphic stabilization of metal complexation overcomes the negative entropy of fixing the random coil conformation. Thinking about the underlying phenomena, we hypothesized that the metal complexes should undergo a dynamic assembly-disassembly process before evolving to a single dominant helical structure, owing to the lability of the Ag(I)-alkyne bonds. Hence, the equilibrium constant calculated is the total value of at least two different but interdependent equilibra (Scheme 35).

---

[288] S. Hecht, A. Khan, *Angew. Chem*. *Int. Ed.* **2003**, *42*, 6021–6024.

[289] V. Dehm, M. Büchner, J. Seibt, V. Engel, F. Würthner, *Chem. Sci.* **2011**, *2*, 2094–2100.

[290] Given the multitude of docking sites of large ligands and their intrinsic flexibility, different metallosupramolecular structures could be formed. For example, oligopyridines-Pb(II) helicates are involved in a fast equilibrium with disassembled grid-type structures. See e.g.: (a) A. M. Garcia, F. J. Romero-Salguero, D. M. Bassani, J.-M. Lehn, G. Baum, D. Fenske, *Chem. Eur. J.* **1999**, *5*, 1803-1808; (b) M. Barboiu, G. Vaughan, R. Graff, J.-M. Lehn, *J. Am. Chem. Soc.* **2003**, *125*, 10257-10265. However, the preferred kinked structures formed by multiple coordination with the silver observed for the other analogs, the lower entropic penalty associated to the helicates, some 2D-ROESY experiments and theoretical calculations make the aboved-depicted hypothesis more probable. For related cases of dynamic constitutional diversity, see e.g.: (c) S. Hiraoka, T. Yi, M. Shiro, M. Shionoya, *J. Am. Chem. Soc.* **2002**, *124*, 14510-14511.

[291] Performed by Dr. Mota. Departamento de Química Inorgánica, Universidad de Granada, Spain.
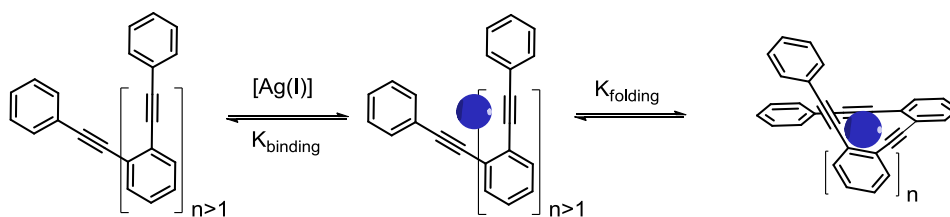
Scheme 35. *Equilibrium in which the foldamers (n=2, 3, 4….) are involved in the presence of Ag(I).*

The structures tested have shown different behaviours depending on its size and, hence, the number of alkynes coordinated to the silver cation. Many electron-rich late transition metals (d^{10} ions) such as Cu(I), Ag(I), Au(I), Zn(II) form stable 2-coordinated complexes. However, other coordination numbers such as 3 or 4 *inter alia* are known for Ag(I) and most of the other cations due to their ability to partially transfer some electron density from its d-orbitals (π-backbonding). Additionally, Ag-Ag bonds have been detected in X-ray structures[292] (2.655-3.187 Å) and confirmed by theoretical calculations.[293] Seeking into the question of how the silver would be coordinated to these foldamers, we have computationally calculated by DFT methods some model structures (**58**, **59** and **60** coordinated to one and/or two Ag(I) cations) in order to evaluate the effect of the helix size and the number of coordinated silver cations on the helical structure.

For example, in complex **58**·Ag(I), the silver adopts a pseudo-tetrahedral geometry (Figure 117). For such complex, the silver cation is simultaneously coordinated to the four alkynes of the ligand but more strongly to three of them almost lying in a plane (av. C-Ag distance of 2.48 Å) and the forth one is apically positioned at a C-Ag distance of 2.71 Å.
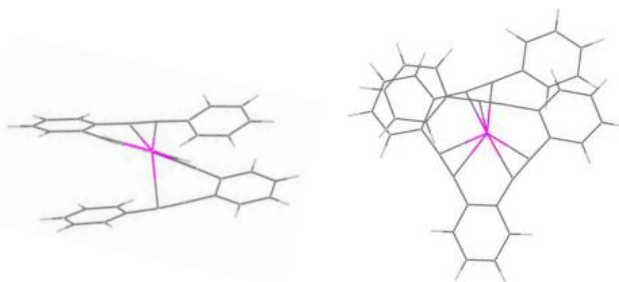
Figure 117. *Optimal geometry calculated for the complex **58**·Ag(I).*

Two different complexes were obtained in the case of **59** depending on the number of silver atoms considered. For only one Ag(I), again a pseudo-tetrahedral coordination (mean basal C-Ag distance 2.57 Å , and mean apical C-Ag distance 2.59 Å) has been obtained for the optimized geometry in which one of the alkynes remains non-coordinated (Figure 118).
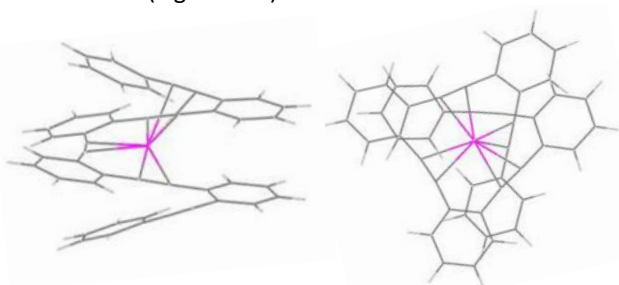
Figure 118. *Optimal geometry calculated for the complex **59**·Ag(I).*

If two Ag(I) cations were planced into the structure of **59**, the calculations predict that each silver would be allocated between three alkynes (Figure 119) giving a distorted trigonal binding motif similar to the one observed in the X-ray structure of [**30a**·Ag]BF$_4$ (Figure 101). In this case, the calculated structure has one Ag(I)-Ag(I) contact.

---

[292] F. A. Cotton, X. Feng, M. Matusz, R. Poli, *J. Am. Chem. Soc*. **1988**, *110*, 7077.

[293] *J. Phys. Chem. A* **1998,** *102,* 2443-2448.
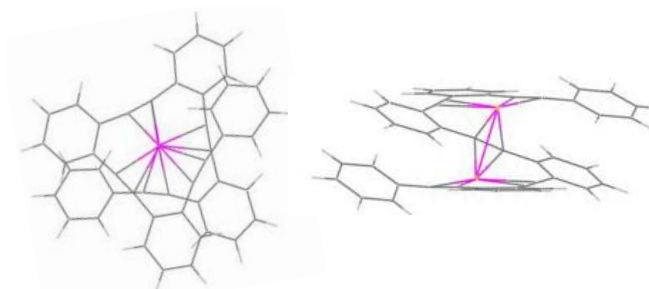
*Figure 119. Optimal geometry calculated for the complex [**59**·Ag$_2$]$^{2+}$*

For compound **60** bearing six triple bonds, two parallel but independent trigonal complexes were predicted as the most stable coordination structures for two silver cations (Figure 120).
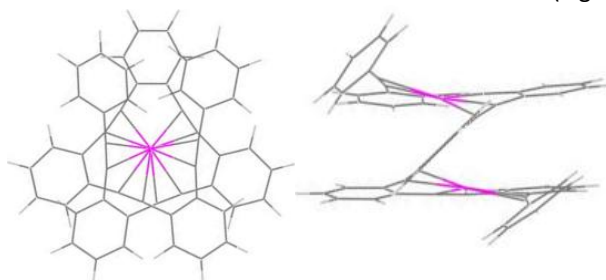
*Figure 120. Optimal geometry calculated for the complex [**60**·Ag$_2$]$^{2+}$*

In order to check, whether silver atoms would stack one above the other in an ideal "infinite" helical *o*PE, we have also calculated the optimal geometry for the next oligomer, following the so-called "3n+1 rule" where n is the number of silver atoms that could be incorporated and 3n+1 the number of benzenes in the *o*PE backbone. For such ligand (n=3, i.e. 3n+1=10 benzene rings), DFT predicted again a trigonal coordination motif (Figure 121). For this complex, at least two of the Ag(I) atoms would be involved in a Ag(I)-Ag(I) interaction. A small distortion from the ideal planar stacking between loops in comparison to the geometry obtained for [**59**·Ag$_2$]$^{2+}$ became evident when the structure was visualized from a side view. Efforts to obtain X-ray quality single crystals are currently underway in order to contrast these theoretical predictions.
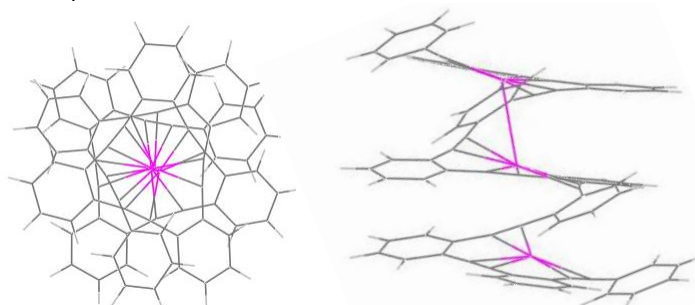
Figure 121. Optimal geometry calculated for the next complex following the "3n+1 rule".

2.3.2.2. oPEOs with UV-distinctive features[294]

The reasonably high association constants obtained for the longer oPEOs raised our interest on developing a family of oPEOs with new UV-features. Pyrene is a prototypical polycyclic aromatic fluorescent molecule which has been frequently used for the synthesis of fluorescent chemical sensors because unique monomer and excimer emissions occur depending on the relative proximity between pyrene fluorophores.[295] π-Stacking interactions between two pyrene units either in the ground state or

---

in the excited state result in the excimer emission upon photoexcitation.[296] Intramolecular interaction of two pyrene units in the ground state through π-π stacking has been observed when pyrene units are attached to a conformationally rigid molecular framework.[297] In molecules with conformational flexibility, metal-ion-mediated conformational changes have resulted in bringing two pyrene units close to undergo a π-stacking interaction.[298]

With these inspirations, we decided to synthesize four fluorogenic oPEs bearing one terminal pyrene and four different terminal rings (Figure 122). In order to check their binding affinities and if the folding could be extended to such family of compounds, NMR titration were firstly recorded following the same strategy.
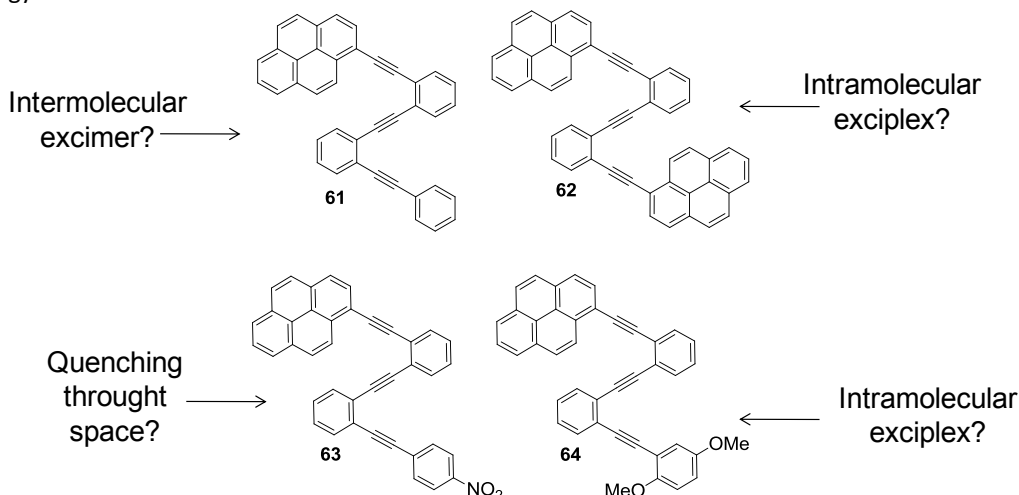
Figure 122. *Target structures **61**-**64** with distinctive UV-vis features to check the Ag(I)-induced assembly.*

2.3.2.2.1. ^{1}H-NMR titrations

For compound **61**, strong shielding of the signals of the terminal benzene could be observed since the beginning of the ^{1}H-NMR titration (Figure 123)). The binding affinity measured for that compound (K_{eq}=46 ± 13 M^{-1}) resulted to be very similar to the one obtained for **31**.[299] Analogous observations and only a slightly higher binding constant (K_{eq}=58 ± 5 M^{-1}) were detected for **62** (Figure 124). Despite the wide π-surface of the acene and the complicate chemical shift pattern, the downfield shift of the diagnostic *ortho*-protons (bright green line Δδ≈0.2 ppm) and the changes registered on the carbon signals for the alkynes supported the coordination of the silver to the alkynes in compound **62** too. Moreover, an accused upfield of some aromatic protons as a consequence of the neighboring ring current experimented by the nucleus stacked on top of the pyrene was also consistent with our previous observations.

---

[296]   Excimers   (or   exciplexes)   are   short-lived dimeric (transient   dimers)   or heterodimeric molecules formed from two species only if one of both molecules is in the electronic excited state.

[297] T.-C. Chou, C.-L. Hwa, J.-J. Lin, K.-C. Liao, J.-C. Tseng, *J. Org.Chem.* **2005**, *70*, 9717-9726.

[298] (a) H. Yuasa, N. Miyagawa, T. Izumi, M. Nakatani, Izumi, Hashimoto. *Org. Lett.* **2004**, *6*, 1489-1492. (b) S. H. Lee, S. H. Kim, S. K. Kim, j. H. Jung, J. S. Kim, *J. Org. Chem.* **2005**, *70*, 9288-9295. (c) For anion-mediated ð stacking, see: I. Suzuki, M. Ui, A. Yamauchi, *J. Am. Chem. Soc*. **2006**, *128*, 4498-4499. (d) S. K. Kim, J. H. Bok, R. A. Bartsch, J. Y. Lee, J. S. Kim, *Org. Lett.* **2005**, *7*, 4839-4842. (e) J.-S. Yang, C.-S. Lin, C.-Y. Hwang, *Org. Lett.* **2001**, *3*, 889-892.

[299] Global fotting using all the signals.

Figure 123. *^{1}H-NMR spectra of **61** by stepwise addition of AgBF_4 (left) and titration curves obtained from the experimental data (right).*
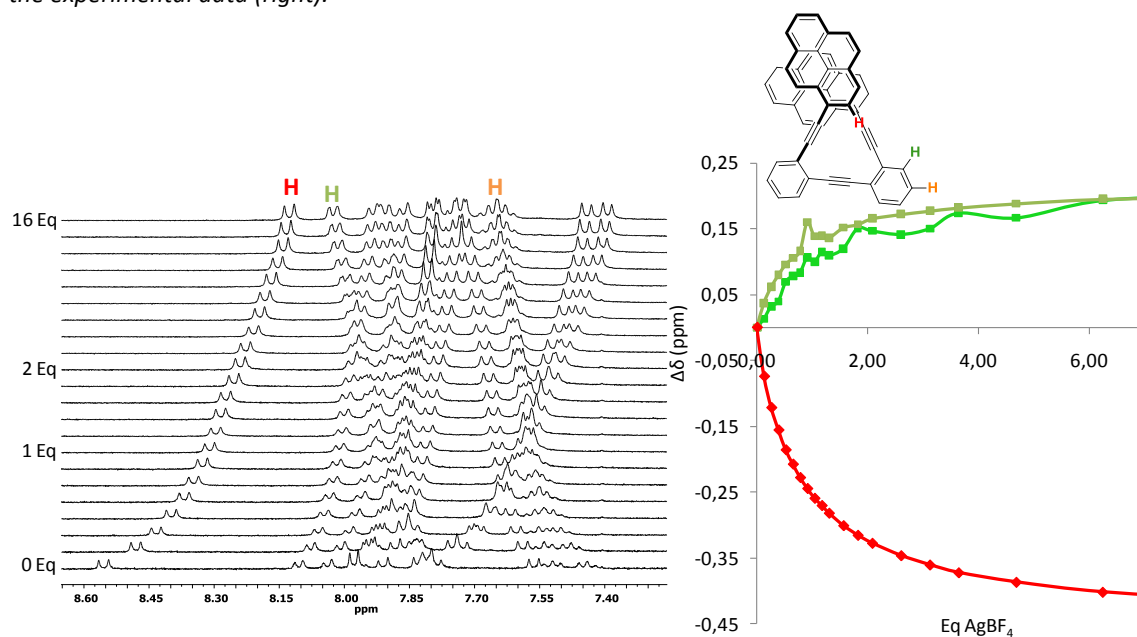
Figure 124. *^{1}H-NMR spectra of **62** by stepwise addition of AgBF_4 (left) and titration curves obtained from the experimental data (right).*

These ^{1}H-NMR spectroscopic studies provided compelling experimental evidence that the Ag(I) can bind to both oPEOs to form helicates in a similar way to the behavior of its unsubstituted and benzyl substituted analogs. We thus decided to investigate metal binding in solution by UV-vis and fluorescence spectroscopic titrations.

2.3.2.2.2.UV-vis titrations

Firstly, to gain insights into their optical properties, we recorded the spectra of the pure ligands (Figure 125 and table 8). Unlike the absorption spectra which were quite similar,[300] the emission spectra of **61**

---

[300] The electronic transitions (i.e. λ_{max}) observed for the two products are aparently the same but they are characterized by different moalr absorption coefficients (i.e. ε).

showed a vibrational fine structure and occurred at shorter wavelengths (λ_{em} from 410 to 450 nm) in comparison to the broad, featureless emission of **62** that occurs at longer wavelengths (λ_{em} from 420 to 520 nm).[301] This long-wavelength band was attributed to the excimer emission formed intramolecularly[302] by the association of electronically excited and unexcited pyrenyl groups in liquid solution. Due to the flexibility and conformational freedom of **62**, π-stacking could be broken and the interplanar distances between the pyrene units became longer, resulting in varying degrees of the π-stacking interaction.[303]
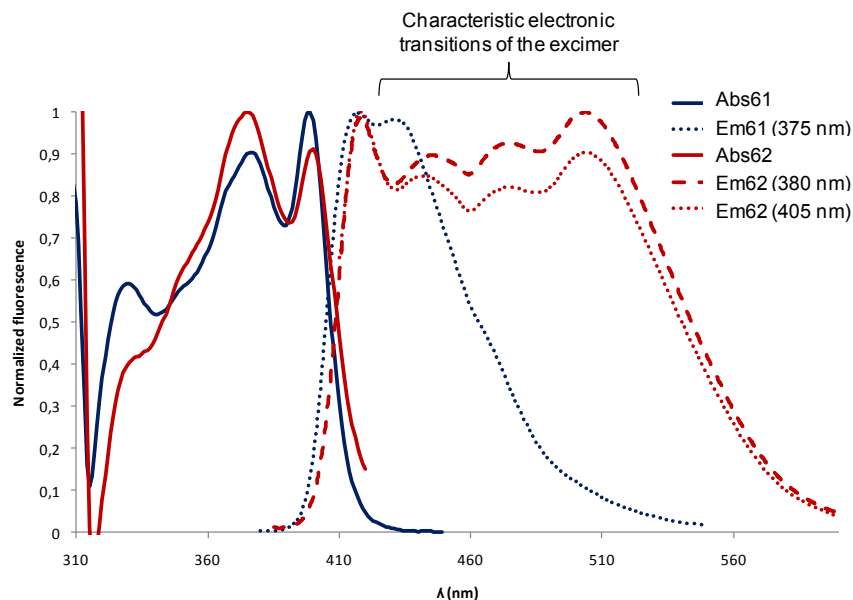
Figure 125. *Absorption (solid line) and emission (dotted and dashed lines) spectra of **61** and **62**.*

λ_{abs} (ε) / nm (cm^{-1}M^{-1})	λ_{em} (λ_{exc})	ϕ
330 (5467) 380 (7436) 400 (8301)	416 (375 nm)	0.59±0.07
330 (1452) 380 (3376) 400 (3276)	418 (380) 446 (380) 475 (380) 504 (380)	0.26±0.03

Table 8

Then, Ag(I)-titration of compounds **61** and **62** were recorded and absorption and fluorescence (λ_{exc}=400 nm) spectra gave together interesting information. Upon addition of only 1 eq. of Ag(I) to a solution of compound **61**, the molar absorptivity of the more energetic transition (λ_{abs}=330 nm) changed drastically while the lower energy electronic transitions (attributed to the pyrene fragment) did not change at all (Figure 126). From 10 equivalents until the end of titration, any additional variation was detected at 330

---

[301] An excimer emission maximum in the range of 490-530 nm is consistent for various pyrene derivatives.

[302] The fluorescence emission maximum was invariant with concentration in the range of 10^{-5}-10^{-7} M, indicating that the emission arises from an intramolecular excimer. A wider study in comparison to other compounds able to for intermolecular excimer was performed to secure this assertion. See esi page XXX

[303] Fluorescence spectrum of **62** is the average spectrum of all the conformations adopted in solution as ocurred in the NMR espectra under fast exchange conditions.

nm but the intensity of the pyrene electronic transition (maxima at 380 and 400 nm) decreased continuously across an isoemissive point at 410 nm.

Analogous observation was made in the fluorescence spectra registered when excitation was fixed at 400nm (Figure 121 middle). However, any distinguishable feature such as the appearance of a new transition, the decrease/increase of the existing bands or Stokes shift of the maximum at λ_{em}=417 nm, became evident when the fluorescence spectra were normalized (Figure 121 left). For this reason, the formation of intermolecular complexes either in the ground and the exited state was rejected as consequence of the excess of silver and the fluorescence quenching was attributed to the intramolecular benzene-pyrene π-π stacking interaction.
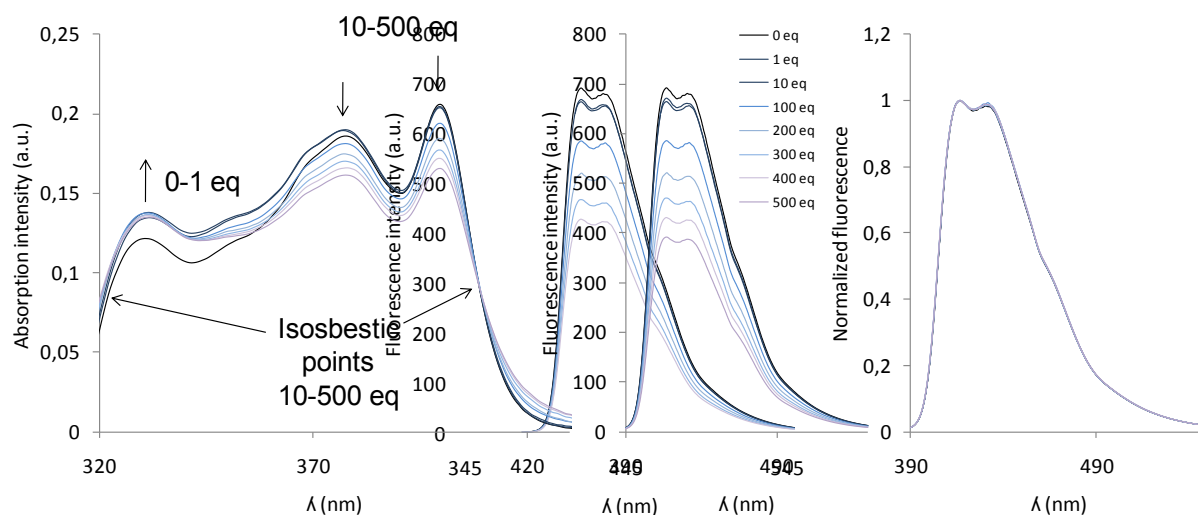
Figure 126. *Absorption and fluorescence spectra registeredupon stepwise addition of AgBF$_4$ ta solution of 61.*

Significantly different results were obtained for **62**. In addition to a gradual decrease in the absorption bands at 380 and 400 nm and increase at 330 nm (Figure 127 right), a significant ratiometric change was evidenced in the fluorescence spectra (Figure 127 middle). As the fluorescence spectrum of **62** is the average spectrum of all the conformations adopted in solution, the experimental observation suggested that the presence of the Ag(I) quenched the fluorecence of the less energetic conformations attibuted to the intramolecular excimer. On the other hand, as the Ag-alkyne is a weak interaction probably involved in a dynamic equilibrium, the formation of the dominant structure required the addition of a big excess of metal due to the highly diluted conditions required in comparison to the NMR experiments.
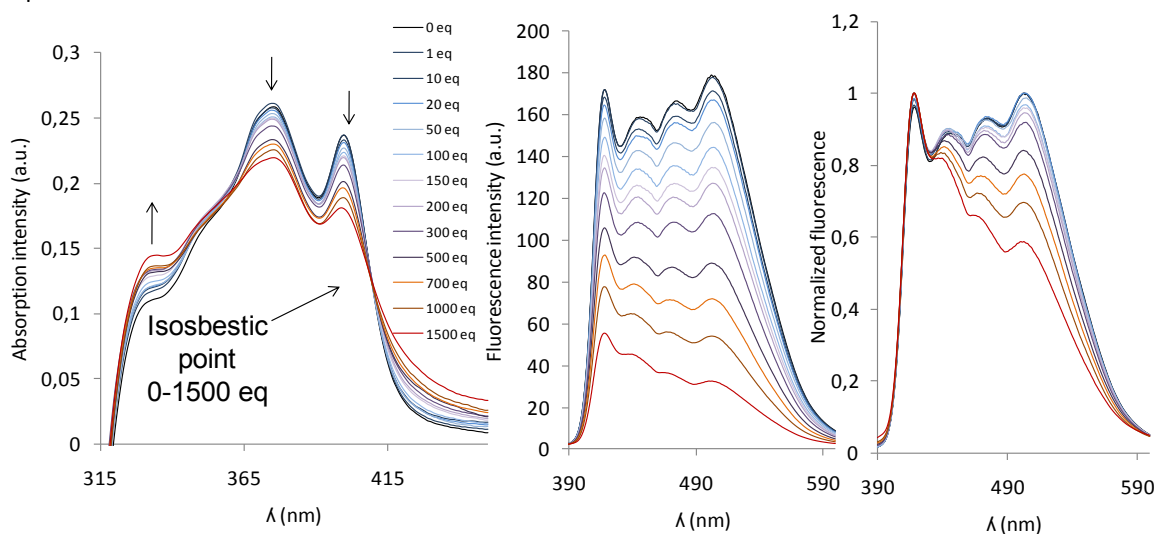
Figure 127. *Absorption and fluorescence spectra registeredupon stepwise addition of AgBF$_4$ ta solution of 62.*

146

2.3.2.2.3.Time-resolved measurements

When a fluorophore is exposed to light, it is transformed into an excited state by promoting electrons to a higher energy level. In contrast to absorption, the length of time that fluorescent molecules remain in the excited state provides valuable information to detect dynamic processes in solution.[304] Furthermore, the phenomenon of quenching is a great opportunity for understanding the role of the excited-state lifetime in time-resolved fluorescence measurements.

Fluorescence measurements can be broadly classified into two types of measurements: steady-state and time-resolved. Steady-state measurements are those performed with constant illumination and observation (i.e. the fluorescence spectra shown in figures 126 and 127). In these types of experiment, when the sample is first exposed to light, steady state is reached almost immediately and the fluorescence observation is simply an average of the time-resolved phenomena e.g. conformational changes. The second type of measurement is time-resolved, which is used for measuring intensity decays or anisotropy decays. In time-resolved measurements, fluorescence decay is given by

$$f(t) = \sum_{n=1}^{\infty} \left(A_n e^{-t/\tau n} \right)$$

where A_n are the preexponential factors which represent the abundance and τ_n the fluorescence lifetime of each excited-state specie. For these measurements the sample is exposed to a pulse of light, where the pulse width is typically shorter than the decay time of the sample. The intensity decay could reveal several decay times τ_i and thus the presence of more than one excited-state specie. Additionally, time-resolved measurements reveal whether quenching is due to diffusion from a fluorophore or to complex formation in the excited-state (excimers or exciplexes) depending on the sign of the preexpenential factors. For all these reasons, we performed time-resolved measurements of both pure ligands **61** and **62** and some metal-ligand mixtures formed during the titration.

Fluorescence decay traces of **61** followed a bi-exponential function for the pure ligand and two metal-ligand mixtures evidencing the existence of at least two excited-state species with a relatively short lifetime of ca. 2.3 ns[305] (Figure 128). The positive sign of the pre-exponential factors confirmed that such species were form in the ground-state in agreement with the steady-state observations. Any significant change was observed for the mean lifetime of the three sample tested.

Lifetime measurements

0 eq. Ag
$\tau_1 = 2.93$ 0.03 ns, $A_1 = 0.73$ ns
$\tau_2 = 1.42$ 0.06ns, $A_2 = 0.38$ ns
$\tau = 2.36$ 0.09 ns

400 eq. Ag
$\tau_1 = 2.96$ 0.04 ns, $A_1 = 0.50$ ns
$\tau_2 = 1.58$ 0.05ns, $A_2 = 0.50$ ns
$\tau = 2.28$ 0.08 ns

1000 eq. Ag
$\tau_1 = 2.90$ 0.02 ns, $A_1 = 0.65$ ns
$\tau_2 = 1.29$ 0.07ns, $A_2 = 0.35$ ns
$\tau = 2.34$ 0.1 ns
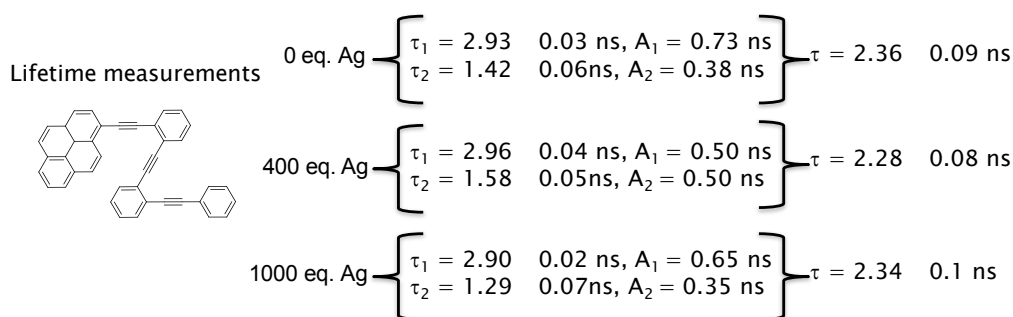
Figure 128. Lifetime results obtained from the fluorescence decays of 61.

Compound **62** able to form intramolecular excimers as the steady-state fluorescence spectra revealed much more information about the dynamic folding of such oPEs (Figure 129). From the time-resolved

---

[304] The fluorescence lifetime and quantum yield are perhaps the most important characteristics of a fluorophore. Quantum yield is defined as the number of emitted photons relative to the number of absorbed photons. Substances with the largest quantum yields, approaching unity, such as rhodamines, display the brightest emissions. The lifetime of the excited state is defined by the average time the molecule spends in the excited state prior to return to the ground state.
[305] Measured at 420, 440 and 460 nm. See experimental section.

measurements for the pure ligand **62**, three lifetime components were calculated.[306] The high and negative value of the pre-exponential A_1 corresponding to the shortest lifetime component τ_1 indicated the formation of the excimer in the excited-state. The two longer lifetimes τ_2 and τ_3 were related to the emission of two different excimers (Figure 129).[307]

$$f(t) = -A_1 \cdot e^{-t/\tau_1} + A_2 \cdot e^{-t/\tau_2} + A_3 \cdot e^{-t/\tau_3} \begin{cases} \tau_1 = 0.71 \quad 0.01 \text{ ns}, A_1 = -36324 \\ \tau_2 = 6.37 \quad 0.14 \text{ ns}, A_2 = 64.3 \\ \tau_3 = 12.36 \quad 0.05 \text{ ns}, A_3 = 35.8 \end{cases}$$

Figure 129. Lifetime results obtained from the fluorescence decays of 62.

Then, fluorescence decays were registered for all the samples of the titration (Figure 130).
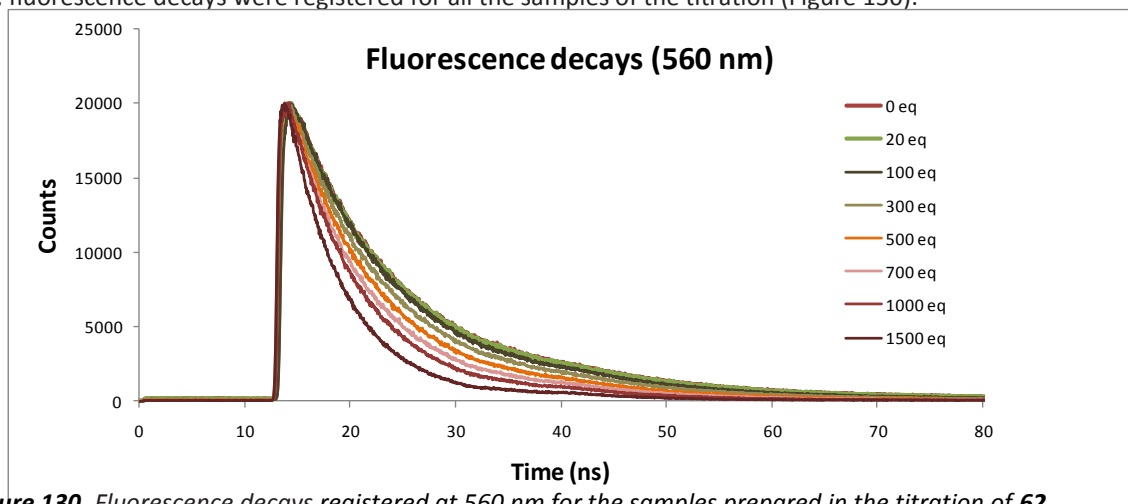
Figure 130. Fluorescence decays registered at 560 nm for the samples prepared in the titration of 62.

Analysis of the fluorescence decays of the ligand-Ag(I) titration mixtures revealed the decrease of all the lifetime components in comparison to the free ligand (Figure 131).
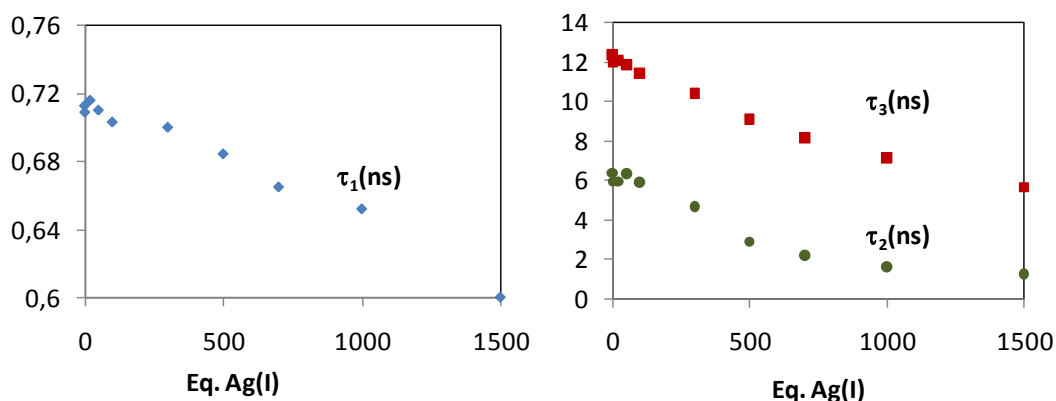
Figure 131. Variation of the lifetime components along the titration of 62.

In the case of τ_1, this value at the typical wavelengths of monomer emission (420 nm) provided an estimation of the excited-state kinetics for excimer formation (k_f). Using an unquenched reference,[308] we calculated the rate constant as follows: $k_f = 1/\tau_{short} - 1/\tau_{ref}$. The progression of the k_f values along of the titration clearly evidenced the faster formation of the excimer due to the presence of the silver (Figure 132).

---

[306] Calculated at different wavelenghts: 420, 440, 460, 480, 500, 520, 540, 560 and 580 nm.
[307] The free rotation of the pyrene and the flexibility of the oPE backbone could reasonably lead to different conformers characterized by different lifetimes. Ikawa et al. reported that carbazole units in a poly(*N*-vinyl carbazole) polymer exhibit distinctive fluorescence features depending on the degree of overlap between the carbazoles. See: Ikawa, T.; Shiga, T.; Okada, A. *J. Appl. Polym. Sci.* **1997**, *66*, 1569.
[308] τ_{ref} = 2.385 ns.
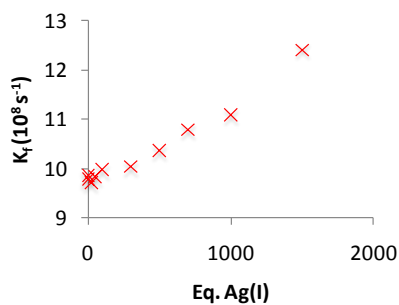
*Figure 132. Progression of the excimer formation rate constant (kf) along the titration of **62**.*

Furthermore, the similar magnitude and the opposite sign of the absolutes abundances measured at the excimer wavelength (560 nm) revealed that only one of such excimers was formed in the excited-state (Figure 133 blue and green points). Thus, the longest lifetime component τ_3 corresponded to a species that was already formed in the ground-state and whose proportion was increased when silver was added (red points).
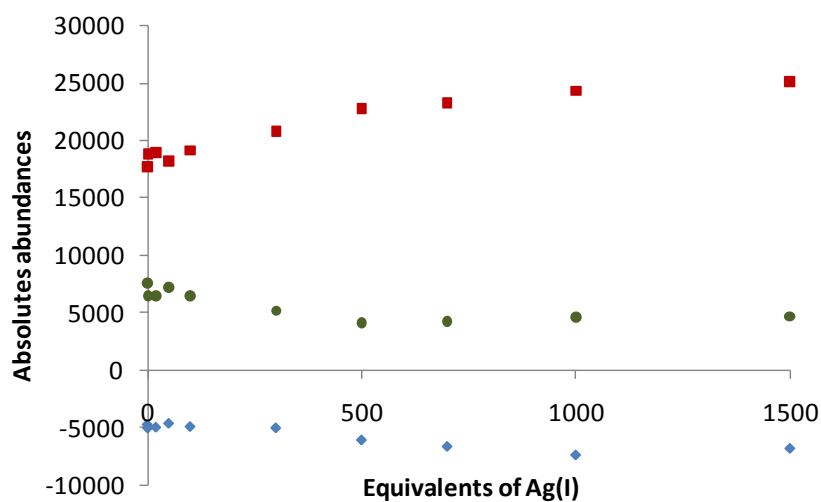
Figure 133. Influence of the Ag(I) addition on the absolutes abundances of the excited state species.

Under the light of these results, we proposed the following model which relates the ground state equilibrium in which compound **62** is involved, and the changes excited-state species and kinetics for excimer formation (Figure 134).

149
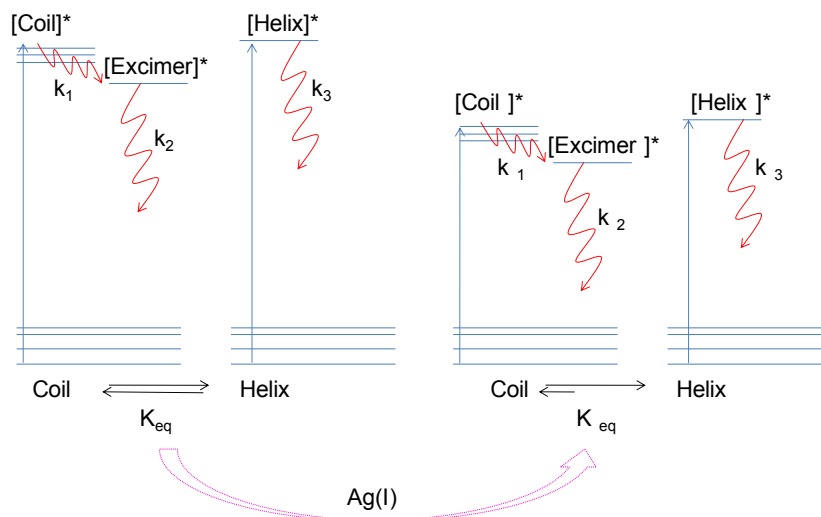
Figure 134. Schematic relation between the influence of the addition of Ag(I) in the random coil-helix equilibrium and the photokinetic data obtained from the time-resolved fluorescence measurements.

In the absence of Ag(I), the folding of compound **62** and hence the formation of the "excimer" and the already folded "helix" were revealed by the florescence decays. Upon addition of Ag(I), together with the changes observed in the absorption spectra and the fluorescence quenching, time-resolved measurements suggested the increase of the excimer formation rates and the major population of the helix in solution consistent with the NMR observations. The shortening of all the lifetime components when silver was added was also in agreement with the fluorescence quenching observed in the ready-state titration.

<u>2.3.2.2.4. Analysis on **63** and **64**</u>

The effects of tuning of the chemical structure of two additional oPEs with electron -rich and electron-poor terminal benzenes (Figure 22, compounds **63** and **64**) were also investigated concerning the performance on the supramolecular organization, i.e., the binging affinity to the Ag(I) and the optoelectronic properties.

Side-chain variation with a nitro-group (compound **63**) resulted in a Δδ ≈ 0.16 ppm (orange) and Δδ ≈ 0.26 ppm (green) deshielding of the NMR signals (Figure 135) but any clear break point was detected in the range of the titration suggesting a very weak coordination (K_{eq}= 8 ± 0.08 M^{-1}).
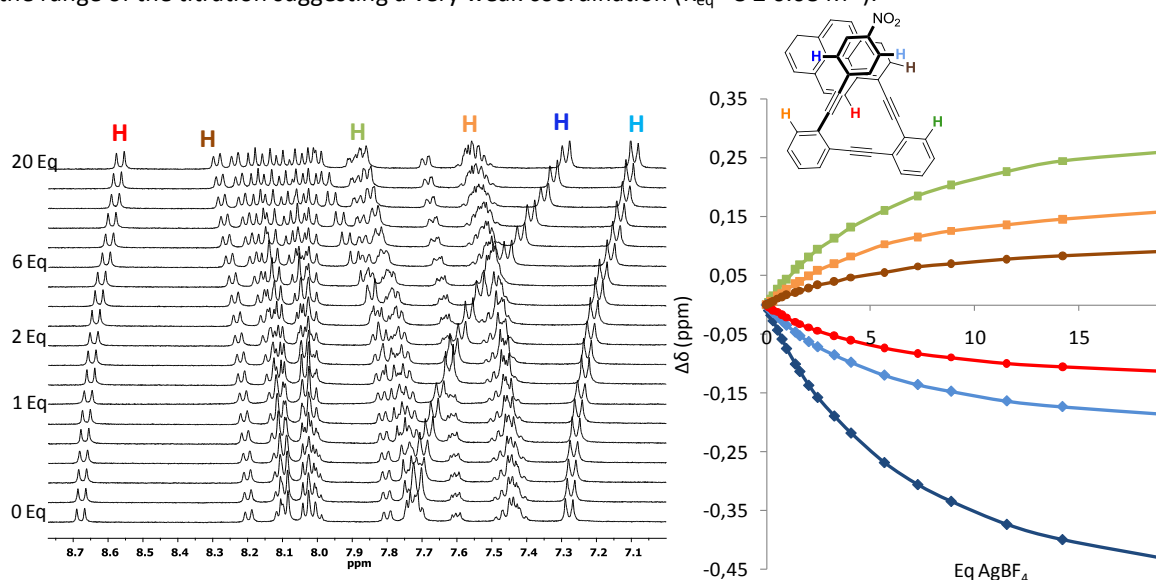
Figure 135.^{1}H-NMR spectra of 63 by stepwise addition of AgBF$_4$ (left) and titration curves obtained from the experimental data (right).

A strong quenching of the fluorescence of **63** due to the electronic communication along the carbon backbone was evidenced by the low fluorescence quantum yield which characterized this compound in comparison to other pyrene derivates (ϕ=0.009±0.005). In this case, UV-vis titrations (Figure 136) gave tiny intensity decrease and the fluorescence decay of the pure ligand could be adjusted to a bi- or tri-exponential process to give very similar values to the one observed for **61** (Figure 137).
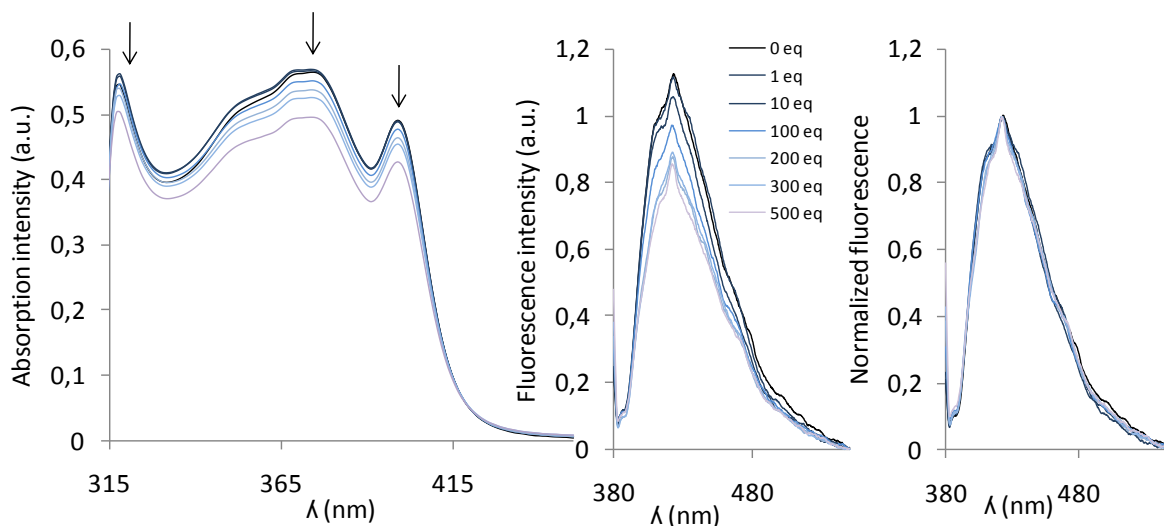
Figure 136. Absorption and fluorescence spectra registered upon stepwise addition of AgBF₄ ta solution of 63.

$\tau_1 = 3.05 \quad 0.06$ ns, $A_1 = 0.54$ns
$\tau_2 = 1.43 \quad 0.03$ ns, $A_2 = 0.46$ ns
$\tau = 2.31 \quad 0.1$ ns

$\tau_1 = 3.82$ ns, $A_1 = 0.16$ ns
$\tau_2 = 2.26$ ns, $A_2 = 0.66$ ns
$\tau_3 = 0.62$ ns, $A_3 = 0.18$ ns
$\tau = 2.22 \quad 0.13$ ns
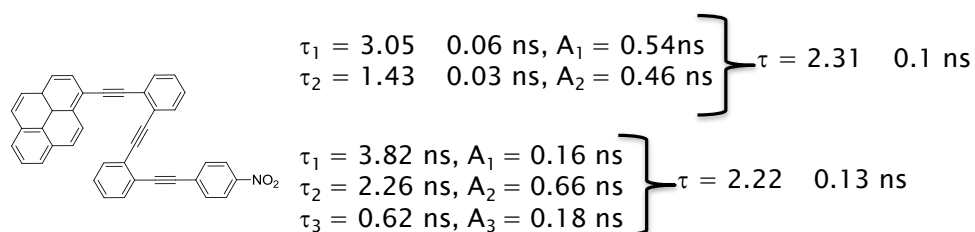
Figure 137. Lifetime results obtained from the fluorescence decays of 63.

Fluorogenic compound **64** bearing two pendent metoxy groups on the benzene ring gave much more interesting information. ^{1}H-NMR titration displayed a completely new phenomemon because the OMe group took part in the complexation (Figure 138). In the beginning of the titration up to 0.5 eq. of Ag(I) the more affected signals were the one corresponding to the dimetoxybenzene ring closely followed by the aromatic protons of the inner benzenes which were poorly resolved in comparison to the pyrene protons. The broadening of the signals meant that a slow exchange process was taking place for such titration range (Figure 138 red box). From 0.5 to 1 equivalent, the protons of the inner benzenes experimented more accused shifts from $\Delta\delta \approx 0.11$ to 0.23 ppm. After 1.2 equivalents the spectra were all identical suggesting that the saturation plateau had been reached. The stronger interaction with the silver was also evidenced by the increase of the binding constant ($K_{eq}= 242 \pm 55$ M^{-1}).[309]

---

[309] Calculated only using the NMR data of the inner benzene in order to compared this value with the parent structures. Higher K values are obtained when the dimetoxy-benzene signals are considered.
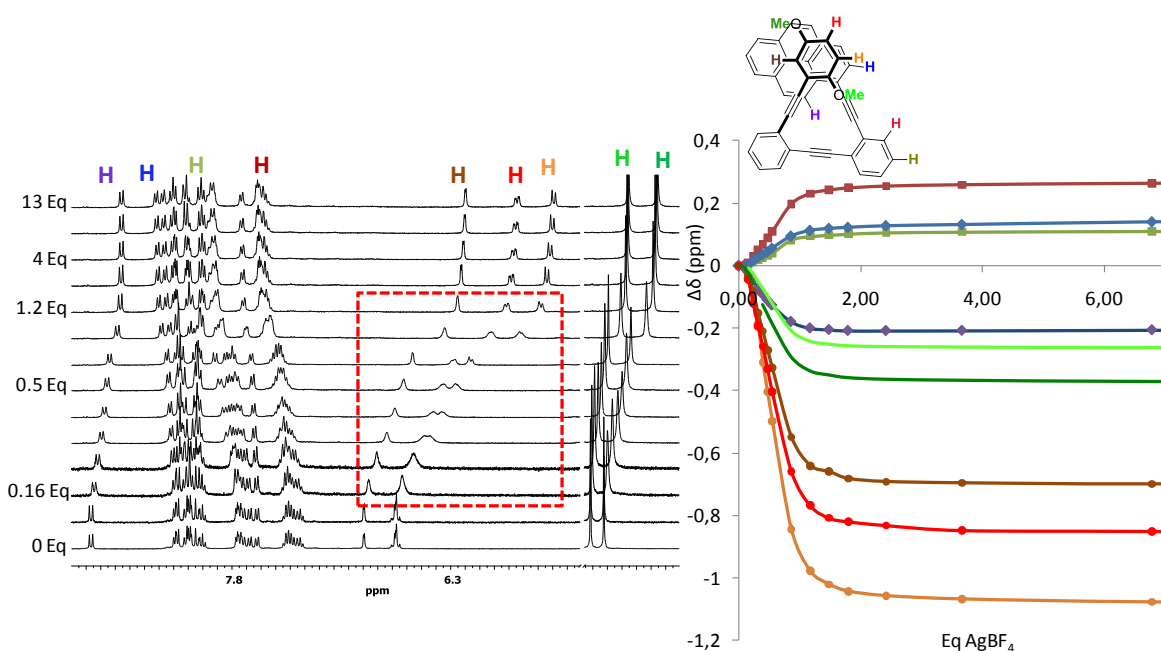
Figure 138. ^{1}H-NMR spectra of **64** by stepwise addition of AgBF$_4$ (left) and titration curves obtained from the experimental data (right). Proton signals affected by slow exchange (red inset).

These evidences prompt us to think that the oxygen initially trapped the Ag(I) probably with the aid of the neighboring alkyne (Scheme 36) to latter adopted a trigonal pyramid coordination geometry involving the three alkynes and the oxygen (guess translocation). In principle when a receptor responds to external (intermolecular) as well as internal (intramolecular) stimuli, the molecule exhibit cooperative functions. Such synergetic interaction was reflected in the sigmoidal movement of the protons (Figure 138 right).
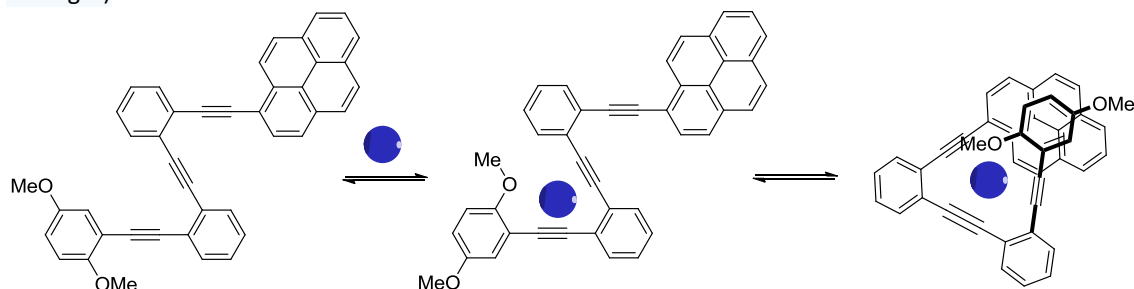
Scheme 36. Hypothetical folding mechanismfor **64** with Ag(I).

Interestingly, the silver template-folded conformation of **64** was evidenced by the ^{13}C shift of the alkynes signals and by several strong 2D-NOESY cross picks (Figure 139). The metoxy group located at ortho position (δ=3.36 ppm) respect to the alkyne (identify due to the cross peak with the doublet at 5.58 ppm) gave a strong NOE with the more deshielded H-10 proton of the pyrene ring together with some other aromatic hydrogens. Complementary cross-peaks between the meta-metoxy group (δ=3.14 ppm) and the pyrene were consistent with a stable relative conformation of both terminal rings in which the ortho-metoxy group was located onto the cavity of the helix probably coordinating the silver ion.

152
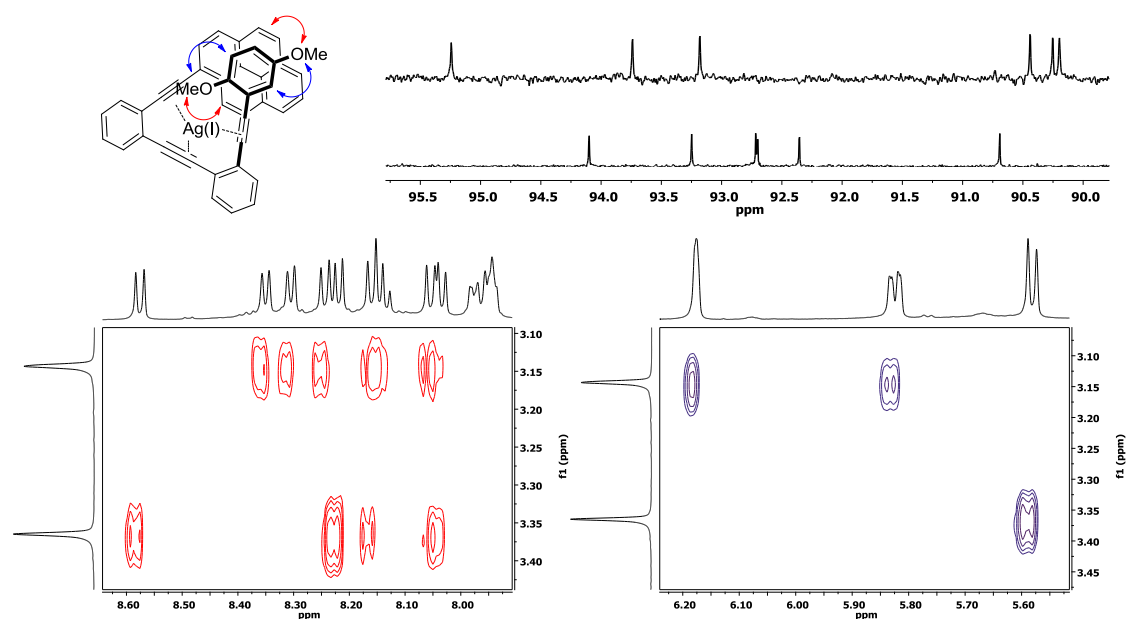
Figure 139. *2D-NOESY cross picks observed for the **64**·Ag(I) complex suggested that the metoxy group located at ortho position respect to the alkyne points to the void of the macrocycle. Changes observed in the ^{13}C-NMR spectra evidenced the coordination of the silver between the alkynes.*

Compared with **63**, **64** displayed a strong emissive profile (ϕ=0.53±0.02). When Ag(I) was added, analogous changes to the one observed for **62** were shown for the absorption.[310] On the other hand, in the fluorescence spectra a homogeneous quenching of the emission was observed (Figure 140).
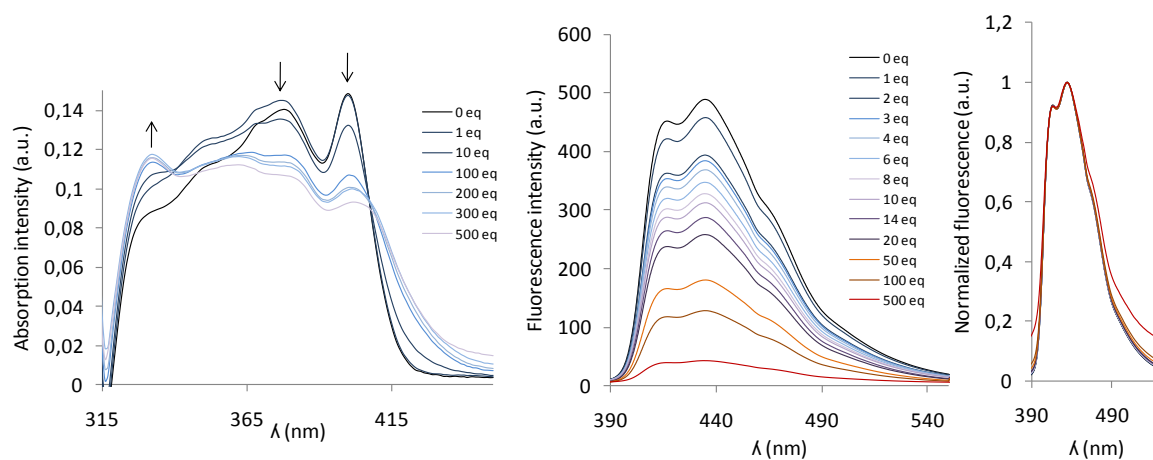
Figure 140. *Absorption and fluorescence spectra registered upon stepwise addition of AgBF$_4$ ta solution of **64**.*

From the fluorescence decay data, three lifetime components were obtained but all the pre-exponential were positive, thus, the three fluorescent species were already formed in the ground state (Figure 141). Comparison of the free ligand and the saturated complex were consistent with the faster formation and the shorter lifetime of the excited-state species.

---

[310] That is a gradual decrease in the absorption bands at 380 and 400 nm and increase at 330 nm (Figure XXX right)
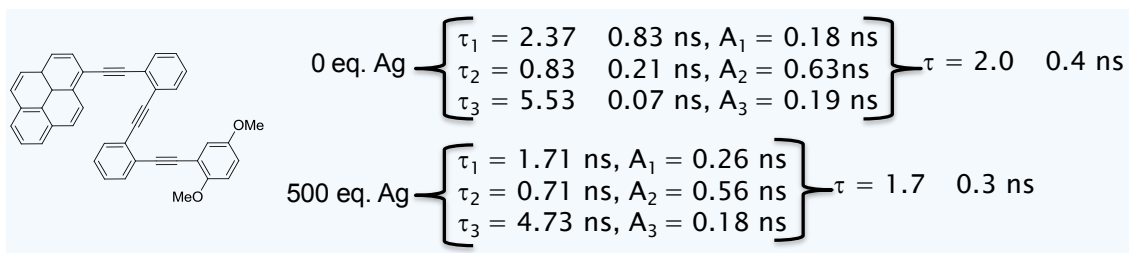
Figure 141. Lifetime results obtained from the fluorescence decays of 64.

Among the four different pyrene combinations tested compound **64** appeared to be a quite promising ligand to obtain the discrete and stable 1:1 Ag(I)-helices. In order to check if the presence of the pyrene had a crucial role in such behaviour, we decided to study its benzene analog **65**.[311] For this compound, again fast exchange was observed during the NMR titration (Figure 136). In this case, coordinated shifts were observed for most of all protons. The inner benzenes and one of the methoxy signals were the most downfield shifted. When the binding constant was calculated from the NMR data,[312] values higher that 10^5 M^{-1} were obtained with good fitting parameters for a 1:1 stochiometry. For this complex a weak NOESY could be detected between the metoxy group located in *ortho* position and the doublet of the stacked benzene (Figure 143).
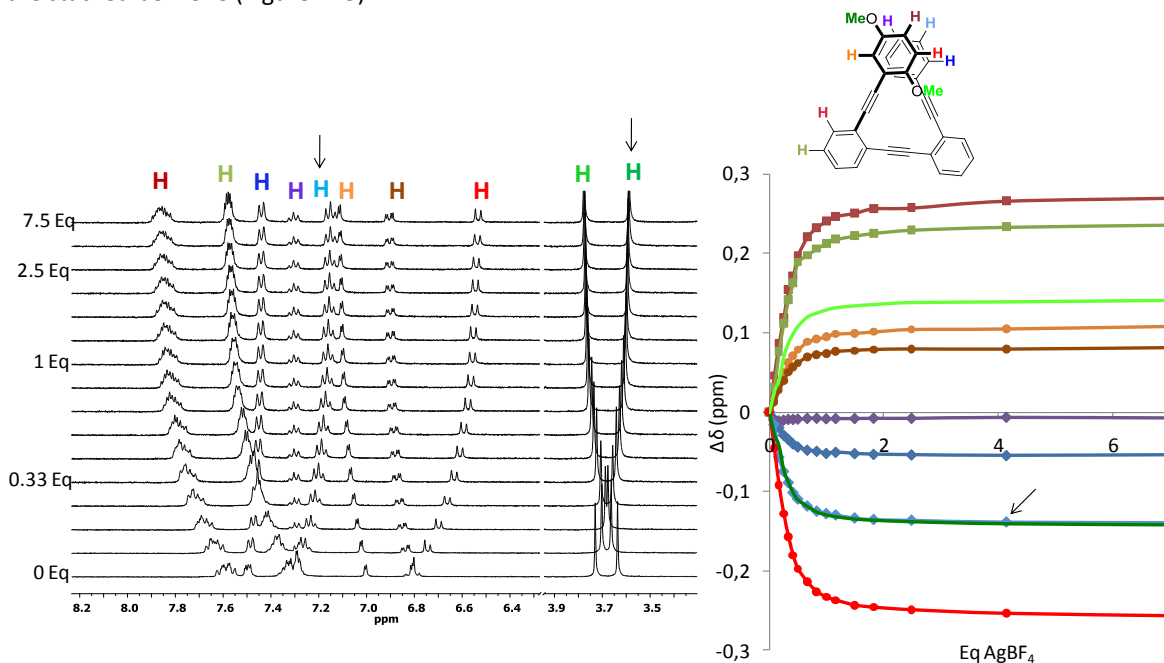
Figure 142. *^{1}H-NMR spectra of **65** by stepwise addition of AgBF$_4$ (left) and titration curves obtained from the experimental data (right).*

---

[311] Nitrobenzene analog was also synthesized and evaluated. See experimental section for details.

[312] Global fitting using all the proton signals.
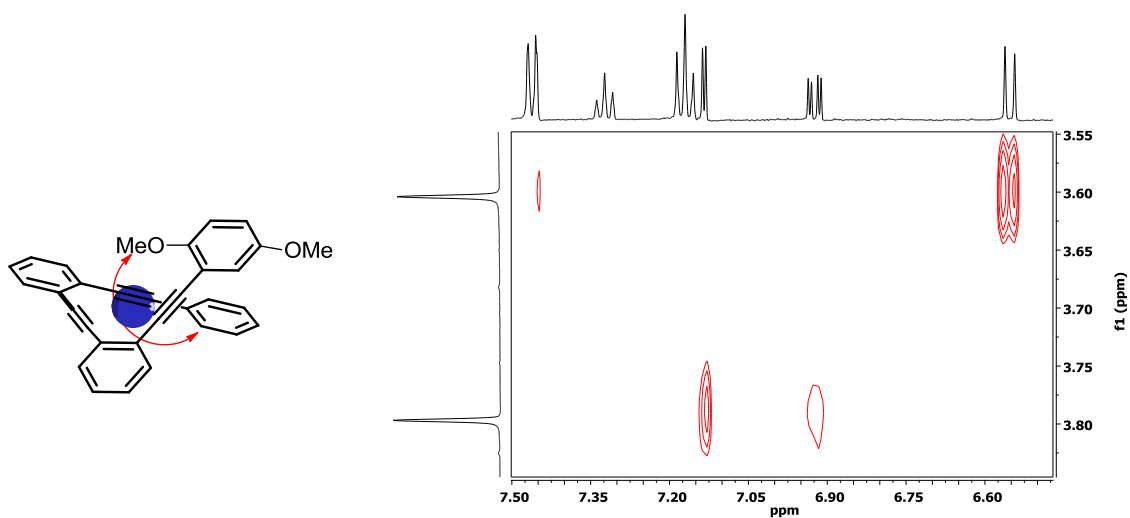
Figure 143. *2D-NOESY cross picks observed for the* **65**·*Ag(I) complex.*

2.3.3. Conclusions and outlook

In this chapter, we have studied the ability of silver(I) to chelate π-bonds in wide variety of flexible oPEOs, macrocyclic oPEOs and some related compounds. Quantitative binding affinities have been determined by ^{1}H-NMR titrations and UV-fluorescence and CD studies could be also used to calculate the binding data. Ag(I) salts has been used to induce the folding of the flexible oPEO backbones into thermodynamically favored helicates which have resulted to be a highly thermodynamically favoured process when the ligands has more that three alkyne bonds. DFT calculations support our findings and point towards the possible formation of larger systems. Using CD spectroscopy, different responses have observed for the chiral mono-stapled isomers. A crystal obtained obtained for the complex of **[30a·Ag]BF₄** revealed a distorted trigonal-pyramidal geometry around the silver ion provided by the planarization of the ligand. The ideal role displayed by the MeO group in flexible oPEOs open the opportunity to get a new family of ditopic ligand able to form much more robust Ag(I) helicates (Figure 144). The possibility to change the alkoxy chain for e.g. a chiral group would potentially be applicable to form a single P or M helicate and to transfer the chirality to the metal center. Additionally, other heteroatoms such as N, S, P located in ortho-position could potentially behave in a similar way widen the scope of the guest metal to for example Au(I). Thus, the possibility to develop chiral metal catalysts would start to become a realistic application for such helicates.
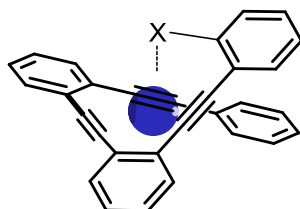
Figure 144. *Chemical structure of the new generation of oPE helical foldamers (ditopic ligands).*

2.3.4. Experimental section[313]

The following known compound was isolated as a pure sample and showed identical NMR spectra to the reported compounds: **31**, **55**, **56**, **31**, **58**, **59**, **60**.[314]

1. *Synthesis and analytical characterization of the new ligands and Ag(I) complexes.*

Silver Complex 29: ^{1}H NMR (401 MHz, 9CD$_2$Cl$_2$:1Acetone) δ 7.89 (d, *J* = 9.2 Hz,21H), 7.83 (d, *J* = 8.8 Hz, 2H), 7.63 – 7.53 (m, 4H), 7.42 (d, *J* = 8.0 Hz, 4H), 7.21 (d, *J* = 8.1 Hz, 4H), 4.68 (s, 4H); ^{13}C NMR (126 MHz, CD$_2$Cl$_2$) δ 145.2 (C), 134.7 (CH), 133.9 (CH), 132.9 (CH), 131.1 (CH), 130.9 (CH), 127.4 (CH), 125.2 (C), 123.2 (C), 96.0 (C), 92.9 (C), 84.8 (C), 64.9 (CH$_2$). One quaternary carbon could not be identified.

Silver Complex 30a: ^{1}H NMR (500 MHz, 9CD$_2$Cl$_2$:1Acetone) δ 7.95 – 7.87 (m, 2H), 7.89 – 7.83 (m, 2H), 7.66 – 7.56 (m, 4H), 7.48 – 7.42 (m, 4H), 7.22 (d, *J* = 8.4 Hz, 4H), 5.18 (s, 4H), 3.57 (s, 2H); ^{13}C NMR (126 MHz, 9CD$_2$Cl$_2$:1Acetone) δ 166.4 (C), 139.3 (C), 135.0 (CH), 134.0 (CH), 133.2 (CHx2), 131.2 (C), 131.1 (C), 129.0 (C), 124.9 (C), 122.6 (C), 118.6 (C), 96.4 (C), 93.1 (C), 85.76, 66.6 (CH$_2$), 42.5 (CH$_2$).

Silver Complex 31: ^{1}H NMR (500 MHz, 9CD$_2$Cl$_2$:1Acetone) δ 7.87 (dd, *J* = 6.0, 3.1 Hz, 2H), 7.80 (dd, *J* = 5.9, 3.2 Hz, 2H), 7.59 – 7.54 (m, 4H), 7.46 – 7.41 (m, 4H), 7.37 (t, *J* = 7.6 Hz, 2H), 7.22 (t, *J* = 7.8 Hz, 4H). ^{13}C NMR (126 MHz, 9DCM:1Acetone) δ 134.4 (CH), 133.8 (CH), 132.7 (CHx2), 131.1 (CH), 131.0 (CH), 130.7 (CH), 129.3 (CHx2), 125.1 (C), 123.1 (C), 119.2 (C), 96.0 (C), 92.6 (C), 85.3 (C).
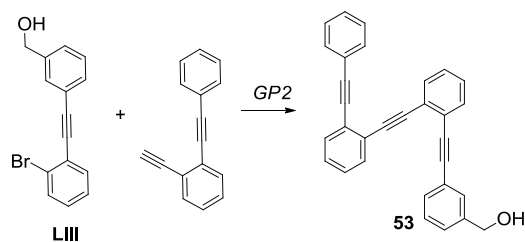
Compound **53** was prepared from **LIII** (300 mg, 1.15 mmol) and 1-ethynyl-2-(phenylethynyl)benzene (436 mg, 1.26 mmol) according to previously described *GP2* to give **53** in 53 % yield (315 mg) as a pale yellow syrup. ^{1}H NMR (600 MHz, 9CD$_2$Cl$_2$:1Acetone) δ 7.64 – 7.55 (m, 4H), 7.52 – 7.48 (m, 3H), 7.39 (d, *J* = 7.4 Hz, 1H), 7.36 – 7.31 (m, 4H), 7.31 – 7.23 (m, 5H), 4.57 (d, *J* = 5.9 Hz, 2H), 3.13 (t, *J* = 5.8 Hz, 1H); ^{13}C NMR (151 MHz, 9CD$_2$Cl$_2$:1Acetone) δ 142.7 (C), 132.6 (CH), 132.5 (CH), 132.4 (CH), 132.3 (CH), 132.1 (CHx2), 130.8 (CH), 130.5 (CH), 129.0 (CH), 129.0 (CH), 129.0 (CH), 128.9 (CHx3), 128.7 (CH), 128.7 (CH), 127.4 (CH), 126.2 (C), 126.2 (C), 126.2 (C), 126.1 (C), 123.6 (C), 123.5 (C), 94.3 (C), 94.2 (C), 92.7 (C), 92.7 (C), 88.6 (C), 88.5 (C), 64.6 (CH$_2$); ESIpos-HRMS calculated for C$_{31}$H$_{21}$O [M+H^{+}]: 409.1597, found: 409.1586.

Silver Complex 53: ^{1}H NMR (500 MHz, 9CD$_2$Cl$_2$:1Acetone) δ 7.84 (dd, *J* = 5.2, 2.4 Hz, 2H), 7.81 – 7.74 (m, 2H), 7.56 (s, 1H), 7.55 – 7.51 (m, 4H), 7.47 – 7.41 (m, 2H), 7.35 (t, *J* = 8.4 Hz, 3H), 7.21 (dd, *J* = 15.0, 7.5 Hz, 3H), 4.55 (s, 2H); ^{13}C NMR (126 MHz, cd$_2$cl$_2$) δ 142.9 (C), 134.1 (CH), 134.1 (CH), 133.6 (CHx2), 132.6 (CHx2), 131.6 (CH), 131.1 (CH), 130.8 (CHx2), 130.7 (CH), 130.5 (CH), 130.5 (CH), 129.4 (CHx2), 129.1 (CHx2), 125.2 (C), 125.2 (C), 123.5 (C), 123.5 (C), 120.0 (C), 119.9 (C), 95.7 (C), 95.6 (C), 92.6 (C), 92.6 (C), 85.9 (C), 85.8 (C), 64.7 (CH$_2$).

Silver Complex 54: ^{1}H NMR (500 MHz, 9CD$_2$Cl$_2$:1Acetone) δ 7.88 (dd, *J* = 6.1, 3.0 Hz, 2H), 7.80 (dd, *J* = 6.0, 3.1 Hz, 2H), 7.56 (dd, *J* = 5.8, 3.3 Hz, 4H), 7.44 (d, *J* = 8.1 Hz, 4H), 7.20 (d, *J* = 8.1 Hz, 4H), 5.07 (s, 4H), 2.12 (s, 6H); ^{13}C NMR (126 MHz, cd$_2$cl$_2$) δ 172.0 (C), 139.5 (C), 134.3 (CH), 133.7 (CH), 132.8 (CHx2), 131.0 (CH), 130.6 (CH), 128.2 (CHx2), 125.0 (C), 123.1 (C), 118.8 (C), 95.4 (C), 92.5 (C), 85.52 (C), 65.8 (CH$_2$), 21.1 (CH$_3$).

---

[313] For general procedures of the Sonogashira reaction see GP1 and GP2.
[314] Grubbs, H. Robert, Kratz, Detlef, *Chemische Berichte*, **1993**, *126*, 149 – 158.

Silver Complex 30b: ^{1}H NMR (600 MHz, 9CD$_2$Cl$_2$:1Acetone) δ 7.63 (dd, *J* = 5.7, 3.3 Hz, 2H), 7.61 (dd, *J* = 5.7, 3.3 Hz, 2H), 7.40 – 7.32 (m, 4H), 7.27 (d, *J* = 8.1 Hz, 4H), 6.98 (d, *J* = 8.1 Hz, 4H), 4.96 (s, 4H), 2.66 (s, 4H); ^{13}C NMR (151 MHz, 9CD$_2$Cl$_2$:1Acetone) δ 176.1 (C), 138.8 (C), 135.4 (CH), 135.1 (CH), 134.3 (CHx2), 131.0 (CH), 130.7 (CH), 130.0 (CHx2), 127.9 (C), 127.7 (C), 125.0 (C), 96.1 (C), 94.4 (C), 90.9 (C), 68.1 (CH2), 31.2 (CH2).

Silver Complex 58: ^{1}H NMR (500 MHz, 9CD$_2$Cl$_2$:1Acetone) δ 7.94 – 7.88 (m, 1H), 7.71 (s, 1H), 7.63 – 7.59 (m, 1H), 7.47 – 7.38 (m, 5H), 7.24 – 7.19 (m, 1H), 7.11 (dd, *J* = 10.5, 4.7 Hz, 2H); ^{13}C NMR (126 MHz, 9CD$_2$Cl$_2$:1Acetone) δ 134.6 (CH), 133.6 (CH), 133.5 (CH), 132.7 (CHx2), 131.4 (CH), 131.3 (CH), 130.9 (CH), 130.4 (CH), 129.2 (CHx2), 125.3 (C), 123.9 (C), 122.(C), 120.2 (C), 97.4 (C), 93.6 (C), 91.8 (C), 87.0 (C).
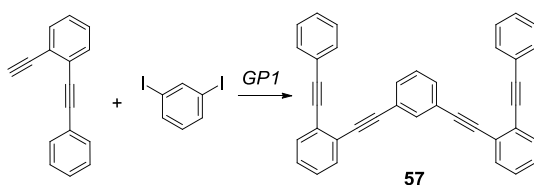
***Compound* 57** was prepared from 1-ethynyl-2-(phenylethynyl)benzene (300 mg, 1.15 mmol) and 1,3-diiodobenzene (436 mg, 1.26 mmol) according to previously described *GP1* to give **57** in 53 % yield (315 mg) as a pale yellow solid. ^{1}H NMR (401 MHz, CDCl$_3$) δ 7.91 (t, *J* = 1.6 Hz, 1H), 7.68 – 7.58 (m, 10H), 7.41 – 7.31 (m, 11H); ^{13}C NMR (101 MHz, CDCl$_3$) δ 134.9 (CH), 131.9 (CHx2), 131.9 (CHx2), 131.7 (CHx4), 131.5 (CHx2), 128.7 (CH), 128.6 (CHx2), 128.5 (CHx4), 128.3 (CHx2), 128.1 (CHx2), 126.1 (C), 125.6 (C), 123.8 (C), 123.2 (C), 93.9 (C), 92.8 (C), 89.2 (C), 88.4 (C); EI-HRMS calculated for C$_{38}$H$_{22}$: 478.1722, found: 478.1721.

Silver Complex 59: ^{1}H NMR (500 MHz, 9CD$_2$Cl$_2$:1Acetone) δ 7.73 (d, *J* = 7.5 Hz, 2H), 7.71 – 7.67 (m, 2H), 7.48 – 7.38 (m, 12H), 7.30 (td, *J* = 7.7, 1.0 Hz, 2H), 7.11 – 7.01 (m, 8H); ^{13}C NMR (126 MHz, , 9CD$_2$Cl$_2$:1Acetone) δ 134.3 (CH), 134.0 (CH), 132.8 (CH), 132.5 (CHx2), 132.4 (CH), 131.1 (CH), 131.1 (CH), 130.8 (CH), 130.7 (CH), 130.1 (CH), 129.0 (CHx2), 125.1 (C), 123.6 (C), 122.9 (C), 122.4 (C), 120.5 (C), 97.6 (C), 94.3 (C), 92.5 (C), 92.0 (C), 87.7 (C).

Silver Complex 60: ^{1}H NMR (500 MHz, 9CD$_2$Cl$_2$:1Acetone) δ 7.91 (td, *J* = 5.6, 2.5 Hz, 2H), 7.73 (dd, *J* = 7.6, 3.6 Hz, 2H), 7.61 (dd, *J* = 13.6, 1.6 Hz, 2H), 7.62 (d, *J* = 9.3 Hz, 2H) 7.49 – 7.40 (m, 4H), 7.38 (m, 1H), 7.33 (d, *J* = 6.9 Hz, 1H), 7.30 (d, *J* = 8.1 Hz, 1H), 7.29 – 7.25 (m, 1H), 7.22 – 7.18 (m, 1H), 7.17 – 7.14 (m, 1H), 7.13 – 7.08 (m, 2H); ^{13}C NMR (126 MHz, , 9CD$_2$Cl$_2$:1Acetone) δ 134.7 (CH), 134.6 (CH), 134.4 (CH), 133.7 (CH), 133.6 (CH), 133.4 (CH), 133.1 (CH), 132.7 (CH), 132.5 (CH), 132.3 (CH), 131.4 (CH), 131.3 (CH), 131.21 (CH), 131.17 (CH), 130.9 (CH), 130.6 (CH), 130.3 (CH), 129.0 (CH), 128.5 (CH), 125.6 (C), 124.9 (C), 124.3 (C), 123.7 (C), 123.53 (C), 122.48 (C), 122.3 (C), 122.0 (C), 119.7 (C), 97.3 (C), 95.2 (C), 93.8 (C), 93.0 (C), 92.2 (C), 91.9 (C), 91.5 (C), 86.7 (C). One CH and seven C could not be detected.
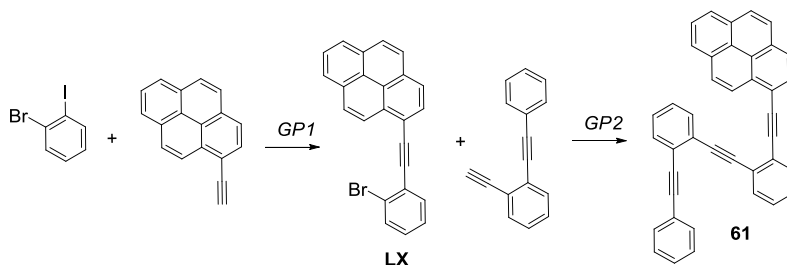
***Compound* LX** was prepared from 1-bromo-2-iodobenzene (200 mg, 0.71 mmol) and 1-ethynyl-pyrene (160 mg, 0.7 mmol) according to previously described *GP1* to give **LX** in 36 % yield (97 mg) as a bright yellow solid. ^{1}H NMR (500 MHz, Chloroform-d) δ 8.82 (d, *J* = 9.0 Hz, 1H), 8.21 (d, *J* = 7.9 Hz, 1H), 8.17 (d, *J* = 7.5 Hz, 1H), 8.11 (d, *J* = 7.5 Hz, 1H), 8.07 (d, *J* = 8.4 Hz, 2H), 8.04 – 7.97 (m, 2H), 7.81 – 7.75 (m, 2H), 7.72 (dd, *J* = 7.6, 1.4 Hz, 1H), 7.68 (d, *J* = 7.6 Hz, 1H), 7.63 (dd, *J* = 7.7, 1.1 Hz, 1H), 7.51 – 7.45 (m, 2H), 7.45 – 7.34 (m, 3H), 7.29 (td, *J* = 7.7, 1.4 Hz, 1H), 7.23 – 7.19 (m, 3H). ^{13}C NMR (126 MHz, cdcl$_3$) δ 132.6 (CH), 132.5 (CH), 132.2 (CH), 132.0 (CH), 131.8 (CHx2), 131.4 (C), 131.3 (C), 131.2 (C), 129.9 (CH), 128.5

(CH), 128.4 (CH), 128.4 (CH), 128.4 (CH), 128.3 (CH), 128.3 (CHx2), 128.1 (CH), 128.0 (CH), 127.3 (CH), 126.4 (C), 126.2 (CH), 126.2 (C), 126.1 (CH), 125.9 (C), 125.8 (C), 125.7 (CH), 125.6 (CH), 124.5 (CH), 124.5 (C), 124.3 (C), 123.3 (C), 117.9 (C), 94.1 (Cx2), 93.2 (C), 92.9 (C), 92.6 (C), 88.5 (C). EI-HRMS calculated for $C_{24}H_{13}Br$: 380.0200, found: 380.0201.

***Compound* 61** was prepared from intermediate **LX** (200 mg, 0.71 mmol) and 1-ethynyl-2-(phenylethynyl)benzene (160 mg, 0.7 mmol) according to previously described *GP2* to give **61** in 82 % yield (39 mg) as a bright yellow solid. ^{1}H NMR (500 MHz, Chloroform-d) δ 8.82 (d, *J* = 9.0 Hz, 1H), 8.21 (d, *J* = 7.9 Hz, 1H), 8.17 (d, *J* = 7.5 Hz, 1H), 8.11 (d, *J* = 7.5 Hz, 1H), 8.07 (d, *J* = 8.4 Hz, 2H), 8.04 − 7.97 (m, 2H), 7.81 − 7.75 (m, 2H), 7.72 (dd, *J* = 7.6, 1.4 Hz, 1H), 7.68 (d, *J* = 7.6 Hz, 1H), 7.63 (dd, *J* = 7.7, 1.1 Hz, 1H), 7.51 − 7.45 (m, 2H), 7.45 − 7.34 (m, 3H), 7.29 (td, *J* = 7.7, 1.4 Hz, 1H), 7.23 − 7.19 (m, 3H); ^{13}C NMR (126 MHz, cdcl$_3$) δ 132.6 (CH), 132.5 (CH), 132.2 (CH), 132.0 (CH), 131.8 (CHx2), 131.4 (C), 131.3 (C), 131.2 (C), 129.9 (CH), 128.5 (CH), 128.4 (CH), 128.4 (CH), 128.4 (CH), 128.3 (CH), 128.3 (CHx2), 128.1 (CH), 128.0 (CH), 127.3 (CH), 126.4 (C), 126.2 (CH), 126.2 (C), 126.1 (CH), 125.9 (C), 125.8 (C), 125.7 (CH), 125.6 (CH), 124.5 (CH), 124.5 (C), 124.3 (C), 123.3 (C), 117.9 (C), 94.1 (Cx2), 93.2 (C), 92.9 (C), 92.6 (C), 88.5 (C).

Silver Complex 61: ^{1}H NMR (500 MHz, 9CD$_2$Cl$_2$:1Acetone $_2$) δ 8.48 (d, *J* = 9.0 Hz, 1H), 8.34 (d, *J* = 7.6 Hz, 1H), 8.29 (d, *J* = 7.5 Hz, 1H), 8.25 (d, *J* = 8.9 Hz, 1H), 8.16 (d, *J* = 8.0 Hz, 1H), 8.13 (t, *J* = 7.6 Hz, 2H), 8.11 (d, *J* = 9.1 Hz, 1H), 8.08 (d, *J* = 8.9 Hz, 1H), 8.01 (d, *J* = 8.0 Hz, 1H), 7.95 (dd, *J* = 5.9, 3.2 Hz, 2H), 7.92 (d, *J* = 8.7 Hz, 1H), 7.72 (d, *J* = 8.6 Hz, 1H), 7.62 (dd, *J* = 5.9, 3.3 Hz, 2H), 7.58 (t, *J* = 7.7 Hz, 1H), 7.54 (t, *J* = 7.6 Hz, 1H), 6.84 (d, *J* = 7.3 Hz, 2H), 6.43 (t, *J* = 7.6 Hz, 1H), 6.27 (t, *J* = 7.8 Hz, 2H); ^{13}C NMR (126 MHz, 9CD$_2$Cl$_2$:1Acetone) δ 134.6 (CH), 134.5 (CH), 134.0 (CH), 133.8 (CH), 133.6 (C), 132.7 (C), 131.6 (CHx2), 131.5 (C), 131.15 (CH), 131.11 (C), 131.0 (CH), 130.8 (CH), 130.7 (CH), 130.1 (CH), 129.9 (CHx2), 128.1 (CHx2), 127.3 (CH), 127.2 (CH), 127.11 (CH), 127.10 (CH), 125.7 (C), 125.3 (CH), 125.2 (C), 124.7 (C), 124.3 (C), 124.2 (CH), 123.41 (C), 123.37 (C), 118.0 (C), 112.4 (C), 95.5 (C), 95.0 (C), 93.3 (C), 92.8 (C), 90.0(C), 84.6 (C).

62
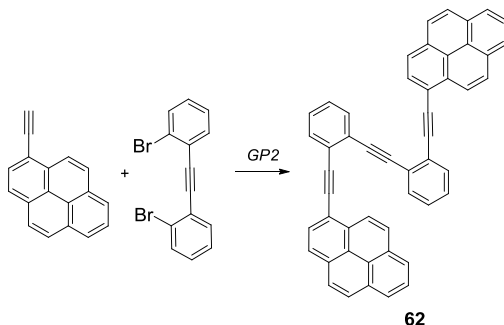
***Compound* 62** was prepared from 1,2-bis(2-bromophenyl)ethyne (30 mg, 0.08 mmol) and 1-ethynyl-pyrene (50 mg, 0.22 mmol) according to previously described *GP2* to give **62** in 53 % yield (27 mg) as a bright yellow solid. ^{1}H NMR (500 MHz, CDCl$_3$) δ 8.57 (d, *J* = 9.0 Hz, 2H), 8.10 (s, 2H), 8.03 (d, *J* = 7.1 Hz, 2H), 7.97 (dd, *J* = 15.0, 7.7 Hz, 4H), 7.90 (d, *J* = 8.9 Hz, 2H), 7.83 − 7.76 (m, 8H), 7.56 (d, *J* = 9.1 Hz, 2H), 7.47 (td, *J* = 7.6, 1.2 Hz, 2H), 7.40 − 7.36 (m, 2H); ^{13}C NMR (126 MHz, CDCl$_3$) δ 132.9 (CH), 132.2 (CH), 131.9 (C), 131.2 (Cx2), 131.1 (C), 131.0 (C), 129.8 (CH), 129.0 (C), 128.5 (CH), 128.1 (CHx2), 128.0 (CH), 127.1 (CH), 126.7 (C), 126.1 (CH), 125.9 (CH), 125.8 (C), 125.6 (CH), 125.4 (CH), 124.2 (CH), 124.1 (C), 117.7 (C), 94.1 (C), 93.5 (C), 93.0 (C); MALDI-HRMS calculated for $C_{50}H_{26}$: 626.2048, found: 626.2029.

Silver Complex 62: ^{1}H NMR (500 MHz, 9CD$_2$Cl$_2$:1Acetone) δ 8.11 (d, *J* = 9.0 Hz, 1H), 8.01 (d, *J* = 9.0 Hz, 1H), 7.92 (d, *J* = 7.5 Hz, 1H), 7.89 (d, *J* = 7.4 Hz, 1H), 7.85 (d, *J* = 7.5 Hz, 1H), 7.78 (d, *J* = 7.9 Hz, 1H), 7.76 (t, *J* = 7.5 Hz, 1H), 7.72 (d, *J* = 8.8 Hz, 1H), 7.71 (d, *J* = 9.0 Hz, 1H)7.65 (td, *J* = 7.7, 1.5 Hz, 1H), 7.62 (td, *J* = 7.5, 1.5 Hz, 1H), 7.43 (d, *J* = 8.8 Hz, 1H), 7.38 (d, *J* = 7.9 Hz, 1H); ^{13}C NMR (126 MHz, 9CD$_2$Cl$_2$:1Acetone) δ 134.8 (CH), 134.0 (CH), 132.8 (C), 132.0 (C), 131.1 (CH), 130.9 (CH), 130.8 (C), 130.4 (C), 129.9 (CH), 129.7 (CH), 129.5 (CH), 126.9 (CH), 126.7 (CH), 126.7 (CH), 126.6 (CH), 125.9 (CH), 124.4 (CH), 123.8 (C), 123.6 (CH), 123.5 (C), 123.1 (C), 11.4 (C), 95.1 (C), 93.5 (C), 89.5 (C).

Compound 63 was prepared from **LXI**[315] (100 mg, 0.4 mmol) and **LX** (111 mg, 0.29 mmol) according to previously described *GP2* to give **63** in 57 % yield (91 mg) as a pale yellow solid. ^{1}H NMR (300 MHz, CDCl$_3$) δ 8.29 – 8.18 (m, 2H), 7.77 – 7.69 (m, 2H), 7.65 (dd, *J* = 7.9, 1.3 Hz, 1H), 7.58 (dd, *J* = 7.7, 1.8 Hz, 1H), 7.34 (td, *J* = 7.6, 1.4 Hz, 1H), 7.25 (td, *J* = 7.6, 1.8 Hz, 1H); ^{13}C NMR (75 MHz, CDCl$_3$) δ 147.3 (C), 133.6 (CH), 132.8 (CH), 132.5 (CHx2), 130.5 (CH), 129.9 (C), 127.3 (CH), 126.0 (C), 124.4 (C), 123.8 (CHx2), 93.1 (C), 91.8 (C). ESIpos-HRMS calculated for C$_{42}$H$_{26}$O$_2$Na [M+Na]$^+$: 585.1847, found: 585.1825.

Silver Complex 63: ^{1}H NMR (401 MHz, 9CD$_2$Cl$_2$:1Acetone) δ 8.56 (d, *J* = 9.0 Hz, 1H), 8.29 (d, *J* = 7.6 Hz, 1H), 8.24 (d, *J* = 7.7 Hz, 1H), 8.19 (d, *J* = 8.0 Hz, 1H), 8.15 (d, *J* = 8.9 Hz, 1H), 8.10 (t, *J* = 7.6 Hz, 1H), 8.05 (d, *J* = 8.0 Hz, 1H), 8.02 (d, *J* = 6.4 Hz, 1H), 8.00 (d, *J* = 6.4 Hz, 1H), 7.92 - 7.86 (m, 3H), 7.69 (d, *J* = 7.5 Hz, 1H), 7.62 – 7.50 (m, 4H), 7.29 (d, *J* = 8.5 Hz, 2H), 7.09 (d, *J* = 8.6 Hz, 2H).

Compound LXII was prepared from 2-bromo-1,4-dimethoxybenzene (500 mg, 2.29 mmol) and TMSA (0.5 mL,3.6 mmol) according to previously described *GP2* to give **LXII** in 71 % yield (263 mg) as a transparent liquid. ^{1}H NMR (300 MHz, CDCl$_3$) δ 7.04 (d, *J* = 2.8 Hz, 1H), 6.90 (dd, *J* = 9.1, 2.7 Hz, 1H), 6.83 (d, *J* = 9.1 Hz, 2H), 3.88 (s, 3H), 3.78 (s, 3H), 3.36 (s, 1H); ^{13}C NMR (75 MHz, CDCl$_3$) δ 155.0 (C), 153.1 (C), 119.0 (C), 118.7 (CH), 116.2 (CH), 111.9 (CH), 111.6 (C), 81.2 (CH), 80.0 (C), 56.3 (CH3), 55.7 (CH3).

Compound LXIII was prepared from **LXII** (263 mg, 1.62 mmol) and 1-bromo-2-iodobenzene (458 mg, 1.62 mmol) according to previously described *GP1* to give **LXIII** in 45 % yield (230 mg) as a transparent liquid. ^{1}H NMR (500 MHz, CDCl$_3$) δ 7.60 (ddd, *J* = 9.6, 7.9, 1.4 Hz, 2H), 7.32 – 7.24 (m, 1H), 7.17 (td, *J* = 7.8, 1.7 Hz, 1H), 7.09 (d, *J* = 3.1 Hz, 1H), 6.89 (dd, *J* = 9.0, 3.0 Hz, 1H), 6.84 (d, *J* = 9.0 Hz, 1H), 3.89 (s, 3H), 3.79 (s, 3H); ^{13}C NMR (126 MHz, CDCl$_3$) δ 154.8 (C), 153.4 (C), 133.5 (CH), 132.5 (CH), 129.4 (CH), 127.1 (CH), 125.7 (C), 125.7 (C), 118.3 (CH), 116.3 (CH), 112.9 (C), 112.5 (CH), 92.0 (C), 90.5 (C), 56.8 (CH3), 55.6 (CH3); EI-HRMS calculated for C$_{16}$H$_{14}$BrO$_2$ [M+H]$^+$: 317.0165, found: 317.0177.

Compound 64. Compound LXIV was prepared from **LXIII** (260 mg, 0.82 mmol) and TMSA (0.2 mL, 1.23 mmol) according to previously described *GP2* to give **LXIV** in 45 % yield (230 mg) as a transparent liquid. This compound **LXIV** (23 mg, 0.09 mmol) was cross-coupled with **LX** (32 mg, 0.0.9 mmol) according to

---

[315] M. S. Wong, J.-F. Nicoud, *Tetrahedron Letters*, **1994**, 35, 6113 – 6116.

previously described *GP2* to give **64** in 51 % yield (25 mg) as a pale yellow solid. ^{1}H NMR (500 MHz, CDCl$_3$) δ 8.80 (d, *J* = 9.0 Hz, 1H), 8.20 – 8.17 (m, 1H), 8.17 (t, *J* = 3.7 Hz, 1H), 8.12 – 8.06 (m, 3H), 8.02 (d, *J* = 8.9 Hz, 1H), 7.99 (t, *J* = 7.6 Hz, 1H), 7.76 – 7.73 (m, 3H), 7.68 – 7.64 (m, 2H), 7.39 (qd, *J* = 7.8, 1.1 Hz, 2H), 7.34 (td, *J* = 7.5, 1.3 Hz, 1H), 7.29 (td, *J* = 7.6, 1.3 Hz,13H), 6.95 (d, *J* = 3.0 Hz, 1H), 6.70 (dd, *J* = 9.0, 3.0 Hz, 1H), 6.65 (d, *J* = 9.0 Hz, 1H), 3.65 (s, 3H), 3.55 (s, 3H); ^{13}C NMR (126 MHz, CDCl$_3$) δ 154.5 (C), 153.1 (C), 132.7 (CH), 132.5 (CH), 132.2 (C), 132.1 (CH), 132.0 (CH), 131.4 (C), 131.3 (C), 131.2 (C), 129.9 (CH), 128.5 (CH), 128.4 (CH), 128.3 (CH), 128.3 (CH), 128.0 (CH), 127.9 (CH), 127.4 (CH), 126.7 (C), 126.2 (CH), 126.2 (C), 126.2 (CH), 125.9 (C), 125.9 (C), 125.7 (CH), 125.5 (CH), 124.5 (CH), 124.5 (C), 124.4 (C), 117.9 (C), 117.7 (CH), 116.6 (CH), 112.9 (C), 112.1 (CH), 94.1 (C), 93.3 (C), 92.7 (C), 92.7 (C), 92.4 (C), 90.7 (C), 56.4 (CH3), 55.6 (CH3); ESIpos-HRMS calculated for C$_{42}$H$_{26}$O$_2$Na [M+Na$^+$]: 585.1847, found: 585.1825.

Silver Complex 64: ^{1}H NMR (600 MHz, 9CD$_2$Cl$_2$:1Acetone) δ 8.56 (d, *J* = 9.0 Hz, 1H), 8.34 (d, *J* = 7.5 Hz, 1H), 8.29 (d, *J* = 7.5 Hz, 1H), 8.23 (d, *J* = 8.8 Hz, 1H), 8.21 (d, *J* = 7.9 Hz, 1H), 8.15 - 8-13 (m, 2H), 8.04 (d, *J* = 8.9 Hz, 1H), 8.02 (d, *J* = 8.0 Hz, 1H), 7.96 (d, *J* = 8.3 Hz, 1H), 7.95 - 7.92 (m, 2H), 7.73 (d, *J* = 7.6 Hz, 1H), 7.65 – 7.55 (m, 4H), 6.16 (s, 1H), 5.81 (dd, *J* = 9.0, 2.7 Hz, 1H), 5.57 (d, *J* = 9.1 Hz, 1H), 3.35 (s, 3H), 3.13 (s, 3H); ^{13}C NMR (151 MHz, 9CD$_2$Cl$_2$:1Acetone) δ 152.9 (C), 151.3 (C), 134.5 (CH), 134.11 (CH), 134.10 (CH), 133.6 (CH), 133.6 (C), 132.5 (C), 131.5 (C), 131.2 (CH), 131.0 (CH), 130.9 (CH), 130.8 (CH), 130.6 (CH), 130.1 (CH), 129.8 (CH), 127.2 (CH), 127.2 (CH), 127.0 (CH), 126.9 (C), 125.5 (C), 125.1 (CH), 124.5 (C), 124.4 (C), 124.2 (C), 124.1 (CH), 123.3 (C), 122.8 (C), 117.4 (CH), 117.1 (CH), 112.5 (C), 110.8 (CH), 106.8 (C), 95.2 (C), 93.7 (C), 93.2 (C), 90.4 (C), 90.3 (C), 90.2 (C), 57.2 (CH3), 55.4 (CH3).
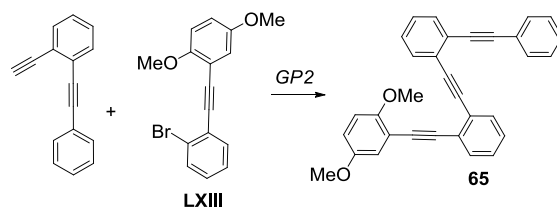
LXIII

***Compound* 65** was prepared from **LXIII** (60 mg, 0.19 mmol) and 1-ethynyl-2-(phenylethynyl)benzene (50 mg, 0.25 mmol) according to previously described *GP2* to give **65** in 33 % yield (27 mg) as a transparent liquid. ^{1}H NMR (500 MHz, CDCl$_3$) δ 7.65 – 7.62 (m, 2H), 7.60 (dd, *J* = 7.5, 1.3 Hz, 1H), 7.58 – 7.55 (m, 1H), 7.53 (dd, *J* = 6.7, 3.0 Hz, 2H), 7.35 – 7.27 (m, 7H), 7.05 (d, *J* = 3.0 Hz, 1H), 6.82 (dd, *J* = 9.0, 3.1 Hz, 1H), 6.77 (d, *J* = 9.0 Hz, 1H), 3.76 (s, 3H), 3.66 (s, 3H). ^{13}C NMR (126 MHz, CDCl$_3$) δ 154.7 (C), 153.3 (C), 132.4 (CH), 132.1 (CH), 132.0 (CH), 131.8 (CHx2), 131.8 (CH), 128.4 (CH), 128.4 (CHx2), 128.2 (CH), 128.2 (CH), 128.0 (CH), 128.0 (CH), 126.2 (C), 126.1 (C), 125.9 (C), 125.9 (C), 123.3 (C), 117.9 (CH), 116.7 (CH), 113.0 (C), 112.3 (CH), 93.9 (C), 92.6 (C), 92.3 (C), 92.3 (C), 90.4 (C), 88.4 (C), 56.6 (CH3), 55.8 (CH3); ESIpos-HRMS calculated for C$_{32}$H$_{22}$O$_2$Na [M+Na$^+$]: 461.1518, found: 461.1512.

Silver Complex 65: ^{1}H NMR (500 MHz, 9CD$_2$Cl$_2$:1Acetone) δ 7.88 (dd, *J* = 6.2, 3.1 Hz, 1H), 7.85 (dd, *J* = 5.9, 3.1 Hz, 2H), 7.83 (dd, *J* = 6.2, 3.0 Hz, 1H), 7.59 – 7.55 (m, 4H), 7.44 (d, *J* = 7.2 Hz, 2H), 7.30 (t, *J* = 7.6 Hz, 1H), 7.15 (t, *J* = 7.8 Hz, 2H), 7.11 (d, *J* = 3.1 Hz, 1H), 6.90 (dd, *J* = 9.2, 3.1 Hz, 1H), 6.53 (d, *J* = 9.2 Hz, 1H), 3.77 (s, 3H), 3.58 (s, 3H); ^{13}C NMR (126 MHz, 9CD$_2$Cl$_2$:1Acetone) δ 154.3 (C), 152.9 (C), 134.5 (CH), 134.2 (CH), 134.0 (CH), 133.7 (CH), 132.7 (CHx2), 131.21 (CH), 131.18 (CH), 131.1 (CH), 130.9 (CH), 130.8 (CH), 129.3 (CHx2), 125.2 (C), 124.7 (C), 123.1 (C), 122.9 (C), 119.3 (CH), 118.7 (CH), 112.6 (CH), 96.5 (C), 93.3 (C), 92.9 (C), 91.0 (C), 90.8 (C), 85.5 (C), 57.2 (CH3), 56.4 (CH3).

2. *Binding studies.*

Titrations were conducted in 1H-NMR, UV-vis and CD spectroscopy but binding constants were only calculated from the NMR data.

<u>1H-NMR titrations:</u>

A stock solution of the ligands (10^{-2}-10^{-3}M) in CD$_2$Cl$_2$/Acetone (v/v, 9:1) was firstly prepared. Using this solution as a solvent, a stock solution of AgBF$_4$ (20-200 mM depending on the ligand) was prepared. Then, 0.5 mL of the purê ligand solution was transferred to a NMR tube and initial spectra was registered. To this solution, small portions of the silver solution were added and the spectra recorded after each addition. Binding constants were determined by non-linear regression curve fitting methods

using Program DynaFit[316] plotting the differences measured between the initial chemical shift of the selected protons[317] against the concentration of the silver added.

UISUV-vis and CD titrations:
The experiments were conducted from stock solutions of the ligands (10^{-4}M) in CD_2Cl_2/Acetone (v/v, 9:1). Two or three solutions of different concentrations of the $AgBF_4$ were prepared in CD_2Cl_2/Acetone (v/v, 9:1). A small portion of the ligand was transferend to a cuvette and diluted with the solvent mixture to 10^{-5}-10^{-6}M. After taking the initial spectra, small portions (from 1-100 µL) of the silver solution were added and the spectra recorded after each addition.

3. *UV-vis studies*
Absorption spectra were measured on a Hewlett-Packard model 8543 spectrophotometer using 1-cm cuvettes. Steady-state fluorescence emission measurements were recorded with a Varian Eclipse spectrofluorometer.

4. *Time-resolved fluorescence studies*
Fluorescence decay studies were recorded on a Fluorotime 200 spectrofluorimeter (Picoquant Inc.) using a laser beam (405 nm) using 1-cm cuvettes.

5. *Computatinal details*
All theoretical calculations were carried out at the DFT level of theory using the hybrid M06 exchange-correlation functional proposed by Truhlar and Zhao (probed to be well adapted for a better description of non-covalent weak interactions), as implemented in the Gaussian 09 program. The Pople standard 6-31G* basis set has been used in all cases. Enthalpies and free energies, where necessary, were determined by the corresponding frequency calculation on each optimized structure.

6. *X-ray structure determinations*
Under inert argon atmosphere, $AgBF_4$ (19.5 mg, 0.1 mmol) was added to a solution of **30a** (50.7 mg, 0.1 mmol) in dry CH_2Cl_2 (10 ml). The mixture was stirred for 4 h with the exclusion of light. A pale brown precipitate formed which was collected by vacuum filtration, dissolved in acetone, filtered through celite and then the solvent removed under reduced pressure to give a pale brown solid (16.4 mg). The filtrate from the initial filtration was filtered through celite and then solvent removed under reduced pressure to give **30a·Ag** as a brown solid (40. 2 mg). Cristals were grown from…

7. *Au(I) studies*
To check if Au(I) gold complexes could be also formed, some experiments have also been carried out. In a first trial, a solution of 30a (10 mg, 0.02 mmol) in CD_2Cl_2 (1 ml) and $AuCl(SMe_2)$ (6mg, 0.02 mmol) under air was sonicated 2 minutes in a vial wrapped with aluminium foil. Then, 0.5 mL of the mixture was transferred to a NMR tube and a ^{1}H-NMR spectra was registered (Figure S1, middle). The appearance of small peaks at lower fields suggested the labile coordination of the AgCl. Then, the tube mixture was poured again into the vial and excess of $AgBF_4$ was added (30 mg, 0.15 mmol). After 5 minutes of sonication, 0.5 mL of the supernatant liquid (some precipitates were formed after addition of the silver salt) evidenced the formation of a new complex which was tentatively assigned to the gold species (Figure S1, top).

---

[316] P. Kuzmic, *Analytical Biochemistry*, **1996**, *237*, 260-273.
[317] For the calculations all the identificable signals were included in a global fitting except for the indicated cases.
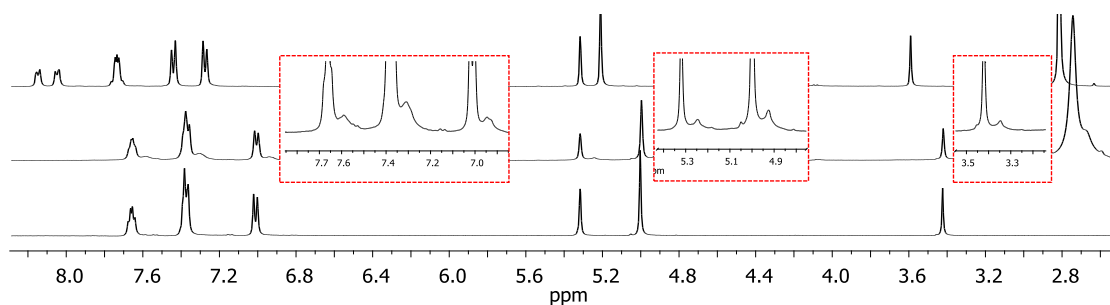
Figure S1

Direct comparison of the ^{1}H-NMR spectra resulting from this experiment with the one obtained using and excess of AgBF$_4$ evidence that all the ligand protons display larger downfield shifts in the gold adduct than in silver adduct (Figure S2).
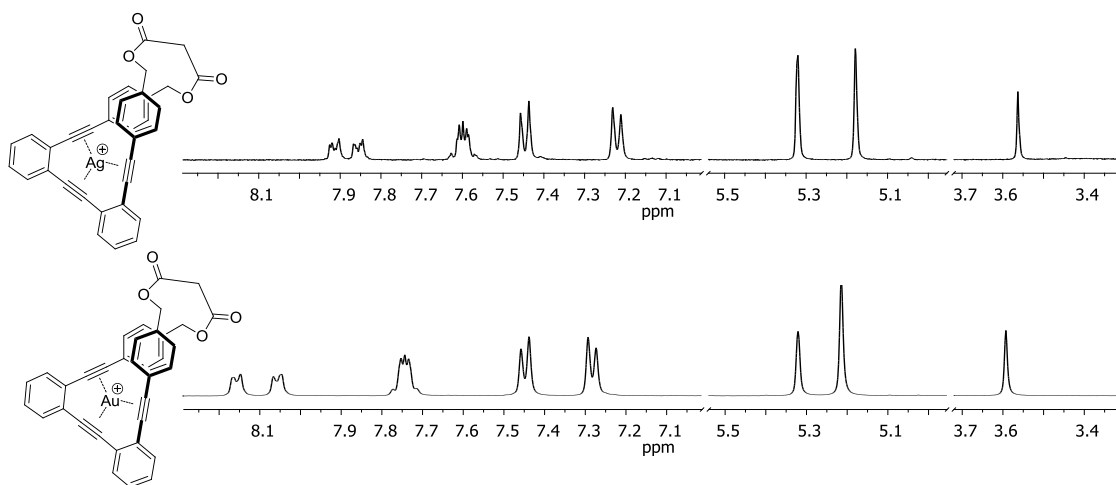
Figure S1

In order to check if we could measure the binding constant of such gold complex, several experiments were performed adding small aliquots of AgBF$_4$ (from a stock solution of the salt prepared in CD$_2$Cl$_2$/Acetone (v/v, 9:1)) to a solution 1:1 of the ligand and the AuCl(SMe$_2$) in CDCl$_3$ (10^{-3}M) but in all the cases (some experimental variations were also tested witout further success), mixtures of both complexes (Figure S2) or only the silver complex were detected.
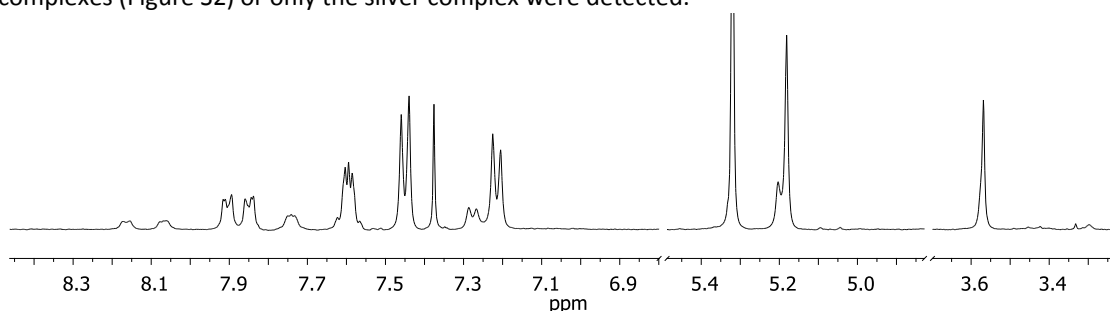
Figure S1

All the troubles faced in this binding experiments could be related with the termal unestability of the Au(I)-alkyne complexes or direct formation of an stable complex.[318] Additional efforts to obtain a crystal structure of the Au(I) complex with the model macrocycle **30a** and other non-stapled ligands are underway in Prof. Echavarren laboratory (Institute of Chemical Research of Catalonia (ICIQ), Tarragona, Spain).

---

[318] R. E. M. Brooner, T. J. Brown, R. A. Widenhoefer, Chem. Eur, J. *Chem. Eur. J.* **2013**, *19*, 8276-8284.

CHAPTER 3. Ti/Pd-mediated free radical conjugated additions

3.1. Introduction

3.1.1. Ti(III)-chemistry

The first organic radical identified was the triphenylmethyl (trityl, Tr) radical discovered by Moses Gomberg in the beginning of the twenty century.[319] During his efforts to prepare the sterically congested hydrocarbon hexaphenylethane, Gomberg attempted the Wurtz coupling of triphenylmethyl chloride (Scheme 34). Seeking to this work, he correctly identified the trityl radical giving, unwittingly, birth to a new fruitful research field.[320]
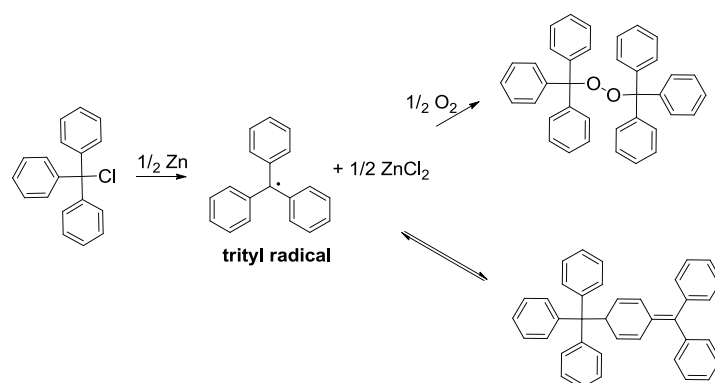
Scheme 37. *Wurtz coupling attempted by Gomberg in which he correctly identified the first radical.*

Radicals play an important role in combustion, polymer chemistry, living organisms and many other chemical processes. In this context, the rapid growth in radical chemistry development is highlighted by the large number of publications dealing with new methods of generation of the radicals as well as their compatibility with various functional groups and reaction conditions.[321] Although the generation of radicals can be directly promoted by light (with an organic initiator) or mediated by transition metals through an oxidative or a reductive process, one reason for the rapid development of this field was the introduction of samarium diiodide as electron-transfer reagent to organic synthesis by Kagan and Namy in 1980.[322]

Tributyltin hydride (Bu₃SnH)[323] and samarium iodide (SmI₂),[324] known as "Kagan's reagent", are probably the most popular reagents to conduct free-radical reactions under reductive conditions closely followed by the bis(cyclopentadienyl)titanocene(III) chloride or [Cp₂TiCl].[325]

This reagent was firstly characterized by Green[326] in 1972 and it can be generated in situ by stirring commercially available bis(cyclopentadienyl)titanium(IV) dichloride (Cp₂TiCl₂) with a reducing agent including metals such as Na, Al, Zn, Mn or Mg.[327] [Cp₂TiCl] crystallizes as trinuclear species together with

[319] M. Gomberg, *J. Am. Chem. Soc.*, **1900**, *22*, 752–757.

[320] C. S. Schoepple, W. E. Bachmann, *J. Am. Chem. Soc.*, **1947**, *12*, 2921–2925.

[321] T. V. RajanBabu, *Acc. Chem. Res.* **1991**, 24, 139-145.

[322] (a) P. Girard, J.-L. Namy, H.B. Kagan, *J. Am. Chem. Soc.* **1980**, *102*, 2693. (b) J.-L. Namy, P. Girard, H.B. Kagan, *New J. Chem*. **1977**, *1*, 5.

[323] J. Iqbal, B. Bhatia, N. K. Nayyar, *Chem. Rev.*, **1994**, *94*, 519–564.

[324] (a) K. C. Nicolaou, S. P. Ellery, J. S. Chen, *Angew. Chem. Int. Ed.* **2009,** *48*, 7140–7165; (b) A. Gansäuer, H. Bluhm, *Chem. Rev.* **2000**, *100*, 2771-2788; (c) G. A. Molander, C. R. Harris, *Chem. Rev.* **1996**, *96*, 307-338.

[325] T. V. RajanBabu, *Acc. Chem. Res.* **1991**, 24, 139-145.

[326] M. L. H. Green, C. R. J. Lucas, *J. Chem. Soc., Dalton Trans*. **1972**, 1000-1003.

[327] (a) R. S. P. Coutts, P. C. Wailes, R. L. Martin, *J. Organomet. Chem.* **1973**, *47*, 375-382; (b) D. J. Sekutowski, G. D. Stucky, *Inorg. Chem*. **1975**, *14*, 2192-2199; (c) R. S. P. Coutts, P. C. Wailes, R. L. Martin, *J. Organomet. Chem.* **1973**, *47*, 375-382; (d) D. W. Stephan, *Organometallics* **1992**, *11*, 996-999.

the salt of the reducing agent (Scheme 38),[328] nevertheless it is generally accepted that in THF solutions [Cp$_2$TiCl] complex is involved in an equilibrium between a monomeric and dimeric form.[329]
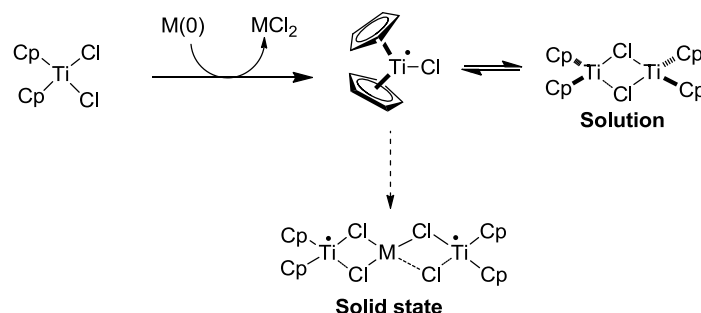
Scheme 38. *Formation of the [Cp$_2$TiCl] species by SET from a reducing metal. Bi- and trinuclear species formed by the radical complex.*

The broad success of [Cp$_2$TiCl] in radical reactions is due to the combination of the following features: 1) [Cp$_2$TiCl] is a single-electron-transfer,[330] 2) a soft Lewis acid and 3) it is highly oxophylic. According to these properties, [Cp$_2$TiCl] plays a multiple role: 1) it activates oxygenated groups by coordination,[331] 2) generates radicals from activated substrates and 3) enforces the reductive termination of radical processes by trapping the final radical and giving rise to a organometallic-Ti(IV) species.[332] The use of a second Lewis acid to compete with the system Cp$_2$TiCl$_2$/M(0) has permitted the development of the catalytic versions of titanoce(III)-mediated processes reintroducing the Ti(IV) into the catalytic cycle and making the process irreversible.[333] Some chiral titanium(IV) catalysts have also been described allowing the development of asymmetric titanocene(III)-mediated reactions (Figure 145).[334]

[328] D. W. Stephan, *Organometallics* **1992**, *11*, 996-999.

[329] R. J. Enemærke, J. Larsen, T. Skrydstrup, K. Daasbjerg, *J. Am. Chem. Soc.* **2004**, *126*, 7853 − 7864.

[330] R. J. Enemærke, J. Larsen, T. Skrydstrup, K. Daasbjerg, J. Am. Chem. Soc. 2004, 126, 7853 − 7864.

[331] A. Fernández- Mateos, P. Herrero Teijón, L. Mateos Burón, R. Rabanedo Clemente, R. Rubio González, *J. Org. Chem.* **2007**, *72*, 9973 − 9982.

[332] (a) M. T. Reetz, R. Steinbach, J. Westerman, R. Peter, *Angew. Chem. Int. Ed. Engl.* **1980**, *19*, 1011-1012; (b) M. T. Reetz, *Top. Curr. Chem.* **1982**, *106*, 1-54.

[333] (a) A. Gansäuer, H. Bluhm, M. Pierobon, *J. Am. Chem. Soc.* **1998**, *120*, 12849–12859; (b) A. F. Barrero, A. Rosales, J. M. Cuerva, J. E. Oltra, *Org. Lett.* **2003**, *5*, 1935–1938; (c) S. Fuse, M. Hanochi, T. Doi, T. Takahashi, *Tetrahedron Lett.* **2004**, *45*, 1961–1964.

[334] (a) A. Hafner, R. O. Duthaler, R. Marti, G. Rihs, P. Rothe-Streit, F. Schwarzenbach, *J. Am. Chem. Soc.* **1992**, *114*, 2321-2336; (b) A. Bensari, J.-L. Renaud, O. Riant, *Org. Lett.* **2001**, *3*, 3863-3865; (c) Z. Chen, R. L. Halterman, *J. Am. Chem. Soc.* **1992**, *114*, 2276-2277; (d) E. Cesarotti, H. B. Kagan, R. Goddard, C. Krüger, *J. Organomet. Chem.* **1978**, *162*, 297-309; (e) F. R. W. P. Wild, L. Zsolnai, G. Huttner, H. H. Brintzinger, *J. Organomet. Chem.* **1982**, *232*, 233-247.
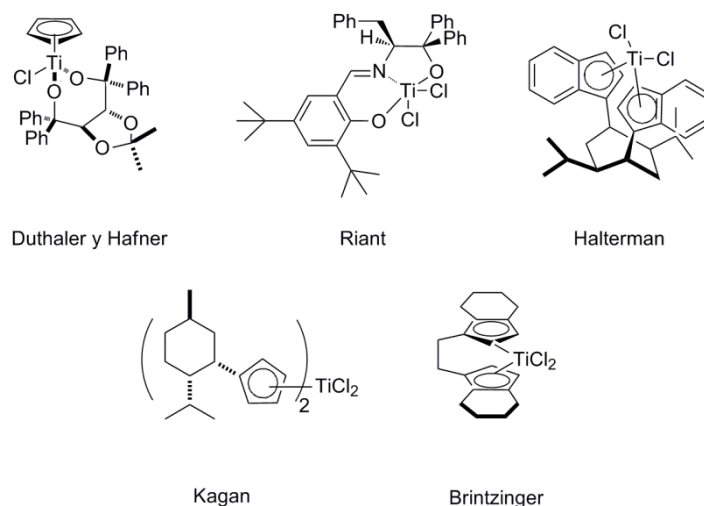
Figure 145. *Some chiral titanium(IV) catalysts.*

3.1.1.1. Epoxides

For the last twenty years, [Cp$_2$TiCl] has proven to be a useful single-electron-transfer (SET) reagent able to promote and to catalyze the homolytic ring opening of epoxides (Scheme 36).[335] This process was firstly described by Rajanbabu and Nugent in the earlies 90´s[336] and it is analogous to the formation of a homoallyl radical from a cyclopropylmethyl radical (Scheme 36) but generating a β-titanoxy radical.
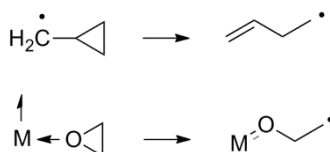
Scheme 39. *Homoallyl radical formation from a cyclopropenyl radical (top). β-Titanoxy radical formation from an epoxyde and a SET reagent (bottom).*

The β-titanoxy radical can be subsequently trapped by a second [Cp$_2$TiCl] species to yield a bimetallic intermediate which eventually evolves to an alkene giving the corresponding deoxygenation product from the original epoxide (Scheme 40, path A).[337] In the presence of a hydrogen-atom donor, the radical is reduced to an alcohol with the opposite regiochemistry to that expected from the reduction with nucleophilmetal hydrides (Scheme 40, path B).[338] New C-C bonds are formed if a β-titanoxy radical undergo inter- and intramolecular radical additions to alkenes (or alkynes). For example, in the presence of an activated olefin such as an acrylate, δ-hydroxycarbonyl molecules are synthesized (Scheme 40, path C).[339]

---

[335] T. V. RajanBabu, W. A. Nugent, *J. Am. Chem. Soc.* **1994**, *116*, 986 –997.

[336] (a) W. A. Nugent, T. V. Rajanbabu, *J. Am. Chem. Soc.* **1988**, *110*, 8591-8562; (b) T. V. Rajanbabu, W. A. Nugent, *J. Am. Chem. Soc.* **1989**, *111*, 4525-4527; (c) T. V. Rajanbabu, W. A. Nugent, M. S. Beattie, *J. Am. Chem. Soc.* **1990**, *112*, 6408-6409; (d) T. V. Rajanbabu, W. A. Nugent, *J. Am. Chem. Soc.* **1994**, *116*, 986-997.

[337] (a) W. A. Nugent, T. V. Rajanbabu, *J. Am. Chem. Soc.* **1988**, *110*, 8591-8562; (b) T. V. Rajanbabu, W. A. Nugent, *J. Am. Chem. Soc.* **1989**, *111*, 4525-4527; (c) T. V. Rajanbabu, W. A. Nugent, M. S. Beattie, *J. Am. Chem. Soc.* **1990**, *112*, 6408-6409; (d) T. V. Rajanbabu, W. A. Nugent, *J. Am. Chem. Soc.* **1994**, *116*, 986-997.

[338] T. V. RajanBabu, W. A. Nugent, J. Am. Chem. Soc. 1994, 116, 986 – 997.

[339] T. V. Rajanbabu, W. A. Nugent, *J. Am. Chem. Soc.* **1989**, *111*, 4525-4527.
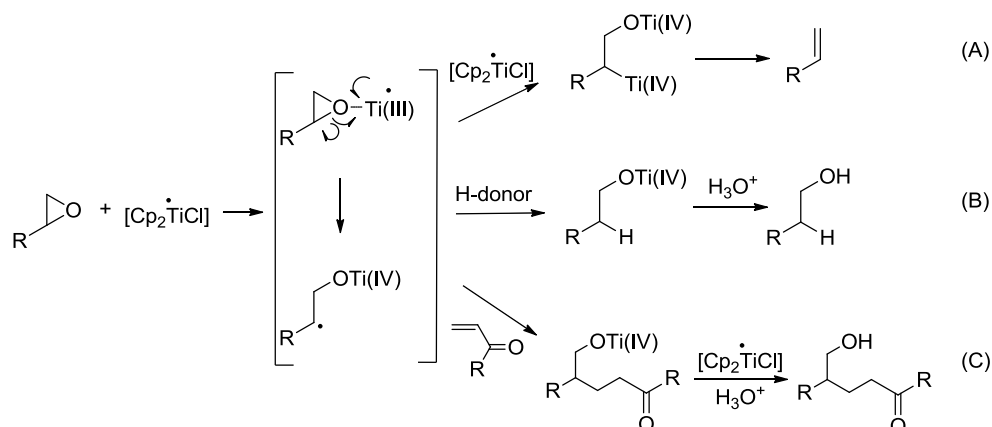
Scheme 40. β-*Titanoxy radical evolution to dehydrogenation products (A), reduction products (B) and addition products (C).*

In addition to deoxygenation, reduction and addition to olefins, titanocene(III) has also been used to promote intramolecular additions of epoxides to carbonyl and nitrile groups by Fernández-Mateos *et al.* (Scheme 41).[340]
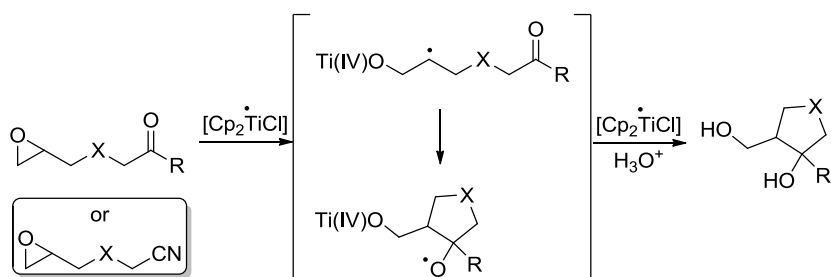
Scheme 41. *Intramolecular additions of epoxides to carbonyl and nitrile groups.*

A conceptually novel approach to radical aromatic substitutions by employing oxidative additions and reductive eliminations in single electron steps has recently been reported by Gansäuer *et al.* (Scheme 42).[341]

---

[340] (a) A. Fernández-Mateos, E. Martín de la Nava, G. Pascual Coca, A. Ramos Silvo, R. Rubio González, *Org. Lett.* **1999**, *1*, 607-609; (b) A. Fernández-Mateos, P. Herrero Teijón, L. Mateos Burón, R. Rabanedo Clemente, R. González Rubio, *J. Org. Chem.* **2007**, *72*, 9973-9982.

[341] A. Gansäuer, M. Behlendorf, D. v. Laufenberg, A. Fleckhaus, C. Kube, D. V. Sadasivam, R. A. Flowers II, *Angew. Chem. Int. Ed.* **2012**, *51*, 4739-4742.
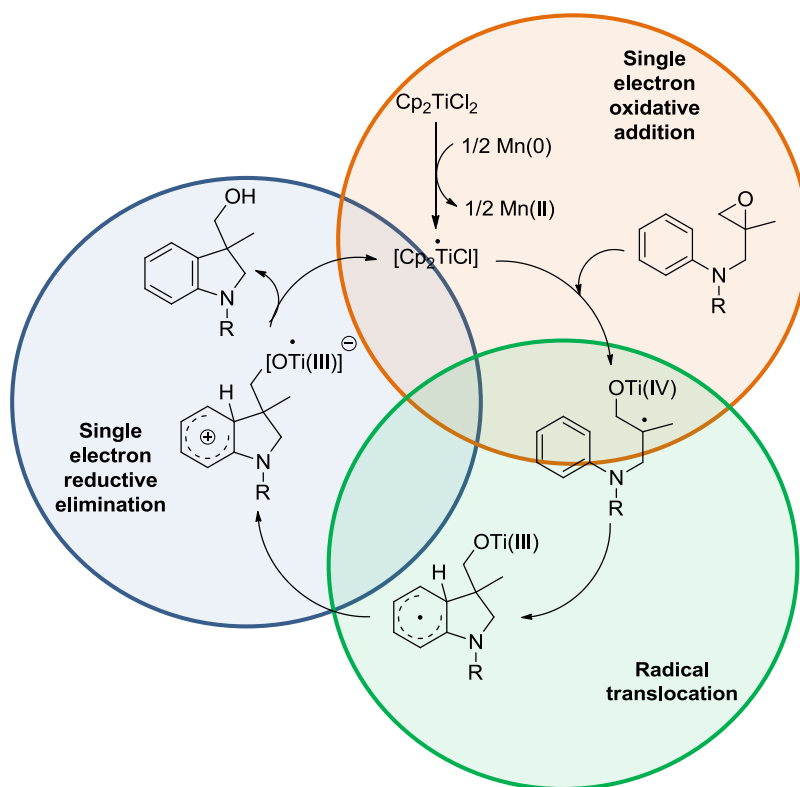
Scheme 42. *Gansäuer et al. mechanistic proporsal for radical aromatic substitutions.*

Since the product of radical addition to an alkene (or alkyne) is itself a radical capable of undergoing further transformations, radical reactions are commonly used to create reaction cascades in which the complexity of the product is much greater than that of the starting materials. These cascade reactions are very useful in total synthesis (Scheme 43).[342]
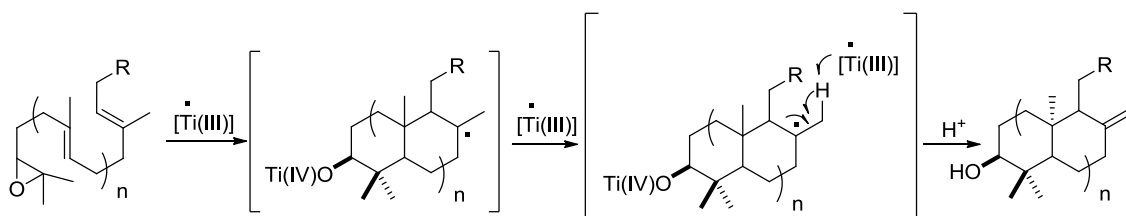
Scheme 43. *Cascade radical cyclization.*

3.1.1.2. Halides

Activated halides are reactive substrates for [Cp₂TiCl] too. Allyl, propargyl and benzyl halides can give Wurtz homocoupling reactions and Barbier-type additions to carbonyl groups. α-Haloketones are also able to undergo Reformatsky-type reactions. In 1990, Yanlong *et al.* reported Wurtz dimerisation of allyl bromides using titanocene(III) (Scheme 44).[343] This reactivity has been further developed by Barrero *et al.*
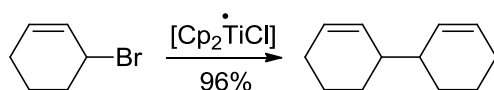
Scheme 44. *Wurtz dimerisation of allyl bromides.*

[342] J. Justicia, L. Álvarez de Cienfuegos, A. G. Campaña, D. Miguel, V. Jakoby, A. Gansäuer, J. M. Cuerva, *Chem. Soc. Rev.* **2011**, *40*, 3525-3537.

[343] Q. Yanlong, L. Guisheng, Y. Huang, *J. Organomet. Chem.* **1990**, *381*, 29-34.

Sato[344] and Teuben[345] groups proved that allyl-titanocene complexes are wonderful allylation reagents (Scheme 45). Enantioselective allylation did not take long to come out from the hand of Collins,[346] Hafner[347] and Duthaler[348] using chiral (η^3-allyl)titanocene(III) complexes (Figure 145).
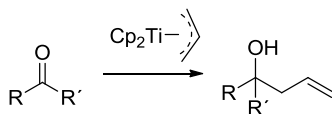
Scheme 45. *Allyl titanocene addition to a carbonyl group.*

However, a major drawback of the enantioselective allylation is the use of stochiometric amounts of titanium complexes. In this context, a catalytic protocol for this allylation using 2,4,6-collidine and Me$_3$SiCl as regenerating agents was developed in our group.[349] Chiral titanium catalysts were also tested but low inductions were observed (Scheme 46).
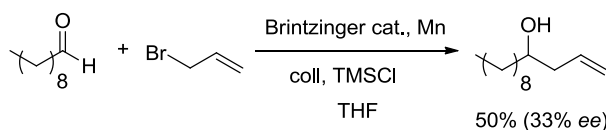
Scheme 46. *Asymmetric aalylation using Britzinger catalyst.*

Analogously, propargylation and α-halo-carbonyl[350] addition to aldehydes and ketones have also been developed (Scheme 47).[351]
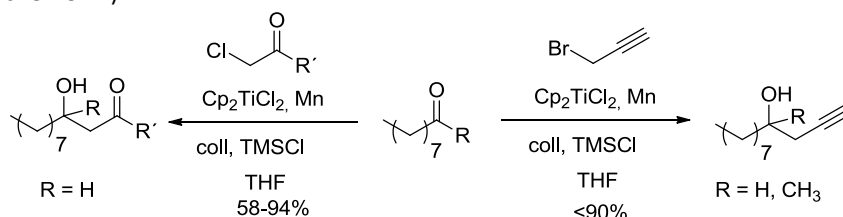
Scheme 47. *Propargylation (right) and crotylation (left) reactions of carbonyl groups catalyzed by Ti(III).*

3.1.1.3. Carbonyl groups

Titanocene(III) complexes can promote the pinacol coupling of conjugated and aromatic aldehydes in good yields and diastereoselectivities (Scheme 45).[352] The high sin-diastereoselectivity has been attributed to the formation of trinuclear or dimeric intermediates in which the ketyl radicals are orientated in opposite sides in order to minimize steric repulsion (Scheme 48, right). The catalytic version of this pinacol coupling methodology was published shortly after Barden and Schwarz communication.[353] Aliphatic aldehydes are also good substrates for this reaction but they lead to lower

---

[344] F. Sato, S. Iijima, M. Sato, *Tetrahedron Lett*. **1981**, *22*, 243-246.

[345] E. Klei, J. H. Teuben, H. J. De Liefde Meijer, *J. Organomet. Chem*. **1982**, 327-339.

[346] S. Collins, B. A. Kuntz, Y. Hong, *J. Org. Chem*. **1989**, *54*, 4154-4158.

[347] A. Hafner, R. O. Duthaler, R. Marti, G. Rihs, P. Rothe-Streit, F. Schwarzenbach, *J. Am. Chem. Soc.* **1992**, *114*, 2321-2336

[348] M. Riediker, R. O. Duthaler, *Angew. Chem. Int. Ed. Engl.* **1989**, *28*, 494-495.

[349] A. Rosales, J. L. Oller-López, J. Justicia, A. Gansäuer, J. E. Oltra, J. M. Cuerva, *Chem. Commun*. **2004**, *22*, 2628-2629.

[350] J. D. Parrish, D. R. Shelton, R. D. Little, *Org. Lett.* **2003**, *5*, 3615-3617.

[351] See appendix.

[352] (a) Y. Handa, J. Inanaga, *Tetrahedron Lett.* **1987**, *28*, 5717 – 5718; (b) M. C. Barden, J. Schwartz, *J. Am. Chem. Soc.* **1996**, *118*, 5484-5485.

[353] A. Gansäuer, *J. Chem. Soc., Chem. Commun.* **1997**, 457-458.

conversions and diastereoselectivities.[354] Using titanium-Brintzinger catalyst, Dunlap and Nicholas obtained moderate enantioselectivities for aromatic aldehydes.[355]
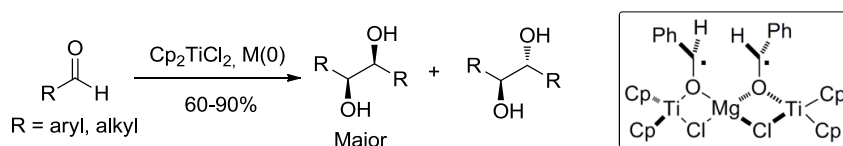
Scheme 48. *Pinacol coupling catalyzed by Ti(III) (right). Proposed intermediate responsible of the diastereoselectivity (left).*

We have recently reported that using Cp_2TiCl_2/Mn(0) mixtures, aromatic ketones can also undergo pinacol coupling in excellent stereoselectivities.[356] If methanol is added, instead of pinacolization the selective reduction of the α,β-unsaturated bond is observed (Scheme 49).[357] On the other hand, when water is used as an additive[358] or as solvent,[359] ketones are reduced to the corresponding alcohols (Scheme 50).
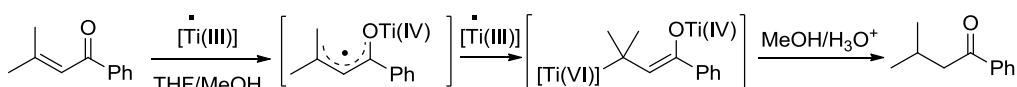
Scheme 49. *Selective reduction of the α,β-unsaturated bonds vs pinacolization in the presence of methanol.*
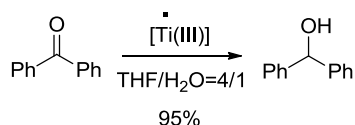
Scheme 50. *Reduction of aromatic ketones to alcohols catalyzed by Ti(III) using water at H donor.*

Aldehydes and conjugated alkenals undergo a stereoselective Michael-type coupling to form γ-lactols in the presence of stoichiometric amounts of [Cp$_2$TiCl].[360] Mechanistic hypothesis is outline below (Scheme 51).
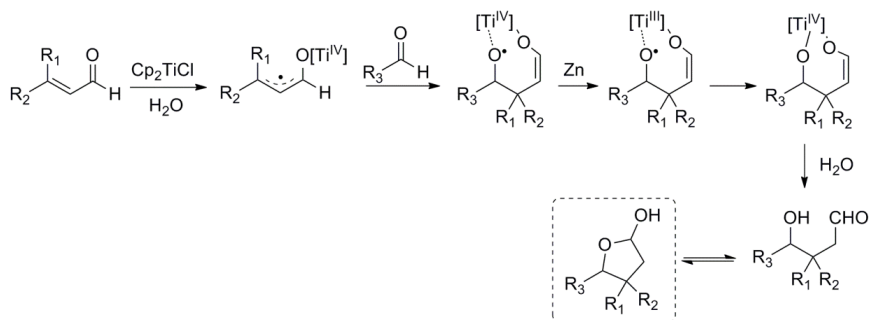
Scheme 51. *Mechanistic hypothesis of the stereoselective Michael-type coupling of aldehydes.*

3.1.1.4. Water

[354] T. Hirao, B. Hatano, M. Ashara, Y. Muguruma, A. Ogawa, *Tetrahedron Lett.* **1998**, *39*, 5247-5248.

[355] (a) M. S. Dunlap, K. M. Nicholas, *Synth. Commun*. **1999**, *29*, 1097-1106; (b) M. S. Dunlap, K. M. Nicholas, *J. Organomet. Chem.* **2001**, *630*, 125-131.

[356] M. Paradas, A. G. Campaña, R. E. Estévez, L. Álvarez de Cienfuegos, T. Jiménez, R. Robles, J. M. Cuerva, J. E. Oltra, *J. Org. Chem.* **2009**, *74*, 3616-3619.

[357] L. Moisan, C. Hardouin, B. Rousseau, E. Doris, *Tetrahedron Lett.* **2002**, *43*, 2013-2015.

[358] A. F. Barrero, A. Rosales, J. M. Cuerva, A. Gansäuer, J. E. Oltra, *Tetrahedron Lett.* **2003**, *44*, 1079-1082.

[359] J. L. Oller-López, A. G. Campaña, J. M. Cuerva, J. E. Oltra, *Synthesis* **2005**, 2619-2622.

[360] R. E. Estévez, J. L. Oller-López, R. Robles, C. R. Melgarejo, A. Gansäuer, J. M. Cuerva, J. E. Oltra, *Org. Lett.* **2006**, *8*, 5433-5436.

Although reduction of radicals is a widely known phenomenon, water was thought to be inert to free radicals.[361] This hypothetical passivity has been attributed to the high H-OH bond-dissociation energy (E=117.59±0.07 kcal mol^{-1}). However, tertiary radicals formed after polyprene cyclization are effectively reduced in the presence of [Cp$_2$TiCl] and water or eliminated to alkene in absence of it (Scheme 52).[362] Between 2001 and 2006, a lot of effort to screen the [Cp$_2$TiCl]-promoted hydrogen-atom transfer (HAT) from water to primary, secondary and tertiary carbon radical was made in our lab.
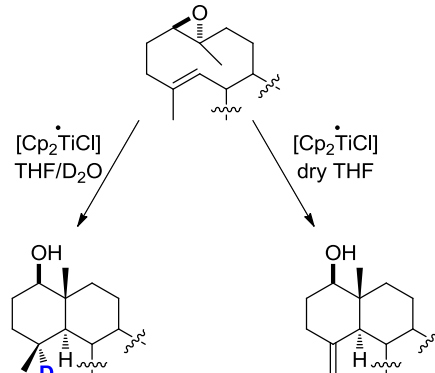
Scheme 52. *Either the reduction or the elimination product can be obtained in the same Ti(II)-mediated radical cyclization depending on the presence or absence of water.*

Theoretical calculations revealed that when [Cp$_2$TiCl] coordinates water, H-OH bond-dissociation energy decrease to 49.4 kcal mol^{-1} (Figure 146, left)[363] Thus, the aquo-complex acts as a hydrogen-atom transfer (Figure 146, right). Despite based on a different mechanism, Wood *et al.* have also described the HAT ability of water in trialkylborane mediated reactions.[364] In 2010, we put some more light into this hydrogen transference studying thoroughly the influence of some additives (alcohols, phenols, amines…).[365] Subsequent works have tried to elucidate the aquo-complex structure using electronic paramagnetic resonance (EPR) and cyclic voltametry (CV) together with theoretical calculations.[366]

$$\Delta(E+ZPE) = 49.4 \text{ kcal mol}^{-1}$$
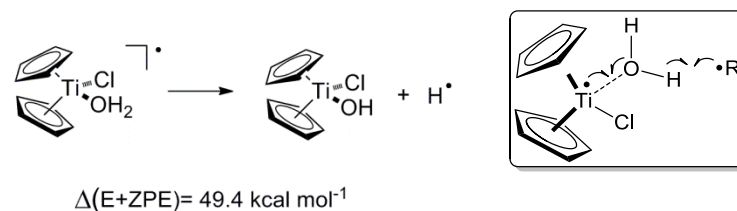
Figure 146. *Calculated H-OH bond-dissociation energy of the Ti(III) aquocomplex.*

3.1.2. Intramolecular Michael-type conjugated additions

[361] *Stereochemistry of Radicals Reactions*, Eds.: D. P. Curran, N. A. Porter, B. Giese, VCH, Weinheim, **1996.**

[362] (a) A. F. Barrero, J. M. Cuerva, M. M. Herrador, M. Valdivia, *J. Org. Chem*. **2001**, *66*, 4074-4078; (b) A. F. Barrero, J. E. Oltra, J. M. Cuerva, A. Rosales, *J. Org. Chem*. **2002**, *67*, 2566-2571; (c) J. Justicia, A. Rosales, E. Buñuel, J. L. Oller-López, M. Valdivia, A. Haïdour, J. E. Oltra, A. F. Barrero, D. J. Cárdenas, J. M. Cuerva, *Chem. Eur. J.* **2004**, *10*, 1778-1788.

[363] J. M. Cuerva, A. G. Campaña, J. Justicia, A. Rosales, J. L. Oller-López, R. Robles, D. J. Cárdenas, E. Buñuel, J. E. Oltra, *Angew. Chem. Int. Ed.* **2006**, *45*, 5522-5526.

[364] (a) D. A. Spiegel, K. B. Wiberg, L. N. Schacherer, M. R. Medeiros, J. L. Wood, *J. Am. Chem. Soc.* **2005**, *127*, 12513-12515; (b) M. R. Medeiros, L. N. Schacherer, D. A. Spiegel, J. L. Wood, *Org. Lett*. **2007**, *9*, 4427-4429.

[365] M. Paradas, A. G. Campaña, T. Jiménez, R. Robles, J. E. Oltra, E. Buñuel, J. Justicia, D. J. Cárdenas, J. M. Cuerva, *J. Am. Chem. Soc.* **2010**, *132*, 12748-12756.

[366] A. Gansäuer, M Behlendorf, A. Cangönül, C. Kube, J. M. Cuerva, J. Friedrich, M. v. Gastel, *Angew. Chem. Int. Ed*. *Engl.* **2012**, *51*, 3266-3270.

Formation of carbon–carbon bonds by intramolecular additions of carbon radicals into alkenes are important reactions in organic synthesis (Figure 147, left).
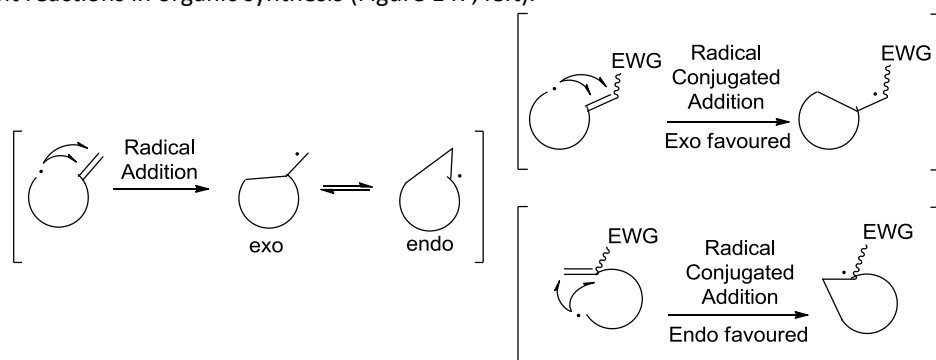
Figure 147. *General schematic representation of an intramolecular radical addition (left) and regioselective radical conjugated addition (right).*

In general, electron donating groups on the radical and electron withdrawing groups (EWG) on the alkene accelerate the cyclization usually referred as Michael-type free radical conjugate addition (Figure 147, right). Frontier molecular orbital (FMO) theory offers a good explanation of the substituent effects. The singularly occupied molecular orbital (SOMO) of the radical interacts with either the lowest unoccupied molecular orbital (LUMO) or the highest occupied molecular orbital (HOMO) of the alkene bond (Figure 148). The addition rate of nucleophilic radicals is increased because the location of an electron widthdrawing group (EWG) at the alkene lowers the LUMO energy, reduces the SOMO–LUMO gap, and also stabilizes the cyclized radical.
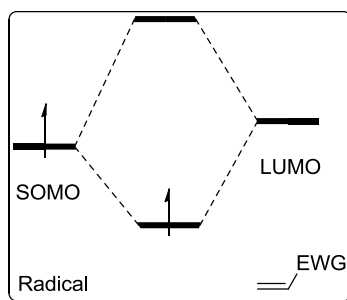
Figure 148. *FMO interaction of a nucleophilic radical with an electron-poor alkene.*

Free radical conjugate additions were first explored in intermolecular fashion in the early 80s by pioneers like Bachi, Danishefsky, Stork, Beckwith, Hanessian, *inter alia*.[367] In every radical cyclization to an alkene, there are two competing pathways. *Endo* cyclization occurs when the radical attacks the terminal end of the multiple bond to form a larger ring, or *exo* cyclization occurs when it attacks the internal end to form a smaller ring. Radical cyclizations are usually regioselective and favor *exo* cyclizations. In the series of intramolecular free radical Michael additions, the position of EWG attached to the radical acceptor has significant influence on the regioselectivity. The *exo* cyclization is enhanced if the EWG is at the terminus of the carbon–carbon double bond, whereas the *endo* cyclizationfor large ring closure is favorable if the EWG is at the inner position (Scheme 147, right).

The largest body of stereoselective radical reactions relates to 5-*exo* cyclizations of the substituted hexenyl radicals. For example, Hanessian and coworkers have demonstrated that cyclizations of α,β-unsaturated esters reduced the endo ring closure byproducts to an undetectable level as analyzed by ^{1}H-NMR spectroscopy (Scheme 53).[368]

[367] W. Zhang, *Tetrahedron* **2001**, 57, 7237-7267.
[368] S. Hanessian, D. S. Dhanoa, P. L. Beaulieu, *Can. J. Chem.* **1987**, *65*, 1859-1866.
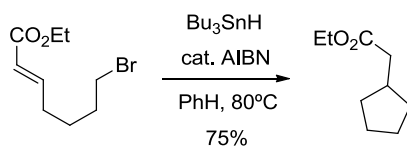
Scheme 53. *Hanessian et al. exo-regioselective radical cyclization.*

As predicted by the Beckwith–Houk model (Scheme 54), the R_1 substituent at the 1-position of hexenyl radicals affords *cis*-1,2-disubstituted cyclopentanes as the major diastereomer. Results from reactions promoted by mercury(II) acetate among others are consistent with the predictions (Scheme 55).
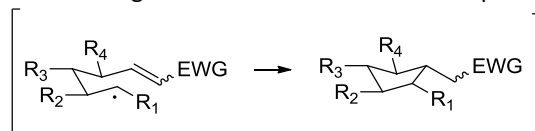
Scheme 54. *Chair-line transition state proposed by Beckwith-Houk model.*
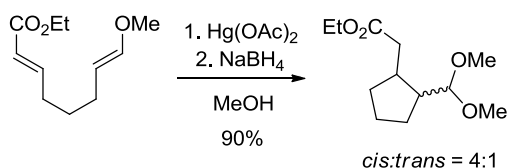
Scheme 55. *Preferred formation of the cis-cyclopentane consistent with the Beckwith rules prediction.*

Higher percentages of *trans*-1,2-disubstituted cyclopentanes have been observed by Enholm and Torii *et al.* suggesting that the bulky organometallic group is axially oriented at the chair-like transition state (Scheme 56).[369]
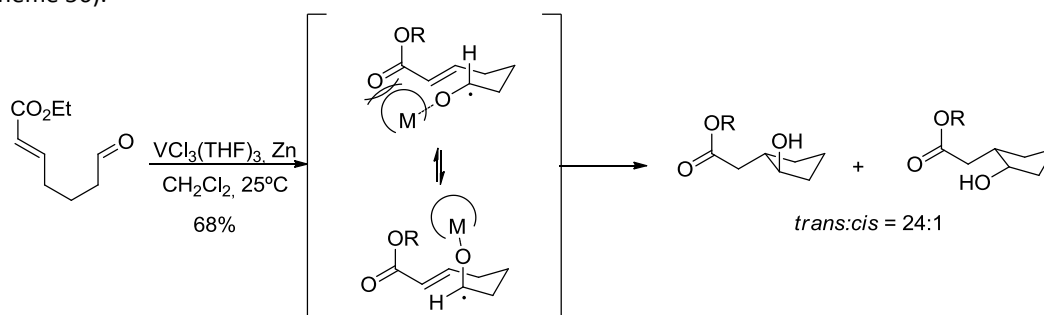
Scheme 56. *Preferred formation of the trans-cyclopentane observed By Enholm and Torii.*

Endo cyclizations are usually minor processes in the formation of standard and medium sized rings. But, as we mentioned before, appropriately assembled radical acceptors change the regioselectivity in favor of *endo* cyclization. This concept has been specially utilized in radical macrocyclizations (Scheme 57) in the groups of Porter,[370] Sonoda[371] and Phillipons.[372]

---

[369] (a) Enholm, E. J.; Kinter, K. S. J. Org. Chem. 1995, 60, 4850. (b) Inokuchi, T.; Kawafuchi, H.; Torii, S. J. Org. Chem.1991, 56, 4983.

[370] (a) Porter, N. A.; Magnin, D. R.; Wright, B. T. J. Am. Chem. Soc. 1986, 108, 2787; (b) Porter, N. A.; Chang, V. H.-T.; Magnin, D. R.; Wright, B. T. J. Am. Chem. Soc. 1988, 110, 3554; (c) Porter, N. A.; Chang, V. H.-T. J. Am. Chem. Soc. 1987, 109, 4976; (d) Porter, N. A.; Lacher, B.; Chang, V. H.-T.; Magnin, D. R. J. Am. Chem. Soc. 1989, 111, 8309.

[371] (a) Ryu, I.; Nagahara, K.; Yamazaki, H.; Tsunoi, S.; Sonoda, N. Synlett 1994, 643. (b) Nagahara, K.; Ryu, I.; Yamazaki, H.; Kambe, N.; Komatsu, M.; Sonoda, N.; Baba, A. Tetrahedron 1997, 53, 14615.

[372] (a) Beckwith, A. L. J.; Drok, K.; Maillard, B.; Degueil-Castaing, M.; Philippon, A. Chem. Commun. 1997, 499; (b) Philippon, A.; Tao, J.; Te´tard, D.; Degueil-Castaing, M.; Maillard, B. Synth. Commun. 1997, 27, 2651. (c) Philippon, A.; Degueil-Castaing, M.; Beckwith, A. L. J.; Maillard, B. J. Org. Chem. 1998, 63, 6814.

n = 10, 50-55%
n = 14, 47-56%
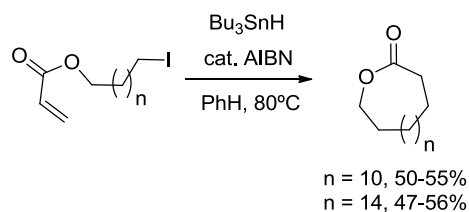
Scheme 57. Endo-radical macrocyclizations.

Unlike in radical reactions, the number of transition metal mediated cyclization procedures in which ring closure results from intramolecular conjugate addition of a nucleophile to a Michael acceptor is rare. The main reasons are competition from retrograde Michael reactions, secondary condensations and the presence of relatively acidic protons. To compensate these constraints, highly stabilized (less basic) nucleophiles have been employed such as phosphonium ylides,[373] the anion of dithiane,[374] and the enolates of β-ketoesteres,[375] adehydes,[376] ketones[377] and esters.[378]

For this reason, analogous cyclization using nonstabilized nucleophiles has received little attention, undoubtedly owing to difficulties associated with the specific generation of an unactivated anion in the presence of the highly reactive electrophilic alkene.[379] One of the few examples for intramolecular Michael-type additions was reported by Cooke.[380] In 1979, this group reported the first intramolecular Michael reaction initiated by an internally generated Grignard reagent (Scheme 58).

60%
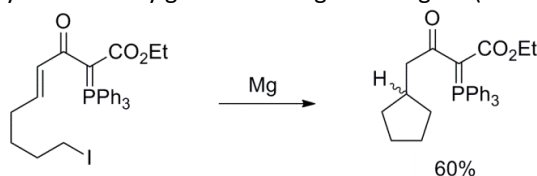
Scheme 58. Example of an intramolecular Michael reaction initiated by a Grignard reagent.

Shortly thereafter, Macdonald and Mahalingam[381] effected ring formation using a latent carbanionic organotin nucleophile and an activated cyclohexenone (Scheme 59).

68%
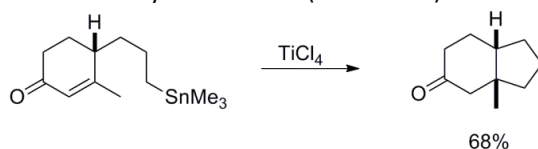
Scheme 59. Michael-type cyclization of a carbanionic organotin nucleophile.

Michael-type intramolecular allylations are less common owing to the difficulties to incorporate the nucleophilic subunit in the starting materials. To the best of our knowledgehe few examples that can be found have been reported by Majetic, Yoo, Patteneden, Werder and Schauss *et al*. In 1988, Majetic work pionerred this area using allylsilanes as allylic carbanion synthons (Scheme 60).[382]

[373] Cory, R. M.; Chan, D. M. *Tetrahedron Lett.* **1975, 4441.**

[374] G rotjahn, D. B.; Andenen, N. H., *J . Chem. SOC.C, hem. Commun.* **1981, 306.**

[375] (a) Stork, **G.;** Taber, D. F.; Marx, M., *Tetrahedron Lett.* **1978,2445.** (b) Stork, G.; Rosen, P.; Goldman, N.; Coombs, R. V.; Tsuji, J. J. **Am. Chem. SOC. 1965,87, 275.** (c) Stork, G.; Winkler, J. D.; Saccomano, N. A. *Tetrahedron Lett.* **1983,24,4934.** (d) Stork, **G.;** Boeckman, R. K., Jr.; Taber, D. F.; Still, W. C.; Sigh, J. J. **Am. Chem. SOC. 1979,101,7107.**

[376] Stork, **G.;** Shiner, C. S.; Winkler, J. D. *J. Am. Chem. SOC.* **1982, 104, 310.**

[377] T rost, B. M.; Shuey, C. D.; DiNimmo, F. J. **Am. Chem. SOC1.9 79,101, 1284.**

[378] Lee, **R. A.** *Tetrahedron Lett.* **1973, 3333.**

[379] G. Majetich, R. W. Desmond, J. J. Soria, *J. Org. Chem.* **1986**, *51*, 1753-1769.

[380] (a) M. P. Cooke, *Tetrahedron Lett.* **1979**, *20*, 2199-2202; (b) M. P. Cooke, *J. Org. Chem.* **1984**, *49*, 1144-1146.

[381] T. L. Macdonald, S. Mahalingam, *J. Am. Chem. Soc.* **1980**, *102*, 2113-2115.

[382] G. Majetich, R. W. Desmond, J. J. Soria, *J. Org. Chem.* **1986**, *51*, 1753-1769.
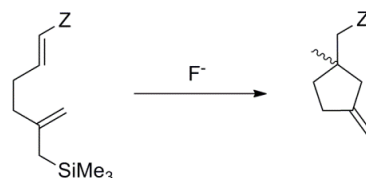
Scheme 60. *Michael-type cyclization of allylsilanes.*

Wender and White studies on organobis(cuprates) provided an efftient access to [4.4], [4.5] and [5.5] spirocompounds in a single step (Scheme 61).[383]

X =Cl, Br, I
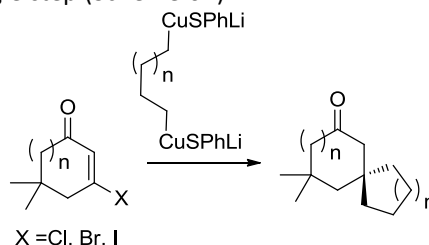
Scheme 61. *Michael-type cyclization of organobis(cuprates).*

A year later, Pattenden *et al.* used a modification of the traditional radical macrocyclization method (Scheme 55) for the synthesis of mukulol and related marine cembranolide lactones (Scheme 62).

E:Z = 3:1
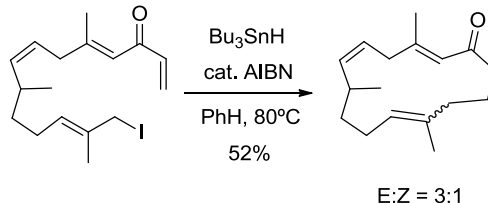
Scheme 62. *Key step for the total synthesis of Mukulol and related Cembranolid lactones.*

Yoo and Fukumoto took advantage of this Bu_3SnH/AIBN catalized Michael-type intramolecular addition as a key intermediate for the total synthesis of meroquinene (Scheme 63).[384]

E = COOEt
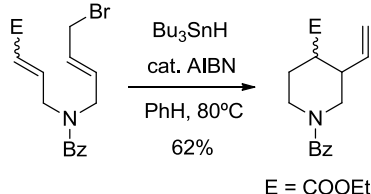
Scheme 63. *Michael-type intramolecular radical allylation.*

More recently, Schaus used an intramolecular version of the Hosori-Sakauri reaction[385] to synthesize the clerodane decaline core of asmarine A and related diterpenes (Scheme 64).[386]

88%
93% *ee*
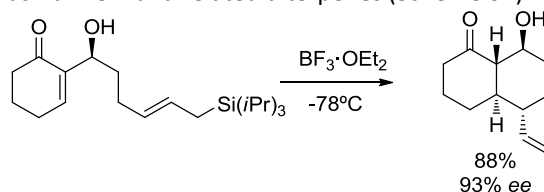
Scheme 64. *Michael-type intramolecular radical allylation using allylsylanes for the synthesis of a clerodane decaline core.*

---

[383] P. A. Wender, A. W. White, J. Am. Chem. Soc. 1988, 110, 2218-2223.

[384] (a) S.-E. Yoo, K. Y. Yi, S.-H. Lee, N. Jeong, *Synlett* **1990**, 575; (b) M. Ihara, F. Setsu, Shohda, N. Taniguchi, Y. Tokunaga, K. Fukumoto, *J. Org. Chem.* **1994**, *59*, 5317.

[385] The Hosomi Sakurai Reaction involves the Lewis acid-promoted allylation of various electrophiles with allyltrimethysilane. Activation by Lewis acids is critical for an efficient allylation to take place.

[386] S. A. Rodgen, S. Schaus, Angew. Chem. Int. Ed. 2006, 45, 4929-4932.

Taking into account the simplicity and the potential usefulness of our radical/transition metal combined protocols, we planned to extent our multimetallic methodology to the synthesis of carbo- and heterocycles based on a Michael-type reaction using allylic carbonates and carboxilates as pronucleophiles.

Our working hypothesis is shown in Scheme 65. An initial oxidative addition step of the starting allylic electrophile **S** to M^0 would yield to the corresponding (η^3-allyl)metal(II) complex **S1**. Monoelectronic reduction of that complex could form a (η^3-allyl)metal(I) intermediate **S2**, which would fragment to the corresponding carbon-centered allyl radical **S3** and a M(0) complex. A subsequent intramolecular free-radical conjugated addition assisted by the coordination of [Cp$_2$TiCl] to the Michael acceptor would end up in the titanocene(IV) intermediate **S4**. Final quenching under acidic conditions would give the cyclic product **P**.

Z = electron withdrawing group
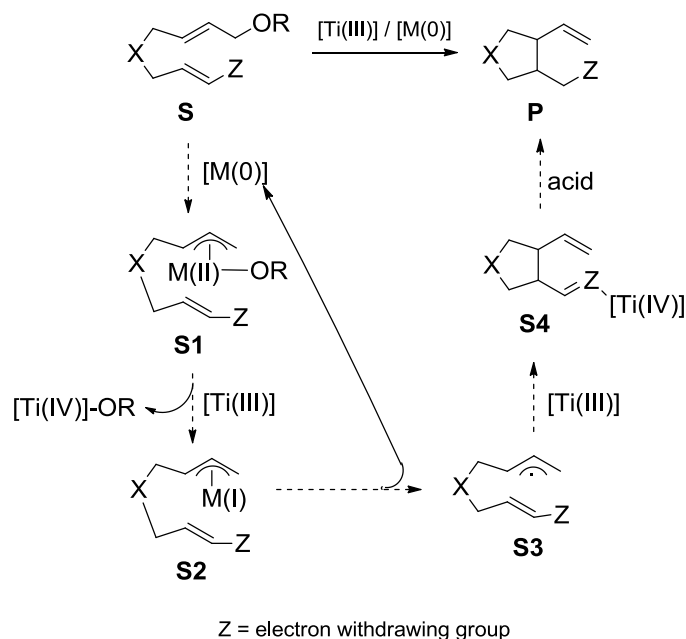
Scheme 65. *Working hypothesis of the Ti/Pd-mediated Michael-type conjugated additions.*

---

[387] This chapter has been developed in collaboration with Dr. Millán and Dr. Miguel.

3.3. Background: Multicomponent redox systems

The use of more than one metal catalyst to mediate organic transformations offers a very interesting potential. Different catalytic properties of metal complexes can be synergistically coupled to induce processes that are otherwise difficult to catalyze with high regio-, chemo-, and stereoselectivity. When one thinks about reactions mediated by two metals, cross-coupling reactions come probably to mind. However, other less popular transformations take advantage of mixed methodologies too.

Free-radical chemistry has several appealing characteristics to synthetic chemists. Reactions are usually clean and fast, high tolerant to functional groups and they proceed under mild conditions.[388] Despite of all these favourable distinctions, free radical reactions present a major limitation: radical generation requires reactive substrates such as epoxides, halides and electron deficient carbonyl groups. Radical/low valent transition metal hybrid strategies provide a viable solution to this problem. However, its potential has so far not been widely explored.[389] Combinations of Ti(III)/Rh(I),[390] Ti(III)/Pd(0), Ti(III)/Ni(0), Cr(II)/Co(II),[391] Mn(II)-Co(II),[392] Mn(II)-Cu(I),[393] Ru(II)-Rh(III)[394] among others has been described in radical reactions.

Typical SET reagent such as SmI_2 combined with transition metal complexes has been studied by Inaga *et al.* (Scheme 66). Using a palladium catalyst, allyl acetates form (η3-allyl)palladium intermediates. SmI_2 release the allyl radical by SET from the (η3-allyl)palladium complex which can be reduced to form alkenes[395] or, in the presence of a carbonyl group, generates a homoallyl alcohol.[396]
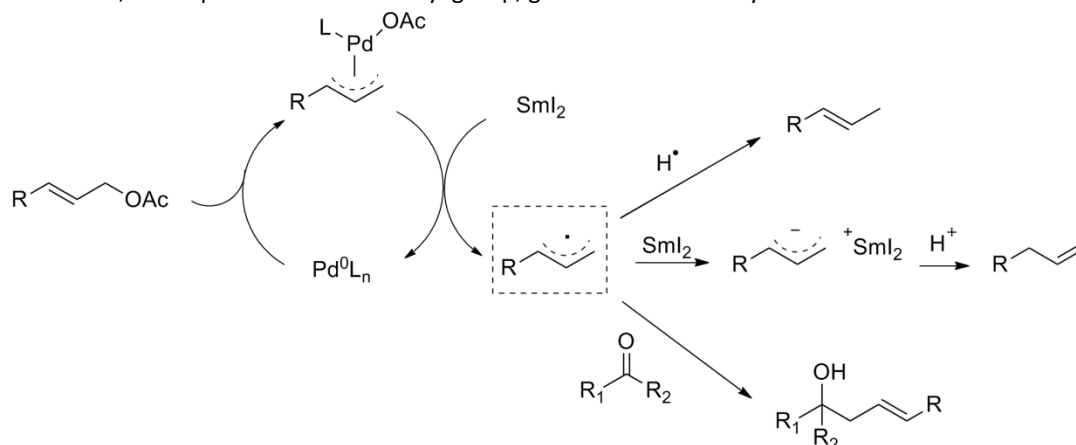
Scheme 66. *Pd(0)/SmI₂-mediated formation of allyl radicals and subsequent reactivity of such intermediate.*

In 2008, Gansäuer *et al.* discovered that after activation by rhodium catalysts molecular hydrogen can be used in hydrogen transfer reactions to radicals. Reductive ring opening of epoxides cocatalyzed by titanocene(III) and the Wilkinson complex ($RhCl(PPh_3)_3$) afforded branched primary alcohols in good yields.[397] This study was later extended to $Cp(CO)_3CrH$ and Vaska's complex ($Ph_3P)_3Ir(CO)Cl$ but with

[388] *Radicals Reactions in Organic Synthesis*, Ed.: S. Z. Zard, Oxford University Press, Oxford, **2003**.

[389] U. Jahn, *Top. Curr. Chem.* **2012**, *320*, 121–190

[390] (a) A. Gansäuer, C.-A. Fan, F. Piestert, *J. Am. Chem. Soc.* **2008**, *130*, 6916; (b) A. Gansäuer, M. Otte, F. Piestert, C.-A. Fan, *Tetrahedron*, **2009**, *65*, 4984-4891.

[391] (a) L. A. Wessjohann, H. S. Schrekker, *Tetrahedron Lett.* **2007**, *48*, 4323; (b) D. L. Usanov, H. Yamamoto, *Angew. Chem. Int. Ed. Engl.* **2010**, *49*, 8169-8172.

[392] (a) F. Recupero, C. Punta, *Chem. Rev.* **2007**, *107*, 3800-3842; (b) T. Kagayama, A. Nakano, S. Sakaguchi, Y. Ishii, *Org. Lett.* **2006**, *8*, 407-409.

[393] E. Riguet, I. Klement, C. K. Reddy, G. Cahiez, P. Knochel, *Tetrahedron Lett.* **1996**, *37*, 5865-5868.

[394] L. Quebatte, R. Scopelliti, K. Severin, *Angew. Chem. Int. Ed. Engl.* **2004**, *43*, 1520-1524.

[395] T. Tabuchi, J. Inanaga, M. Yamaguchi, *Tetrahedron Lett.* **1986**, *27*, 601-602.

[396] T. Tabuchi, J. Inanaga, M. Yamaguchi, *Tetrahedron Lett.* **1986**, *27*, 1195-1196.

[397] Gansäuer A, Fan C-A, Piestert F (2008) J Am Chem Soc 130:6916

worse results.[398] Three years later, the use of titanocene(III) in combination with and iridium hydride complex was successfully employed in cascade cyclization (Scheme 67).[399]
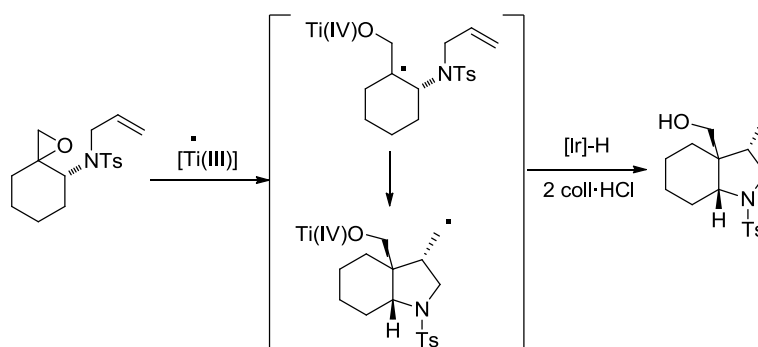
Scheme 67. *Epoxide-ring-opening mediated by Ti(III), radical addition and reduction of the primary radical reported by Gansäuer et al.*

The addition of organic halides to carbonyl compounds in a "one-pot" Barbier[400]-type fashion has been efficiently and conveniently mediated by different reducing agents as B,[401] Zn,[402] In,[403] Sn,[404] Cr[405] (Nozaki-Hiyama-Kishi), SmI$_2$[406] among others. With regard to the nucleophile, a wide range of substrates including allyl, propargyl, vinyl, alkynyl, and aryl halides, carbonates, carboxilates, fosfates and even alcohols were found to be suitable precursors for the formation of organometallic intermediates.

Multimetallic systems have also been developed to improve these Barbier-type reactions. For example, Usanov and Yamamoto recently found that catalytic amounts of Co(TPP) led to a dramatic rate acceleration of Nozaki-Hiyama-Kishi reactions catalyzed by a chromium complex (Scheme 68).[407]

[398] Gans€auer A, Otte M, Piestert F, Fan C-A (2009) Tetrahedron 65:4984

[399] A. Gansäuer, M. Otte, L. Shi, *J. Am. Chem. Soc*. **2011**, *133*, 416-417.

[400] P. Barbier, *Comp. Rend.* **1899**, *128*, 110-111.

[401] (a) M. Kimura, I. Kiyama, T. Tomizawa, Y. Horino, S. Tanaka, Y. Tamaru, *Tetrahedron Lett*. **1999**, *40*, 6795-6798; (b) S. Sebelius, O. A. Wallner, K. J. Szabó, *Org. Lett.* **2003**, *5*, 3065-3068; (c) S.-F. Zhu, Y. Yang, L.-X. Wang, B. Liu, Q.-L. Zhou, *Org. Lett*. **2005**, *7*, 2333-2335.

[402] (a) S. Médégan, F. Hélion, J.-L. Namy, *Eur. J. Org. Chem.* **2005**, 4715-4722; (b) Y. Masuyama, N. Kinagawa, Y. Kurusu, *J. Org. Chem.* **1987**, *52*, 3702-3704; (c) W. Qui, Z. Wang, *J. Chem. Soc., Chem. Commun.* **1989**, 356-357; (d) M. Shimizu, M. Kimura, S. Tanaka, Y. Tamaru, *Tetrahedron Lett.* **1988**, *39*, 609-612; (e) K. Yasui, Y. Goto, T. Yajima, Y. Taniseki, K. Fugami, A. Tanaka, Y. Tamaru, *Tetrahedron Lett.* **1993**, *34*, 7619-7622; (f) M. Kimura, M. Shimizu, K. Shibata, M. Tazoe, Y. Tamaru, *Angew. Chem. Int. Ed.* **2003**, *42*, 3392-3395; (g) Y. Tamaru, *Eur. J. Org. Chem.* **2005**, 2647-2656; (h) G. Zanoni, S. Gladiali, A. Marchetti, P. Piccinini, I. Tredici, G. Vidari, *Angew. Chem. Int. Ed.* **2004**, *43*, 846-849.

[403] S. Araki, T. Kamei, H. Hirashita, H. Yamamura, M. Kawai, *Org. Lett.* **2000**, *2*, 847-849.

[404] (a) B. M. Trost, J. W. Herndon *J. Am. Chem. Soc.* **1984**, *106*, 6835-6837; (b) Y. Masuyama, R. Hayashi, K. Otake, Y. Kurusu, *J. Chem. Soc., Chem. Commun.* **1988**, 44-45; (c) Y. Masuyama, K. Otake, Y. Kurusu, *Tetrahedron Lett*. **1988**, *29*, 3563-3565; (d) Y. Masuyama, J. P. Takahara, Y. Kurusu, *J. Am. Chem. Soc.* **1988**, *110*, 4473-4474; (e) J. P. Takahara, Y. Masuyama, Y. Kurusu, *J. Am. Chem. Soc.* **1992**, *114*, 2577-2586.

[405] (a) Y. Okude, S. Hirano, T. Hiyama, H. Nozaki, *J. Am. Chem. Soc.* **1977**, *99*, 3179-3181; (b) G. C. Hargaden, P. J. Guiry, *Adv. Synth. Catal.* **2007**, *349*, 2407-2424; (c) M. Bandini, P. G. Cozzi, P. Melchiorre, A. Umani-Ronchi, *Angew. Chem. Int. Ed.* **1999**, *38*, 3357-3359; (d) H. Jin, J.-i. Uenishi, W. J. Christ, Y. Kishi, *J. Am. Chem. Soc.* **1986**, *108*, 5644-5646; (e) K. Takai, M. Tagashira, T. Kuroda, K. Oshima, K. Utimoto, H. Nozaki, *J. Am. Chem. Soc.* **1986**, *108*, 6048-6050; (f) A. Fürstner, N. Shi, *J. Am. Chem. Soc.* **1996**, *118,* 2533-2534; (g) A. Fürstner, N. Shi, *J. Am. Chem. Soc.* **1996**, *118,* 12349-12357; (h) K. Takai, K. Kimura, T. Kuroda, T. Hiyama, H. Nozaki, *Tetrahedron Lett.* **1983**, *24*, 5281-5284.

[406] (a) S. Médégan, F. Hélion, J.-L. Namy, *Eur. J. Org. Chem.* **2005**, 4715-4722; (b) T. Tabuchi, J. Inanaga, M. Yamaguchi, *Tetrahedron Lett.* **1986**, *27*, 601-602; (c) T. Tabuchi, J. Inanaga, M. Yamaguchi, *Tetrahedron Lett.* **1986**, *27*, 1195-1196.

[407] Usanov DL, Yamamoto H (2010) Angew Chem Int Ed 49:8169
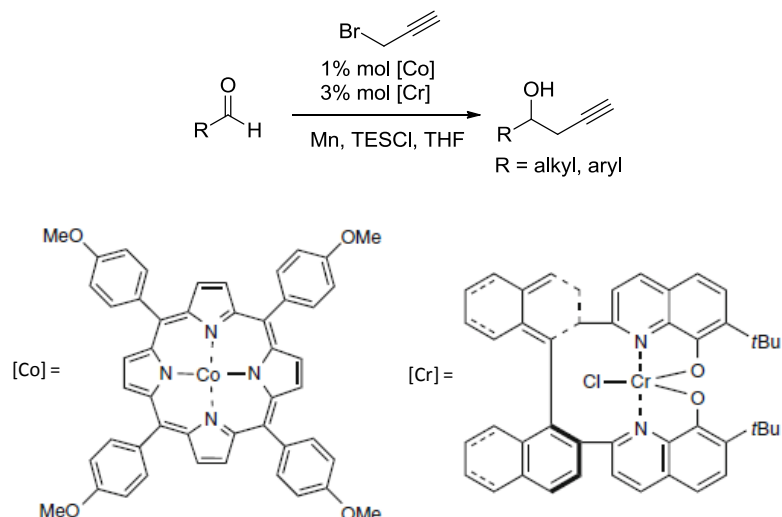
Scheme 68. *Barbier-type propargylation of aldehydes mediated by the multimetallic Co/Cr system.*

As far as the electrophile is concerned, Barbier-type additions are usually limited to aldehydes. The ability of titanocene complexes to catalyze the addition of allyl, prenyl and crotyl groups to aldehydes and ketones was demonstrated in our group in 2009. This α-regioselective allylation has been used as a key step in the synthesis of polyhydroxylated terpenes.[408]

At the same time, divergent titanium(III)-mediated transformations modulated by Ni or Pd to form C-C bonds were studied in our lab (Scheme 69). Using these transition metals in combination with titanocene(III), pronucleophiles such as allylic carbonates and carboxylates became reactive substrates for subsequent radical reactions. Ni organometallic intermediates evolve giving a metallo-ene cyclization (Process B) while (η^3-allyl)palladium(II) complexes are smoothly reduced by a single electron- transfer (SET) reagent such as [[Cp$_2$TiCl][409] or Mn(0) leading to radical allylations (Process A).
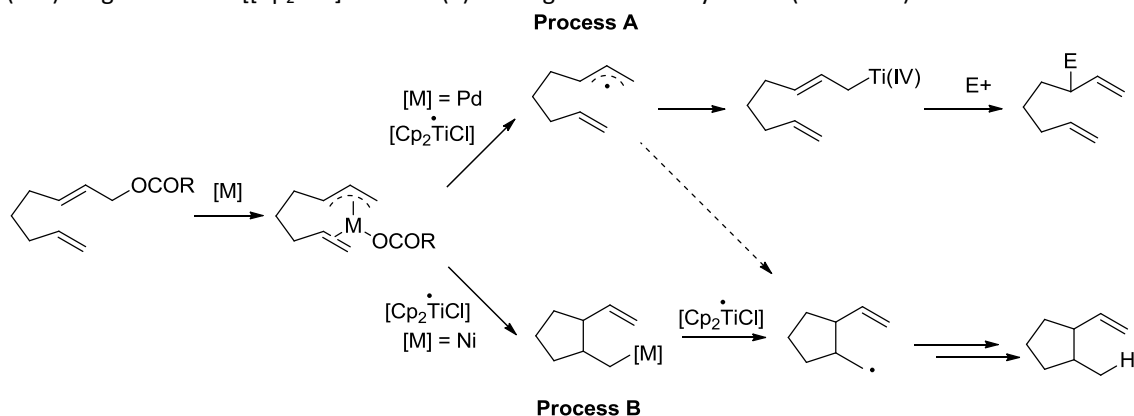
Scheme 69. *Divergent titanium(III)-mediated transformation modulated by Pd (Process A) or Ni (Process B).*

Both Ti/Pd and Ti/Ni protocols outlined above have paved the way for further investigations. For example, Wurtz-type dimerization reaction from allyl carbonates and carboxylates has been optimized using Pd/Ti mixtures (Scheme 70).[410]

---

[408] See appendices A3 and A4.
[409] R. J. Enemærke, J. Larsen, T. Skrydstrup, K. Daasbjerg, *J. Am. Chem. Soc.* **2004**, *126*, 7853 – 7864.
[410] Millán, A.; Campaña, A. G.; Bazdi, B.; Miguel, D.; Álvarez de Cienfuegos, L.; Echavarren, A. M.; Cuerva, J. M. *Chem.;Eur. J.* **2011**, *17*, 3985–3994.
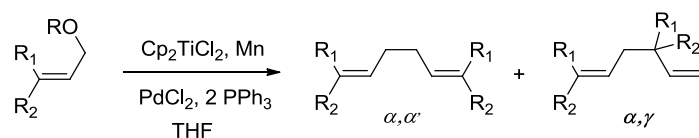
10 examples
49-100% yield
α,α' major regioisomer

Scheme 70. *Wurtz-type dimerization reaction from allyl carbonates and carboxylates.*

When [Cp$_2$TiCl] is added in a big excess, resultant (η1-allyl)titanium(IV) complexes are formed leading to the reduction of the allylic substrates.[410] As the excellent HAT capabilities of the Ti(III)-aqua complexes have been demonstrated,[411] the presence of deuterated water allowed the synthesis of deuterated derivatives of great interest in the food and pharmaceutical industries (Scheme 71).

Scheme 71. *Reduction of allyl carbonates and carboxylates to the corresponding deuterated products.*

Allylation, crotylation and prenylation of aldehydes and ketones has also been afforded with this multimetallic system.[410] It is well worth to highlight the allylation of ketones which are infrequent substrates and the possibility to conduct the reaction intramolecularly to synthesize five- and six-membered rings with good stereoselectivities (Schemes 72 y 73).

R$_3$, R$_4$ = H (Allyl)
13 examples
54-99% yield

R$_3$ = H, R$_4$ = CH$_3$ (Crotyl)
10 examples
36-96% yield

R$_3$, R$_4$ = CH$_3$ (Prenyl)
5 examples
54-84% yield
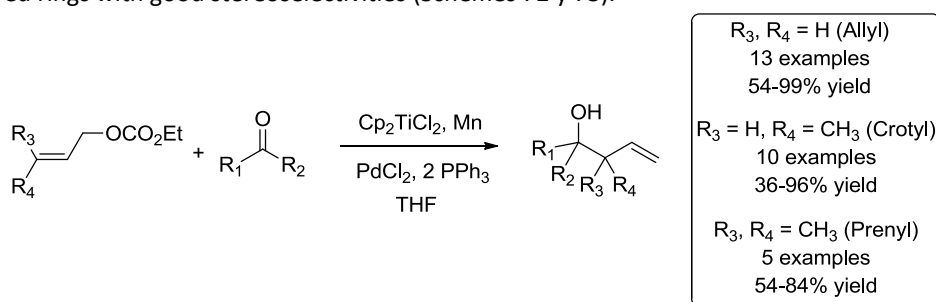
Scheme 72. *Allylation, prenylation and crotylation of carbonates and carboxylates mediated by the multimetallic Ti(III)/Pd system.*

Z = Malonate, sulfone, sulfonamide

8 examples
46-95% yield
n = 0, *trans* major
n = 1, *cis* major
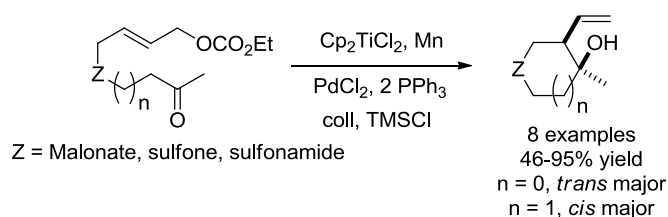
Scheme 73. *Intramolecular allylation of ketones.*

This multimetallic Ti/Pd protocol can also be used to perform the efficient synthesis of homopropargylic alcohols with an excellent regioselectivity toward the homopropargylic alcohol (Scheme 74).[412,413]

[411] (a) J. Jin, M. Newcomb, *J. Org. Chem.* **2008**, *73*, 7901–7905. (b) Cuerva, J. M.; Campaña, A. G.; Justicia, J.; Rosales, A.; Oller-López, J. L.; Robles, R.; Cárdenas, D. J.; Buñuel, E.; Oltra, J. E. *Angew. Chem., Int. Ed*. **2006***, 45*, 5522–5526. (c) Paradas, M.; Campaña, A. G.; Jiménez, T.; Robles, R.; Oltra, J. E.; Buñuel, E.; Justicia, J.; Cárdenas, D. J.; Cuerva, J. M. *J. Am. Chem. Soc.* **2010**, *132*, 12748–12756. (d) Gansäuer, A.; Cangönül, A.; Behlendorf, M.; Kube, C.; Cuerva, J. M.; Friedrich, J.; van Gastel, M. *Angew. Chem., Int. Ed.* **2012**, *51*, 3266–3270.
[412] A. Millán, L. Álvarez de Cienfuegos, A. Martín-Lasanta, A. G. Campaña, J. M. Cuerva, *Adv. Synth. Catal.* **2011**, *353*, 73–78.
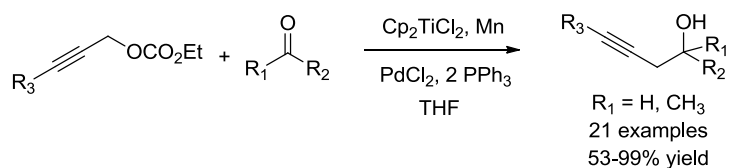
Scheme 74. *Ti/Pd-mediated propargylation of ketones and aldehydes.*

On the other hand, Ni/Ti system has been optimized to perform allylation of carbonyl compounds in the presence of crotyl- and prenyl- carbonates in high yields meanwhile fragmentation products are observed with palladium (Scheme 75).[414]
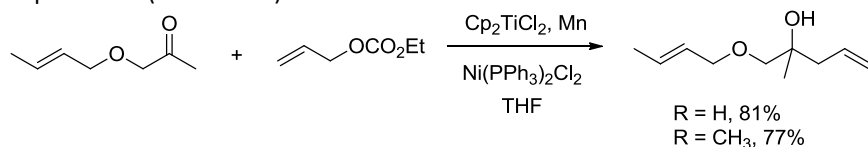
Scheme 75. *Ti/Ni-mediated allylation of a carbonyl compound bearing a crotyl chain.*

Our last synthetic application of this hybrid methodology has outlined the excellent HAT capabilities of the Ti(III)-aqua complexes combined with a Ti/Ni/Mn multiredox system.[415] In this work, cyclizations of alkyl iodides and simple alkenes were driven to the reduced or Heck-type products just because of the presence or absence of water (Scheme 76).
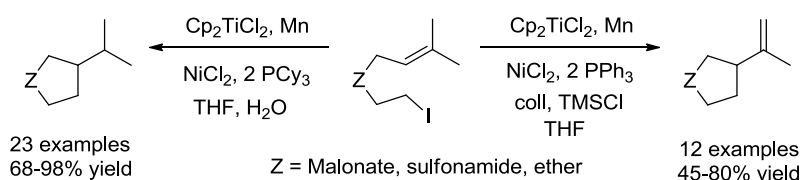
Scheme 76. *Divergent Ti/Ni-mediated methodology.* Heck-type cyclization (right) occurrs under anhydride concitions while the tertiary cabon radical is reducted in the presence of water (left).

[413] See appendix A3.

[414] A. Martínez-Peragón, A. Millán, A. G. Campaña, I. Rodríguez-Márquez, S. Resa, D. Miguel, L. Álvarez de Cienfuegos, J. M. Cuerva, *Eur. J. Org. Chem.* **2012**, 1499–1503.

[415] A. Millán, L. Álvarez de Cienfuegos, D. Miguel, A. G. Campaña, J. M. Cuerva, *Org. Lett.*, **2012**, *14*, 5984-5987.

3.4. Results and discussion

In order to check the viability of our initial hypothesis (Scheme 65), we synthesized the model substrate **Z-66** bearing an allyl-carboxylate and a Michael acceptor (Scheme 77).
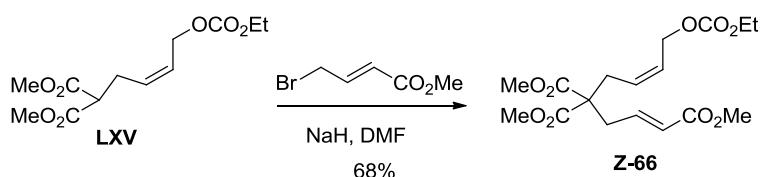
Scheme 77. *Synthesis of the model compound **Z-66**.*

Using this model compound **Z-66**, we started our investigation screening the behavior of multimetallic systems Ti/Ni/Mn able to perform carbocyclizations (Scheme 78).[416] The intramolecular Michael addition product (formal 1,4-addition) **67** was obtained in the first trial using [Cp$_2$TiCl$_2$] (200 mmol%), NiCl$_2$(PPh$_3$)$_2$ (20 mmol%), Mn (800 mmol%) in 28% yield. This preliminary result which yields to the α-reduced products of the regioselective favor 5-exo-trig cyclization, confirmed the validity of our original hypothesis. However, [Cp$_2$TiCl] was used in excess (200 mmol %) facilitating side reactions. Hence, we subsequently tried the substoichiometric version of this multicomponent redox reaction using titanocene-regenerating agent 2,4,6-collidine and trimethylsilyl chloride.[417] Carbocycle **67** was obtained in 38% yield (83 % yield based on recovered starting material or brsm). At that point, a major drawback was pending: the combination of Ti/Ni/Mn was not efficiently catalyzing the cyclization.

Stoichiometric Ti	28%
Catalytic Ti	38%, 83%brsm
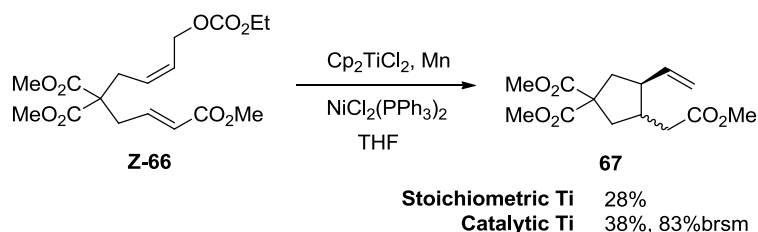
Scheme 78. *Initial screening with the Ti/Ni multimetallic system.*

On the other hand, it is known that Pd(0) complexes can also activate allylic carbonates and carboxylates.[418] Therefore, we subsequently assayed the palladium-catalyzed version using stoichiometric and substoichiometric amounts of titanium catalyst (Scheme 79). For this metal combination using stoichiometric amounts of [Cp$_2$TiCl], the α,β-unsaturated ester **67** was converted into the desired cycle (20% yield) but the allyl radical homocoupling product **68** was the major compound isolated (26% yield). The use of allylic esters in Wurtz-type reactions was rather unusual so this reaction was concurrently studied in our lab.[419] Finally, the palladium/titanium catalytic protocol afforded the desired intramolecular Michael-type allylation product **67** in a good yield (72% yield) as a 4:1 mixture of *cis:trans* stereoisomers. Similar *cis:trans* ratios were previously observed in Ti(III)-promoted intramolecular addition of allyl-halides to carbonyl compounds.[420]

[416] A. G. Campaña, B. Bazdi, N. Fuentes, R. Robles, J. M. Cuerva, J. E. Oltra, S. Porcel, A. M. Echavarren, *Angew. Chem. Int. Ed.* **2008**, *47*, 7515-7519.

[417] (a) A. Gansäuer, H. Bluhm and M. Pierobon, J. Am. Chem. Soc., 1998, 120, 12849–12859; (b) A. F. Barrero, A. Rosales, J. M. Cuerva and J. E. Oltra, Org. Lett., 2003, 5, 1935–1938; (c) S. Fuse, M. Hanochi, T. Doi and T. Takahashi, Tetrahedron Lett., 2004, 45, 1961–1964.

[418] (a) W. Oppolzer in Comprehensive Organic Synthesis, Vol. 5 (Eds.: B. M. Trost, I. Fleming), Pergamon, Oxfod, 1991, chap. 1.2; (b) E. Gomez-Bengoa, J. M. Cuerva, A. M. Echavarren, G. Martorell, Angew. Chem. Int. Ed. Engl. 1997, 36, 767 – 769.

[419] A. Millán, A. G. Campaña, B. Bazdi, D. Miguel, L. Álvarez de Cienfuegos, A. M. Echavarren, L. M. Cuerva, *Chem.;Eur. J.* **2011**, *17*, 3985–3994.

[420] R. E. Estévez, J. Justicia, B. Bazdi, N. Fuentes, M. Paradas, D. Choquesillo-Lazarte, J. M. García-Ruiz, R. Robles, A. Gansäuer, J. M. Cuerva, J. E. Oltra, *Chem. Eur. J.* **2009**, *15*, 2774-2791.
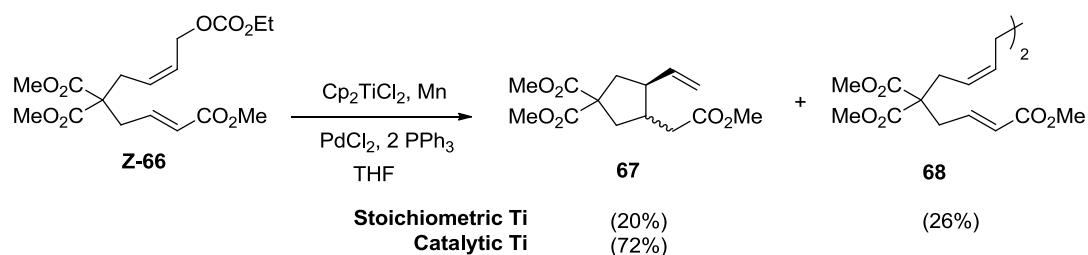
Scheme 79. *Initial screening with the Ti/Pd multimetallic system.*

Then, a set of control experiments were run in order to optimize the reaction conditions (Table 9). Control experiments showed that Mn dust, palladium catalyst and at least one Lewis acid ([Cp$_2$TiCl] or TMSCl) were indispensable in this transformation (Table 9, entries 4-7 and 9). Nevertheless, improved yields and clean reactions were obtained in the presence of [Cp$_2$TiCl] as Lewis acid (Table 9, entries 2 and 3). This fact can be related with [Cp$_2$TiCl] ability to activate the Michael acceptor by coordination and to trap radical species, avoiding undesirable side reactions and/or decomposition of these highly active intermediates. Addition of 2,4,6-collidine had little influence on the yield (Table 9, entry 8) but it allowed smoother reaction conditions hence it was also maintained in subsequent reactions. Both Ti and Pd catalyst loadings could be down to 10 mol% with similar yields (Table 9, entry 10). Bulkier titanocene-based catalysts with higher steric hindrance did not have a significant impact on the *cis:trans* stereoselectivity (Table 9, entries 11 and 12). This result agrees with related multimetallic allylations[421] and is inconsistent with a mechanism based on an *in situ* generation of nucleophilic (η^1-allyl)Ti(IV) intermediates.[422]

Entry	Ti catalyst (mol%)	Ligand (mol%)	Pd catalyst (mol%)	Mn (mol%)	TMSCl (mol%)	2,4,6-Collidine (mol%)	Yield (*trans:cis*)
1	Cp$_2$TiCl$_2$ (200)	PdCl$_2$ (20)	PPh$_3$ (40)	800	-	-	20 (4:1)
2	Cp$_2$TiCl$_2$ (40)	PdCl$_2$ (20)	PPh$_3$ (40)	800	400	700	72 (4:1)
3	-	PPh$_3$ 40)	PdCl$_2$ (20)	800	400	-	62
4	Cp$_2$TiCl$_2$ (40)	-	PdCl$_2$ (20)	800	400	700	0
5	Cp$_2$TiCl$_2$ (40)	PPh$_3$ (40)	-	800	400	700	0
6	Cp$_2$TiCl$_2$ (40)	PPh$_3$ 40)	PdCl$_2$ (20)	-	400	700	0
7	-	PPh$_3$ (40)	PdCl$_2$ (20)	800	-	-	0
8	Cp$_2$TiCl$_2$ (40)	PPh$_3$ 40)	PdCl$_2$ (20)	800	400	-	71
9	-	-	Pd(PPh$_3$)$_4$	-	-	-	0
10	Cp$_2$TiCl$_2$ (10)	PdCl$_2$ (10)	PPh$_3$ (40)	800	400	700	80 (4:1)

[421] Millán, Alba. *Tesis Doctoral*, 2012, UGR.
[422] (a) M. T. Reetz, R. Steinbach, J. Westerman, R. Peter, *Angew. Chem. Int. Ed. Engl.* **1980**, *19*, 1011-1012; (b) M. T. Reetz, *Top. Curr. Chem.* **1982**, *106*, 1-54; (c) F. Sato, H. Urabe, S. Okamoto, *Chem. Rev.* **2000**, *100*, 2835-2886; (d) T. Takeda, I. Miura, Y. Horikawa, T. Fujiwara, *Tetrahedron Lett*. **1995**, *36*, 1495-1498.
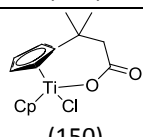
11	(tBuCp)₂TiCl₂ (150)	PPh₃ (40)	PdCl₂ (20)	800	-	-	54 (4:1)
12	[Ti complex structure] Cp–Ti(Cl)–O... (150)	PPh₃ (40)	PdCl₂ (20)	800	-	-	62 (4:1)

Table 9

Phosphines and phosphites screening with different electronic and steric characteristics did not improve the catalytic activity obtained using simple PPh₃.[423] Recently the enhancement of the metalation efficiency between [Cp₂TiCl] and a low-valent transition metal as Zn(0) at low temperatures by the use of phosphine additives for addition of allyl halides has been reported.[424] Although the exact role of phosphine is unclear for the aforementioned reaction, which failed for carboxilated and carbonates, the positive effect of the simple PPh₃ appears quite general suggesting it stabilizes the intermediate allyl organometallic species.

After the screening of the optimal reaction conditions (Table 9, entry 2), we synthesized the *E*-stereoisomer **E-66** which led to the same products revealing the stereoconvergent nature of the process (Scheme 80). This observation was also found in related titanocene-mediated intramolecular allylations. However, significantly different results have been obtained by Fand *et al.* from the radical conjugated addition of aliphatic radical precursors with 5,7-substituents.[425]

MeO₂C, MeO₂C ... OCO₂Et / CO₂Me **E-66** — [Ti(III)], [Pd(II)] — 73% → MeO₂C, MeO₂C ... CO₂Me **67**   *cis:trans* = 4:1
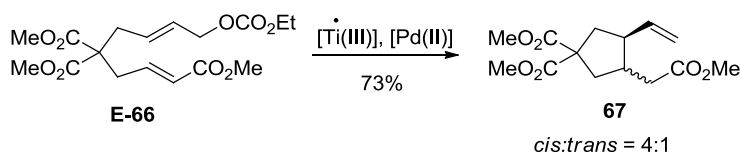
Scheme 79. Ti/Pd-mediated cyclization of E-66 led to the same 4:1 mixtures of stereoisomers.

Three different carboxylates synthesized by a common route were equally adequate pro-nuclephiles (Scheme 80). It is worth noting that chiral (*R*)-2-(6-methoxynaphthalen-2-yl)propanoate (shortened as ONp or naproxene) gave any enatioinduction what suggested that neither the Pd nor the Ti complexes were involved in the C-C bond step.

MeO₂C, MeO₂C ... OH — 1. Alkylation 2. Oxidation → MeO₂C, MeO₂C ... OR / CO₂Me
68 R = OAc (79%)
69 R = OBz (75%)
70 R = ONp (61%)

ONp = —O—C(=O)—CH(CH₃)— naphthyl—OMe

— [Ti(III)], [Pd(II)] → MeO₂C, MeO₂C ... CO₂Me **67**
R = OAc (73%)
R = OBz (95%)
R = CNp (52%)
cis:trans = 4:1
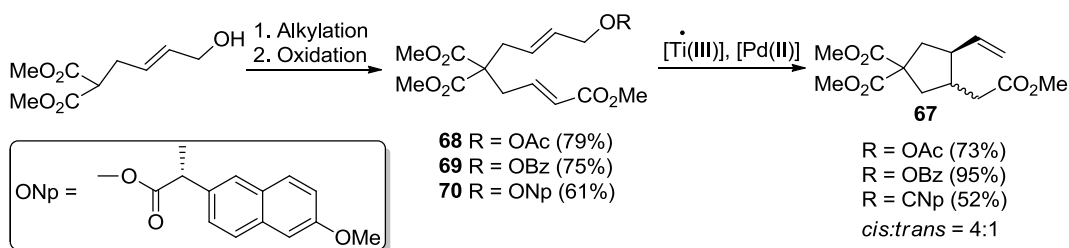
Scheme 80. Changing the allyl carboxylate.

Substrates bearing different Michael acceptors were synthesized by olefin metathesis of the dimethyl 2-allylmalonate with the corresponding vinyl reagents and alkylation with methyl-(E)-4-bromo crotonate (Scheme 81). This retrosynthetic analysis was planned in order to introduce different Michael acceptors by cross metatesis to a common backbone. However, cross metathesis using second generation Grubbs catalyst failed with acrylonitrile, acrylamide and vinylsulfone. Slightly higher cis-diastereoselection was observed for tert-butyl ester **72** and ketone **74** compared to the methyl ester **66**.

[423] Millán, Alba. *PhD Thesis*, **2012**, UGR.
[424] L. M. Fleury, A. D. Kosal, J. T. Masters, B. L. Ashfeld *J. Org. Chem.* **2013**, *78*, 253–269.
[425] J.-M. Fang, H.-T. Chang, C.-C. Lin, *J. Chem. Soc., Chem. Commun.* **1988**, *1385*.
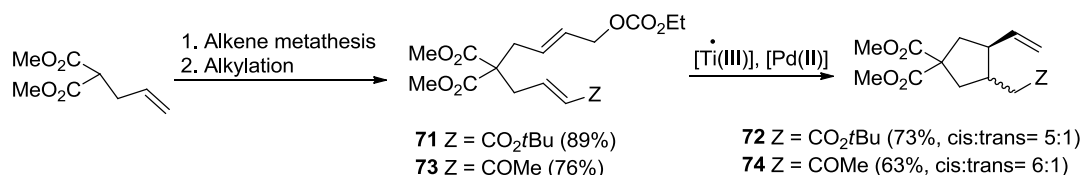
Scheme 81. *Changing the Michael acceptor.*

A different route consisting on alkylation and oxidation using Dess-Martin Periodinane was followed to obtain the α,β-unsaturated aldehyde **75** (Scheme 82). In the cyclization step, several reaction paths strongly competed dropping significantly the cyclization yield to 26%. The ability of [Cp$_2$TiCl] to catalyzed pinacol coupling of carbonyl group is known.[426] On the other hand, α,β-unsaturated aldehydes react with titanocene to form allyl-titanoxy radicals.[427] The Grignard-type alcohol formed by the fast transfer of a Cp group from [Cp$_2$TiCl] to the aldehyde was also isolated as a by-product.
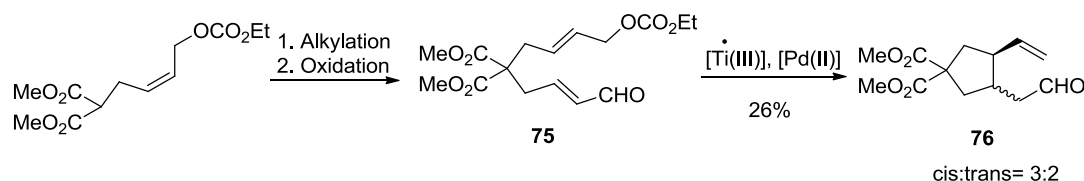
Scheme 82. *Cyclization of an α,β-unsaturated aldehyde.*

Methyl-substituted alkenes are also compatible using our methodology. *α*-Methyl-substituted carbonate **77** was synthesized by palladium catalyzed monoalkylation with isoprene monoxide, esterification with ethylchloroformiate and second alkylation with the methyl-(E)-4-bromo crotonate (Scheme 83). Final, cyclization step yielded to a 5:2 mixture of cis:trans diastereosimers in 68% yield brsm (compound **78**).
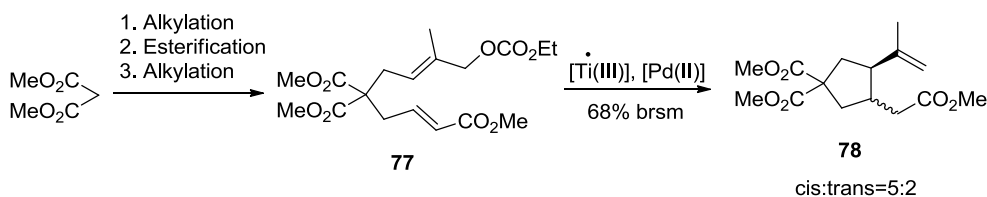
Scheme 83. *Cyclization of an α-methyl-substituted carbonate.*

The β-methyl-carbonate **79** was obtained after two alkylaton steps (Scheme 84). Although cyclization step proceed, the steric hindrance at the newly formed C–C bond decreased drastically the cyclization yield (35% yield for compound **80**) and stereoselectivity (*cis:trans*=3:2) as predicted the second Beckwith´s rule.[428]

---

[426] (a) Y. Handa, J. Inanaga, *Tetrahedron Lett.* **1987**, *28*, 5717 – 5718; (b) A. Gansäuer, Chem. Commun. 1997, 457 –458; (c) A. Gansäuer, D. Bauer, *J. Org. Chem*. **1998**, *63*, 2070 –2071; d) A. Gansäuer, D. Bauer, Eur. *J. Org.Chem.* **1998**, 2673–2676; (e) T. Hirao, B. Hatano, M. Asahara, Y. Muguruma, A. Ogawa, *Tetrahedron Lett.* **1998**, *39*, 5247 – 5248; (f) M. S. Dunlap, K. M. Nicholas, *J. Organomet. Chem.* **2001**, *630*, 125 –131; (g) M. Paradas, A. G. Campaña, R. E. Estévez, L. Álvarez de Cienfuegos, T. Jiménez, R. Robles, J. M. Cuerva*, J. E. Oltra, J. Org. Chem.* **2009**, *74*, 3616-3619.

[427] (REF OL 2006).

[428] Summary of the Beckwith rules: 1) Intramolecular addition under kinetic control in lower alkenyl and alkynyl radicals and related species occurs preferentially in the exo-mode. 2) Substituents on an olefinic bond disfavour homolitic addition at the substituted position. The effect, which is probably mainly steric in origin, accounts more satisfactorily than do thermodynamic criteria for the rates and regioselectivity of homolytic inter- and intra-molecular addition to substituted olefins except when the substituent exerts a strong stabilizing effect. 3) Homolytic cleavage is favoured when the bond concerned lies close to the plane of an adjacent semi-occupied orbital or of an adjacent filled non-bonding or pi-orbital. 4) 1,5-Ring closures of substituted 5-hexenyl and related radicals are stereoselective, mainly *cis*-disubstituted products is obtained for 1- or 3-substituted systems, whereas 2- or 4-substituted systems give mainly *trans*-products. The preferential formation of the *cis*-product from l-substituted hexenyl
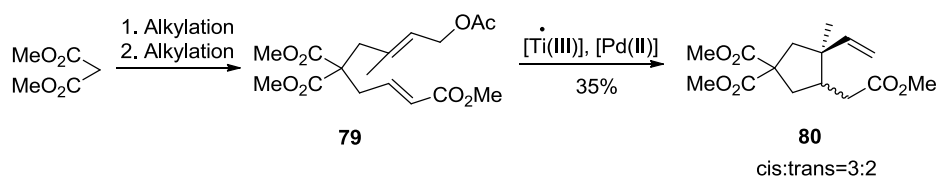
Scheme 84. *Cyclization of a β-methyl-substituted carbonate.*

Both *α*-methyl and *β*-methyl-*α*,β-unsaturated esters were also synthesized following similar procedures to the previously described (Scheme 85). After Pd-catalyzed alkylation, oxidation with Dess-Martin Periodinane, Pinnick oxidation and esterification, compound **81** was transformed into the carbocycle **82** was obtained as a single *cis*-diasteromer in 64% yield.
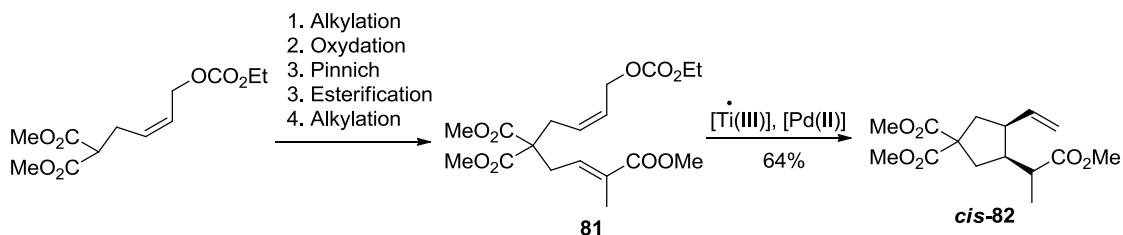
Scheme 85. *Cyclization of a α-methyl-α,β-unsaturated ester led to a single cis-stereoisomer.*

β-Methyl-α,β-unsaturated ester **83** was obtained in 7% global yield in a six step sequence from dimethylmalonate: alkylation with *trans*-4-acetoxy-1-bromo-2-methyl-2-butene, desacetilation, oxidation with Dess-Martin Periodinane, Pinnick oxidation, esterification and final alkylation with methyl-(E)-4-bromo crotonate (Scheme 86). Unfortunately, carbonate **83** did not form the carbocycle under our conditions probably due to the slow addition to the radical to the disubstitued olefin.[429] 6-endo-trig cycle was neither observed probably due to the inadequate orientation of the radical[430] and the void effect of the EWG on this position.
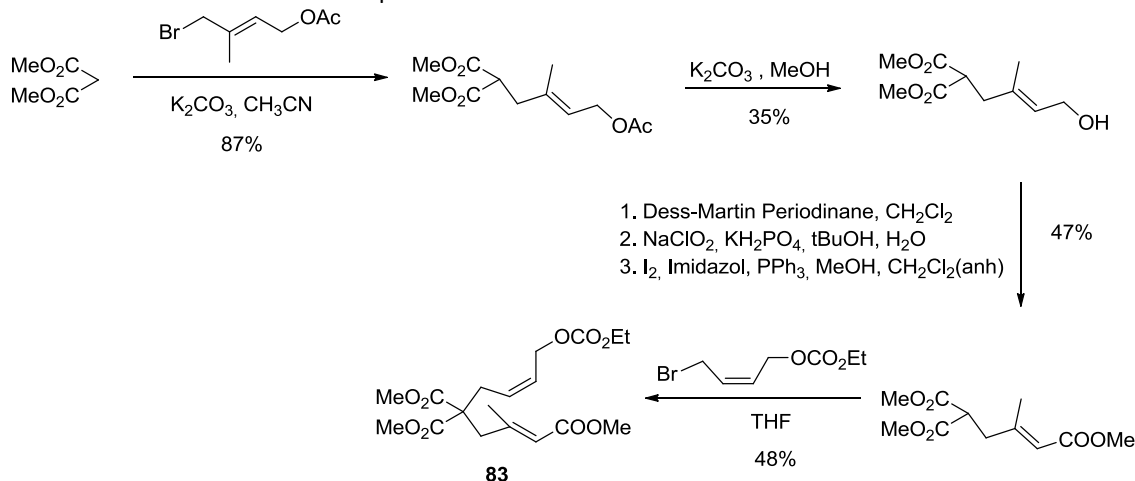
Scheme 86. *Synthesis of the β-methyl-α,β-unsaturated ester. Any cyclization occurred when 83 was submitted to the standard conditions.*

In our earlier work on carbocyclization catalyzed by the multimetallic system Ti/Ni, we were unable to form six-member rings. These results were not surprising because it is generally accepted that compared

---

radicals has been ascribed to the effects of orbital symmetry. This 4th guideline may fail when the substituent at C-1 is bulky. The stereoselectivity of ring closure of 2-3-, or 4-substituted hexenyl radicals reflects the conformational preference of the transition state and therefore is likely to be more pronounced for systems containing bulky substituents. Read more in: Beckwith, A. L. J.; Easton, C. J.; Serelis, A. K. J. Chem. Soc., Chem. Commun. 1980, 482.

[429] Giese, B. Angew. Chem., Int. Ed. Engl. 1983, 22, 753.

[430] Tedder, M.; Walton, J. C. Acc. Chem. Res. 1976, 9, 183.

to *exo* cyclizations, *endo* cyclizations are usually minor processes in the formation of standard and medium sized rings. However, the position of the EWG attached to the radical acceptor has the capability to change the regioselectivity in favor of *endo* cyclization.[431] Moreover, in almost all cases radicals add preferentially to the unsubstituted double bonds. Thus, we synthesize compound **84** to check if Michael-type conjugated addition was favoured (Scheme 87). As a matter of fact, cyclization afforded the cyclohexane **85** in a good yield.
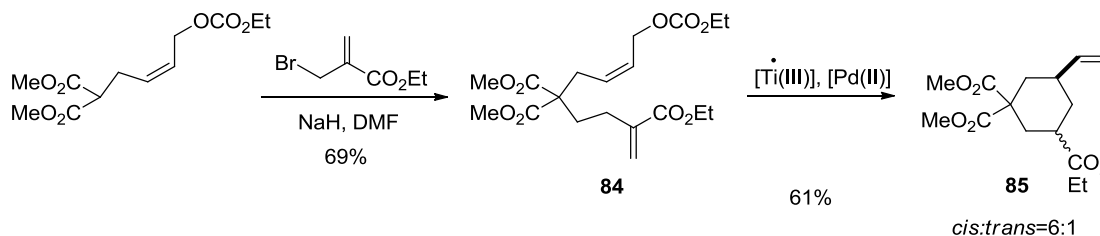
Scheme 87. *6-Endo cyclization controlled by the position of the EWG.*

Bis-sulfones are challenging substrates due to their high tendency to eliminate under the reductive conditions used and the relatively acid γ-protons of the Michael acceptor.[432] Related SET reagent as SmI_2 are known to catalyzed the reductive elimination of sulfones to the corresponding alkenes.[433] As a proof of the mild conditions of our multimetallic protocol, we prepared compounds **86** and **88** following similar synthetic sequences to the ones we have shown (Scheme 88). In both cases, cycles were obtained in moderate yields. Higher yields and stereoselectivities were obtained for the 6-*endo-trig* product **89**.[434] All this facts strongly outline the relevance of the electron-withdrawing substituents on the reaction rate and thermodynamics.[435]
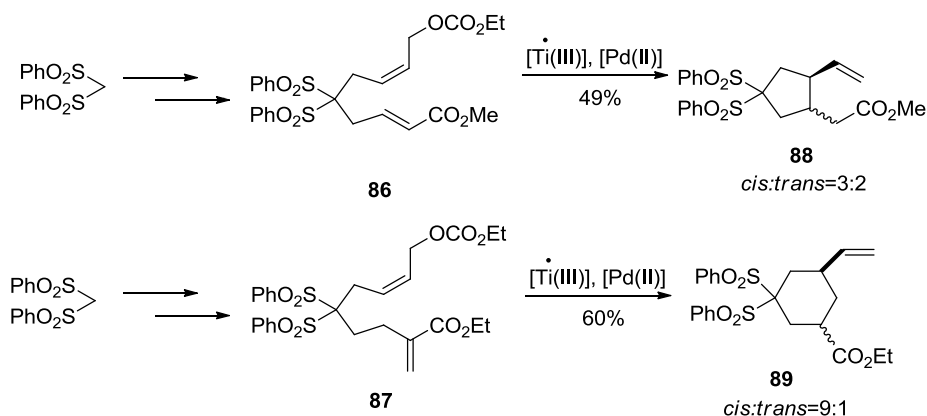
Scheme 88. *5-Exo and 6-endo Michael-type cyclizations of bis-sulfone derivates depending on the position of the EWG.*

Cyclopentanes were also obtained in good yields from α,β-γ,δ-unsaturated ester **90** and ketone **92** leading to the residual non-conjugated E double bond. Starting materials were synthesized following a

---

[431] (a) Munt, S. P.; Thomas, E. J. J. Chem. Soc., Chem. Commun. 1989, 480. (b) Colombo, L.; Giacomo, M. D.; Scolastico, C.; Manzoni, L.; Belvisi, L.; Molteni, V. Tetrahedron Lett. 1995, 36, 625. (c) Morikawa, T.; Nishiwaki, T.; Kobayashi, Y. Tetrahedron Lett. 1989, 30, 2407. (d) Negishi, E.-I.; Ma, S.; Sugihara, T.; Noda, Y. J. Org. Chem. 1997, 62, 1922.

[432] G. Majetich, R. W. Desmond, J. J. Soria, *J. Org. Chem.* **1986**, *51*, 1753-1769.

[433] Markó, I; Murphy, Fiona; Dolan, Simon (1996). *Tetrahedron Letters* 37 (12): 2089.

[434] Better *cis*-stereoselectivity for 6-endo-trig cyclization was attributed the additional pseudoequatorial location of the EWG in a chair-like transition state.

[435] Lower reaction barriers have been theoretically calculated for alkenes with electron-withdrawing substituents which increase the reaction exothermicity and therefore reactivity in radical additions. Read more: Wong, M. W.; Pross, A.; Radom, L.J. Am. Chem. Soc.1993,115, 11050.

common synthetic path (Scheme 89). As the Michael addition happened in δ-position of the unsaturated ester, cascade cyclization could follow but any bicyclic product was isolated.
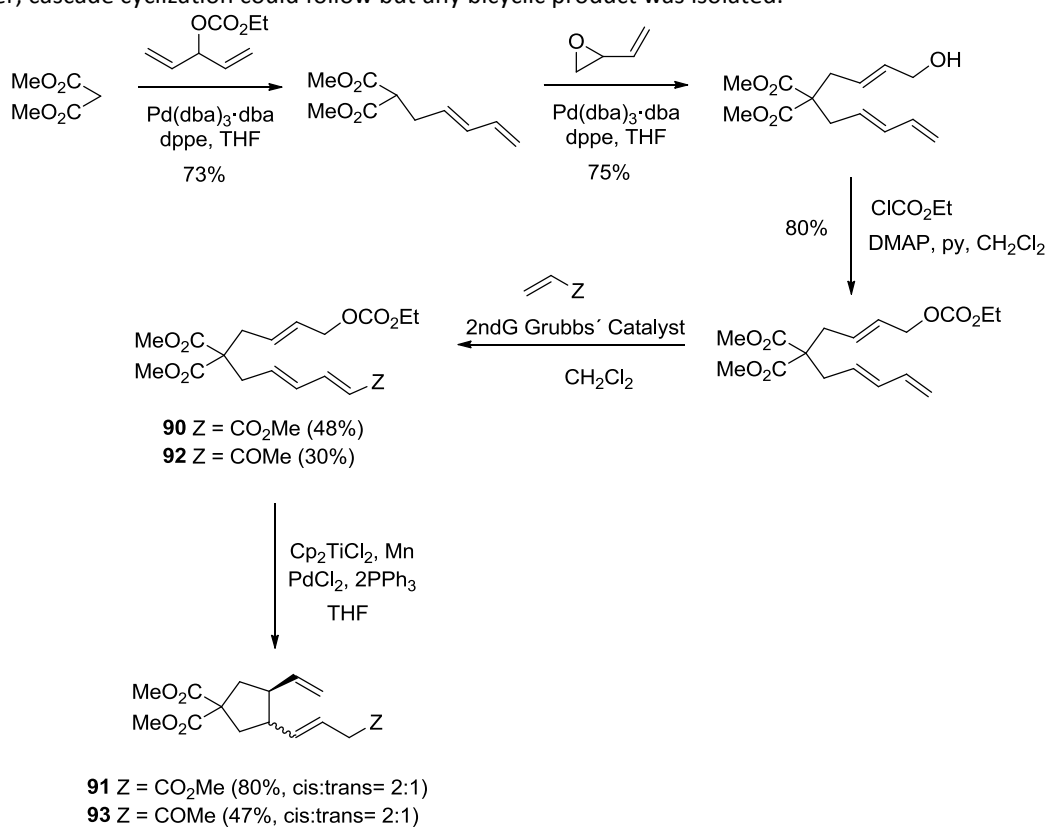
Scheme 89. *5-Exo Michael-type cyclizations of α,β-γ,δ-unsaturated ester and ketone.*

Additionally, using this methodology 1-protected pyrrolidines **96** and **97** were obtained protected in moderate yields and diastereoselectivities (Scheme 90).
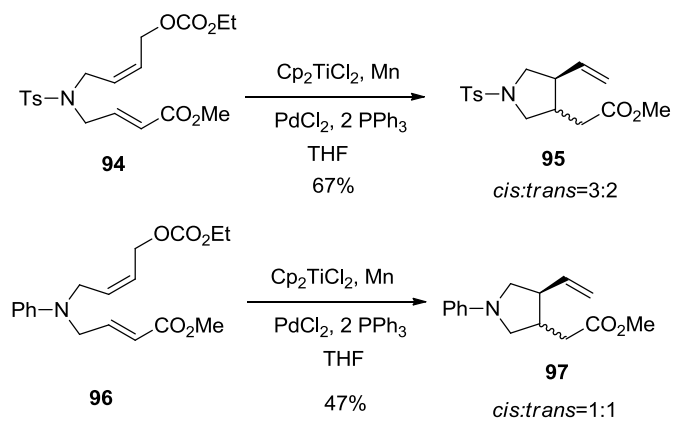
Scheme 90. *Synthesis of five membered N-protected heterocycles.*

Unfortunately, the synthesis of other heterocycles such as tetrahydrofurans was unsuccessful (Scheme 91). When compound **98** was submitted to our standard conditions, fragmentation products were identified after short reaction times by TLC and ^{1}H-NMR analysis of the crude. This fact suggested that β-hydride elimination of the (η3-allyl)palladium and/or fragmentation of β-oxygenated transient

radicals[436] species prevailed on the cyclization step. In a subsequent work, the simple addition of acetone has been proved to benefit conceptually related radical cyclization.[437]
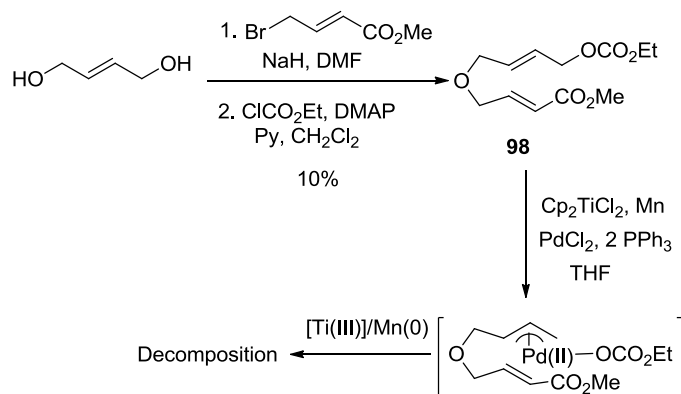
Scheme 91. *Fragmentation of O-allyl ethers.*

Finally, we run some experiments in order to envisage the reaction mechanism. In the light of results, three different pathways may be operative after the formation of the (η^3-allyl)palladium(II) intermediate **S1** (Scheme 92).
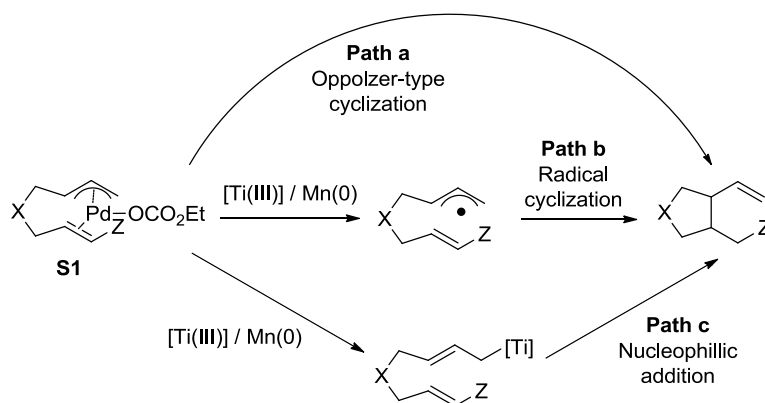
Scheme 92. *Mechanistic hypothesis.*

No example of Oppolzer carbocyclizations of activated alkenes has been described in literature. Therefore, we carried out the Oppolzer cyclization of compound **Z-66** using two different conditions. Under the original Oppolzer conditions, we obtained the carbocycle **99** in 14% with an additional double bond derived from β-hydride-elimination (Scheme 93).
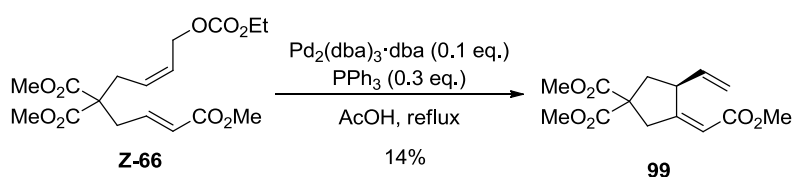
Scheme 93. *Oppolzer cyclization of compound Z-66.*

Under our conditions (THF, rt) no cyclization was observed, isolating only a diene derived from the elimination of the ethyl carbonate group (Scheme 94). These two experiments ruled out a palladium-catalyzed Oppolzer-type mechanism.

[436] José Justicia *, Tania Jiménez, Sara P. Morcillo, Juan M. Cuerva *, J. Enrique Oltra, Tetrahedron 65 (2009) 10837–10841

[437] A. Millán, L. Álvarez de Cienfuegos, D. Miguel, A. G. Campaña, J. M. Cuerva, Org. Lett., 2012, 14, 5984-5987.
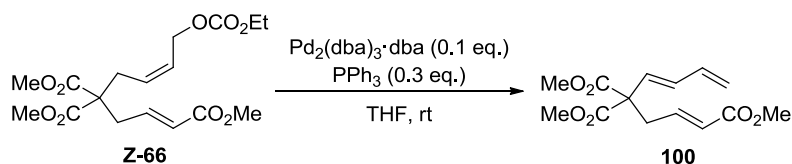
Scheme 94. *Oppolzer-type cyclization of compound* **Z-66** *using THF at rt.*

A mechanism based on an *in situ* generation of nucleophilic titanocene(IV)-complexes (Scheme 81, path c) was ruled out taking into account that an increase in the steric hinderance in the titanocene(III)-complex was not correlated with a variation in the diastereoselectivity (Table 9, entries 11 and 12). Therefore, a direct radical addition seemed to be the only able to explain the experimental results. The small influence of the titanium catalyst and phosphine estereoelectronic characteristics catched sight of the free radical nature of the underlying mechanism.

It is worth noting that few examples of allyl radical additions to α,β-unsaturated carbonyl compounds have been described in literature owing to their tendency to dimerize.[438] High dilution and/or slow addition using syringe pump are usually required. Accordingly, a control radical cyclization was made using the corresponding bromide (Figure 95) in our standard concentrations (10mM) and no cyclization products were obtained. This fact suggests that this multimetallic protocol generates tiny amounts of the allyl radicals hindering any potential side dimerization process.
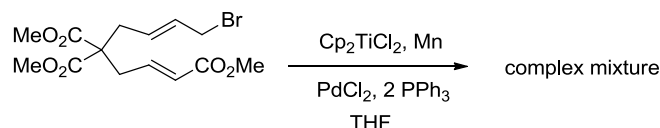
Scheme 95. *Cyclization of the allylbromide under our standard conditions failed.*

Although free radical addition to olefins depend on the complex interplay of polar, steric, and bond-strength terms,[439] higher *cis*-stereoselectivities can be understood by invoiking a Beckwith–Houk envelope-like transition state[440] where the side chains occupy pseudoequatorial positions to minimize unfavorable 1,3-diaxial interactions.[441] The initial stereoselectivity (4:1) could be substantially improved carrying out the reaction at -20ºC. At this lower temperature, the cis-stereoisomer was exclusively isolated in 61% yield (Figure 96).
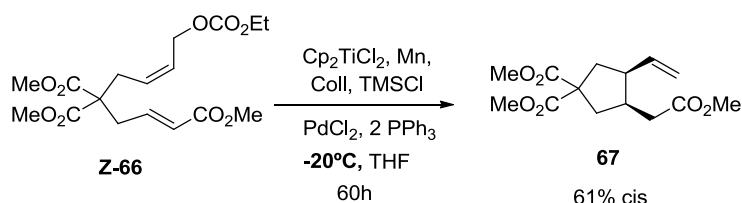
Scheme 96.*Cyclization stereoselectivity was improved carrying out the reaction at -20⁰C.*

3.5.Conclusions and outlook

We have developed a novel [Ti]/[Pd] mediated intramolecular Michael-type allylation reaction using stable allyl carbonates and carboxylates as pronucleophiles. This reaction takes place using catalytic

---

[438] See intro: (a) Cox, N. J. G.; Pattenden, G. Tetrahedron Lett. 1989, 30, 621-624. (b) Mandal, S. K.; Jana, S.; Roy, S. C. Tetrahedron Lett. 2005, 46, 6115-6117. (c) Morikawa, T.; Uchida, J.; Imoto, K.; Taguchi, T. J. Fluorine Chem. 1992, 58, 119-125; (d) Stork, G.; Reynolds, M. E. J. Am. Chem. Soc. 1988, 110, 6911; (e) Yoo, S.-E.; Yi, K. Y.; Lee, S.-H.; Jeong, N. Synlett 1990, 575.

[439] Tedder, M.; Walton, J. C. Acc. Chem. Res. 1976, 9, 183.

[440] (a) Beckwith, A. L. J.; Schiesser, C. H. Tetrahedron 1985, 41, 3925. (b) Spellmeyer, D. C.; Houk, K. N. J. Org. Chem. 1987, 52, 959. (c) Tripp, J. C.; Schiesser, C. H.; Curran, D. P. J. Am. Chem. Soc. 2005, 127, 5518.

441 J. P. Takahara, Y. Masuyama, Y. Kurusu, *J. Am. Chem. Soc.* **1992**, *114* (7), pp 2577–2586.

amounts of Ti and Pd at room temperature and allows the formation of five- and six-membered carbo- and heterocycles in one step with good yields and moderate diastereoselectivities. Cis-stereoisomer of the model compound **Z-66** was exclusively isolated when the reaction was performed at -20ºC. From a mechanistic point of view, the small influence of the titanium catalyst used and phosphine estereoelectronic characteristics suggested that the cyclization occurs via direct radical addition to the Michael acceptor. It is worth noting that few examples of allyl radical additions to α,β-unsaturated carbonyl compounds have been described in literature owing to their tendency to dimerize.

3.6. Experimental section

The following known compounds were isolated as pure samples and showed NMR spectra identical to reported data: **Z-LXV**,[442] **E-LXV,**[443] **E-LXXIII** and **E-LXXIV,**[444] (*Z*)-BrCH$_2$CH=CHCH$_2$CO$_2$Et,[445] **Z-LXXXV,**[446] *trans*-4-acetoxy-1-bromo-2-methyl-2-butene[447] and ethyl penta-1,4-dien-3-yl carbonate**.**[448]

1. *General procedures:*

Representative protocol for the intramolecular Michael-type addition of allylic carboxylates to activated alkenes. **(GP8)**
Rigorously deoxygenated THF (10 mL) was added to a mixture of Cp$_2$TiCl$_2$ (0.1 mmol), PdCl$_2$ (0.05 mmol), PPh$_3$ (0.1 mmol) and Mn dust (2 mmol) under Ar atmosphere, and the suspension was stirred at room temperature until it turned dark green (about 15 min). A solution of the activated alkene (0.25 mmol) and 2,4,6-collidine (1.75 mmol) in THF (2 mL) and Me$_3$SiCl (1 mmol) was then added. The mixture was stirred at room temperature for 21 h and then diluted with AcOEt, washed with HCl (10%), dried over anhydrous Na$_2$SO$_4$ and the solvent removed. The residue was submitted to flash chromatography (EtOAc/Hexane mixtures) to give the corresponding cyclic products.

2. *Synthesis and analytical characterization of the compounds*
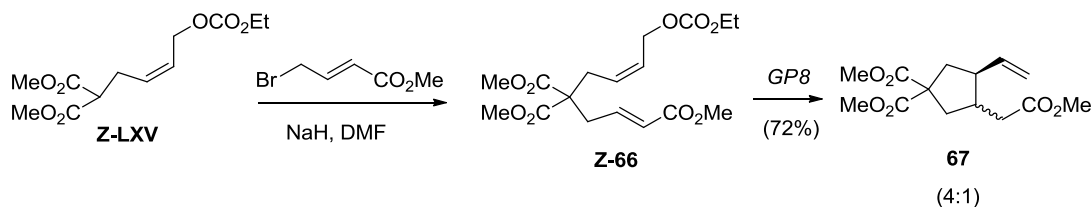
Compound **Z-66.** Methyl 4-bromocrotonate (230mg, 1.1 mmol) was added to a mixture of NaH (44 mg, 1.1 mmol) and dimethylmalonate derivative **Z-LXV** (274 mg, 1 mmol) in DMF (10 mL) at 0ºC. The resulting solution was stirred at room temperature for 16 h. Then the mixture was diluted with EtOAc, washed with HCl (10%) and dried over anhydrous Na$_2$SO$_4$.The residue was submitted to flash chromatography (EtOAc: Hexane, 2:8) to give **Z-66** (253 mg, 68 %) as a colourless oil. ^{1}H-NMR (500 MHz, CDCl$_3$): δ (ppm) = 6.76 (dt, *J* = 15.4, 7.6 Hz, 1H), 5.91 − 5.81 (m, 1H), 5.74 − 5.60 (m, 1H), 5.50 (ddd, *J* = 11.1, 8.5, 4.5 Hz, 1H), 4.63 (d, *J* = 6.8 Hz, 2H), 4.18 (q, *J* = 7.1 Hz, 2H), 3.72 (s, *J* = 3.3 Hz, 6H), 3.70 (s, *J* = 3.3 Hz, 3H), 2.76 (d, *J* = 7.7 Hz, 2H), 2.70 (d, *J* = 7.7 Hz, 2H), 1.29 (t, *J* = 7.1 Hz, 3H); ^{13}C-NMR (126 MHz, CDCl$_3$): δ (ppm) = 170.5 (C), 166.2 (C), 155.1 (C), 142.4 (CH), 127.8 (CH), 127.6 (CH), 125.1 (CH), 64.2

[442] A. G. Campaña, N. Fuentes, E. Gómez-Bengoa, C. Mateo, J. E. Oltra, A. M. Echavarren, J. M. Cuerva, *J. Org. Chem.,* **2007**, *72*, 8127-8130.

[443] A. G. Campaña, B. Bazdi, N. Fuentes, R. Robles, J. M. Cuerva, J. E. Oltra, S. Porcel, A. M. Echavarren, *Angew. Chem. Int. Ed.,* **2008**, *47*, 7515-7519.

[444] C. Fernández-Rivas, M. Méndez, C. Nieto-Oberhuber, A. M. Echavarren, *J. Org. Chem.*, **2002**, *67*, 5197-5201.

[445] W. Oppolzer, A. Fürstner., *Helv. Chim. Acta.,* **1993**, *69*, 2369-2337.

[446] R. E. Estévez, J. Justicia, B. Bazdi, N. Fuentes, M. Paradas, D. Choquesillo-Lazarte, J. M. García-Ruiz, R. Robles, A. Gansaüer, J. M. Cuerva, J. E. Oltra, *Chem. Eur. J.,* **2009**, *15*, 2774-2791.

[447] K. Sato, S. Inoue, S. Ota, Y. Fujita, *J. Org. Chem.,* **1972**, *37*, 462-466.

[448] B. M. Trost, J. I. Luengo, *J. Am. Chem. Soc* **1988,** *110* ,8239-8241.

(CH$_2$), 63.1 (CH$_2$), 57.3 (C), 52.9 (CH$_3$), 51.7 (CH$_3$), 35.8 (CH$_2$), 31.3 (CH$_2$), 14.4 (CH$_3$); EI-HRMS calcd. for C$_{17}$H$_{24}$O$_9$ [M]$^+$: 372.1420; found: 372.1403.

Compound 67 was prepared from **Z-66** according to previously described *GP8* to give **67** in 72 % yield. Mixture of isomers ≈ 4:1 (*cis:trans*). ^{1}H-NMR (500 MHz, CDCl$_3$): δ (ppm) = 5.58 (ddt, *J* = 13.3, 8.3, 6.7 Hz, 1H), 5.00 – 4.88 (m, 2H), 3.65 (s, 3H), 3.64 (s, 3H), 3.56 (s, 3H), 2.79 – 2.68 (m, 1H), 2.51 – 2.37 (m, 1H), 2.25 (dd, *J* = 16.0, 7.0 Hz, 2H), 2.17 – 2.09 (m, 2H), 1.99 – 1.91 (m, 2H); ^{13}C-NMR (126 MHz, CDCl$_3$): δ (ppm) = 173.2 (2xC), 172.9 (C), 137.4 (CH), 116.5 (CH$_2$), 59.0 (C), 52.94 (CH$_3$), 52.90 (CH$_3$), 51.6 (CH$_3$), 45.9 (CH), 39.2 (CH$_2$), 39.1 (CH), 38.8 (CH$_2$), 35.3 (CH$_2$); EI-HRMS calcd. for C$_{14}$H$_{20}$O$_6$ [M]$^+$: 284.1260; found: 284.1265.
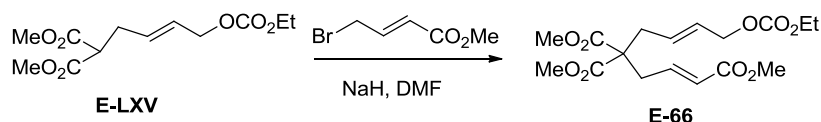
Compound E-66. Methyl 4-bromocrotonate (979mg, 5.5 mmol) was added to a mixture of NaH (219 mg, 5.5 mmol) and dimethylmalonate derivative **E-LXV** (1 g, 3.7 mmol) in DMF (25 mL) at 0ºC. The resulting solution was stirred at room temperature for 16 h. Then the mixture was diluted with EtOAc, washed with HCl (10%) and dried over anhydrous Na$_2$SO$_4$. The residue was submitted to flash chromatography (EtOAc: Hexane, 2:8) to give **E-66** (253 mg, 68 %) as a colourless oil. ^{1}H-NMR (300 MHz, CDCl$_3$): δ (ppm) = 6.75 (dt, *J* = 15.3, 7.6 Hz, 1H), 1H), 5.85 (d, *J* = 15.6 Hz, 1H), 5.72 - 5.52 (m, 2H), 4.53 (d, *J* = 4.9 Hz, 2H), 4.17 (q, *J* = 7.1 Hz, 2H), 3.72 (s, 6H), 3.70 (s, 3H), 2.79 - 2.67 (m, 2H), 2.64 (d, *J* = 5.9 Hz, 2H), 1.27 (t, *J* = 7.1 Hz, 3H); ^{13}C-NMR (75 MHz, CDCl$_3$): δ (ppm) = 170.4 (C), 166.2 (C), 154.9 (C), 142.4 (CH), 129.2 (CH), 128.7 (CH), 124.9 (CH), 67.5 (CH$_2$), 64.0 (CH$_2$), 57.3 (C), 52.7 (CH$_3$), 51.6 (CH$_3$), 36.0 (CH$_2$), 35.6 (CH$_2$), 14.3 (CH$_3$); EI-HRMS *m/z* calcd. for C$_{17}$H$_{24}$O$_9$ [M]$^+$: 372.1420; found: 372.1418.
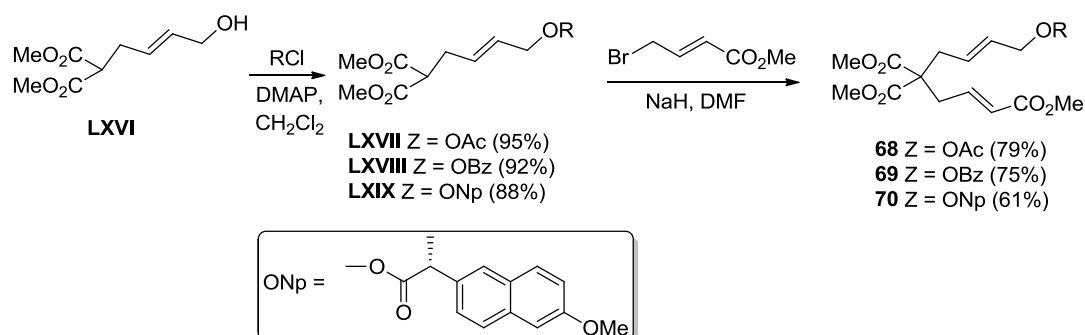
Compound LXVII. Ac$_2$O (102 mg, 1 mmol) was added to a solution of compound **LXVI** (202 mg, 1 mmol) and DMAP (121 mg, 1mmol) in CH$_2$Cl$_2$ (15mL). The mixture was stirred for 1h and then solvent was removed. The residue was submitted to flash chromatography (EtOAc:Hexane, 2:8) to give **LXVII** (232 mg, 95%) as a colourless oil. ^{1}H NMR (300 MHz, CDCl$_3$): δ (ppm) = 5.72 - 5.64 (m, 2H), 4.48 (d, *J* = 4.9 Hz, 2H), 3.73 (s, 6H), 3.44 (t, *J* = 7.5 Hz, 1H), 2.69 - 2.60 (m, 2H), 2.04 (s, 3H); ^{13}C NMR (75 MHz, CDCl$_3$): δ (ppm) = 169.2 (C), 130.8 (CH), 127.4 (CH), 64.6 (CH$_2$), 52.7 (CH$_3$), 51.4 (CH), 31.6 (CH$_2$), 21.1 (CH$_3$); EI-HRMS *m/z* calcd. for C$_{11}$H$_{17}$O$_6$ [M+1]$^+$: 245.1025; found: 245.1017

Compound LXVIII. Benzoyl chloride (140 mg, 1mmol) was added to a solution of compound **LXVI** (202 mg, 1 mmol) and DMAP (121 mg, 1 mmol) in CH$_2$Cl$_2$ (15mL). The mixture was stirred for 1h and then solvent was removed. The residue was submitted to flash chromatography (EtOAc:Hexane, 2:8) to give **LXVIII** (281 mg, 92%) as a colourless oil. ^{1}H NMR (300 MHz, CDCl$_3$): δ (ppm) = 8.02 (d, *J* = 8.4 Hz, 2H), 7.54 (t, *J* = 7.4 Hz, 1H), 7.42 (t, *J* = 7.6 Hz, 2H), 5.80 (m, 2H), 4.74 (d, *J* = 4.0 Hz, 2H), 3.72 (s, 6H), 3.47 (t, *J* = 7.5 Hz, 1H), 2.70-2.62 (m, 2H); ^{13}C NMR (75 MHz, CDCl$_3$): δ (ppm) = 169.2 (2xC), 166.3 (C), 133.1 (CH), 130.9 (CH), 130.3 (C), 129.7 (2xCH), 128.5 (2xCH), 127.5 (CH), 65.0 (CH$_2$), 52.6 (2xCH$_3$), 51.4 (CH), 31.6 (CH$_2$); EI-HRMS *m/z* calcd. for C$_{16}$H$_{18}$O$_6$ [M]$^+$: 306.1103; found: 306.1103.

Compound LXIX. (*R*)-2-(6-Methoxynaphthalen-2-yl)propanoyl chloride (248 mg, 1mmol) was added to a solution of compound **LXVI** (202 mg, 1 mmol) and DMAP (121 mg, 1 mmol) in CH$_2$Cl$_2$ (15mL). The mixture was stirred for 3h and then solvent was removed. The residue was submitted to flash chromatography (EtOAc:Hexane, 2:8) to give **LXIX** (364 mg, 88%) as a colourless oil. ^{1}H NMR (300 MHz,

CDCl$_3$): δ (ppm) = 7.68 (m, 2H), 7.41 (d, J = 1.7 Hz, 1H), 7.38 (d, J = 1.7 Hz, 1H), 7.15 (d, J = 2.4 Hz, 1H), 7.12 (d, J = 3.8 Hz, 1H), 5.59 (m, 2H), 4.55 - 4.40 (m, 2H), 3.90 (s, 3H), 3.84 (q, J = 7.1 Hz, 1H), 3.68 (s, 6H), 3.36 (t, J = 7.6 Hz, 1H), 2.63 - 2.54 (m, 2H), 1.57 (d, J = 7.2 Hz, 3H). ^{13}C NMR (75 MHz, CDCl$_3$): δ (ppm) = 174.3 (C), 169.1 (2xC), 157.7 (C), 135.7 (C), 133.8 (C), 130.5 (CH), 129.3 (CH), 129.0 (C), 127.3 (CH), 127.2 (CH), 126.3 (CH), 126.0 (CH), 119.1 (CH), 105.7 (CH), 64.8 (CH$_2$), 55.4 (CH$_3$), 52.5 (2xCH$_3$), 51.3 (CH), 45.8 (CH), 31.5 (CH$_2$), 18.6 (CH$_3$); EI-HRMS m/z calcd. for C$_{23}$H$_{26}$O$_7$ [M]$^+$: 414.1679; found: 414.1681.

Compound 68. Methyl 4-bromocrotonate (220 mg, 1.23 mmol) was added to a mixture of NaH (49 mg, 1.23 mmol) and **LXVII** (200 mg, 0.82 mmol) in DMF (15 mL) at 0ºC. The resulting solution was stirred at room temperature for 16 h. Then the mixture was diluted with EtOAc, washed with HCl (10%) and dried over anhydrous Na$_2$SO$_4$. The residue was submitted to flash chromatography (EtOAc:Hexane, 2:8) to give **68** (221 mg, 79%) as a colourless oil. ^{1}H NMR (300 MHz, CDCl$_3$): δ (ppm) = 6.73 (dt, J = 15.3, 7.6 Hz, 1H), 5.84 (d, J = 15.5 Hz, 1H), 5.68 - 5.49 (m, 2H), 4.46 (d, J = 4.2 Hz, 2H), 3.70 (bs, 9H), 2.72 (d, J = 7.2 Hz, 2H), 2.61 (d, J = 5.6 Hz, 2H), 2.02 (s, 3H); ^{13}C NMR (75 MHz, CDCl$_3$): δ (ppm) = 170.5 (3xC), 166.2 (C), 142.5 (CH), 129.3 (CH), 128.6 (CH), 125.0 (CH), 64.4 (CH$_2$), 57.3 (C), 52.7 (2xCH$_3$), 51.6 (CH$_3$), 36.0 (CH$_2$), 35.6 (CH$_2$), 20.9 (CH$_3$); EI-HRMS m/z calcd. for C$_{16}$H$_{22}$O$_8$ [M]$^+$: 342.1315; found: 342.1304

Compound 69. Methyl 4-bromocrotonate (220 mg, 1.23 mmol) was added to a mixture of NaH (49 mg, 1.23 mmol) and **LXVIII** (250 mg, 0.82 mmol) in DMF (15 mL) at 0ºC. The resulting solution was stirred at room temperature for 16 h. Then the mixture was diluted with EtOAc, washed with HCl (10%) and dried over anhydrous Na$_2$SO$_4$. The residue was submitted to flash chromatography (EtOAc:Hexane, 2:8) to give **69** (248 mg, 75%) as a colourless oil. ^{1}H NMR (300 MHz, CDCl$_3$): δ (ppm) = 7.96 (d, J = 8.4 Hz, 2H), 7.43 (t, J = 7.4 Hz, 1H), 7.33 (t, J = 7.6 Hz, 2H), 6.72 (dt, J = 15.3, 7.6 Hz, 1H), 5.82 (d, J= 15.5 Hz, 1H), 5.76 - 5.56 (m, 2H), 4.68 (d, J = 4.2 Hz, 2H), 3.65 (bs, 9H), 2.72 (d, J = 7.2 Hz, 2H), 2.62 (d, J = 5.6 Hz, 2H). ^{13}C NMR (75 MHz, CDCl$_3$): δ (ppm) = 170.3 (3xC), 165.9 (C), 142.3 (CH), 132.8 (CH), 130.1 (C), 129.4 (2xCH), 129.1 (CH), 128.6 (CH), 128.3 (2xCH), 124.8 (CH), 64.7 (CH$_2$), 57.1 (C), 52.5 (2xCH$_3$), 51.3 (CH$_3$), 35.9 (CH$_2$), 35.5 (CH$_2$); EI-HRMS m/z calcd. for C$_{21}$H$_{24}$O$_8$ [M]$^+$: 404.1471; found: 404.1755.

Compound 70. Methyl 4-bromocrotonate (193 mg, 1.08 mmol) was added to a mixture of NaH (43 mg, 1.08 mmol) and **LXIX** (300 mg, 0.72 mmol) in DMF (15 mL) at 0ºC. The resulting solution was stirred at room temperature for 16 h. Then the mixture was diluted with EtOAc, washed with HCl (10%) and dried over anhydrous Na$_2$SO$_4$. The residue was submitted to flash chromatography (EtOAc:Hexane, 2:8) to give **5** (225 mg, 61%) as a colourless oil. ^{1}H NMR (300 MHz, CDCl$_3$): δ (ppm) = 7.66 (m, 2H), 7.41 (d, J = 1.8 Hz, 1H), 7.38 (d, J = 1.8 Hz, 1H), 7.14 (d, J = 2.4 Hz, 1H), 7.11 (d, J = 2.2 Hz, 1H), 6.71 (m, 1H), 5.78 (d, J = 15.5 Hz, 1H), 5.66 - 5.41 (m, 2H), 4.50 (d, J = 5.7 Hz, 2H), 3.90 (s, 3H), 3.85 (q, J = 7.1 Hz, 1H), 3.71 (s, 3H), 3.66 (s, 3H), 3.65 (s, 3H), 2.63 (d, J = 6.9 Hz, 2H), 2.58 (d, J = 6.8 Hz, 2H), 1.57 (d, J = 7.2 Hz, 3H); ^{13}C NMR (75 MHz, CDCl$_3$): δ (ppm) = 174.2 (C), 170.4 (2xC), 166.2 (C), 157.7 (C), 142.4 (CH), 135.6 (C), 133.7 (C), 129.3 (CH), 129.1 (CH), 128.9 (C), 128.3 (CH), 127.2 (CH), 126.2 (CH), 126.0 (CH), 124.8 (CH), 119.0 (CH), 105.6 (CH), 64.6 (CH$_2$), 57.3 (C), 55.3 (CH$_3$), 52.6 (2xCH$_3$), 51.6 (CH), 45.5 (CH$_3$), 35.9 (CH$_2$), 35.4 (CH$_2$), 18.5 (CH$_3$); EI-HRMS m/z calcd. for C$_{28}$H$_{32}$O$_9$ [M]$^+$: 512.2046; found: 512.2042.

LXX Z = CO$_2$tBu (78%)
LXXI Z = COMe (95%)

71 Z = CO$_2$tBu (89%)
73 Z = COMe (76%)

GP8

72 Z = CO$_2$tBu (73%, cis:trans= 5:1)
74 Z = COMe (63%, cis:trans= 6:1)
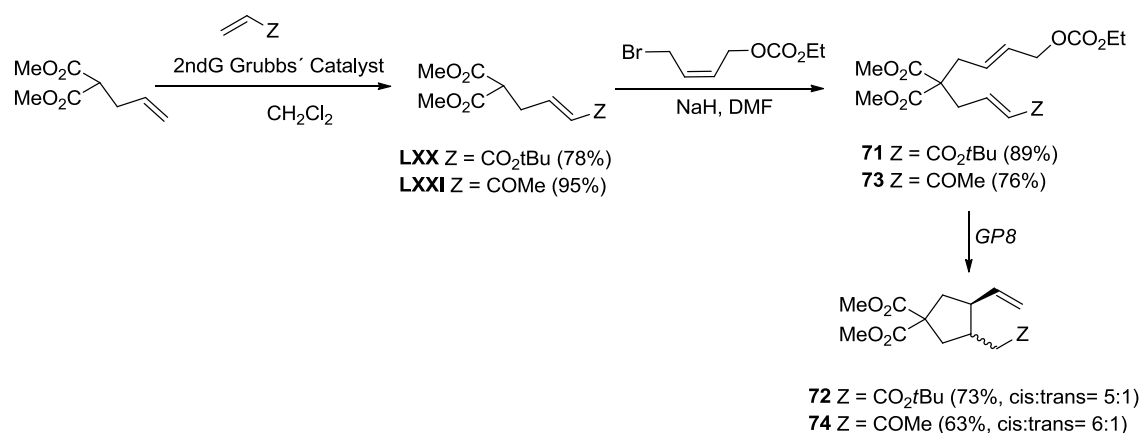
Compound LXX. *Tert*-butylacrylate (0.192 g, 1.5 mmol) was added to a solution of Grubb´s 2nd generation catalyst (21 mg, 0.025 mmol) and allyldimethylmalonate (86 mg, 0.5 mmol) in CH$_2$Cl$_2$ (5 ml) and the mixture was stirred under reflux for 24h. The solvent was removed and the residue was submitted to flash chromatography (EtOAc: Hexane, 2:8) to give **LXX** (106 mg, 78 %) as a colourless oil.

^{1}H-NMR (400 MHz, CDCl$_3$): δ (ppm) = 6.71 (dt, J = 15.2, 7.1 Hz, 1H), 5.77 (d, J = 15.6 Hz, 1H), 3.71 (s, 6H), 3.47 (t, J = 7.4 Hz, 1H), 2.73 (dd, J = 10.4, 4.0 Hz, 2H), 1.43 (d, J = 6.3 Hz, 9H); ^{13}C-NMR (101 MHz, CDCl$_3$): δ (ppm) = 168.8 (2xC), 165.4 (C), 142.3 (CH), 125.7 (CH), 80.5 (C), 52.8 (2xCH$_3$), 50.5 (CH), 31.0 (CH$_2$), 28.1 (3xCH$_3$); EI-HRMS m/z calcd. for C$_{13}$H$_{21}$O$_6$ [M+1]$^+$: 273.1338; found: 273.1344.

Compound 71. A sample of (Z)-BrCH$_2$CH=CHCH$_2$CO$_2$Et[445] (120 mg, 0.54 mmol) was added to a mixture of NaH (22 mg, 0.54 mmol) and **LXX** (98 mg, 0.36 mmol) in DMF (5 mL) at 0ºC. The resulting solution was stirred at room temperature for 16h. Then the mixture was diluted with EtOAc, washed with HCl (10%) and dried over anhydrous Na$_2$SO$_4$. The residue was submitted to flash chromatography (EtOAc: Hexane, 2:8) to give **71** (132 mg, 89 %) as a colourless oil. ^{1}H-NMR (500 MHz, CDCl$_3$): δ (ppm) = 6.63 (dtd, J = 12.1, 7.7, 4.4 Hz, 1H), 5.79 (d, J = 15.5 Hz, 1H), 5.73 – 5.64 (m, 1H), 5.56 – 5.47 (m, 1H), 4.64 (d, J = 6.8 Hz, 2H), 4.18 (q, J = 7.1 Hz, 2H), 3.73 (s, J = 3.7 Hz, 6H), 2.75 (d, J = 7.7 Hz, 2H), 2.70 (d, J = 7.8 Hz, 2H), 1.46 (s, 9H), 1.29 (t, J = 7.1 Hz, 3H); ^{13}C-NMR (126 MHz, CDCl$_3$): δ (ppm) = 170.6 (2xC=O), 165.2 (C=O), 155.2 (C=O), 140.7 (CH), 128.0 (CH), 127.5 (CH), 127.3 (CH), 80.6 (C), 64.2 (CH$_2$), 63.2 (CH$_2$), 57.3 (C), 52.9 (CH$_3$), 52.8 (CH$_3$), 35.7 (CH$_2$), 31.3 (CH$_2$), 28.2 (3x CH$_3$), 14.4 (CH$_3$); EI-HRMS m/z calcd. for C$_{20}$H$_{31}$O$_9$ [M+1]$^+$: 415.1958; found: 415.1960.

Compound 72 was prepared from **71** according to previously described *GP8* to give **72** in 73 % yield. Mixture of isomers ≈ 5:1 (*cis:trans*). ^{1}H-NMR (500 MHz, CDCl$_3$): δ (ppm) = 5.66 (ddd, J = 16.7, 10.6, 8.7 Hz, 1H, major isomer), 5.62 – 5.56 (m, 1H, minor isomer), 5.06 – 4.97 (m, 2H), 3.71 (s, 3H), 3.71 (s, 3H), 2.83 – 2.75 (m, 1H, major isomer), 2.66 – 2.60 (m, 1H, minor isomer), 2.52 (d, J = 7.4 Hz, 1H), 2.50 – 2.47 (m, 2H), 2.45 (t, J = 6.5 Hz, 1H), 2.23 (dd, J = 15.9, 6.9 Hz, 1H), 2.17 (dd, J = 14.1, 6.3 Hz, 1H), 2.09 (dd, J = 16.0, 8.0 Hz, 1H), 2.06 – 1.97 (m, 2H); ^{13}C-NMR (126 MHz, CDCl$_3$): δ (ppm) = 173.1 (C, minor isomer) 173.01 (C, major isomer), 172.97 (C, major isomer), 172.9 (C, minor isomer), 172.1 (C, major isomer), 172.0 (C, minor isomer), 139.4 (CH, minor isomer), 137.6 (CH, major isomer), 116.4 (CH$_2$), 80.5 (C, minor isomer), 80.4 (C, major isomer), 59.0 (C, major isomer), 58.5 (C, minor isomer), 52.92 (CH$_3$, minor isomer), 52.87 (2xCH$_3$, major isomer), 52.85 (CH$_3$, minor isomer), 50.1 (CH, minor isomer), 45. 9 (CH, major isomer), 41.7 (CH, minor isomer), 40.5 (CH$_2$, minor isomer), 39.9 (CH$_2$, minor isomer), 39.3 (CH, major isomer), 39.2 (CH$_2$, major isomer), 39.1 (CH$_2$, minor isomer), 38.9 (CH$_2$, major isomer), 36.8 (CH$_2$, major isomer), 28.23 (CH$_3$), 28.21 (CH$_3$, major isomer); EI-HRMS calcd for C$_{17}$H$_{27}$O$_6$ [M$^+$+1]: 327.1808; found:327.1806.

Compound 73. Methyl vinyl ketone (0.43 g, 5.2 mmol) was added to a solution of the Grubb´s 2nd generation catalyst ((210 mg, 0.25 mmol)) and the allyldimethylmalonate derivative **LXXI** (300 mg, 1.74 mmol) in CH$_2$Cl$_2$ (10 mL) and the mixture was stirred under reflux for 24h. The solvent was removed and the residue was submitted to flash chromatography (EtOAc: Hexane, 2:8) to give **73** (353 mg, 95 %) as a colourless oil. ^{1}H-NMR (500 MHz, CDCl$_3$): δ (ppm) = 6.68 – 6.58 (m, 1H), 6.09 (d, J = 15.9 Hz, 1H), 5.73 – 5.59 (m, 2H), 4.55 (d, J = 5.6 Hz, 2H), 4.19 (q, J = 7.1 Hz, 2H), 3.73 (s, 6H), 2.75 (dd, J = 7.6, 0.9 Hz, 2H), 2.66 (d, J = 6.6 Hz, 2H), 2.23 (s, J = 4.6 Hz, 3H), 1.30 (t, J = 7.1 Hz, 3H).^{13}C-NMR (126 MHz, CDCl$_3$): δ (ppm) = 198.1 (C), 170.6 (2xC), 155.1 (C), 141.4 (CH), 134.7 (CH), 129.3 (CH), 128.9 (CH), 67.6 (CH$_2$), 64.2 (CH$_2$), 57.5 (C), 52.9 (2xCH$_3$), 36.4 (CH$_2$), 36.2 (CH$_2$), 27.2 (CH$_3$), 14.4 (CH$_3$); EI-HRMS m/z calcd. for C$_{14}$H$_{18}$O$_5$ [M - OCO$_2$Et]$^+$: 266.1154; found: 266.1150.

Compound 74 was prepared from **72** according to previously described *GP8* to give **74** in 63 % yield. Mixture of isomers ≈ 6:1 (*cis:trans*). ^{1}H-NMR (500 MHz, CDCl$_3$): δ (ppm) = 5.69 – 5.58 (m, 1H), 5.07 – 4.94 (m, 2H), 3.721 (s, 3H), 3.716 (s, 3H), 2.85 – 2.76 (m, 1H), 2.62 (ddd, J = 19.5, 10.2, 6.1 Hz, 1H), 2.55 (dd, J = 13.9, 7.2 Hz, 1H), 2.50 – 2.41 (m, 2H), 2.33 (dd, J = 17.4, 7.4 Hz, 1H), 2.13 (dd, J = 12.5, 4.9 Hz, 1H), 2.09 (s, 3H), 1.97 (dd, J = 13.7, 9.2 Hz, 1H); ^{13}C-NMR (126 MHz, CDCl$_3$): δ (ppm) = 207.7 (C), 173.2 (C), 173.0 (C), 137.9 (CH), 116.3 (CH$_2$), 58.9 (C), 53.0 (CH$_3$), 52.9 (CH$_3$), 45.7 (CH$_2$), 44.5 (CH$_2$), 39.3 (CH$_2$), 38.89 (CH$_2$), 38.0 (CH$_2$), 30.6 (CH$_3$).
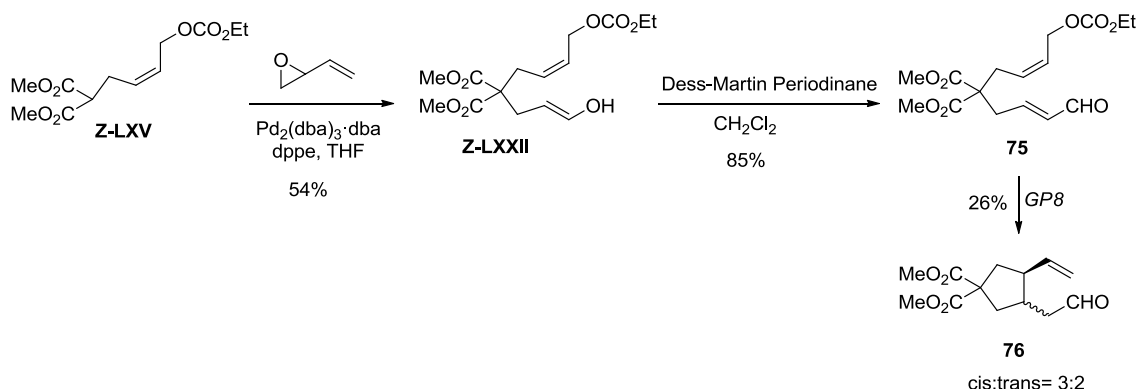
Compound Z-LXXII. Butadiene monoxide (0.02 mL, 0.38 mmol) was added to a solution of **Z-LXV** (100 mg, 0.38 mmol), Pd(dba)$_3$·dba (3 mg, 0.019 mmol) and dppe (8 mg, 0.019 mmol) in THF (10 mL). The resulting mixture was stirred at room temperature for 16 h and then solvent was removed. The residue was filtered through a short silica pad to give **Z-LXXII** (71 mg, 54 %) as a colourless oil. ^{1}H-NMR (400 MHz, CDCl$_3$): δ (ppm) = 5.77 – 5.49 (m, 4H), 4.54 (d, J = 4.2 Hz, 2H), 4.19 (q, J = 14.2, 7.1 Hz, 2H), 4.08 (d, J = 5.6 Hz, 2H), 3.71 (s, 6H), 2.64 (m, J = 12.3, 8.5 Hz, 4H), 1.30 (t, J = 7.1 Hz, 3H); ^{13}C-NMR (101 MHz, CDCl$_3$): δ (ppm) = 171.2 (2xC), 155.2 (C), 134.6 (CH), 130.1 (CH), 128.4 (CH), 125.2 (CH), 67.8 (CH$_2$), 64.2 (CH$_2$), 63.1 (CH$_2$), 58.0 (C), 52.8 (CH$_3$), 52.7 (CH$_3$), 35.8 (CH$_2$), 35.7 (CH$_2$), 14.5 (CH$_3$); EI-HRMS m/z calcd. for C$_{14}$H$_{21}$O$_6$ [M-CO$_2$Me]$^+$: 285.1338; found: 285.1341.

Compound 75. Dess-Martin periodinane (DMP) (148 mg, 0.35 mmol) was added to a solution of **Z-LXXII** (100 mg, 0.29 mmol) in CH$_2$Cl$_2$ (20 mL). The resulting mixture was stirred for 3 h at room temperature and then washed with saturated aqueous solution of Na$_2$S$_2$O$_3$ and NaHCO$_3$ in 1:1 proportion, dried over anhydrous Na$_2$SO$_4$ and the solvent removed. The residue was submitted to flash chromatography (EtOAc: Hexane, 2:8) to give **75** (84 mg, 85 %) as a colourless oil; ^{1}H-NMR (500 MHz, CDCl3): δ (ppm) = 9.49 (d, J = 7.8 Hz, 1H), 6.77 – 6.65 (m, 1H), 6.13 (d, J = 7.8 Hz, 1H), 5.66 (dd, J = 10.5, 6.1 Hz, 2H), 4.54 (d, J = 5.6 Hz, 2H), 4.19 (q, J = 7.1 Hz, 2H), 3.73 (s, 6H), 2.85 (d, J = 7.4 Hz, 2H), 2.67 (d, J = 6.8 Hz, 2H), 1.30 (t, J = 7.1 Hz, 3H); ^{13}C-NMR (126 MHz, CDCl$_3$): δ (ppm) = 193.4 (C), 170.4 (2xC), 155.9 (C), 151.4 (CH), 136.1 (CH), 129.1 (CH), 129.0 (CH), 67.5 (CH$_2$), 64.2 (CH$_2$), 57.4 (C), 53.0 (CH$_3$), 52.9 (CH$_3$), 36.6 (CH$_2$), 36.3 (CH$_2$), 14.4 (CH$_3$); EI-HRMS m/z calcd. for C$_{13}$H$_{17}$O$_5$ [M-OCO$_2$Et]$^+$: 253.1076; found: 253.1071.

Compound 76 was prepared from **75** according to previously described *GP8* to give **75** in 26 % yield. Mixture of isomers ≈ 3:2 (*cis:trans*). ^{1}H-NMR (500 MHz, CDCl$_3$): δ (ppm) = 9.75 (t, J = 2.0 Hz, 1H, minor isomer), 9.74 (t, J = 1.4 Hz, 1H, major isomer), 5.63 (dddd, J = 18.2, 17.2, 10.2, 8.4 Hz, 1H), 5.10 – 4.98 (m, 2H), 3.74 (s, 3H, major isomer), 3.73 (s, 3H, minor isomer), 3.73 (s, 3H), 2.88 – 2.80 (m, 1H), 2.70 – 2.60 (m, 2H), 2.56 (dd, J = 14.2, 7.4 Hz, 1H), 2.53 – 2.46 (m, 2H), 2.38 – 2.29 (m, 1H), 2.21 – 2.14 (m, 1H), 2.04 (ddd, J = 19.4, 13.6, 10.0 Hz, 1H); ^{13}C-NMR (126 MHz, CDCl$_3$): δ (ppm) = 201.5 (C), 201.4 (C), 173.0 (2xC), 172.9 (C), 172.8 (C), 139.1 (CH, minor isomer), 137.6 (CH, major isomer), 116.9 (CH$_2$, minor isomer), 116.8 (CH$_2$, major isomer), 59.0 (C), 58.7 (C), 53.03 (CH$_3$), 52.98 (CH$_3$), 50.4 (CH), 47.5 (CH$_2$), 45.9 (CH), 45.1 (CH$_2$), 40.4 (CH$_2$), 40.0 (CH$_2$), 39.5 (CH), 39.3 (CH$_2$), 38.9 (CH$_2$), 37.1 (CH), 29.8 (CH$_2$); EI-HRMS m/z calcd. for C$_{13}$H$_{18}$O$_5$ [M]$^+$: 254.1154; found: 254.1155.

195
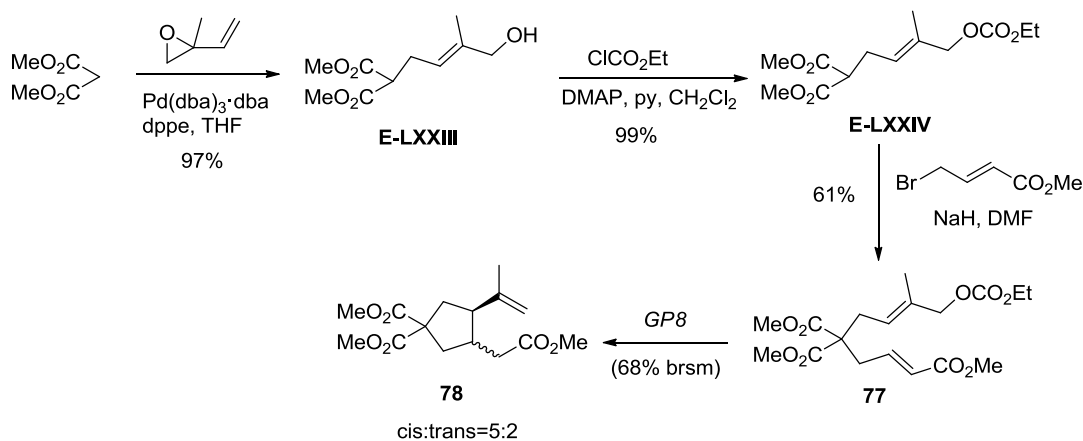
Compound E-LXXIII. Isoprene monoxide (191 mg, 2.27 mmol) was added to a solution dimethylmalonate (300 mg, 2.27 mmol), Pd$_2$(dba)$_3$·dba (20 mg, 0.11 mmol) and dppe (44 mg, 0.11 mmol) in THF (10 mL). The resulting mixture was stirred at room temperature for 3 h and then solvent was removed. The residue was filtered through a short silica pad to give **E-LXXIII** (476 mg, 97%) as colourless oil.

Compound E-LXXIV. Ethyl chloroformiate (285 mg, 2.64 mmol) was added to a solution of **E-LXXIII** (476 mg, 2.20 mmol), dimethylaminopyridine (DMAP) (81 mg, 0.66 mmol), pyridine (521 mg, 6.6 mmol) in CH$_2$Cl$_2$, and it was stirred at room temperature for 16 h. Then the mixture was diluted with CH$_2$Cl$_2$, washed with HCl (10%), NaOH (10%) and brine and dried over anhydrous Na$_2$SO$_4$. The residue was submitted to flash chromatography (EtOAc:Hexane, 4:6) to give **E-LXXIV** (628 mg, 99%) as a colourless oil. Its spectroscopic data were identical to the reported compound.

Compound 77. Methyl 4-bromocrotonate (585 mg, 3.27 mmol) was added to a mixture of NaH (131 mg, 3.27 mmol) and **E-LXXIV** (628 mg, 2.18 mmol) in DMF (15 mL) at 0ºC. The resulting solution was stirred at room temperature for 16 h. Then the mixture was diluted with EtOAc, washed with HCl (10%) and dried over anhydrous Na$_2$SO$_4$. The residue was submitted to flash chromatography (EtOAc:Hexane, 4:6) to give **77** (513 mg, 61%) as a yellow oil (mixture of isomers ≈1.5:1). ^{1}H NMR (500 MHz, CDCl$_3$): δ (ppm) = 6.81 - 6.73 (m, 2H), 5.87 (dd, J = 3.9, 2.5 Hz, 1H, major isomer), 5.84 (dd, J = 3.9, 2.5 Hz, 1H, minor isomer), 5.33 (dd, J = 8.1, 6.8 Hz, 1H, minor isomer), 5.25 (dd, J = 8.1, 6.8 Hz, 1H, major isomer), 4.59 (s, 2H, major isomer), 4.48 (s, 2H, minor isomer), 4.20 (q, J = 7.1 Hz, 4H), 3.73 (s, 12H), 3.71 (s, 6H), 2.76 (d, J = 7.7 Hz, 4H), 2.70 (d, J = 7.8 Hz, 2H, major isomer), 2.66 (d, J = 7.1 Hz, 2H, minor isomer), 1.78 (s, 3H, major isomer), 1.67 (s, 3H, minor isomer), 1.31 (t, J = 7.1 Hz, 6H); ^{13}C NMR (126 MHz, CDCl$_3$): δ (ppm) = 170.8 (2xC), 166.3 (C), 155.3 (C), 142.7 (CH), 134.4 (C), 125.0 (CH), 123.6 (CH, major isomer), 122.5 (CH, minor isomer), 72.9 (CH$_2$), 65.9 (CH$_2$, major isomer), 64.2 (CH$_2$, minor isomer), 57.5 (C), 52.9 (2xCH$_3$), 51.7 (CH$_3$), 35.7(CH$_2$), 31.6 (CH$_2$), 21.7 (CH$_3$), 14.4 (CH$_3$). EI-HRMS m/z calcd. for C$_{18}$H$_{26}$O$_9$ [M]$^+$: 386.1577; found: 386.1581.

Compound 78 was prepared from **77** according to previously described *GP8* to give **78** in 68 % yield. Mixture of isomers ≈ 5:2 (*cis:trans*). ^{1}H NMR (500 MHz, CDCl$_3$): δ (ppm)= 4.86 (s, 1H, major isomer), 4.79 (s, 1H, minor isomer), 4.76 (s, 1H, minor isomer), 4.69 (s, 1H, major isomer), 3.73 (s, 6H, minor isomer), 3.72 (s, 6H, major isomer), 3.64 (s, 3H, major isomer), 3.63 (s, 3H, minor isomer), 2.72 − 2.58 (m, 2H), 2.54 (dd, J = 14.4, 7.0 Hz, 1H), 2.45 (dd, J = 15.4, 4.3 Hz, 1H, minor isomer), 2.39 (dd, J = 13.4, 6.1 Hz, 1H, major isomer), 2.25 − 2.18 (m, 2H), 2.17 (d, J = 4.4 Hz, 1H), 2.14 (d, J = 4.1 Hz, 1H), 2.04 (dd, J = 16.1, 10.4 Hz, 1H, major isomer) 1.97 − 1.89 (m, 1H, minor isomer), 1.71 (s, 3H, major isomer), 1.67 (s, 3H, minor isomer); ^{13}C NMR (126 MHz, CDCl$_3$): δ (ppm)= 173.7 (C), 173.1 (2xC), 144.0 (C, minor isomer), 143.6 (C, major isomer), 112.9 (CH$_2$, minor isomer), 111.8 (CH$_2$, major isomer), 58.3 (C), 53.1 (CH3, minor isomer), 53.0 (CH$_3$, major isomer), 51.6 (CH), 48.9 (2xCH$_3$), 39.9 (CH$_2$, minor isomer), 39.4 (CH$_2$), 39.1 (CH$_2$, minor isomer), 38.9 (CH, minor isomer), 37.9 (CH$_2$, minor isomer), 37.1 (CH major isomer), 36.1 (CH$_2$), 34.4 (CH$_2$), 23.2 (CH$_3$); EI-HRMS m/z calcd. for C$_{15}$H$_{22}$O$_6$ [M]$^+$: 298.1416; found: 298.1412.
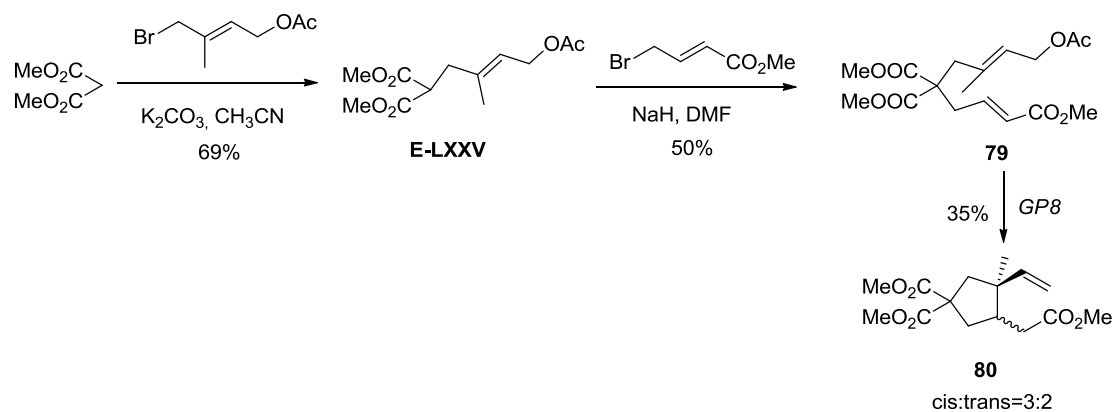
Compound E-LXXV. In a round-bottom flask dimethylmalonate (660 mg, 5 mmol), K$_2$CO$_3$ (760 mg, 5.5 mmol), *trans*-4-acetoxy-1-bromo-2-methyl-2-butene (1.13 g, 5.5 mmol), and CH$_3$CN (15 mL) were placed. The resulting mixture was stirred under reflux for 16 h. Then K$_2$CO$_3$ was filtered and the solvent was removed. The residue was submitted to flash chromatography (EtOAc: Hexane, 2:8) to give **E-LXXV**

(894mg, 69 %) as a colourless oil. ^{1}H-NMR (400 MHz, CDCl$_3$): δ (ppm) = 5.34 (t, J = 6.3 Hz, 1H), 4.50 (d, J = 6.9 Hz, 2H), 3.69 (s, 6H), 3.55 (t, J = 7.9 Hz, 1H), 2.60 (d, J = 7.7 Hz, 2H), 1.99 (s, 3H), 1.68 (s, 3H); ^{13}C-NMR (101 MHz, CDCl$_3$): δ (ppm) = 170.9 (C), 169.3 (2xC), 137.6 (C), 121.4 (CH), 60.9 (CH$_2$), 52.6 (CH$_3$), 50.3 (CH), 38.3 (CH$_2$), 21.0 (CH$_3$), 16.3 (CH$_3$).

Compound 79. Methyl 4-bromocrotonate (107mg, 0.6 mmol) was added to a mixture of NaH (30 mg, 0.75 mmol) and **E-LXXV** (125 mg, 0.5 mmol) in DMF (5 mL) at 0ºC. The resulting solution was stirred at room temperature for 16 h. Then the mixture was diluted with EtOAc, washed with aqueous NH$_4$Cl, dried over anhydrous Na$_2$SO$_4$, and the solvent removed. The residue was submitted to flash chromatography (EtOAc: Hexane, 2:8) to give **79** (90 mg, 50%) as a colourless oil. ^{1}H-NMR (500 MHz, CDCl$_3$): δ (ppm) = 6.78 (tt, J = 15.4, 7.6 Hz, 1H), 5.87 (t, J = 15.9 Hz, 1H), 5.43 – 5.33 (m, 1H), 4.55 (d, J = 6.8 Hz, 2H), 3.72 (s, 6H), 3.72 (s, 3H), 2.75 (dd, J = 7.6, 1.2 Hz, 2H), 2.72 (d, J = 6.0 Hz, 2H), 2.04 (s, 3H), 1.62 (s, 3H); ^{13}C-NMR (126 MHz, CDCl$_3$): δ (ppm) = 171.0 (2xC), 166.3 (C), 142.9 (CH), 136.0 (C), 125.0 (CH), 124.9 (CH), 124.2 (C), 61.0 (CH$_2$), 57.3 (C), 52.8 (2xCH$_3$), 51.7 (CH$_3$), 42.8 (CH$_2$), 35.7 (CH$_2$), 21.0 (CH$_3$), 17.2 (CH$_3$); EI-HRMS m/z calcd. for C$_{17}$H$_{24}$O$_8$ [M]$^+$: 356.1471; found: 356.1462.

Compound 80 was prepared from **79** according to previously described *GP8* to give **80** in 35 % yield. Mixture of isomers ≈ 3:2 (*cis:trans*). ^{1}H-NMR (500 MHz, CDCl$_3$): δ (ppm) = 5.73 (dd, J = 17.4, 10.8 Hz, 1H), 5.06 – 4.94 (m, 2H), 3.72 (s, 6H, minor isomer), 3.72 (s, 6H, major isomer), 3.65 (s, 3H, minor isomer), 3.63 (s, 3H, major isomer), 2.61 – 2.43 (m, 2H), 2.35 (d, J = 14.0 Hz, 1H), 2.28 (dt, J = 9.0, 3.8 Hz, 2H), 2.25 – 2.03 (m, 5H), 1.13 (s, J = 12.7 Hz, 2H), 0.88 (s, J = 14.0 Hz, 2H); ^{13}C-NMR (126 MHz, CDCl$_3$): δ (ppm) = 173.5 (C), 173.3 (C), 173.2 (C), 173.04 (C), 172.97 (C), 145.7 (CH, major isomer), 141.5 (CH, minor isomer), 113.8 (CH$_2$, minor isomer), 113.09 (CH$_2$, major isomer), 57.9 (C), 57.8 (C), 53.1 (CH$_3$), 52.9 (CH$_3$), 51.69 (CH$_3$), 51.66 (CH$_3$), 47.6 (CH$_2$), 47.4 (C), 47.3 (C), 46.2 (CH$_2$), 46.11 (CH), 44.7 (CH), 39.4 (CH$_2$), 38.7 (CH$_2$), 34.8 (CH$_2$), 34.1 (CH$_2$), 24.1 (CH$_3$), 17.6 (CH$_3$); EI-HRMS m/z calcd. for C$_{15}$H$_{22}$O$_6$ [M]$^+$: 298.1416; found:298.1420.
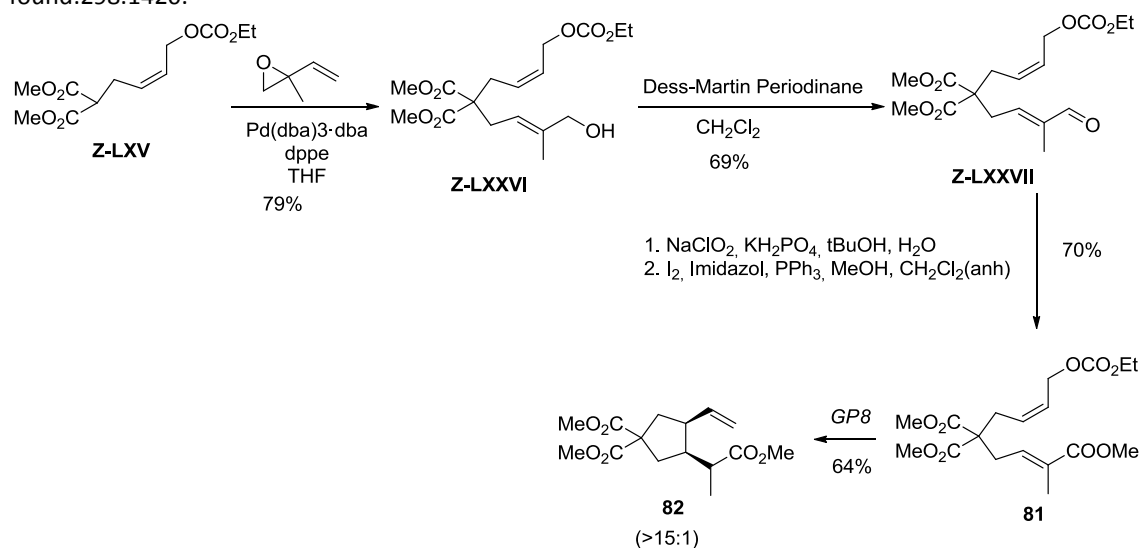
Compound Z-LXXVI. Isoprene monoxide (0.04 mL, 0.38 mmol) was added to a solution of the dimethylmalonate derivative **Z-LXV** (100 mg, 0.038 mmol), Pd(dba)$_3$·dba (6 mg, 0.1 mmol) and dppe (16 mg, 0.038 mmol) in THF (10 mL) and the mixture was stirred at room temperature for 16 h. The solvent was removed and the residue was submitted to flash chromatography (EtOAc: Hexane,) to give **Z-LXXVI** (105 mg, 79 %) as a colourless oil. ^{1}H-NMR (400 MHz, CDCl$_3$): δ (ppm) = 5.74 – 5.58 (m, J = 5.5 Hz, 2H), 5.11 (t, J = 8.3 Hz, 1H), 4.53 (d, J = 4.8 Hz, 2H), 4.17 (q, J = 7.2 Hz, 2H), 4.07 (d, J = 2.3 Hz, 2H), 3.71 (s, 6H), 2.68 – 2.56 (m, 4H), 1.79 (s, 3H), 1.30 (t, J = 7.2 Hz, 3H); ^{13}C-NMR (101 MHz, CDCl$_3$): δ (ppm) = 171.3 (C), 154.9 (C), 139 (C), 129.9 (CH), 128.1 (CH), 120.5 (CH), 120.4 (CH), 67.6 (CH$_2$), 64.0 (CH$_2$), 61.2 (CH$_2$), 57.8 (C), 52.6 (CH$_3$), 52.6 (CH$_3$), 35.8 (CH$_2$), 31.0 (CH$_2$), 21.7 (CH$_3$), 14.2 (CH$_3$); EI-HRMS m/z calcd. for C$_{14}$H$_{21}$O$_5$ [M-OCO$_2$Et]$^+$: 269.1389; found: 269.1361.

Compound Z-LXXVII. Dess-Martin periodinane (DMP) (77 mg, 0.17 mmol) was added to a solution of **Z-LXXVI** (29 mg, 0.08 mmol) in CH$_2$Cl$_2$ (5 mL). The resulting mixture was stirred for 3 h at room temperature and then washed with saturated aqueous solution of Na$_2$S$_2$O$_3$ and NaHCO$_3$ in 1:1 proportion, dried over anhydrous Na$_2$SO$_4$ and the solvent removed. The residue was submitted to flash

chromatography (EtOAc: Hexane,) to give **Z-LXXVII** (20 mg, 69 %) as a colourless oil. ^{1}H-NMR (500 MHz, CDCl$_3$): δ (ppm) = 9.39 (s, 1H), 6.35 (t, *J* = 7.3 Hz, 1H), 5.66 (m, 2H), 4.54 (d, *J* = 4.7 Hz, 2H), 4.18 (q, *J* = 7.1 Hz, 2H), 3.74 (s, 6H), 2.90 (d, *J* = 7.3 Hz, 2H), 2.69 (d, *J* = 5.8 Hz, 2H), 1.74 (s, 3H), 1.29 (t, *J* = 7.1 Hz, 3H); ^{13}C-NMR (126 MHz, CDCl$_3$): δ (ppm) = 193.4 (CH), 170.4 (2xC), 155.0 (C), 151.4 (CH), 136.1 (CH), 129.1 (CH), 129.0 (CH), 67.5 (CH$_2$), 64.2 (CH$_2$), 57.4 (C), 52.9 (2xCH$_3$), 36.6 (CH$_2$), 36.3 (CH$_2$), 29.8 (CH$_3$), 14.4 (CH$_3$); EI-HRMS *m/z* calcd. for C$_{15}$H$_{21}$O$_6$ [M-CO$_2$Me]$^+$: 297.1338; found: 297.1347.

Compound **81.** Sodium chlorite (660 mg, 7.25 mmol) and potassium dihydrogen phosphate (720 mg, 5.28 mmol) were added to a solution of **Z-LXXVII** (190 mg, 0.55 mmol) in water (4 mL) and *t*-butanol (10 mL). The resulting solution was stirred at room temperature for 16 h. Then the mixture was diluted with diethyl ether, washed with water, dried over anhydrous Na$_2$SO$_4$, and the solvent removed. In a separated flask equipped with a magnetic stir bar, a solution of iodine (183 mg, 1.05 mmol) in dry CH$_2$Cl$_2$ (10 mL) and triphenylphosphine (275 mg, 1.5 mmol) was prepared. Then, imidazole (160 mg, 3.3 mmol) was added and a white solid appeared. Subsequently, the carboxylic acid without further purification (160 mg, 0.7 mmol) and dissolved in dry CH$_2$Cl$_2$ (5 mL) was added. The resulting misture was stirred at room temperature for 16 h. Then the mixture was diluted with CH$_2$Cl$_2$, washed with 2 N HCl, dried over anhydrous Na$_2$SO$_4$, and the solvent removed. The residue was submitted to flash chromatography (EtOAc: Hexane,) to give **81** (148 mg, 70%) as a colourless oil. ^{1}H-NMR (500 MHz, CDCl$_3$): δ (ppm) = 6.53 (t, *J* = 7.4 Hz, 1H), 5.70 – 5.62 (m, 1H), 5.51 – 5.43 (m, 1H), 4.58 (d, *J* = 6.8 Hz, 2H), 4.13 (q, *J* = 7.1 Hz, 2H), 3.68 (s, 6H), 3.67 (s, 3H), 2.73 (d, *J* = 7.5 Hz, 2H), 2.68 (d, *J* = 7.7 Hz, 2H), 1.78 (s, 3H), 1.24 (t, *J* = 7.1 Hz, 3H); ^{13}C-NMR (126 MHz, CDCl$_3$): δ (ppm) = 170.7 (2xC), 167.9 (C), 155.0 (C), 134.8 (CH), 131.1 (C), 128.0 (CH), 127.4 (CH), 64.0 (CH$_2$), 63.0 (CH$_2$), 57.1 (C), 52.8 (2xCH$_3$), 51.9 (CH$_3$), 32.0 (CH$_2$), 31.2 (CH$_2$), 14.3 (CH$_3$), 12.6 (CH$_3$); EI-HRMS *m/z* calcd. for C$_{18}$H$_{26}$O$_9$ [M]$^+$: 386.1577; found: 386.1575.

Compound **82** was prepared from **81** according to previously described *GP8* to give **82** in 64 % yield. Mixture of isomers ≈ >15:1 (*cis:trans*). Only one isomer could be characterized and a C-3, C-7-*trans* stereochemistry was tentatively assigned. The stereochemistry at C-8 could not be determined. ^{1}H-NMR (300 MHz, CDCl$_3$): δ (ppm) = 5.66 (dd, *J* = 16.6, 10.1 Hz, 1H), 5.04 (d, *J* = 10.1 Hz, 1H), 5.00 (s, 1H), 3.70 (s, 6H), 3.65 (s, 3H), 2.77 (m, 1H), 2.58 (dd, *J* = 14.3, 7.3 Hz, 1H), 2.36 – 2.09 (m, 5H), 1.12 (d, *J* = 6.7 Hz, 3H). ^{13}C-NMR (75 MHz, CDCl$_3$): δ (ppm) = 176.62 (C), 173.05 (C), 172.98 (C), 137.01 (CH), 116.46 (CH2), 58.81 (C), 53.01 (CH$_3$), 52.92 (CH$_3$), 51.64 (CH$_3$), 46.64 (CH), 45.24 (CH), 40.88 (CH), 39.88 (CH$_2$), 37.32 (CH$_2$), 16.05 (CH$_3$); EI-HRMS *m/z* calcd. for C$_{15}$H$_{22}$O$_6$ [M]$^+$: 298.1416; found: 298.1415.
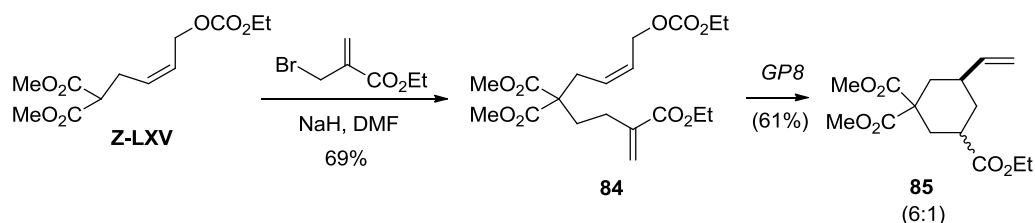
Compound **84.** Ethyl (2-bromomethyl)acrylate (212 mg, 1.1 mmol) was added to a mixture of NaH (44 mg, 1.1 mmol) and **Z-LXV** (274 mg, 1 mmol) in DMF (10 mL) at 0ºC. The resulting solution was stirred at room temperature for 24 h. Then the mixture was diluted with EtOAc, washed with aqueous NH$_4$Cl, dried over anhydrous Na$_2$SO$_4$, and the solvent removed. The residue was submitted to flash chromatography (EtOAc: Hexane, 2:8) to give **84** (211 mg, 52%) as a colourless oil. ^{1}H-NMR (500 MHz, CDCl$_3$): δ (ppm) = 6.26 (d, *J* = 1.2 Hz, 1H), 5.68 (dt, *J* = 13.4, 6.7 Hz, 1H), 5.61 (s, 1H), 5.63 – 5.56 (m, 1H), 4.64 (d, *J* = 6.6 Hz, 2H), 4.171 (q, *J* = 7.1 Hz, 2H), 4.166 (q, *J* = 7.1 Hz, 2H), 3.69 (s, 6H), 2.97 (d, *J* = 11.9 Hz, 2H), 2.64 (d, *J* = 7.3 Hz, 2H), 1.29 (t, *J* = 7.1 Hz, 3H), 1.27 (t, *J* = 7.1 Hz, 3H); ^{13}C-NMR (126 MHz, CDCl$_3$): δ (ppm) = 170.9 (2xC), 166.9 (C), 155.2 (C), 136.1 (C), 129.1 (CH$_2$), 128.5 (CH), 127.0 (CH), 64.1 (CH$_2$), 63.3 (CH$_2$), 61.1 (CH$_2$), 57.8 (C), 52.6 (2xCH$_3$), 34.2 (CH$_2$), 31.1 (CH$_2$), 14.4 (CH$_3$), 14.3 (CH$_3$); EI-HRMS *m/z* calcd. for C$_{18}$H$_{26}$O$_9$ [M]$^+$: 386.1577; found: 386.1577.

Compound **85** was prepared from **84** according to previously described *GP8* to give **85** in 61 % yield. Mixture of isomers ≈ 6:1 (*cis:trans*). ^{1}H-NMR (500 MHz, CDCl$_3$): δ (ppm) = 5.72 (ddd, *J* = 23.4, 10.9, 5.7 Hz, 1H), 5.07 – 4.96 (m, 2H), 4.19 – 4.03 (m, 2H), 3.69 (s, 3H), 3.68 (s, *J* = 2.6 Hz, 3H), 2.89 (dq, *J* = 11.8, 6.0 Hz, 1H), 2.68 (dd, *J* = 4.1, 1.7 Hz, 1H), 2.34 – 2.24 (m, 3H), 1.95 – 1.87 (m, 1H), 1.74 (dt, *J* = 19.0, 9.6 Hz, 1H), 1.58 (ddd, *J* = 13.3, 8.3, 4.7 Hz, 1H), 1.25 (td, *J* = 7.1, 2.5 Hz, 3H); ^{13}C-NMR (126 MHz, CDCl$_3$): δ (ppm) = 174.8 (C), 172.3 (C), 171.8 (C), 141.4 (CH), 114.0 (CH$_2$), 60.6 (CH$_2$), 52.8 (CH$_3$), 54.9 (C), 52.70

(CH$_3$), 52.66 (CH$_3$), 36.4 (CH), 35.7 (CH$_2$), 34.0 (CH), 31.7 (CH$_2$), 31.2 (CH$_2$), 14.3 (CH$_3$); EI-HRMS m/z calcd. for C$_{15}$H$_{22}$O$_6$ [M-CH$_2$]$^+$: 298.1416; found: 298.1408.
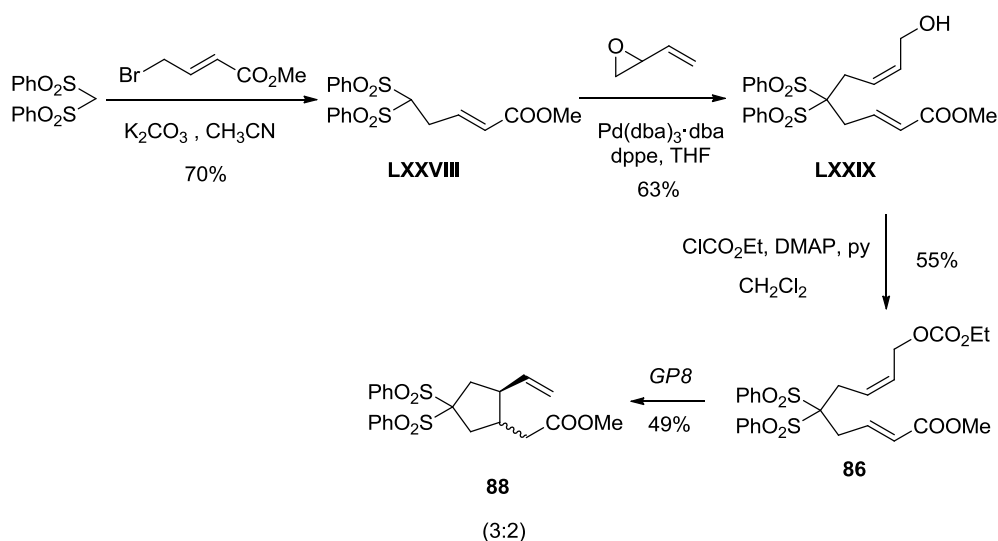
Compound LXXVIII. In a round-bottom flask methyl 4-bromocrotonate (230mg, 1.1 mmol), bis(phenylsulfonyl)methane (296 mg, 1 mmol), K$_2$CO$_3$ (152 mg, 1.1 mmol) and CH$_3$CN (10 mL) were placed. The resulting mixture was stirred under reflux for 3 h. Then K$_2$CO$_3$ was filtered and the solvent was removed. The residue was submitted to flash chromatography (EtOAc: Hexane, 3:7) to give **LXXVIII** (276mg, 70 %) as a colourless oil. ^{1}H-NMR (400 MHz, CDCl$_3$): δ (ppm) = 7.85 (d, J = 7.4 Hz, 4H), 7.61 (t, J = 7.3 Hz, 2H), 7.49 (t, J = 7.5 Hz, 4H), 6.71 (dt, J = 14.3, 7.0 Hz, 1H), 5.69 (d, J = 15.5 Hz, 1H), 4.53 (t, J = 5.9 Hz, 1H), 3.61 (s, 3H), 3.00 (t, J = 6.4 Hz, 2H); ^{13}C-NMR (101 MHz, CDCl$_3$): δ (ppm) = 165.9 (C), 141.7 (CH), 137.6 (2xC), 134.9 (2xCH), 129.7 (4xCH), 129.3 (4xCH), 124.4 (CH), 82.3 (CH), 51.7 (CH$_3$), 28.3 (CH$_2$); EI-HRMS m/z calcd. for C$_{18}$H$_{18}$O$_6$S$_2$ [M$^+$]: 394.0545; found: 394.0537.

Compound LXXIX: Butadiene monoxide (35mg, 0.5mmol) was added to a solution of **LXXVIII** (197mg, 0.5mmol), Pd(dba)3·dba (4mg, 0.025mmol) and dppe (10mg, 0.025mmol) in THF (10mL). The resulting mixture was stirred at room temperature for 16 h and then solvent was removed. The residue was filtered through a short silica pad to give **LXXIX** (47mg, 63%) as a white solid. ^{1}H-NMR (400 MHz, CDCl$_3$): δ (ppm) = 7.95 (d, J = 7.8 Hz, 4H), 7.64 (t, J = 7.4 Hz, 2H), 7.51 (t, J = 7.5 Hz, 4H), 7.00 – 6.89 (m, 1H), 5.80 (d, J = 15.7 Hz, 1H), 5.74 (t, J = 6.5 Hz, 1H), 5.68 (dd, J = 9.5, 4.7 Hz, 1H), 4.00 (d, J = 4.6 Hz, 2H), 3.64 (s, 3H), 3.04 (d, J = 6.9 Hz, 2H), 2.94 (d, J = 6.2 Hz, 2H), 2.18 (s, 1H); ^{13}C-NMR (101 MHz, CDCl$_3$): δ (ppm) = 166.0 (C), 140.3 (CH), 136.4 (2xC), 136.2 (CH), 135.0 (2xCH), 131.5 (4xCH), 128.8 (4xCH), 125.5 (CH), 122.3 (CH), 89.6 (C), 62.8 (CH$_2$), 51.8 (CH$_3$), 32.9 (CH$_2$), 32.4 (CH$_2$); EI-HRMS m/z calcd. for C$_{22}$H$_{25}$O$_7$S$_2$ [M+1]$^+$: 465.1042; found: 465.1044.

Compound 86. Ethyl chloroformiate (31 mg, 0.29 mmol) was added to a solution of **LXXIX** (122 mg, 0.26 mmol), dimethylaminopyridine (DMAP) (10 mg, 0.08 mmol), pyridine (62 mg, 0.8 mmol) in CH$_2$Cl$_2$ (5 mL), and it was stirred at room temperature for 16 h. Then the mixture was diluted with CH$_2$Cl$_2$, washed with HCl (10%), NaOH (10%) and brine and dried over anhydrous Na$_2$SO$_4$. The residue was submitted to flash chromatography (EtOAc: Hexane, 4:6) to give **86** (85 mg, 55%) as a colorless foam. ^{1}H-NMR (500 MHz, CDCl$_3$): δ (ppm) = 8.03 (d, J = 8.3 Hz, 4H), 7.72 (t, J = 7.1 Hz, 2H), 7.60 (t, J = 7.8 Hz, 4H), 7.05 – 6.95 (m, 1H), 5.98 – 5.90 (m, 1H), 5.88 (d, J = 15.5 Hz, 1H), 5.75 – 5.67 (m, 1H), 4.55 (d, J = 6.1 Hz, 2H), 4.20 (q, J = 7.1 Hz, 2H), 3.73 (s, 3H), 3.11 (d, J = 6.9 Hz, 2H), 3.02 (d, J = 6.7 Hz, 2H), 1.31 (t, J = 7.1 Hz, 3H); ^{13}C-NMR (126 MHz, CDCl$_3$): δ (ppm) = 165.8 (C), 155.0 (C), 139.9 (CH), 136.5 (2xC), 135.1 (2xCH), 131.7 (4xCH), 130.4 (CH), 128.9 (4xCH), 126.7 (CH), 125.9 (CH), 89.6 (C), 67.3 (CH$_2$), 64.3 (CH$_2$), 51.8 (CH$_3$), 33.1 (CH$_2$), 32.6 (CH$_2$), 14.4 (CH$_3$); EI-HRMS m/z calcd. for C$_{25}$H$_{28}$O$_9$S$_2$ [M]$^+$: 536.1175; found: 536.1176.

Compound 88 was prepared from **86** according to previously described *GP8* to give **88** in 50 % yield. Mixture of isomers ≈ 3:2 (*cis:trans*). ^{1}H-NMR (500 MHz, CDCl$_3$): δ (ppm) = 8.06 (dd, J = 13.3, 4.9 Hz, 4H), 7.75 – 7.68 (m, 2H), 7.60 (tdd, J = 10.7, 6.1, 4.5 Hz, 4H), 5.81 – 5.71 (m, 1H, minor isomer), 5.48 (ddd, J = 17.0, 10.2, 8.5 Hz, 1H, major isomer), 5.09 – 4.98 (m, 2H), 3.65 (s, 3H, minor isomer), 3.64 (s, 3H, major

isomer), 3.06 – 2.96 (m, 1H, minor isomer), 2.86 (dt, J = 21.8, 9.1 Hz, 1H, major isomer), 2.74 – 2.66 (m, 2H), 2.53 (ddd, J = 14.3, 6.8, 4.2 Hz, 1H), 2.47 (dd, J = 15.8, 4.0 Hz, 1H), 2.40 (d, J = 11.4 Hz, 1H), 2.36 – 2.32 (m, 2H), 2.32 – 2.24 (m, 1H), 2.17 – 2.08 (m, 1H), 2.02 – 1.95 (m, 1H); ^{13}C-NMR (126 MHz, CDCl$_3$): δ (ppm) = 172.9 (C), 172.3 (C), 137.6 (CH), 136.6 (CH), 136.3 (C), 136.1 (C), 134.8 (2xCH), 134.7 (CH), 134.6 (CH), 131.6 (2xCH), 131.5 (2xCH), 131.46 (2xCH), 131.45 (2xCH), 129.8 (C), 129.2 (C), 128.94 (2xCH), 128.89 (2xCH), 128.87 (2xCH), 128.8 (2xCH), 118.1 (CH$_2$), 117.3 (CH$_2$), 93.8 (C), 91.8 (C), 51.73 (CH$_3$), 51.71 (CH$_3$), 49.9 (CH), 46.5 (CH), 41.5 (CH), 39.1 (CH), 38.2 (CH$_2$), 37.9 (CH$_2$), 36.9 (CH$_2$), 36.8 (CH$_2$), 36.5 (CH$_2$), 35.0 (CH$_2$); EI-HRMS m/z calcd. for C$_{22}$H$_{24}$O$_6$S$_2$ [M]$^+$: 448.1014; found:448.1011.

(9:1)
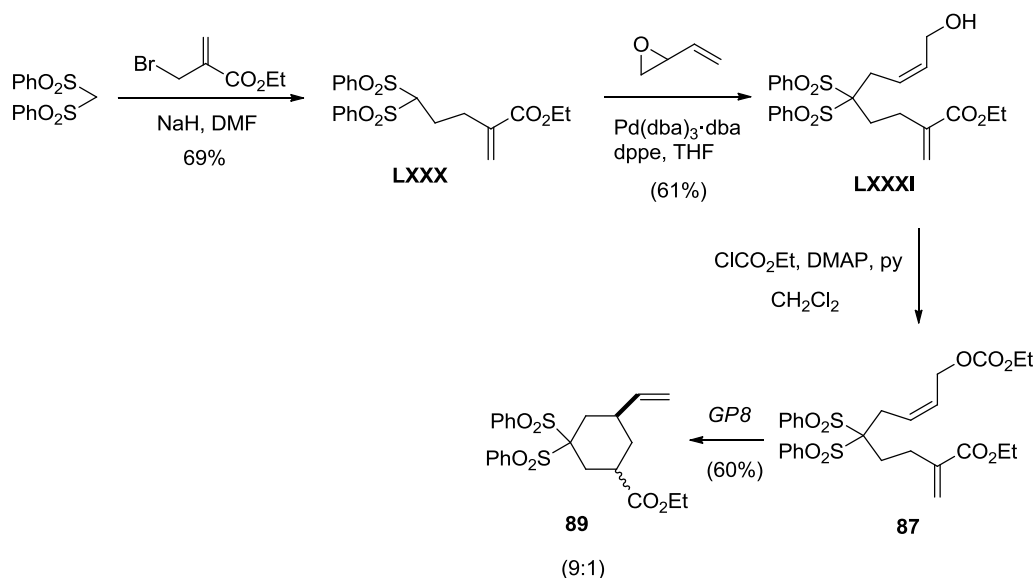
Compound LXXX. In a round-bottom flask ethyl (2-bromomethyl)acrylate (213mg, 1.1 mmol), bis(phenylsulfonyl)methane (296 mg, 1 mmol), K$_2$CO$_3$ (152 mg, 1.1 mmol) and CH$_3$CN (10 mL) were placed. The resulting mixture was stirred under reflux for 5 h. Then K$_2$CO$_3$ was filtered and the solvent was removed. The residue was submitted to flash chromatography (EtOAc: Hexane, 3:7) to give **LXXX** (320 mg, 79 %) as a colourless oil. ^{1}H-NMR (300 MHz, CDCl$_3$): δ (ppm) = 7.97 – 7.85 (m, 4H), 7.68 (t, J = 7.4 Hz, 2H), 7.55 (t, J = 7.6 Hz, 4H), 6.24 (s, 1H), 5.73 (s, 1H), 5.32 (t, J = 7.0 Hz, 1H), 4.11 (q, J = 7.1 Hz, 2H), 3.18 (d, J = 7.0 Hz, 2H), 1.25 (t, J = 7.1 Hz,3H); ^{13}C-NMR (75 MHz, CDCl$_3$): δ (ppm) = 138.4 (C), 134.6 (2xCH), 134.1 (C), 132.0 (C), 129.70 (CH$_2$), 129.67 (4xCH), 129.2 (4xCH), 128.7 (C), 81.2 (CH), 61.2 (CH$_2$), 29.6 (CH$_2$), 14.2 (CH$_3$); EI-HRMS m/z calcd. for C$_{19}$H$_{20}$O$_6$S$_2$ [M]$^+$: 408.0701; found: 408.0703.

Compound LXXXI. Butadiene monoxide (53mg, 0.75mmol) was added to a solution of **LXXX** (306 mg, 0.75mmol), Pd(dba)3·dba (6 mg, 0.0375mmol) and dppe (15 mg, 0.0375mmol) in THF (10mL) and the mixture was stirred at room temperature for 16h. The solvent was removed and the residue was submitted to flash chromatography (EtOAc: Hexane, 4:6) to give **LXXXI** (230mg, 64%) as a colorless oil. ^{1}H-NMR (300 MHz, CDCl$_3$): δ (ppm) = 6.26 (d, J = 1.2 Hz, 1H), 5.68 (dt, J = 13.4, 6.7 Hz, 1H), 5.61 (s, 1H), 5.63 – 5.56 (m, 1H), 4.64 (d, J = 6.6 Hz, 2H), 4.171 (q, J = 7.1 Hz, 2H), 4.166 (q, J = 7.1 Hz, 2H), 3.69 (s, 6H), 2.97 (d, J = 11.9 Hz, 2H), 2.64 (d, J = 7.3 Hz, 2H), 1.29 (t, J = 7.1 Hz, 3H), 1.27 (t, J = 7.1 Hz, 3H); ^{13}C-NMR (75 MHz, CDCl$_3$) δ (ppm) = 167.4 (C), 137.3 (2xC), 134.8 (2xCH), 134.5 (CH), 133.7 (C), 132.7 (CH$_2$), 131.8 (4xCH), 128.8 (4xCH), 124.5 (CH), 90.8 (C), 63.2 (CH$_2$), 61.5 (CH$_2$), 33.7 (CH$_2$), 31.6 (CH$_2$), 14.1 (CH$_3$); EI-HRMS m/z calcd. for C$_{23}$H$_{26}$O$_7$S$_2$ [M]$^+$: 478.1120; found: 478.1119.

Compound 87. Ethyl chloroformiate (52 mg, 0.48 mmol) was added to a solution of **LXXXI** (208 mg, 0.44 mmol), dimethylaminopyridine (DMAP) (16 mg, 0.13 mmol), pyridine (103 mg, 1.3 mmol) in CH$_2$Cl$_2$ (10 mL), and it was stirred at room temperature for 16 h. Then the mixture was diluted with CH$_2$Cl$_2$, washed with saturated NH$_4$Cl and dried over anhydrous Na$_2$SO$_4$. The residue was submitted to flash chromatography (EtOAc: Hexane, 3:7) to give **32** (110 mg, 49%) as a colorless oil. ^{1}H-NMR (500 MHz, CDCl$_3$): δ (ppm) = 8.04 (d, J = 7.9 Hz, 4H), 7.71 (t, J = 7.4 Hz, 2H), 7.58 (t, J = 7.8 Hz, 4H), 6.46 (s, 1H), 6.12 (s, 1H), 6.02 – 5.94 (m, 1H), 5.68 – 5.60 (m, 1H), 4.49 (d, J = 6.3 Hz, 2H), 4.20 (q, J = 7.1 Hz, 2H), 4.13 (q, J = 7.1 Hz, 2H), 3.38 (s,2H), 3.00 (d, J = 6.4 Hz, 2H), 1.31 (t, J = 7.1 Hz,3H), 1.22 (t, J = 7.1 Hz, 3H); ^{13}C-NMR (126 MHz, CDCl$_3$): δ (ppm) = 167.1 (C), 155.1 (C), 137.4 (2xC), 134.8 (2xCH), 133.5 (C), 132.6 (CH$_2$), 131.9

(4xCH), 128.8 (4xCH), 128.7 (CH), 128.6 (CH), 90.7 (C), 67.7 (CH$_2$), 64.2 (CH$_2$), 61.4 (CH$_2$), 33.9 (CH$_2$), 31.9 (CH$_2$), 14.4 (CH$_3$), 14.2 (CH$_3$); EI-HRMS (EI, 70 eV) *m/z* calcd. for C$_{26}$H$_{30}$O$_9$S$_2$ [M]$^+$: 550.1331; found: 550.1331.

Compound 89 was prepared from **87** according to previously described *GP8* to give **89** in 60 % yield. Mixture of isomers ≈ 9:1 (*cis:trans*). Only one isomer isolated. ^{1}H NMR (300 MHz, CDCl$_3$): δ (ppm) = 8.05 (m, 4H), 7.77 − 7.67 (m, 2H), 7.65 − 7.52 (m, 4H), 5.70 (ddd, *J* = 16.7, 10.8, 7.0 Hz, 1H), 5.04 − 4.91 (m, 2H), 4.18 (qd, *J* = 7.1, 1.9 Hz, 2H), 3.15 − 3.02 (m, 2H), 2.71-2.47 (ddd, *J* = 20.9, 15.6, 7.4 Hz, 2H), 2.39-1.99 (m, 2H), 1.60-1.49 (m, 2H), 1.26 (t, *J* = 7.1 Hz, 3H); ^{13}C NMR (75 MHz, CDCl$_3$): δ (ppm) = 174.0 (C), 140.8 (CH), 136.2 (2xC), 134.8 (2xCH), 131.7 (2xCH), 131.5 (2xCH), 128.9 (2xCH), 128.8 (2xCH), 114.9 (CH$_2$), 87.1 (C), 61.1 (CH$_2$), 35.6 (CH), 33.2 (CH), 30.1 (CH$_2$), 29.6 (CH$_2$), 26.4 (CH$_2$), 14.3 (CH$_3$); EI-HRMS *m/z* calcd. for C$_{23}$H$_{27}$O$_6$S$_2$ [M+1]$^+$: 463.1249; found: 463.1241.

90 Z = CO2Me (48%)
92 Z = COMe (30%)

91 Z = CO$_2$Me (80%, cis:trans= 2:1)
93 Z = COMe (47%, cis:trans= 2:1)
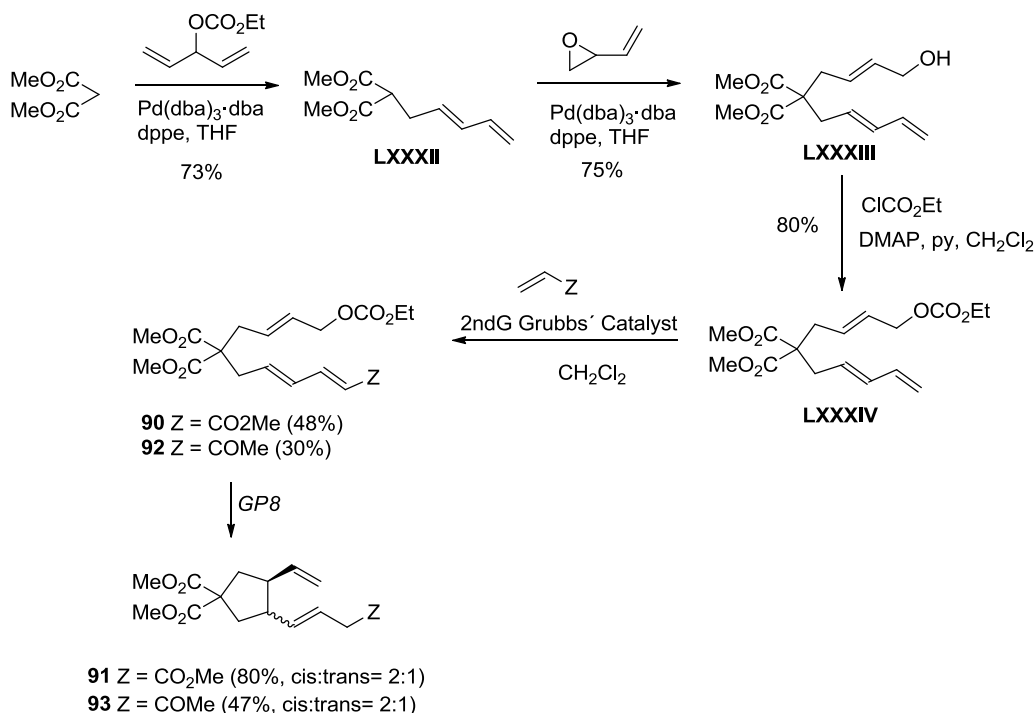
Compound LXXXII. Ethyl penta-1,4-dien-3-yl carbonate (590 mg, 3.79 mmol) was added to a solution of dimethylmalonate (500 mg, 2.27 mmol), Pd$_2$(dba)$_3$·dba (33 mg, 0.19 mmol) and dppe (75 mg, 0.19 mmol) in THF (10 mL). The resulting mixture was stirred at room temperature for 3 h and then solvent was removed. The residue was submitted to flash chromatography (EtOAc:Hexane, 2:8) to give **LXXXII** (549 mg, 73%) as a colourless oil. ^{1}H NMR (500 MHz, CDCl$_3$): δ (ppm) = 6.34 6.20 (m, 1H), 6.17 - 6.01 (m, 1H), 5.62 (dt, *J* = 14.9, 7.3 Hz, 1H), 5.13 (dd, *J* = 16.7, 1.6 Hz, 1H), 5.02 (dd, *J* = 10.1, 1.6 Hz, 1H), 3.73 (s, 6H), 3.44 (t, *J* = 7.6 Hz, 1H), 2.66 (dd, *J* = 13.8, 7.4 Hz, 2H); ^{13}C NMR (125 MHz, CDCl$_3$): δ (ppm) = 169.7 (2xC), 137.0 (CH), 134.3 (CH), 129.8 (CH), 117.1 (CH$_2$), 53.0 (2xCH$_3$), 52.1 (CH), 32.3 (CH$_2$).

Compound LXXXIII. Butadiene monoxide (176 mg, 2.52 mmol) was added to a solution of compound **LXXXII** (500 mg, 2.52 mmol), Pd$_2$(dba)$_3$·dba (22 mg, 0.13 mmol) and dppe (50 mg, 0.13 mmol) in THF (10 mL). The resulting mixture was stirred at room temperature for 16 h and then solvent was removed. The residue was submitted to flash chromatography (EtOAc:Hexane, 4:6) to give **LXXXIII** (506 mg, 75%) as colourless oil. ^{1}H NMR (500 MHz, CDCl$_3$): δ (ppm) = 6.26 (dt, *J* = 17.0, 10.3 Hz, 1H), 6.12 - 6.03 (m, 1H), 5.75 - 5.64 (m, 1H), 5.51 (ddt, *J* = 18.1, 15.2, 7.5 Hz, 2H), 5.12 (dd, *J* = 16.6, 4.5 Hz, 1H), 5.02 (dd, *J* = 9.9, 5.3 Hz, 1H), 4.07 (d, *J* = 5.4 Hz, 2H), 3.70 (s, 6H), 2.64 (m, 4H); ^{13}C NMR (125 MHz, CDCl$_3$): δ (ppm) = 171.1 (2xC), 136.5 (CH), 135.2 (CH), 134.0 (CH), 127.6 (CH), 125.8 (CH), 116.6 (CH$_2$), 63.2 (CH$_2$), 58.0 (C), 52.4 (2xCH$_3$), 35.9 (CH$_2$), 35.6 (CH$_2$).

Compound LXXXIV. Ethyl chloroformiate (245 mg, 2.27 mmol) was added to a solution of **LXXXIII** (506 mg, 1.89 mmol), dimethylaminopyridine (DMAP) (70 mg, 0.57 mmol) and pyridine (448 mg, 5.67 mmol) in CH$_2$Cl$_2$, and it was stirred at room temperature for 16 h. Then the mixture was diluted with CH$_2$Cl$_2$,

washed with HCl (10%), NaOH (10%) and brine and dried over anhydrous Na_2SO_4. The residue was submitted to flash chromatography (EtOAc:Hexane, 2:8) to give **LXXXIV** (513 mg, 80%) as a colourless oil. ^{1}H NMR (300 MHz, CDCl$_3$): δ (ppm) = 6.23 (dt, J = 16.9, 10.2 Hz, 1H), 6.03 (dd, J = 14.6, 10.7 Hz, 1H), 5.65 - 5.58 (m, 2H), 5.44 (dt, J = 15.1, 7.6 Hz, 1H), 5.09 (d, J = 16.8 Hz, 1H), 4.98 (d, J = 10.1 Hz, 1H), 4.55 - 4.42 (m, 2H), 4.15 (q, J = 7.2 Hz, 2H), 3.67 (s, 6H), 2.63 - 2.55 (m, 4H), 1.26 (t, J = 7.1 Hz, 3H). ^{13}C NMR (75 MHz, CDCl$_3$): δ (ppm) = 171.5 (2xC), 155.5 (C), 137.1 (CH), 135.9 (CH), 130.5 (CH), 128.8 (CH), 128.1 (CH), 117.2 (CH$_2$), 68.2 (CH$_2$), 64.6 (CH$_2$), 58.4 (C), 53.0 (2xCH$_3$), 36.6 (CH$_2$), 36.3 (CH$_2$), 14.9 (CH$_3$); EI-HRMS m/z calcd. for $C_{17}H_{24}O_7$ [M]$^+$: 340.1522; found: 340.1527

Compound 90. Methylacrilate (163 mg, 1.90 mmol) was added to a deoxygenated solution of Grubb´s 2nd generation catalyst (11 mg, 0.03 mmol) and compound **LXXXIV** (215 mg, 0.63 mmol) in dry CH$_2$Cl$_2$ (2 mL). The resulting mixture was refluxed for 16 hours and the solvent was removed. The residue was submitted to flash chromatography (EtOAc:Hexane, 2:8) to give **90** (120 mg, 48%) as a colourless oil. ^{1}H NMR (500 MHz, CDCl$_3$): δ (ppm) = 7.20 (dd, J = 15.4, 11.0 Hz, 1H), 6.24 - 6.10 (m, 1H), 5.98 - 5.86 (m, 1H), 5.81 (d, J = 15.4 Hz, 1H), 5.70 - 5.57 (m, 2H), 4.53 (d, J = 4.9 Hz, 2H), 4.18 (q, J = 7.1 Hz, 2H), 3.72 (s, 3H), 3.70 (s, 6H), 2.72 - 2.68 (m, 2H), 2.67 - 2.54 (m, 2H), 1.29 (t, J = 7.1 Hz, 3H); ^{13}C NMR (125 MHz, CDCl$_3$): δ (ppm) = 170.8 (2xC), 167.5 (C), 155.1 (C), 144.1 (CH), 137.0 (CH), 132.4 (CH), 129.7 (CH), 128.7 (CH), 120.8 (CH), 67.7 (CH$_2$), 64.2 (CH$_2$), 57.8 (C), 52.8 (2xCH$_3$), 51.7 (CH$_3$), 36.7 (CH$_2$), 36.2 (CH$_2$), 14.5 (CH$_3$). EI-HRMS m/z calcd. for $C_{19}H_{26}O_9$ [M]$^+$: 398.1577; found: 398.1566.

Compound 91 was prepared from **90** according to previously described *GP8* to give **91** in 80 % yield. Mixture of isomers ≈ 2:1 (*cis:trans*). ^{1}H NMR (500 MHz, CDCl$_3$): δ (ppm) = 5.73 - 5.60 (m, 1H), 5.59 - 5.48 (m, 1H), 5.48 - 5.38 (m, 1H), 4.99 (m, 2H), 3.73 (s, 6H), 3.67 (s, 3H), 3.03 (d, J = 6.4 Hz, 2H), 2.82 - 2.71 (m, 1H), 2.59 - 2.52 (m, 1H), 2.48 (dd, J = 13.8, 6.8 Hz, 1H), 2.34 - 2.27 (m, 1H), 2.23 - 2.15 (m, 1H), 2.08 - 1.98 (m, 1H); ^{13}C NMR (125 MHz, CDCl$_3$): δ (ppm) = 173.2 (2xC), 173.0 (C), 139.2 (CH, minor isomer), 138.3 (CH, major isomer), 135.0 (CH, minor isomer), 134.3 (CH, major isomer), 123.1 (CH, minor isomer), 122.9 (CH, major isomer) 115.6 (CH$_2$), 59.2 (C), 53.0 (2xCH$_3$), 51.9 (CH$_3$), 49.8 (CH, major isomer), 48.6 (CH, major isomer), 47.3 (CH, minor isomer), 46.1 (CH, major isomer), 40.4 (CH$_2$, minor isomer), 40.2 (CH$_2$, major isomer), 39.2 (CH$_2$, minor isomer) 39.1 (CH$_2$, major isomer), 38.0 (CH$_2$); EI-HRMS m/z calcd. for $C_{16}H_{22}O_6$ [M]$^+$: 310.1416; found: 310.1420.

Compound 92. Methylvinylketone (185 mg, 2.65 mmol) was added to a deoxygenated solution of Grubb´s 2nd generation catalyst (15 mg, 0.05 mmol) and compound **LXXXIV** (300 mg, 0.88 mmol) in dry CH$_2$Cl$_2$ (2 mL). The resulting mixture was refluxed for 16 hours and the solvent was removed. The residue was submitted to flash chromatography (EtOAc:Hexane, 2:8) to give **92** (100 mg, 30%) as a colourless oil. ^{1}H NMR (500 MHz, CDCl$_3$): δ (ppm) = 7.02 (dd, J = 15.7, 10.7 Hz, 1H), 6.25 - 6.12 (m, 1H), 6.03 (d, J = 15.7 Hz, 1H), 6.03 - 5.91 (m, 1H), 5.65 - 5.59 (m, 2H), 4.52 (d, J = 4.9 Hz, 2H), 4.16 (q, J = 7.1 Hz, 2H), 3.69 (s, 6H), 2.74 - 2.65 (m, 2H), 2.65 - 2.57 (m, 2H), 2.23 (s, 3H), 1.27 (t, J = 7.1 Hz, 3H); ^{13}C NMR (125 MHz, CDCl$_3$): δ (ppm) = 198.9 (C), 171.03 (2xC), 155.3 (C), 143.0 (CH), 138.0 (CH), 133.1 (CH), 130.6 (CH), 129.8 (CH), 128.9 (CH), 67.9 (CH$_2$), 64.4 (CH$_2$), 58.0 (C), 53.0 (2xCH$_3$), 37.0 (CH$_2$), 36.4 (CH$_2$), 27.5 (CH$_3$), 14.7 (CH$_3$); EI-HRMS m/z calcd. for $C_{19}H_{26}O_8$ [M]$^+$: 382.1628; found: 382.1624.

Compound 93 was prepared from **92** according to previously described *GP8* to give **93** in 47 % yield. Mixture of isomers ≈ 2:1 (*cis:trans*). ^{1}H NMR (400 MHz, CDCl$_3$) δ (ppm) = 5.74 - 5.57 (m, 1H), 5.60 - 5.47 (m, 1H), 5.48 – 5.35 (m, 1H), 4.99 (dd, J = 15.6, 5.5 Hz, 2H), 3.73 (s, 6H), 3.10 (d, J = 6.7 Hz, 2H), 2.78 (dt, J = 14.1, 7.0 Hz, 1H), 2.57 – 2.43 (m, 2H), 2.39 – 2.23 (m, 1H), 2.25 – 2.14 (m, 1H), 2.13 (s, 3H), 2.07 – 1.97 (m, 1H); ^{13}C NMR (101 MHz, CDCl$_3$) δ 207.3 (C), 172.9 (C), 139.2 (CH, minor isomer), 138.3 (CH, major isomer), 135.6 (CH, minor isomer), 134.7 (CH, major isomer), 123.4 (CH, minor isomer), 123.2 (CH, major isomer), 115.8 (CH$_2$, minor isomer), 115.6 (CH$_2$, major isomer), 59.1 (C, major isomer), 58.4 (C, minor isomer), 53.0 (2xCH$_3$), 49.9 (CH, minor isomer), 48.7 (CH, major isomer), 47.7(CH$_2$), 47.3 (CH, major isomer), 46.1 (CH, minor isomer), 40.4 (CH$_2$, minor isomer), 40.2 (CH$_2$, major isomer), 39.3 (CH$_2$, major isomer) , 38.9, (CH$_2$, minor isomer) 29.8 (CH$_3$, major isomer), 29.4 (CH$_3$, minor isomer); EI-HRMS calcd. for $C_{16}H_{21}O_5$ [M-1]$^+$: 293.1389; found: 293.1390.
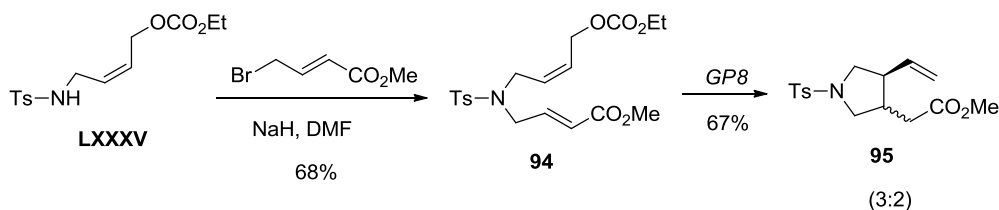
Compound 94. In a round-bottom flask methyl 4-bromocrotonate (230mg, 1.1 mmol), the tosyl amide derivative **LXXXV** (341 mg, 1 mmol), K_2CO_3 (152 mg, 1.1 mmol) and CH_3CN (10 mL) were placed. The resulting mixture was stirred under reflux for 3 h. Then K_2CO_3 was filtrated and the solvent was removed. The residue was submitted to flash chromatography (EtOAc: Hexane, 2:8) to give **94** (298 mg, 68 %) as a colourless oil. ^{1}H-NMR (300 MHz, CDCl$_3$): δ (ppm) = 7.69 (dt, J = 8.3, 2.1 Hz, 2H), 7.30 (dd, J = 8.5, 2.5 Hz, 2H), 6.73 (dt, J = 15.6, 5.8 Hz, 1H), 5.93 (dt, J = 15.6, 1.7 Hz, 1H), 5.75 – 5.45 (m, 2H), 4.56 (dd, J = 7.0, 1.4 Hz, 2H), 4.23 – 4.12 (m, 2H), 3.91 (dd, J = 5.7, 1.7 Hz, 2H), 3.87 (d, J = 1.4 Hz, 2H), 3.71 (s, 3H), 2.42 (s, 3H), 1.28 (t, J = 7.1 Hz, 3H); ^{13}C-NMR (75 MHz, CDCl$_3$): δ (ppm) = 166.1(C), 143.9 (C), 142.8 (C), 136.7 (C), 130.0 (2xCH), 129.9 (CH), 127.6 (CH), 127.4 (2xCH), 127.3 (CH), 123.7 (CH), 64.3 (CH$_2$), 62.5 (CH$_2$), 51.8 (CH$_3$), 48.2 (CH$_2$), 44.8 (CH$_2$), 21.6 (CH$_3$), 14.3 (CH$_3$); EI-HRMS m/z calcd. for C$_{19}$H$_{26}$NO$_7$S [M+1]$^+$: 412.1430; found: 412.1430.

Compound 95 was prepared from **94** according to previously described *GP8* to give **95** in 67 % yield. Mixture of isomers ≈ 3:1 (*cis:trans*). ^{1}H-NMR (500 MHz, CDCl$_3$): δ (ppm) = 7.71 (d, J = 8.1 Hz, 4H), 7.32 (d, J = 7.7 Hz, 4H), 5.45 (dt, J = 18.7, 9.6 Hz, 2H), 5.10 – 4.94 (m, 4H), 3.62 (s, 6H), 3.50 (ddd, J = 22.4, 10.0, 7.5 Hz, 1H), 3.38 (dd, J = 10.0, 6.6 Hz, 1H), 3.23 (dd, J = 10.0, 4.4 Hz, 1H), 3.03 (dd, J = 10.0, 7.8 Hz, 1H), 2.94 (dd, J = 18.6, 9.0 Hz, 1H), 2.80 (dt, J = 13.0, 6.5 Hz, 1H), 2.51 (tt, J = 14.3, 7.2 Hz, 1H), 2.43 (s, 6H), 2.31 – 2.22 (m, 2H), 2.15 – 2.03 (m, 2H); Data of the major isomer: ^{13}C-NMR (126 MHz, CDCl$_3$): δ (ppm) = 172.4 (C), 143.62 (C), 134.5 (CH), 134.1 (C), 129.82 (2xCH), 127.57 (2xCH), 118.1 (CH$_2$), 52.5 (CH$_2$), 51.8 (CH$_3$), 51.7 (CH$_2$), 45.1 (CH), 38.4 (CH), 33.2 (CH$_2$), 21.63 (CH$_3$). Data of the minor isomer: ^{13}C-NMR (126 MHz, CDCl$_3$): δ (ppm) = 172.2 (C), 143.64 (C), 136.0 (CH), 134.0 (C), 129.83 (2xCH), 127.63 (2xCH), 118.2 (CH$_2$), 53.0 (CH$_2$), 51.9 (CH$_2$), 51.8 (CH$_3$), 48.9 (CH), 40.5 (CH), 35.9 (CH$_2$), 21.64 (CH$_3$). EI-HRMS m/z calcd. for C$_{16}$H$_{22}$NO$_4$S [M+1]$^+$: 324.1270; found: 324.1271.
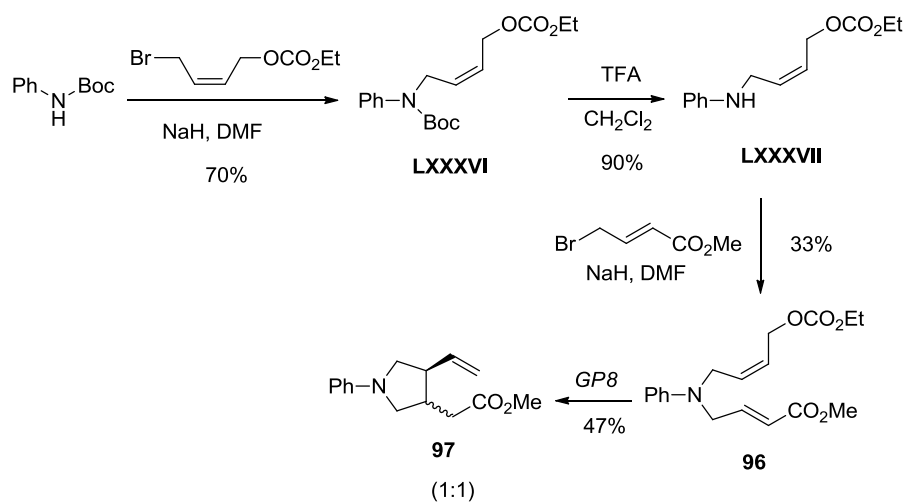
Compound LXXXVI. A sample of (Z)-BrCH$_2$CH=CHCH$_2$CO$_2$Et (1 g, 4.5 mmol) was added to a mixture of NaH (270 mg, 6.8 mmol) and *N*-Boc aniline (878 mg, 4.5 mmol) in DMF (20 mL) at 0ºC. The resulting solution was stirred at 60ºC for 15 h. Then the mixture was diluted with EtOAc, washed with HCl (10%), dried over anhydrous Na$_2$SO$_4$, and the solvent removed. The residue was submitted to flash chromatography (EtOAc: Hexane, 1:9) to give **LXXXVI** (1 g, 70 %) as a colorless oil. ^{1}H-NMR (300 MHz, CDCl$_3$): δ (ppm) = 7.34 – 7.28 (m, 2H), 7.24 – 7.16 (m, 3H), 5.99 – 5.85 (m, 1H), 5.80 – 5.64 (m, 1H), 4.62 (dd, J = 6.0, 1.0 Hz, 2H), 4.28 – 4.15 (m, 4H), 1.46 (s, 9H), 1.32 (t, J = 7.1 Hz, 3H); ^{13}C-NMR (75 MHz, CDCl$_3$): δ (ppm) = 155.2 (C), 154.6 (C), 142.9 (C), 131.7 (CH), 128.9 (3xCH), 126.7 (CH), 126.1 (CH), 125.9 (CH), 80.7 (C), 67.6 (CH$_2$), 64.2 (CH$_2$), 51.9 (CH$_2$), 28.5 (3xCH$_3$), 14.5 (CH$_3$); EI-HRMS m/z calcd. for C$_{18}$H$_{25}$NO$_5$ [M]$^+$: 335.1733; found: 335.1733.

Compound LXXXVII. An excess of trifluoroacetic acid (TFA) was added to a solution of **LXXXVI** (502 mg, 1.5mmol) in CH_2Cl_2 (15 mL). The resulting mixture was stirred at room temperature for 2h and then the solvent was removed. The residue was submitted to flash chromatography chromatography (EtOAc: Hexane, 2:8) to give **LXXXVII** (318 mg, 90%) as a colourless oil. ^{1}H-NMR (400 MHz, CDCl$_3$): δ (ppm) = 7.21 – 7.15 (m, 2H), 6.72 (t, J = 7.3 Hz, 1H), 6.61 (d, J = 7.8 Hz, 2H), 5.98 – 5.90 (m, 1H), 5.89 – 5.80 (m, 1H), 4.62 (d, J = 5.9 Hz, 2H), 4.20 (q, J = 7.1 Hz, 2H), 3.79 (d, J = 5.1 Hz, 2H), 1.31 (t, J = 7.1 Hz, 3H); ^{13}C-NMR (101 MHz, CDCl$_3$) δ (ppm) = 155.1 (C), 132.8 (CH), 129.3 (2xCH), 128.8 (C), 125.3 (CH), 117.8 (CH), 113.1 (2xCH), 67.6 (CH$_2$), 64.1 (CH$_2$), 45.3 (CH$_2$), 14.4 (CH$_3$); EI-HRMS m/z calcd. for $C_{13}H_{17}NO_3$ [M]$^+$: 235.1208; found: 235.1210.

Compound 96. Methyl 4-bromocrotonate (314mg, 1.5 mmol) was added to a mixture of NaH (60 mg, 1.5 mmol) and **LXXXVII** (235 mg, 1 mmol) in DMF (10 mL) at 0ºC. The resulting solution was stirred at room temperature for 16 h. Then the mixture was diluted with EtOAc, washed with HCl (10%) and dried over anhydrous Na$_2$SO$_4$. The residue was submitted to flash chromatography (EtOAc: Hexane, 4:6) to give **96** (111 mg, 33 %) as a colourless oil. ^{1}H-NMR (400 MHz, CDCl$_3$): δ (ppm) = 7.21 (t, J = 7.2 Hz, 2H), 6.97 (d, J = 14.4 Hz, 1H), 6.74 (t, J = 7.2 Hz, 1H), 6.67 (d, J = 7.8 Hz, 2H), 5.96 (d, J = 16.2 Hz, 1H), 5.80 – 5.68 (m, 2H), 4.72 (d, J = 3.7 Hz, 2H), 4.26 – 4.18 (m, 2H), 4.08 – 4.01 (m, 4H), 3.72 (s, 3H), 1.32 (t, J = 7.1 Hz, 3H); ^{13}C-NMR (101 MHz, CDCl$_3$): δ (ppm) = 166.7 (C), 155.2 (C), 144.9 (C), 132.1 (CH), 129.5 (3xCH), 125.8 (CH), 121.9 (CH), 117.6 (CH), 112.9 (2xCH), 64.3 (CH$_2$), 63.0 (CH$_2$), 51.9 (CH$_2$), 51.7 (CH$_3$), 48.0 (CH$_2$), 14.4 (CH$_3$); EI-HRMS m/z calcd. for $C_{18}H_{23}NO_5$ [M]$^+$: 333.1576; found: 335.1575.

Compound 97 was prepared from **96** according to previously described *GP8* to give **97** in 47 % yield. Mixture of isomers ≈ 1:1 (*cis:trans*). ^{1}H-NMR (500 MHz, CDCl$_3$): δ (ppm) = 7.25 – 7.20 (m, 2H), 6.68 (t, J = 7.3 Hz, 1H), 6.55 (d, J = 7.3 Hz, 2H), 5.83 – 5.70 (m, 1H), 5.22 – 5.07 (m, 2H), 3.70 (s, 3H, one isomer), 3.69 (s, 3H, one isomer), 3.51 (ddd, J = 12.1, 9.6, 4.5 Hz, 2H), 3.28 (dd, J = 9.4, 4.0 Hz, 1H, one isomer), 3.18 – 3.08 (m, 1H), 3.05 (t, J = 9.0 Hz, 1H), 2.83 (dt, J = 13.8, 6.9 Hz, 1H, one isomer), 2.63 (dt, J = 10.6, 5.3 Hz, 1H, one isomer), 2.56 (dt, J = 16.7, 8.4 Hz, 1H, one isomer), 2.53 – 2.44 (m, 1H), 2.41 – 2.28 (m, 1H); ^{13}C-NMR (126 MHz, CDCl$_3$): δ (ppm) = 173.2 (C), 172.9 (C), 147.7 (C), 147.5 (C), 137.9 (CH), 136.3 (CH), 129.3 (4xCH), 117.5 (CH$_2$), 117.2 (CH$_2$), 116.0 (CH), 115.9 (CH), 111.6 (4xCH), 53.4 (CH$_2$), 53.0 (CH$_2$), 52.2 (CH$_2$), 52.0 (CH$_2$), 51.8 (2xCH$_3$), 49.2 (CH), 45.3 (CH), 40.7 (CH), 38.4 (CH), 36.6 (CH$_2$), 34.1 (CH$_2$); EI-HRMS m/z calcd. for $C_{15}H_{19}NO_2$ [M]$^+$: 245.1416; found: 254.1410

CONCLUSIONES GENERALES

En el capítulo 1 objetivo 1, hemos diseñado y abordado la síntesis de una red bidimensional anisotrópica que podría comportarse como un conductor molecular plano. La síntesis de la subunidad structural menor se llevó a cabo con éxito pero este diseño original no ha permitido la síntesis de estructuras más extensas. Para ello, se propone un nuevo diseño de malla que permite obtener una estructura plana conductora menos rígida y más soluble.

En el capítulo 1 objetivo 2, hemos comenzado a estudiar sistemas modelo funcionalizadas con las bases nitrogenadas adenina y timina, que podría autoensamblarse en una superficie mediante enlaces de hidrógeno para dar estructuras 2D supramoleculares conductoras. Aunque los resultados son esperanzadores, el empleo de téncicas de síntesis en fase sólida así como otros motivos de unión más estables serán claves para la terminar con éxito esta nueva aproximación.

En el capítulo 2 objetivo 1, hemos desarrollado una familia de macrociclos conductores basados en oligómeros de fenilacetileno. Para fijar la estructura de la hélice de forma chiral hemos utilizado un derivado del acido tartárico. El aislamiento de una única hélice de quiralidad M, se consiguió cerrando un esqueleto de oPE, primero con una "grapa" quiral que definió un eje preferente y, después, haciendo más rígida la estructura con una segunda "grapa" formada mediante la reacción de metátesis de alquenos.

En el capítulo 2 objetivo 2, hemos estudiado la integración de metales en la cavidad de un "poro molecular". De entre los distintos metales probados, los metales carbófilos Ag(I) y Au(I) dieron lugar a los productos organometálicos. Con el fin de estudiar la fortaleza de la interacción Ag(I)-alquino, hemos realizado valoraciones utilizando ^{1}H-RMN, espectroscopia de *UV-vis* y CD. Los resultados de las valoraciones sugieren que la capacidad de coordinación de estos macrociclos es discreta en términos de energía libre y depende en gran parte del tamaño de la cavidad que generan, de la flexibilidad del esqueleto cíclico y de la geometría de coordinación preferente de la Ag(I).

Durante los estudios de quelación de las hélices con el ión Ag(I), observamos que este metal parecía inducir el plegamiento helicoidal de los oligómeros abiertos de oPE. Mediante un estudio sistemástico experimental y teórico, hemos cooborabado que las sales de Ag(I) pueden utilizarse para inducir el plegamiento de oligómeros de oPE para dar helicatos. Además hemos hecho un estudio fotocinético que ha proporcionado información cuantitativa sobre la velocidad de plegamiento de estos foldámero en presencia y ausencia de Ag(I). Además, hemos comenzado el estudio de una nueva familia de *helicatos* ditópicos más estables de los cuales se podrían desarrollar versiones chirales y capaces de coordinarse otros metales.

En el capítulo 3, hemos desarrollado un método eficiente para la alilación intramolecular tipo Michael de grupos carbonilo α,β-insaturados, a partir de carbonatos y carboxilatos alílicos (pronucleófilos). El uso combinado en cantidades catalíticas de complejos de Ti/Pd ha permitido la síntesis de carbo- y heterociclos de cinco y seis miembros con rendimientos moderados y generalmente buenas diastereoselecciones. Además, hemos realizado varias pruebas mecanísticas que confirman que esta reacción transcurre mediante una vía radicalaria.

APPENDICES

A1. Influence of the Number of Anchoring Groups on the Electronic and Mechanical Properties of Benzene-, Anthracene- and Pentacene-Based Molecular Devices[449]

Intuitively, if an organic molecule were bound to a metallic electrode through more than one linking group, both an increase in the conductivity and better mechanical stability would be expected. Several linkers could act collectively to reduce possible molecule–electrode disconnections due to thermal or mechanical stress, and thus improve system reliability.

Based on this hypothesis, we decided to theoretically study three new single-molecule devices in which simple bencene (B), antracene (A) and pentacene (P) are bound to the gold electrodes by means of a sandwich-type junction with different numbers of sulfur-anchoring groups. Anthracene and pentacene can be considered as the smallest member of the family of zig-zag graphene nanoribbons,(ZGNRs) and larger systems have been successfully synthesized by several groups.
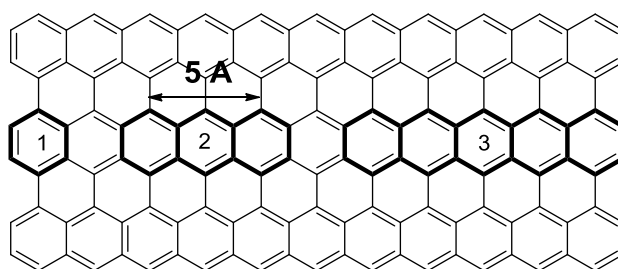
To survey the consequences of increasing the number of S-linker on the electronic and mechanical behavior of our conceptual single-molecule device, the current profiles and the analysis of the transmission data and current stability were calculated by NEGF and SIESTA code.
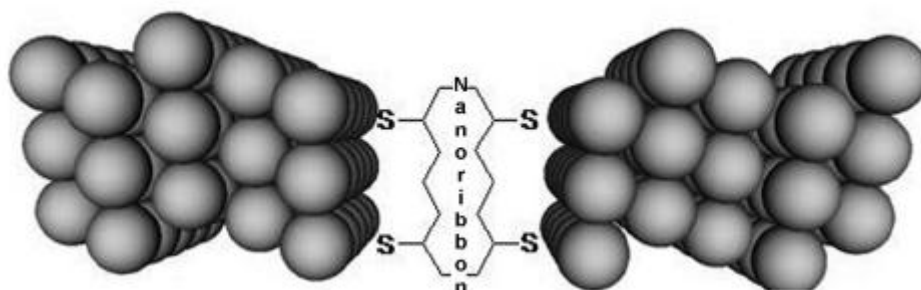
[449] A. Martín-Lasanta, D. Miguel, T. García, J. A. López-Villanueva, S. Rodríguez-Bolivar, F. M. Gómez-Campos, E. Buñuel, D. J. Cárdenas, L. Álvarez de Cienfuegos, J. M. Cuerva, *ChemPhysChem* **2012,** *13*, 860-868. DOI: 10.1002/cphc.201100582.

A2. Organic-based molecular switches for Molecular Electronics[450]

Molecular electronics (ME) is the branch of nanotechnology which studies the application of molecular building blocks for the fabrication of electronic components. In many cases an emulation of the properties of macroscopic devices is intended. Thus, a typical example in conventional computing and digital information storage is the condition of having clearly different states. This requirement is usually related to the 0 or 1 values (a bit) set by the defined measure of a property. Molecular switches are defined as species which can change between two or more states with distinct properties due to an external triggering stimulus. The switching process could serve to reproduce circuit elements at the molecular level, as the tiniest unit for information storage or as basic elements for more complex logic operations. In this context, the control of electron transport (ET) through nanomaterials and even single molecules is highly valuable. Hence, molecular switches able to produce changes in their electronic properties (mainly conductivity) are primary targets. The switching event must satisfy some basic requirements to be useful: (a) to have high differences in the magnitude of the initial and final value of the properties, (b) to be stable enough to take information of the states without disrupting them, and (c) the interconversion barrier between the states has to be higher than the thermal energy at the working temperature.

A3. Titanium/Palladium-Mediated Regioselective Propargylation of Ketones using Propargylic Carbonates as Pronucleophiles[451]

In recent years alkynes have become versatile building blocks in organic synthesis. Therefore, reactions able to efficiently introduce this functional group in a given structure are indispensable. A careful inspection of the described protocols shows that methods for the propargylation of carbonyl compounds using propargylic organometallic species exist in literature. Nevertheless, most of them have some drawbacks derived from their high reactivity, complex preparation and/or poor regioselectivity, usually yielding mixtures of homopropargylic and allenylic alcohols.

Propargylic carbonates are readily available compounds but inert under the classical Barbier conditions. Combining the reactivity of Ti/Pd complexes, we have developed a novel and mild propargylation method which works effitiently with terminal and internal alkynes to give exclusively the homopropagylic alcohol. The only exception to the regioselectivity was observed when the reaction was carried out intramolecularly. In that case, the conformational restrictions favor the formation of the corresponding six-membered carbocycle bearing an allenyl side chain.
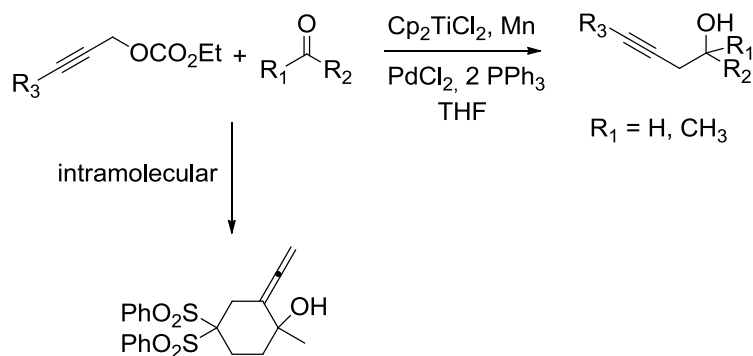
[451] A. Millán, L. Álvarez de Cienfuegos, A. Martín-Lasanta, A. G. Campaña, J. M. Cuerva, *Adv. Synth. Catal.* **2011,** *353*, 73-78. DOI: 10.1002/adsc.201000655.

A4. Combining the Power of Ti(III)-mediated Processes for an Easy Access to Hydroxylated Polycyclic Terpenoids. Synthesis of Sesterstatin 1 and C-D Rings of Aspergilloxide[452]

Radical cascade cyclizations are excellent methods for the stereoselective synthesis of polycyclic terpenes from relatively simple acyclic precursors. Within this context, radical cyclization of epoxypolyprenes catalyzed by titanocene(III) complex [Cp$_2$TiCl] has been reported in the preparation of several C-3 hydroxylated terpenoids such as sesquiterpenoids, diterpenoids, polycyclic triterpenoids, and meroterpenes in racemic and enantioselective forms.
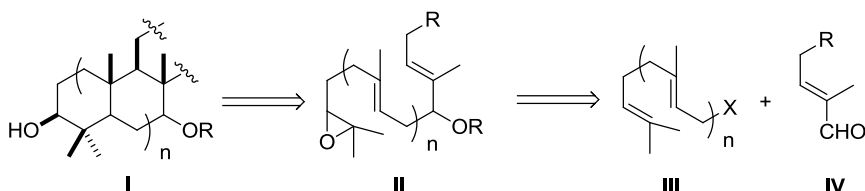
(Poly)hydroxylated terpenes are widespread in nature and they exhibit diverse biological properties such as anti-inflammatory, cytotoxic, antifeedant, platelet aggregation, and antimicrobial effects. In this work, we explored the usefulness and versatility of Ti(III) chemistry for the preparation of functionalized (poly)hydroxylated epoxy(poly)prenes and (poly)hydroxylated terpenes. The success of this approach is based on the excellent a-regioselective of Barbier-type reactions mediated by a bulk Ti(III) complex [(tBuC$_5$H$_4$)$_2$TiCl] and the straightforward bioinspired radical cyclization catalyzed by the classical Ti(III) reagent [Cp$_2$TiCl]. To demonstrate the potential interest of this methodology, the pentacyclic scalarane sesterstatin 1 and a model of the C-D rings of the marine natural sesterterpenoid aspergilloxide were prepared.

Sesterstatine 1

Model compound 3 for
the C and D rings of 2
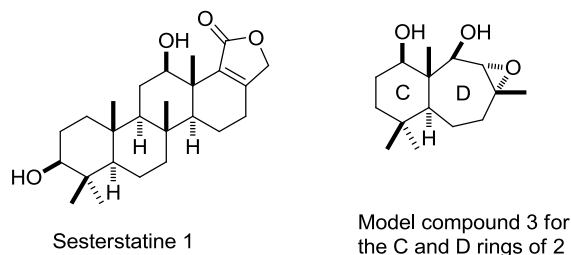
[452] T. Jiménez, S. P. Morcillo, A. Martín-Lasanta, D. Collado-Sanz, D. J. Cárdenas, A. Gansäuer, J. Justicia, J. M. Cuerva, *Chem., Eur. J.* **2012**, *18*, 12825-12833. DOI: 10.1002/chem.201201534.

A5. Ti(III)-catalyzed cyclizations of ketoepoxypolyprenes: frustrated polycyclizations and unexpected stereoselectivities[453]

In the present work, we have described a new strategy to control Ti(III)-catalyzed bioinspired radical cyclizations using α,β-unsaturated ketones placed in appropriate positions in the starting ketoepoxypolyene. Based on our previuos results on Michael-type conjugated additions, we thought that the simple oxidation of the hydroxylated polyprene to the α,β-unsaturated ketone could stop the radical cascade at a desired point due to the reduction of the intermediate enol radical. Surprisingly, some bicycles presented a very uncommon *cis* fusion between A and B rings. This results was reasoned afterwards due to a template effect exerted by the titanium catalyst which can be simultaneously coordinated to the epoxide and the ketone group. The mechanistic hypothesis proposed for this unexpected cis-regioselectivity was confirmed by theoretical calculation. This procedure has allowed us to synthesize several polycyclic terponoids with acceptable yields meeting the demand for selectivity and atom- and step economy required for any modern synthesis.

453

INDEX OF SCHEMES

216

LIST OF PUBLICATIONS FROM THE PhD PERIOD

• *Titanium/Palladium-Mediated Regioselective Propargylation of Ketones Using Propargylic Carbonates as Pronucleophiles.* A. Millán, L. Álvarez de Cienfuegos, A. Martín-Lasanta, A. G. Campaña, J. M. Cuerva, *Adv. Synth. Catal.* **2011,** *353*, 73-78.

• *Ti/Pd-Catalyzed Intramolecular Michael-type Addition of Allylic Carboxylates to Activated Alkenes.* A. Millán, A. Martín-Lasanta, D. Miguel, L. Álvarez de Cienfuegos, J. M. Cuerva, *Chem.Comm.* **2011***, 47,* 10470-10472*.*

• *Organic-based molecular switches for Molecular Electronics.* N. Fuentes, A. Martín-Lasanta, L. Álvarez de Cienfuegos, M. Ribagorda, A. Parra, J. M. Cuerva, *Nanoscale* **2011**, *353,* 73-78.

• *Influence of the Number of Anchoring Groups in the Electronic and Mechanical Properties of Benzene-, Anthracene- and Pentacene-Based Molecular Devices* A. Martín-Lasanta, D. Miguel, T. García, J. A. López-Villanueva, S. Rodríguez-Bolivar, F. M. Gómez-Campos, E. Buñuel, D. J. Cárdenas, L. Álvarez de Cienfuegos, J. M. Cuerva, *ChemPhysChem* **2012,** *13*, 860-868.

• *Combining the Power of TiIII-mediated Processes for an Easy Access to Hydroxylated Polycyclic Terpenoids. Synthesis of Sesterstatin 1 and C-D Rings of Aspergilloxide,* T. Jiménez, S. P. Morcillo, A. Martín-Lasanta, D. Collado-Sanz, D. J. Cárdenas, A. Gansäuer, J. Justicia, J. M. Cuerva, *Chem., Eur. J.* **2012**, *18*, 12825-12833.

• *A versatile bottom-up approach to stapled π-conjugated helical scaffolds: Synthesis and chiroptical properties of cyclic o-phenylene ethynylene oligomers,* N. Fuentes, A. Martín-Lasanta, L. Álvarez de Cienfuegos, R. Robles, D. Choquesillo-Lazarte, J. M. García-Ruiz, A. J. Mota, L. Martínez-Fernández, I. Corral, D. J. Cárdenas, M. Ribagorda, M. C. Carreño, J. M. Cuerva, *Angew. Chem. Int. Ed.* **2012**, *51*, 1-6.

• *Ti(III)-catalyzed cyclizations of ketoepoxypolyprenes: frustrated polycyclizations and unexpected stereoselectivities* S. P. Morcillo, D. Miguel, S. Resa, A. Millán, A. Martin-Lasanta, D. Choquesillo-Lazarte, J. M. García-Ruiz, A. J. Mota, J. Justicia, J. M. Cuerva, *manuscript in preparison*